Transition Metal-Catalyzed Oxidative Cross Coupling for Synthesis and Functionalization of Diverse Molecules

By

Aristidis Vasilopoulos

A dissertation submitted in partial fulfillment

of the requirements for the degree of

Doctor of Philosophy

(Chemistry)

at the

University of Wisconsin – Madison

2021

Date of Final Oral Examination: 02/02/2021

The dissertation is approved by the following members of the Final Oral Committee:
Shannon S. Stahl, Professor, Chemistry
Tehshik P. Yoon, Professor, Chemistry
Clark R. Landis, Professor, Chemistry
Daniel J. Weix, Professor, Chemistry

Transition Metal-Catalyzed Oxidative Cross Coupling for Synthesis and Functionalization of Diverse Molecules

Aristidis Vasilopoulos

Under the supervision of Professor Shannon S. Stahl

At the University of Wisconsin-Madison

Abstract

Modular C–H functionalization methods offer a direct approach to molecular derivatization. In "radical relay" C–H functionalization reactions, a C(sp^3)–H bond can be abstracted by an H atom transfer (HAT) reagent to form an alkyl radical. It has been demonstrated that alkyl radicals can be cross coupled with nucleophilic coupling partners in the presence of transition metal catalysts or reacted directly with compatible radical traps to form new bonds. Such oxidative coupling reactions allow bond construction from otherwise unreactive C–H sites enabling conversion of simple molecular building blocks into value added product libraries and generation of structural analogues of important molecules that can be tested for improved properties. This thesis discloses the development, mechanistic understanding, and application of several oxidative cross coupling methods including C(sp^3)–H arylation, fluorination, and methylation reactions as well as an aerobic oxidative amidation reaction between alcohols and amines.

Chapter 2 discusses our initial efforts in C(sp^3)–H bond functionalization, which were inspired by the Kharasch-Sosnovsky reaction (1958), an allylic C–H bond functionalization method for C–O/C–N bond formation using Cu with a peroxide oxidant. We targeted the expansion of this reaction paradigm towards direct formation of C–C bonds, which had yet to be achieved

intermolecularly. We developed a Cu-catalyzed oxidative C–C coupling of benzylic C–H bonds with arylboronic esters to form 1,1-diarylalkanes employing a peroxide oxidant. The reaction tolerates numerous functional groups, including several that are usually sensitive to oxidizing conditions.

Chapters 3 and 4 cover related studies on radical relay C(sp^3)–H functionalization reactivity again using Cu as the catalyst, but now with N-fluorobenzenesulfonimide (NFSI) as the oxidant. Using this system in concert with a boronate sacrificial reductant, we discovered a benzylic C–H fluorination reaction (chapter 3). In contrast to aliphatic fluorides, benzyl monofluorides are relatively unstable in the presence of hydrogen-bond donors and Lewis acids. Alkylarene fluorination products were converted into diverse structures via catalyzed displacement of the fluoride in the presence of oxygen, nitrogen, and carbon nucleophiles that would otherwise be incompatible with a direct oxidation reaction pathway (chapter 4).

Successful development of the Kharasch-type C(sp^3)–C(sp^2) coupling reaction from chapter 2 led us to pursue a peroxide-based C(sp^3)–C(sp^3) cross coupling variant in chapter 5. This time, we sought to develop a peroxide-based C–C coupling reaction that uses the C–H substrate as the limiting reagent. We hypothesized that this goal could be achieved by controlling β-Me scission reactivity of *t*BuO• from the peroxide by accessing the radical at low temperatures (*vide infra*). We targeted the development of a C(sp^3)–H methylation reaction that employs photosensitization to activate the peroxide at room temperature. Photosensitization was effective for the activation of *t*BuOO*t*Bu at room temperature, leading to *t*BuO• fragments that served as both HAT reagents and methyl radical sources. A Ni catalyst facilitated cross coupling of the alkyl radical, resulting from HAT, with a methyl radical, resulting from β-Me scission, to form the C(sp^3)–Me bond. The

optimized C–H methylation reaction demonstrates broad functional group tolerance and is able to use the C–H substrate as limiting reagent.

Chapter 6, although not directly related to chapters 2-5, details the development of a unique oxidative cross coupling reaction for the synthesis of complex α-heteroamides. Our research group reported a Cu/ABNO-catalyzed aerobic oxidative amidation method that couples alcohols with amines. In chapter 6, alcohols bearing β-electron-withdrawing atoms were recognized as strategic substrates for this method. By targeting these alcohols as coupling partners, a simplified yet improved catalyst system was identified that can be used to form densely functionalized amides from functionally rich alcohols and amines in high yields. In addition to the excellent reactivity, the method demonstrates high chemoselectivity for the amidation of primary amines in the presence of secondary amines due to steric constraints of the catalyst system.

Collectively, these methods contribute to the breadth of oxidation reactions available for the synthesis and functionalization of diverse molecules. The C–H arylation, fluorination/fluoride displacement, and amide coupling all are opportunities to apply oxidative coupling directly to the synthesis of important molecules. Complementarily, the fluorination and methylation reactions present opportunities to functionalize existing molecules to allow derivatized compositions of matter to be accessed for testing. Both forms of methodology are appealing for application in synthesis-driven specialties, where rapid and direct access to new structures is essential to solving complex challenges.

Acknowledgements

In chemistry, I did not realize how lucky I was to work with Prof. Jeff Byers as an undergraduate until I finished my degree and realized that it is uncommon for an assistant professor to directly mentor an undergraduate. Jeff personally taught me how to run a column in the lab! Working with Jeff for 3 years allowed me to experience the struggles of being a young graduate student before I ever set foot in Madison. In Jeff's lab, I was also fortunate enough to work with Jessica Drake and Dr. Hilan Kaplan, both of whom were gracious mentors.

Working with Prof. Shannon Stahl at UW has been a formative experience. Shannon's mentorship has imparted me with vastly improved communication skills (written and verbal), leadership skills, and time-management skills. Shannon also ignited an attention to detail in myself that I had never known before. When I joined Shannon's group, I was a student, and from his guidance, I now feel like a scientist. Shannon was not without help in fostering my growth. Dr. Susan Zultanski, Dr. Scott McCann, and Dr. Shane Krska are three individuals that I owe immensely for any success that I have experienced at UW-Madison. Each of them taught me irreplaceable lessons about how to be a good researcher. I am grateful for the time that they have invested in me and I largely attribute my scientific approach to their teachings. In addition to these individuals, there are others who have contributed significantly to my training: Dr. Spring Knapp, Dr. Mycah Uehling, Kevin Dykstra, Bing Li, Dr. Damian Hruszkewycz, Prof. Alastair Lennox, Prof. Dian Wang, and Dr. Yuriy Slutskyy are just a few people that I have looked up to over the past few years. Each have taught me lessons about being a good scientist, co-worker, and person. I also thank my committee for their guidance through my Ph.D. Brainstorming through ideas with Prof. Tehshik Yoon and Prof. Clark Landis at key intervals in my graduate training has helped ensure that my research was always pointing in the right direction.

I owe a lot of my development to my co-workers as well, who have taught me to be a better team member and taught me to think outside my comfort zone. I always enjoyed my scientific discussions with Sijie Chen, David Bruns, Alexios Stamoulis, Kristine Golden, Prof. Joshua Buss, and Paige Piszel. In addition to spending time in the Stahl labs, I spent a lot of time in the mass spectrometry lab with Dr. Martha Vestling and she always made UPLC data analysis more pleasant. I have also enjoyed my experiences with other staff including Dr. Heike Hofstetter, Mike Bradley, Steve Myers, Kendall Schneider, and Karen Stephens, among others. Lastly, I have to thank my friends from graduate school for always being there to decompress. Dr. Zeb Girvin, Ben Grabow, Dr. Chase Salazar, Kevin Garcia, and Lauren Whitmire are some of my best friends and between them and anyone that has been to a dock party, Halloween party, tailgate, game night, friendsgiving, costume party, or bachelor party with me, they turned the difficult and trying experience that is graduate school into some of the most enjoyable years of my life.

From my personal life, I need to thank my family. My dad taught me how to work hard, how to challenge myself, and, how to believe in myself. My mom taught me how to have fun, how to treat people that I care about, and how to balance my work with my life. My sisters, cousins, friends, and friends' families have all had important influences on me along the way as well. I am thankful to have spent so much time with them all. Finally, I have to thank my ever-supportive significant other Leslie Mei and her lovely family for being so caring and inclusive the past several years. My inner circle was dealt a massive toll when my father was diagnosed with advanced Alzheimer's disease in late 2018, and my sisters and I needed all of the support that we could get in order to emotionally pull through the experience. So, thank you to the Mei family for being my family away from family when I needed it the most.

I dedicate this thesis to my father, John Vasilopoulos.

Table of Contents

List of Figures

List of Schemes

List of Tables

Abbreviations and Acronyms

HAT	hydrogen atom transfer
NFSI	*N*-fluorobenzenesulfonimide
NHSI	*N*-(phenylsulfonyl)benzenesulfonamide
NSI	bis(phenylsulfonyl)amide (anion)
Bdiol	4,4,6-trimethyl-1,3,2-dioxaborinane
Bpin	pinacolboron
BOX	bisoxazoline
CAS	chemical abstracts service
$^{t\text{Bu}}$bpy	4,4′-di-*tert*-butyl-2,2′-dipyridyl
CuI•DMS	copper iodide dimethyl sulfide complex
$NiCl_2$•dme	Nickel(II) chloride ethylene glycol dimethyl ether complex
phd	1,10-phenanthroline-5,6-dione
phen	1,10-phenanthroline
Bphen	4,7-diphenyl-1,10-phenanthroline
acac	acetylacetone
PTFE	polytetrafluoroethylene
tpy	terpyridine
$^{t\text{Bu}}$tpy	4,4′,4″-tri-*tert*-Butyl-2,2′:6′,2″-terpyridine
ABNO	9-azabicyclo[3.3.1]nonane N-oxyl
TEMPO	(2,2,6,6-tetramethylpiperidin-1-yl)oxyl
TPA	tris(2-pyridylmethyl)amine
Ir–F	$Ir[dF(CF_3)ppy]_2{}^{t\text{Bu}}bpyPF_6$

DTBP	di-*tert*-butyl peroxide
DCP	dicumyl peroxide
TFE	2,2,2-trifluoroethanol
DCE	1,2-dichloroethane
RSM	remaining starting material
% conv	percent conversion of the C–H substrate
THF	tetrahydrofuran
DMSO	dimethyl sulfoxide
DCM	dichloromethane
HFIP	hexafluoroisopropanol
ACN	acetonitrile
PEG	polyethylene glycol
TFAA	trifluoroacetic anhydride
TFA	trifluoroacetate
•TFA	trifluoroacetic acid
Selectfluor	1-chloromethyl-4-fluoro-1,4-diazoniabicyclo[2.2.2]octane bis(tetrafluoroborate)
TFAH	trifluoroacetic acid
DBU	1,8-diazabicyclo[5.4.0]undec-7-ene
TMG	1,1,3,3-tetramethylguanidine
UV-Vis	ultraviolet-visible
LC-AP	liquid chromatography area percent
GC-MS	gas chromatography mass spectrometer
LC-MS	liquid chromatography mass spectrometer

UPLC-MS	ultra performance liquid chromatography mass spectrometer
PCET	proton-coupled electron transfer
ETPT	electron transfer proton transfer
ee	enantiomeric excess
d.r	diastereomeric ratio
r.r	regioisomeric ratio

Chapter 1.

C(sp^3)–H Functionalization: Introduction and Recent Developments

1.1. Emergence of practical C(sp^3)–H functionalization reactivity

In synthetic organic disciplines there is a constant demand for practical synthetic methods. The importance of practical, robust reactivity is evident from the most commonly used reactions in the pharmaceutical industry: acylation, Suzuki cross coupling and substitution reactions make up 50% of all reactions used.[1] Popularity of these reactions is due to their ease of setup, reliability, and ability to couple structural buildings blocks, which enables generation of cross coupling libraries for exploring new products and expeditious routes for target-oriented synthesis.[2] The synthetic utility of these reactions is supplemented by their use of naturally abundant functional groups including carboxylic acids, amines, alcohols, boronic acids/esters, and aryl/alkyl halides. While coupling reactions between building blocks with pre-functionalized groups has proven to be reliable and robust, efforts are being made to engage C–H bonds in cross coupling (Scheme 1.1A).[3,4] C(sp^3)–H bonds are ubiquitous in organic molecules and their selective activation and coupling would unlock countless opportunities for synthesis of bonds at new sites (Scheme 1.1B).[5,6] Despite the promise of C(sp^3)–H functionalization, synthetic limitations have caused it to be used sparingly in the synthetic organic community. Historically, common limitations of C–H functionalization included narrow substrate and functional group compatibility, requirement of excess C–H substrate, utilization of exotic or dangerous reagents, and uncontrollable substrate-dependent site-selectivity.[7] Recent discoveries in C–H functionalization have begun to address these issues and some new methods demonstrate levels of practicality that rival that of coupling reactions between pre-functionalized substrates.[8,9,10] The enclosed thesis research strives to further

minimize the gap in practicality between traditional coupling reactions and C(sp^3)–H functionalization.

Scheme 1.1. Practical C(sp^3)–H functionalization unlocks opportunities in synthesis

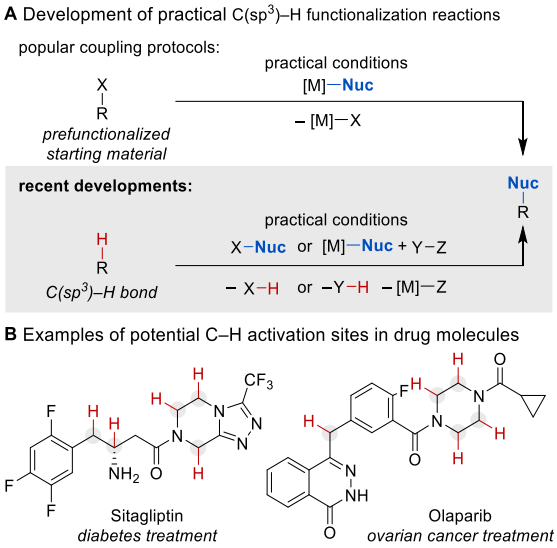

The field of C–H functionalization is burgeoning with success and is led by developments in the disciplines of photoredox, radical rebound, radical relay, directed C–H activation, and C–H insertion chemistry.[11-16] In this preamble, advances in practical C–H functionalization from 2015-2020 will be discussed to serve as a contextual medium for the enclosed research. A reaction is considered "practical" if it is able to utilize the valuable coupling partner as limiting reagent, it tolerates and/or installs at least two functional groups commonly used in coupling reactions, and ideally has a convenient reaction protocol with respect to reaction setup and availability of reagents. The chemistries summarized here are only a small subset of those that fit this description, but are a representative sample of leading developments. The reactions are organized into two groups, C–H functionalization for synthesis (Scheme 1.2A) and C–H functionalization for molecular derivatization (Scheme 1.2B). In the synthesis section, reactions that couple two building blocks > 75 molecular weight are grouped while the molecular derivatization section contains reactions where only the C–H substrate is structurally complex. Within these divisions,

the reactions are subdivided between direct C–H functionalization, where the final product is obtained in one step, and indirect C–H functionalization, where the C–H bond is transformed into a group that is converted to the product(s). This collection of reactions reveals that the limitations of narrow substrate and functional group compatibility, requirement of excess C–H substrate, and utilization of exotic or dangerous reagents are being overcome in modern chemistries. However, controlling site-selectivity of C–H activation remains a major challenge for the field. After summarizing the leading reactions, the latest developments for controlling site-selectivity are briefly reviewed.[17] Collectively, this information provides a basis for comparison for the following thesis research on oxidative C(sp^3)–H functionalization.

Scheme 1.2. C(sp^3)–H functionalization can be used broadly via direct or indirect approaches

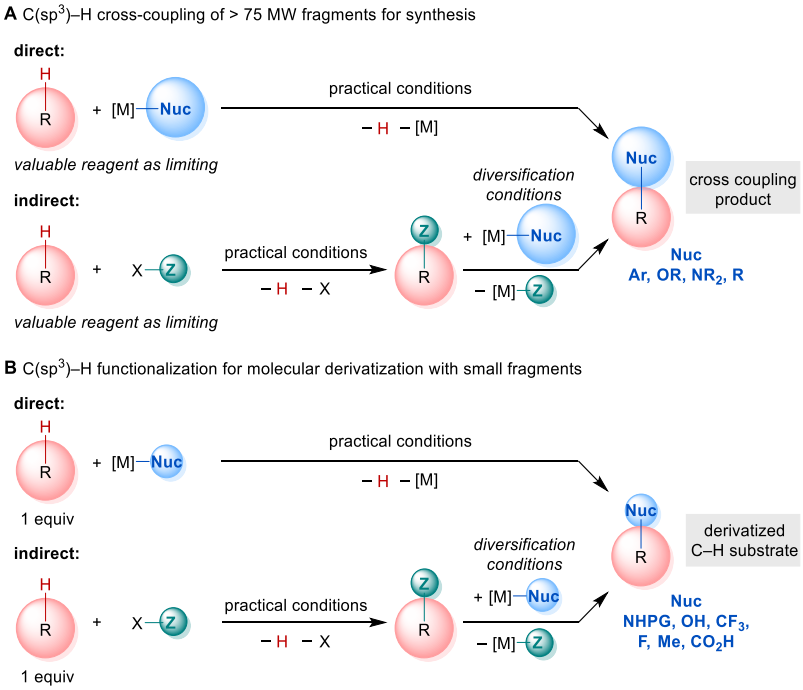

1.2. C(sp^3)–H functionalization for synthesis – C–H cross coupling

C(sp^3)–H cross coupling reactions that are able to couple two partners with a molecular weight > 75 are privileged for the generation of compound libraries and in some cases are useful for target-

oriented synthesis. In medicinal chemistry, implementation of these technologies allows a pharmaceutical core fragment that has demonstrated some biological activity to be chosen as a substrate for C–H functionalization that is cross coupled with hundreds or even thousands of different coupling partners at a C–H site. Submission of the coupling products to biological assays could lead to the identification of a new and improved lead compound that could serve as the basis for further synthetic optimization studies.[18] An alternative application of C–H functionalization for synthesis is in target-oriented synthesis, where the desired structure is known. In this scenario, C–H functionalization can be enabling for a retrosynthetic analysis that allows a synthon to be conveniently coupled at a C–H site of another synthon to streamline a synthetic route.[19,20] Development of C–H functionalization for synthesis has flourished in recent years and some leading examples are outlined in the following sections.

1.2.1. List of direct C(sp^3)–H functionalization reactions for synthesis

The Liu lab published a study on benzylic C–H arylation using a Cu catalyst with arylboronic acids as aryl source and N-fluorobenzenesulfonimide (NFSI) as oxidant (Scheme 1.3A). The reaction proceeds via radical intermediates, wherein NFSI is activated by Cu to form a sulfonimidyl radical capable of undergoing HAT on the C–H substrate to form a substrate radical. The substrate radical is functionalized by a Cu^{II}–Ar species to yield the 1,1-diarylalkane product.[21] Although the substrate scope is limited to activated alkylarenes and electron-deficient arylboronic acids, this reaction is unique in that it can use the C–H substrate as limiting reagent in a non-directed C(sp^3)–H arylation reaction. A follow-up study has since been published describing an enantioselective, albeit less practical, variation of this reaction (> 4 day reaction time).[22]

The Stahl lab reported a benzylic C–H etherification reaction using alcohols as nucleophiles that also uses a Cu/NFSI catalyst system (Scheme 1.3B). Like the arylation reaction, this reaction proceeds via radical intermediates. A substrate radical is formed by HAT from the sulfonimidyl radical from NFSI and a Cu^{II}–OR species is able to catalyze etherification of the radical species to form product. Use of a phosphite sacrificial reductant was crucial for identifying good reactivity in this method.[23] The reaction tolerates significant complexity in both the alkylarene and alcohol coupling partners and uses commercially available starting materials.

Direct C–H amidation reactions that use C–H substrate as limiting reagent are uncommon in the synthetic literature. A metal-free reaction was reported that uses *N*-iodosuccinimide and visible light to promote benzylic sulfonamidation using 2 equivalents of C–H substrate (Scheme 1.3C).[24] The reaction is proposed to proceed via radical intermediates. A benzylic radical is formed by HAT and iodinated under the reaction conditions. The resulting benzyl iodide is then displaced *in situ* by diverse acidic nitrogen nucleophiles to yield the sulfonamide products. The reaction conditions are simplistic and a few examples of late-stage functionalization are highlighted.

$C(sp^3)$–H alkylation using limiting C–H substrate is another rare transformation. By using a tunable iridium photocatalyst in tandem with a phosphate base, a report revealed that C–H alkylation could be achieved using limiting C–H substrate with alkene coupling partners (Scheme 1.3D).[25] The reaction proceeds via a proton-coupled electron transfer pathway that allows net H atom abstraction to form a substrate radical for addition to alkenes via a Giese reaction mechanism. The photocatalyst engages in electron transfer with the alkene addition product to complete the transformation. The scope of alkene coupling partners in this particular report is small, but the developed methodology is a promising platform for extension to new alkene substrates.

Over the past several decades, directed C–H activation protocols have been the focus of hundreds of reports.[15] Directed C–H functionalization strategies rely on the use of chelating, usually heteroatomic, groups that can bind to a transition metal and guide it to a C–H bond. The transition metal then undergoes C–H activation, at which point the C–H site is poised for functionalization by a reductive elimination step. Various classes of coupling partners can be installed at a C–H site using this approach. The study summarized here describes an example of this form of catalysis wherein a primary amine is transiently functionalized to a potent directing group to enable a distal C–H arylation with an aryl iodide coupling partner (Scheme 1.3E).[26] Forgoing the requirement of having a covalently installed directing group greatly amplifies the appeal of this type of C–H functionalization for synthesis.

In contrast to the above studies, which all utilize the C–H substrate as limiting reagent or in minor excess, some reactions use a coupling partner that is sufficiently valuable to justify the use of a high excess of C–H substrate. In a Cu-catalyzed N–H alkylation reaction, cyclohexane and other low-cost C–H substrates were used as alkylating reagents for the functionalization of valuable amides and nitrogen heterocycles (Scheme 1.3F).[27] The reaction is proposed to proceed via photolysis of di-*tert*-butyl peroxide that yields a pair of *tert*-butoxyl radicals that undergo HAT on the alkane to form alkyl radicals for cross coupling. The alkyl radicals react with a Cu^{II}–NRR species, leading to formation of *N*-alkylated products. The use of excess C–H substrate in this reaction was justified based on the relative value of the coupling partners used.

Scheme 1.3. C(sp^3)–H functionalization for synthesis – direct coupling

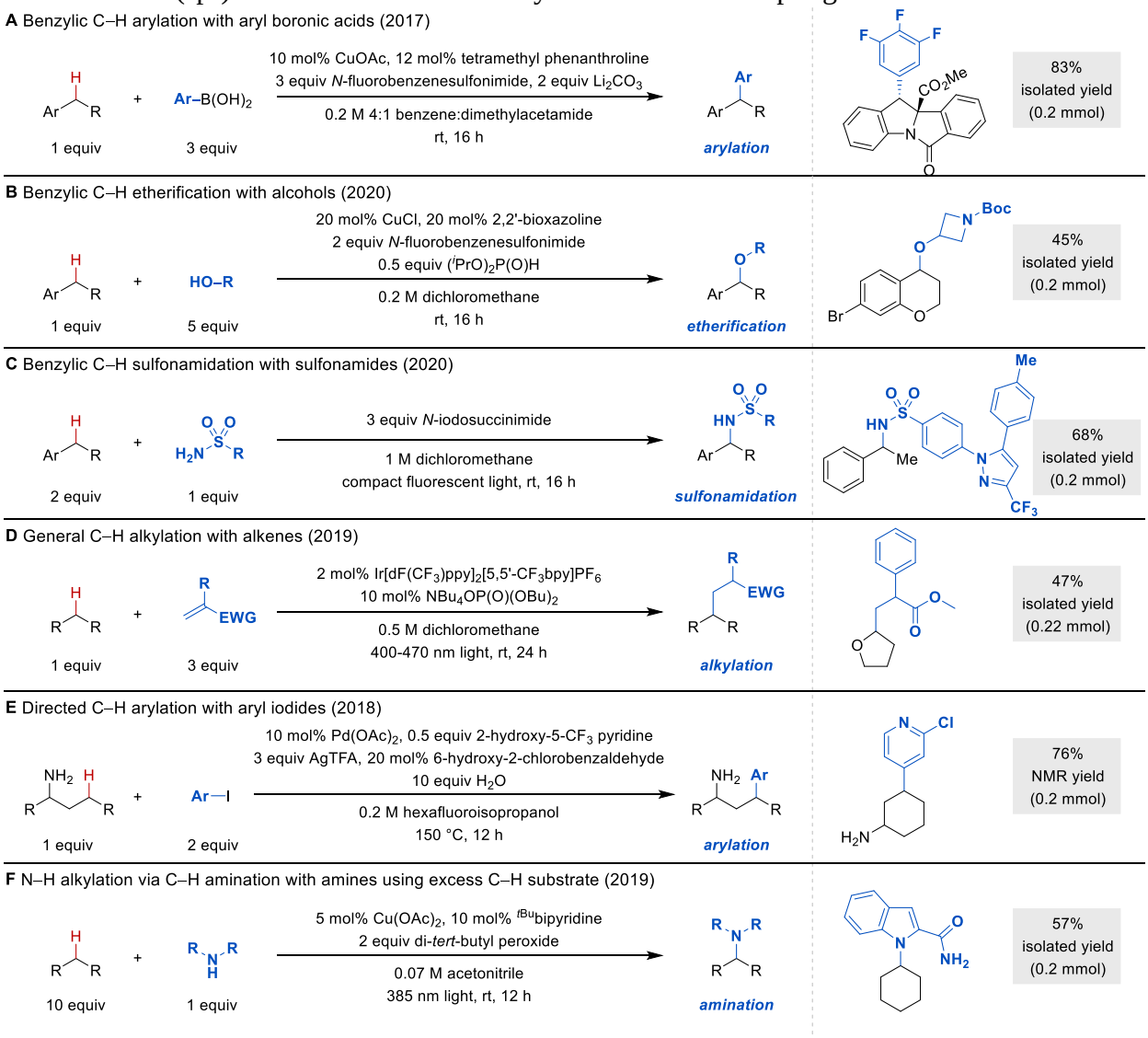

1.2.2. List of indirect C(sp^3)–H functionalization reactions for synthesis

The concept of indirect C–H functionalization has become increasingly interesting in the past several years due to the discovery of several synthetic platforms.[28] A reaction that embodies this indirect approach is the photocatalytic C(sp^3)–H xanthylation reaction from the Alexanian lab (Scheme 1.4A).[29] The reaction employs an N-xanthylamide as a source of HAT reagent and xanthyl radical. When the *N*-xanthylamide is irradiated, the N–S bond homolyzes to form an *N*-

centered radical that undergoes HAT on a C–H substrate and an S-centered radical that is able to react with the incipient substrate radical to form the product. The xanthylation product can be subjected to a variety of diversification reactions, including thiolation, vinylation, and amination, among others. The breadth of transformations from the product combined with the ability to use the C–H substrate as limiting reagent makes this reaction appealing for use in synthesis.

A traditional sequence for indirect C–H functionalization is a C–H bromination/displacement sequence. Bromination reactions are numerous in the literature and the first examples were reported over 100 years ago.[30] One example of this reaction is a recently reported photochemical iridium-catalyzed benzylic bromination reaction employing CBr_4 as bromine source in a radical bromination reaction (Scheme 1.4B).[31] While the reaction conditions are not particularly optimized compared to those using N-bromosuccinimide as bromine source, the authors of this report highlight the utility of bromination followed by one-pot displacement with a secondary amine for a net C(sp^3)–H amination reaction. Electron-rich secondary amines are prone to undergo direct oxidation via single-electron transfer and decoupling the C–H activation step (bromination) from the C–N bond forming step (substitution) allows these sensitive nucleophiles to be engaged as coupling partners.

Alkyl boronate esters are a common synthetic handle that are readily engaged in coupling to form new products. A C(sp^3)–H borylation reaction of unactivated C–H bonds using B_2pin_2 with an iridium catalyst was disclosed and the reaction uses C–H substrate as limiting reagent (Scheme 1.4C).[32] The optimized reaction conditions lead to borylation of primary C–H bonds in the presence of secondary C–H bonds due to steric constraints of the iridium catalyst during the C–H activation step. Non-directed borylation reactivity with limiting C(sp^3)–H substrate was unprecedented, and the authors highlighted the synthetic utility of the borylated products for

downstream functionalization by demonstrating transformations including arylation, vinylation, amination, hydroxylation, and fluorination on one of the isolated alkyl boronate products.

Another form of indirect C–H functionalization relies on the use of a strong base to deprotonate a C–H bond to form a carbanion for reaction with an electrophile. The carbanion is often stabilized by lithium as an organolithium species. This form of reactivity has a long history and advances are still being made with respect to compatible coupling partners and selectivity.[33] In Scheme 1.4D, the α-amino C–H site is zincated using *n*-butyl lithium and a zinc salt. Usually, the carbanion complex would be used in a direct reaction with an electrophile, but in this report, the carbanion is instead functionalized via palladium-catalyzed cross coupling with an aryl-pseudohalide to form a C–C bond.[34] Efficient C–H to C–C coupling reactions are highly appealing and once more mild deprotonation conditions are identified, this reaction class could become valuable for late-stage synthesis.

The aforementioned reports emphasize indirect C–H functionalization strategies wherein a C–X bond is accessed from a C–H bond, and the C–X bond is reacted via direct or catalytic pathways to form new C–X bonds. An alternative strategy was explored by the Groves lab in a manganese catalyzed C–H isocyanation study (Scheme 1.4E).[35] The isocyanate is installed by a radical rebound pathway at a C–H site using a manganese catalyst and amines are added to the resulting alkyl isocyanate to form unsymmetrical ureas. This indirect C–H functionalization approach allows rapid and selective formation of benzyl urea libraries from the isocyanate intermediate while leveraging the installed C–N bond of the isocyanate.

C–H azidation presents another opportunity where the C–N bond formed during functionalization is preserved in conversion to other valuable products. One study demonstrated a tertiary C–H azidation reaction using an iron catalyst with a bisoxazoline ligand that is able to

azidate C–H bonds in a radical process (Scheme 1.4F).[36] The alkyl azide products were converted to a variety of amination products in a second step including a primary amine, triazole, and amide, among other groups.

Scheme 1.4. C(sp^3)–H functionalization for synthesis – indirect coupling

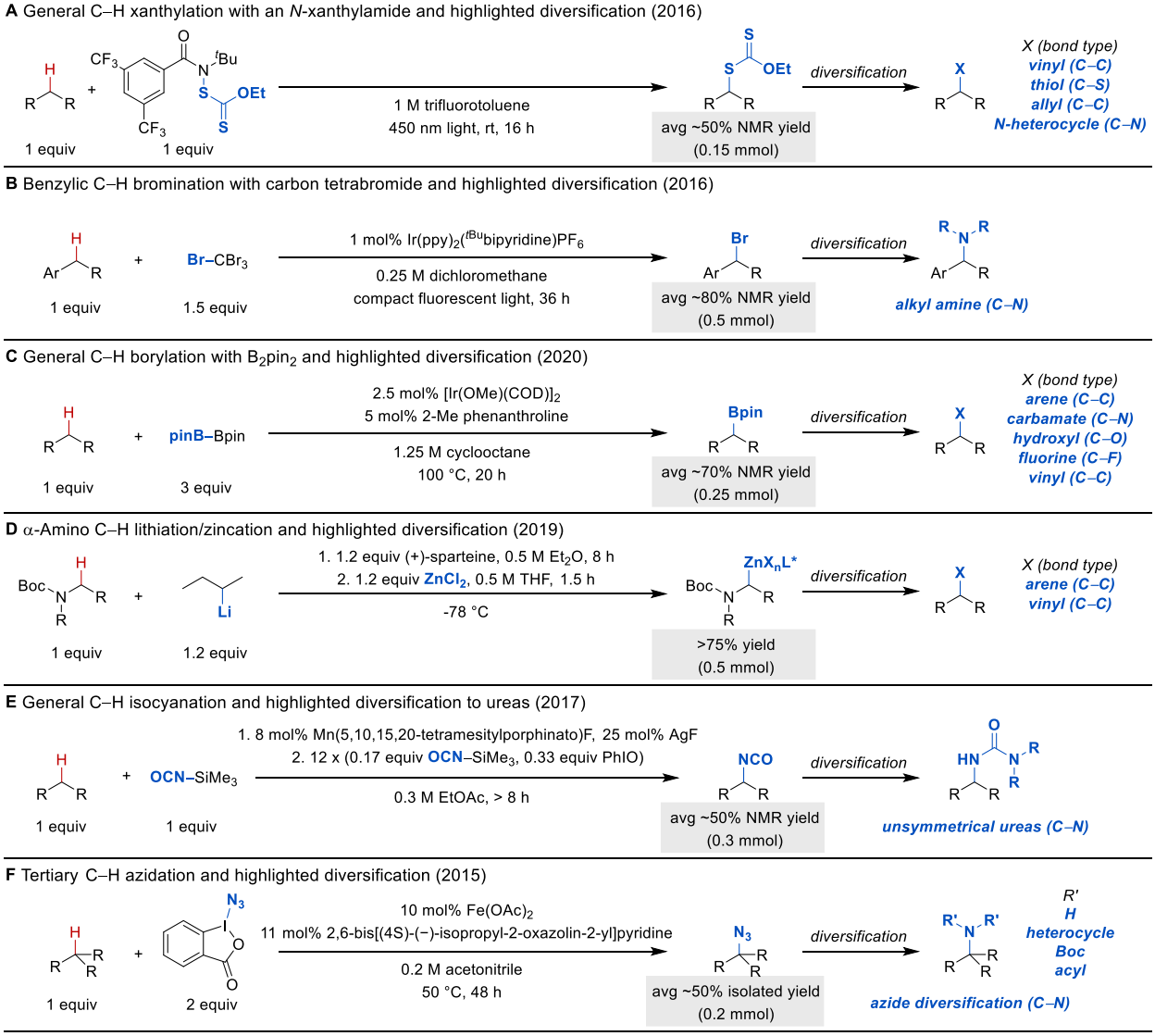

1.3. C(sp^3)–H functionalization for late-stage molecular derivatization

Some C–H functionalization reactions are not well-suited for the installation of large (> 75 molecular weight) coupling fragments. This limitation can make these reactions unappealing for

library syntheses, but there are other important use-cases for installing small functional groups at C–H sites. In medicinal chemistry, it is common to begin the drug development process with a library of tens of thousands of compounds that is eventually narrowed down to less than ten leads. At that stage, identified structures must be iteratively derivatized in search of improved variants. In the lead optimization stage, the ability to substitute a C–H bond for a small molecular weight fragment is invaluable. Ideally a fragment could be added at the C–H site that might affect the solubility or stability of the drug lead, without having a significant enough effect to be detrimental to the mechanism of action.[4,37] Ideal transformations include late-stage C–H methylation, fluorination, oxygenation, amination, trifluoromethylation, or deuteration, among others. By exploring all of the C–H modified variants, researchers can be assured of their decision to move on with a drug candidate. The following reactions enumerate important advances in late-stage C–H functionalization that allow for derivatization of optimized structures.

1.3.1. List of direct C(sp^3)–H functionalization reactions for derivatization

A popular C(sp^3)–H functionalization reaction is C–H oxygenation to form a carbonyl. There are numerous reaction pathways that are able to generate oxygenation products, including oxygenation by a peroxide, oxygenation by a metal-oxo species, and oxygenation by direct reaction of an alkyl radical with O_2 (*vide infra*). A report from the Stahl lab revealed an improved reaction for C–H oxygenation with O_2 that uses a manganese catalyst with N-hydroxyphthalimide (Scheme 1.5A).[38] The reaction proceeds by manganese-catalyzed generation of the *N*-hydroxy radical, which is able to abstract a benzylic C–H bond to form an alkyl radical that is oxygenated under aerobic reaction conditions. The reaction is useful for the oxygenation of simple alkylarenes

as well as a few pharmaceutical precursors. Several other oxygenation reactions have also been developed in the past five years with varying degrees of synthetic utility.[39]

Another frequently studied reaction is C(sp^3)–H amination with amine surrogates using limiting C–H substrate.[40] Installation of protected amino groups at C–H sites allows for facile deprotection to form the C–H aminated product. There are a variety of mechanistic approaches that have been used to achieve this type of transformation.[41,42,43] One example is a C–H amination reaction that utilizes iodine catalysis to functionalize benzylic C–H bonds with primary triflamide (Scheme 1.5B).[44] The study suggests that the reaction proceeds by *in situ* formation of an N–I bond that is homolyzed by light to create an HAT reagent for abstracting a benzylic C–H bond, which forms an alkyl radical for iodination. The benzyl iodide is subsequently substituted by the primary triflamide to generate the product. A complementary report on C–H to C–N functionalization has demonstrated that C–N bond formation can also be achieved enantioselectively by instead using a chiral rhodium catalyst to install the C–N bond in a nitrene insertion reaction.[45]

Fluorination of C–H bonds is a common goal in late-stage C–H functionalization and numerous advances are made in C–H fluorination technology each year.[46,47] One example from the Britton group uses NFSI as oxidant and F source with a decatungstate catalyst serving as a radical chain initiator and propagator (Scheme 1.5C).[48] The decatungstate catalyst undergoes HAT to form an alkyl radical that can react directly with NFSI to become fluorinated. The fluorination process results in formation of a sulfonimidyl radical that either reoxidizes the decatungstate catalyst or engages in chain propagation by undergoing HAT on another substrate molecule. Most examples of C(sp^3)–H fluorination rely upon a radical chain mechanism and the oxidant "Selectfluor" is commonly used in these reactions.[47] Non-radical processes are also competent for

fluorination reactivity, with some directed C–H activation reactions demonstrating fluorination reactivity with broad substrate scope and good enantioselectivities.[47,49]

C–H trifluoromethylation is also an important target in C(sp^3)–H functionalization. Unlike C–H fluorination, where fluorine is akin to an electronically distinct isostere of hydrogen, trifluoromethyl groups impart significant steric effects on the functionalized product.[50] One example of C(sp^3)–H trifluoromethylation reaction uses a Cu/NFSI catalyst system to activate the benzylic C–H site of a substrate via HAT, which forms an alkyl radical that reacts with an *in situ* generated Cu^{II}–CF_3 species to yield the trifluoromethylated product (Scheme 1.5D).[51] This reaction has impressive substrate scope that highlights application to numerous drug molecules.

Photoredox catalysis can be used to directly access benzylic C–H carboxylation products with CO_2 gas as the carboxyl source (Scheme 1.5E).[52] The reaction proceeds by oxidation of a catalytic thiol by tetracarbazolyl isophthalonitrile followed by deprotonation to form a thiyl radical. The thiyl radical undergoes HAT on limiting benzylic C–H substrate to form an alkyl radical that is reduced by the photocatalyst to form a carbanion. Reaction of the carbanion with pressurized CO_2 from the reaction headspace followed by proton transfer leads to formation of the carboxylic acid. These products could be innately desirable for testing and otherwise may also be converted to other products via simple amidation reactions or novel decarboxylative coupling protocols.[53]

Scheme 1.5. C(sp^3)–H functionalization for derivatization – direct functionalization

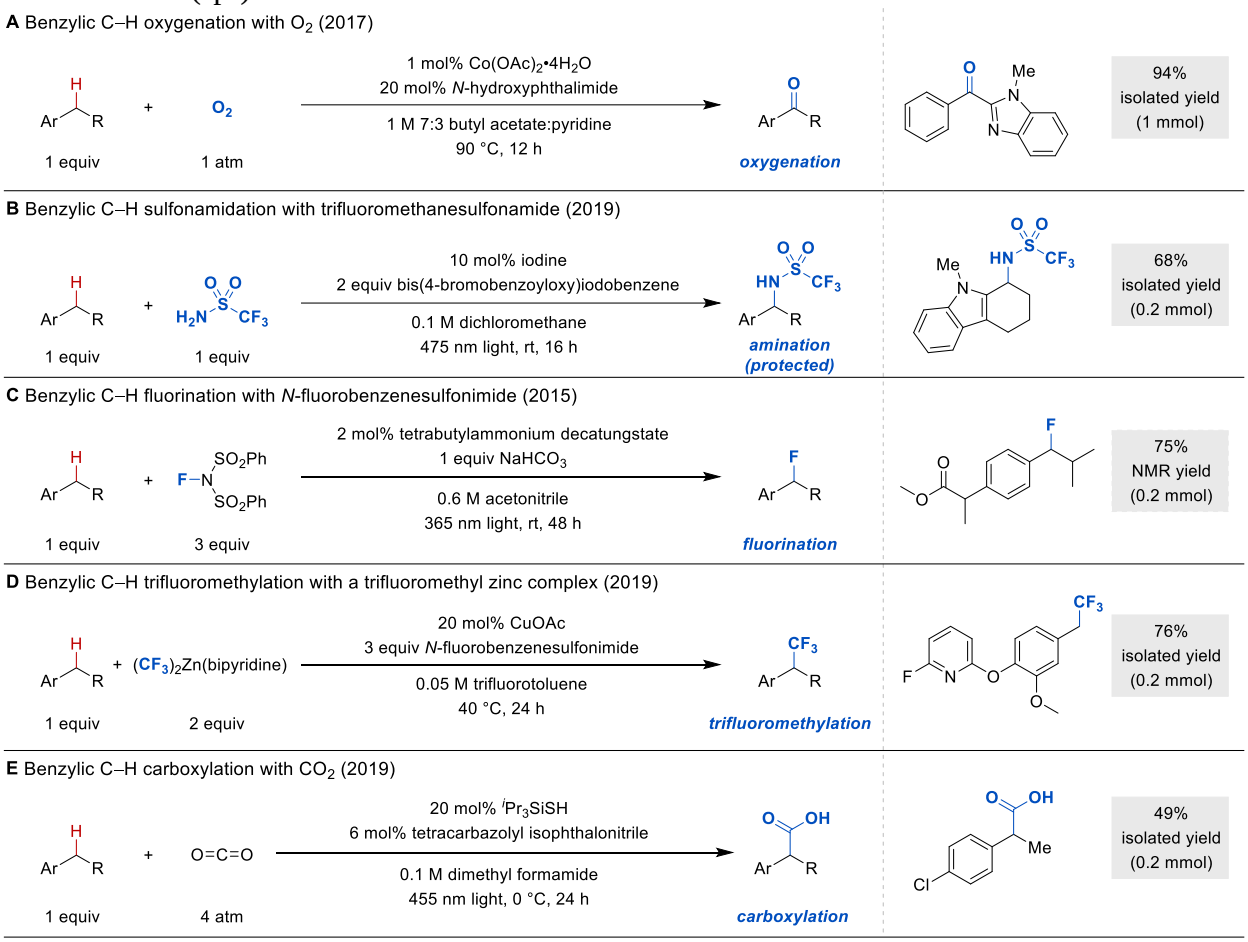

1.3.2. List of indirect C(sp^3)–H functionalization reactions for derivatization

Indirect C–H functionalization reactions have also been identified for use in molecular derivatization. One such reaction is an asymmetric benzylic C–H cyanation reaction from the Liu lab and Stahl lab (Scheme 1.6A). In their study, enantioselective C–H cyanation of a variety of substrates using NFSI with trimethyl silyl cyanide and a chiral copper catalyst was reported.[54] The alkyl cyanide products tend to be toxic in biological systems but are readily converted to carboxylic acids in hydrolysis processes that result in formation of enantioenriched benzyl carboxylic acids. The cyanide may also be converted to a methylamino group by using reducing conditions. This study was a seminal work in the development of benzylic C–H functionalization using limiting C–H substrate.

An appealing, yet challenging C–H functionalization reaction is the hydroxylation of primary and secondary C–H bonds. This reaction is challenging because under oxidizing conditions the hydroxylated product is prone to oxidation to a ketone. To address this competing reactivity, a reaction was designed that uses homolysis of di-mesyl-peroxide to form an oxyl radical that can undergo activation of a benzylic C–H bond to form an alkyl radical that can engage in radical coupling with another oxyl radical to form an alkyl mesylate (Scheme 1.6B).[55] The mesylate group is then hydrolyzed with water in hexafluoroisopropanol to yield hydroxylated product in 2 steps. Formation of C–H hydroxylation products is important to the pharmaceutical industry since the products tend to match up with important metabolites that are formed by biological metabolism.[56]

A recent study demonstrated the ability to enact an indirect C–H methylation reaction on α-heteroatomic C–H bonds (Scheme 1.6C). C(sp^3)–H methylation is a desired transformation because "magic methyl" effects have been observed in the development of some pharmaceutical molecules where installation of a methyl group results in a > 100-fold improvement in potency of a drug.[57] Indirect C–H methylation was achieved by using a manganese-oxo catalyst that can oxygenate α-amino C–H bonds to hemiaminals. The hemiaminals were then converted to iminium species by addition of an activator followed by addition of trimethyl aluminum, which methylates the iminium and forms the methylated product. The reaction is used on a variety of α-heteroatomic C–H sites using limiting C–H substrate and it was also shown to be compatible with methylation of late-stage compounds.[58]

Scheme 1.6. C(sp^3)–H functionalization for derivatization – indirect functionalization

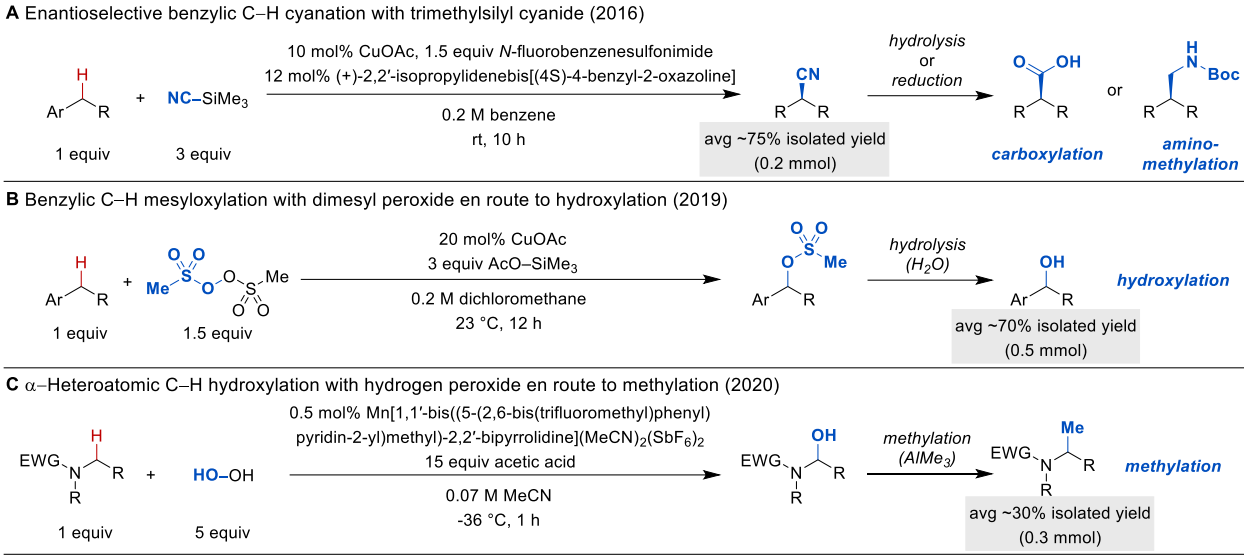

1.4. Selectivity remains as a key challenge for state-of-the-art C–H functionalization

The previous sections indicate that C–H functionalization has grown significantly in the past 5 years with respect to functional group compatibility, breadth of coupling partner scope, ease of reaction operation, and ability to utilize C–H substrate as limiting reagent. One significant challenge that remains for the field is the ability to apply these powerful methods to any target C–H bond in a molecule. In many cases, the reactions are initiated by an HAT reaction on the weakest or most kinetically available C–H site in a substrate, which leads to functionalization at that site. It is possible that the C–H site of interest might not have the characteristics necessary to promote the desired functionalization. For these substrates alternative C–H activation strategies and reaction conditions must be explored. Studies focused on addressing site-selectivity are being actively developed by researchers in the field. A few strategies for enabling site-selective C–H functionalization are summarized below.

Methods employing Cu/NFSI catalyst systems are typically used for functionalization of benzylic C–H sites. In a benzylic C–H azidation reaction, it was demonstrated that the Cu/NFSI catalyst system is site-selective for azidation of a benzylic site in the presence of an electron-rich

tertiary C–H site (Scheme 1.7A).[59] It is proposed that the steric effects of the bulky sulfonimidyl radical HAT reagent promoted abstraction of the methylene C–H bond preferentially to the methine C–H bond.

Another C–H functionalization method that leverages the importance of steric effects on C–H activation is a rhodium-catalyzed C–H insertion reaction that employs diazo compounds to form C–C bonds.[16] The Davies lab has studied numerous variations of this reaction, and by utilizing a sufficiently bulky and chiral rhodium paddlewheel complex, they are able to obtain enantioenriched C–H functionalization products selectively at primary C–H sites (Scheme 1.7B).[60] The reactivity is not especially practical due to limitations in coupling partner scope, functional group compatibility, and the cost of the catalyst, however the reaction does demonstrate exceptional site- and enantio- selectivity.

The importance of modifying the electronic and steric properties of an HAT reagent was shown in a Cu-catalyzed allylic C–H cyanation reaction using N–F reagents.[61] The reaction was based upon the Cu/NFSI benzylic C–H cyanation reaction described above, however NFSI proved to be too reactive for use with alkene substrates. By increasing the electron-density on nitrogen in the N–F reagent, the potency of the hydrogen atom abstractor was sufficiently tempered to allow selective HAT on allylic C–H bonds in the presence of benzylic C–H bonds (Scheme 1.7C). This concept of changing site selectivity through electronic modification of HAT reagents was previously explored in a pair of studies on C–H bromination and C–H chlorination using synthesized N–X reagents.[62,63] In those studies the authors identified a *tert*-butyl amide that possessed ideal steric and electronic properties for maximizing site-selectivity in the halogenation reactions.

In an HAT reaction, both a proton and electron are removed simultaneously. This simultaneous process levels out the influence of electronic effects like acidity of the H atom vs reduction potential of the electron during HAT.[64] However, decoupling the proton and electron transfer processes can unlock opportunities for accessing alternative site-selectivities. One example of this approach was demonstrated in a photochemical Cu-catalyzed benzylic C–H etherification reaction (Scheme 1.7D).[65] In contrast to the Cu/NFSI benzylic etherification reaction that proceeds by HAT, this reaction utilizes an electron-transfer – proton-transfer pathway (ETPT). The substrate undergoes single electron oxidation to form a radical cation, followed by deprotonation to yield a benzylic radical for functionalization by Cu^{II}–OR. This strategy can allow selective C–H activation of electron-rich alkylarene benzylic sites in the presence of other activated C–H bonds with similar or lower bond dissociation energies.

Conversely to an ETPT pathway, where functionalization is guided towards the most oxidizable functional group, a reaction may also selectively functionalize at the most acidic C–H site in a molecule. A report demonstrated that it is possible to transiently amplify the acidity of a C–H site to govern site-selectivity. In a heterobenzylic C–H fluorination reaction, it was determined that the sulfonyl group from NFSI could be transferred to a Lewis basic heteroaromatic nitrogen, which drastically reduced electron-density of the ring system and boosted acidity of the heterobenzylic C–H bond.[66] This resulted in facile deprotonation to yield an enamine/carbanion that reacts with NFSI in a 2-electron process to become fluorinated preferentially to fluorination of benzylic C–H sites (Scheme 1.7E). This approach combined with the ETPT approach to C–H functionalization presents two viable alternatives to HAT for benzylic C–H functionalization with varied selectivity.

Strategies for modifying site-selectivity for functionalization of different alkyl C–H sites have been discussed, but it is also important to consider the effects of heteroatoms on site-selectivity. α-Heteroatomic C–H bonds tend to be more reactive to C–H activation than alkane C–H bonds. In some cases α-heteroatomic C–H bonds can even be more reactive towards C–H activation than benzylic C–H bonds that have lower bond dissociation energies.[67] The origin of this selectivity relationship is explained by the "radical polarities". HAT reagents are typically electron-deficient X radicals. If C–H abstraction results in formation of another electron-deficient radical, the polarity is a mismatch and will be kinetically disfavored. If the HAT forms an electron-rich radical, the polarities are considered a match and the HAT will be kinetically facile. This concept has been discussed in numerous studies, but further synthetic-oriented research is needed to unlock its potential for controlling and predicting site-selectivity in C–H functionalization reactions.[68]

Rather than strictly relying on innate steric and electronic effects to govern site selectivity between alkyl and α-heteroatomic C–H bonds, it is also possible to modify the relative reactivities of the sites by changing the reaction medium. The effects of hydrogen-bond donors on the reactivity of α-heteroatomic C–H sites is dramatic. It has been shown that the rate of HAT on an α-amido C–H site is reduced by over an order of magnitude by changing the solvent from MeCN to hexafluoroisopropanol (HFIP).[69] This is attributed to hydrogen-bond donation of HFIP to the amido carbonyl, which removes electron density from N and thus deactivates the adjacent C–H site. Oxidation of alcohols is similarly affected by this phenomenon. These solvent effects were demonstrated in a report that showed a complete change in site-selectivity of a metal-oxo oxygenation reaction from favoring the α-amido position to favoring the tertiary position by changing the reaction solvent to HFIP (Scheme 1.7F).[70]

Relative rates of HAT on alkyl C–H sites and α-heteroatomic C–H bonds is affected to an even greater extent when the heteroatom can be protonated. Protonation of an amine by a strong acid like trifluoroacetic acid or sulfuric acid results in sufficient deactivation of the group that even unactivated alkyl C–H bonds can be functionalized preferentially. This technique has been applied in several synthetic methodology papers including examples of C–H oxygenation (Scheme 1.7G), hydroxylation, fluorination, and trifluoromethylation at unactivated C–H sites.[71-75]

Scheme 1.7. Site-selective C(sp^3)–H functionalization reactions

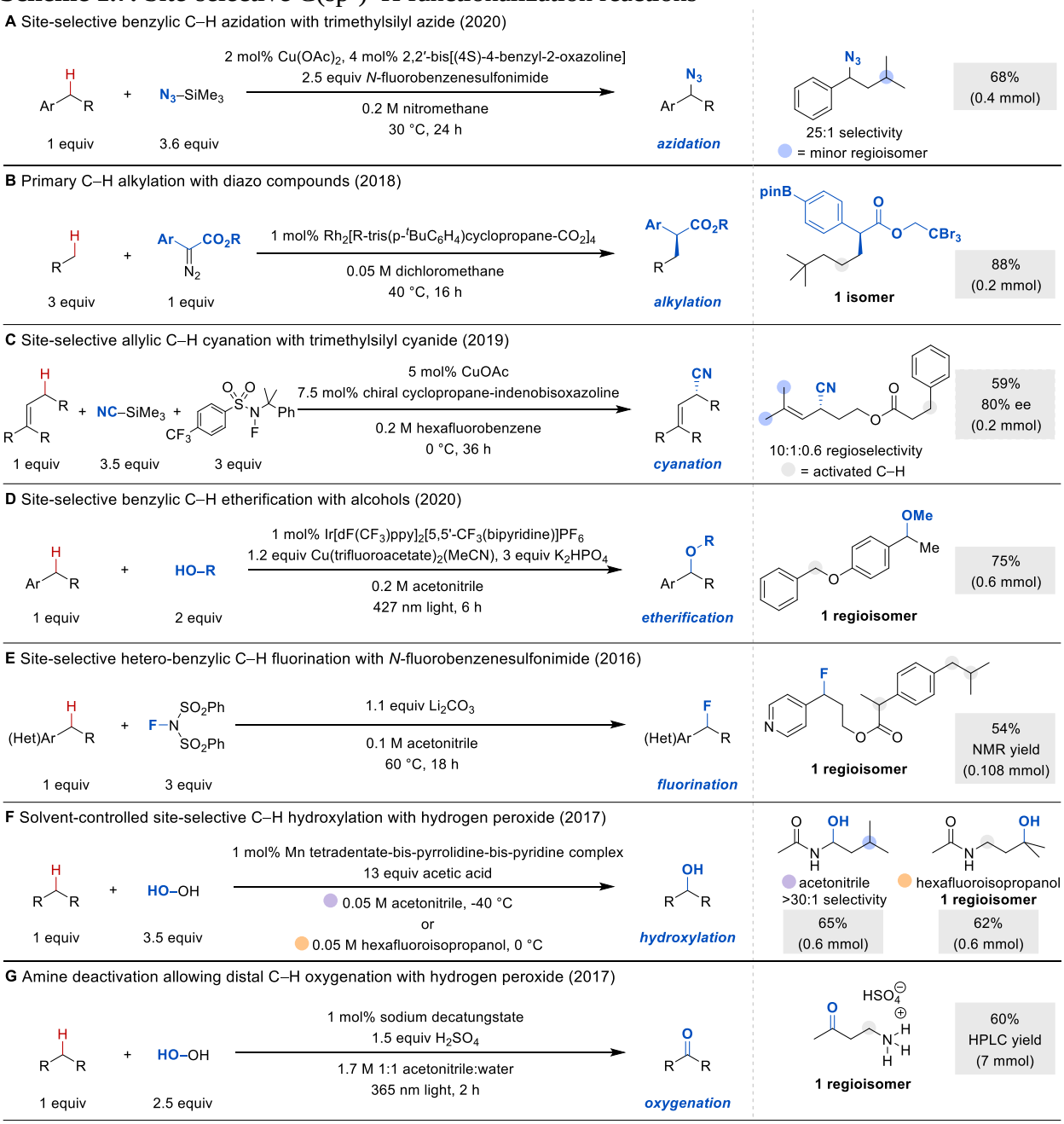

Two other approaches for controlling site-selectivity of C–H functionalization rely on the use of directing groups to guide C–H activation to a preferred site or use of extensive substrate-specific small molecule or enzyme catalyst tuning. While both of these are effective means to solving the issue of site-selectivity, the two lack practicality for some applications, since utilization of a directing group may not be feasible in a given synthesis and designing new catalysts for

functionalization of different C–H sites can be a cumbersome task. However, in the right scenarios, these two strategies offer the most upside when excellent site-selectivity and reactivity are needed.[76,77,78]

1.5. Thesis scope

The enclosed thesis research describes three C(sp^3)–H functionalization reactions. One reaction is a benzylic C–H arylation reaction that would be classified as a direct C–H functionalization reaction for synthesis. The reaction utilizes valuable aryl boronate esters as limiting reagent while using inexpensive alkylarene C–H substrates as alkylating reagents (chapter 2). The next reaction is a benzylic C–H fluorination/functionalization reaction. It was initially anticipated that the transformation of a C–H bond into a C–F bond would be inherently valuable as a derivatization reaction. It was later determined that many benzyl fluorides have quite poor stability (chapter 3). To address the instability of these molecules, the fluoride products were used in acid-catalyzed substitution reactions to form diverse C–O, C–N, and C–C bonded products in an indirect C–H functionalization reaction for synthesis (chapter 4). The final C–H functionalization reaction of this thesis is a late-stage C–H methylation reaction that is a direct C–H functionalization reaction for derivatization (chapter 5). In that study, the use of strong acids to deactivate α-heteroatomic C–H sites for chemoselective methylation of late-stage C–H substrates is explored. Overall, the enclosed studies add to the other advances to C–H functionalization that were discussed in this introductory section.

1.6. References

1. Roughley, S. D.; Jordan, A. M. The Medicinal Chemist's Toolbox: An Analysis of Reactions Used in the Pursuit of Drug Candidates. *J. Med. Chem.* **2011**, *54*, 3451–3479.
2. Brown, D. G.; Boström, J. Where Do Recent Small Molecule Clinical Development Candidates Come From? *J. Med. Chem*. **2018**, *61*, 9442-9468.
3. Brown, D. G.; Boström, J. Analysis of Past and Present Synthetic Methodologies on Medicinal Chemistry: Where Have All the New Reactions Gone? *J. Med. Chem.* **2016**, *59*, 4443–4458.
4. Cernak, T.; Dykstra, K. D.; Tyagarajan, S.; Vachal, P.; Krska, S. W. The Medicinal Chemist's Toolbox for Late Stage Functionalization of Drug-Like Molecules. *Chem. Soc. Rev.* **2016**, *45*, 546-576.
5. Blakemore, D. C.; Castro, L.; Churcher, I.; Rees, D. C.; Thomas, A. W.; Wilson, D. M.; Wood, A. Organic Synthesis Provides Opportunities to Transform Drug Discovery. *Nat. Chem.* **2018**, *10*, 383-394.
6. Shaw, M. H.; Shurtleff, V. W.; Terrett, J. A.; Cuthbertson, J. D.; MacMillan, D. W.C. Native functionality in triple catalytic cross-coupling: sp^3 C−H bonds as latent nucleophiles. *Science* **2016,** *352*, 1304−1308.
7. Labinger, J. A.; Bercaw, J. E. Understanding and exploiting C–H bond activation. *Nature* **2002,** *417*, 507–514.
8. Wencel-Delord, J.; Glorius, F. C–H bond activation enables the rapid construction and late-stage diversification of functional molecules. *Nat. Chem.* **2013**, *5*, 369-375.
9. Dénès, F. Intermolecular Radical C–H Bond Activation: A Powerful Tool for Late Stage Functionalization. *Chimia* **2020**, *74*, 23-32.

10. Lam, N. Y. S.; Wu, K.; Yu, J.-Q. Advancing the logic of chemical synthesis: C–H activation as strategic and tactical disconnections for C–C bond constructions. *Angew. Chem. Int. Ed.* **2020**, *Accepted Article*, https://doi.org/10.1002/anie.202011901.
11. Prier, C. K.; Rankic, D. A.; MacMillan, D. W. C. Visible light photoredox catalysis with transition metal complexes: applications in organic synthesis. *Chem. Rev.* **2013,** *113*, 5322−5363.
12. Romero, N. A.; Nicewicz, D. A. Organic photoredox catalysis. *Chem. Rev*. **2016,** *116*, 10075−10166.
13. Huang, X.; Groves, J. T. Beyond ferryl-mediated hydroxylation: 40 years of rebound mechanism and C−H activation. *J. Biol. Inorg. Chem*. **2017**, *22*, 185−207.
14. H. Yi, G. Zhang, H. Wang, Z. Huang, J. Wang, A. K. Singh, A. Lei, Recent advances in radical C−H activation/radical cross-coupling. *Chem. Rev.* **2017**, *117*, 9016-9085.
15. He, J.; Wasa, M.; Chan; K. S. L.; Shao, Q.; Yu, J.-Q. Palladium-catalyzed transformations of alkyl C−H bonds. *Chem. Rev.* **2017,** *117*, 8754−8786.
16. Davies, H. M. L.; Manning, J. R. Catalytic C−H functionalization by metal carbenoid and nitrenoid insertion. *Nature* **2008,** *451*, 417−424.
17. White, M. C.; Zhao, J. Aliphatic C−H oxidations for late-stage functionalization. *J. Am. Chem. Soc.* **2018,** *140*, 13988−14009.
18. Mortenson, P. N.; Erlanson, D. A.; Esch, I. J. P.; Jahnke W.; Johnson, C. N. Fragment-to-lead medicinal chemistry publications in 2017. *J. Med. Chem.* **2019**, *62*, 3857-3872.
19. Gutekunst, W. R.; Baran, P. S. C–H functionalization logic in total synthesis. *Chem. Soc. Rev.* **2011**, *40*, 1976-1991.

20. Abrams, D. J.; Provencher, P. A.; Sorensen, E. J. Recent applications of C–H functionalization in complex natural product synthesis. *Chem. Soc. Rev.* **2018**, *47*, 8925-8967.
21. Zhang, W.; Chen, P.; Liu, G. Copper-catalyzed arylation of benzylic C−H bonds with alkylarenes as the limiting reagents. *J. Am. Chem. Soc*. **2017,** *139*, 7709−7712.
22. Zhang, W.; Wu, L.; Chen, P.; Liu, G. Enantioselective arylation of benzylic C−H bonds by copper-catalyzed radical relay. *Angew. Chem. Int. Ed*. **2019,** *58*, 6425−6429.
23. Hu, H.; Chen, S.-J.; Mandal, M.; Pratik, S. M.; Buss, J. A.; Krska, S. W.; Cramer, C. J.; Stahl, S. S. Copper-Catalyzed Benzylic C–H Coupling with Alcohols via Radical Relay Enabled by Redox Buffering. *Nat. Catal.* **2020**, *3*, 358-367.
24. Wu, F.; Ariyarathna, J. P.; Kaur, N.; Alom, N.-E.; Kennell, M. L.; Bassiouni, O. H.; Li, W. Halogen-Bond-Induced Consecutive Csp^3−H Aminations via Hydrogen Atom Transfer Relay Strategy. *Org. Lett.* **2020**, *22*, 2135-2140.
25. Morton, C. M.; Zhu, Q.; Ripberger, H.; Troian-Gautier, L.; Toa, Z. S. D.; Knowles, R. R.; Alexanian, E. J. C−H Alkylation via Multisite-Proton-Coupled Electron Transfer of an Aliphatic C−H Bond. *J. Am. Chem. Soc.* **2019**, *141*, 13253-13260.
26. Chen, Y.-Q.; Wang, Z.; Wu, Y.; Wisniewski, S. R.; Qiao, J. X.; Ewing, W. R.; Eastgate, M. D.; Yu, J -Q. Overcoming the Limitations of γ- and δ-C−H Arylation of Amines through Ligand Development. *J. Am. Chem. Soc.* **2018**, *140*, 17884−17894.
27. Zheng, Y.-W.; Narobe, R.; Donabauer, K.; Yakubov, S.; König, B. Copper(II)-Photocatalyzed N–H Alkylation with Alkanes. *ACS Catal.* **2020**, *10*, 8582-8589.
28. The following $C(sp^2)$–H functionalization is particularly notable: Berger, F.; Plutschack, M. B.; Riegger, J.; Yu, W.; Speicher, S.; Ho, M.; Frank, N.; Ritter, T. Site-selective and versatile aromatic C–H functionalization by thianthrenation. *Nature*, **2019**, *567*, 223-228.

29. Czaplyski, W. L.; Na; C. G.; Alexanian, E. J. C−H Xanthylation: a synthetic platform for alkane functionalization. *J. Am. Chem. Soc.* **2016,** *138*, 13854−13857.

30. Saikia, I.; Borah, A. J.; Phukan, P. Use of Bromine and Bromo-Organic Compounds in Organic Synthesis. *Chem. Rev.* **2016**, *116*, 6837-7042.

31. Hou, T.; Lu, P.; Li, P. Visible-light-mediated benzylic sp^3 C–H bond functionalization to C–Br or C–N bond. *Tetrahedron Lett.* **2016**, *57*, 2273-2276.

32. Oeschger, R.; Su, B.; Yu, I.; Ehinger, C.; Romero, E.; He, S.; Hartwig, J. Diverse Functionalization of Strong Alkyl C–H Bonds by Undirected Borylation. *Science* **2020**, *368*, 736-741.

33. Campos, K. R. Direct sp^3 C–H bond activation adjacent to nitrogen in heterocycles. *Chem. Soc. Rev.* **2007**, *36*, 1069-1084.

34. Lin, W.; Zhang, K.-F.; Baudoin, O. Regiodivergent enantioselective C–H functionalization of Boc-1,3-oxazinanes for the synthesis of β^2- and β^3-amino acids. *Nat. Catal.* **2019**, *2*, 882-888.

35. Huang, X.; Zhuang, T.; Kates, P. A.; Gao, H.; Chen, X.; Groves, J. T. Alkyl Isocyanates via Manganese-Catalyzed C–H Activation for the Preparation of Substituted Ureas. *J. Am. Chem. Soc.* **2017**, *139*¸15407-15413.

36. Sharma, A.; Hartwig, J. F. Metal-catalyzed azidation of tertiary C−H bonds suitable for late-stage functionalization. *Nature* **2015,** *517*, 600−604.

37. Campos, K. R.; Coleman, P. J.; Alvarez, J. C.; Dreher, S. D.; Garbaccio, R. M.; Terrett, N. K.; Tillyer, R. D.; Truppo, M. D.; Parmee, E. R. The importance of synthetic chemistry in the pharmaceutical industry. *Science* **2019**, *363*, 10.1126/science.aat0805.

38. Hruszkewycz, D. P.; Miles, K. C.; Thiel, O. R.; Stahl, S. S. Co/NHPI-mediated aerobic oxygenation of benzylic C–H bonds in pharmaceutically relevant molecules. *Chem. Sci.* **2017**, *8*, 1282-1287.

39. Sterckx, H.; Morel, B.; Maes, B. U. W. Catalytic Aerobic Oxidation of C(sp^3)–H Bonds. *Angew. Chem. Int. Ed.* **2019**, *58*, 7946-7970.

40. Park, Y.; Kim, Y.; Chang, S. Transition Metal-Catalyzed C–H Amination: Scope, Mechanism, and Applications. *Chem. Rev.* **2017**, *117*, 9247-9301.

41. Clark, J. R.; Feng, K.; Sookezian, A.; White, M. C. Manganese-catalysed benzylic C(sp^3)−H amination for late-stage functionalization. *Nature Chem*. **2018,** *10*, 583−591.

42. Chiappini, N. D.; Mack, J. B. C.; Du Bois, J. Intermolecular C(sp^3)–H Amination of Complex Molecules. *Angew. Chem. Int. Ed.* **2018**, *57*, 4956-4959.

43. Bakhoda, A.; Jian, Q.; Badiei, Y. M.; Bertke, J. A.; Cundari, T. R.; Warren, T. H. Copper Catalyzed sp^3 C–H Amidation: Sterically Driven Primary and Secondary C–H Site-Selectivity. *Angew. Chem. Int. Ed.* **2019**, *58*, 3421-3425.

44. Bosnidou, A. E.; Muñiz, K. Intermolecular Radical C(sp^3)–H Amination under Iodine Catalysis. *Angew. Chem. Int. Ed.* **2019**, *58*, 7485-7489.

45. Nasrallah, A.; Boquet, V.; Hecker, A.; Retailleau, P.; Darses, B.; Dauban, P. Catalytic Enantioselective Intermolecular Benzylic C(sp^3)–H Amination. *Angew. Chem. Int. Ed.* **2019**, *58*, 8192-8196.

46. Yerien, D. E.; Bonesi, S.; Postigo, A. Fluorination Methods in Drug Discovery. *Org. Biomol. Chem.* **2016**, *14*, 8398-8427.

47. Szpera, R.; Moseley, D. F. J.; Smith, L. B.; Sterling, A. J.; Gouverneur, V. The Fluorination of C–H Bonds: Developments and Perspectives. *Angew. Chem. Int. Ed.* **2019**, *58*, 14824-14848.

48. Nodwell, M. B.; Bagai, A.; Halperin, S. D.; Martin, R. E.; Knust, H.; Britton, R. Direct Photocatalytic Fluorination of Benzylic C–H Bonds with *N*-Fluorobenzenesulfonimide. *Chem. Commun.* **2015**, *51*, 11783-11786.

49. Park, H.; Verma, P.; Hong, K; Yu, J.-Q. Controlling Pd(IV) reductive elimination pathways enables Pd(II)-catalysed enantioselective C(sp^3)−H fluorination. *Nat. Chem.* **2018**, *10*, 755–762.

50. Wang, J.; Sánchez-Roselló, M.; Aceña, J. L.; Pozo, C. D.; Sorochinsky, A. E.; Fustero, S.; Soloshonok, V. A.; Liu, H. Fluorine in pharmaceutical industry: fluorine-containing drugs introduced to the market in the last decade (2001−2011). *Chem. Rev.* **2014**, *114*, 2432–2506.

51. Xiao, H.; Liu, Z.; Shen, H.; Zhang, B.; Zhu, L.; Li, C. Copper-Catalyzed Late-Stage Benzylic C(sp^3)–H Trifluoromethylation. *Chem* **2019**, *5*, 940-949.

52. Meng, Q.-Y.; Schirmer, T. E.; Berger, A. L.; Donabauer, K.; König, B. Photocarboxylation of benzylic C−H bonds. *J. Am. Chem. Soc.* **2019,** *141*, 11393−11397.

53. Murarka, S. N-(Acyloxy)phthalimides as Redox-Active Esters in Cross-Coupling Reactions. *Adv. Synth. Catal.* **2018**, *360*, 1735-1753.

54. Zhang, W.; Wang, F.; McCann, S. D.; Wang, D.; Chen, P.; Stahl, S. S.; Liu, G. Enantioselective Cyanation of Benzylic C–H Bonds via Copper-Catalyzed Radical Relay. *Science* **2016**, *353*, 1014-1018.

55. Tanwar, L.; Börgel, J.; Ritter, T. Synthesis of benzylic alcohols by C−H oxidation. *J. Am. Chem. Soc*. **2019,** *141*, 17983−17988.

56. Montellano, P. R. O. D. Hydrocarbon Hydroxylation by Cytochrome P450 Enzymes. *Chem. Rev.* **2010**, *110*, 932–948.

57. H. Schönherr, T. Cernak, Profound methyl effects in drug discovery and a call for new C–H methylation reactions. *Angew. Chem. Int. Ed.* **2013**, *52*, 12256-12267.

58. K. Feng, R. E. Quevedo, J. T. Kohrt, M. S. Oderinde, U. Reilly, M. C. White, Late-stage oxidative C(sp^3)–H methylation. *Nature* **2020**, *580*, 621-627.

59. Suh, S.-E. Chen, S.-J. Mandal, M.; Guzei, I. A.; Cramer, C. J.; Stahl, S. S. Site-Selective Copper-Catalyzed Azidation of Benzylic C–H Bonds. *J. Am. Chem. Soc.* **2020**, *142*, 11388-11393.

60. Liao, K.; Yang, Y.-F.; Li, Y.; Sanders, J. N.; Houk, K. N.; Musaev, D. G.; Davies, H. M. L. Design of catalysts for site-selective and enantioselective functionalization of non-activated primary C–H bonds. *Nat. Chem.* **2018**, *10*, 1048-1055.

61. Li, J.; Zhang, Z.; Wu, L.; Zhang, W.; Chen, P.; Lin, Z.; Liu, G. Site-specific allylic C−H bond functionalization with a copper-bound N-centered radical. *Nature* **2019**, *574*, 516−521.

62. Schmidt, V. A.; Quinn, R. K.; Brusoe, A. T.; Alexanian, E. J. Site-selective aliphatic C−H bromination using *N*-bromoamides and visible light. *J. Am. Chem. Soc.* **2014,** *136*, 14389−14392.

63. Quinn, R. K.; Könst, Z. A.; Michalak, S. E.; Schmidt, Y.; Szklarski, A. R.; Flores, A. R.; Nam, S.; Horne, D. A.; Vanderwal, C. D.; Alexanian, E. J. Site-selective aliphatic C−H chlorination using *N*-chloroamides enables a synthesis of chlorolissoclimide. *J. Am. Chem. Soc.* **2016**, *138*, 696−702

64. Rafiee, M., Wang, F.; Hruszkewycz, D. P.; Stahl, S. S. *N*-hydroxyphthalimide-mediated electrochemical iodination of methylarenes and comparison to electron-transfer-initiated C−H functionalization. *J. Am. Chem. Soc*. **2018,** *140*, 22−25.

65. Lee, B. J.; DeGlopper, K. S.; Yoon, T. P. Site-Selective Alkoxylation of Benzylic C–H Bonds by Photoredox Catalysis. *Angew. Chem. Int. Ed.* **2020**, *59*, 197-202.

66. Meanwell, M.; Nodwell, M. B.; Martin, R. E.; Britton, R. A Convenient Late-Stage Fluorination of Pyridylic C–H Bonds with *N*-Fluorobenzenesulfonimide. *Angew. Chem. Int. Ed.* **2016**, *55*, 13244-13248.

67. Milan, M.; Salamone, M.; Costas, M.; Bietti, M. The Quest for Selectivity in Hydrogen Atom Transfer Based Aliphatic C–H Bond Oxygenation. *Acc. Chem. Res.* **2018**, *51*, 1984-1995.

68. Note: The MacMillan lab cited this phenomenon as being active in a C(sp^3)–H alkylation reaction that they developed. However, the examined substrates did not sufficiently explore the question of selectivity, since the "polarity matched" C–H substrates were always used in excess relative to the "polarity mismatched" alkyl halide coupling partners: Le, C.; Liang, Y.; Evans, R. W.; Li, X.; MacMillan, D. W. C. Selective sp^3 C−H alkylation via polarity-match-based cross-coupling. *Nature* **2017,** *547*, 79−83.

69. Bietti, M. Activation and deactivation strategies promoted by medium effects for selective aliphatic C–H bond functionalization. *Angew. Chem. Int. Ed.* **2018**, *57*, 16618-16637.

70. Dantignana, V.; Milan, M.; Cussó, O.; Company, A.; Bietti, M.; Costas, M. Chemoselective Aliphatic C–H Bond Oxidation Enabled by Polarity Reversal. *ACS Cent. Sci.* **2017**, *3*, 1350-1358.

71. Schultz, D. M.; Lévesque, F.; DiRocco, D. A.; Reibarkh, M.; Ji, Y.; Joyce, L. A.; Dropinski, J. F.; Sheng, H.; Sherry, B. D.; Davies, I. W. Oxyfunctionalization of the Remote C–H Bonds

of Aliphatic Amines by Decatungstate Photocatalysis. *Angew. Chem. Int. Ed.* **2017**, *56*, 15274-15278.

72. Lee, M.; Sanford M. S. Platinum-catalyzed, terminal-selective C(sp^3)–H oxidation of aliphatic amines. *J. Am. Chem. Soc.* **2015**, *137*, 12796-12799.
73. J. M. Howell, K. Feng, J. R. Clark, L. J. Trzepkowski, M. C. White, Remote oxidation of aliphatic C–H bonds in nitrogen-containing molecules. *J. Am. Chem. Soc.* **2015**, *137*, 14590-14593.
74. Nodwell, M. B.; Yang, H.; Čolovic, M.; Yuan, Z.; Merkens, H.; Martin, R. E.; Bénard, F.; Schaffer, P.; Britton, R. ^{18}F-Fluorination of Unactivated C–H Bonds in Branched Aliphatic Amino Acids: Direct Synthesis of Oncological Positron Emission Tomography Imaging Agents. *J. Am. Chem. Soc.* **2017**, *139*, 3595-3598.
75. Sarver, P. J.; Bacauanu, V.; Schultz, D. M.; DiRocco, D. A.; Lam, Y.-H.; Sherer, E. C.; MacMillan, D. W. C. The merger of decatungstate and copper catalysis to enable aliphatic C(sp^3)−H trifluoromethylation. *Nat. Chem.* **2020,** *12*, 459−467.
76. Gornisky, P. E.; White, M. C. Catalyst-controlled aliphatic C−H oxidations with a predictive model for site-selectivity. *J. Am. Chem. Soc.* **2013,** *135*, 14052−14055.
77. Alderson, J. M.; Corbin, J. R.; Schomaker, J. M. Tunable, Chemo- and Site-Selective Nitrene Transfer Reactions through the Rational Design of Silver(I) Catalysts. *Acc. Chem. Res.* **2017**, *50*, 2147-2158.
78. Chen, K.; Arnold, F. H. Engineering new catalytic activities in enzymes. *Nat. Catal.* **2020**, *3*, 203-213.

Chapter 2.

Feedstocks to Pharmacophores: Cu-Catalyzed Oxidative Arylation of Inexpensive Alkylarenes Enabling Direct Access to Diarylalkanes

2.1. Abstract

A Cu-catalyzed method has been identified for selective oxidative arylation of benzylic C−H bonds with boronic esters (Figure 2.1). The resulting 1,1-diarylalkanes are accessed directly from inexpensive alkylarenes containing primary and secondary benzylic C−H bonds, such as toluene or ethylbenzene. All catalyst components are commercially available at low cost, and the arylboronic esters are either commercially available or easily accessible from the commercially available boronic acids. The potential utility of these methods in medicinal chemistry applications is highlighted.

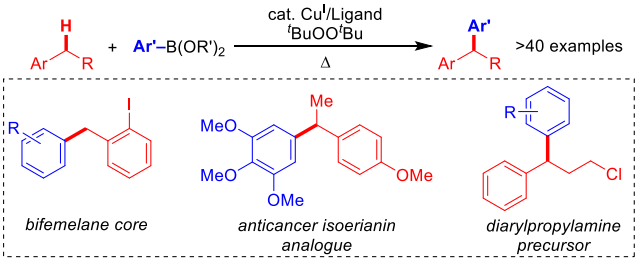

Figure 2.1. Cu-Catalyzed Benzylic C–H Arylation Summarization of Reactivity

2.2. Introduction

Toluene, xylenes, and ethylbenzene are amongst the largest-volume platform chemicals in the commodity chemical industry, and the low cost of these molecules underlies their use as industrial solvents and components of gasoline. In addition to these basic feedstocks, many other alkylarenes are abundant and inexpensive relative to reagents commonly used in organic chemistry and, therefore, represent ideal starting materials for the preparation of complex molecules, such as pharmaceuticals and agrochemicals.[1] Catalytic methods for selective functionalization of benzylic C–H bonds, particularly those capable of forming carbon-carbon bonds, would provide a strategic means to utilize this resource.[1-3] Diarylalkanes, also known as benzyhydryls, represent an important pharmacophore in drugs and other bioactive molecules (Scheme 2.1),[4,5] and arylation of

benzylic C–H bonds would provide an efficient route to such compounds. Precedents for such reactivity are rare,[6-8] and a synthetically versatile method for benzylic C–H arylation could have significant impact.

Scheme 2.1. Pharmaceutically Important Diarylalkanes

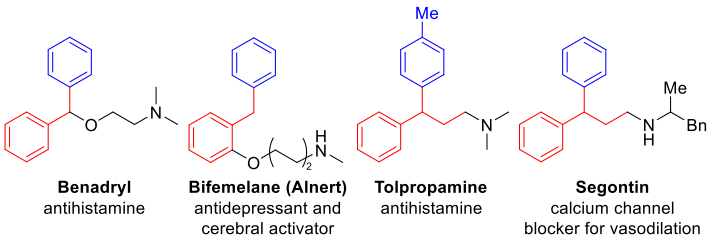

Kharasch-Sosnovsky reactions, which use a Cu catalyst in combination with a peroxide-based oxidant (originally *t*BuOOBz) to achieve allylic oxygenation,[9,10] provided key inspiration for this study (Scheme 2.2A/B). These reactions are proposed to be initiated by abstraction of an allylic C–H bond by an alkoxy radical, followed by reaction of the carbon-centered radical with a Cu^{II}–OR species to form the C–O bond (Scheme 2.2C, left cycle).[11] Related methods for benzylic C–H oxidation have also been developed,[12] and, in collaboration with Liu and coworkers, we recently reported a method for Cu-catalyzed cyanation of benzylic C–H bonds.[13] We speculated that benzylic arylation could be achieved via transmetalation from an arylboronic acid to the Cu^{II}–OR species within the catalytic cycle en route to an aryl(benzyl)copper species that undergoes C–C coupling (Scheme 2.2C, right cycle).[14] The results presented below validate this hypothesis and show that a wide range of readily available methyl- and alkylarenes undergo arylation with diverse arylboronic esters, including heterocyclic derivatives, to afford medicinally important benzhydryl derivatives.

Scheme 2.2. Cu-Catalyzed Benzylic C–H Arylation Method and Its Relationship to the Kharasch-Sosnovsky Reaction

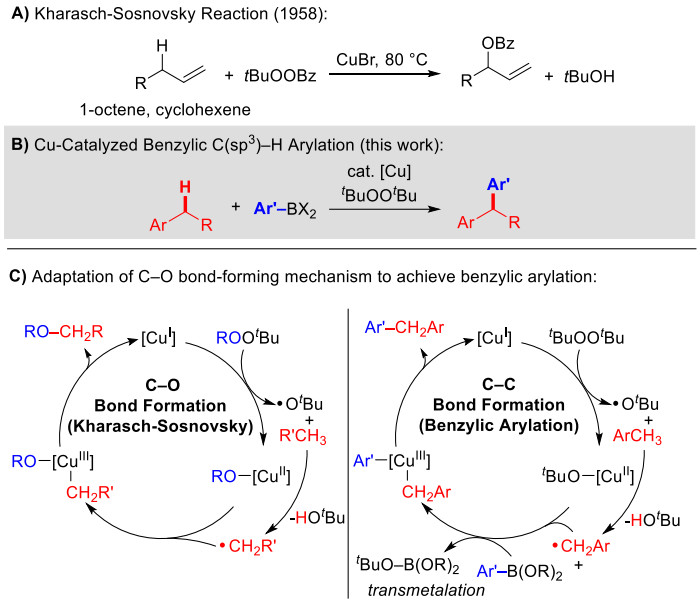

2.3. Results and Discussion

We initiated our investigation by examining toluene as a prototypical benzylic C–H substrate in the presence of commonly used catalyst components for Kharasch-type oxidations: a copper source (CuI), ligand (phenanthroline), and peroxide-based oxidant (Table 2.1). Testing of trimethoxyphenylsilane and phenylboronic acid did not lead to appreciable C–C coupling product (entries 1 and 2), but use of phenylboronic pinacol ester, PhBpin, afforded a 50% yield of diphenylmethane, with respect to PhBpin (entry 3). Increasing the ligand loading decreased formation of the biphenyl byproduct, while simultaneously increasing the product yield to 68% (entry 4; see Figure 2A.2 in Appendix A for full analysis of the product distributions at different ligand:Cu ratios). This improvement in yield may be rationalized by attenuation of the rate of aryl transmetalation from boron to Cu, thereby decreasing the steady-state concentration of a Cu–Ar intermediate, which could undergo unproductive biphenyl formation. A number of other Cu^{I} sources (e.g., CuBr, CuCl, CuCN) were effective, with only a moderate drop in yield (see

Appendix A for full screening data), but we chose to proceed with CuI•DMS (copper iodide dimethyl sulfide complex; entry 5) because it has good solubility, has good physical properties for weighing and dispensing, and led to reproducibly good yields. A final improvement in yield was achieved by using the 4,4,6-trimethyl-1,3,2-dioxaborinane ester, PhBdiol. This boronic ester led to a 9% increase in yield relative to PhBpin (entry 6) and is readily accessed in one step from 2-methyl-2,4-pentanediol and the corresponding commercially available aryl boronic acid (see Figure 2A.3 in Appendix A for a comparison of their reactivity). 1,10-Phenanthroline-5,6-dione (phd) was screened for efficacy as a ligand, as it has higher solubility in toluene, but it led to a lower yield of the desired product. In selected reactions described below, however, use of phd as a ligand proved to be advantageous.

Table 2.1. Cu-Catalyzed Benzylic C−H Arylation: Optimization of the Reaction Conditions

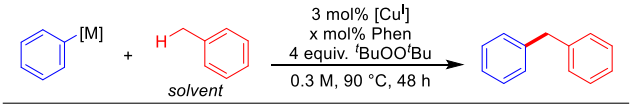

entry[a]	Ph-[M]	Cu(I)	mol % Phen	% Ph-Ph	% Ph-H	% yield[b]
1	$PhSi(OMe)_3$	CuI	3	0	1	6
2	$PhB(OH)_2$	CuI	3	1	48	3
3	PhBpin	CuI	3	32	1	50
4	PhBpin	CuI	15	12	1	68
5	PhBpin	CuI•DMS	15	13	2	69
6	**PhBdiol**	**CuI•DMS**	**15**	**6**	**2**	**78**
7[c]	PhBdiol	CuI•DMS	15	1	1	26

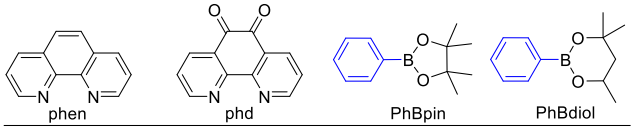

[a]Reactions at 0.5 mmol scale in 1.6 mL PhMe under N_2. [b]Calibrated GC yield with tetradecane as the internal standard. [c]Phd used as the ligand instead of phen.

The optimized reaction conditions were then tested with a number of different Bdiol-derived boronic esters bearing diverse functional groups. The reaction appears to be relatively insensitive to electronic properties of the boronic ester: both electron-rich (e.g., **2** and **3**) and electron-deficient

(e.g., **4**, **6**, and **23**) boronic esters undergo effective coupling in similarly good yields. This favorable outcome was not necessarily expected, as rates of transmetalation of aryl groups from arylboronic esters to Cu^{II} have been shown to exhibit relatively strong electronic effects,[14a] and different relative rates of transmetalation could favor formation of biaryl and/or bibenzyl side products owing to changes in steady state concentrations of organocopper intermediates. Reactive functional groups, including methylester (**13**), *N*-methylamide (**16**), methylthioether (**25**), and halides (F, Cl, Br, I; **5**–**8**) are conserved in the reactions and provide potential points for further elaboration of the 1,1-diarylmethane products. Steric effects were also evaluated. The reactions tolerate both *para* and *meta* substitution well, but the presence of an *ortho* substituent reduces the yield (cf. **3** vs. **9**). Boronic esters bearing heterocycles are also competent coupling partners (cf. **11**, **12**, **15**, **18**–**22**). Benzofuran derivative **18** is a key intermediate en route to a sphingosine-1 phosphate receptor subtype-1 agonist,[15] and a single-step route to this and other heterocyclic diarylmethane derivatives offers an appealing alternative to traditional pathways to these molecules.

Table 2.2. Cu-Catalyzed Arylation of Primary Benzylic C–H Bonds: Substrate Scope

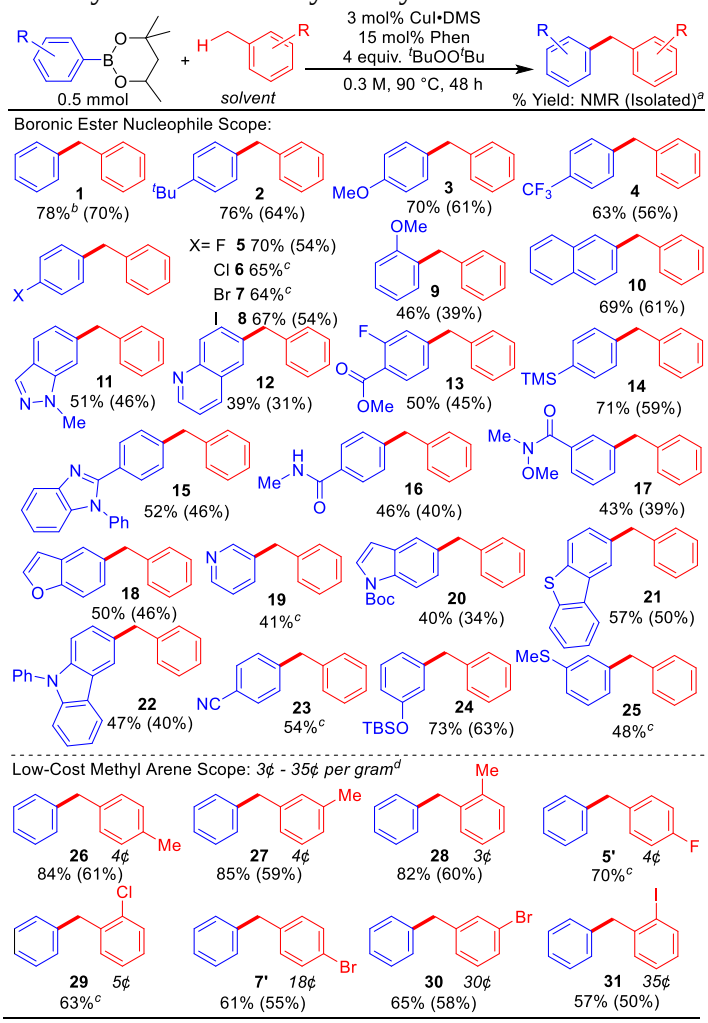

[a]Calibrated ^{1}H NMR yields using dibromomethane as an internal standard (isolated yields in parentheses). [b]Reaction yield at 74% by ^{1}H NMR after 24 h. [c]Product obtained as a mixture with biphenyl or biaryl byproduct; see Appendix A for details. [d]Prices obtained from vendors listed on SciFinder.

In addition to toluene, many other methylarene derivatives are very inexpensive (2–35¢/gram), which makes them amenable to use in large excess relative to the valuable boronic esters. The xylene isomers (cf. **26**, **27**, and **28**) proved to be even more effective coupling partners with PhBdiol than toluene. Because xylene is the solvent, this outcome could reflect an increase in the effective concentration of benzylic C–H bonds. Toluene derivatives with dimethylamino and acetyl functional groups are not effective oxidative coupling partners with PhBdiol (<10% yield);

however, halogenated toluene derivatives are quite effective (**5'**, **7'**, **29**–**31**). Halogens at the *ortho*, *meta*, and *para* positions are all well tolerated. The importance of the latter results is readily apparent in the context of the active pharmaceuticals shown in Scheme 2.1. For example, use of *o*-iodotoluene as a C–H substrate provides an opportunity to access derivatives of bifemelane[5a] by employing different Bdiol coupling partners and through coupling reactions of the aryl iodide. In other cases, the halogen substituents themselves are valuable. For example, the potency of a diarylalkane-derived antihistamine increases by an order of magnitude upon introducing a *p*-Cl or *p*-Br substitutent.[16] More generally, the activated methylene position in all of the products in Table 2.2 provides a site for elaboration, as demonstrated by a number of recent carbon-carbon[17] and carbon-heteroatom[18] bond forming methods.

After assessing the reactivity of methylarenes, we chose to examine other alkylarenes. Anticipating that such substrates will typically have higher cost than the methyl arenes in Table 2.2, we investigated these reactions with only 10 equiv of the alkylarene partner. Optimization of the reagent concentration and ligand:Cu ratio resulted in a 69% yield of cross-coupled product in the reaction of PhBdiol and ethylbenzene (see Appendix A for full optimization data). These reactions are similarly compatible with substituted boronic esters (**35** and **36**). For certain C–H substrates, however, modified conditions proved to be optimal. For example, the highest yields of **34**, **37**, and **38** were obtained with phd as the ligand rather than phen. These conditions provide a single-step route to the racemic anti-cancer isoerianin analogue **34**.[5b,c] In order to demonstrate the preparative utility of the method, we performed this reaction on half-gram scale (Scheme 2.3). The reaction was conducted on the benchtop to demonstrate that the typical protocol of loading reagents in a glovebox was not needed. This larger-scale reaction proceeded in 70% yield, which is even higher than the small-scale reaction. The good yield and ease of recovery of the unreacted

alkylarene starting material (see Appendix A for details) suggests that this reaction could be used in the arylation of other valuable alkylarenes.

Table 2.3. Cu-Catalyzed Arylation of Secondary Benzylic C–H Bonds: Substrate Scope

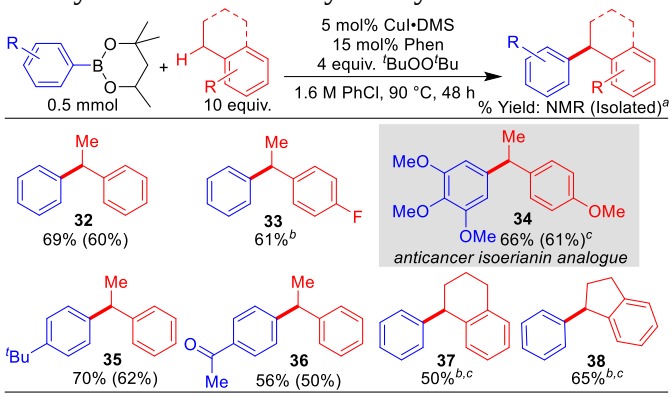

[a]Calibrated ^{1}H NMR yields using dibromomethane as an internal standard (isolated yields in parentheses). [b]Product obtained as a mixture with homocoupled C–H substrate; see Appendix A for details. [c]Reaction run using 3 mol% CuI•DMS with 15 mol% phd as the ligand instead of phen.

Scheme 2.3. Half-Gram Scale, Glove-Box-Free Synthesis of an Isoerianin Analogue (**34**)

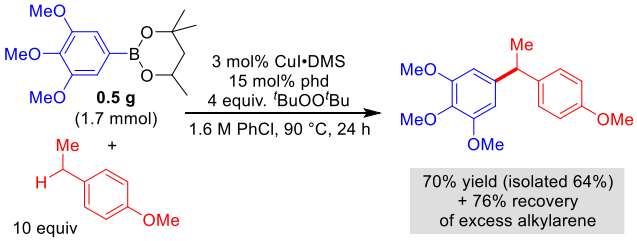

Finally, we examined the functionalization of 3-chloro-1-phenylpropane, another inexpensive arylalkane substrate (28¢/gram). The product of the arylation reaction is a direct precursor to pharmaceutically relevant 3,3-diarylpropylamine derivatives (cf. Scheme 2.1).[4b-e,19] Slightly modified reaction conditions, most notably the use of a higher concentration of oxidant, enabled optimized yields to be attained for the benzylic arylation reaction. Reaction with the parent PhBdiol affords **39** in good yield, and similar reactivity was observed with other boronic ester

derivatives. As observed in Table 2.2, potentially reactive functional groups, such as an aryl iodide and a ketone, are compatible with the reaction (cf. **40**, **42**, and **43**). These results further demonstrate how direct benzylic C–H arylation method could be used in the discovery of new drug candidates.

Table 2.4. Direct Access to Derivatized 1,1-Diarylalkane Pharmacophores

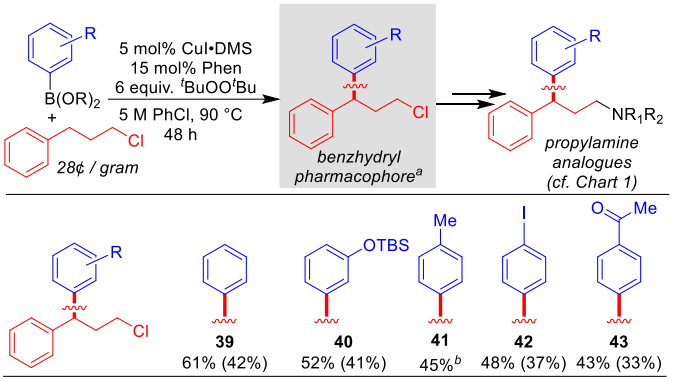

[a]Reactions run on 0.5 mmol scale with 10 equiv. of 3-phenyl-1-chloropropane. Isolated yields in parentheses. [b]Product obtained as a mixture with homocoupled C–H substrate; see Appendix A for details.

Mechanistic studies are the focus of ongoing investigation, but several observations are worth noting. As might be expected, several factors contribute to the selectivity of the reactions, including substrate sterics, electronics, and stoichiometry. Competition studies reveal that the relative reactivity of alkyl arenes follow the order: 2° (ethyl) > 1° (methyl) >> 3° (isopropyl) (see Figure 2A.5). Further experiments with toluene and diphenylmethane, however, show that the diarylmethanes are comparatively unreactive and do not undergo arylation in the presence of excess toluene (Figure 2A.6). Further control experiments show that tertiary diarylalkanes do not react under the catalytic conditions (Figure 2A.7). Collectively, these observations rationalize selective formation of the products in Tables 2.2–4.

2.4. Conclusion

In summary, the Cu-catalyzed oxidative arylation reactions described herein provide efficient access to highly important diarylalkane derivatives from inexpensive, readily available methyl- and alkylarenes. This new C–C coupling method represents an important extension of traditional Kharasch-Sosnovsky methods for C−H functionalization, and they offer a compelling complement to benzylic arylation reactions that employ more-traditional nucleophile/electrophile coupling partners.[20]

2.5. Acknowledgements

The authors thank Scott McCann for valuable discussions and assistance with data collection. This work was supported by the DOE (DE-FG02-05ER15690) and the NIH (Ruth L. Kirschstein National Research Service Award F32-GM109569 to S.L.Z). Spectroscopic instrumentation was partially supported by the NIH (1S10 OD020022-1) and the NSF (CHE-1048642).

2.6. Author Contributions

Vasilopoulos, A: experimental work and manuscript preparation

Zultanski, S. L: reaction ideation and preliminary results

2.7. References

1. Vanjari, R.; Singh, K. N. *Chem. Soc. Rev.* **2015**, *44*, 8062–8096.
2. (a) Borduas, N.; Powell, D. A. *J. Org. Chem.* **2008**, *73*, 7822-7825. (b) Guin, S.; Rout, S. K.; Banerjee, A.; Nandi, S.; Patel, B. K. *Org. Lett.* **2012**, *14*, 5294–5297. (c) Wu, Y.; Choy, P.

Y.; Mao, F.; Kwong, F. Y. *Chem. Commun.*, **2013**, *49*, 689-691. (d) Xiong, F.; Qian, C.; Lin, D.; Zeng, W.; Lu, X. *Org. Lett.* **2013**, *15*, 5444-5447. (e) Xu, Z.; Xiang, B.; Sun, P. *RSC Adv.*, **2013**, *3*, 1679-1682. (f) Curto, J. M.; Kozlowski, M. C. *J. Am. Chem. Soc.* **2015**, *137*, 18-21. (g) Tang, S.; Wang, P.; Li, H.; Lei, A. *Nat. Commun.* **2016**, *7*, 11676.

3. For related C–C bond-forming reactions, see: (a) Li, C.-J. *Acc. Chem. Res.* **2009**, *42*, 335–344. (b) Liu, D.; Li, Y.; Qi, X.; Liu, C.; Lan, Y.; Lei, A. *Org. Lett.* **2015**, *17*, 998-1101.
4. For examples of bioactive propylamines and other benzhydryls, see: (a) Loew, E. R.; MacMillan, R.; Kaiser, M. E. *J. Pharm. Exp. Ther.* **1945**, *86*, 229-238. (b) Jones, G.; Maisey, R. F.; Somerville, A. R.; Whittle, B. A. *J. Med. Chem.* **1971**, *14*, 161-164. (c) Emanuel, M. B. *Clin. Exp. Allergy* **1999**, *29*, 1-11. (d) Mueller, A. L.; Balandrin, M. F.; Van Wagenen, B. C.; DelMar, E. G.; Moe, S. T.; Artman, L. D.; Barmore, R. M. US6051610A, April 18, 2000. (e) Church, D. S.; Church, M. K. *World Allergy Organ. J.* **2011**, *4*, S22-S27.
5. For medicinal studies on bifemelane and isoerianin, see: (a) Kuriyama, S.; Saitoh, M. EP0103897 A1, March 28, 1984. (b) Messaoudi, S.; Hamze, A.; Provot, O.; Tréguier, B.; De Losada, J. R.; Bignon, J.; Liu, J.-M.; Wdzieczak-Bakala, J.; Thoret, S.; Dubois, J.; Brion, J.-D.; Alami, M. *ChemMedChem*. **2011**, *6*, 488-497. (c) Rasolofonjatovo, E.; Provot, O.; Hamze, A.; Rodrigo, J.; Bignon, J.; Wdzieczak-Bakala, J.; Desravines, D.; Dubois, J.; Brion, J.-D.; Alami, M. *Eur. J. Med. Chem.* **2012**, *52*, 22-32.
6. For use of chelate-directed aryl C–H activation in benzylic C–H coupling reactions, see: (a) Aihara, Y.; Tobisu, M.; Fukumoto, Y.; Chatani, N. *J. Am. Chem. Soc.* **2014**, *136*, 15509–15512. (b) Kubo, T.; Aihara, Y.; Chatani, N. *Chem. Lett.* **2015**, *44*, 1365–1367. (c) Zhang, H.-J.; Su, F.; Wen, T.-B. *J. Org. Chem.* **2015**, *80*, 11322-11329.

7. For photoinduced 4-pyridination of benzylic C–H bonds with 4-cyanopyridines: Hoshikawa, T.; Inoue, M. *Chem. Sci.* **2013**, *4*, 3118-3123.

8. The following examples of Ir photoredox catalysis focus on functionalization of other C–H bonds, but they include one example each of a benzylic C–H arylation: (a) Shields, B. J.; Doyle, A. G. *J. Am. Chem. Soc.* **2016**, *138*, 12719–12722. (b) Heitz, D. R.; Tellis, J. C.; Molander, G. A. *J. Am. Chem. Soc.* **2016**, *138*, 12715–12718. (c) Shaw, M. H.; Shurtleff, V. W.; Terrett, J. A.; Cuthbertson, J. D.; MacMillan, D. W. C. *Science* **2016**, *352*, 1304–1308.

9. (a) Sosnovsky, G.; Kharasch, M. S. *J. Am. Chem. Soc.* **1958**, *80*, 756. (b) Fono, A.; Kharasch, M. S. *J. Org. Chem.* **1958**, *23*, 325-326

10. For reviews, see: (a) Rawlinson, D. J.; Sosnovsky, G. *Synthesis* **1972**, *1*, 1-28. (b) Eames, J.; Watkinson, M. *Angew. Chem., Int. Ed.* **2001**, *40*, 3567-3571. (c) Andrus, M. B.; Lashley, J. C. *Tetrahedron*. **2002**, *58*, 845-866.

11. For mechanistic considerations, see the following leading refs: (a) Kochi, J. K.; Mains, H. E. *J. Org. Chem.* **1965**, *30*, 1862-1872. (b) Jenkins, C. L.; Kochi, J. K. *J. Am. Chem. Soc.* **1972**, *94*, 856–865. (c) Gephart, III, R. T.; McMullin, C. L.; Sapiezynski, N. G.; Jang, E. S.; Aguila, M. J. B.; Cundari, T. R.; Warren, T. H. *J. Am. Chem. Soc.* **2012**, *134*, 17350–17353. (d) Tran, B. L.; Driess, M.; Hartwig, J. F. *J. Am. Chem. Soc.* **2014**, *136*, 17292–17301. (e) Tran, B. A.; Li, B.; Driess, M.; Hartwig, J. F. *J. Am. Chem. Soc.* **2014**, *136*, 2555-2563.

12. (a) Powell, D. A.; Fan, H. *J. Org. Chem.* **2010**, *75*, 2726-2729. (b) García-Cabeza, A. L.; Marín-Barrios, R.; Moreno-Dorado, F. J.; Ortega, M. J.; Massanet, G. M.; Guerra, F. M. *Org. Lett.* **2014**, *16*, 1598–1601. (c) Zeng, H.-T.; Huang, J.-M. *Org. Lett.* **2015**, *17*, 4276-4279. (d) Lu, B.; Zhu, F.; Sun, H.-M.; Shen, Q. *Org. Lett.* **2017**, *19*, 1132–1135.

13. Zhang, W.; Wang, F.; McCann, S. D.; Wang, D.; Chen, P.; Stahl, S. S.; Liu, G. *Science* **2016**, *353*, 1014-1018.

14. (a) King, A. E.; Ryland, B. L.; Brunold, T. C.; Stahl, S. S. *Organometallics*, **2012**, *31* 7948–7957. (b) Wang, F.; Wang, D.; Mu, X.; Chen, P.; Liu, G. *J. Am. Chem. Soc.* **2014**, *136*, 10202–10205.

15. Saha, A. K.; Yu, X.; Lin, J.; Lobera, M.; Sharadendu, A.; Chereku, S.; Schutz, N.; Segal, D.; Marantz, Y.; McCauley, D.; Middleton, S.; Siu, J.; Bürli R. W.; Buys, J.; Horner, M.; Salyers, K.; Schrag, M.; Vargas, H. M.; Xu, Y.; McElvain, M.; Xu, H. *ACS Med. Chem. Lett.* **2011**, *2*, 97-101.

16. *Analytical toxicology: for clinical, forensic and pharmaceutical chemists*; Brandenberger, H.; Maes, R. A. A., Eds.; Walter de Gruyter: Berlin, 1997, pp. 549-550.

17. See, for example: (a) Gopishetty, B.; Gogoi, S.; Dutta, A. K. *Tetrahedron: Asymmetry* **2011**, *22*, 1081–1086. (b) Zhang, J.; Bellomo, A.; Creamer, A. D.; Dreher, S. D.; Walsh, P. J. *J. Am. Chem. Soc.* **2012**, *134*, 13765–13772. (c) Zhang, J.; Bellomo, A.; Trongsiriwat, N.; Jia, T.; Carroll, P. J.; Dreher, S. D.; Tudge, M. T.; Yin, H.; Robinson, J. R.; Schelter, E. J.; Walsh, P. J. *J. Am. Chem. Soc.* **2014**, *136*, 6276–6287.

18. See, for example: (a) Shaw, H.; Perlmutter, H. D.; Gu, C.; Arco, S. D.; Quibuyen, T. O. *J. Org. Chem.* **1997**, *62*, 236–237. (b) Yi, H.; Liu, Q.; Liu, J.; Zeng, Z.; Yang, Y.; Lei, A. *ChemSusChem* **2012**, *5*, 2143–2146. (c) Cantillo, D.; de Frutos, O.; Rincon, J. A.; Mateos, C.; Kappe, C. O. *J. Org. Chem.* **2014**, *79*, 223–229. (d) Huang, H.; Chen, W.; Xu, Y.; Li, J. *Green Chem.* **2015**, *17*, 4715–4719. (e) Hruszkewycz, D. P.; Miles, K. C.; Thiel, O. R.; Stahl, S. S. *Chem. Sci.* **2017**, *8*, 1282–1287.

19. (a) Hong, W.; Xueyan, Y.; Tang, C. CN101941911 A, 2011. (b) Estevez, C. C.; Bayarri, F. N.; Castells, B. J.; Echeverria, B. B. EP2357172 B1, 2011.

20. For leading references, see: (a) Do, H.-Q.; Chandrashekar, E. R. R.; Fu, G. C. *J. Am. Chem. Soc.* **2013**, *135*, 16288–16291. (b) Maity, P.; Shacklady-McAtee, D. M.; Yap, G. P. A.; Sirianni, E. R.; Watson, M. P. *J. Am. Chem. Soc.* **2013**, *135*, 280–285. (c) Zhou, Q.; Srinivas, H. D.; Dasgupta, S.; Watson, M. P. *J. Am. Chem. Soc.* **2013**, *135*, 3307–3310. (d) Shacklady-McAtee, D. M.; Roberts, K. M.; Basch, C. H.; Song, Y.-G.; Watson, M. P. *Tetrahedron.* **2014**, *70*, 4257–4263. (e) Tellis, J. C.; Primer, D. N.; Molander, G. A. *Science* **2014**, *345*, 433–436.

Chapter 3.

Copper-Catalyzed Functionalization of Benzylic C–H Bonds with N-Fluorobenzenesulfonimide: Switch from C–N to C–F Bond Formation Promoted by a Redox Buffer and Brønsted Base

Reproduced with permission from: Joshua A. Buss, **Aristidis Vasilopoulos**, Dung L. Golden, Shannon S. Stahl. Copper-Catalyzed Functionalization of Benzylic C–H Bonds with *N*-Fluorobenzenesulfonimide: Switch from C–N to C–F Bond Formation Promoted by a Redox Buffer and Brønsted Base. *Org. Lett.* **2020**, *22*, 5749-5752. Copyright 2020 American Chemical Society.

3.1. Abstract

A copper catalyst in combination with *N*-fluorobenzenesulfonimide (NFSI) has been reported to functionalize benzylic C–H bonds to the corresponding benzylic sulfonimides via C–N coupling. Here, we reported a closely related Cu-catalyzed method with NFSI that instead leads to C–F coupling (Figure 3.1). This switch in selectivity arises from changes to the reaction conditions (Cu:ligand ratio, temperature, addition of base) and further benefits from inclusion of $MeB(OH)_2$ to the reaction. $MeB(OH)_2$ is shown to serve as a "redox buffer" in the reaction, responsible for rescuing inactive Cu(II) for continued promotion of fluorination reactivity.

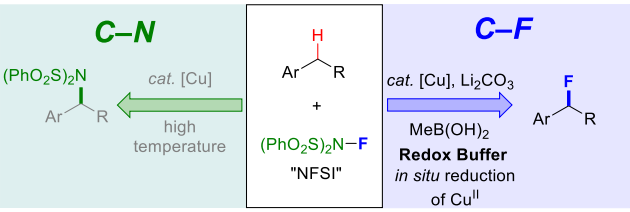

Figure 3.1. Switch from Benzylic C–H Sulfonimidation to Benzylic C–H Fluorination

3.2. Introduction

N–Fluorobenzenesulfonimide (NFSI) is a widely used reagent in organic synthesis. It is commonly used as a terminal oxidant in transition metal-catalyzed oxidations[1] and as a group-transfer reagent for sulfonylation, fluorination, and sulfonimidation of organic molecules.[2,3] The majority of these methods take advantage of the reactive N–F bond. For example, NFSI is commonly featured in electrophilic and radical fluorination of carbanions, carbon-centered radicals, and acidic C–H bonds,[4] while complementary methods and mechanisms have been identified for C–N bond formation with the sulfonimide group.[5] This bifurcation in reactivity between C–F and C–N bond formation is well documented in C(sp^2)–H functionalization of (hetero)arenes with NFSI (Scheme 3.1A).[3] We and others have recently been exploring Cu

catalyzed methods for site-selective functionalization of benzylic C(sp^3)–H bonds.[6,7] These reactions employ NFSI in a radical-relay mechanism that enables oxidative C–H coupling with diverse nucleophilic partners, including cyanide, azide, trifluoromethyl, alcohols, and arylboronic acids (Scheme 3.1B). The earliest example of this reactivity featured direct transfer of the sulfonimide group from NFSI to the benzylic position (Scheme 3.1C, top).[6] Here, we show that variation of the Cu/NFSI C–H sulfonimidation reaction conditions leads to C–F rather than C–N bond formation, complementing other benzylic C–H fluorination methods in the literature.[8] Mechanistic studies provide insights into the origin of this switch in selectivity, highlighting the role of $MeB(OH)_2$ as a "redox buffer" and Li_2CO_3 as a Brønsted base in the reaction. Additional studies reveal the intrinsic lability of secondary benzylic fluorides, making them susceptible to nucleophilic substitution. The latter reactivity is noted here, but provides basis for a complementary effort, leading to a versatile new class of benzylic C–H cross-coupling reactions.[9]

Scheme 3.1. C–N to C–F Bond Formation when Using NFSI in C(sp^2) and C(sp^3) C–H Functionalization

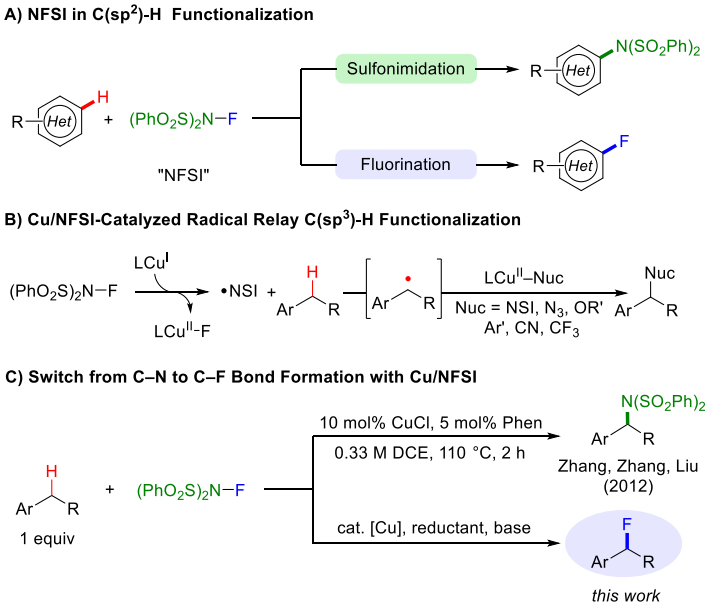

3.3. Results and Discussion

The present study was initiated by investigating the original Cu/NFSI-catalyzed sulfonimidation reaction (Scheme 3.1C).[6] This reaction takes place at much higher temperatures than more recent Cu/NFSI reactions, which often proceed near room temperature.[7] Attempting the sulfonimidation of *p*-bromoethylbenzene at lower temperature led to low conversion, but led to small quantities of C–F, in addition to C–N, bond formation product (Table 3.1, entry 2). The formation of a C–F bond could arise from reaction of an intermediate benzylic radical with a Cu^{II}–F species[10] or via a Cu-promoted radical-chain process involving NFSI.[8g,11] Addition of $MeB(OH)_2$ as an in situ reductant for the Cu catalyst[7e] (see further discussion below) led to complete substrate conversion, but only moderate yield of the C–N product was observed, with no C–F product (Table 3.1, entry 3). Further variation of the conditions, however, including addition of Li_2CO_3 as a base, using PhCl as the solvent, and lowering the catalyst loading, led to C–H fluorination in good yield (81%, Table 3.1, entry 7), with no C–N product formation (see additional screening data in Appendix B). Difluorination of the benzylic position is the primary side reaction.

Table 3.1. Fluorination Reaction Optimizations

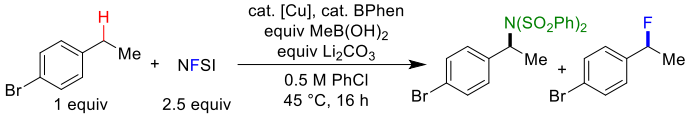

entry	[Cu] (mol%)	BPhen (mol%)	$MeB(OH)_2$ (equiv)	Li_2CO_3 (equiv)	conv (%)	C–N (%)	C–F (CF_2)[a] (%)
1[b,c]	CuCl (10)	*see Scheme 3.1A for conditions*			nd	**76**	nd
2[c]	CuCl (10)	5	-	-	24	19	4
3[c]	CuCl (10)	5	2	-	100	42	-
4[c]	CuCl (10)	5	2	3	100	44	21 (4)
5	CuCl (10)	5	2	3	100	25	40 (6)
6	CuCl (2)	1	2	3	86	4	74 (4)
7	CuOAc (2)	2.4	2	3	100	-	**81 (11)**

[a]0.3 mmol scale. ^{1}H NMR yields; int. std. = CH_2Br_2. [b]Reported results with ethylbenzene (ref. 7a). [c]1,2-dichloroethane (DCE) used as the solvent.

Several fundamental studies were undertaken to gain insights into the observed reactivity and the role of $MeB(OH)_2$ and other reaction components. Copper(I) is proposed to react with NFSI, forming a Cu^{II}–F species and an imidyl radical, •NSI (Scheme 3.1B). The imidyl radical can promote hydrogen atom transfer from the benzylic C–H bond, but it can react even more rapidly with another Cu^I center,[7e,12] generating a second equivalent of Cu^{II} and halting catalysis. To probe Cu/NFSI reactivity, NFSI was titrated into a solution of $BPhenCu^I(OAc)$ in PhCl (Bphen = bathophenanthroline). Nearly isosbestic behavior was observed by UV-visible spectroscopy, corresponding to oxidation of Cu^I to Cu^{II} species by NFSI (Figure 3.2A, step 1). Complete consumption of Cu^I was observed upon addition of 0.5 equiv of oxidant. This oxidation is rapid at room temperature, occurring on the timescale of mixing. Addition of NFSI beyond 0.5 equiv has no effect on the UV-visible spectrum, suggesting that Cu^{II} does not react further with NFSI.

The Cu^{II} species generated by NFSI is reduced by $MeB(OH)_2$. Addition of 5 equiv of $MeB(OH)_2$ to a solution of Cu^{II} generated from a combination of $BPhenCu^I(OAc)$ and 0.5 equiv of NFSI in PhCl slowly regenerates Cu^I over approximately 1 h (Figure 3.2A, step 2). This process

generates Me–$N(SO_2Ph)_2$ as a byproduct of the reaction, resembling the previously reported Chan-Lam amidation of alkylboronic acids[13] (see Figure 3B.2 in Appendix B).

The impact of $MeB(OH)_2$ on the catalytic reaction is clearly evident in Figure 3.2B. Virtually no reaction is observed in the absence of $MeB(OH)_2$. In contrast, full substrate conversion occurs in the presence of 2 equiv of $MeB(OH)_2$, leading to an 84% yield of the benzyl fluoride. This behavior is rationalized by the ability of $MeB(OH)_2$ to serve as a "redox buffer" for the Cu catalyst, slowly reducing Cu^{II} during the reaction. A mechanistic framework for these observations is illustrated in Figure 3.2C. Cu^{I} is oxidized rapidly to Cu^{II} by NFSI at the beginning of the reaction, but slow reduction of Cu^{II} by $MeB(OH)_2$ (dashed arrow, Figure 3.2C) generates small amounts of Cu^{I} that can react with additional NFSI. Generation of •NSI at this stage can lead to hydrogen atom transfer (HAT) from the benzylic C–H with only limited competitive quenching of •NSI by Cu^{I}, due to the low Cu^{I} concentration.

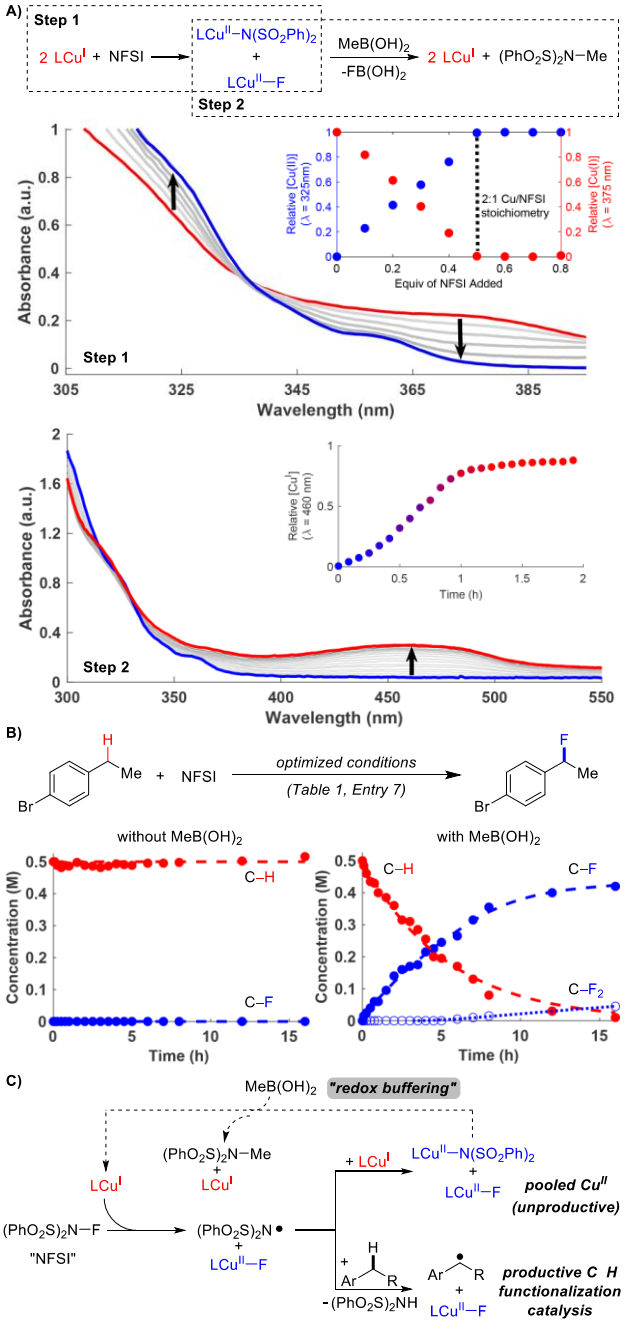

Figure 3.2. Fundamental insights into Cu/NFSI-catalyzed fluorination reactions. (A) Spectroscopic analysis of stoichiometric oxidation of Cu^{I} by NFSI and reduction of Cu^{II} by $MeB(OH)_2$. (B) Reaction time course data demonstrating the effect of $MeB(OH)_2$ redox buffering in the catalytic fluorination reaction. (C) Mechanism depicting the redox buffering role of $MeB(OH)_2$ in benzylic fluorination. Conditions: (A) Step 1 – 0.33 mM $BPhenCu^{I}OAc$ + 0.1 equiv NFSI (×8) in PhCl. Step 2 – [Cu^{II}] (from 0.33 mM $BPhenCu^{I}(OAc)$ + 0.5 equiv NFSI) + 5 equiv $MeB(OH)_2$, 15 equiv Li_2CO_3 in PhCl. (B) See Table 3.1, entry 7.

The synthetic scope of this reactivity is the focus of a separate study;[9] however, testing of representative substrates showed that isolation of benzyl monofluorides can be rather challenging, with poor mass balance and the appearance of new byproducts (see Appendix B, Section 3B.V). Similar challenges are evident from previous C–H fluorination methods,[8] and other studies show that benzyl monofluorides undergo facile displacement in the presence of Brønsted and Lewis acids or hydrogen-bond donors.[14] The latter insights prompted us to assess the role of Li_2CO_3 in the reaction, which was also used in a previous benzylic C–H fluorination method.[8g] A time course for the optimized reaction conditions in Figure 3.2B (right) may be compared to the time course obtained without added Li_2CO_3 (Scheme 3.2A). The rate of substrate conversion is virtually identical in the presence and absence of Li_2CO_3; however, very little C–F product is observed after the first few hours of the reaction without Li_2CO_3, and the major products arise from C–O and C–N bond formation. NHSI is a strong acid and will build up as the fluorination reaction proceeds, and it could promote acidolysis of the benzyl fluoride.[15] In a control experiment, 1 equiv of NHSI was added to a solution of benzyl fluoride obtained from the catalytic reaction, following filtration through a silica plug to remove the Li_2CO_3. This reaction results in rapid formation of 1-phenylethanol (Scheme 3.2B). The hydroxy group presumably originates from adventitious water from the solvent or reagents present in the original reaction mixture. The net C–H fluorination/hydrolysis sequence resembles the recently reported C–H mesylation/hydrolysis strategy to achieve C–H hydroxylation, reported by Ritter and coworkers.[16]

Scheme 3.2. Li_2CO_3 Effect on Benzyl Fluoride Lability

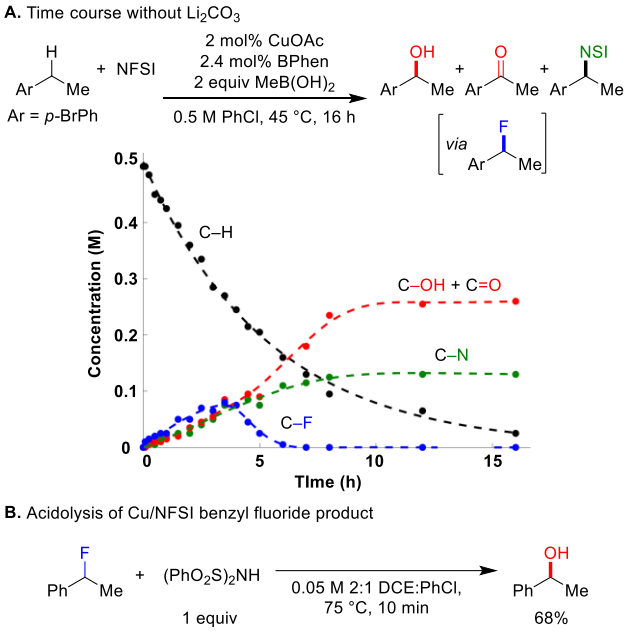

3.4. Conclusion

The results presented herein reveal an unusual switch in selectivity, from C–N to C–F bond formation, in Cu/NFSI-promoted oxidative functionalization of benzylic C–H bonds. Mechanistic studies show how two new reaction additives contribute to formation of the fluorination product. $MeB(OH)_2$ serves as a redox buffer[7e] that promotes steady-state reduction of Cu^{II} to the active Cu^{I} species during the catalytic reaction. Li_2CO_3 serves as a Brønsted base that prevents acid-promoted displacement of the fluoride during the reaction. While the observed substitutional lability of the products undermines the accessibility and practical utility of isolated benzyl monofluorides, this property introduces the possibility of using benzyl fluorides as strategic intermediates in a C–H fluorination/substitution sequence. Development and elaboration of the latter C–H cross-coupling strategy is the focus of a parallel report.[9]

3.5. Acknowledgements

The authors thank Scott McCann and Si-Jie Chen (UW-Madison) for valuable discussions leading to the development of redox buffering in Cu/NFSI systems. This work was supported by the NIH (R01 GM126832, R35 GM134929), including a Ruth L. Kirschstein NRSA fellowship (F32 GM129909, to JAB). Spectroscopic instrumentation was partially supported by the NIH (1S10 OD020022-1) and the NSF (CHE-1048642).

3.6. Author Contributions

Buss, J. A: leading experimental work and manuscript preparation

Vasilopoulos, A: experimental work and manuscript preparation

Golden, D. L: manuscript preparation

3.7. References

1. Engle, K. M.; Mei, T.-S.; Wang, X.; Yu, J.-Q. Bystanding F^+ Oxidants Enable Selective Reductive Elimination from High-Valent Metal Centers in Catalysis. *Angew. Chem. Int. Ed.* **2011**, *50*, 1478-1491.
2. (a) Roy, A.; Schneller, S. W. An Unusual Occurrence on Attempted Purine C-8 Electrophilic Fluorination of 5'-Noraristeromycin. *Org. Lett.* **2005**, *7*, 3889-3891. (b) Jing, L.; Yu, X.; Guan, M.; Wu, X.; Wang, Q.; Wu, X. An Efficient Method for Sulfonylation of Amines, Alcohols, and Phenols with *N*-Fluorobenzenesulfonimide Under Mild Conditions. *Chem. Res. Chin. Univ.* **2018**, *34*, 191-196. (c) Jie, K.; Wang, Y.; Huang, L.; Guo, S.; Cai, H. Convenient Sulfonylation of Imidazoles and Triazoles Using NFSI. *J. Sulfur Chem.* **2018**, *39*, 465-471.

3. Gu, Q.; Vessally, E. *N*-Fluorobenzenesulfonimide: A Useful and Versatile Reagent for The Direct Fluorination and Amination of (Hetero)Aromatic C–H Bonds. *RSC Adv.* **2020**, *10*, 16756-16768.

4. For recent reviews of fluorination chemistry, see: (a) Champagne, P. A.; Desroches, J.; Hamel, J.-D.; Vandamme, M.; Paquin, J.-F. Monofluorination of Organic Compounds: 10 Years of Innovation. *Chem. Rev.* **2015**, *115*, 9073-9174. (b) Yerien, D. E.; Bonesi, S.; Postigo, A. Fluorination Methods in Drug Discovery. *Org. Biomol. Chem.* **2016**, *14*, 8398-8427. (c) Szpera, R.; Moseley, D. F. J.; Smith, L. B.; Sterling, A. J.; Gouverneur, V. The Fluorination of C–H Bonds: Developments and Perspectives. *Angew. Chem. Int. Ed.* **2019**, *58*, 14824-14848.

5. Li, Y.; Zhang, Q. *N*-Fluorobenzenesulfonimide: An Efficient Nitrogen Source for C–N Bond Formation. *Synthesis* **2015**, *47*, 159-174.

6. Ni, Z.; Zhang, Q.; Xiong, T.; Zheng, Y.; Li, Y.; Zhang, H.; Zhang, J.; Liu, Q. Highly Regioselective Copper-Catalyzed Benzylic C–H Amination by *N*-Fluorobenzenesulfonimide. *Angew. Chem. Int. Ed.* **2012**, *51*, 1244-1247.

7. (a) Zhang, W.; Wang, F.; McCann, S. D.; Wang, D.; Chen, P.; Stahl, S. S.; Liu, G. Enantioselective Cyanation of Benzylic C–H Bonds via Copper-Catalyzed Radical Relay. *Science* **2016**, *353*, 1014-1018. (b) Zhang, W.; Chen, P.; Liu, G. Copper-Catalyzed Arylation of Benzylic C–H Bonds with Alkylarenes as the Limiting Reagents. *J. Am. Chem. Soc.* **2017**, *139*, 7709-7712. (c) Xiao, H.; Liu, Z.; Shen, H.; Zhang, B.; Zhu, L.; Li, C. Copper-Catalyzed Late-Stage Benzylic C(sp^3)–H Trifluoromethylation. *Chem* **2019**, *5*, 940-949. (d) Wang, A.; DeOliveira, C. C.; Emmert, M. Non-Directed, Copper Catalyzed Benzylic C–H Amination Avoiding Substrate Excess. *ChemRxiv* **2019**, https://doi.org/10.26434/chemrxiv.8792243. (e)

Hu, H.; Chen, S.-J.; Mandal, M.; Pratik, S. M.; Buss, J. A.; Krska, S. W.; Cramer, C. J.; Stahl, S. S. Copper-Catalyzed Benzylic C–H Coupling with Alcohols via Radical Relay Enabled by Redox Buffering. *Nat. Catal.* **2020**, *3*, 358-367. (f) Suh, S.-E. Chen, S.-J. Mandal, M.; Guzei, I. A.; Cramer, C. J.; Stahl, S. S. Site-Selective Copper-Catalyzed Azidation of Benzylic C–H Bonds. *J. Am. Chem. Soc.* **2020**, *142*, 11388-11393.

8. For selected primary references describing benzylic fluorination, see: (a) Bloom, S.; Pitts, C. R.; Miller, D. C.; Haselton, N.; Holl, M. G.; Urheim, E.; Lectka, T. A Polycomponent Metal-Catalyzed Aliphatic, Allylic, and Benzylic Fluorination. *Angew. Chem. Int. Ed.* **2012**, *51*, 10580-10583. (b) Xia, J.-B.; Zhu, C.; Chen, C. Visible Light-Promoted Metal-Free C–H Activation: Diarylketone-Catalyzed Selective Benzylic Mono- and Difluorination. *J. Am. Chem. Soc.* **2013**, *135*, 17494-17500. (c) Bloom, S.; Pitts, C. R.; Woltornist, R.; Griswold, A.; Holl, M. G.; Lectka, T. Iron(II)-Catalyzed Benzylic Fluorination. *Org. Lett.* **2013**, *15*, 1722-1724. (d) Amaoka, Y.; Nagatomo, M.; Inoue, M. Metal-Free Fluorination of C(sp^3)−H Bond Using a Catalytic *N*-Oxyl Radical. *Org. Lett*. **2013**, *15*, 2160-2163. (e) Cantillo, D.; de Frutos, O.; Rincón, J. A.; Mateos, C.; Kappe, C. O. A Continuous-Flow Protocol for Light-Induced Benzylic Fluorinations. *J. Org. Chem.* **2014**, *79*, 8486-8490. (f) Xu, P.; Guo, S.; Wang, L.; Tang, P. Silver-Catalyzed Oxidative Activation of Benzylic C–H Bonds for the Synthesis of Difluoromethylated Arenes. *Angew. Chem. Int. Ed.* **2014**, *53*, 5955-5958. (g) Nodwell, M. B.; Bagai, A.; Halperin, S. D.; Martin, R. E.; Knust, H.; Britton, R. Direct Photocatalytic Fluorination of Benzylic C–H Bonds with *N*-Fluorobenzenesulfonimide. *Chem. Commun.* **2015**, *51*, 11783-11786. (h) Groendyke, B. J.; AbuSalim, D. I.; Cook, S. P. Iron-Catalyzed, Fluoroamide-Directed C–H Fluorination. *J. Am. Chem. Soc.* **2016**, *138*, 12771-12774. (i) Meanwell, M.; Nodwell, M. B.; Martin, R. E.; Britton, R. A Convenient Late-Stage

Fluorination of Pyridylic C–H Bonds with *N*-Fluorobenzenesulfonimide. *Angew. Chem. Int. Ed.* **2016**, *55*, 13244-13248. (j) Xiang, M.; Xin, Z.-K.; Chen, B.; Tung, C.-H.; Wu, L.-Z. Exploring the Reducing Ability of Organic Dye (Acr^+-Mes) for Fluorination and Oxidation of Benzylic C(sp^3)−H Bonds under Visible Light Irradiation. *Org. Lett.* **2017**, *19*, 3009-3012. (k) Hua, A. M.; Mai, D. N.; Martinez, R.; Baxter, R. D. Radical C–H Fluorination Using Unprotected Amino Acids as Radical Precursors. *Org. Lett.* **2017**, *19*, 1949-1952.

9. Vasilopoulos, A.; Golden, D. L.; Buss, J. A.; Stahl, S. S. Copper-Catalyzed C–H Fluorination/Functionalization Sequence Enabling Benzylic C–H Cross Coupling with Diverse Nucleophiles. *Org. Lett.* **2020**, *22*, 5753-5757.
10. Bower, J. K.; Cypcar, A. D.; Henriquez, B.; Stieber, S. C. E.; Zhang, S. C(sp^3)–H Fluorination with a Copper(II)/(III) Redox Couple. *J. Am. Chem. Soc.* **2020**, *142*, 8514-8521.
11. (a) Rueda-Becerril, M.; Sazepin, C. C.; Leung, J. C. T.; Okbinoglu, T.; Kennepohl, P.; Paquin, J.-F.; Sammis, G. M. Fluorine Transfer to Alkyl Radicals. *J. Am. Chem. Soc.* **2012**, *134*, 4026-4029. (b) Pitts, C. R.; Bloom, S.; Woltornist, R.; Auveshine, D. J.; Ryzhkov, L. R.; Siegler, M. A.; Lectka, T. Direct, Catalytic Monofluorination of sp^3 C–H Bonds: A Radical-Based Mechanism with Ionic Selectivity. *J. Am. Chem. Soc.* **2014**, *136*, 9780-9791. (c) Li, M.; Xue, X.-S.; Chen, J.-P. Establishing Cation and Radical Donor Ability Scales of Electrophilic F, CF_3, and SCF_3 Transfer Reagents. *Acc. Chem. Res.* **2020**, *53*, 182-197.
12. Haines, B. E.; Kawakami, T.; Murakami, K.; Itami, K.; Musaev, D. G. Cu-Catalyzed Aromatic C–H Imidation with *N*-Fluorobenzenesulfonimide: Mechanistic Details and Predictive Models. *Chem. Sci.* **2017**, *8*, 988-1001.

13. Rossi, S. A.; Shimkin, K. W.; Xu, Q.; Mori-Quiroz, L. M.; Watson, D. A. Selective Formation of Secondary Amides via the Copper-Catalyzed Cross-Coupling of Alkylboronic Acids with Primary Amides. *Org. Lett.* **2013**, *15*, 2314-2317.
14. (a) Amii, H.; Uneyama, K. C–F Bond Activation in Organic Synthesis. *Chem. Rev.* **2009**, *109*, 2119-2183. (b) Hamel, J.-D.; Paquin, J.-F. Activation of C–F Bonds α to C–C Multiple Bonds. *Chem. Commun.* **2018**, *54*, 10224-10239.
15. (a) Bernstein, J.; Roth, J. S.; Miller Jr., W. T. The Preparation and Properties of Some Substituted Benzyl Fluorides. *J. Am. Chem. Soc.* **1948**, *70*, 2310-2314. (b) Swain, C. G.; Spalding, R. E. T. III. Mechanism of Acid Catalysis of the Hydrolysis of Benzyl Fluoride. *J. Am. Chem. Soc.* **1960**, *82*, 6104-6107.
16. Tanwar, L.; Börgel, J.; Ritter, T. Synthesis of Benzylic Alcohols by C–H Oxidation. *J. Am. Chem. Soc.* **2019**, *141*, 17983-17988.

Chapter 4.

Copper-Catalyzed C–H Fluorination/Functionalization Sequence Enabling Benzylic C–H Cross Coupling with Diverse Nucleophiles

Reproduced with permission from: **Aristidis Vasilopoulos**, Dung L. Golden, Joshua A. Buss, Shannon S. Stahl. Copper-Catalyzed C–H Fluorination/Functionalization Sequence Enabling Benzylic C–H Cross Coupling with Diverse Nucleophiles. *Org. Lett.* **2020**, *22*, 5753-5757.

4.1. Abstract

Site-selective transformation of benzylic C–H bonds into diverse functional groups is achieved via Cu-catalyzed C–H fluorination with *N*-fluorobenzenesulfonimide (NFSI), followed by substitution of the resulting fluoride with various nucleophiles (Figure 4.1). The benzyl fluorides generated in these reactions are reactive electrophiles in the presence of hydrogen-bond donors or Lewis acids, allowing them to be used without isolation in C–O, C–N, and C–C coupling reactions.

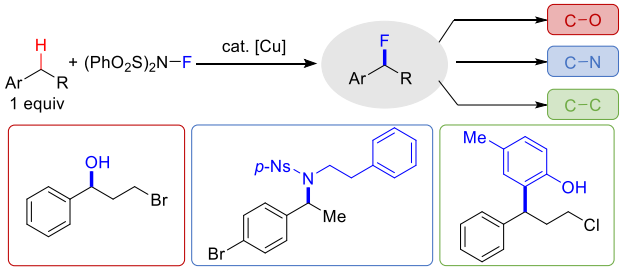

Figure 4.1. Summary of Benzylic C–H Fluorination/Functionalization Reactivity

4.2. Introduction

Medicinal chemistry and drug discovery efforts greatly benefit from synthetic coupling reactions that facilitate access to analogs of pharmaceutical building blocks and core structures. Functional groups that participate in efficient coupling, such as carboxylic acids, aryl halides, and boronic acids, provide the foundation for these methods.[1] Expansion of latent functionalities that participate in coupling could greatly increase the scope of synthetic diversity.[2] Benzylic C–H bonds are an appealing target in this context as they are prevalent in drug-like molecules and are susceptible to site-selective activation owing to their enhanced reactivity (e.g., reduced bond strength, higher acidity). Recent studies demonstrate that benzylic C–H substrates may be used as the limiting reagent in cross-coupling reactions with a number of different reaction partners,

including alcohols,[3] amides,[4] and arylboronic acids.[5] Cu catalysts in combination with *N*-fluorobenzenesulfonimide (NFSI) are particularly effective in these reactions as they exhibit unique selectivity for benzylic C–H bonds and promote a radical relay mechanism that enables coupling with diverse reaction partners (Scheme 4.1).[3a,4b,5a,6] We recently discovered that a Cu/NFSI-based catalyst system switches selectivity, from C–N to C–F bond formation, when the reaction is conducted with $MeB(OH)_2$ as a redox buffer and Li_2CO_3 as a Brønsted base.[7] These observations provide the foundation for the present study in which we demonstrate a C–H fluorination/substitution sequence that enables benzylic C–H cross-coupling with diverse oxygen, nitrogen, and carbon nucleophiles (Scheme 4.1). This strategy, which takes advantage of the intrinsic lability of benzyl monofluorides,[8,9] contrasts the many C–H fluorination efforts motivated by the inertness of the C–F bond.[10,11] This approach allows for successful benzylic C–H cross coupling with reaction partners that are oxidatively sensitive or otherwise incompatible with direct Cu/NFSI-catalyzed methods, thereby greatly expanding the synthetic scope and versatility of benzyl C–H cross coupling.

Scheme 4.1. C–H Cross-Coupling via a Benzyl Fluoride

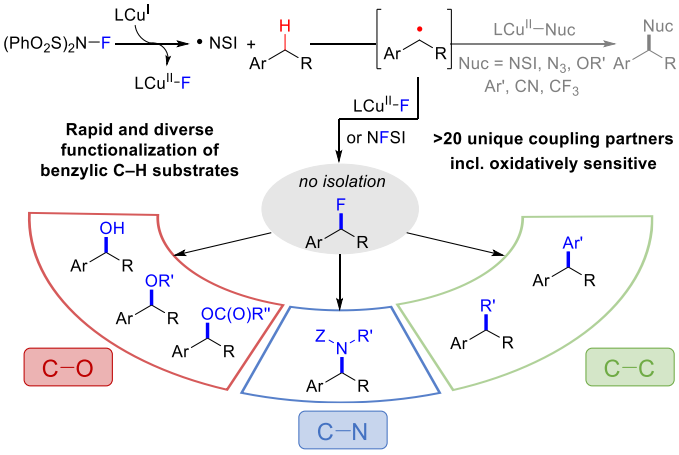

4.3. Results and Discussion

The present study began by testing the previously optimized fluorination conditions[7] with a variety of benzylic C–H substrates (Table 4.1). *para*-Bromoethylbenzene proceeds effectively in 81% to the corresponding benzyl fluoride product **1** (Table 4.1). Use of *ortho*-bromoethylbenzene resulted in low conversion of the starting material (<20%), presumably reflecting the deleterious steric or σ-electron withdrawing effect of the *o*-halogen on HAT. Empirical modification of the conditions, including use of 4 equiv of NFSI, replacement of $MeB(OH)_2$ with B_2pin_2 as the reductant, and operating at 75 °C, led to a 50% yield of the desired product **2**. The modified conditions, either at 55 °C or 75 °C, also proved effective with other electron- deficient substrates (**2**, **4**, **5**, **6**, **9**, **13**, **17**, **19**), while the original conditions were favored for more reactive substrates (**3**, **7**, **8**, **10**, **11**, **12**, **14**). The latter group also includes celestolide, which underwent fluorination in 86% yield (**18**), and substrates with tertiary C–H bonds, leading to **23** and **24** in 92% and 84% yields. Overoxidation to ketone or styrene-derived side products, was observed with more activated C–H substrates, necessitating the identification of milder conditions (35 °C, 0.5 equiv $MeB(OH)_2$). These conditions allowed several benzyl fluorides to be obtained in good yield (**15**, **16**, **20**), including a bromochroman derivative. Methylarenes appear to favor C–H sulfonimidation rather than fluorination, as observed by the formation of **21** and **22**. A collection of other less successful substrates is provided in Table 4C.9 of Appendix C, but, overall, these results show that the catalytic conditions may be tuned to access good fluorination reactivity for a broad range of benzylic C–H substrates.[12]

Table 4.1. Cu/NFSI Fluorination of Benzylic C–H Bonds

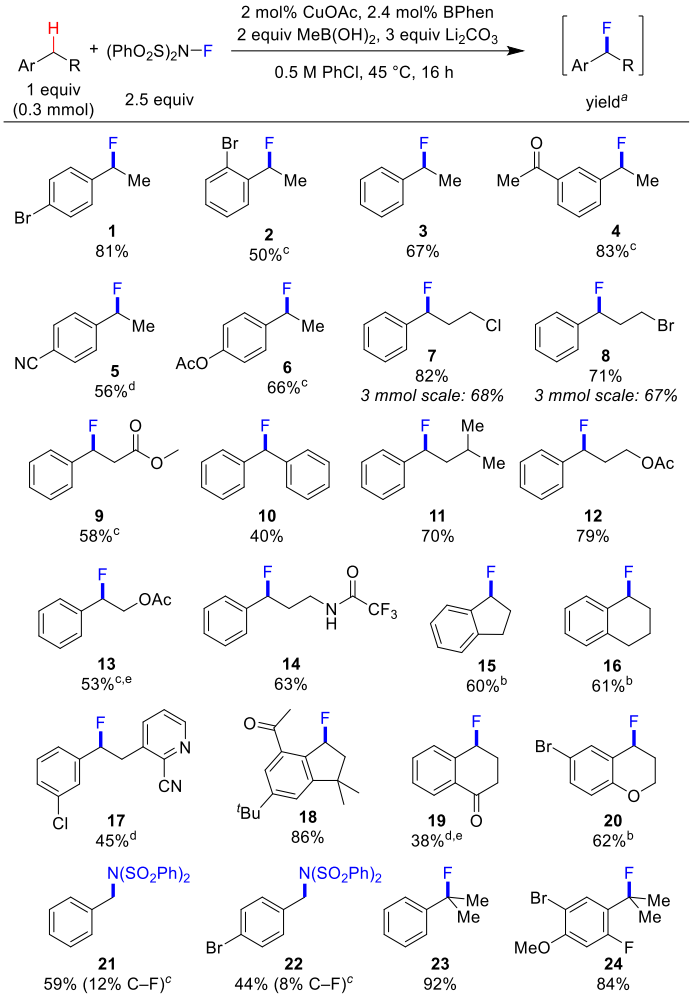

[a]^{1}H NMR yields; CH_2Br_2 or $PhCF_3$ as int. stds. [b]35 °C, 0.5 equiv $MeB(OH)_2$. [c]55 °C, 1 mol% Cu/1.2 mol% BPhen, 4 equiv NFSI, 1 equiv B_2pin_2 instead of $MeB(OH)_2$. [d]75 °C 1 mol% Cu/1.2 mol% BPhen, 4 equiv NFSI, 1 equiv B_2pin_2 instead of $MeB(OH)_2$. [e]Acetone solvent.

Complications were encountered during product isolation. Many of the products decomposed in the presence of silica gel, and even when stored in glass vessels. These observations belie the frequent incorporation of fluorine in organic molecules to inhibit reactivity at specific sites, for example, to slow drug metabolism.[10] Separately, benzylic monofluorides have been shown to undergo nucleophilic substitution in the presence of acids or hydrogen-bond donors.[8,9] These insights suggest that monofluorination of benzylic C–H bonds is not a compelling end-goal for

many substrates. On the other hand, they suggest that benzyl fluorides could serve as strategic intermediates in a sequential approach to benzylic C–H functionalization.

Efforts to explore sequential C–H fluorination/functional-ization were initiated by testing hexafluoroisopropanol (HFIP, 10 equiv) as a hydrogen bond donor to activate the benzyl fluoride (Table 4.2).[9f] Initial results demonstrated conversion of benzyl fluorides to benzyl alcohols by including water as a nucleophile in the reaction mixture (**25-27**). Formation of **25** shows that hydrogen-bond activation supports displacement of the fluoride, even in the presence of a primary alkyl bromide. This fluorination/water-substitution sequence to access benzylic alcohols is noteworthy because C–H oxygenation strategies will typically proceed directly to ketones, reflecting the higher reactivity of alcohols relative to C–H bonds.[13]

Analogous efforts were effective for the formation of benzylic ethers and esters (**28**–**36**). For less nucleophilic alcohols, like *tert*-butanol, more forcing conditions were needed to form the product, using BF_3•OEt_2 as a Lewis acid catalyst (**28** and **33**).[9i] This approach also enabled reactivity with alcohols bearing Boc-pyrrolidine or pyridine substituents (**31** and **32**). These results expand the scope of accessible products relative to the recently reported method for direct Cu/NFSI-catalyzed benzylic etherification,[3a] which shows limited compatibility with basic heterocycles, such as pyridines, and Boc-protected pyrrolidines. Carboxylic acids were also effective coupling partners (**34-36**). These substrates have innate acidity, but the reactions were more effective with HFIP or BF_3 additives. The presence of allylic and benzylic C–H bonds in the carboxylic acids used to prepare **34** and **36** would likely complicate direct C–H carboxylation methods with these partners.

We then targeted C–N coupling reactions. Direct C–H amidation reactions typically feature primary sulfonamides or other stabilized ammonia surrogates capable of generating nitrenoid

intermediates.[14] Few precedents exist for oxidative coupling of C–H bonds with carbamates or secondary sulfonamides.[4b,15] *tert*-Butyl carbamate itself proved to be an effective coupling partner when using BF_3•Et_2O to activate the benzyl fluoride (**37**). Then a range of secondary sulfonamides were shown to undergo effective displacement of the benzyl fluoride, with BF_3•Et_2O as an activator (**38**-**43**). The good reactivity with less nucleophilic, but more readily deprotected, nosylamides is noteworthy. Competitive Friedel-Crafts reactivity with chlorobenzene was observed in some of these reactions, but this complication was resolved by using dichloromethane as the solvent for the fluorination step (**40**-**43)**.

The observation of Friedel-Crafts reactivity highlights opportunities for coupling with electron-rich arenes and other carbon nucleophiles that would not be compatible with a direct Cu/NFSI-catalyzed C–H coupling reaction. Such reactivity was demonstrated with phenols (**44**-**46**), *N*-sulfonyl indole (**47**-**48**), and a silyl enol ether and allyl silane (**49**-**50**).

Each of the reactions highlighted above proceeds via a straightforward two-step protocol, without isolation of the benzyl fluoride intermediate. Following the fluorination step, sodium dithionite is added to quench any unreacted NFSI. The slurry is then diluted with dichloromethane and filtered. Subsequent addition of the nucleophile and HFIP/BF_3 promoter initiates the displacement reaction. As conveyed in several instances above, this two-step C–H cross-coupling sequence greatly expands the scope of useful reaction partners. Many of the electron-rich substrates and nucleophiles bearing oxidatively sensitive substituents would decompose or undergo deleterious side reactions with NFSI in a direct oxidative coupling reaction.[11c,16]

Table 4.2. Benzylic C–H Cross-Coupling to C–O, C–N, and C–C Bonds via a Benzyl Fluoride

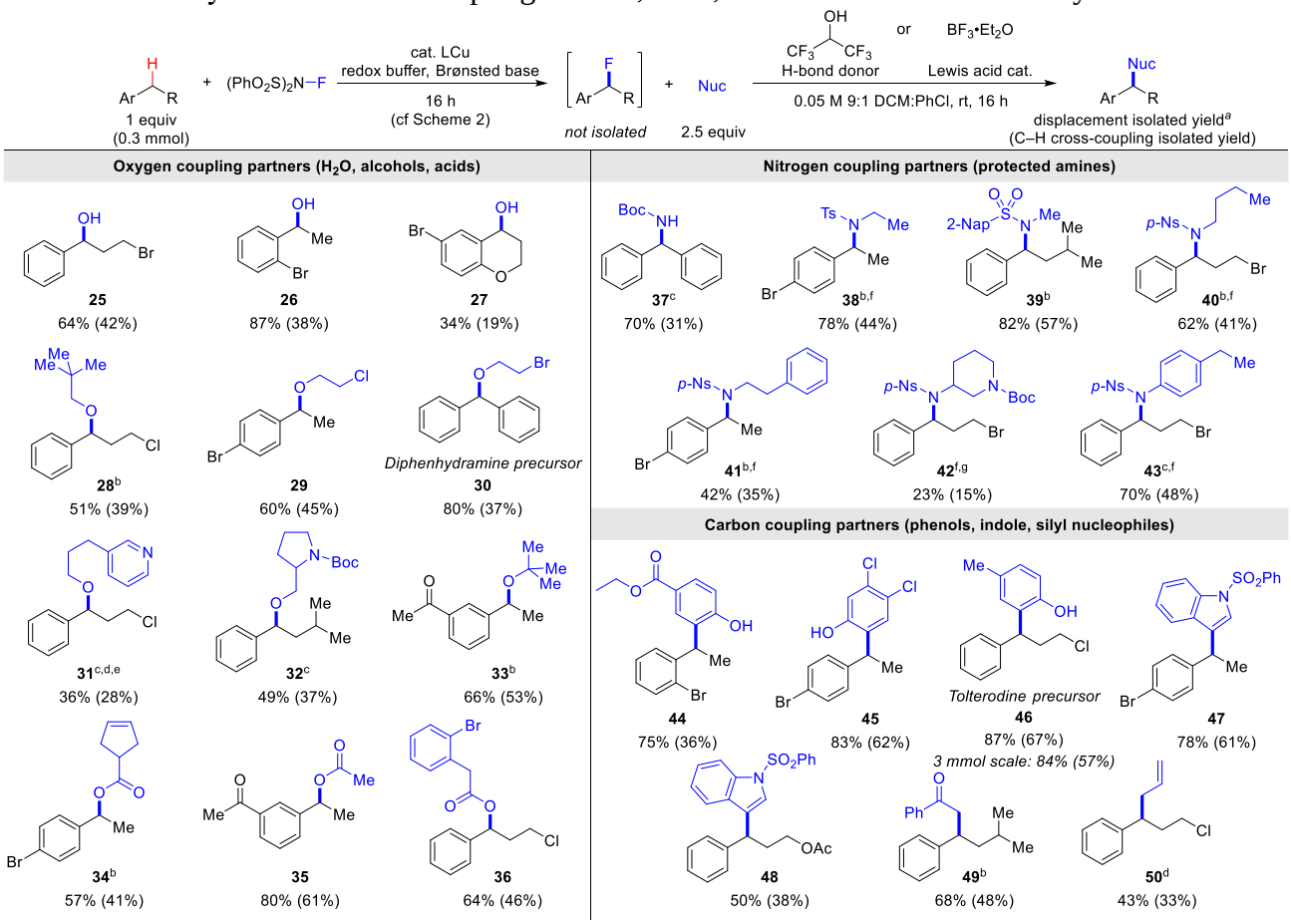

[a]Reaction uses 10 equiv HFIP as a H-bond donor. Isolated yields calculated with respect to the ^{1}H NMR yield of the benzyl fluoride (or the C–H substrate, in parentheses). [b]10 mol% BF_3•Et_2O used instead of HFIP. [c]50 mol% BF_3•Et_2O used instead of HFIP [d]Both HFIP and BF_3•Et_2O used. [e]2.5 equiv MsOH added to the nucleophile. [f]Used dichloromethane as the fluorination reaction solvent. [g]1.5 equiv BF_3•Et_2O used instead of HFIP. Isolated as the amine.

4.4. Conclusion

In summary, the results described above introduce a new strategy to achieve selective benzylic C–H cross-coupling with diverse reaction partners. The use of Cu/NFSI conditions that may be tuned to accommodate different substrate electronic properties allowed formation of benzyl fluorides that may be used without isolation as coupling partners to access products with new C(sp^3)–O, –N, and –C bonds. This method joins a number of emerging strategies for C(sp^3)–H

cross-coupling that involve formation of strategic intermediates, such as xanthate esters, isocyanates, lactones, alkylboronates,[17] that allow rapid access to diversified products.

4.5. Acknowledgements

This work was supported by the NIH (R01 GM126832, R35 GM134929), including a Ruth L. Kirschstein NRSA fellowship (F32 GM129909, to JAB). Spectroscopic instrumentation was partially supported by the NIH (1S10 OD020022-1) and the NSF (CHE-1048642).

4.6. Author Contributions

Vasilopoulos, A: reaction ideation, leading experimental work, and manuscript preparation

Golden, D. L: experimental work and manuscript preparation

Buss, J. A: preliminary results

4.7. References

1. Brown, D.G.; Boström, J. Analysis of Past and Present Synthetic Methodologies on Medicinal Chemistry: Where Have All the New Reactions Gone? *J. Med. Chem.* **2016**, *59*, 4443-4458.
2. (a) Cernak, T.; Dykstra, K. D.; Tyagarajan, S.; Vachal, P.; Krska, S. W. The Medicinal Chemist's Toolbox for Late Stage Functionalization of Drug-Like Molecules. *Chem. Soc. Rev.* **2016**, *45*, 546-576. (b) Blakemore, D. C.; Castro, L.; Churcher, I.; Rees, D. C.; Thomas, A. W.; Wilson, D. M.; Wood, A. Organic Synthesis Provides Opportunities to Transform Drug Discovery. *Nat. Chem.* **2018**, *10*, 383-394.

3. (a) Hu, H.; Chen, S.-J.; Mandal, M.; Pratik, S. M.; Buss, J. A.; Krska, S. W.; Cramer, C. J.; Stahl, S. S. Copper-Catalyzed Benzylic C–H Coupling with Alcohols via Radical Relay Enabled by Redox Buffering. *Nat. Catal.* **2020**, *3*, 358-367. (b) Lee, B. J.; DeGlopper, K. S.; Yoon, T. P. Site-Selective Alkoxylation of Benzylic C–H Bonds by Photoredox Catalysis. *Angew. Chem. Int. Ed.* **2020**, *59*, 197-202.

4. (a) Zhang, Y.; Dong, J.; Liu, L.; Liu, L.; Zhou, Y.; Yin, S.-F. Manganese(III) Acetate Catalyzed Oxidative Amination of Benzylic C(sp^3)–H Bonds with Nitriles. *Org. Biomol. Chem.* **2017**, *15*, 2897-2901. (b) Wang, A.; DeOliveira, C. C.; Emmert, M. Non-Directed, Copper Catalyzed Benzylic C–H Amination Avoiding Substrate Excess. *ChemRxiv* **2019**, https://doi.org/10.26434/chemrxiv.8792243.

5. (a) Zhang, W.; Chen, P.; Liu, G. Copper-Catalyzed Arylation of Benzylic C–H Bonds with Alkylarenes as the Limiting Reagents. *J. Am. Chem. Soc.* **2017**, *139*, 7709-7712. (b) Yazaki, R.; Ohshima, T. Recent Strategic Advances for the Activation of Benzylic C–H Bonds for the Formation of C–C Bonds. *Tet. Lett.* **2019**, *60*, 151225.

6. (a) Ni, Z.; Zhang, Q.; Xiong, T.; Zheng, Y.; Li, Y.; Zhang, H.; Zhang, J.; Liu, Q. Highly Regioselective Copper-Catalyzed Benzylic C–H Amination by *N*-Fluorobenzenesulfonimide. *Angew. Chem. Int. Ed.* **2012**, *51*, 1244-1247. (b) Zhang, W.; Wang, F.; McCann, S. D.; Wang, D.; Chen, P.; Stahl, S. S.; Liu, G. Enantioselective Cyanation of Benzylic C–H Bonds via Copper-Catalyzed Radical Relay. *Science* **2016**, *353*, 1014-1018. (c) Xiao, H.; Liu, Z.; Shen, H.; Zhang, B.; Zhu, L.; Li, C. Copper-Catalyzed Late-Stage Benzylic C(sp^3)–H Trifluoromethylation. *Chem* **2019**, *5*, 940-949. (d) Suh, S.-E. Chen, S.-J. Mandal, M.; Guzei, I. A.; Cramer, C. J.; Stahl, S. S. Site-Selective Copper-Catalyzed Azidation of Benzylic C–H Bonds. *J. Am. Chem. Soc.* **2020**, *142*, 11388-11393.

7. Buss, J. A.; Vasilopoulos, A.; Golden, D. L.; Stahl, S. S. Copper-Catalyzed Functionalization of Benzylic C–H Bonds with *N*-Fluorobenzenesulfonimide: Switch from C–N to C–F Bond Formation Promoted by a Redox Buffer and Brønsted Base. *Org. Lett.* **2020**, *22*, 5749-5752.

8. (a) Amii, H.; Uneyama, K. C–F Bond Activation in Organic Synthesis. *Chem. Rev.* **2009**, *109*, 2119-2183. (b) Hamel, J.-D.; Paquin, J.-F. Activation of C–F Bonds α to C–C Multiple Bonds. *Chem. Commun.* **2018**, *54*, 10224-10239.

9. For leading primary references, see: (a) Bernstein, J.; Roth, J. S.; Miller Jr., W. T. The Preparation and Properties of Some Substituted Benzyl Fluorides. *J. Am. Chem. Soc.* **1948**, *70*, 2310-2314. (b) Swain, C. G.; Spalding, R. E. T. III. Mechanism of Acid Catalysis of the Hydrolysis of Benzyl Fluoride. *J. Am. Chem. Soc.* **1960**, *82*, 6104-6107. (c) Toteva, M. M.; Richard, J. P. Hydrogen Bonding and Catalysis of Solvolysis of 4-Methoxybenzyl Fluoride. *J. Am. Chem. Soc.* **2002**, *124*, 9798-9805. (d) Blessley, G.; Holden, P.; Walker, M.; Brown, J. M.; Gouverneur, V. Palladium-Catalyzed Substitution and Cross-Coupling of Benzylic Fluorides. *Org. Lett.* **2012**, *14*, 2754-2757. (e) Champagne, P. A.; Pomarole, J.; Thérien, M.-E.; Benhassine, Y.; Beaulieu, S.; Legault, C. Y.; Paquin, J.-F. Enabling Nucleophilic Substitution Reactions of Activated Alkyl Fluorides Through Hydrogen Bonding. *Org. Lett.* **2013**, *15*, 2210-2213. (f) Champagne, P. A.; Benhassine, Y.; Desroches, J.; Paquin, J.-F. Friedel-Crafts Reaction of Benzyl Fluorides: Selective Activation of C–F Bonds as Enabled by Hydrogen Bonding. *Angew. Chem. Int. Ed.* **2014**, *53*, 13835-13839. (g) Pryyma, A.; Bu, Y. J.; Wai, Y.; Patrick, B. O.; Perrin, D. M. Synthesis and Activation of Bench-Stable 3a-Fluoropyrroloindolines as Latent Electrophiles for the Synthesis of C-2-Thiol-Substituted Tryptophans and C-3a-Substituted Pyrroloindolines. *Org. Lett.* **2019**, *21*, 8234-8238. (h) Zhu, J.; Pérez, M.; Stephan, D. W. C–C Coupling of Benzyl Fluorides Catalyzed by an

Electrophilic Phosphonium Cation. *Angew. Chem. Int. Ed.* **2016**, *55*, 8448-8451. (i) Zhou, X.; Ding, H.; Chen, P.; Liu, L.; Sun, Q.; Wang, X.; Wang, P.; Lv, Z.; Li, M. Radical Dehydroxymethylative Fluorination of Carbohydrates and Divergent Transformations of the Resulting Reverse Glycosyl Fluorides. *Angew. Chem. Int. Ed.* **2020**, *59*, 4138-4144.

10. Szpera, R.; Moseley, D. F. J.; Smith, L. B.; Sterling, A. J.; Gouverneur, V. The Fluorination of C–H Bonds: Developments and Perspectives. *Angew. Chem. Int. Ed.* **2019**, *58*, 14824-14848.
11. For selected primary references directed toward benzylic fluorination, see: (a) Xia, J.-B.; Zhu, C.; Chen, C. Visible Light-Promoted Metal-Free C–H Activation: Diarylketone-Catalyzed Selective Benzylic Mono- and Difluorination. *J. Am. Chem. Soc.* **2013**, *135*, 17494-17500. (b) Bloom, S.; Pitts, C. R.; Woltornist, R.; Griswold, A.; Holl, M. G.; Lectka, T. Iron(II)-Catalyzed Benzylic Fluorination. *Org. Lett.* **2013**, *15*, 1722-1724. (c) Nodwell, M. B.; Bagai, A.; Halperin, S. D.; Martin, R. E.; Knust, H.; Britton, R. Direct Photocatalytic Fluorination of Benzylic C–H Bonds with *N*-Fluorobenzenesulfonimide. *Chem. Commun.* **2015**, *51*, 11783-11786. (d) Meanwell, M.; Nodwell, M. B.; Martin, R. E.; Britton, R. A Convenient Late-Stage Fluorination of Pyridylic C–H Bonds with *N*-Fluorobenzenesulfonimide. *Angew. Chem. Int. Ed.* **2016**, *55*, 13244-13248.
12. For previous studies of benzylic fluorination, see refs. 7, 10, 11 and references cited therein.
13. For important alternative strategies to convert 2° C–H bonds to alcohols, see: (a) Li, G.-X.; Morales-Rivera, C. A.; Gao, F.; Wang, Y.; He, G.; Liu, P.; Chen, G. A Unified Photoredox-Catalysis Strategy for C(sp^3)–H Hydroxylation and Amidation using Hypervalent Iodine. *Chem. Sci.* **2017**, *8*, 7180-7185. (b) Dantignana, V.; Milan, M.; Cussó, O.; Company, A.; Bietti, M.; Costas, M. Chemoselective Aliphatic C–H Bond Oxidation Enabled by Polarity

Reversal. *ACS Cent. Sci.* **2017**, *3*, 1350-1358. (c) Tanwar, L.; Börgel, J.; Ritter, T. Synthesis of Benzylic Alcohols by C–H Oxidation. *J. Am. Chem. Soc.* **2019**, *141*, 17983-17988.

14. (a) Clark, J. R.; Feng, K.; Sookezian, A.; White, M. C. Manganese-Catalysed Benzylic C(sp^3)–H Amination for Late-Stage Functionalization. *Nat. Chem.* **2018**, *10*, 583-591. (b) Chiappini, N. D.; Mack, J. B. C.; Du Bois, J. Intermolecular C(sp^3)–H Amination of Complex Molecules. *Angew. Chem. Int. Ed.* **2018**, *57*, 4956-4959. (c) Nasrallah, A.; Boquet, V.; Hecker, A.; Retailleau, P.; Darses, B.; Dauban, P. Catalytic Enantioselective Intermolecular Benzylic C(sp^3)–H Amination. *Angew. Chem. Int. Ed.* **2019**, *58*, 8192-8196. (d) Bakhoda, A.; Jian, Q.; Badiei, Y. M.; Bertke, J. A.; Cundari, T. R.; Warren, T. H. Copper Catalyzed sp^3 C–H Amidation: Sterically Driven Primary and Secondary C–H Site-Selectivity. *Angew. Chem. Int. Ed.* **2019**, *58*, 3421-3425.
15. Each of the following has an example of a secondary (sulfon)amide as a coupling partner: (a) Pelletier, G.; Powell, D. A. Copper-Catalyzed Amidation of Allylic and Benzylic C−H Bonds. *Org. Lett.* **2006**, *8*, 6031-6034. (b) Ye, Y.-H.; Zhang, J.; Wang, G.; Chen, S.-Y.; Yu, X.-Q. Cobalt-Catalyzed Benzylic C–H Amination via Dehydrogenative-Coupling Reaction. *Tetrahedron* **2011**, *67*, 4649-4654. (c) Bosnidou, A. E.; Muñiz, K. Intermolecular Radical C(sp^3)–H Amination under Iodine Catalysis. *Angew. Chem. Int. Ed.* **2019**, *58*, 7485-7489.
16. (a) Jing, L.; Yu, X.; Guan, M.; Wu, X.; Wang, Q.; Wu, X. An Efficient Method for Sulfonylation of Amines, Alcohols, and Phenols with *N*-Fluorobenzenesulfonimide Under Mild Conditions. *Chem. Res. Chin. Univ.* **2018**, *34*, 191-196. (b) Rozatian, N.; Ashworth, I. W.; Sandford, G.; Hodgson, D. R. W. A Quantitative Reactivity Scale for Electrophilic Fluorinating Reagents. *Chem. Sci.* **2018**, *9*, 8692-8702.

17. For examples of C(sp^3)–H functionalization sequences, see: (a) Czaplyski, W. L.; Na, C. G.; Alexanian, E. J. C–H Xanthylation: A Synthetic Platform for Alkane Functionalization. *J. Am. Chem. Soc.* **2016**, *138*, 13854-13857. (b) Huang, X.; Zhuang, T.; Kates, P. A.; Gao, H.; Chen, X.; Groves, J. T. Alkyl Isocyanates via Manganese-Catalyzed C–H Activation for the Preparation of Substituted Ureas. *J. Am. Chem. Soc.* **2017**, *139*¸15407-15413. (c) Zhuang, Z.; Yu, J.-Q. Lactonization as a General Route to β-C(sp^3)–H Functionalization. *Nature* **2020**, *577*, 656-659. (d) Oeschger, R.; Su, B.; Yu, I.; Ehinger, C.; Romero, E.; He, S.; Hartwig, J. Diverse Functionalization of Strong Alkyl C–H Bonds by Undirected Borylation. *Science* **2020**, *368*, 736-741.

Chapter 5.

C(sp^3)–H Methylation Enabled by Peroxide Photosensitization and Ni-Mediated Radical Coupling

Reproduced with permission from: **Aristidis Vasilopoulos**, Shane W. Krska, Shannon S. Stahl. C(sp^3)–H Methylation Enabled by Peroxide Photosensitization and Ni-Mediated Radical Coupling. *Manuscript in preparation*.

5.1. Abstract

The "magic methyl" effect describes the profound influence of a single methyl group on the potency, selectivity, and/or metabolic stability of a drug candidate. This phenomenon motivates the development of synthetic methods capable of adding methyl groups to molecules, preferably at a late stage in the synthetic route. Here, we exploit triplet-energy transfer to promote oxygen-oxygen bond homolysis of di-*tert*-butyl or dicumyl peroxide under mild conditions. The resulting alkoxyl radicals undergo divergent reactivity: hydrogen-atom transfer from a substrate C–H bond or methyl radical generation via *beta*-scission, with relative rates that can be tuned by varying the reaction conditions or the peroxide identity. Nickel-catalyzed coupling of the substrate and methyl radicals affords the methylated product.

5.2. Introduction

Molecular derivatization enables structural modifications to bioactive compounds that improve the overall physicochemical and drug-like properties while preserving and enhancing the key pharmacological interactions.[1,2] Converting an H atom to a methyl group is a structural change to drug candidates that has been shown in cases to result in a more than 400-fold improvement in drug potency. This dramatic effect has been coined as the “magic methyl” effect.[3] Improvements in potency are attributed to changes in molecular conformation, lipophilicity, and 3-dimensional character.[4,5] It is ideal to test for “magic methyl” effects through direct methylation of drug candidates, yet limitations in methylation chemistry often require early-stage introduction of the group. In many cases, a methyl group is incorporated by purchasing the commercially available methylated building block and rebuilding the molecule *de novo*.[6,7] Methods capable of installing methyl groups at pre-functionalized sites are becoming more prevalent, but are not typically

utilized in synthesis.[8-11] A few reactions are able to achieve C(sp^3)–H methylation, however they either require a directing-group, use of excess C–H substrate, or use a methyl source with undesirable sensitivity to acidic or Lewis basic functional groups.[3,9-14] Identification of a versatile direct C(sp^3)–H methylation reaction would facilitate production of methylated drug analogs that otherwise might never be synthesized for biological testing, potentially leading to identification of new transformative "magic methyl" effects (Figure 5.1A). Here we report an oxidative Ni-catalyzed photochemical method for direct C(sp^3)–H methylation with limiting reagent that is enabled by photosensitization of alkyl peroxides (Figure 5.1B). We hypothesized that direct C(sp^3)–H methylation should be possible by generating a substrate radical from hydrogen atom transfer (HAT) in the presence of a metal methyl species that could capture the incipient radical and form a new C–C bond. Di-*tert*-butyl peroxide (DTBP) has the ability to act as both the HAT reagent and methyl source for this reaction: *tert*-butoxyl radicals generated from O–O homolysis readily participate in HAT with C–H bonds to form substrate alkyl radicals or undergo β-scission to form a methyl radical and acetone (Figure 5.1C).[15] If β-scission of the oxyl radical and HAT with the C–H substrate occur concurrently, transient methyl radical and substrate radical species will form that might coupled together. Coupling two transient radical species is challenging, however one could envision employment of a Ni catalyst to enhance the persistence of the partners to allow C–C coupling for net C(sp^3)–H methylation.[16]

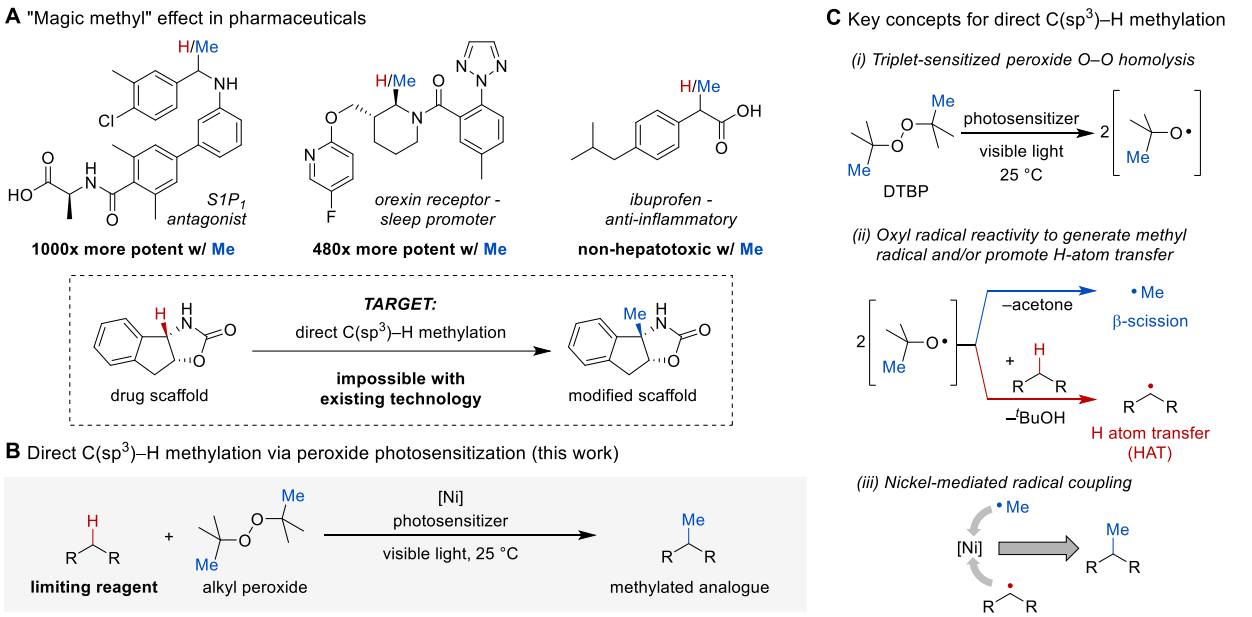

Figure 5.1. Direct C(sp^3)–H methylation via photochemical activation of peroxides. (A) Benefits of single methyl groups on drug properties motivate the development of a synthetic method for direct C(sp3)–H methylation. (B) General reaction equation for the methods described in this report. (C) Concepts that underlie Ni-catalyzed C(sp3)–H methylation via photosensitization of di-tert-butyl peroxide.

5.3. Results and Discussion

In order to realize this transformation using the C–H substrate as limiting reagent, inefficient HAT from the *tert*-butoxyl radical would need to be addressed, as existing peroxide-based C–H coupling reactions typically use 10 or more equivalents of C–H substrate to overcome deficiencies in first-order HAT reactivity compared to the zero-order β-scission process.[17-21] We hypothesized that it would be possible to change the relative rates of these processes by modifying the temperature that the oxyl radical is formed. According to a study by Walling, HAT with an oxyl radical becomes increasingly favored over β-scission at reduced temperatures, with a 14-fold improvement in HAT at 25 °C compared to 100 °C.[22] This relative rate enhancement at reduced temperatures could allow for use of limiting C–H substrate in peroxide-based C–H functionalization reactions. However, the vast majority of C(sp^3)–H functionalization reactions

using DTBP as oxidant employ thermal activation of the peroxide and thus are conducted at temperatures in excess of 90 °C. To generate *tert*-butoxyl radicals at room temperature, we decided to evaluate O–O bond cleavage using triplet energy transfer from an excited photosensitizer. Excited photosensitizers with sufficient triplet energy levels are rapidly quenched by DTBP, resulting in relaxation of the photosensitizer and cleavage of the peroxide O–O bond to form *tert*-butoxyl radicals.[23-25] This activation approach has yet to be applied to C–H functionalization using limiting C–H substrate but is expected to be an effective strategy based on the relative rate enhancement of HAT at room temperature.

We sought to determine whether room temperature photochemical oxyl radical formation will allow efficient HAT with limiting C–H substrate. Photochemical peroxide activation and HAT studies were initiated by irradiating vials containing DTBP, limiting alkylarene substrate, and 1 to 10 mol% of photosensitizer at room temperature with a "Tuna blue" 400-470 nm LED lamp (Figure 5.2A). Reaction performance was evaluated based on conversion of the benzylic C–H substrate by monitoring disappearance of the benzylic C–H signal using ^{1}H NMR, which indicates successful peroxide activation and competent HAT reactivity. These experiments revealed that peroxide photosensitization at room temperature could lead to >70% conversion of the limiting alkylarene using photosensitizers with excited state triplet energy levels over 55 kcal/mol. The reaction dependence on high triplet energy level of the photosensitizer and the observation of 12% conversion of alkylarene from direct photolysis of the peroxide in the absence of a photosensitizer are suggestive of a triplet energy transfer activation pathway as opposed to a photoredox pathway.[23] Based on these experiments Ir[dF(CF_3)ppy]$_2$($^{t\text{Bu}}$bpy)PF_6 (Ir–F) was chosen as photosensitizer for development of the photochemical C(sp^3)–H methylation reaction. Ir–F is a practical choice because it readily absorbs blue and violet light, has demonstrated robustness in

other photocatalytic synthetic methods, and efficiently catalyzed peroxide activation and HAT. With an effective means for oxyl radical formation at room temperature, we began studying tunability of HAT vs β-scission.

In a systematic study of reaction parameter effects on HAT vs β-scission with 1 equiv DTBP, photoactivation at mild temperatures was confirmed to be crucial: C–H substrate conversion more than doubled at room temperature as compared to reactions run at 100 °C (Figure 5.2B).[26] Further increases in HAT efficiency were achieved by increasing the reaction concentration to 0.6 M, resulting in 74% conversion of alkylarene using only 1 equiv of oxidant. However, an effective C–H methylation reaction would require that both HAT and β-scission processes are operating simultaneously with high efficiency. Literature reports focused on modifying β-scission from oxyl radicals suggested that use of a polar protic reaction solvent like 2,2,2-trifluoroethanol (TFE) and/or use of dicumyl peroxide (DCP) as the methyl radical source should improve β-scission reactivity.[15,27] Indeed, both of these approaches dramatically increased the efficiency of β-scission and allowed high rates of both HAT and β-scission to be achieved under the same reaction conditions, critical to the success of the desired C(sp^3)–H methylation reaction. With these conditions, we pursued development of the target C(sp^3)–H methylation reaction.

In the absence of a metal catalyst, only trace C–H methylation product could be detected under DTBP/TFE conditions with 2 equivalents of DTBP. By adding catalytic $NiCl_2$•dimethoxyethane and *tert*-butyl terpyridine ($^{t\text{Bu}}$tpy) to the reaction, a 5% yield of the C–H methylation product could be formed. Empirical additive screening led to the discovery that addition of an acid to the reaction enabled a 36% yield of C–H methylation under these conditions, which was further increased to 60% yield by using 6 equiv of DTBP (Figure 5.2C, see Appendix D for other screening data). The low cost of DTBP and ease of removal of associated by-products (acetone and gas), made the use

of excess peroxide a reasonable approach for optimization of the reaction. We sought to further understand the role of the Ni catalyst by evaluating the gasses that formed during the reaction.

Headspace analysis experiments were conducted using a sealed system with a pressure transducer to quantify the amount of gas formed in the reaction, and the gas composition was evaluated using gas chromatography (Figure 5.2D). Conducting the peroxide activation reaction in the absence of Ni using 0.6 mmol of DTBP resulted in formation of 0.36 mmol of gas that was 97% methane, suggesting efficient generation of Me radicals via β-scission (Figure 5.2D, pathway A). Addition of the Ni catalyst caused ethane formation to be favored 10.5:1 over the formation of methane gas, indicative of Ni-catalyzed homocoupling of Me radicals (Figure 5.2D, pathway B).[28] Finally, addition of 0.3 mmol C–H substrate to the reaction with Ni caused ethane formation to be reduced by 0.11 mmol, while 0.11 mmol of methylation product was formed (Figure 5.2D, pathways B and C). These experiments showed that methyl radicals from β-scission only efficiently coupled to ethane in the presence of the Ni catalyst and otherwise favored pathways leading to methane formation. The reduction in ethane formation with added C–H substrate implied that the same Me radicals that lead to gas formation could instead be incorporated at the C–H site of the substrate. Taken together, these data suggested that Ni was serving as an agnostic alkyl radical coupling catalyst wherein methyl radicals from β-scission could be captured to methylate incoming alkyl radicals to form either ethane or desired product (Figure 5.2D).

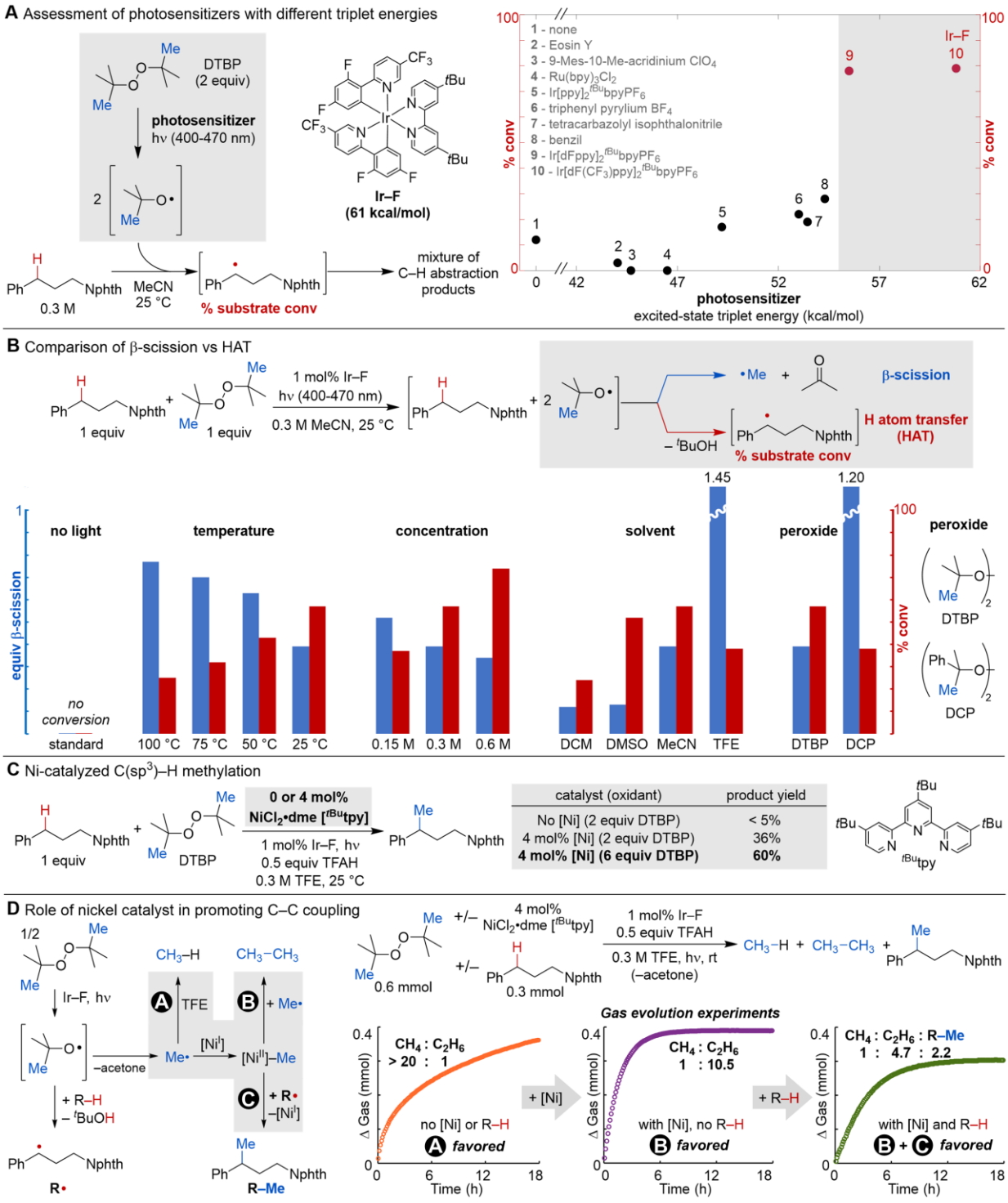

Figure 5.2. Mechanistic insights and reaction guide for Ni-catalyzed C–H methylation. (A) Assessment of photosensitizers. (B) Survey of different reaction parameters, showing their influence on the relative rates of β-methyl scission (blue) and HAT from the substrate C–H bond (red). (C) Demonstration that a Ni catalyst is required to promote substrate/methyl radical coupling. (D) Mechanistic insights into the fate of the methyl radical in the absence and presence of the Ni catalyst and the substrate. Reactions in panels A-C were conducted on 0.1 mmol scale and yields were determined by ^{1}H NMR (mesitylene standard).

Developing these initial observations into a general C–H methylation protocol would require the identification of complementary sets of reaction conditions that could be tuned to account for changes in intrinsic HAT rates across new substrates, maintaining the correct balance of HAT vs β-scission rates needed for good reactivity. Extensive exploration of various ligands, acids, solvents, and concentrations using high-throughput experimentation on different C–H substrates led to a starting point for optimization studies that allowed four sets of conditions to be identified for application in the methylation scope (see Appendix D for select screening tables). For benzylic and α-amido substrates, $^{t\text{Bu}}$tpy was the optimal ligand, paired with either DTBP/TFE or DCP/MeCN as oxidant and reaction solvent. For more electron-rich C–H substrates, like carbamates and ethers, trispicolyl amine (TPA) was the optimal ligand, also using either DTBP/TFE or DCP/MeCN. Reaction concentration was a key variable that could be tuned to optimize reaction performance: higher concentration was used for substrates demonstrating recalcitrance to methylation while lower concentration was used for substrates that were prone to overoxidation (Table 5.1A). These four sets of reaction conditions and ensuing concentration modifications were used to develop the methylation reaction substrate scope.

A wide range of C–H substrates were methylated at benzylic and α-heteroatomic C–H sites (Table 5.1B). Simple alkylarene substrates **1** and **2** with protected functional groups gave good (59%) isolated yields of the desired mono-methylated products. In these reactions and others, the remaining mass balance was primarily remaining starting material and multi-methylation products (UPLC-MS traces are available in Appendix D). Substrates **3** and **4** showed that the reaction tolerates both aryl and alkyl chlorides. Substrate **5** could only be methylated in low yields using DTBP with TFE, likely due to interference by the primary amide, but switching to DCP with MeCN enabled a 38% yield of the desired product.[29] Benzylic C–H sites in **7** and **12** were

preferentially methylated over acidic and chelating heteroatoms despite precedents for methylation of such groups in other metal-catalyzed methylation reactions.[9] Popular cross-coupling partners like aryl boronates and aryl bromides were preserved under the reaction conditions (**8**, **9**, **10**, **11**). The silyl protected alcohol in substrate **9** was unaffected by the methylation reaction. Surprisingly no Minisci addition products are observed in either pyridine-containing substrate (**6** and **9**), despite the mildly acidic conditions and generation of methyl radicals from β-scission.[30] The method was also competent for formation of quaternary centers (**8**, **13**, **15**). In addition to benzylic and α-amino sites, an α-oxy and tertiary C–H site were methylated under optimized reaction conditions using TPA as the ligand (**14**, **15**). For commentary on ineffective substrates, see Table 5D.14 of Appendix D.

α-Amino C–H sites of Boc-protected amines were highly reactive towards the C–H methylation reaction conditions. For these substrates, TFE with DTBP was typically found to be most effective, possibly due to a relevant hydrogen-bonding interaction with the carbamate protecting group that contributed to partial deactivation of the highly reactive C–H sites.[29] Use of TPA as a ligand in these reactions minimized deleterious side product formation (dehydrogenation and other decomposition products). Substrates **16** and **17** showed installation of tertiary and quaternary methyl groups α to protected primary amines. Methylation of C–H sites in protected 4-, 5-, and 6- membered rings was also demonstrated (**18**, **19**, **20**, **21**). In all cases, the mass balance was comprised of starting material, monomethylated isomers, dimethylated isomers, and in some cases multi-methylation isomers or dehydrogenation products. Several different functional groups were tolerated in the methylation of protected piperidine rings, including a quaternary alcohol, ester, benzisoxazole, and lactam (**22**, **23**, **24**, **25**, respectively). In substrate **25**, dimethylation reactivity was favored. The robustness of the methylation reaction allowed for its application

to several late-stage drug molecules. In these examples, high densities of potentially reactive functional groups were tolerated, including a ketone, primary sulfonamide, trifluoroacetamide, and quaternary carboxylic acid, among previously mentioned functionalities (**26**-**30**). Methylation of the doubly activated C–H site in TFA-protected sitagliptin led to a 61% yield of product. Dimethyl sulfoxide could be used as co-solvent in some reactions to overcome substrate solubility issues. In the glyburide precursor (**27**), bezafibrate (**29**), and agomelatine (**30**), α-amino C–H sites were preferentially methylated over benzylic C–H sites. The observed chemoselectivity led us to question whether selectivity could be modified in the methylation reactions by changing the reaction medium.

Table 5.1. Methylation substrate scope.

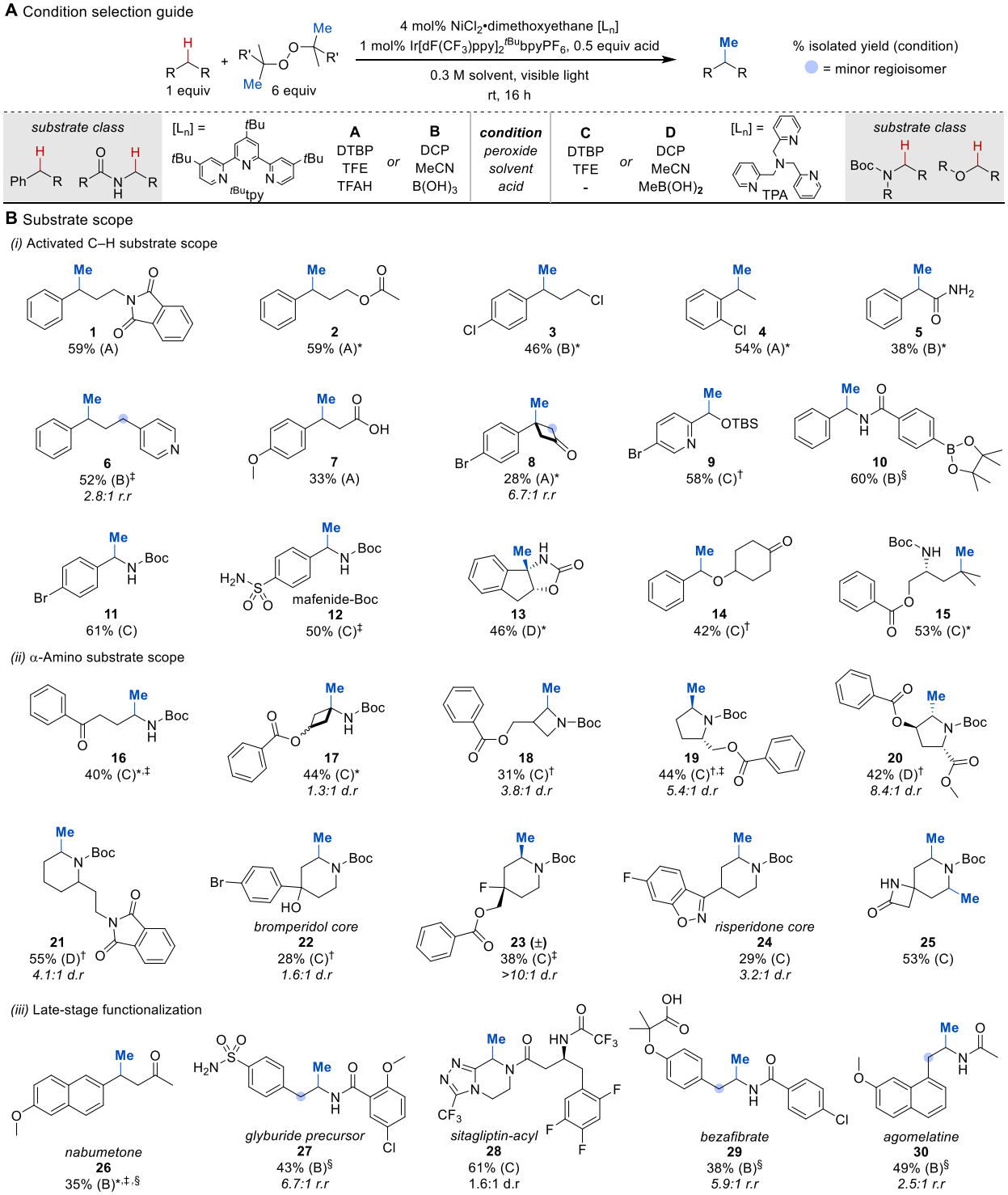

(A) Different substrate classes and their preferred reaction conditions. (B) Reaction outcome with various substrates. Reactions run on 0.3 mmol scale, isolated yields of combined regio- and stereoisomers are shown. Sites of secondary methylation are designated by blue circles. * 0.6 M concentration. † 0.15 M concentration. ‡ 0.5 equiv $MeB(OH)_2$ used as acid. § 1:1 MeCN:DMSO used as solvent.

Protonation of basic amines by Brønsted acids provides a means to deactivate adjacent C–H sites, resulting in reactivity to more remote C–H sites.[29,31,32] We decided to test this deactivation strategy by conducting a competition experiment between methylation of a Boc piperidine and an alkylarene. In a non-hydrogen-bonding solvent at low concentration, the Boc-piperidine was preferentially methylated over the benzylic C–H substrate. If the Boc group was removed *in situ* and the amine protonated, the reaction instead favored methylation of the benzylic C–H site (Table 5.2A). This selectivity switch could serve as the basis for enabling chemoselective methylation of complex substrates containing basic amines. We tested this hypothesis by methylating a variety of C–H substrates that possessed both a basic amine and distal benzylic C–H site in the presence of trifluoroacetic acid (Table 5.2B). Methylation of Boc amine **32** revealed selective methylation of the α-amino position, whereas deprotection and protonation of the amine led to regioselective methylation of the benzylic position (**31**). This reactivity was extended to the methylation of more complex amine salts including safinamide (**33**), trimethobenzamide (**34**), and cinacalcet (**35**). The unnatural amino acid homo-phenylalanine was also methylated in moderate yield (**36**). Pharmaceutical molecules often have basic sites, and this Brønsted acid deactivation approach should allow for widespread application of the methylation reaction to these compounds.

Table 5.2. Control over site-selectivity with a Brønsted acid.

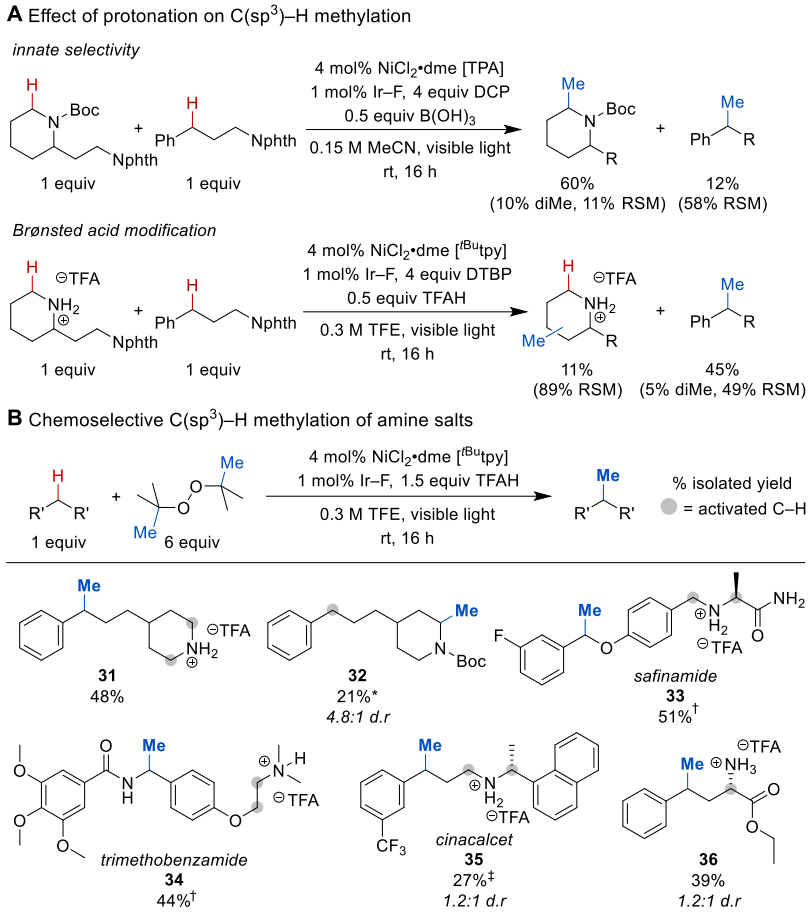

(A) α-Amino C–H sites are deactivated by protonation. (B) Chemoselective C–H methylation. Reactions run on 0.3 mmol scale, isolated yields are shown. * No acid added, used 3 equiv DCP, TPA as the ligand, and 0.15 M MeCN as the solvent. † 4 equiv of DCP and MeCN used in place of DTBP and TFE. ‡ 0.6 M concentration.

5.4. Conclusion

In summary, the first direct and general C(sp^3)–H methylation reaction has been identified by implementing triplet energy transfer activation of alkyl peroxides. Photosensitization allows the alkyl peroxide O–O bond to be homolyzed at room temperature to form oxyl radicals that exhibit good reactivity for HAT with limiting C–H substrate and use of TFE or DCP allows for sufficient β-scission to concurrently occur to form Me radical for use in methylation by the Ni catalyst. These results led to development of a mild and robust methylation reaction capable of methylating a wide

variety of substrates including drugs and drug substructures relevant to the pharmaceutical industry. Continued development of new C–H methylation methods will facilitate discoveries of transformative “magic methyl” effects in drug discovery programs.[33] Additionally, the peroxide photoactivation mechanism holds promise for use in future radical relay C–H functionalization reactions with limiting C–H substrate, and expanded studies in this area will contribute to the reputation of weak C–H bonds as reliable synthetic disconnections in synthesis and molecular derivatization.

5.5. Acknowledgements

The authors thank Bing Li, Kevin Dykstra, Mycah Uehling, Scott Borges, and Dani Schultz among other Merck colleagues for valuable discussions, feedback, and training pertaining to the implementation of experimentation techniques used for development of this chemistry. The authors also thank Chase Salazar and Will McDermott for assistance with gas evolution experiments. This work was supported by the NIH (R01 GM126832, R35 GM134929). Spectroscopic instrumentation was partially supported by the NIH (1S10 OD020022-1) and the NSF (CHE-1048642).

5.6. References

1. P. N. Mortenson, D. A. Erlanson, I. J. P. Esch, W. Jahnke, C. N. Johnson, Fragment-to-lead medicinal chemistry publications in 2017. *J. Med. Chem.* **2019**, *62*, 3857-3872.

2. T. Cernak, K. D. Dykstra, S. Tyagarajan, P. Vachal, S. W. Krska, The medicinal chemist's toolbox for late stage functionalization of drug-like molecules. *Chem. Soc. Rev.* **2016**, *45*, 546-576.

3. H. Schönherr, T. Cernak, Profound methyl effects in drug discovery and a call for new C–H methylation reactions. *Angew. Chem. Int. Ed.* **2013**, *52*, 12256-12267.

4. E. J. Barreiro, A. E. Kümmerle, C. A. M. Fraga, The methylation effect in medicinal chemistry. *Chem. Rev.* **2011**, *111*, 5215-5246.

5. S. Sun, J. Fu, Methyl-containing pharmaceuticals: methylation in drug design. *Bioorganic Med. Chem. Lett.* **2018**, *28*, 3283-3289.

6. J. Quancard, B. Bollbuck, P. Janser, D. Angst, F. Berst, P. Buehlmayer, M. Streiff, C. Beerli, V. Brinkmann, D. Guerini, P. A. Smith, T. J. Seabrook, M. Traebert, K. Seuwen, R. Hersperger, C. Bruns, F. Bassilana, M. Bigaud, A potent and selective $S1P_1$ antagonist with efficacy in experimental autoimmune encephalomyelitis. *Chem. Biol.* **2012**, *19*, 1142-1151.

7. P. J. Coleman, J. D. Schreier, C. D. Cox, M. J. Breslin, D. B. Whitman, M. J. Bogusky, G. B. McGaughey, R. A. Bednar, W. Lemaire, S. M. Doran, S. V. Fox, S. L. Garson, A. L. Gotter, C. M. Harrell, D. R. Reiss, T. D. Cabalu, D. Cui, T. Prueksaritanont, J. Stevens, P. L. Tannenbaum, R. G. Ball, J. Stellabott, S. D. Young, G. D. Hartman, C. J. Winrow, J. J. Renger, Discovery of [(2R,5R)-5-{[(5-fluoropyridin-2-yl)oxy]methyl}-2-methylpiperidin-1-yl][5-methyl-2-(pyrimidin-2-yl)phenyl]methanone (MK-6096): a dual orexin receptor antagonist with potent sleep-promoting properties. *ChemMedChem* **2012**, *7*, 415-424.

8. Z. Liang, W. Xue, K. Lin, H. Gong, Nickel-catalyzed reductive methylation of alkyl halides and acid chlorides with methyl p-tosylate. *Org. Lett.* **2014**, *16*, 5620-5623.

9. G. Yan, A. J. Borah, L. Wang, M. Yang, Recent advances in transition metal-catalyzed methylation reactions. *Adv. Synth. Catal.* **2015**, *357*, 1333-1350.

10. Y. Chen, Advances in the synthesis of methylated products through indirect approaches. *Adv. Synth. Catal.* **2020**, *362*, 998-1014.

11. R. W. Pipal, K. T. Stout, P. Z. Musacchio, S. Ren, T. J. A. Graham, S. Verhoog, L. Gantert, T. G. Lohith, A. Schmitz, H. S. Lee, D. Hesk, E. D. Hostetler, I. W. Davies, D. W. C. MacMillan, Metallaphotoredox aryl and alkyl radiomethylation for PET ligand discovery. *Nature* **2020,** https://doi.org/10.1038/s41586-020-3015-0.

12. C. Le, Y. Liang, R. W. Evans, X. Li, D. W. C. MacMillan, Selective sp^3 C–H alkylation via polarity-match-based cross-coupling. *Nature* **2017**, *547*, 79-83.

13. Y. Chen, Recent advances in methylation: a guide for selecting methylation reagents. *Chem. Eur. J.* **2019**, *25*, 3405-3439.

14. K. Feng, R. E. Quevedo, J. T. Kohrt, M. S. Oderinde, U. Reilly, M. C. White, Late-stage oxidative C(sp^3)–H methylation. *Nature* **2020**, *580*, 621-627.

15. C. Walling, P. J. Wagner, Positive halogen compounds. X. Solvent effects in the reactions of *t*-butoxy radicals[1]. *J. Am. Chem. Soc.* **1964**, *86*, 3368-3375.

16. S. Wang, S. Tang, A. Lei, Tuning radical reactivity for selective radical/radical cross-coupling. *Sci. Bull.* **2018**, *63*, 1006-1009.

17. M. S. Kharasch, G. Sosnovsky, The reactions of t-butyl perbenzoate and olefins–a stereospecific reaction. *J. Am. Chem. Soc.* **1958**, *80*, 756.

18. R. D. Small, J. C. Scaiano, Absolute rates of hydrogen abstraction by tert-butoxy radicals. *J. Am. Chem. Soc.* **1978**, *100*, 296-298.

19. B. L. Tran, B. Li, M. Driess, J. F. Hartwig, Copper-catalyzed intermolecular amidation and imidation of unactivated alkanes. *J. Am. Chem. Soc.* **2014**, *136*, 2555-2563.

20. A. Vasilopoulos, S. L. Zultanski, S. S. Stahl, Feedstocks to pharmacophores: Cu-catalyzed oxidative arylation of inexpensive alkylarenes enabling direct access to diarylalkanes. *J. Am. Chem. Soc.* **2017**, *139*, 7705-7708.

21. H. Yi, G. Zhang, H. Wang, Z. Huang, J. Wang, A. K. Singh, A. Lei, Recent advances in radical C−H activation/radical cross-coupling. *Chem. Rev.* **2017**, *117*, 9016-9085.

22. P. Wagner, C. Walling, Positive halogen compounds. XII.[1] Relative reactivities of hydrocarbons toward alkoxy radicals determined by direct and indirect methods[2]. *J. Am. Chem. Soc.* **1965**, *87*, 5179-5185.

23. J. C. Scaiano, G. G. Wubbels, Photosensitized dissociation of di-tert-butyl peroxide. Energy transfer to a repulsive excited state. *J. Am. Chem. Soc.* **1981**, *103*, 640-645.

24. M. V. Encinas, E. A. Lissi, Quenching of excited singlets by peroxides and hydroperoxides. *J. Photochem.* **1982**, *20*, 153-161.

25. P. S. Engel, T. L. Woods, M. A. Page, Quenching of excited triplet sensitizers by organic peroxides. *J. Phys. Chem.* **1983**, *87*, 10-13.

26. No conversion is observed in the absence of light.

27. D. V. Avila, C. E. Brown, K. U. Ingold, J. Lusztyk, Solvent effects on the competitive β-scission and hydrogen atom abstraction reactions of the cumyloxyl radical. Resolution of a long-standing problem. *J. Am. Chem. Soc.* **1993**, *115*, 466-470.

28. G. D. Jones, C. McFarland, T. J. Anderson, D. A. Vicic, Analysis of key steps in the catalytic cross-coupling of alkyl electrophiles under Negishi-like conditions. *Chem. Commun.* **2005**, *33*, 4211-4213.

29. M. Bietti, Activation and deactivation strategies promoted by medium effects for selective aliphatic C–H bond functionalization. *Angew. Chem. Int. Ed.* **2018**, *57*, 16618-16637.

30. D. A. DiRocco, K. Dykstra, S. Krska, P. Vachal, D. V. Conway, M. Tudge, Late-stage functionalization of biologically active heterocycles through photoredox catalysis. *Angew. Chem. Int. Ed.* **2014**, *53*, 4802-4806.

31. M. Lee, M. S. Sanford, Platinum-catalyzed, terminal-selective C(sp^3)–H oxidation of aliphatic amines. *J. Am. Chem. Soc.* **2015**, *137*, 12796-12799.

32. J. M. Howell, K. Feng, J. R. Clark, L. J. Trzepkowski, M. C. White, Remote oxidation of aliphatic C–H bonds in nitrogen-containing molecules. *J. Am. Chem. Soc.* **2015**, *137*, 14590-14593.

33. S. D. Friis, M. J. Johansson, L. Ackermann, Cobalt-catalysed C–H methylation for late-stage drug diversification. *Nat. Chem.* **2020**, *12*, 511-519.

Chapter 6.

Oxidative Amide Coupling from Functionally Diverse Alcohols and Amines using Aerobic Copper/Nitroxyl Catalysis

6.1. Abstract

The aerobic Cu/ABNO catalyzed oxidative coupling of alcohols and amines is highlighted here in the synthesis of amide bonds in diverse drug-like molecules (ABNO = 9-azabicyclo[3.3.1]nonane *N*-oxyl). The robust method leverages the privileged reactivity of alcohols bearing electronegative heteroatoms (O, F, N, Cl) in the β-position. The reaction tolerates over 20 unique functional groups and is demonstrated on a 15 mmol scale under air (Figure 6.1). Steric constraints of the catalyst allow for chemoselective amidation of primary amines in the presence of secondary amines. All catalyst components are commercially available, and the reaction proceeds under mild conditions with retention of stereocenters in both reaction partners, while producing only water as a by-product.

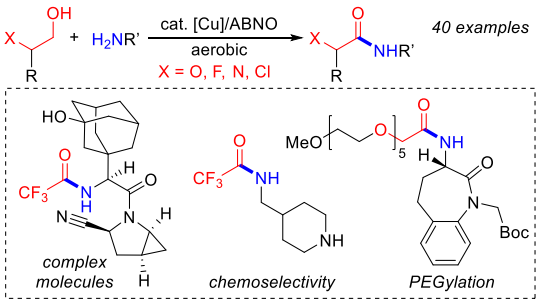

Figure 6.1. Cu/ABNO-catalyzed oxidative amidation summarization of reactivity

6.2. Introduction

Amide coupling reactions account for 16% of all reactions performed in pharmaceutical syntheses.[1] Typical methods use stoichiometric coupling reagents to activate a carboxylic acid for nucleophilic attack by the amine coupling partner.[2] Several catalytic methods for amide coupling have been reported, but none yet exhibit the synthetic utility of methods that use stoichiometric coupling reagents. Recent efforts have explored catalytic methods for amide bond formation with reaction partners other than carboxylic acids.[3] Prominent examples include oxidative or dehydrogenative coupling of amines with primary alcohols, which often produce only water or H_2

as a by-product. In spite of the potential appeal of these reactions,[4] the precedents lack the functional-group compatibility, efficiency, or synthetic reliability needed to compete with traditional amide coupling methods. Herein, we demonstrate highly practical applications of Cu/ABNO-catalyzed aerobic oxidative coupling of primary alcohols and amines for the synthesis of diverse α-heteroatom-substituted amides (ABNO = 9-azabicyclo[3.3.1] nonane *N*-oxyl).

Heteroatom-substituted amides and α-substituted derivatives, in particular (Figure 6.2), are an important class of molecules due to their prevalence in pharmaceuticals and related bioactive compounds.[5] For example, a recent survey of over 3500 pharmaceuticals revealed that the majority of alkyl amides feature an oxygen or nitrogen atom α, β, or γ to the carbonyl.[1b] The heteroatom linkage at these positions has a beneficial effect on bioactivity and/or pharmacological properties of the molecule due to changes in enzyme binding and solubility. In light of these considerations, new strategies to access such structures could have broad impact.

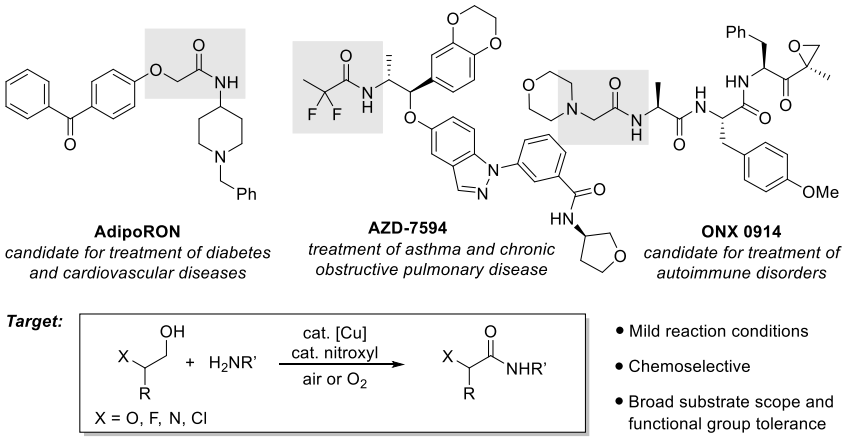

Figure 6.2. α-Heteroatom-substituted amides in pharmaceuticals and targeted strategy for their preparation.

6.3. Results and Discussion

Cu/nitroxyl catalyst systems have been identified as highly effective catalyst systems for aerobic alcohol oxidation,[6,7] and we recently demonstrated that analogous catalyst systems could

support aerobic oxidative coupling of alcohols and amines.[4o] The latter reactions, however, were subject to many of the synthetic limitations noted above. The oxidative amidation begins with alcohol oxidation to the aldehyde, followed by trapping by an amine to form a hemiaminal, which is then oxidized further to the corresponding amide (Figure 6.3A). Insights from mechanistic studies of Cu/nitroxyl-catalyzed alcohol oxidation[8] suggested that β-heteroatom-substituted primary alcohols could be a privileged substrate class for oxidative coupling due to their enhanced acidity (e.g., the aqueous pK_a values for EtOH, ethylene glycol, and trifluoroethanol are 15.9,[9] 15.1,[10] and 12.4,[11] respectively). The previous studies showed that more acidic alcohols undergo more rapid oxidation, an effect attributed to their more favorable reaction with the Cu^{II}–hydroxide intermediate.[8b] For example, competition studies showed that electron-deficient benzyl alcohol derivatives react more rapidly than electron-rich analogs. In addition, the aldehyde intermediate with an α-heteroatom substituent will have enhanced electrophilicity that will promote formation of a hemiaminal and disfavor formation of an imine,[12] which is not a productive intermediate to the amide (Figure 6.3B). Improved reactivity in these fundamental steps should allow these methods to be particularly effective for the preparation of pharmaceutically relevant α-heteroatom-substituted amides.

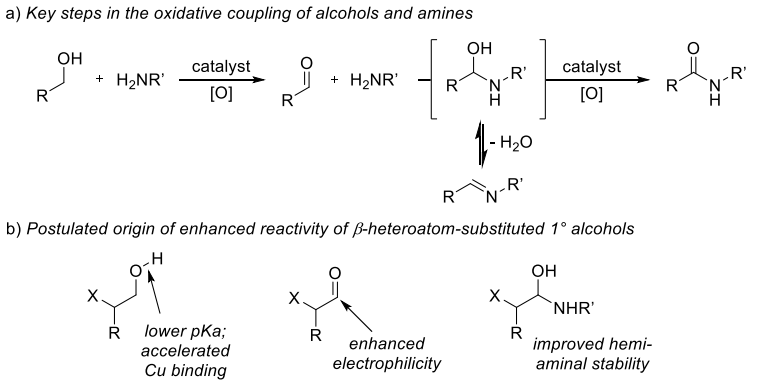

Figure 6.3. (A) General mechanism for the oxidative coupling of alcohols and amines to prepare amides. (B) Basis for enhanced reactivity of α-heteroatom-substituted alcohols in catalytic Cu/nitroxyl-catalyzed oxidative amidation.

The present study was initiated by testing the oxidative amidation of tetrahydropyran-2-methanol with 3-phenylpropylamine. Screening of multiple conditions and catalyst compositions revealed that use of CuI/$^{t\text{Bu}}$bpy (4,4'-di-*tert*-butyl-2,2'-bipyridine) in combination with ABNO in MeCN produced the desired amide **8** (Table 3.1) in 94% yield under O_2 (see Supporting Information for full screening data). While an improved yield was obtained with pure O_2 as the source of oxidant, a yield of 77% was still retained with air as the oxidant. This simplified 3-component catalyst system provided the starting point to evaluate the scope and functional group tolerance of the method with other alcohols and amines.

A variety of β-heteroatom-substituted alcohols were tested in the oxidative coupling reaction with 3-phenylpropylamine (Table 3.1A). Relevant β-heteroatom-substituted alcohol starting materials are readily available from glycol derivatives, amino alcohols, and halohydrins. Five β-fluorinated alcohols (**1**-**5**) were coupled under the optimized conditions, and each coupling resulted in >90% yield of the corresponding amide product. The trifluoroethanol-derived product **3** was prepared in a 15 mmol scale reaction using ambient air as the oxidant (92% isolated yield). A number of other noteworthy results were obtained from these reactions. The mild conditions allowed for preservation of the Boc protecting group on the piperidine in **5**. A high yield was retained when using β-chloroethanol (**6**) as the substrate, indicating that the amidation outcompetes S_N2 displacement of a primary alkyl chloride. In contrast, β-bromoethanol was not an effective substrate due to competing S_N2 reactivity. (The latter result and other examples of unsuccessful substrates are documented in the Supporting Information; see Tables 6E.9 and 6E.10). Alcohols with alkyl ethers, aryl ethers, and acetonides at the β position also were converted effectively to the corresponding amide products (**7**, **8**, **9**, **11**, **14**). Boc-protected 2-(*S*)-morpholinemethanol

afforded the corresponding amide in 92% yield (**10**). β-Nitrogen containing alcohols are more challenging substrates, possibly reflecting their reduced electron-withdrawing effect and/or deleterious chelation of the Cu center and inhibition of catalytic turnover.[7b] Despite this challenge, tertiary amine (**12**) was isolated in modest yield. Acylation of the β-nitrogen atom, including conversion to a phthalimide (**15**) or Boc-protected amino alcohol (**17**), led to product formation in high-yield. Similarly, alcohols bearing β-heteroaromatic rings, oxazole (**13**) and imidazole (**16**), formed the amidation product in 80% and 81% isolated yields, respectively. The β-oxazolidinone of an alcohol fragment in tedizolid (**18**) was well tolerated under the optimal conditions. The antibiotic metronidazole is insoluble in acetonitrile (**16**); however, conducting the reaction in DMF led to an 81% yield of the desired product.[13]

After assessing the alcohol substrate scope, we explored different amine coupling partners (Table 3.1B). We elected 2,2,2-trifluorethanol (TFE) as the coupling partner for coupling with different amines, resulting in formation of the corresponding trifluoroacetamide derivative.[14] An initial set of substrates (**19**-**26**) was selected to probe the compatibility of various functional groups, while a second set features an expanded set of functional groups within specific pharmaceutically relevant molecules (**27**-**34**). Functional groups in the first set include oxygen-containing groups (ethers, *t*Bu ester, and acetonide **19**-**22**), and aromatic heterocycles (thiophene, pyridine, and thiazole **23**-**25**), all of which formed the desired amide product in very good-to-excellent yields. The catalyst system favors reaction with the primary amine over the sterically encumbered secondary amine, leading to formation of **26**. The reaction tolerated a primary amide[15] and a free tertiary alcohol (**30** and **33**; 89% and 94% yields, respectively), showing that this protocol could have advantages over the use of trifluoroacetic anhydride, which can lead to competitive functionalization of other groups in a molecule.[16] Compatible functional groups

evident from reactions with the second set of molecules include nitriles, alkenes, nitro groups, imides, cyclopropyl rings, and lactams. The effectiveness of the reaction with substrates as complex as the anti-diabetic drugs alogliptin (**32**) and saxagliptin (**33**) and antiviral oseltamivir (**34**), all of which underwent oxidative coupling in >90% yield, shows that this oxidative coupling strategy represents a compelling complement, and in some cases may be superior, to traditional amide coupling reactions.[17]

Table 6.1. Substrate scope of alcohols and amines for aerobic Cu/ABNO catalyzed α-heteroatom-substituted amide formation.

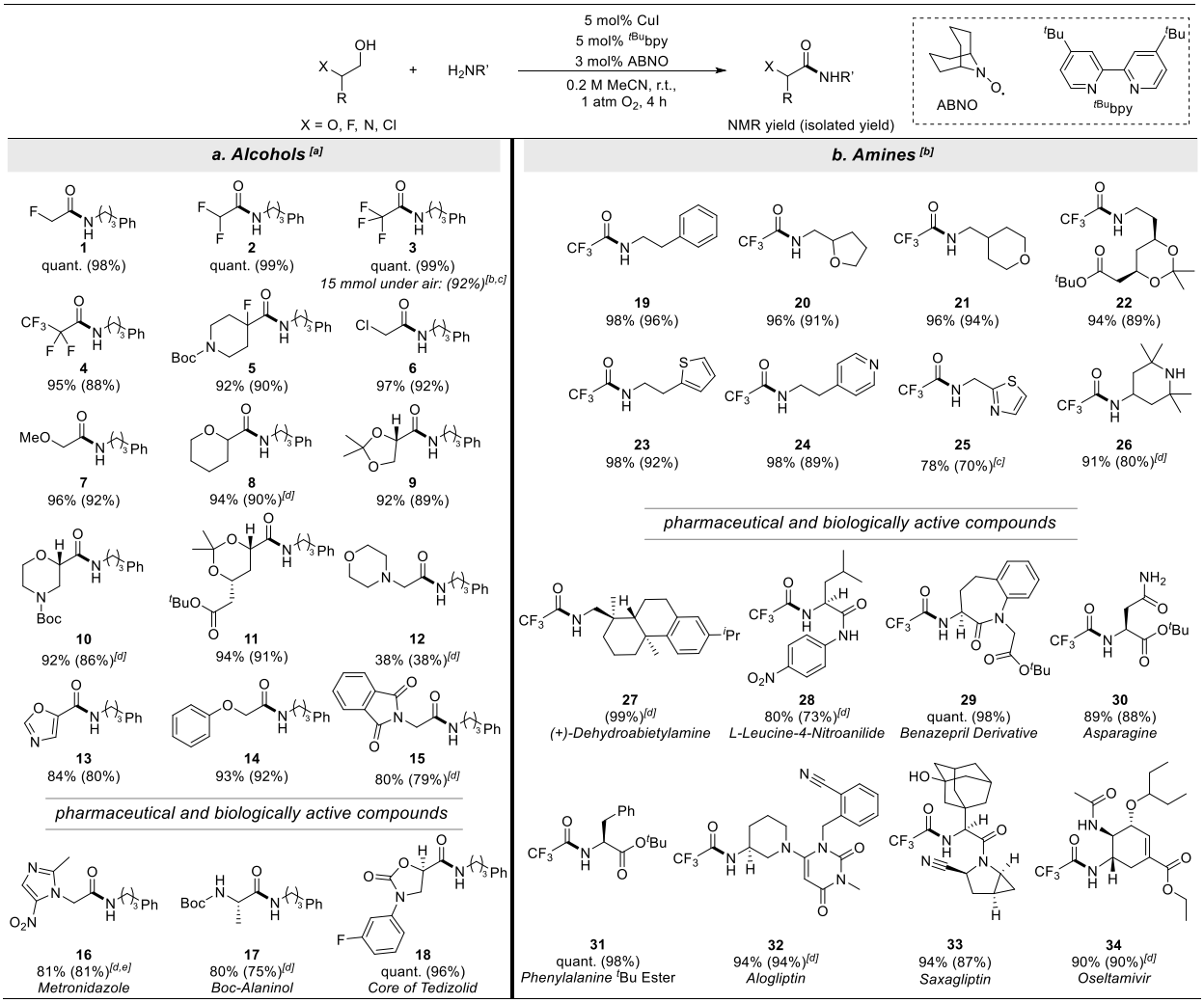

Reactions at 0.5 mmol scale. Calibrated 1H NMR yields using dimethyldiphenylsilane as an internal standard. tBubpy = 4,4'-di-tert-butyl-2,2'-bipyridine, ABNO [a]1 equiv alcohol with 1.1 equiv amine. [b]1 equiv amine with 1.5 equiv alcohol. [c]Under air. [d]Catalyst loading: 10 mol% CuI, 10 mol% tBubpy, and 6 mol% ABNO. [e]DMF used as solvent.

The chemoselective functionalization of the primary amine over the secondary amine in substrate **26** prompted us to explore this issue further.[18] Cu/nitroxyl catalyst systems show good sterically controlled selectivity in oxidations of two different alcohols,[7b,19] owing to the closed 6-membered transition state involved in the H-transfer between bound alkoxide and nitroxyl ligands.[20] We reasoned that analogous selectivity could be achieved in reactions of hemiaminals derived from primary and secondary amines due to the steric differences between the intermediates. A competition experiment between 3-phenylpropylamine and piperidine in the presence of 1 equiv of TFE exhibited >15:1 selectivity for the primary amine (94% yield) over the secondary amine (Figure 6.4A). In contrast, use of traditional trifluoroacetylation conditions with trifluoroacetic anhydride (TFAA)[21] resulted in low selectivity (primary:secondary ≤ 2:1), again favoring reaction with the primary amine. These results were then extended to the reaction of 4-(aminomethyl)piperidine (Figure 6.4B). Chemoselective trifluoroacetylation of the primary amine was again achieved with the Cu/ABNO catalyst system (primary:secondary > 30:1, with very little difunctionalization; 64% yield). Traditional trifluoroacetylation conditions with TFAA exhibited poor selectivity, with preferential formation of the difunctionalized product. In addition to the steric argument these observations also could arise from the relative stability of the hemiaminal intermediate, which is more stable when derived from a primary amine.

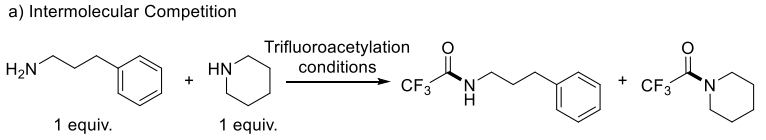

Trifluoroacetylation Conditions:	*2° amide*	*3° amide*
TFAA, DBU, DCM [a]	66%	34%
TFAA, TMG, MeCN [b]	53%	34%
Cu/ABNO [c]	***94%***	*6%*

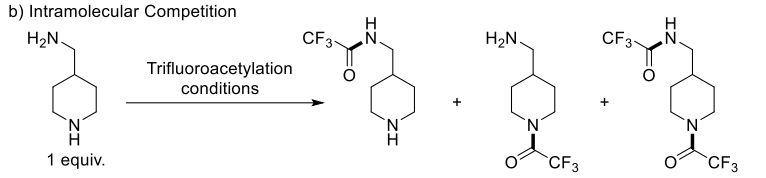

Trifluoroacetylation Conditions:	*2° amide*	*3° amide*	*di-functionalized*
TFAA, DBU, DCM [a]	16%	3%	29%
TFAA, TMG, MeCN [b]	30%	3%	33%
Cu/ABNO [c]	***64%***	*1%*	*2%*

Figure 6.4. Intermolecular (A) and Intramolecular (B) competition experiments between a primary and secondary amine under optimized conditions and using typical trifluoroacetylation protocols. [a]1 equiv TFAA, 1.5 equiv DBU, DCM (0.6 M), 0 ºC to rt, overnight. [b]1 equiv TFAA, 1.5 equiv TMG, MeCN (0.6 M), 0 ºC to rt, overnight. [c]1 equiv TFE, 10 mol% CuI, 10 mol% $^{t\text{Bu}}$bpy, 6 mol% ABNO, MeCN (0.2 M), air, rt, 4 h. TFAA = trifluoroacetic acid, DBU = 1,8-Diazabicyclo5.4.0undec-7-ene, TMG = 1,1,3,3-Tetramethylguanidine, TFE = 2,2,2-trifluoroethanol.

Finally, we sought to demonstrate that the coupling method could be effective for cases in which both coupling partners exhibit significant molecular complexity (Table 6.2). Reactions of this type lack precedent among prior oxidative amidation methods. Each of the examples in Table 6.2 feature reactions in which both reaction partners contain two or more heteroatom substituents. Noteworthy examples include amide coupling with saxagliptin, as the resulting amide product contains 10 unique heteroatoms (**35**). Formation of a dipeptide was achieved via the coupling of a *t*Bu-ester amino acid with an *N*-Boc-protected amino alcohol (**38**).

Polyethylene glycols (PEGs) are a prominent class of β-heteroatom-substituted alcohols, and PEGylation of pharmaceuticals can lead to enhanced pharmacological properties by changing their solubility or membrane permeability.[22,23] The Cu/ABNO-catalyzed method proved to be effective

in coupling mPEG–OH units with benazepril F,[24] affording excellent product yields in both cases (**40**, **41**).

Table 6.2. Synthesis of complex molecules using bioactive coupling partners in Cu/ABNO catalyzed alcohol-amine coupling.

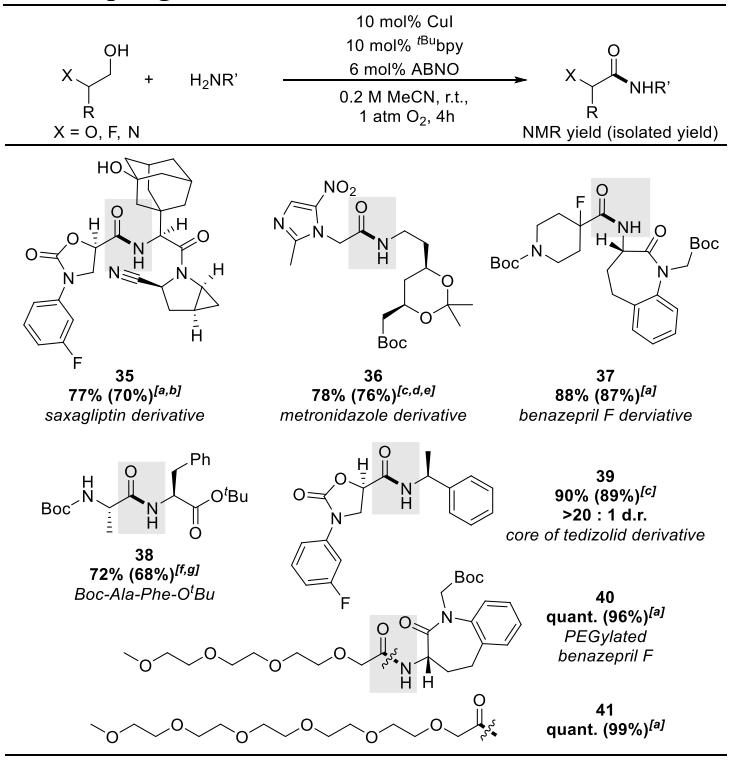

Reactions at 0.5 mmol scale. [a]1.1 equiv of alcohol used. [b]5 mol% CuI, 5 mol% tBubpy, and 3 mol% ABNO. [c]1.1 equiv of amine used. [d]DMF used as solvent. [e]Catalyst loading doubled. [f]1.5 equiv of amine used. [g]15 mol% CuI, 15 mol% tBubpy, and 9 mol% ABNO.

6.4. Conclusion

The results described herein demonstrate that the Cu/ABNO catalyst system exhibits broad scope and synthetic utility for the oxidative coupling of alcohols and amines to form amides. The reactions take advantage of the unique activating properties of β-heteroatom-substituted alcohols to afford pharmaceutically important α-substituted amides. The reaction yields, even with complex substrates, are commonly >90%, suggesting that these methods represent an important complement to traditional amide coupling methods. For example, the efficiency and

chemoselectivity evident in the trifluoroacetylation of primary amines suggests that this method offers an appealing alternative to methods that use trifluoroacetic anhydride. More broadly, these methods could find extensive use in medicinal chemistry, enabling rapid diversification of simple building blocks or core structures containing a primary alcohol or amine. And, the lack of requirement for a stoichiometric coupling reagent offers potential advantages in large scale amide coupling reactions.

6.5. Acknowledgements

Financial support for this project was provided by a grant from the National Institutes of Health (R01-GM100143). This material is based upon work supported by the National Science Foundation Graduate Research Fellowship Program under Grant No. DGE-1747503 (PEP). Any opinions, findings, and conclusions or recommendations expressed in this material are those of the author(s) and do not necessarily reflect the views of the National Science Foundation. Support was also provided by the Graduate School and the Office of the Vice Chancellor for Research and Graduate Education at the University of Wisconsin-Madison with funding from the Wisconsin Alumni Research Foundation. NMR instrumentation was supported by the NSF (CHE-1048642) and by a generous gift from Paul J. and Margaret M. Bender. Mass spectrometry instrumentation was supported by the NIH (1S10 OD020022-1).

6.6. Author Contributions

Piszel, P. E: manuscript preparation and leading experimental work

Vasilopoulos, A: preliminary results, manuscript preparation, and experimental work

6.7. References

1. (a) J. S. Carey; D. Laffan; C. Thomson; M. T. Williams, *Org. Biomol. Chem.* **2006**, *4*, 2337–2347. (b) S. D. Roughley; A. M. Jordan, *J. Med. Chem.* **2011**, *54*, 3451–3479. (c) D. G. Brown; J. Boström, *J. Med. Chem.* **2016**, *59*, 4443–4458.
2. (a) E. Valeur; M. Bradley, *Chem. Soc. Rev.* **2009**, *38*, 606–631. (b) H. Lundberg; F. Tinnis; H. Adolfsson, *Synlett* **2012**, *23*, 2201–2204. (c) H. Lundberg; F. Tinnis; H. Adolfsson, *Chem. Eur. J.* **2012**, *18*, 3822–3826. (d) R. M. Lanigan; P. Starkov; T. D. Sheppard, *J. Org. Chem.* **2013**, *78*, 4512–4523. (e) B. Basavaprabhu; K. Muniyappa; N. R. Panguluri; P. Veladi; V. V. Sureshbabu, *New J. Chem.* **2015**, *39*, 7746–7749.
3. (a) C. A. G. N. Montalbetti; V. Falque, *Tetrahedron* **2005**, *61*, 10827–10852. (b) K. Ekoue-Kovi; C. Wolf, *Chem. Eur. J.* **2008**, *14*, 6302–6315. (c) V. R. Pattabiraman; J. W. Bode, *Nature* **2011**, *480*, 471–479 (d) C. L. Allen; J. M. J. Williams, *Chem. Soc. Rev.* **2011**, *40*, 3405–3415. (e) A. M. Whittaker; V. M. Dong, *Angew. Chem. Int. Ed.* **2015**, *54*, 1312–1315 (f) H. Miyamura; H. Min; J.-F. Soulé; S. Kobayashi, *Angew. Chem. Int. Ed.* **2015**, *54*, 7564–7567; *Angew. Chem.* **2015**, *127*, 7674–7677. (g) T. T. Nguyen; K. L. Hull, *ACS Catal*. **2016**, *6*, 8214–8218. (h) R. M. de Figueiredo; J.-S. Suppo; J.-M. Campagne, *Chem. Rev.* **2016**, *116*, 12029–12122. (i) J. R. Dunetz; J. Magano; G. Weisenburger, *Org. Process Res. Dev.* **2016**, *20*, 140–177.
4. (a) C. Gunanathan; Y. Ben-David; D. Milstein, *Science* **2007**, *317*, 790–792. (b) L. U. Nordstrøm; H. Vogt; R. Madsen, *J. Am. Chem. Soc.* **2008**, *130*, 17672–17673. (c) J. H. Dam; G. Osztrovszky; L. U. Nordstrøm; R. Madsen, *Chem. Eur. J.* **2010**, *16*, 6820–6827. (d) Y. Zhang; C. Chen; S. C. Ghosh; Y. Li; S. H. Hong, *Organometallics* **2010**, *29*, 1374–1378. (e)

A. Prades; E. Peris; M. Albrecht, *Organometallics* **2011**, *30*, 1162–1167. (f) N. D. Schley; G. E. Dobereiner; R. H. Crabtree, *Organometallics* **2011**, *30*, 4174–4179. (g) C. Chen; Y. Zhang; S. H. Hong, *J. Org. Chem.* **2011**, *76*, 10005–10010. (h) J.-F. Soulé; H. Miyamura; S. Kobayashi, *J. Am. Chem. Soc.* **2011**, *133*, 18550–18553. (i) X. Bantreil; C. Fleith; J. Martinez; F. Lamaty, *ChemCatChem* **2012**, *4*, 1922–1925. (j) S. C. Ghosh; J. S. Y. Ngiam; A. M. Seayad; D. T. Tuan; C. W. Johannes; A. Chen, *Tetrahedron Lett.* **2013**, *54*, 4922–4925. (k) N. Ortega; C. Richter; F. Glorius, *Org. Lett.* **2013**, *15*, 1776–1779 (l) X. Bantreil; N. Kanfar; N. Gehin; E. Golliard; P. Ohlmann; J. Martinez; F. Lamaty, *Tetrahedron* **2014**, *70*, 5093–5099. (m) X. Xie; H. V. Huynh, *ACS Catal.* **2015**, *5*, 4143–4151. (n) B. Kang; S. H. Hong, *Adv. Synth. Catal.* **2015**, *357*, 834–840. (o) S. L. Zultanski; J. Zhao; S. S. Stahl, *J. Am. Chem. Soc.* **2016**, *138*, 6416–6419. (p) S. Selvamurugan; R. Ramachandran; G. Prakash; P. Viswanathamurthi; J. G. Malecki; A. Endo, *J. Organomet. Chem.* **2016**, *803*, 119–127. (q) E. M. Lane; K. B. Uttley; N. Hazari; W. Bernskoetter, *Organometallics* **2017**, *36*, 2020–2025. (r) A. Kumar; N. A. Espinosa-Jalapa; G. Leitus; Y. Diskin-Posner; L. Avram; D. Milstein, *Angew. Chem. Int. Ed.* **2017**, *56*, 14992–14996; *Angew. Chem.* **2017**, *129*, 15188–15192.

5. (a) E. M. Huber; M. Basler; R. Schwab; W. Heinemeyer; C. J. Kirk; M. Groettrup; M. Groll, *Cell* **2012**, *148*, 727–738. (b) W. L. Holland; P. E. Scherer, *Science* **2013**, *342*, 1460–1461. (c) M. Golden; N. P. R. Mon; V. Nandialath; A. Muthusamy; R. Neppalli; R. H. Vasudev (Astra Zeneca), WO 2016124722, **2016**.
6. For reviews, see: (a) B. L. Ryland; S. S. Stahl, *Angew. Chem. Int. Ed.* **2014**, *53*, 8824–8838; *Angew. Chem.* **2014**, *126*, 8968–8983 (b) Y. Seki; K. Oisaki; M. Kanai, *Tet. Lett.* **2014**, *55*, 3738–3746. (c) Q. Cao; L. M. Dornan; L. Rogan; N. L. Hughes; M. J. Muldoon, *Chem. Commun.* **2014**, *50*, 4524 (d) K. C. Miles; S. S. Stahl, *Aldrichimica Acta* **2015**, *48*, 8–10.

7. For leading references, see: (a) P. Gamez; I. W. C. E. Arends; R. A. Sheldon; J. Reedijk, *Adv. Synth. Catal.* **2004**, *346*, 805–811 (b) E. T. T. Kumpulainen, A. M. P. Koskinen, *Chem. Eur. J.* **2009**, *15*, 10901–10911. (c) J. M. Hoover; S. S. Stahl, *J. Am. Chem. Soc.* **2011**, *133*, 16901–16910. (d) J. E. Steves; S. S. Stahl, *J. Am. Chem. Soc.* **2013**, *135*, 15742–15745. (e) Y. Sasano; S. Nagasawa; M. Yamazaki; M. Shibuya; J. Park; Y. Iwabuchi, *Angew. Chem. Int. Ed.*, **2014**, *53*, 3236–3240.
8. (a) J. M. Hoover; B. L. Ryland; S. S. Stahl, *ACS Catal.* **2013**, *3*, 2599–2605. (b) J. M. Hoover; B. L. Ryland; S. S. Stahl, *J. Am. Chem. Soc.* **2013**, *135*, 2357–2367.
9. W. N. Olmstead, Z. Margolin, F. G. Bordwell, *J. Org. Chem.* **1980**, *45*, 3295–3299.
10. E. P. Serjeant, B. Dempsey. *Ionisation Constants of Organic Acids in Aqueous Solution*, Pergamon Press, **1979**, 22.
11. F. G. Bordwell, *Acc. Chem. Res.* **1988**, *21*, 456–463.
12. See, for example: G. Blond; T. Billard; B. R. Langlois, *J. Org. Chem.* **2001**, *66*, 4826–4830.
13. N. A. Kasim; M. Whitehouse; C. Ramachandran; M. Bermejo; H. Lennernäs; A. S. Hussain; H. E. Junginger; S. A. Stavchansky; K. K. Midha; V. P. Shah; G. L. Amidon, *Mol. Pharm.* **2004**, *1*, 85–96.
14. P. G. M. Wuts; T. W. Greene, *Greene's Protecting Groups in Organic, Fourth Edition*, Wiley-VCH, **2006**, 781–783.
15. A recent report showed that Cu/nitroxyl catalyst systems can promote imide formation from amides: K. Kataoka; K. Wachi; X. Jin; K. Suzuki; Y. Sasano; Y. Iwabuchi; J.-Y. Hasegawa; N. Mizuno; K. Yamaguchi *Chem. Sci.* **2018**, *9*, 4756–4768.
16. J. M. Tedder, *Chem. Rev.* **1955**, *55*, 787–827.

17. For discoveries of the drugs, see: (a) A. Moscona, *N. Engl. J. Med.* **2005**, *353*, 1363–1373. (b) D. J. Augeri; J. A. Robl; D. A. Betebenner; D. R. Magnin; A. Khanna; J. G. Robertson; A. Wang; L. M. Simpkins; P. Taunk; Q. Huang; S.-P. Han; B. Abboa-Offei; M. Cap; L. Xin; L. Tao; E. Tozzo; G. E. Welzel; D. M. Egan; J. Marcinkeviciene; S. Y. Chang; S. A. Biller; M. S. Kirby; R. A. Parker; L. G. Hamann, *J. Med. Chem.* **2005**, *48*, 5025–5037. (c) J. Feng; Z. Zhang; M. B. Wallace; J. A. Stafford; S. W. Kaldor; D. B. Kassel; M. Navre; L. Shi; R. J. Skene; T. Asakawa; K. Takeuchi; R. Xu; D. R. Webb; S. L. Gwaltney, *J. Med. Chem.* **2007**, *50*, 2297–2300.

18. For previous studies directed toward chemoselective acylation of amines, see the following: (a) S.-I. Murahashi; T. Naota; N. Nakajima, *Chem. Lett.* **1987**, 879–882. (b) A. O. Gálvez; C. P. Schaack; H. Noda; J. W. Bode, *J. Am. Chem. Soc.* **2017**, *139*, 1826–1829. (c) F. Piazzolla; A. Temperini, *Tetrahedron Lett.* **2018**, *59*, 2615–2621.

19. X. Xie; S. S. Stahl, *J. Am. Chem. Soc.* **2015**, *137*, 3767–3770.

20. B. L. Ryland, S. D. McCann, T. C. Brunold, S. S. Stahl, *J. Am. Chem. Soc.* **2014**, *136*, 12166–12173.

21. Trifluoroacetylation conditions obtained from: A. Welle; F. Billard; J. Marchand-Brynaert, *Synthesis* **2012**, *44*, 2249–2254.

22. J. M. Harris; R. B. Chess, *Nat. Rev. Drug Discov.* **2003**, *2*, 214–221.

23. S. M. Ryan; G. Mantovani; X. Wang; D. M. Haddleton; D. J. Brayden, *Expert Opin. Drug Discov.* **2008**, *5*, 371–383.

24. For discovery of benazepril F, see: W. H. Parsons; A. A. Patchett; M. K. Holloway; G. M. Smith; J. L. Davidson; V. J. Lotti; R. S. L. Chang, *J. Med. Chem.* **1989**, *32*, 1681–1685.

Appendix A: Supporting Information Chapter 2

2A.I. General Considerations

All reagents were purchased and used as received unless otherwise noted. Cu salts were purchased from Aldrich. Boronic acids and C–H substrates were purchased from Oakwood, Combi-Blocks, Chem-Impex, or Aldrich. Ligands were purchased from Aldrich. 2-Methyl-2,4-pentanediol was purchased from TCI America. Toluene was used from a solvent system dried by molecular sieves. All peroxides and oxidants were used as received from Aldrich and Combi-Blocks. In the experimental section, "readily purchasable" refers to availability from a vendor for less than $500.00 per gram, without a special order.

All coupling reactions were set up in an LC Technology Solutions nitrogen-filled glovebox, except where specifically noted. ^{1}H and ^{13}C NMR spectra were recorded on a Bruker 400 spectrometer or a Bruker 500 spectrometer and chemical shifts are reported in parts per million (ppm), referenced to $CDCl_3$ at 7.26 ppm (^{1}H) and 77.16 (^{13}C). Chromatography was performed using an automated Biotage Isolera® with reusable 120g or 60g Biotage® SNAP Ultra C-18 cartridges or standard silica cartridges. High-resolution mass spectra were obtained using a Thermo Q Exactive™ Plus via (ASAP-MS) by the mass spectrometry facility at the University of Wisconsin (funded by NIH grant: 1S10OD020022-1). GC analyses were performed on a Shimadzu gas chromatograph (GC-2010 Plus) using a Phenomenex® Zebron™ ZB-Wax capillary column (30 m x 0.25 mm x 0.25 μm film thickness).

2A.II. General Procedure for 2-Aryl-4,4,6-trimethyl-1,3,2-dioxaborinane (ArBdiol) Synthesis

Set-up: To a 15 mL vial was added boronic acid (1 equiv.), 2-methyl-2,4-pentanediol (1.1 equiv.), and dichloromethane (0.5 M). The reaction was then capped and stirred for 16 h at r.t.
Work-up: The reaction mixture was washed 1x with saturated $NaHCO_3$, and the aqueous phase was then extracted with dichloromethane. The organics were combined and washed 1x with saturated $NaHCO_3$ and 1x with brine. After washing, the organics were combined, dried with $MgSO_4$, and concentrated to afford the product. Products showing discoloration were passed through a silica plug with 90% pentane/Et_2O to remove trace impurities. If a precipitate formed from the pentane/Et_2O, the precipitate was filtered, and either the filtered material or filtrate was isolated as the product (without further purification).

2A.III. General Procedure for Cu-Catalyzed Intermolecular Methylarene C–H Arylation

Set-up: In a nitrogen-filled glovebox, a disposable 15 mL glass vial was charged with CuI•DMS complex (0.015 mmol, 3.6 mg, 0.03 equiv.), 1,10-phenanthroline (0.075 mmol, 13.5 mg, 0.15 equiv.), the requisite aryl dioxaborinane (0.5 mmol, 1.0 equiv.), the methyl arene coupling partner (1.6 mL, 0.3 M), di-*tert*-butyl peroxide (2.0 mmol, 366 μL, 4.0 equiv.), and a Teflon stir bar. The vial was then capped with a PTFE-lined pierceable cap and removed from the glovebox. After taping the cap with electrical tape, the vial was placed in an aluminum heating block on a heated stir plate, and the mixture was stirred at 90 °C for 48 h.
Work-up: At the end of the reaction, the mixture turned a red/brown color. The vial was then removed from the heat/stir plate and allowed to cool to room temperature. Dibromomethane was

then added via syringe as ^{1}H NMR internal standard (0.5 mmol, 35 μL, 1 equiv.), and an aliquot of the reaction mixture was taken for analysis by ^{1}H NMR to determine the calibrated yield. The reaction was then condensed by rotary evaporation (taking care not to remove the desired product). The methyl arene starting material is sometimes removed in this step. The crude reaction mixture was then diluted with 100:1 pentane:EtOAc and a portion of it was passed over a silica plug, yielding a colorless or red/yellow solution (for normal phase columns, the crude reaction mixture was instead diluted with 9:1 pentane:EtOAc and then filtered over a syringe filter). The pentane:EtOAc was removed by rotary evaporation, and the mixture was then purified using automated reverse phase column chromatography (Biotage; MeOH/H_2O with 0.1% TFA gradient; DCM was used to load the sample) or automated normal phase column chromatography (Biotage; pentane:EtOAc gradient). For reverse phase columns, the purified product fractions were collected and extracted 2x with 9:1 pentane:Et_2O and brine. These organic layers were collected, dried by $MgSO_4$, and the solvent was removed to yield the desired 1,1-diarylmethane.

2A.IV. General Procedure for Cu-Catalyzed Intermolecular Alkyl Arene C–H Arylation

Set-up: In a nitrogen-filled glovebox, a disposable 15 mL glass vial was charged with either 5 or 3 mol% CuI•DMS complex (0.025 mmol, 6.0 mg, 0.05 equiv. or 0.015 mmol, 3.6 mg, 0.03 equiv.), 1,10-phenanthroline or 1,10-phenanthroline-5,6-dione ligand (0.075 mmol, 13.5 mg or 15.8 mg respectively, 0.15 equiv.), the requisite aryl dioxaborinane (0.5 mmol, 1.0 equiv.), the alkyl arene coupling partner (5 mmol, 10.0 equiv.), di-*tert*-butyl peroxide (2.0 mmol, 366 μL, 4.0 equiv.), chlorobenzene solvent (313 μl, 1.6 M), and a Teflon stir bar. The vial was then capped with a PTFE-lined pierceable septum cap and removed from the glovebox. After taping the cap with electrical tape, the vial was placed on an aluminum heating block on a heated stir plate, and the reaction mixture was stirred at 90 °C for 48 h.
Work-up: Identical to that in III. Reactions sometimes needed to be filtered with a syringe filter before they are passed through the silica plug with 100:1 pentane:EtOAc (particularly for the 1-chloro-3-phenylpropane substrates).

2A.V. Procedure for Glovebox-Free Cu-Catalyzed Benzylic C–H Arylation of 4-Ethylanisole

Set-up: In a fume hood, a disposable 24 mL glass vial was charged with CuI•DMS complex (12.3 mg, 0.051 mmol, 0.03 equiv.), 1,10-phenanthroline-5,6-dione (53.7 mg, 0.255 mmol, 0.15 equiv.), 2-(3,4,5-methoxyphenyl)-4,4,6-trimethyl-1,3,2-dioxaborinane (500 mg, 1.7 mmol, 1.0 equiv.), 4-ethylanisole (2.4 mL, 17 mmol, 10.0 equiv.), di-*tert*-butyl peroxide (1.2 mL, 6.8 mmol, 4.0 equiv.), chlorobenzene solvent (1 ml, 1.6 M), and a Teflon stir bar. The vial was then capped with a PTFE-lined pierceable septum cap and taped with electrical tape. The septum was pierced and the vial was evacuated and then backfilled with N_2 three times (evacuate/backfill quickly or freeze-pump-thaw to avoid bumping). It was then placed on an aluminum heating block on a heated stir plate and stirred at 90 °C for 24 h.
Work-up: Identical to that in III, except dichloromethane was used as the eluent for the silica plug. This product was isolable using normal-phase flash chromatography. The first several fractions of the column contained pure 4-ethylanisole starting material (76% of the unreacted starting material, i.e. 12 mmol of 15.81 mmol, was recovered)

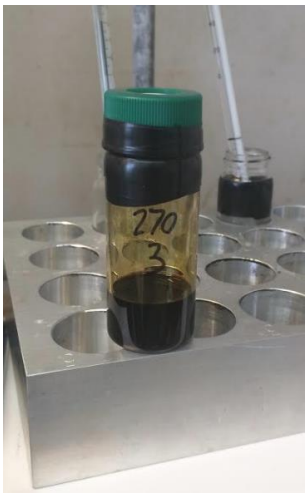

Figure 2A.1. Glovebox-free arylation reaction after 24 h.

2A.VI. Screening Tables

Table 2A.1. Nucleophile Screening Table

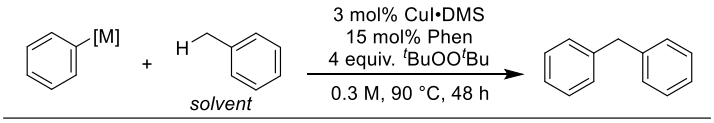

entry	Ph-[M]	% yield[a]
1	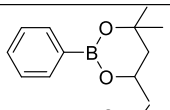	76
2	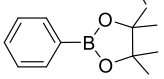	61
3	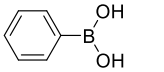	1
4	w/ 1 equiv. NaOMe	3
5	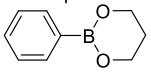	2
6	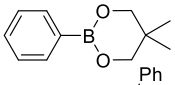	0
7	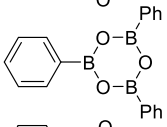	0
8	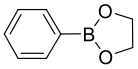	0
9	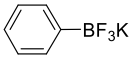	2
10	w/ 1 equiv. NaOMe	13
11	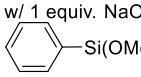	6
12	w/ 1 equiv. CsF	3

[a]Reactions run on 0.4 mmol scale and yields analyzed by calibrated GC using 1 eq. tetradecane as an internal standard.

Table 2A.2. Copper Source Screening Table

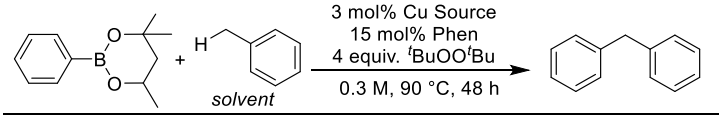

entry	Cu Source	% yield[a]
1	CuI•DMS	76
2	CuI	74
3	CuBr•DMS	67
4	CuBr	73
5	CuCl	61
6	CuCN	69

[a]Reactions run on 0.4 mmol scale and yields analyzed by calibrated GC using 1 eq. tetradecane as an internal standard.

Table 2A.3. Ligand Screening Table

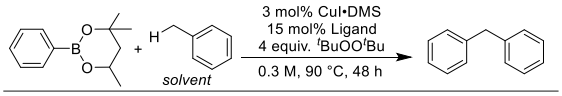

entry	Ligand	% yield[a]
1	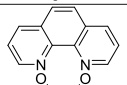	76
2	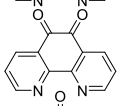	29[b]
3	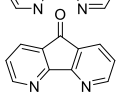	23
4	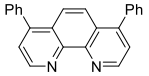	55
5	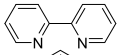	8
6	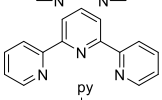	32
7		4
8	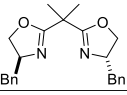	3

[a]Reactions run on 0.4 mmol scale and yields analyzed by calibrated GC using 1 eq. tetradecane as an internal standard. [b]Affords a 60% yield if 4 mol% Cu and 12 mol% phd are used rather than 3 mol% and 15 mol%.

Table 2A.4. Chiral Ligand Screening

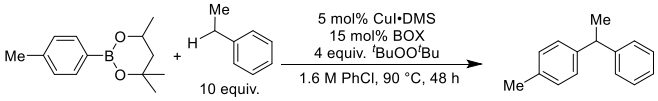

entry	Box Ligand	% yield[a]
1	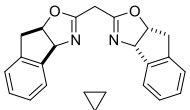	1
2	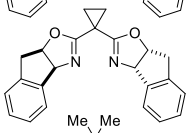	8
3	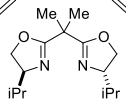	0
4	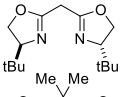	11
5	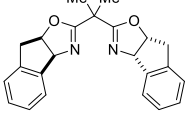	0

[a]Reactions run on 0.4 mmol scale and yields analyzed by ^{1}H NMR with 1 eq.CH_2Br_2 as the internal standard.

Table 2A.5. Oxidant Screening Table

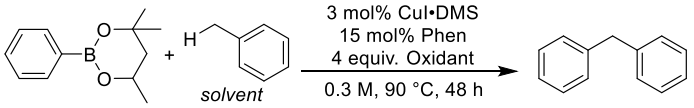

entry	Oxidant	% yield[a]
1	^{t}BuOO^{t}Bu	76
2	^{t}BuOOH (6 M in decane)	10
3	^{t}BuOOBz	3
4	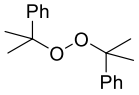	24
5	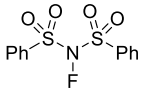	3
6	Oxone	2
7	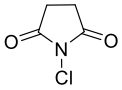	2
8	$K_2S_2O_8$	2

[a]Reactions run on 0.4 mmol scale and yields analyzed by calibrated GC using 1 eq. tetradecane as an internal standard.

Table 2A.6. Control Reactions (Temperature, Time, Air, Concentration, Catalyst)

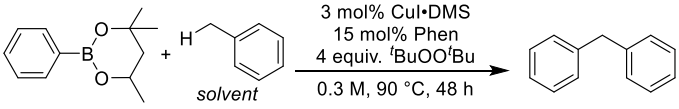

entry	Variation to Conditions	% yield[a]
1	70 °C instead of 90 °C	22
2	24 h instead of 48 h	76[b]
3	Set up on bench under air	60[c]
4	10 eq. Toluene, Same Volume (0.43 mL Toluene + 0.87 mL PhCl)	35[d]
5	No CuI•DMS	5
6	No phen	4
7	No Oxidant	0
8	No Nucleophile	0
9	1 eq. Product Added at Start (no PhBDiol)	77

[a]Reactions run on 0.4 mmol scale and yields analyzed by calibrated GC using 1 eq. tetradecane as an internal standard. [b]In this screen, the 48h reaction gave 80% yield by GC. [c]Components weighed out on bench, and then capped. [d]See caption in table 7 for better conditions with 10 equiv.

Table 2A.7. Ethyl Benzene Optimization of Ligand/Cu Ratio

entry	mol% Ligand	mol% Cu	Ligand:Cu Ratio	% yield[a]
1	10	5	2	52%
2	12	4	3	66%
3	**15**	**5**	**3**	**68%[b]**
4	30	10	3	64%
5	20	5	4	52%

[a]Reactions run on 0.4 mmol scale and yields analyzed by calibrated GC using 1 eq. tetradecane as an internal standard. [b]63% yield using toluene as the C–H substrate.

Table 2A.8. Alkyl Arene (Indane) Optimized Conditions w/ phd

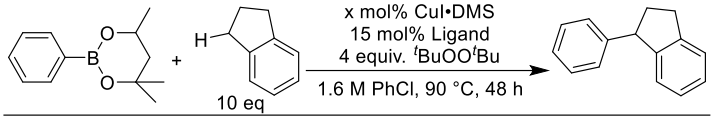

entry	Ligand	mol% Cu	Ligand:Cu Ratio	% yield[a]
1	Phen	5	3	45%
2	Phen	3	5	52%
3	phd	5	3	40%
4	**phd**	**3**	**5**	**65%**

[a]Reactions run on 0.4 mmol scale and yields analyzed by calibrated GC using 1 eq. tetradecane as an internal standard.

2A.VII. Additional Experiments and Observations

Figure 2A.2 shows the effect of increasing the ligand:Cu ratio in the benzylic arylation reaction. As the ligand:Cu ratio increases from 0.5 to 6, formation of the desired product **B** increases and biaryl side-product **C** decreases. Only trace amounts of protodeboronation of the boronic ester is detected (**D**). The only other product that consumes >5% of the boronic ester is **E**, which is likely the result of arylation of in situ-generated bibenzyl. The amount of **E** is relatively constant once the ligand:Cu ratio exceeds 1.

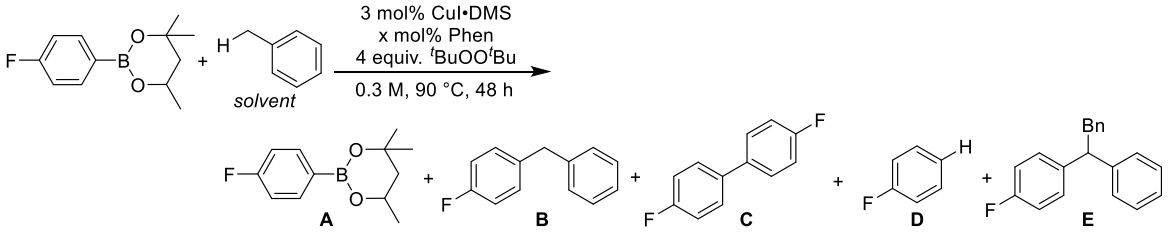

entry	x mol% Phen	Equiv. **A**	Equiv. **B**	2*Equiv. **C**	Equiv. **D**	Equiv. **E**	mass balance
1	1.5%	0	0.15	0.82	0	0.03	100%
2	3%	0.02	0.19	0.78	0.02	0.05	106%
3	6%	0	0.54	0.36	0	0.10	100%
4	9%	0.02	0.64	0.26	0.02	0.14	108%
5	12%	0.03	0.67	0.13	0.01	0.12	96%
6	15%	0.03	0.72	0.09	0.02	0.11	97%
7	18%	0.02	0.76	0.07	0	0.12	97%
8	21%	0.02	0.74	0.07	0.02	0.12	97%
9	24%	0.02	0.76	0.05	0.01	0.09	93%

Figure 2A.2. Product Distribution as a Function of the Ligand:Cu Ratio. [a]Reactions run on 0.4 mmol scale and yields analyzed by ^{1}H NMR and ^{19}F NMR with 1 eq.CH_2Br_2 and 1 eq. CF_3Ph as internal standards.

Figure 2A.3 compares the distribution of ArBdiol- and ArBpin-derived products. The data show that more biaryl is generated with ArBpin than with ArBdiol. This outcome may arise from more-rapid transmetalation by ArBpin, resulting in a higher concentration of a Cu–Ar species that could undergo disproportionation to generate biaryl. Similar to the data in Figure 2A.2, **E** is also the only major byproduct when using ArBpin as the nucleophile (only trace amount of protodeboronation to **D** is observed).

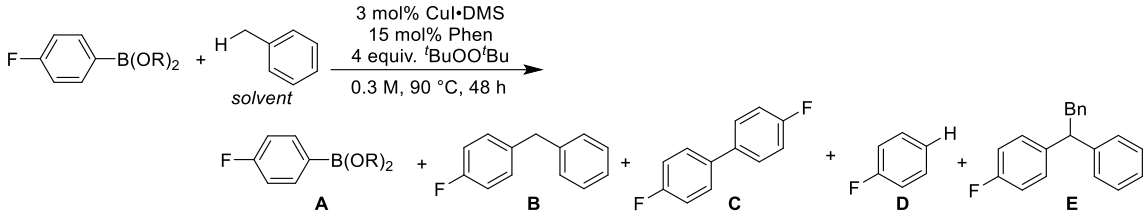

entry	Boronic Ester	Equiv. A	Equiv. B	2*Equiv. C	Equiv. D	Equiv. E	M.B.
1	Bdiol	0.03	0.72	0.09	0.02	0.11	97%
2	Bpin	0.03	0.50	0.32	0.01	0.08	94%

Figure 2A.3. Distribution of Products for ArBdiol vs ArBpin. [a]Reactions run on 0.4 mmol scale and yields analyzed by ^{1}H NMR and ^{19}F NMR with 1 eq.CH_2Br_2 and 1 eq. CF_3Ph as internal standards. M. B. = mass balance.

Several competition exepriments were carried out to probe the selectivity with respect to the arylboron nucleophile. The effect of the electronic property of the arylboronic ester showed a slight preference for the more-electron-rich aryl boronic ester nucleophile (Figure 2A.4A). The effect of the diol fragment in the aryl boronic ester showed a slight preference for the Bpin derivative over the "Bdiol" derivative (i.e., the 4,4,6-trimethyl-1,3,2-dioxaborinane) (Figure 2A.4B). Comparison of Bdiol vs. BF_3K shows exclusive selectivity for 4-F-PhBdiol over $PhBF_3K$ (Figure 2A.4C).

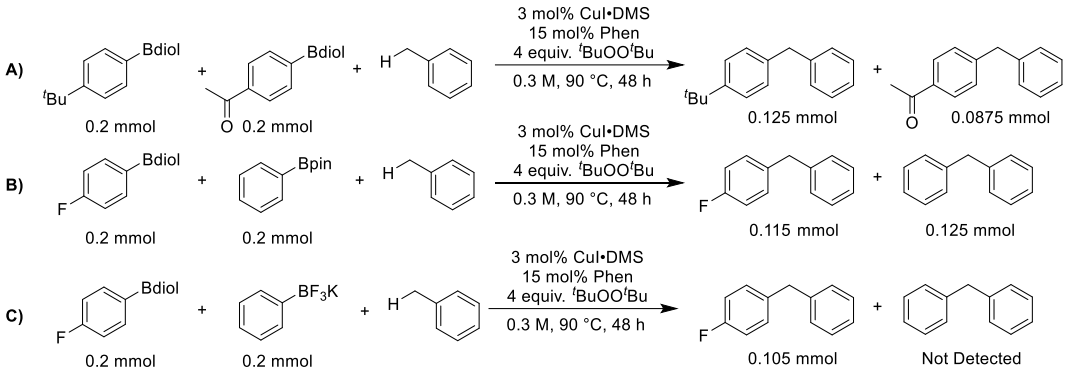

Figure 2A.4. Competition Experiments Between Boron Nucleophiles. [a]Reactions run on 0.4 mmol scale and yields analyzed by ^1H NMR and ^{19}F NMR with 1 eq.CH_2Br_2 and 1 eq. CF_3Ph as internal standards.

Figure 2A.5A depicts a competition reaction between toluene and ethyl benzene and shows that ethyl benzene undergoes preferential benzylic arylation over toluene in a ratio of 2.3 to 1. Figure 2A.5B depicts an intramolecular competition reaction between the primary and tertiary C–H bonds of cumene. No observed oxidation of the tertiary C–H bond, while 0.33 equiv. of the diaryl methane of cumene was detected by ^{1}H NMR. Tertiary C–H bonds appear to be unreactive under the catalytic conditions (See Figure 2A.7).

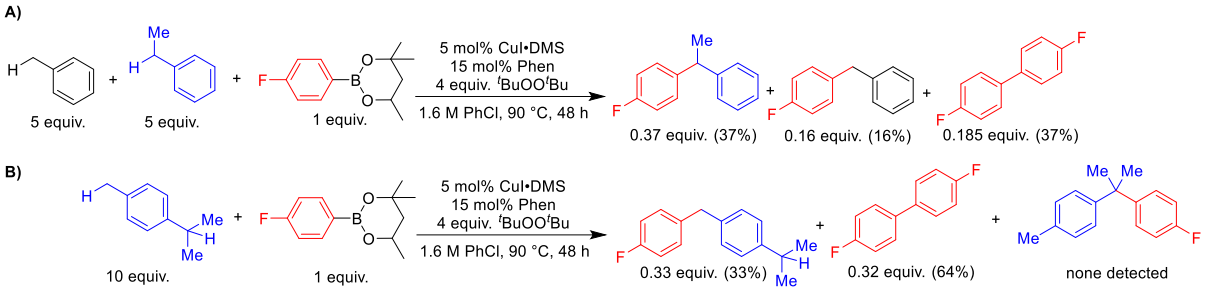

Figure 2A.5. Selectivity Experiment for Primary vs Secondary and Primary vs Tertiary C–H Functionalization. [a]Reactions run on 0.4 mmol scale and yields analyzed by ^{1}H NMR and ^{19}F NMR with 1 eq.CH_2Br_2 and 1 eq. CF_3Ph as internal standards.

In Figure 2A.6 depicts experiments to assess the relative reactivity of methyl arene and diarylmethane C–H bonds. In reaction A, a control experiment is conducted with toluene. In reaction B, diphenylmethane undergoes 25% conversion under standard catalytic conditions, generating primarily 1,1,2,2-tetraphenylethane as the product (via homocoupling of the benzylic radical). In a competition experiment between toluene and diphenylmethane, under conditions reflecting typical reaction conditions, only 10% of diphenylmethane conversion is observed. These observations suggest that the diarylmethane products of the benzylic arylation reactions are not especially susceptible to overoxidation.

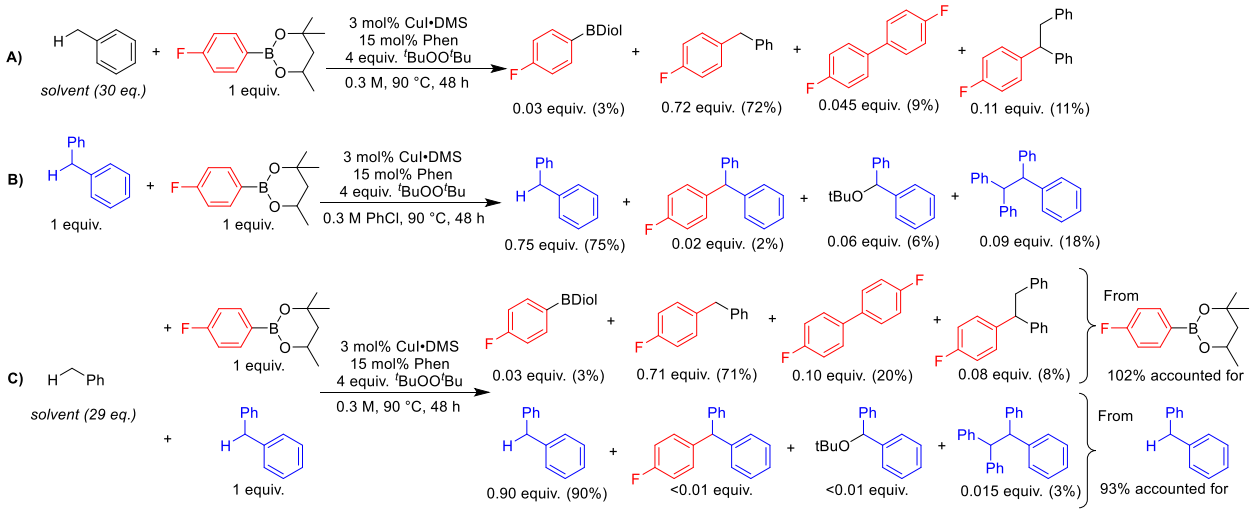

Figure 2A.6. Selectivity Experiment for C–H Arylation of a Methyl Arene vs a Diarylmethane. [a]Reactions run on 0.4 mmol scale and yields analyzed by ^{1}H NMR and ^{19}F NMR with 1 eq.CH_2Br_2 and 1 eq. CF_3Ph as internal standards.

Figure 2A.7 provides information on the relative reactivity of secondary and tertiary benzylic C–H bonds, using ethylbenzene and 1,1-diphenylpropane as the substrate. Even in the absence of ethylbenzene, only 1% conversion of the benzylic tertiary C–H bond is observed. When 9 equivalents of ethylbenzene is present (reflecting typical reaction conditions), no conversion of 1,1-diphenylpropane is detected, while ethylbenzene is converted into the corresponding diarylalkane in 57% yield.

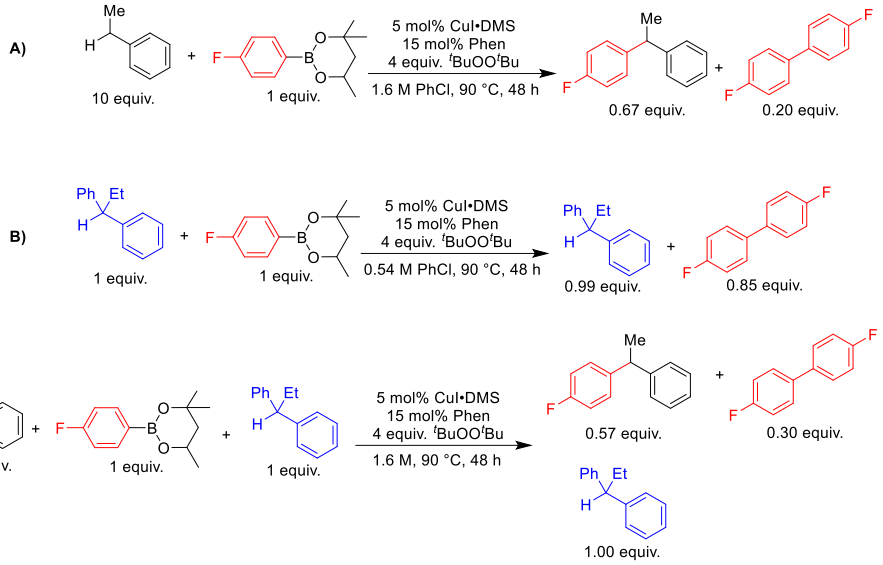

Figure 2A.7. Comparative reactivity of ethylbenzene and 1,1-diphenylpropane. [a]Reactions run on 0.4 mmol scale and yields analyzed by ^{1}H NMR and ^{19}F NMR with 1 eq.CH_2Br_2 and 1 eq. CF_3Ph as internal standards.

2A.VIII. Experimental Data for the ArBdiol Products (Compounds 1a-28a)

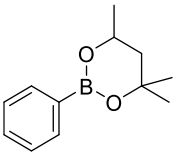

(1a) 2-Phenyl-4,4,6-trimethyl-1,3,2-dioxaborinane: Prepared according to the general procedure in Section II using Phenylboronic acid (40 mmol, 4.88 g).
Reaction duration: 16 h. Purification: Extraction and a SiO_2 plug, 90% pentane/Et_2O.
Yield: 95% (7.72 g), colorless oil.
Readily Purchasable (CAS): Yes (15961-35-0). As the BPin (CAS): Yes (24388-23-6)
Spectra Available in the Literature: Yes[1]
^{1}H NMR (500 MHz, $CDCl_3$) δ 7.83 (d, J = 6.6 Hz, 2H), 7.41 (t, J = 7.3 Hz, 1H), 7.35 (t, J = 7.2 Hz, 2H), 4.36 (dqd, J = 12.3, 6.2, 2.9 Hz, 1H), 1.88 (dd, J = 13.9, 3.0 Hz, 1H), 1.61 (dd, 1H), 1.39 (s, 3H), 1.38 (s, 3H), 1.36 (d, J = 6.2 Hz, 3H).
^{13}C NMR (126 MHz, $CDCl_3$) δ 133.73, 130.31, 127.43, 70.96, 64.96, 46.05, 31.30, 28.17, 23.23.

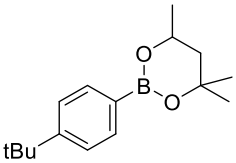

(2a) 2-(4-*tert*-Butylphenyl)-4,4,6-trimethyl-1,3,2-dioxaborinane: Prepared according to the general procedure in Section II using 4-*tert*-Butylphenylboronic acid (5 mmol, 890 mg).
Reaction duration: 16 h. Purification: Extraction.
Yield: 98% (1.27 g), white solid.
Readily Purchasable (CAS): No (N/A) As the BPin (CAS): Yes (214360-66-4)
Spectra Available in the Literature: Yes[2]
^{1}H NMR (500 MHz, $CDCl_3$) δ 7.75 (d, J = 8.2 Hz, 2H), 7.37 (d, J = 8.2 Hz, 2H), 4.33 (dqd, J = 12.2, 6.2, 2.9 Hz, 1H), 1.85 (dd, J = 13.9, 2.9 Hz, 1H), 1.57 (dd, J = 13.9, 11.6 Hz, 1H), 1.36 (s, 3H), 1.35 (s, 3H), 1.34 (d, J = 6.2 Hz, 3H), 1.32 (s, 9H).
^{13}C NMR (126 MHz, $CDCl_3$) δ 153.35, 133.60, 124.38, 70.78, 64.86, 46.09, 34.72, 31.31, 31.24, 28.12, 23.26.
HRMS (ESI) Calculated for $C_{16}H_{25}BO_2$ ($[M+H]^+$): 260.2057, measured: 260.2053.

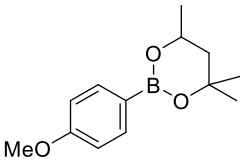

(3a) 2-(4-Methoxyphenyl)-4,4,6-trimethyl-1,3,2-dioxaborinane: Prepared according to the general procedure in Section II using 4-Methoxyphenylboronic acid (7.5 mmol, 1.14 g).
Reaction duration: 4 h. Purification: Extraction.
Yield: 94% (1.65 g), colorless oil.
Readily Purchasable (CAS): Yes (934558-31-3) As the BPin (CAS): Yes (171364-79-7)
Spectra Available in the Literature: Yes[1]
^{1}H NMR (500 MHz, $CDCl_3$) δ 7.76 (d, J = 8.6 Hz, 2H), 6.87 (d, J = 8.6 Hz, 2H), 4.33 (dqd, J = 12.3, 6.2, 2.9 Hz, 1H), 3.82 (s, 3H), 1.85 (dd, J = 13.8, 3.0 Hz, 1H), 1.58 (dd, J = 13.5, 11.7 Hz, 1H), 1.36 (s, 3H), 1.35 (s, 3H), 1.34 (d, J = 6.2 Hz, 3H).
^{13}C NMR (126 MHz, $CDCl_3$) δ 161.49, 135.41, 113.00, 70.81, 64.86, 55.06, 46.08, 31.36, 28.18, 23.29.

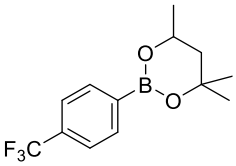

(4a) 2-(4-Trifluoromethylphenyl)-4,4,6-trimethyl-1,3,2-dioxaborinane: Prepared according to the general procedure in Section II using 4-Trifluoromethylphenylboronic acid (2.5 mmol, 475 mg).
Reaction duration: 16 h. Purification: Extraction.
Yield: 91% (622 mg), white solid.
Readily Purchasable (CAS): No (1214273-27-4) As the BPin (CAS): Yes (214360-65-3)
Spectra Available in the Literature: Yes[2]
^{1}H NMR (500 MHz, $CDCl_3$) δ 7.91 (d, J = 7.5 Hz, 2H), 7.57 (d, J = 8.7 Hz, 2H), 4.37 (dqd, J = 12.3, 6.2, 2.9 Hz, 1H), 1.89 (dd, J = 13.9, 2.9 Hz, 1H), 1.61 (dd, J = 13.9, 11.6 Hz, 1H), 1.39 (s, 3H), 1.38 (s, 3H), 1.36 (d, J = 6.2 Hz, 3H).
^{13}C NMR (126 MHz, $CDCl_3$) δ 133.98, 131.90 (q, J = 31.9 Hz), 124.35 (q, J = 272.2 Hz), 123.98 (q, J = 3.8 Hz), 71.38, 65.24, 45.96, 31.18, 28.13, 23.10.
^{19}F NMR (377 MHz, $CDCl_3$) δ -62.83.
HRMS (ESI) Calculated for $C_{13}H_{16}BO_2F_3$ ($[M+H]^+$): 272.1305, measured: 272.1303.

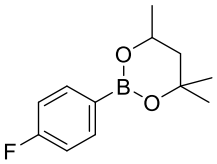

(5a) 2-(4-Fluorophenyl)-4,4,6-trimethyl-1,3,2-dioxaborinane: Prepared according to the general procedure in Section II using 4-Fluorophenylboronic acid (7.5 mmol, 1.05 g).
Reaction duration: 16 h. Purification: Extraction and a SiO_2 plug, 90% pentane/Et_2O.
Yield: 80% (1.34 g), slightly yellow oil.
Readily Purchasable (CAS): Yes (1029653-69-7) As the BPin (CAS): Yes (214360-58-4)
Spectra Available in the Literature: Yes[2]
^{1}H NMR (500 MHz, $CDCl_3$) δ 7.80 (dd, J = 8.5, 6.4 Hz, 2H), 7.01 (t, J = 9.0 Hz, 2H), 4.34 (dqd, J = 12.3, 6.2, 2.9 Hz, 1H), 1.87 (dd, J = 13.9, 3.0 Hz, 1H), 1.58 (dd, J = 14.1, 11.8 Hz, 1H), 1.37 (s, 3H), 1.36 (s, 3H), 1.34 (d, J = 6.2 Hz, 3H).
^{13}C NMR (126 MHz, $CDCl_3$) δ 164.64 (d, J = 248.4 Hz), 135.85 (d, J = 8.0 Hz), 114.38 (d, J = 19.9 Hz), 71.06, 65.01, 45.99, 31.26, 28.14, 23.18.
^{19}F NMR (377 MHz, $CDCl_3$) δ -110.55.
HRMS (ESI) Calculated for $C_{12}H_{16}BFO_2$ ($[M+H]^+$): 222.1336, measured: 222.1336.

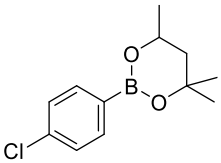

(6a) 2-(4-Chlorophenyl)-4,4,6-trimethyl-1,3,2-dioxaborinane: Prepared according to the general procedure in Section II using 4-Chlorophenylboronic acid (7.5 mmol, 1.17 g).
Reaction duration: 16 h. Purification: Extraction and a SiO_2 plug, 90% pentane/Et_2O.
Yield: 75% (1.34 g), yellow oil.
Readily Purchasable (CAS): No (N/A) As the BPin (CAS): Yes (195062-61-4)
Spectra Available in the Literature: Yes[2]
^{1}H NMR (500 MHz, $CDCl_3$) δ 7.73 (d, J = 8.3 Hz, 2H), 7.30 (d, J = 8.3 Hz, 2H), 4.34 (dqd, J = 12.3, 6.2, 2.9 Hz, 1H), 1.87 (dd, J = 13.9, 2.9 Hz, 1H), 1.58 (dd, J = 13.9, 11.6 Hz, 1H), 1.37 (s, 3H), 1.36 (s, 3H), 1.34 (d, J = 6.2 Hz, 3H).
^{13}C NMR (126 MHz, $CDCl_3$) δ 136.45, 135.18, 127.63, 71.16, 65.08, 45.97, 31.23, 28.15, 23.16.
HRMS (ESI) Calculated for $C_{12}H_{16}BClO_2$ ($[M+H]^+$): 238.1041, measured: 238.1041.

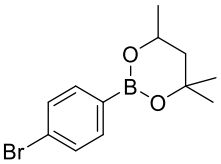

(7a) 2-(4-Bromophenyl)-4,4,6-trimethyl-1,3,2-dioxaborinane: Prepared according to the general procedure in Section II using 4-Bromophenylboronic acid (2.5 mmol, 502 mg).
Reaction duration: 16 h. Purification: Extraction.
Yield: 96% (677 mg), colorless oil.
Readily Purchasable (CAS): Yes (1092060-78-0) As the BPin (CAS): Yes (68716-49-4)
Spectra Available in the Literature: Yes[3]
^{1}H NMR (500 MHz, $CDCl_3$) δ 7.66 (d, J = 8.2 Hz, 2H), 7.46 (d, J = 8.2 Hz, 2H), 4.33 (dqd, J = 12.3, 6.2, 2.9 Hz, 1H), 1.87 (dd, J = 13.9, 2.9 Hz, 1H), 1.58 (dd, J = 13.9, 11.6 Hz, 1H), 1.36 (s, 3H), 1.35 (s, 3H), 1.34 (d, J = 6.2 Hz, 3H).
^{13}C NMR (126 MHz, $CDCl_3$) δ 135.43, 130.57, 125.15, 71.18, 65.09, 45.96, 31.23, 28.14, 23.15.

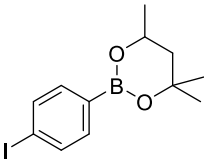

(8a) 2-(4-Iodophenyl)-4,4,6-trimethyl-1,3,2-dioxaborinane: Prepared according to the general procedure in Section II using 4-Iodophenylboronic acid (2.5 mmol, 619.7 mg).
Reaction duration: 16 h. Purification: Extraction and a SiO_2 plug, 90% pentane/Et_2O.
Yield: 90% (745 mg), thick off-white oil.
Readily Purchasable (CAS): Yes (1279115-53-5) As the BPin (CAS): Yes (73852-88-7)
Spectra Available in the Literature: Yes[4]
^{1}H NMR (500 MHz, $CDCl_3$) δ 7.67 (d, J = 8.0 Hz, 2H), 7.51 (d, J = 8.0 Hz, 2H), 4.33 (dqd, J = 12.2, 6.2, 2.9 Hz, 1H), 1.86 (dd, J = 13.9, 2.8 Hz, 1H), 1.58 (dd, J = 13.9, 11.6 Hz, 1H), 1.36 (s, 3H), 1.35 (s, 3H), 1.33 (d, J = 6.1 Hz, 3H).
^{13}C NMR (126 MHz, $CDCl_3$) δ 136.56, 135.48, 97.68, 71.18, 65.09, 45.95, 31.21, 28.14, 23.14.

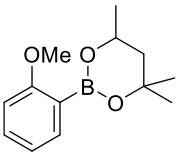

(9a) 2-(2-Methoxyphenyl)-4,4,6-trimethyl-1,3,2-dioxaborinane: Prepared according to the general procedure in Section II using 4-Methoxyphenylboronic acid (2.5 mmol, 380 mg).
Reaction duration: 16 h. Purification: Extraction.
Yield: 95% (554 mg), white solid.
Readily Purchasable (CAS): Yes (934558-37-9) As the BPin (CAS): Yes (190788-60-4)
Spectra Available in the Literature: Yes[1]
^{1}H NMR (500 MHz, $CDCl_3$) δ 7.60 (dd, J = 7.3, 1.9 Hz, 1H), 7.32 (ddd, J = 8.2, 7.3, 1.9 Hz, 1H), 6.92 (td, J = 7.3, 0.9 Hz, 1H), 6.83 (dd, J = 8.3, 0.9 Hz, 1H), 4.38 (ddh, J = 12.4, 6.2, 3.0 Hz, 1H), 3.81 (s, 3H), 1.86 (dd, J = 13.9, 3.0 Hz, 1H), 1.64 (dd, J = 13.8, 11.7 Hz, 1H), 1.39 (s, 3H), 1.38 (s, 3H), 1.35 (d, J = 6.2 Hz, 3H).
^{13}C NMR (126 MHz, $CDCl_3$) δ 163.50, 135.45, 131.14, 120.27, 110.90, 71.13, 65.18, 55.83, 45.96, 31.28, 28.17, 23.20.

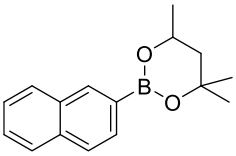

(10a) 2-(2-Napthyl)-4,4,6-trimethyl-1,3,2-dioxaborinane: Prepared according to the general procedure in Section II using Naphthalene-2-boronic acid (2.5 mmol, 430 mg).
Reaction duration: 16 h. Purification: Extraction.
Yield: 98% (630 mg), viscous slightly yellow oil.
Readily Purchasable (CAS): Yes (1260068-92-5) As the BPin (CAS): Yes (256652-04-7)
Spectra Available in the Literature: Yes[6]
^{1}H NMR (500 MHz, $CDCl_3$) δ 8.35 (s, 1H), 7.89 (t, J = 7.4 Hz, 2H), 7.85 – 7.77 (m, 2H), 7.51 – 7.43 (m, 2H), 4.41 (dqd, J = 12.2, 6.2, 2.9 Hz, 1H), 1.91 (dd, J = 13.9, 2.9 Hz, 1H), 1.65 (dd, J = 13.8, 11.6 Hz, 1H), 1.43 (s, 3H), 1.42 (s, 3H), 1.41 (d, J = 5.9 Hz, 3H).
^{13}C NMR (126 MHz, $CDCl_3$) δ 134.73, 134.72, 132.91, 130.06, 128.63, 127.61, 126.58, 126.34, 125.39, 71.14, 65.11, 46.09, 31.35, 28.24, 23.27.

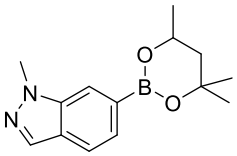

(11a) 2-(6-Methylindazole)-4,4,6-trimethyl-1,3,2-dioxaborinane: Prepared according to the general procedure in Section II using 1-Methylindazole-6-boronic acid (2.5 mmol, 440 mg).
Reaction duration: 16 h. Purification: Extraction.
Yield: 69% (445 mg), white solid.
Readily Purchasable (CAS): No (N/A) As the BPin (CAS): Yes (1256359-09-7)
Spectra Available in the Literature: Yes[2]
^{1}H NMR (500 MHz, $CDCl_3$) δ 7.95 (d, J = 1.0 Hz, 1H), 7.89 (d, J = 1.0 Hz, 1H), 7.68 (dd, J = 8.2, 1.0 Hz, 1H), 7.58 (dd, J = 8.1, 0.8 Hz, 1H), 4.40 (dqd, J = 12.3, 6.2, 2.9 Hz, 1H), 4.12 (s, 3H), 1.91 (dd, J = 13.9, 2.9 Hz, 1H), 1.64 (dd, J = 13.7, 11.9 Hz, 1H), 1.41 (s, 3H), 1.40 (s, 3H), 1.39 (d, J = 6.2 Hz, 3H).
^{13}C NMR (126 MHz, $CDCl_3$) δ 139.89, 132.42, 125.41, 125.16, 119.75, 114.74, 71.25, 65.20, 46.08, 35.59, 31.34, 28.23, 23.27.
HRMS (ESI) Calculated for $C_{14}H_{19}BN_2O_2$ ($[M+H]^+$): 258.1649, measured: 258.1651.

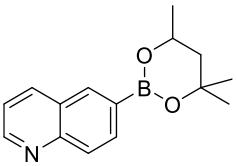

(12a) 2-(6-Quinoline)-4,4,6-trimethyl-1,3,2-dioxaborinane: Prepared according to the general procedure in Section II using Quinoline-6-boronic acid (3 mmol, 519 mg).
Reaction duration: 16 h. Purification: Extraction.
Yield: 64% (490 mg), colorless oil.
Readily Purchasable (CAS): No (N/A) As the BPin (CAS): Yes (406463-06-7)
Spectra Available in the Literature: Yes[2]
^{1}H NMR (500 MHz, $CDCl_3$) δ 8.93 (dd, J = 4.4, 1.7 Hz, 1H), 8.33 (d, J = 1.3 Hz, 1H), 8.21 (dd, J = 8.4, 1.6 Hz, 1H), 8.14 (dd, J = 8.5, 1.4 Hz, 1H), 8.07 (d, J = 8.4 Hz, 1H), 7.39 (dd, J = 8.2, 4.2 Hz, 1H), 4.43 (dqd, J = 12.3, 6.2, 2.9 Hz, 1H), 1.93 (dd, J = 13.9, 2.9 Hz, 1H), 1.67 (dd, J = 13.9, 11.6 Hz, 1H), 1.45 (s, 3H), 1.43 (s, 3H), 1.42 (d, J = 6.2 Hz, 3H).
^{13}C NMR (126 MHz, $CDCl_3$) δ 150.84, 149.57, 136.69, 134.62, 133.92, 128.05, 127.66, 120.83, 71.37, 65.26, 46.05, 31.31, 28.24, 23.23.
HRMS (ESI) Calculated for $C_{15}H_{18}BNO_2$ ($[M+H]^+$): 255.1540, measured: 255.1540.

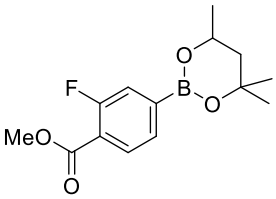

(13a) 2-(3-Fluoro-4-Methoxycarbonylphenyl)-4,4,6-trimethyl-1,3,2-dioxaborinane: Prepared according to the general procedure in Section II using 3-Fluoro-4-Methoxycarbonylphenyl boronic acid (3 mmol, 594 mg).
Reaction duration: 16 h. Purification: Extraction.
Yield: 90% (758 mg), colorless oil.
Readily Purchasable (CAS): No (1214273-29-6) As the BPin (CAS): Yes (603122-52-7)
Spectra Available in the Literature: Yes[2]
^{1}H NMR (500 MHz, $CDCl_3$) δ 7.89 (t, J = 7.4 Hz, 1H), 7.62 (dd, J = 7.6, 1.0 Hz, 1H), 7.55 (dd, J = 11.6, 1.0 Hz, 1H), 4.37 (dqd, J = 12.3, 6.2, 2.9 Hz, 1H), 3.95 (s, 3H), 1.91 (dd, J = 14.0, 3.0 Hz, 1H), 1.69 – 1.57 (m, 1H), 1.40 (s, 3H), 1.39 (s, 3H), 1.37 (d, J = 6.2 Hz, 3H).
^{13}C NMR (126 MHz, $CDCl_3$) δ 165.25 (d, J = 3.6 Hz), 161.46 (d, J = 259.4 Hz), 130.96, 128.94 (d, J = 3.7 Hz), 121.69 (d, J = 20.6 Hz), 119.70 (d, J = 10.0 Hz), 71.62, 65.39, 52.26, 45.92, 31.14, 28.15, 23.06.
^{19}F NMR (377 MHz, $CDCl_3$) δ -112.13.
HRMS (ESI) Calculated for $C_{14}H_{18}BFO_4$ ($[M+H]^+$): 280.1391, measured: 280.1390.

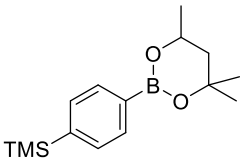

(14a) 2-(4-Trimethylsilylphenyl)-4,4,6-trimethyl-1,3,2-dioxaborinane: Prepared per the general procedure in Section II using 4-Trimethylsilylphenylboronic acid (2.5 mmol, 485 mg).
Reaction duration: 16 h. Purification: Extraction.
Yield: 96% (662 mg), white solid (becomes pink over time on the shelf).
Readily Purchasable (CAS): No (N/A) As BPin (CAS): Yes (1186026-67-4)
Spectra Available in the Literature: Yes[2]
^{1}H NMR (500 MHz, $CDCl_3$) δ 7.78 (d, J = 7.8 Hz, 2H), 7.50 (d, J = 8.1 Hz, 2H), 4.34 (dqd, J = 12.3, 6.2, 3.0 Hz, 1H), 1.86 (dd, J = 13.8, 2.9 Hz, 1H), 1.58 (dd, J = 14.2, 11.6 Hz, 1H), 1.37 (s, 3H), 1.36 (s, 3H), 1.34 (d, J = 6.2 Hz, 3H), 0.26 (s, 9H).
^{13}C NMR (126 MHz, $CDCl_3$) δ 142.79, 132.87, 132.36, 70.90, 64.94, 46.07, 31.28, 28.13, 23.23, -1.21.
HRMS (ESI) Calculated for $C_{15}H_{25}BO_2Si$ ($[M+H]^+$): 276.1826, measured: 276.1824.

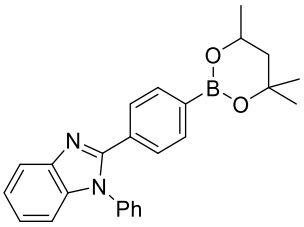

(15a) 2-(4-(1-Phenyl-1*H*-benzimidazol-2-yl)phenyl)-4,4,6-trimethyl-1,3,2-dioxaborinane: Prepared according to the general procedure in Section II using 4-(1-Phenyl-1H-benzimidazol-2-yl)phenylboronic acid (2 mmol, 628 mg).
Reaction duration: 16 h. Purification: Extraction.
Yield: 68% (808 mg), white solid.
Readily Purchasable (CAS): No (N/A) As the BPin (CAS): No (1146340-38-6)
Spectra Available in the Literature: Yes[2]
^{1}H NMR (500 MHz, $CDCl_3$) δ 7.92 (dt, J = 8.0, 0.9 Hz, 1H), 7.79 – 7.74 (m, 2H), 7.60 – 7.54 (m, 2H), 7.54 – 7.44 (m, 3H), 7.39 – 7.23 (m, 5H), 4.35 (dqd, J = 12.3, 6.2, 2.9 Hz, 1H), 1.88 (dd, J = 13.9, 2.9 Hz, 1H), 1.60 (dd, J = 13.9, 11.6 Hz, 1H), 1.38 (s, 3H), 1.37 (s, 3H), 1.35 (d, J = 6.2 Hz, 3H).
^{13}C NMR (126 MHz, $CDCl_3$) δ 152.68, 143.06, 137.29, 137.11, 133.61, 131.45, 129.82, 128.47, 127.45, 123.29, 122.94, 119.86, 110.43, 71.21, 65.11, 45.99, 31.25, 28.19, 23.17.
HRMS (ESI) Calculated for $C_{25}H_{25}BN_2O_2$ ($[M+H]^+$): 396.2118, measured: 396.2115.

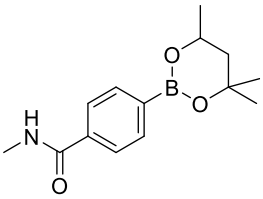

(16a) 2-(4-(N-Methylaminocarbonyl)phenyl)-4,4,6-trimethyl-1,3,2-dioxaborinane: Prepared according to the general procedure in Section II using 4-(N-Methylaminocarbonyl)phenyl boronic acid (2.5 mmol, 450 mg).
Reaction duration: 16 h. Purification: Extraction.
Yield: 90% (587 mg), white solid.
Readily Purchasable (CAS): No (N/A) As the BPin (CAS): Yes (214360-57-3)
Spectra Available in the Literature: Yes[2]
^{1}H NMR (500 MHz, $CDCl_3$) δ 7.78 (d, J = 8.2 Hz, 2H), 7.64 (d, J = 8.2 Hz, 2H), 6.08 (s, 1H), 4.28 (dqd, J = 12.3, 6.2, 2.9 Hz, 1H), 2.95 (d, J = 4.8 Hz, 3H), 1.81 (dd, J = 13.9, 2.9 Hz, 1H), 1.56 – 1.48 (m, 1H), 1.31 (s, 3H), 1.30 (s, 3H), 1.28 (d, J = 6.2 Hz, 3H).
^{13}C NMR (126 MHz, $CDCl_3$) δ 168.41, 135.96, 133.97, 125.70, 71.30, 65.18, 46.00, 31.24, 28.19, 26.82, 23.16.
HRMS (ESI) Calculated for $C_{14}H_{20}BNO_3$ ($[M+H]^+$): 261.1645, measured: 261.1647.

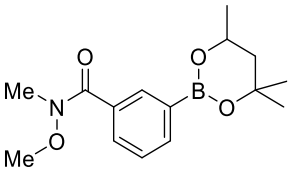

(17a) 2-(3-(N,O-Dimethylhydroxylaminocarbonyl)phenyl)-4,4,6-trimethyl-1,3,2-dioxaborinane: Prepared according to the general procedure in Section II using 3-(N,O-Dimethylhydroxylaminocarbonyl)phenylboronic acid (3 mmol, 627 mg).
Reaction duration: 16 h. Purification: Extraction.
Yield: 93% (809 mg), colorless oil.
Readily Purchasable (CAS): No (N/A) As the BPin (CAS): Yes (957061-17-5)
Spectra Available in the Literature: Yes[2]
^{1}H NMR (500 MHz, $CDCl_3$) δ 8.10 (d, J = 1.7 Hz, 1H), 7.90 (dd, J = 7.5, 1.5 Hz, 1H), 7.69 (dt, J = 7.8, 1.6 Hz, 1H), 7.38 (t, J = 7.5 Hz, 1H), 4.36 (dqd, J = 12.3, 6.2, 2.9 Hz, 1H), 3.58 (s, 3H), 3.36 (s, 3H), 1.89 (dd, J = 13.9, 2.9 Hz, 1H), 1.60 (dd, J = 13.9, 11.6 Hz, 1H), 1.39 (s, 3H), 1.38 (s, 3H), 1.36 (d, J = 6.2 Hz, 3H).
^{13}C NMR (126 MHz, $CDCl_3$) δ 170.68, 135.89, 133.42, 133.32, 129.79, 127.03, 71.18, 65.10, 60.95, 46.02, 31.27, 28.18, 23.19.
HRMS (ESI) Calculated for $C_{15}H_{22}BNO_4$ ($[M+H]^+$): 291.1751, measured: 291.1749.

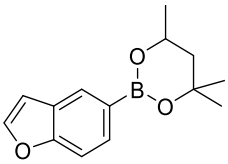

(18a) 2-(5-Benzofuran)-4,4,6-trimethyl-1,3,2-dioxaborinane: Prepared according to the general procedure in Section II using Benzofuran-5-boronic acid (2.5 mmol, 405 mg).
Reaction duration: 16 h. Purification: Extraction.
Yield: >99% (609 mg), slightly yellow oil.
Readily Purchasable (CAS): No (N/A) As the BPin (CAS): Yes (519054-55-8)
Spectra Available in the Literature: Yes[2]
^{1}H NMR (500 MHz, $CDCl_3$) δ 8.11 (s, 1H), 7.78 (d, J = 8.3 Hz, 1H), 7.59 (d, J = 2.2 Hz, 1H), 7.48 (d, J = 8.4 Hz, 1H), 6.77 (d, J = 1.2 Hz, 1H), 4.38 (dqd, J = 12.4, 6.2, 2.9 Hz, 1H), 1.88 (dd, J = 13.8, 2.9 Hz, 1H), 1.62 (dd, J = 13.8, 11.6 Hz, 1H), 1.40 (s, 3H), 1.39 (s, 3H), 1.38 (d, J = 6.2 Hz, 3H).
^{13}C NMR (126 MHz, $CDCl_3$) δ 156.71, 144.56, 129.93, 127.41, 126.91, 110.46, 106.74, 71.00, 65.01, 46.08, 31.38, 28.22, 23.30.
HRMS (ESI) Calculated for $C_{14}H_{17}BO_3$ ($[M+H]^+$): 244.1380, measured: 244.1379.

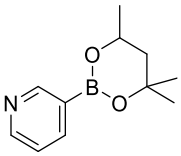

(19a) 2-(3-Pyridyl)-4,4,6-trimethyl-1,3,2-dioxaborinane: Prepared according to the general procedure in Section II using Pyridine-3-boronic acid (2 mmol, 246 mg) with methanol as the solvent instead of dichloromethane.
Reaction duration: 16 h. Purification: Extraction and a filtration over a frit with 90% pentane/Et_2O (collected the filtrate).
Yield: 50% (205 mg), yellow oil.
Readily Purchasable (CAS): No (N/A) As the BPin (CAS): Yes (329214-79-1)
Spectra Available in the Literature: Yes[2]
^{1}H NMR (500 MHz, $CDCl_3$) δ 8.92 (t, J = 1.3 Hz, 1H), 8.60 (dd, J = 4.9, 1.9 Hz, 1H), 8.03 (dt, J = 7.5, 1.9 Hz, 1H), 7.22 (ddd, J = 7.5, 4.9, 1.0 Hz, 1H), 4.35 (dqd, J = 12.3, 6.2, 2.9 Hz, 1H), 1.88 (dd, J = 14.0, 3.0 Hz, 1H), 1.60 (dd, J = 14.0, 11.6 Hz, 1H), 1.37 (s, 3H), 1.36 (s, 3H), 1.34 (d, J = 6.2 Hz, 3H).
^{13}C NMR (126 MHz, $CDCl_3$) δ 154.86, 151.12, 141.36, 122.83, 71.41, 65.24, 46.02, 31.19, 28.15, 23.12.
HRMS (ESI) Calculated for $C_{11}H_{16}BNO_2$ ($[M+H]^+$): 205.1383, measured: 205.1385.

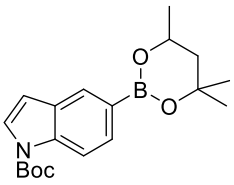

(20a) 2-(5-H-Indole)-4,4,6-trimethyl-1,3,2-dioxaborinane: Prepared according to the general procedure in Section II using 1H-Indole-5-boronic acid (1 mmol, 161 mg).
Reaction duration: 16 h. Purification: Extraction and a SiO_2 plug, 90% pentane/Et_2O.
Yield: 82%
Boc Protection[5]: The H-IndoleBdiol (0.82 mmol, 200 mg, 1 equiv.) was stirred with Boc_2O (1.97 mmol, 429 mg, 2.4 equiv.), Triethylamine (0.98 mmol, 137 µL, 1.2 equiv.), and 4-Dimethylaminopyridine (0.082 mmol, 10 mg, 0.1 equiv.) in dichloromethane (1 mL, 0.8 M).
Reaction duration: 24 h. Purification: Acidic extraction and a SiO_2 plug, 90% pentane/Et_2O.
Overall Yield: 63% (82% and 77% respectively, yielding 216 mg of product), white solid.
Readily Purchasable (CAS): No (N/A) As the BPin (CAS): Yes (777061-36-6)
Spectra Available in the Literature: Yes[2]
^{1}H NMR (500 MHz, $CDCl_3$) δ 8.09 (d, J = 8.3 Hz, 1H), 8.04 (d, J = 1.0 Hz, 1H), 7.77 (dd, J = 8.4, 1.2 Hz, 1H), 7.55 (d, J = 3.8 Hz, 1H), 6.57 (d, J = 3.8 Hz, 1H), 4.37 (dqd, J = 12.3, 6.2, 2.9 Hz, 1H), 1.88 (dd, J = 13.9, 2.9 Hz, 1H), 1.67 (s, 9H), 1.62 (dd, J = 13.9, 11.6 Hz, 1H), 1.40 (s, 3H), 1.39 (s, 3H), 1.37 (d, J = 6.2 Hz, 3H).
^{13}C NMR (126 MHz, $CDCl_3$) δ 149.84, 136.83, 130.11, 129.76, 127.05, 125.53, 114.15, 107.70, 83.51, 70.94, 64.96, 46.10, 31.39, 28.24, 28.23, 23.31.
HRMS (ESI) Calculated for $C_{19}H_{26}BNO_4$ ($[M+H]^+$): 343.2064, measured: 343.2060.

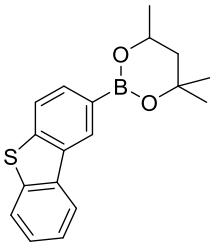

(21a) 2-(2-Dibenzothiophene)-4,4,6-trimethyl-1,3,2-dioxaborinane: Prepared according to the general procedure in Section II using Dibenzothiophene-2-boronic acid (3 mmol, 684 mg).
Reaction duration: 16 h. Purification: Extraction.
Yield: 85% (792 mg), white solid.
Readily Purchasable (CAS): No (N/A) As the BPin (CAS): No (890042-21-4)
Spectra Available in the Literature: Yes[2]
^{1}H NMR (500 MHz, $CDCl_3$) δ 8.64 (d, J = 7.6 Hz, 1H), 8.39 – 8.28 (m, 1H), 7.94 (d, J = 7.9 Hz, 1H), 7.87 (td, J = 7.2, 2.3 Hz, 2H), 7.48 (tt, J = 4.6, 1.8 Hz, 2H), 4.44 (dqd, J = 12.3, 6.1, 3.2 Hz, 1H), 1.94 (dd, J = 13.9, 2.9 Hz, 1H), 1.68 (dd, J = 13.8, 11.7 Hz, 1H), 1.49 – 1.41 (m, 9H).
^{13}C NMR (126 MHz, $CDCl_3$) δ 141.80, 139.17, 135.87, 134.95, 131.95, 127.21, 126.43, 124.29, 122.70, 121.80, 71.22, 65.17, 46.12, 31.38, 28.26, 23.31.

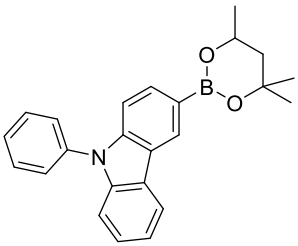

(22a) 2-(3-(9-Phenyl-9H-carbazole))-4,4,6-trimethyl-1,3,2-dioxaborinane: Prepared according to the general procedure in Section II using 9-Phenyl-9H-carbazole-3-boronic acid (4 mmol, 1.15 g).
Reaction duration: 16 h. Purification: Extraction.
Yield: 93% (1.366 g), white solid.
Readily Purchasable (CAS): No (N/A) As the BPin (CAS): Yes (1126522-69-7)
Spectra Available in the Literature: Yes[2]
^{1}H NMR (500 MHz, $CDCl_3$) δ 8.55 (t, J = 0.9 Hz, 1H), 8.13 (dt, J = 7.6, 1.0 Hz, 1H), 7.80 (dd, J = 8.3, 1.1 Hz, 1H), 7.56 – 7.47 (m, 4H), 7.41 – 7.36 (m, 1H), 7.34 – 7.26 (m, 3H), 7.21 (ddd, J = 8.0, 5.5, 2.6 Hz, 1H), 4.34 (dqd, J = 12.3, 6.2, 2.9 Hz, 1H), 1.83 (dd, J = 13.8, 2.9 Hz, 1H), 1.58 (dd, J = 13.8, 11.6 Hz, 1H), 1.37 (s, 3H), 1.35 (s, 3H), 1.34 (d, J = 6.2 Hz, 3H).
^{13}C NMR (126 MHz, $CDCl_3$) δ 142.61, 140.96, 137.74, 131.62, 129.82, 127.38, 127.12, 126.50, 125.60, 123.80, 122.94, 120.49, 119.98, 109.66, 108.81, 70.96, 65.01, 46.20, 31.46, 28.27, 23.39.
HRMS (ESI) Calculated for $C_{24}H_{24}BNO_2$ ($[M+H]^+$): 369.2009, measured: 369.2007.

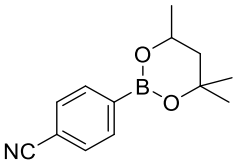

(23a) 2-(4-Cyanophenyl)-4,4,6-trimethyl-1,3,2-dioxaborinane: Prepared according to the general procedure in Section II using 4-Cyanophenylboronic acid (2.5 mmol, 367 mg).
Reaction duration: 16 h. Purification: Extraction.
Yield: 87% (498 mg), white solid.
Readily Purchasable (CAS): Yes (1092060-81-5) As the BPin (CAS): (171364-82-2)
Spectra Available in the Literature: Yes[3]
^{1}H NMR (500 MHz, $CDCl_3$) δ 7.88 (d, J = 8.1 Hz, 2H), 7.59 (d, J = 6.3 Hz, 2H), 4.36 (dqd, J = 12.3, 6.2, 2.9 Hz, 1H), 1.89 (dd, J = 14.0, 2.9 Hz, 1H), 1.60 (dd, J = 14.0, 11.7 Hz, 1H), 1.37 (s, 3H), 1.36 (s, 3H), 1.35 (d, J = 6.2 Hz, 3H).
^{13}C NMR (126 MHz, $CDCl_3$) δ 134.17, 130.91, 119.29, 113.55, 71.62, 65.40, 45.93, 31.16, 28.16, 23.08.

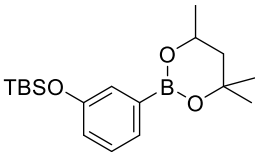

(24a) 2-(3-*tert*-Butyldimethylsilyloxyphenyl)-4,4,6-trimethyl-1,3,2-dioxaborinane: Prepared according to the general procedure in Section II using 3-(*tert*-Butyldimethylsilyloxy)-phenylboronic acid (2.5 mmol, 630 mg).
Reaction duration: 16 h. Purification: Extraction.
Yield: 87% (725 mg), colorless oil.
Readily Purchasable (CAS): No (N/A) As the BPin (CAS): Yes (902120-00-7)
Spectra Available in the Literature: Yes[2]
^{1}H NMR (500 MHz, $CDCl_3$) δ 7.40 (dd, J = 7.3, 1.1 Hz, 1H), 7.27 (d, J = 2.6 Hz, 1H), 7.20 (t, J = 7.6 Hz, 1H), 6.87 (ddd, J = 7.9, 2.7, 1.2 Hz, 1H), 4.33 (dqd, J = 12.3, 6.2, 2.9 Hz, 1H), 1.85 (dd, J = 13.9, 3.0 Hz, 1H), 1.58 (dd, J = 14.0, 11.8 Hz, 1H), 1.36 (s, 3H), 1.35 (s, 3H), 1.34 (d, J = 6.2 Hz, 3H), 0.99 (s, 9H), 0.20 (s, 6H).
^{13}C NMR (126 MHz, $CDCl_3$) δ 154.99, 128.49, 126.64, 125.09, 121.99, 70.92, 64.93, 46.01, 31.26, 28.15, 25.75, 23.19, 18.21, -4.16, -4.38, -4.61.
HRMS (ESI) Calculated for $C_{18}H_{31}BO_3Si$ ($[M+H]^+$): 334.2245, measured: 334.2244.

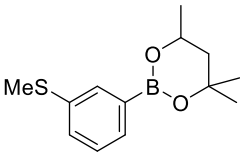

(25a) 2-(3-Methylthiophenyl)-4,4,6-trimethyl-1,3,2-dioxaborinane: Prepared according to the general procedure in Section II using 3-Methylthiophenylboronic acid (2.5 mmol, 420 mg).
Reaction duration: 16 h. Purification: Extraction and a SiO_2 plug, 90% pentane/Et_2O.
Yield: 94% (587 mg), off-white solid.
Readily Purchasable (CAS): No (N/A) As the BPin (CAS): Yes (710348-63-3)
Spectra Available in the Literature: Yes[2]
^{1}H NMR (500 MHz, $CDCl_3$) δ 7.73 (dd, J = 2.0, 1.0 Hz, 1H), 7.59 (dt, J = 7.3, 1.3 Hz, 1H), 7.32 (ddd, J = 7.8, 2.2, 1.4 Hz, 1H), 7.26 (dd, J = 8.6, 6.4 Hz, 1H), 4.34 (dqd, J = 12.3, 6.2, 2.9 Hz, 1H), 2.50 (s, 3H), 1.87 (dd, J = 13.9, 2.9 Hz, 1H), 1.58 (dd, J = 14.1, 11.4 Hz, 1H), 1.37 (s, 3H), 1.36 (s, 3H), 1.35 (d, J = 6.2 Hz, 3H).
^{13}C NMR (126 MHz, $CDCl_3$) δ 137.16, 132.37, 130.66, 128.88, 127.98, 71.11, 65.07, 46.02, 31.26, 28.16, 23.20, 16.18.
HRMS (ESI) Calculated for $C_{13}H_{19}BO_2S$ ($[M+H]^+$): 250.1308, measured: 250.1310.

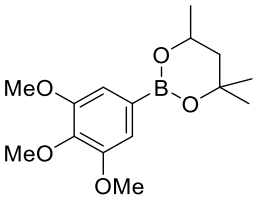

(26a) 2-(3,4,5-Methoxyphenyl)-4,4,6-trimethyl-1,3,2-dioxaborinane: Prepared according to the general procedure in Section II using 3,4,5-Methoxyphenylboronic acid (1.5 mmol, 318 mg).
Reaction duration: 16 h. Purification: Extraction.
Yield: 76% (337 mg), white solid.
Readily Purchasable (CAS): No (N/A) As the BPin (CAS): Yes (214360-67-5)
Spectra Available in the Literature: Yes[2]
^{1}H NMR (500 MHz, $CDCl_3$) δ 7.04 (s, 2H), 4.34 (dqd, J = 12.3, 6.2, 2.9 Hz, 1H), 3.90 (s, 6H), 3.85 (s, 3H), 1.86 (dd, J = 13.9, 2.9 Hz, 1H), 1.57 (dd, J = 13.9, 11.6 Hz, 1H), 1.38 (s, 3H), 1.36 (s, 3H), 1.35 (d, J = 6.2 Hz, 3H).
^{13}C NMR (126 MHz, $CDCl_3$) δ 152.70, 140.17, 110.32, 71.10, 65.08, 60.75, 56.07, 46.04, 31.27, 28.14, 23.23.
HRMS (ESI) Calculated for $C_{15}H_{23}BO_5$ ($[M+H]^+$): 294.1748, measured: 294.1747.

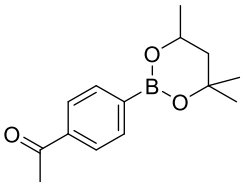

(27a) 2-(4-Acetylphenyl)-4,4,6-trimethyl-1,3,2-dioxaborinane: Prepared according to the general procedure in Section II using 4-Acetylphenylboronic acid (2.5 mmol, 408 mg).
Reaction duration: 16 h. Purification: Extraction and a SiO_2 plug, 90% pentane/Et_2O.
Yield: 95% (587 mg), colorless oil.
Readily Purchasable (CAS): Yes (934558-34-6) As the BPin (CAS): Yes (171364-81-1)
Spectra Available in the Literature: Yes[6]
^{1}H NMR (500 MHz, $CDCl_3$) δ 7.92 – 7.87 (m, 4H), 4.36 (dqd, J = 12.3, 6.2, 2.9 Hz, 1H), 2.60 (s, 3H), 1.89 (dd, J = 14.0, 2.9 Hz, 1H), 1.60 (dd, J = 13.7, 11.8 Hz, 1H), 1.38 (s, 3H), 1.37 (s, 3H), 1.36 (d, J = 6.2 Hz, 3H).
^{13}C NMR (126 MHz, $CDCl_3$) δ 198.70, 138.33, 133.93, 127.11, 71.38, 65.24, 45.99, 31.23, 28.19, 26.77, 23.15.

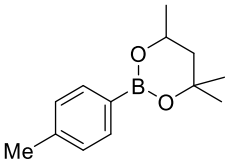

(28a) 2-(4-Methylphenyl)-4,4,6-trimethyl-1,3,2-dioxaborinane: Prepared according to the general procedure in Section II using 4-Methylphenylboronic acid (7.5 mmol, 1.02 g).
Reaction duration: 4 h. Purification: Extraction.
Yield: 83% (1.36 g), colorless oil (with some suspended white solid in the oil).
Readily Purchasable (CAS): Yes (1092060-77-9) As BPin (CAS): Yes (195062-57-8)
Spectra Available in the Literature: Yes[3]
^{1}H NMR (500 MHz, $CDCl_3$) δ 7.72 (d, J = 7.6 Hz, 2H), 7.16 (d, J = 7.5 Hz, 2H), 4.34 (dqd, J = 12.4, 6.2, 2.9 Hz, 1H), 2.36 (s, 3H), 1.86 (dd, J = 13.8, 2.9 Hz, 1H), 1.59 (dd, J = 14.3, 12.2 Hz, 1H), 1.38 (s, 3H), 1.37 (s, 3H), 1.35 (d, J = 6.2 Hz, 3H).
^{13}C NMR (126 MHz, $CDCl_3$) δ 140.23, 133.82, 128.26, 70.85, 64.89, 46.09, 31.35, 28.19, 23.28, 21.67.

2A.IX. Experimental Data for 1,1-Diarylalkane Products (Compounds 1-43)

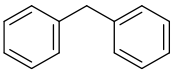

(1) Diphenylmethane: Prepared from **1a** (0.5 mmol, 102.1 mg) and toluene (0.3 M, 1.6 mL) according to Section III.
Reaction duration: 48 h. Purification: Removed solvent, SiO_2 plug w/ 100:1 pentane/EtOAc, reverse-phase column MeOH/H_2O with 0.1% TFA 89%→100%, extraction with 90% pentane/Et_2O.
Yield: 78% (70%, 58.8 mg), colorless oil.
Readily Purchasable (CAS): Yes (101-81-5)
Spectra Available in the Literature: Yes[7]
^{1}H NMR (500 MHz, $CDCl_3$) δ 7.35 – 7.28 (m, 4H), 7.25 – 7.20 (m, 6H), 4.02 (s, 2H).
^{13}C NMR (126 MHz, $CDCl_3$) δ 141.12, 128.94, 128.46, 126.07, 41.95.

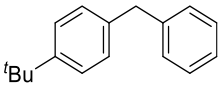

(2) 4-*tert*-Butyldiphenylmethane: Prepared from **2a** (0.5 mmol, 130.1 mg) and toluene (0.3 M, 1.6 mL) according to Section III.
Reaction duration: 48 h. Purification: Removed solvent, SiO_2 plug w/ 100:1 pentane/EtOAc, reverse-phase column MeOH/H_2O with 0.1% TFA 89%→100%, extraction with 90% pentane/Et_2O.
Yield: 76% (64%, 71.7 mg), colorless oil.
Readily Purchasable (CAS): No (16251-99-3)
Spectra Available in the Literature: Yes[7]
^{1}H NMR (500 MHz, $CDCl_3$) δ 7.35 – 7.28 (m, 4H), 7.25 – 7.19 (m, 3H), 7.14 (d, J = 8.0 Hz, 2H), 3.98 (s, 2H), 1.33 (s, 9H).
^{13}C NMR (126 MHz, $CDCl_3$) δ 148.82, 141.27, 138.07, 128.96, 128.50, 128.42, 125.99, 125.34, 41.44, 34.37, 31.40.

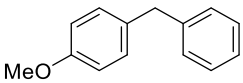

(3) 4-Methoxydiphenylmethane: Prepared from **3a** (0.5 mmol, 117.1 mg) and toluene (0.3 M, 1.6 mL) according to Section III.
Reaction duration: 48 h. Purification: Removed solvent, SiO_2 plug w/ 100:1 pentane/EtOAc, reverse-phase column MeOH/H_2O with 0.1% TFA 80%→100%, extraction with 90% pentane/Et_2O.
Yield: 70% (61%, 60.5 mg), cloudy oil.
Readily Purchasable (CAS): Yes (834-14-0)
Spectra Available in the Literature: Yes[7]
^{1}H NMR (500 MHz, $CDCl_3$) δ 7.32 – 7.27 (m, 2H), 7.23 – 7.17 (m, 3H), 7.12 (d, J = 8.7 Hz, 2H), 6.85 (d, J = 8.6 Hz, 2H), 3.94 (s, 2H), 3.80 (s, 3H).
^{13}C NMR (126 MHz, $CDCl_3$) δ 157.97, 141.60, 133.26, 129.88, 128.83, 128.44, 125.99, 113.88, 55.27, 41.05.

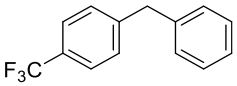

(4) 4-Trifluoromethyldiphenylmethane: Prepared from **13a** (0.5 mmol, 136.0 mg) and toluene (0.3 M, 1.6 mL) according to Section III.
Reaction duration: 48 h. Purification: Removed solvent, SiO_2 plug w/ 100:1 pentane/EtOAc, reverse-phase column MeOH/H_2O with 0.1% TFA 89%→100%, extraction with 90% pentane/Et_2O.
Yield: 63% (56%, 66.1 mg), off-white solid.
Readily Purchasable (CAS): Yes (34239-04-8)
Spectra Available in the Literature: Yes[7]
^{1}H NMR (500 MHz, $CDCl_3$) δ 7.54 (d, J = 8.0 Hz, 2H), 7.34 – 7.28 (m, 4H), 7.24 (t, J = 7.4 Hz, 1H), 7.18 (d, J = 7.1 Hz, 2H), 4.04 (s, 2H).
^{13}C NMR (126 MHz, $CDCl_3$) δ 145.20 (q, J = 1.6 Hz), 143.25, 139.98, 129.19, 128.94, 128.67, 128.48 (q, J = 32.4 Hz), 126.47, 125.40 (q, J = 3.8 Hz), 41.73.
^{19}F NMR (377 MHz, $CDCl_3$) δ -62.37.

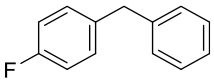

(5) 4-Fluorodiphenylmethane: Prepared from **5a** (0.5 mmol, 111.1 mg) and toluene (0.3 M, 1.6 mL) according to Section III.
Reaction duration: 48 h. Purification: Removed solvent, SiO_2 plug w/ 100:1 pentane/EtOAc, reverse-phase column MeOH/H_2O with 0.1% TFA 85%→100%, extraction with 90% pentane/Et_2O.
Yield: 70% (54%, 50.2 mg), slightly yellow oil.
OR
(5') Prepared from **1a** (0.5 mmol, 102.1 mg) and 4-fluorotoluene (0.3 M, 1.6 mL) according to Section III.
Reaction duration: 48 h. Purification: Removed solvent, SiO_2 plug w/ 100:1 pentane/EtOAc, reverse-phase column MeOH/H_2O with 0.1% TFA 89%→100%, extraction with 90% pentane/Et_2O.
Yield: 70%, slightly yellow oil. The product was obtained from the column as a mixture with <10% biaryl.
Readily Purchasable (CAS): Yes (587-79-1)
Spectra Available in the Literature: Yes[7]
^{1}H NMR (500 MHz, $CDCl_3$) δ 7.20 (t, J = 7.5 Hz, 2H), 7.14 – 7.10 (m, 1H), 7.10 – 7.02 (m, 4H), 6.88 (t, J = 8.7 Hz, 2H), 3.86 (s, 2H).
^{13}C NMR (126 MHz, $CDCl_3$) δ 161.44 (d, J = 243.9 Hz), 140.96, 136.79 (d, J = 3.2 Hz), 130.30 (d, J = 7.9 Hz), 128.85, 128.56, 126.23, 115.23 (d, J = 21.2 Hz), 41.11.
^{19}F NMR (377 MHz, $CDCl_3$) δ -117.44.

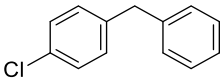

(6) 4-Chlorodiphenylmethane: Prepared from **6a** (0.5 mmol, 119.2 mg) and toluene (0.3 M, 1.6 mL) according to Section III.
Reaction duration: 48 h. Purification: Removed solvent, SiO_2 plug w/ 100:1 pentane/EtOAc, reverse-phase column MeOH/H_2O with 0.1% TFA 89%→100%, extraction with 90% pentane/Et_2O.
Yield: 65%, light yellow oil. The product was obtained from the column as a mixture with 12% bibenzyl.
Readily Purchasable (CAS): Yes (831-81-2)
Spectra Available in the Literature: Yes[8]
^{1}H NMR (500 MHz, $CDCl_3$) δ 7.30 (t, J = 7.5 Hz, 2H), 7.26 (d, J = 8.4 Hz, 2H), 7.24 – 7.20 (m, 1H), 7.17 (d, J = 7.0 Hz, 2H), 7.12 (d, J = 8.4 Hz, 2H), 3.96 (s, 2H).
^{13}C NMR (126 MHz, $CDCl_3$) δ 140.54, 139.57, 131.88, 130.24, 128.85, 128.56, 128.55, 126.28, 41.24.

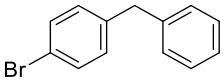

(7) 4-Bromodiphenylmethane: Prepared from **7a** (0.5 mmol, 141.5 mg) and toluene (0.3 M, 1.6 mL) according to Section III.
Reaction duration: 48 h. Purification: Removed solvent, SiO_2 plug w/ 100:1 pentane/EtOAc, reverse-phase column MeOH/H_2O with 0.1% TFA 89%→100%, extraction with 90% pentane/Et_2O.
Yield: 64%, off-white oil. The product was obtained from the column as a mixture with ~20% bibenzyl.
OR
(7') Prepared from **1a** (0.5 mmol, 102.1 mg) and 4-bromotoluene (0.3 M, 1.6 mL) per Section III.
Reaction duration: 48 h. Purification: Removed solvent, SiO_2 plug w/ 100:1 pentane/EtOAc, reverse-phase column MeOH/H_2O with 0.1% TFA 89%→100%, extraction with 90% pentane/Et_2O.
Yield: 61% (55%, 67.7 mg), off-white oil.
Readily Purchasable (CAS): Yes (2116-36-1)
Spectra Available in the Literature: Yes[8]
^{1}H NMR (500 MHz, $CDCl_3$) δ 7.40 (d, J = 8.4 Hz, 2H), 7.30 (t, J = 7.4 Hz, 2H), 7.24 – 7.19 (m, 1H), 7.16 (d, J = 7.0 Hz, 2H), 7.06 (d, J = 8.4 Hz, 2H), 3.94 (s, 2H).
^{13}C NMR (126 MHz, $CDCl_3$) δ 140.43, 140.08, 131.50, 130.65, 128.84, 128.56, 126.29, 119.92, 41.29.

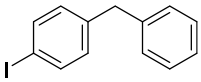

(8) 4-Iododiphenylmethane: Prepared from **8a** (0.5 mmol, 165 mg) and toluene (0.3 M, 1.6 mL) according to Section III.
Reaction duration: 48 h. Purification: Removed solvent, SiO_2 plug w/ 100:1 pentane/EtOAc, reverse-phase column MeOH/H_2O with 0.1% TFA 89%→100%, extraction with 90% pentane/Et_2O.
Yield: 67% (54%, 79.3 mg), colorless oil (decomposes to pink compound over time on bench).
Readily Purchasable (CAS): Yes (35444-94-1)
Spectra Available in the Literature: Yes[9] (Authors are missing some peaks)
^{1}H NMR (500 MHz, $CDCl_3$) δ 7.60 (d, J = 8.4 Hz, 2H), 7.29 (t, J = 7.4 Hz, 2H), 7.21 (t, J = 7.4 Hz, 1H), 7.16 (d, J = 7.5 Hz, 2H), 6.94 (d, J = 7.8 Hz, 2H), 3.92 (s, 2H).
^{13}C NMR (126 MHz, $CDCl_3$) δ 140.78, 140.38, 137.48, 131.00, 128.85, 128.56, 126.29, 91.28, 41.40.
HRMS (ESI) Calculated for $C_{13}H_{11}I$ ($[M+H]^+$): 293.9900, measured: 293.9892.

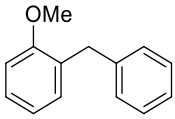

(9) 2-Methoxydiphenylmethane: Prepared from **18a** (0.5 mmol, 117.1 mg) and toluene (0.3 M, 1.6 mL) according to Section III.
Reaction duration: 48 h. Purification: Removed solvent, SiO_2 plug w/ 100:1 pentane/EtOAc, reverse-phase column MeOH/H_2O with 0.1% TFA 70%→100%, extraction with 90% pentane/Et_2O.
Yield: 46% (39%, 38.2 mg), yellow oil.
Readily Purchasable (CAS): No (883-90-9)
Spectra Available in the Literature: Yes[7]
^{1}H NMR (500 MHz, $CDCl_3$) δ 7.30 – 7.24 (m, 2H), 7.24 – 7.15 (m, 4H), 7.09 – 7.05 (m, 1H), 6.91 – 6.84 (m, 2H), 3.98 (s, 2H), 3.82 (s, 3H).
^{13}C NMR (126 MHz, $CDCl_3$) δ 157.30, 140.99, 130.28, 129.63, 128.93, 128.22, 127.37, 125.73, 120.43, 110.36, 55.32, 35.83.

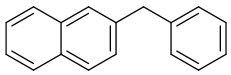

(10) 2-Benzylnapthalene: Prepared from **19a** (0.5 mmol, 127.1 mg) and toluene (0.3 M, 1.6 mL) according to Section III.
Reaction duration: 48 h. Purification: Removed solvent, SiO_2 plug w/ 100:1 pentane/EtOAc, reverse-phase column MeOH/H_2O with 0.1% TFA 89%→100%, extraction with 90% pentane/Et_2O.
Yield: 69% (61%, 66.6 mg), colorless oil.
Readily Purchasable (CAS): No (613-59-2)
Spectra Available in the Literature: Yes[7]
^{1}H NMR (500 MHz, $CDCl_3$) δ 7.85 – 7.76 (m, 3H), 7.67 (s, 1H), 7.46 (pd, J = 6.9, 1.5 Hz, 2H), 7.37 – 7.30 (m, 3H), 7.29 – 7.22 (m, 3H), 4.18 (s, 2H).
^{13}C NMR (126 MHz, $CDCl_3$) δ 140.99, 138.61, 133.62, 132.09, 129.04, 128.51, 128.09, 127.65, 127.63, 127.56, 127.11, 126.16, 125.99, 125.36, 42.13.

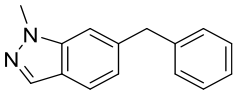

(11) N-Methyl-6-benzylindazole: Prepared from **9a** (0.5 mmol, 129.1 mg) and toluene (0.3 M, 1.6 mL) according to Section III.
Reaction duration: 48 h. Purification: Removed solvent, syringe filtered w/ 9:1 pentane/EtOAc, normal-phase column EtOAc/Pentane 10%→90%. The product was obtained with <10% of the over-benzylated product (analogous to **E** in Figure 2A.1). Reverse-phase column (MeOH/H_2O with 0.1% TFA 89%→100%) was used on that sample to get a pure sample for characterization (with higher yield than the previous method).
Yield: 52% (46%, 52.1 mg), white solid.
Readily Purchasable (CAS): No (N/A)
Spectra Available in the Literature: Yes[2]
^{1}H NMR (500 MHz, $CDCl_3$) δ 7.92 (s, 1H), 7.63 (d, J = 8.3 Hz, 1H), 7.34 – 7.27 (m, 2H), 7.25 – 7.20 (m, 3H), 7.18 (s, 1H), 7.01 (d, J = 8.3 Hz, 1H), 4.14 (s, 2H), 4.03 (s, 3H).
^{13}C NMR (126 MHz, $CDCl_3$) δ 140.93, 140.38, 139.74, 132.55, 128.94, 128.55, 126.24, 122.59, 122.47, 120.95, 108.55, 42.39, 35.48.
HRMS (ESI) Calculated for $C_{15}H_{14}N_2$ ($[M+H]^+$): 223.1230, measured: 223.1229.

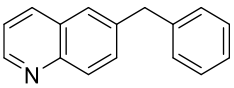

(12) 6-Benzylquinoline: Prepared from **12a** (0.5 mmol, 128 mg) and toluene (0.3 M, 1.6 mL) according to Section III.
Reaction duration: 48 h. Purification: Removed solvent, syringe filtered w/ 9:1 pentane/EtOAc, normal-phase column EtOAc/Pentane 10%→90%. The product was obtained with 13% of the over-benzylated product (analogous to **E** in Figure 2A.1). Reverse-phase column (MeOH/H_2O with 0.1% TFA 89%→100%) was used on that sample to get a pure sample for characterization.
Yield: 39% (31%, 33.8 mg), colorless oil.
Readily Purchasable (CAS): No (54884-99-0)
Spectra Available in the Literature: Yes[2]
^{1}H NMR (500 MHz, $CDCl_3$) δ 8.79 (dd, *J* = 4.2, 1.7 Hz, 1H), 8.00 (dd, *J* = 8.3, 0.9 Hz, 1H), 7.95 (d, *J* = 8.6 Hz, 1H), 7.52 – 7.48 (m, 2H), 7.29 (dd, *J* = 8.3, 4.2 Hz, 1H), 7.27 – 7.21 (m, 2H), 7.20 – 7.12 (m, 3H), 4.10 (s, 2H).
^{13}C NMR (126 MHz, $CDCl_3$) δ 149.90, 147.22, 140.43, 139.58, 135.70, 131.27, 129.54, 129.05, 128.63, 126.79, 126.38, 121.18, 41.90.
HRMS (ESI) Calculated for $C_{16}H_{13}N$ ($[M+H]^+$): 220.1121, measured: 220.1119.

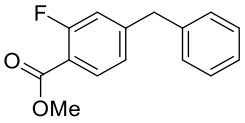

(13) 3-Fluoro-4-methoxycarbonyldiphenylmethane : Prepared from **13a** (0.5 mmol, 140 mg) and toluene (0.3 M, 1.6 mL) according to Section III, except using 20 mol% Phen.
Reaction duration: 48 h. Purification: Removed solvent, syringe filtered w/ 9:1 pentane/EtOAc, normal-phase column EtOAc/Pentane 10%→90%. The product was obtained with <10% of the over-benzylated product. Reverse-phase column (MeOH/H_2O with 0.1% TFA 89%→100%) was used on that sample to get a pure sample for characterization.
Yield: 50% (45%, 54.7 mg), colorless oil.
Readily Purchasable (CAS): No (N/A)
Spectra Available in the Literature: Yes[2]
^{1}H NMR (500 MHz, $CDCl_3$) δ 7.78 (t, *J* = 7.8 Hz, 1H), 7.27 – 7.21 (m, 2H), 7.20 – 7.14 (m, 1H), 7.09 (d, *J* = 6.9 Hz, 2H), 6.96 (d, *J* = 8.0 Hz, 1H), 6.87 (d, *J* = 11.8 Hz, 1H), 3.93 (s, 2H), 3.83 (s, 3H).
^{13}C NMR (126 MHz, $CDCl_3$) δ 164.87 (d, *J* = 3.9 Hz), 163.08, 161.01, 149.04 (d, *J* = 8.4 Hz), 139.22, 132.21 (d, *J* = 1.4 Hz), 128.86 (d, *J* = 28.6 Hz), 126.67, 124.51 (d, *J* = 3.4 Hz), 117.25 (d, *J* = 22.6 Hz), 116.33 (d, *J* = 10.0 Hz), 52.23, 41.63 (d, *J* = 1.5 Hz).
^{19}F NMR (377 MHz, $CDCl_3$) δ -109.62.
HRMS (ESI) Calculated for $C_{15}H_{13}FO_2$ ($[M+H]^+$): 245.0972, measured: 245.0971.

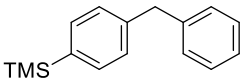

(14) 4-Trimethylsilyldiphenylmethane: Prepared from **20a** (0.5 mmol, 138.1 mg) and toluene (0.3 M, 1.6 mL) according to Section III.
Reaction duration: 48 h. Purification: Removed solvent, SiO_2 plug w/ 100:1 pentane/EtOAc, reverse-phase column MeOH/H_2O with 0.1% TFA 89%→100%, extraction with 90% pentane/Et_2O.
Yield: 71% (59%, 70.8 mg), colorless oil.
Readily Purchasable (CAS): No (17964-29-3)
Spectra Available in the Literature: Yes[7]
^{1}H NMR (500 MHz, $CDCl_3$) δ 7.47 (d, J = 8.1 Hz, 2H), 7.34 – 7.27 (m, 2H), 7.25 – 7.19 (m, 5H), 4.00 (s, 2H), 0.27 (d, J = 1.0 Hz, 9H).
^{13}C NMR (126 MHz, $CDCl_3$) δ 141.73, 140.96, 137.72, 133.54, 128.97, 128.46, 128.32, 126.08, 41.94, -1.06.

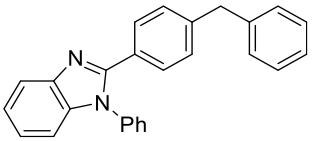

(15) 4-(1-Phenyl-1*H*-benzimidazol-2-yl)diphenylmethane : Prepared from **15a** (0.5 mmol, 198 mg) and toluene (0.3 M, 1.6 mL) according to Section III.
Reaction duration: 48 h. Purification: Removed solvent, syringe filtered w/ 9:1 pentane/EtOAc, normal-phase column EtOAc/Pentane 10%→90%. The product was obtained with <10% of the over-benzylated product. Reverse-phase column (MeOH/H_2O with 0.1% TFA 89%→100%) was used on that sample to get a pure sample for characterization.
Yield: 52% (46%, 82.1 mg), white solid.
Readily Purchasable (CAS): No (N/A)
Spectra Available in the Literature: Yes[2]
^{1}H NMR (500 MHz, $CDCl_3$) δ 7.80 (d, *J* = 7.9 Hz, 1H), 7.49 – 7.36 (m, 5H), 7.26 – 7.10 (m, 8H), 7.08 (d, *J* = 6.7 Hz, 2H), 7.04 (d, *J* = 8.2 Hz, 2H), 3.89 (s, 2H).
^{13}C NMR (126 MHz, $CDCl_3$) δ 152.34, 143.00, 142.64, 140.38, 137.30, 137.10, 129.87, 129.51, 129.00, 128.91, 128.57, 128.51, 127.48, 126.24, 123.22, 122.93, 119.75, 110.40, 41.68.
HRMS (ESI) Calculated for $C_{26}H_{20}N_2$ ($[M+H]^+$): 361.1699, measured: 361.1694.

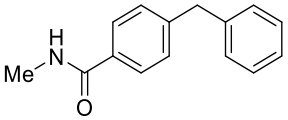

(16) 4-(N-Methylaminocarbonyl)diphenylmethane : Prepared from **16a** (0.5 mmol, 131 mg) and toluene (0.3 M, 1.6 mL) according to Section III, except using 27 mol% Phen.
Reaction duration: 48 h. Purification: Removed solvent, syringe filtered w/ 9:1 pentane/EtOAc, normal-phase column EtOAc/Pentane 10%→90%. The product was obtained with <10% of the over-benzylated product. Reverse-phase column (MeOH/H_2O with 0.1% TFA 89%→100%) was used on that sample to get a pure sample for characterization.
Yield: 46% (40%, 45.2 mg), white solid.
Readily Purchasable (CAS): No (N/A)
Spectra Available in the Literature: Yes[2]
^{1}H NMR (500 MHz, $CDCl_3$) δ 7.60 (d, *J* = 8.2 Hz, 2H), 7.26 – 7.12 (m, 5H), 7.10 (d, *J* = 6.9 Hz, 2H), 3.94 (s, 2H), 2.93 (d, *J* = 4.8 Hz, 2H).
^{13}C NMR (126 MHz, $CDCl_3$) δ 168.09, 144.77, 140.30, 132.51, 129.10, 128.93, 128.59, 127.05, 126.34, 41.75, 26.82.
HRMS (ESI) Calculated for $C_{15}H_{15}NO$ ($[M+H]^+$): 226.1226, measured: 226.1224.

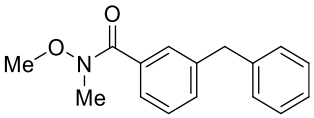

(17) 3-(N,O-Dimethylhydroxylaminocarbonyl)diphenylmethane : Prepared from **17a** (0.5 mmol, 146 mg) and toluene (0.3 M, 1.6 mL) according to Section III.
Reaction duration: 48 h. Purification: Removed solvent, syringe filtered w/ 9:1 pentane/EtOAc, normal-phase column EtOAc/Pentane 10%→90%. The product was obtained with <10% of the over-benzylated product. Reverse-phase column (MeOH/H_2O with 0.1% TFA 89%→100%) was used on that sample to get a pure sample for characterization.
Yield: 43% (39%, 49.7 mg), white solid.
Readily Purchasable (CAS): No (422550-69-4)
Spectra Available in the Literature: Yes[10]
^{1}H NMR (500 MHz, $CDCl_3$) δ 7.42 (dt, *J* = 4.0, 1.8 Hz, 2H), 7.27 – 7.17 (m, 4H), 7.15 – 7.07 (m, 3H), 3.94 (s, 2H), 3.43 (s, 3H), 3.25 (s, 3H).
^{13}C NMR (126 MHz, $CDCl_3$) δ 170.09, 141.03, 140.60, 134.29, 131.13, 128.97, 128.63, 128.53, 128.17, 126.24, 125.90, 60.99, 41.76.

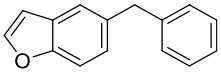

(18) 5-Benzylbenzofuran: Prepared from **12a** (0.5 mmol, 122.0 mg) and toluene (0.3 M, 1.6 mL) according to Section III.
Reaction duration: 48 h. Purification: Removed solvent, SiO_2 plug w/ 100:1 pentane/EtOAc, reverse-phase column MeOH/H_2O with 0.1% TFA 89%→100%, extraction with 90% pentane/Et_2O.
Yield: 50% (46%, 47.8 mg), colorless oil.
Readily Purchasable (CAS): No (939050-19-8)
Spectra Available in the Literature: Yes[11]
^{1}H NMR (500 MHz, $CDCl_3$) δ 7.59 (d, J = 2.2 Hz, 1H), 7.42 (d, J = 8.5 Hz, 1H), 7.40 (d, J = 1.7 Hz, 1H), 7.33 – 7.26 (m, 2H), 7.24 – 7.20 (m, 3H), 7.14 (dd, J = 8.4, 1.8 Hz, 1H), 6.70 (dd, J = 2.2, 1.0 Hz, 1H), 4.08 (s, 2H).
^{13}C NMR (126 MHz, $CDCl_3$) δ 153.66, 145.15, 141.63, 135.62, 128.87, 128.44, 127.59, 126.02, 125.42, 121.10, 111.17, 106.45, 41.78.

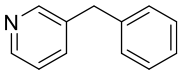

(19) 3-Benzylpyridine: Prepared from **11a** (0.5 mmol, 102.5 mg) and toluene (0.3 M, 1.6 mL) according to Section III.
Reaction duration: 48 h. Purification: Removed solvent, SiO_2 plug w/ 100:1 pentane/EtOAc, reverse-phase column MeOH/H_2O with 0.1% TFA 89%→100%, extraction with 90% pentane/Et_2O.
Yield: 41%, light yellow oil. Product was obtained from the column with <10% impurity of arylated bibenzyl byproduct.
Readily Purchasable (CAS): Yes (620-95-1)
Spectra Available in the Literature: Yes[7]
^{1}H NMR (500 MHz, $CDCl_3$) δ 8.51 (s, 1H), 8.46 (d, J = 4.7 Hz, 1H), 7.46 (d, J = 7.8 Hz, 1H), 7.31 (t, J = 7.4 Hz, 2H), 7.23 – 7.16 (m, 4H), 3.98 (s, 2H).
^{13}C NMR (126 MHz, $CDCl_3$) δ 150.17, 147.65, 139.78, 136.45, 136.28, 128.84, 128.66, 126.47, 123.41, 39.04.

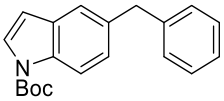

(20) N-Boc-5-benzylindole: Prepared from **10a** (0.5 mmol, 171.6 mg) and toluene (0.3 M, 1.6 mL) according to Section III.
Reaction duration: 48 h. Purification: Removed solvent, SiO_2 plug w/ 100:1 pentane/EtOAc, reverse-phase column MeOH/H_2O with 0.1% TFA 75%→100%, extraction with 90% pentane/Et_2O.
Yield: 40% (34%, 52.4 mg), slightly yellow oil.
Readily Purchasable (CAS): No (2031240-78-3)
Spectra Available in the Literature: Yes[7]
^{1}H NMR (500 MHz, $CDCl_3$) δ 8.04 (d, J = 8.2 Hz, 1H), 7.57 (d, J = 3.7 Hz, 1H), 7.37 (d, J = 1.6 Hz, 1H), 7.32 – 7.25 (m, 2H), 7.23 – 7.19 (m, 3H), 7.16 (dd, J = 8.5, 1.7 Hz, 1H), 6.50 (d, J = 3.9 Hz, 1H), 4.08 (s, 2H), 1.67 (s, 9H).
^{13}C NMR (126 MHz, $CDCl_3$) δ 149.78, 141.72, 135.47, 130.84, 128.87, 128.40, 126.08, 125.95, 125.45, 120.96, 115.04, 107.17, 83.53, 41.79, 29.70, 28.19.

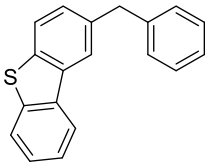

(21) 4-Benzyldibenzothiophene: Prepared from **21a** (0.5 mmol, 155 mg) and toluene (0.3 M, 1.6 mL) according to Section III.
Reaction duration: 48 h. Purification: Removed solvent, syringe filtered w/ 9:1 pentane/EtOAc, normal-phase column EtOAc/Pentane 10%→90%. The product was obtained with <10% of the over-benzylated product. Reverse-phase column (MeOH/H_2O with 0.1% TFA 89%→100%) was used on that sample to get a pure sample for characterization.
Yield: 57% (50%, 69.0 mg), colorless oil.
Readily Purchasable (CAS): No (98882-23-6)
Spectra Available in the Literature: Yes[2]
^{1}H NMR (500 MHz, $CDCl_3$) δ 8.06 – 8.01 (m, 1H), 7.91 (d, *J* = 0.8 Hz, 1H), 7.79 – 7.73 (m, 1H), 7.69 (d, *J* = 8.2 Hz, 1H), 7.40 – 7.32 (m, 2H), 7.27 – 7.20 (m, 3H), 7.19 – 7.11 (m, 3H), 4.10 (s, 2H).
^{13}C NMR (126 MHz, $CDCl_3$) δ 141.20, 139.83, 137.48, 137.22, 135.83, 135.42, 128.93, 128.55, 128.08, 126.63, 126.20, 124.24, 122.85, 122.75, 121.82, 121.58, 41.92.

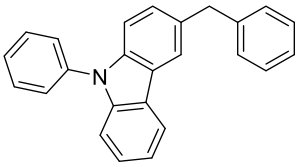

(22) 3-(9-Phenyl-9H-carbazole)diphenylmethane : Prepared from **22a** (0.5 mmol, 184.5 mg) and toluene (0.3 M, 1.6 mL) according to Section III.
Reaction duration: 48 h. Purification: Removed solvent, syringe filtered w/ 9:1 pentane/EtOAc, normal-phase column EtOAc/Pentane 10%→90%. The product was obtained with <10% of the over-benzylated product. Reverse-phase column (MeOH/H_2O with 0.1% TFA 89%→100%) was used on that sample to get a pure sample for characterization.
Yield: 47% (40%, 66.3 mg), white solid.
Readily Purchasable (CAS): No (857503-81-2)
Spectra Available in the Literature: Yes[2]
^{1}H NMR (500 MHz, $CDCl_3$) δ 8.01 (d, *J* = 7.7 Hz, 1H), 7.88 (s, 1H), 7.56 – 7.43 (m, 4H), 7.36 (t, *J* = 7.2 Hz, 1H), 7.33 – 7.09 (m, 10H), 4.11 (s, 2H).
^{13}C NMR (126 MHz, $CDCl_3$) δ 142.15, 141.18, 139.62, 137.88, 132.79, 129.89, 128.96, 128.52, 127.37, 127.29, 127.07, 126.03, 125.93, 123.62, 123.32, 120.49, 120.37, 119.86, 109.82, 109.83, 42.03.

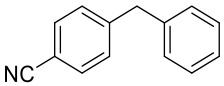

(23) 4-Cyanodiphenylmethane: Prepared from **14a** (0.5 mmol, 114.6 mg) and toluene (0.3 M, 1.6 mL) according to Section III.
Reaction duration: 48 h. Purification: Removed solvent, SiO_2 plug w/ 100:1 pentane/EtOAc, reverse-phase column MeOH/H_2O with 0.1% TFA 89%→100%, extraction with 90% pentane/Et_2O.
Yield: 54%, colorless oil. The product was obtained from the column as a mixture with <10% biaryl.
Readily Purchasable (CAS): No (23450-31-9)
Spectra Available in the Literature: Yes[8]
^{1}H NMR (500 MHz, $CDCl_3$) δ 7.57 (d, J = 8.3 Hz, 2H), 7.34 – 7.27 (m, 4H), 7.26 – 7.22 (m, 1H), 7.16 (d, J = 8.1 Hz, 2H), 4.04 (s, 2H).
^{13}C NMR (126 MHz, $CDCl_3$) δ 146.72, 139.31, 132.29, 129.62, 128.94, 128.75, 126.66, 118.98, 110.03, 41.96.

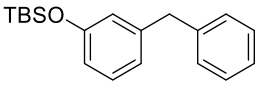

(24) 3-*tert*-Butyldimethylsiloxydiphenylmethane: Prepared from **15a** (0.5 mmol, 167.1 mg) and toluene (0.3 M, 1.6 mL) according to Section III.
Reaction duration: 48 h. Purification: Removed solvent, SiO_2 plug w/ 100:1 pentane/EtOAc, reverse-phase column MeOH/H_2O with 0.1% TFA 89%→100%, extraction with 90% pentane/Et_2O.
Yield: 73% (63%, 93.9 mg), colorless oil.
Readily Purchasable (CAS): No (N/A)
Spectra Available in the Literature: Yes[2]
^{1}H NMR (500 MHz, $CDCl_3$) δ 7.47 (t, J = 7.4 Hz, 2H), 7.41 – 7.34 (m, 3H), 7.32 (t, J = 7.7 Hz, 1H), 6.97 (d, J = 7.1 Hz, 1H), 6.90 – 6.83 (m, 2H), 4.12 (s, 2H), 1.15 (s, 9H), 0.35 (s, 6H).
^{13}C NMR (126 MHz, $CDCl_3$) δ 155.71, 142.56, 141.01, 129.27, 128.89, 128.39, 126.02, 121.94, 120.79, 117.70, 41.77, 25.70, 18.21, -4.42.
HRMS (ESI) Calculated for $C_{19}H_{26}OSi$ ($[M+H]^+$): 299.1826, measured: 299.1823.

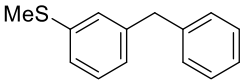

(25) 3-Methylthiodiphenylmethane: Prepared from **16a** (0.5 mmol, 125.0 mg) and toluene (0.3 M, 1.6 mL) according to Section III.
Reaction duration: 48 h. Purification: Removed solvent, SiO_2 plug w/ 100:1 pentane/EtOAc, normal-phase column EtOAc/pentane 10%→40%.
Yield: 48%, colorless oil. The product was obtained from the column as a mixture with 25% bibenzyl. Note: in order to obtain the spectrum for characterization, two additional reverse-phase column purifications were performed (MeOH/H_2O with 0.1% TFA 89%→100%), which led to considerable mass loss.
Readily Purchasable (CAS): No (N/A)
Spectra Available in the Literature: Yes[2]
^{1}H NMR (500 MHz, $CDCl_3$) δ 7.29 (t, J = 7.5 Hz, 2H), 7.24 – 7.17 (m, 4H), 7.12 – 7.08 (m, 2H), 6.96 (d, J = 7.5 Hz, 1H), 3.96 (s, 2H), 2.46 (s, 3H).
^{13}C NMR (126 MHz, $CDCl_3$) δ 141.75, 140.66, 138.45, 128.90, 128.48, 127.11, 126.16, 125.78, 124.20, 41.81, 29.70, 15.78.
HRMS (ESI) Calculated for $C_{14}H_{14}S$ ($[M+H]^+$): 215.0889, measured: 215.0888.

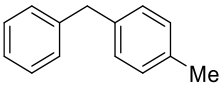

(26) 4-Methyldiphenylmethane: Prepared from **1a** (0.5 mmol, 102.1 mg) and *p*-xylene (0.3 M, 1.6 mL) according to Section III.
Reaction duration: 48 h. Purification: Removed solvent, SiO_2 plug w/ 100:1 pentane/EtOAc, reverse-phase column MeOH/H_2O with 0.1% TFA 89%→100%, extraction with 90% pentane/Et_2O.
Yield: 82% (61%, 55.5 mg), colorless oil.
Readily Purchasable (CAS): Yes (620-83-7)
Spectra Available in the Literature: Yes[7]
^{1}H NMR (500 MHz, $CDCl_3$) δ 7.31 – 7.26 (m, 2H), 7.23 – 7.17 (m, 3H), 7.13 – 7.07 (m, 4H), 3.96 (s, 2H), 2.33 (s, 3H).
^{13}C NMR (126 MHz, $CDCl_3$) δ 141.40, 138.06, 135.53, 129.13, 128.85, 128.79, 128.41, 125.96, 41.51, 21.00.

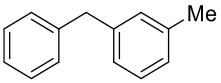

(27) 3-Methyldiphenylmethane: Prepared from **1a** (0.5 mmol, 102.1 mg) and *m*-xylene (0.3 M, 1.6 mL) according to Section III.
Reaction duration: 48 h. Purification: Removed solvent, SiO_2 plug w/ 100:1 pentane/EtOAc, reverse-phase column MeOH/H_2O with 0.1% TFA 89%→100%, extraction with 90% pentane/Et_2O.
Yield: 85% (59%, 53.7 mg), colorless oil.
Readily Purchasable (CAS): Yes (620-47-3)
Spectra Available in the Literature: Yes[8]
^{1}H NMR (500 MHz, $CDCl_3$) δ 7.32 – 7.27 (m, 2H), 7.23 – 7.16 (m, 4H), 7.05 – 6.99 (m, 3H), 3.96 (s, 2H), 2.33 (s, 3H).
^{13}C NMR (126 MHz, $CDCl_3$) δ 141.24, 141.01, 138.02, 129.70, 128.91, 128.42, 128.33, 126.81, 125.99, 125.96, 41.89, 21.41.

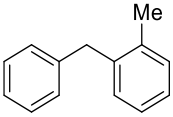

(28) 2-Methyldiphenylmethane: Prepared from **1a** (0.5 mmol, 102.1 mg) and *o*-xylene (0.3 M, 1.6 mL) according to Section III.
Reaction duration: 48 h. Purification: Removed solvent, SiO_2 plug w/ 100:1 pentane/EtOAc, reverse-phase column MeOH/H_2O with 0.1% TFA 89%→100%, extraction with 90% pentane/Et_2O.
Yield: 84% (60%, 54.6 mg), colorless oil.
Readily Purchasable (CAS): Yes (713-36-0)
Spectra Available in the Literature: Yes[8]
^{1}H NMR (500 MHz, $CDCl_3$) δ 7.28 (t, J = 7.6 Hz, 2H), 7.22 – 7.09 (m, 7H), 4.00 (s, 2H), 2.25 (s, 3H).
^{13}C NMR (126 MHz, $CDCl_3$) δ 140.37, 138.90, 136.62, 130.26, 129.92, 128.72, 128.36, 126.43, 125.96, 125.89, 39.43, 19.67.

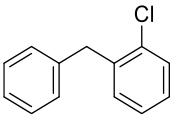

(29) 2-Chlorodiphenylmethane: Prepared from **1a** (0.5 mmol, 102.1 mg) and 2-chlorotoluene (0.3 M, 1.6 mL) according to Section III.
Reaction duration: 48 h. Purification: Removed solvent, SiO_2 plug w/ 100:1 pentane/EtOAc, reverse-phase column MeOH/H_2O with 0.1% TFA 85%→100%, extraction with 90% pentane/Et_2O.
Yield: 63%, slightly yellow oil. The product was obtained from the column as a mixture with <10% bibenzyl.
Readily Purchasable (CAS): Yes (29921-41-3)
Spectra Available in the Literature: Yes[12]
^{1}H NMR (500 MHz, $CDCl_3$) δ 7.40 – 7.37 (m, 1H), 7.30 (t, J = 7.5 Hz, 2H), 7.25 – 7.13 (m, 6H), 4.12 (s, 2H).
^{13}C NMR (126 MHz, $CDCl_3$) δ 139.49, 138.66, 134.22, 131.00, 129.51, 128.93, 128.45, 127.63, 126.80, 126.22, 39.17.

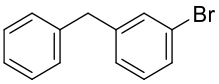

(30) 3-Bromodiphenylmethane: Prepared from **1a** (0.5 mmol, 102.1 mg) and 3-bromotoluene (0.3 M, 1.6 mL) according to Section III.
Reaction duration: 48 h. Purification: Removed solvent, SiO_2 plug w/ 100:1 pentane/EtOAc, reverse-phase column MeOH/H_2O with 0.1% TFA 89%→100%, extraction with 90% pentane/Et_2O.
Yield: 65% (58%, 71.6 mg), colorless oil.
Readily Purchasable (CAS): Yes (27798-39-6)
Spectra Available in the Literature: Yes[13]
^{1}H NMR (500 MHz, $CDCl_3$) δ 7.36 – 7.28 (m, 4H), 7.23 (t, J = 7.4 Hz, 1H), 7.18 (d, J = 7.3 Hz, 2H), 7.17 – 7.10 (m, 2H), 3.95 (s, 2H).
^{13}C NMR (126 MHz, $CDCl_3$) δ 143.43, 140.15, 131.90, 129.99, 129.22, 128.90, 128.60, 127.56, 126.37, 122.54, 41.53.

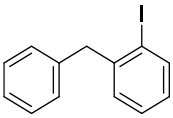

(31) 2-Iododiphenylmethane: Prepared from **1a** (0.5 mmol, 102.1 mg) and 2-iodotoluene (0.3 M, 1.6 mL) according to Section III.
Reaction duration: 48 h. Purification: Removed solvent, SiO_2 plug w/ 100:1 pentane/EtOAc, reverse-phase column MeOH/H_2O with 0.1% TFA 89%→100%, extraction with 90% pentane/Et_2O.
Yield: 57% (50%, 71.6 mg), colorless oil.
Readily Purchasable (CAS): No (35444-93-0)
Spectra Available in the Literature: Yes[14]
^{1}H NMR (500 MHz, $CDCl_3$) δ 7.87 (dd, J = 7.9, 1.3 Hz, 1H), 7.34 – 7.17 (m, 6H), 7.12 (dd, J = 7.6, 1.7 Hz, 1H), 6.92 (td, J = 7.6, 1.7 Hz, 1H), 4.12 (s, 2H).
^{13}C NMR (126 MHz, $CDCl_3$) δ 143.61, 139.55, 138.93, 130.35, 129.08, 128.48, 128.33, 128.01, 126.27, 101.30, 46.48.

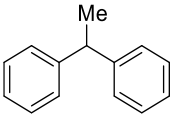

(32) 1,1-Diphenylethane: Prepared from **1a** (0.5 mmol, 102.1 mg) and ethylbenzene (5.0 mmol, 612 µL) according to Section IV. Uses phen as the ligand with 5 mol% Cu.
Reaction duration: 48 h. Purification: Removed solvent, SiO_2 plug w/ 100:1 pentane/EtOAc, reverse-phase column MeOH/H_2O with 0.1% TFA 89%→100%, extraction with 90% pentane/Et_2O.
Yield: 69% (60%, 54.6 mg), colorless oil.
Readily Purchasable (CAS): No (612-00-0)
Spectra Available in the Literature: Yes[14]
^{1}H NMR (500 MHz, $CDCl_3$) δ 7.30 (t, J = 7.6 Hz, 4H), 7.25 – 7.22 (m, 4H), 7.19 (t, J = 7.2 Hz, 2H), 4.17 (q, J = 7.2 Hz, 1H), 1.66 (d, J = 7.2 Hz, 3H).
^{13}C NMR (126 MHz, $CDCl_3$) δ 146.35, 128.34, 127.61, 126.00, 44.76, 21.85.

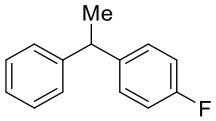

(33) 1-(4-Fluorophenyl)-1-phenylethane: Prepared from **1a** (0.5 mmol, 102.1 mg) and 1-ethyl-4-fluorobenzene (5.0 mmol, 625 µL) according to Section IV. Uses phen as the ligand with 5 mol% Cu.

Reaction duration: 48 h. Purification: Removed solvent, SiO_2 plug w/ 100:1 pentane/EtOAc, reverse-phase column MeOH/H_2O with 0.1% TFA 89%→100%, extraction with 90% pentane/Et_2O.

Yield: 61%, light yellow oil. The product was obtained from the column as a mixture with 15% biaryl.

Readily Purchasable (CAS): No (1192278-61-7)

Spectra Available in the Literature: Yes[15]

^{1}H NMR (500 MHz, $CDCl_3$) δ 7.33 – 7.26 (m, 2H), 7.22 – 7.15 (m, 5H), 6.97 (t, J = 8.7 Hz, 2H), 4.14 (q, J = 7.2 Hz, 1H), 1.63 (d, J = 7.2 Hz, 3H).

^{13}C NMR (126 MHz, $CDCl_3$) δ 161.26 (d, J = 243.9 Hz), 146.17, 142.04 (d, J = 3.2 Hz), 128.98 (d, J = 7.8 Hz), 128.44, 127.52, 126.15, 115.06 (d, J = 21.1 Hz), 44.04, 22.03.

^{19}F NMR (377 MHz, $CDCl_3$) δ -117.54.

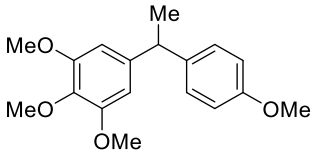

(34) 1-(3,4,5-Methoxyphenyl)-1-(4-methoxyphenyl)-ethane: Prepared from **17a** (0.5 mmol, 147.1 mg) and 4-ethylanisole (5.0 mmol, 731 µL) according to Section IV. Uses phd as the ligand with 3 mol % Cu.

Reaction duration: 48 h. Purification: Removed solvent, SiO_2 plug w/ dichloromethane, normal-phase column EtOAc/pentane 10%→100%.

Yield: 66%, (61%, 91.4 mg), light orange oil.

OR

Prepared from **17a** (1.7 mmol, 500 mg) and 4-ethylanisole (17 mmol, 2.4 mL) according to Section V. Uses phd as the ligand with 3 mol % Cu.

Reaction duration: 24 h. Purification: Removed solvent, SiO_2 plug w/ dichloromethane, normal-phase column EtOAc/pentane 10%→100%.

Yield: 70% (64%, 331 mg), light orange oil.

Readily Purchasable (CAS): No (1199256-72-8)

Spectra Available in the Literature: Yes[16]

^{1}H NMR (500 MHz, $CDCl_3$) δ 7.15 (d, J = 8.5 Hz, 2H), 6.84 (d, J = 8.7 Hz, 2H), 6.42 (s, 2H), 4.04 (q, J = 7.2 Hz, 1H), 3.82 (s, 3H), 3.81 (s, 6H), 3.79 (s, 3H), 1.60 (d, J = 7.2 Hz, 3H).

^{13}C NMR (126 MHz, $CDCl_3$) δ 157.86, 153.02, 142.45, 138.30, 136.15, 128.35, 113.70, 104.57, 60.81, 56.05, 55.22, 44.19, 22.19.

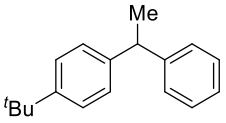

(35) 1-(4-*tert*-Butylphenyl)-1-phenylethane: Prepared from **2a** (0.5 mmol, 130.1 mg) and ethylbenzene (5.0 mmol, 612 µL) according to Section IV. Uses phen as the ligand with 5 mol% Cu.

Reaction duration: 48 h. Purification: Removed solvent, SiO_2 plug w/ 100:1 pentane/EtOAc, reverse-phase column MeOH/H_2O with 0.1% TFA 89%→100%, extraction with 90% pentane/Et_2O.

Yield: 70% (62%, 73.8 mg), colorless oil.

Readily Purchasable (CAS): No (94788-62-2)

Spectra Available in the Literature: Yes[17]

^{1}H NMR (500 MHz, $CDCl_3$) δ 7.32 – 7.27 (m, 4H), 7.25 – 7.22 (m, 2H), 7.20 – 7.14 (m, 3H), 4.13 (q, J = 7.2 Hz, 1H), 1.64 (d, J = 7.2 Hz, 3H), 1.30 (s, 9H).

^{13}C NMR (126 MHz, $CDCl_3$) δ 148.67, 146.58, 143.21, 128.30, 127.60, 127.14, 125.92, 125.19, 44.31, 34.32, 31.38, 21.89.

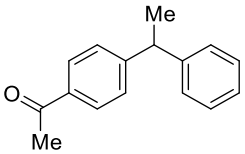

(36) 1-(4-Acetylphenyl)-1-phenylethane: Prepared from **4a** (0.5 mmol, 136.0 mg) and ethylbenzene (5.0 mmol, 612 µL) according to Section IV. Uses phen as the ligand with 5 mol% Cu.

Reaction duration: 48 h. Purification: Removed solvent, syringe filtered w/ 9:1 pentane/EtOAc, normal-phase column EtOAc/Pentane 10%→90%. The product was obtained with <10% of arylated bibenzyl product (analogous to **E** in Figure 2A.1). Reverse-phase column chromatography (MeOH/H_2O with 0.1% TFA 89%→100%) was used on that sample to get a pure sample for characterization (with higher yield than the previous method).

Yield: 56% (50%, 55.9 mg), off-white oil.

Readily Purchasable (CAS): No (94788-60-0)

Spectra Available in the Literature: Yes[18]

^{1}H NMR (500 MHz, $CDCl_3$) δ 7.88 (d, J = 8.4 Hz, 2H), 7.34 – 7.27 (m, 4H), 7.23 – 7.18 (m, 3H), 4.21 (q, J = 7.2 Hz, 1H), 2.57 (s, 3H), 1.66 (d, J = 7.2 Hz, 3H).

^{13}C NMR (126 MHz, $CDCl_3$) δ 197.77, 151.99, 145.30, 135.17, 128.56, 128.51, 127.81, 127.56, 126.35, 44.80, 26.56, 21.53.

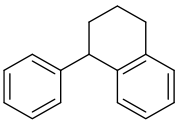

(37) 1-Phenyl-1,2,3,4-tetrahydronaphthalene: Prepared from **1a** (0.5 mmol, 102.1 mg) and 1,2,3,4-tetrahydronaphthalene (5.0 mmol, 680 µL) according to Section IV. Uses phd as the ligand with 3 mol % Cu.
Reaction duration: 48 h. Purification: Removed solvent, SiO_2 plug w/ 100:1 pentane/EtOAc, reverse-phase column MeOH/H_2O with 0.1% TFA 89%→100%, extraction with 90% pentane/Et_2O.
Yield: 50%, colorless oil. The product was obtained from the column as a mixture with <10% of the tetrahydronapthalene homocoupling product.
Readily Purchasable (CAS): Yes (3018-20-0)
Spectra Available in the Literature: Yes[19]
^{1}H NMR (500 MHz, $CDCl_3$) δ 7.28 (t, J = 7.5 Hz, 2H), 7.20 (t, J = 7.3 Hz, 1H), 7.17 – 7.09 (m, 4H), 7.07 – 7.00 (m, 1H), 6.84 (d, J = 7.7 Hz, 1H), 4.12 (t, J = 6.8 Hz, 1H), 2.99 – 2.80 (m, 2H), 2.23 – 2.12 (m, 1H), 1.96 – 1.83 (m, 2H), 1.84 – 1.70 (m, 1H).
^{13}C NMR (126 MHz, $CDCl_3$) δ 147.50, 139.36, 137.57, 130.16, 128.93, 128.82, 128.19, 125.91, 125.87, 125.60, 45.61, 33.24, 29.77, 20.95.

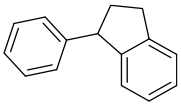

(38) 1-Phenylindane: Prepared from **1a** (0.5 mmol, 102.1 mg) and indane (5.0 mmol, 613 µL) according to Section IV. Uses phd as the ligand with 3 mol % Cu.
Reaction duration: 48 h. Purification: Removed solvent, SiO_2 plug w/ 100:1 pentane/EtOAc, reverse-phase column MeOH/H_2O with 0.1% TFA 89%→100%, extraction with 90% pentane/Et_2O.
Yield: 65%, colorless oil. The product was obtained from the column as a mixture with 35% of the indane homocoupling product.
Readily Purchasable (CAS): No (26461-03-0)
Spectra Available in the Literature: Yes[20]
^{1}H NMR (500 MHz, $CDCl_3$) δ 7.34 – 7.28 (m, 4H), 7.22 – 7.10 (m, 4H), 6.96 (d, J = 7.4 Hz, 1H), 4.34 (t, J = 8.3 Hz, 1H), 3.06 (ddd, J = 15.8, 8.6, 3.7 Hz, 1H), 3.00 – 2.88 (m, 1H), 2.68 – 2.54 (m, 1H), 2.13 – 2.01 (m, 1H).
^{13}C NMR (126 MHz, $CDCl_3$) δ 146.82, 145.39, 144.31, 128.43, 128.09, 126.51, 126.34, 126.32, 124.89, 124.32, 51.63, 36.55, 31.82.

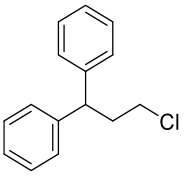

(39) 1-Chloro-3,3-diphenylpropane: Prepared from **1a** (0.5 mmol, 102.1 mg) and 1-chloro-3-phenylpropane (5.0 mmol, 716 µL) according to Section IV. Uses less chlorobenzene (100 µl, 5.0M) and more di-*tert*-butyl peroxide (3.0 mmol, 549 µL, 6.0 equiv.), using phen as the ligand with 5 mol% Cu.
Reaction duration: 48 h. Purification: Removed solvent, syringe filtered w/ 100:1 pentane/EtOAc, passed over an SiO_2 plug, ran a reverse-phase column with MeOH/H_2O with 0.1% TFA 70%→100%, extraction with 90% pentane/Et_2O.
Yield: 61% (42%, 47.9 mg), colorless oil.
Readily Purchasable (CAS): No (29648-95-1)
Spectra Available in the Literature: Yes[21]
^{1}H NMR (500 MHz, $CDCl_3$) δ 7.34 – 7.27 (m, 4H), 7.28 – 7.24 (m, 4H), 7.21 (t, J = 7.2 Hz, 2H), 4.23 (t, J = 7.8 Hz, 1H), 3.47 (t, J = 6.6 Hz, 2H), 2.51 (dt, J = 7.9, 6.6 Hz, 2H).
^{13}C NMR (126 MHz, $CDCl_3$) δ 143.52, 128.62, 127.86, 126.51, 47.87, 43.21, 38.14.

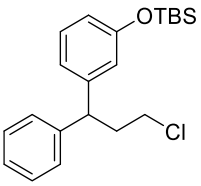

(40) 1-Chloro-3-(3-*tert*-butyldimethylsiloxyphenyl)-3-phenylpropane: Prepared from **15a** (0.5 mmol, 167.1 mg) and 1-chloro-3-phenylpropane (5.0 mmol, 716 µL) according to Section IV. Uses less chlorobenzene (100 µl, 5.0M) and more di-*tert*-butyl peroxide (3.0 mmol, 549 µL, 6.0 equiv.), using phen as the ligand with 5 mol% Cu.
Reaction duration: 48 h. Purification: Removed solvent, syringe filtered w/ 100:1 pentane/EtOAc, passed over an SiO_2 plug, ran a reverse-phase column with MeOH/H_2O with 0.1% TFA 70%→100%, extraction with 90% pentane/Et_2O.
Yield: 52% (41%, 73.5 mg), colorless oil.
Readily Purchasable (CAS): No (N/A)
Spectra Available in the Literature: Yes[2]
^{1}H NMR (500 MHz, $CDCl_3$) δ 7.29 (t, J = 6.5 Hz, 2H), 7.25 – 7.22 (m, 2H), 7.20 (t, J = 7.2 Hz, 1H), 7.14 (t, J = 7.9 Hz, 1H), 6.83 (d, J = 7.7 Hz, 1H), 6.72 (t, J = 2.1 Hz, 1H), 6.68 (ddd, J = 8.0, 2.5, 1.0 Hz, 1H), 4.15 (t, J = 7.8 Hz, 1H), 3.45 (t, J = 6.6 Hz, 2H), 2.47 (dt, J = 7.8, 6.6 Hz, 2H), 0.96 (s, 9H), 0.15 (d, J = 1.5 Hz, 6H).
^{13}C NMR (126 MHz, $CDCl_3$) δ 155.78, 145.03, 143.45, 129.45, 128.55, 127.79, 126.47, 120.88, 119.73, 118.14, 47.65, 43.19, 38.04, 25.69, 18.22, -4.41, -4.43.
HRMS (ESI) Calculated for $C_{21}H_{29}OClSi$ ($[M+H]^+$): 361.1749, measured: 361.1749

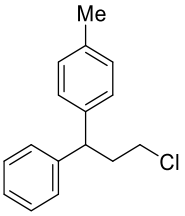

(41) 1-Chloro-3-(*p*-tolyl)-3-phenylpropane: Prepared from **21a** (0.5 mmol, 109.1 mg) and 1-chloro-3-phenylpropane (5.0 mmol, 716 µL) according to Section IV. Uses less chlorobenzene (100 µl, 5.0M) and more di-*tert*-butyl peroxide (3.0 mmol, 549 µL, 6.0 equiv.), using phen as the ligand with 5 mol% Cu.
Reaction duration: 48 h. Purification: Removed solvent, syringe filtered w/ 100:1 pentane/EtOAc, passed over an SiO_2 plug, ran a reverse-phase column with MeOH/H_2O with 0.1% TFA 70%→100%, extraction with 90% pentane/Et_2O.
Yield: 45%, white solid. The product was obtained from the column as a mixture with <10% of the 1-chloro-3-phenylpropane homocoupling product.
Readily Purchasable (CAS): No (55707-02-3)
Spectra Available in the Literature: Yes[21]
^{1}H NMR (500 MHz, $CDCl_3$) δ 7.29 – 7.08 (m, 9H), 4.17 (t, J = 7.8 Hz, 1H), 3.45 (t, J = 6.6 Hz, 2H), 2.48 (dt, J = 7.9, 6.6 Hz, 2H), 2.30 (s, 3H).
^{13}C NMR (126 MHz, $CDCl_3$) δ 143.79, 140.49, 136.03, 129.29, 128.58, 127.77, 127.70, 126.51, 47.48, 43.22, 38.18, 20.96.

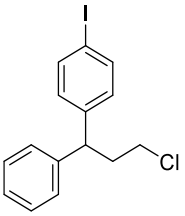

(42) 1-Chloro-3-(4-iodophenyl)-3-phenylpropane: Prepared from **8a** (0.5 mmol, 165 mg) and 1-chloro-3-phenylpropane (5.0 mmol, 716 µL) according to Section IV. Uses less chlorobenzene (100 µl, 5.0M) and more di-*tert*-butyl peroxide (3.0 mmol, 549 µL, 6.0 equiv.), using phen as the ligand with 5 mol% Cu.
Reaction duration: 48 h. Purification: Removed solvent, syringe filtered w/ 100:1 pentane/EtOAc, passed over an SiO_2 plug, ran a reverse-phase column with MeOH/H_2O with 0.1% TFA 70%→100%, extraction with 90% pentane/Et_2O.
Yield: 48% (37%, 65.8 mg), off-white oil.
Readily Purchasable (CAS): No (N/A)
Spectra Available in the Literature: Yes[2]
^{1}H NMR (500 MHz, $CDCl_3$) δ 7.62 (d, J = 8.4 Hz, 2H), 7.33 – 7.28 (m, 2H), 7.24 – 7.19 (m, 3H), 7.00 (d, J = 8.3 Hz, 2H), 4.18 (t, J = 7.8 Hz, 1H), 3.44 (t, J = 6.5 Hz, 2H), 2.46 (dq, J = 7.8, 6.4 Hz, 2H).
^{13}C NMR (126 MHz, $CDCl_3$) δ 143.28, 142.79, 137.66, 129.91, 128.74, 127.76, 126.75, 91.80, 47.30, 42.93, 37.80.
HRMS (ESI) Calculated for $C_{15}H_{14}ICl$ ($[M+H]^+$): 355.9823, measured: 355.9820

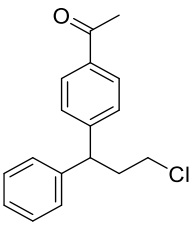

(43) 1-Chloro-3-(4-acetylphenyl)-3-phenylpropane: Prepared from **4a** (0.5 mmol, 123.1 mg) and 1-chloro-3-phenylpropane (5.0 mmol, 716 µL) according to Section IV. Uses less chlorobenzene (100 µl, 5.0M) and more di-*tert*-butyl peroxide (3.0 mmol, 549 µL, 6.0 equiv.), using phen as the ligand with 5 mol% Cu.
Reaction duration: 48 h. Purification: Removed solvent, syringe filtered w/ 100:1 pentane/EtOAc, passed over an SiO_2 plug w/ 9:1 pentane/EtOAc, normal-phase column EtOAc/pentane 10%→100%.
Yield: 43% (33%, 45 mg), slightly orange solid.
Readily Purchasable (CAS): No (N/A)
Spectra Available in the Literature: Yes[2]
^{1}H NMR (500 MHz, $CDCl_3$) δ 7.90 (d, J = 8.3 Hz, 2H), 7.35 (d, J = 8.2 Hz, 2H), 7.35 – 7.27 (m, 2H), 7.25 – 7.20 (m, 3H), 4.30 (t, J = 7.8 Hz, 1H), 3.45 (t, J = 6.5 Hz, 2H), 2.57 (s, 3H), 2.52 (dtd, J = 7.7, 6.5, 3.3 Hz, 2H).
^{13}C NMR (126 MHz, $CDCl_3$) δ 197.62, 149.11, 142.47, 135.57, 128.80, 128.76, 128.07, 127.84, 126.87, 47.76, 42.86, 37.73, 26.57.
HRMS (ESI) Calculated for $C_{17}H_{17}OCl$ ($[M+H]^+$): 273.1041, measured: 273.1041

2A.X. References

1. Murata, M.; Oda, T.; Watanabe, S.; Masuda, Y. *Synthesis* **2007**, *3*, 351-354.
2. Vasilopoulos, A.; Zultanski, S. L.; Stahl, S. S. *J. Am. Chem. Soc.* **2017**, *139*, 7705-7708.
3. PraveenGanesh, N.; Chavant, P. Y. *Eur. J. Org. Chem.* **2008**, *27*, 4690-4696.
4. Demory, E.; Blandin, V.; Einhorn, J.; Chavant, P. Y. *Org. Process. Res. Dev.* **2011**, *15*, 710-716.
5. Kirchberg, S.; Fröhlich, R.; Studer, A. *Angew. Chem., Int. Ed.* **2009**, *48*, 4235-4238.
6. Chavant, P.; PraveenGanesh, N.; Demory, E.; Gamon, C.; Blandin, V.; Chavant, P. Y. *Synlett* **2010**, *16*, 2403-2406.
7. Xia, Y.; Hu, F.; Xia, Y.; Liu, Z.; Ye, F.; Zhang, Y.; Wang, J. *Synthesis* **2017**, *49*, 1073–1086.
8. Chen, C.-R.; Zhou, S.; Biradar, D. B.; Gau, H.-M. *Adv. Synth. Catal.* **2010**, *352*, 1718-1727.
9. Wilson, S. R.; Jacob, L. A. *J. Org. Chem.* **1986**, *51*, 4833–4836.
10. Zhuang, L.; Wai, J. S.; Embrey, M. W.; Fisher, T. E.; Egbertson, M. S.; Payne, L. S.; Guare, J. P., Jr.; Vacca, J. P.; Hazuda, D. J.; Felock, P. J.; Wolfe, A. L.; Stillmock, K. A.; Witmer, M. V.; Moyer, G.; Schleif, W. A.; Gabryelski, L. J.; Leonard, Y. M.; Lynch, J. J., Jr.; Michelson, S. R.; Young, S. D. *J. Med. Chem.* **2003**, *46*, 453-456.
11. Saha, A. K.; Yu, X.; Lin, J.; Lobera, M.; Sharadendu, A.; Chereku, S.; Schutz, N.; Segal, D.; Marantz, Y.; McCauley, D.; Middleton, S.; Siu, J.; Bürli R. W.; Buys, J.; Horner, M.; Salyers, K.; Schrag, M.; Vargas, H. M.; Xu, Y.; McElvain, M.; Xu, H. *ACS Med. Chem. Lett.* **2011**, *2*, 97-101.
12. Srimani, D.; Bej, A.; Sarkar, A. *J. Org. Chem.* **2010**, *75*, 4296-4299.
13. Henry, N.; Enguehard-Gueiffier, C.; Thery, I.; Gueiffier, A. *Eur. J. Org. Chem.* **2008**, *28*, 4824-4827.
14. Dunsford, J. J.; Clark, E. R.; Ingleson, M. J. *Angew. Chem., Int. Ed.* **2015**, *54*, 5688–5692.
15. López-Pérez, A.; Adrio, J.; Carretero, J. C. *Org. Lett.* **2009**, *11*, 5514-5517.
16. Messaoudi, S.; Hamze, A.; Provot, O.; Tréguier, B.; De Losada, R. J.; Bignon, J.; Liu, J.-M.; Wdzieczak-Bakala, J.; Thoret, S.; Dubois, J.; Brion, J.-D.; Alami, M. *ChemMedChem* **2011**, *6*, 488-497.
17. Nakamura, R.; Obora, Y.; Ishii, Y. *Chem. Comm.* **2008**, *29*, 3417-3419.
18. Saini, V.; Liao, L.; Wang, Q.; Jana, R.; Sigman, M. S. *Org. Lett.* **2013**, *15*, 5008–5011.
19. Bandaranayake, W. M.; Riggs, N. V. *Aust. J. Chem.* **1981**, *34*, 115-129.
20. Deng, R.; Sun, L.; Li, Z. *Org. Lett.* **2007**, *9*, 5207-5210.
21. Miyai, T.; Onishi, Y.; Baba, A. *Tetrahedron* **1999**, *55*, 1017–1026.

Appendix B: Supporting Information Chapter 3

3B.I. General Considerations

All reagents were purchased from commercial sources and used as received. Nearly identical performance was observed when using reagents from different commercial sources. Cu salts were purchased from Strem Chemicals and Sigma-Aldrich. C–H substrates were purchased from Oakwood, Combi-Blocks, TCI America, Ambeed, or Sigma-Aldrich. NFSI was purchased from Ark-Pharm and Oakwood. Bathophenanthroline was purchased from Aldrich and Ambeed. $MeB(OH)_2$ was purchased from Sigma-Aldrich and Combi-Blocks.

All fluorination reaction solids were weighed out on the benchtop, while liquids were added in an inert atmosphere (N_2) glovebox. Retention in performance can be obtained by setting up the fluorination reaction on the benchtop with backfilling or sparging of the reaction vessel with N_2. ^1H, ^{13}C, and ^{19}F NMR spectra were recorded on a Bruker Avance III 400 spectrometer at 25 °C (^1H 400.1 MHz, ^{13}C 100.6 MHz, ^{19}F 376.5 MHz) or a Bruker Avance III 500 spectrometer at 25 °C (^1H 500.1 MHz, ^{13}C 125.7 MHz, ^{19}F 470.6 MHz), except where noted otherwise, and chemical shifts are reported in parts per million (ppm). NMR spectra were referenced to residual $CHCl_3$ at 7.26 ppm (^1H) and $CDCl_3$ at 77.16 ppm (^{13}C). All ^{19}F NMR spectra were absolutely referenced to their respective solvent peaks in the ^1H NMR spectrum. Chromatography was performed using an automated Biotage Isolera® with reusable 25 g Biotage® Sfär Silica HC D cartridges for normal phase or 60 g Biotage® SNAP Ultra C18 cartridges for reversed phase. UV-visible data were collected with an Agilent Technologies stainless steel DIP probe equipped with a 1 mm Immersion Fiber Optic Probe Tip. High-resolution mass spectra were obtained using a Thermo Q Exactive™ Plus via (ASAP-MS) by the mass spectrometry facility at the University of Wisconsin.

3B.II. General Procedure for Benzylic C–H Fluorination and NMR Quantitation

Warning: This reaction evolves gas from protonation of Li_2CO_3, which is able to pressurize the reaction vial. Be sure to take appropriate safety precautions.

Set-up: On the benchtop, a disposable 4 mL glass vial was charged with $MeB(OH)_2$ (0.6 mmol, 35.9 mg, 2 equiv), Li_2CO_3 (0.9 mmol, 66.5 mg, 3 equiv), N-fluorobenzenesulfonimide (NFSI; 0.75 mmol, 236.5 mg, 2.5 equiv), and a Teflon stir bar. The vial was sealed by a PTFE-lined pierceable cap. Bathophenanthroline (BPhen, 0.0216 mmol, 7.2 mg, 0.072 equiv) was weighed into a secondary vial with a Teflon stir bar. Both vials were then transferred to a purging glovebox under N_2(g). In the glovebox, CuOAc (0.018 mmol, 2.2 mg, 0.06 equiv) was weighed into the vial containing BPhen. Chlorobenzene (1.8 mL) was added to this vial and the vial is stirred to form a deep red 0.01 M stock solution of copper catalyst. The C–H substrate (0.3 mmol, 1 equiv) was weighed into the vial containing the rest of the reaction components, and then 0.6 mL of the copper catalyst solution was transferred to the reaction vial to give a 0.5 M mixture with a 2 mol% catalyst loading. The solution color changes from red to blue/green. This reaction vial is then removed from the glovebox and set to stir at 45 °C on a stir plate at 450 rpm for 16 h.

Work-up: At the end of the reaction, the mixture often becomes a light blue paste. The cap of the vial is loosened to vent the pressure build-up from the reaction. Dibromomethane (0.3 mmol, 21 µL, 1 equiv) and trifluorotoluene (0.3 mmol, 37 µL, 1 equiv) are then added as ^1H and ^{19}F NMR standards, respectively. The mixture is then diluted with $CDCl_3$ (0.6 mL), mixed, and a 30 µL aliquot is taken and filtered over a 1-inch celite plug directly into an NMR tube using $CDCl_3$ (in a few cases, dilution was done with dichloromethane or $CHCl_3$). The amount of benzyl fluoride product is then quantified relative to the two added internal standards. For purifications, sodium dithionite (1 equiv with respect to the amount of NFSI used, ~150-250 mg) is added with 100 µL water directly to the reaction vial. The reaction is then stirred for 15 min to quench the remaining NFSI (*warning*: dithionite oxidation results in protonation of Li_2CO_3, leading to further pressure build-up). This typically changes the reaction to a red color. The chunky mixture is then filtered over a 3-inch pad of silica into a disposable 24 mL glass vial using dichloromethane as the eluent. The vial is then carefully concentrated to prevent accidental evaporation of desired product and the remaining chlorobenzene solution is added directly to a silica gel column for separation of the product by column chromatography (0% pentane to 10% EtOAc, followed by ramping). Concentration of the product-containing fractions allows collection of the final product.

Reaction tip:

- The fluorination reaction is temperature sensitive, so it is recommended to use a hot plate with a thermocouple.

Reaction picture:

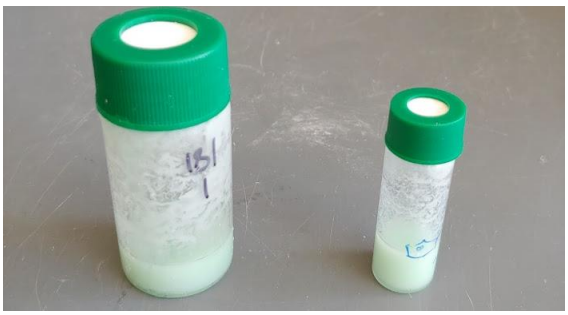

3B.III. Screening Tables

Table 3B.1. Control Experiments Table

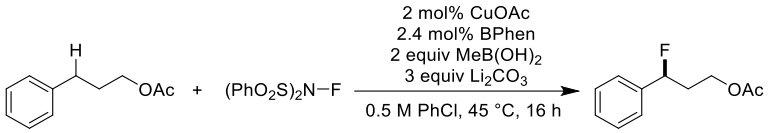

entry	control	MB	% SM	% C-N	% C-F(F_2)[a]
1	No CuOAc	102	102	--	--
2	No BPhen	101	77	--	24
3	No NFSI	102	102	--	--
4	No Li_2CO_3	70	70	--	--
5	No $MeB(OH)_2$	103	103	--	--
6[b]	No $MeB(OH)_2$ w/ 0.5 equiv diisopropyl phosphite	99	95	--	4
7	Under Air	66	42	--	24

[a]Reactions run at 0.2 mmol scale. Calibrated ^{1}H NMR yields using mesitylene as an internal standard. [b]Reaction used 3-phenyl-1-bromopropane as the C–H substrate.

Table 3B.2. Reaction Stoichiometry Screening Table

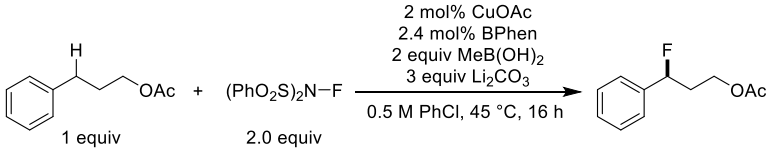

entry	variation	MB	% SM	% C-N	% C-F(F_2)[a]
1	standard cond.	95	2	--	80(5)
2	35 °C	93	44	--	48(1)
3	55 °C	92	3	--	74(10)
4	1 equiv. NFSI	90	34	--	52(2)
5	3 equiv. NFSI	98	7	--	89(5)
6	1 equiv. Li_2CO_3	95	13	--	78(4)
7	2 equiv. Li_2CO_3	93	5	--	82(6)
8	1 equiv. $MeB(OH)_2$	95	12	--	79(4)
9	2.5 equiv. $MeB(OH)_2$	97	3	--	87(7)
10	1 mol% BPhen	100	12	--	83(5)
11	4 mol% BPhen	103	103	--	0
12	1 mol% CuOAc/ 1 mol% BPhen	96	12	--	80(4)
13	10 mol% CuOAc/ 10 mol% BPhen	83	13	--	47(3)
14	10 mol% CuOAc/ 5 mol% BPhen	92	18	--	63(2)

[a]Reactions run at 0.2 mmol scale. Calibrated ^{1}H NMR yields using mesitylene as an internal standard. Mass balance in this table also accounts for formation of the benzyl ketone.

3B.IV. Additional Experiments and Observations

3B.IV.1. UV-Visible Titration of NFSI Addition to BPhenCu^{I}(OAc)

A 50 mL three-neck round-bottom flask was charged with a stir bar and sealed with two septa and a 90° ground-glass joint. The flask was deoxygenated via three evacuation/refill cycles and placed under an atmosphere of N_2. The fiber-optic UV-Visible dip-probe (1 mm path length) was pierced through the center neck of the flask and positioned directly above the stir bar (Figure 3B.1). Degassed PhCl (32 mL) was added to the flask via syringe. The 100% transmittance baseline spectrum was collected.

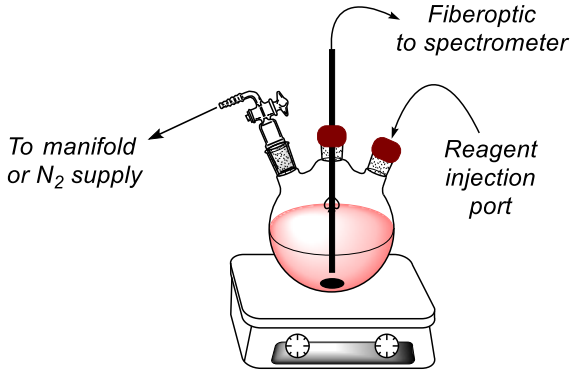

Figure 3B.1. Representative schematic for the experimental set-up used in the BPhenCu^{I}(OAc)/ NFSI titration experiments.

In the glovebox, a stock solution of BPhenCu^{I}(OAc) was prepared by dissolving BPhen (40.0 mg, 0.120 mmol) and Cu^{I}(OAc) (12.3 mg, 0.100 mmol) in PhCl (10 mL). The resulting deep red solution was loaded into a 1 mL syringe and the needle sealed by septum. A second stock solution of NFSI (31.5 mg, 0.100 mmol) in PhCl (10 mL) was prepared in a septum-capped vial.

The BPhenCu^{I}(OAc) solution was injected into the round-bottom flask with a positive counterpressure of N_2, affording a homogeneous red/brown solution with a total [Cu^{I}] of 0.33 mM. A UV-visible spectrum was collected. With stirring, multiple 100 µL aliquots of the NFSI stock solution was injected (0.001 mmol, 0.1 equiv per aliquot). Spectra were collected after each subsequent addition up to a total of eight additions (Table 3B.3). Isosbestic conversion of Cu^{I} to Cu^{II} is observed through five additions. Additional oxidant resulted in no change to the UV-visible spectrum. Representative wavelengths for Cu^{I} (375 nm) and Cu^{II} (325 nm) were selected for tracking conversion.

Table 3B.3. UV-visible data for the Cu/NFSI titration shown in Figure 3.2B.

Equiv NFSI	Abs @ 375 nm	Relative % [Cu^{I}]	Abs @ 325 nm	Relative % [Cu^{II}]
0.0	0.218	100	0.609	0.0
0.1	0.183	81.6	0.653	22.8
0.2	0.142	61.0	0.688	41.4
0.3	0.101	39.8	0.720	57.7
0.4	0.059	18.2	0.755	76.2
0.5	0.024	0.0	0.801	100
0.6	0.024	0.0	0.801	100
0.7	0.024	0.0	0.801	100
0.8	0.024	0.0	0.801	100

3B.IV.2. UV-Visible Spectroscopic Analysis of NFSI Addition to Cu^{I} in the Presence of $MeB(OH)_2$ and Base

A 50 mL three-neck round-bottom flask was charged with $MeB(OH)_2$ (3 mg, 0.05 mmol, 5 equiv), Li_2CO_3 (11.1 mg, 0.15 mmol, 15 equiv), and a stir bar and sealed with two septa and a 90° ground-glass joint. The flask was deoxygenated via three evacuation/refill cycles (*nb*. care must be taken not to pump off the $MeB(OH)_2$ under high vacuum; *ca.* 200 mtorr is acceptable) and placed under an atmosphere of N_2. The reaction vessel was fashioned with the fiber-optic dip-probe analogous to the experimental setup described in Experiment 3B.IV.1 (*cf.* Fig. 3B.1). Degassed PhCl (32 mL) was added to the flask via syringe. The 100% transmittance baseline spectrum was collected.

A deep red $BPhenCu^{I}(OAc)$ stock solution (1 mL at 10 mM) was injected via syringe under a counterflow of N_2, affording a homogeneous red/brown solution. A UV-visible spectrum was recorded to benchmark authentic 0.33 mM [$BPhenCu^{I}(OAc)$] (Table 3B.4). With stirring, NFSI (0.005 mmol, 0.5 equiv) was added as a stock solution in PhCl (0.5 mL), resulting in an immediate color change to light blue. UV-visible spectra (270 to 670 nm) were collected at five-minute intervals, monitoring the reduction of Cu^{II} to Cu^{I} (Table 3B.4). The spectra were baseline corrected using the absorbance value at 670 nm, where the copper species present have negligible background absorption.

Table 3B.4. UV-visible data for the $MeB(OH)_2$-mediated reduction of Cu^{II} (*cf.* Fig. 3.2B).

Time	λ (nm)		% Recovery of Cu^{I}	Time	λ (nm)		% Recovery of Cu^{I}
	460	670			460	670	
(pre NFSI)	0.305	0.039	N/A	60	0.247	0.042	77
0	0.037	0.036	0	65	0.254	0.041	80
5	0.046	0.035	4	70	0.257	0.041	81
10	0.053	0.033	7	75	0.261	0.042	82
15	0.067	0.037	11	80	0.265	0.042	84
20	0.084	0.038	17	85	0.266	0.040	85
25	0.102	0.040	23	90	0.268	0.040	86
30	0.129	0.044	32	95	0.271	0.042	86
35	0.143	0.037	40	100	0.271	0.040	87
40	0.170	0.040	49	105	0.271	0.040	87
45	0.188	0.041	54	110	0.273	0.042	87
50	0.214	0.040	65	115	0.274	0.040	88
55	0.234	0.041	73	120	0.276	0.039	89

3B.IV.3. Stoichiometric Reactivity of $MeB(OH)_2$ with NFSI in the Presence of Cu

According to the UV-visible data, NFSI rapidly oxidizes Cu^{I} to Cu^{II} and $MeB(OH)_2$ slowly reduces the Cu^{II} species back to Cu^{I}. One diagnostic product that we attribute to this reduction is the formation of Me–NSI. Me–NSI is readily observed in the optimized fluorination reaction as a singlet near 3.3 ppm in the ^1H NMR spectrum.[1]

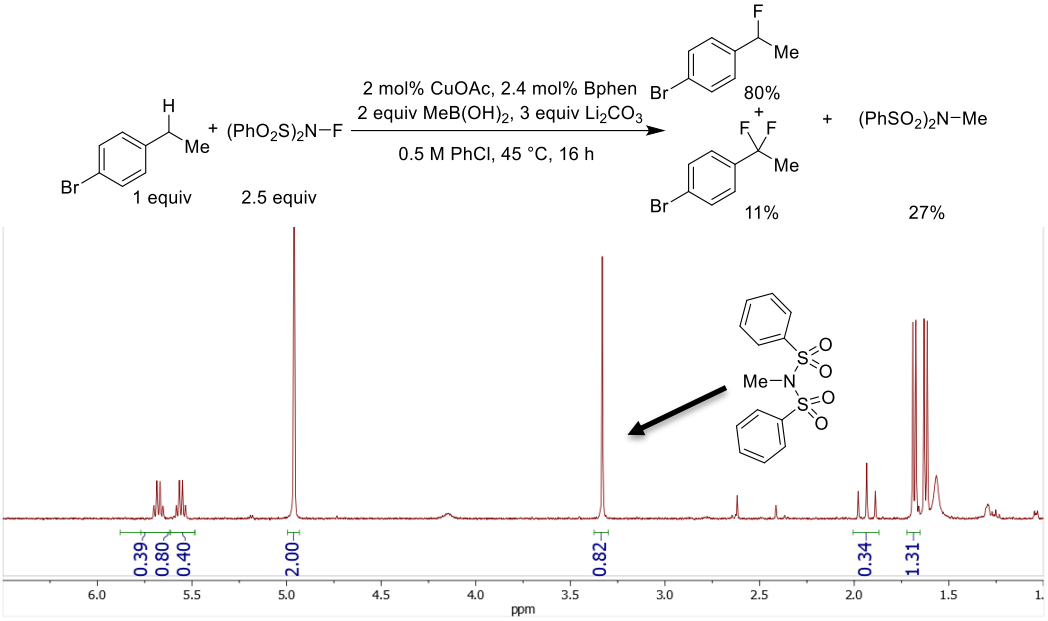

Figure 3B.2. ^1H NMR Spectrum ($CDCl_3$, 400 MHz, 25 °C) of the fluorination reaction with 0.3 mmol of CH_2Br_2 (21 µL) added as an internal standard (4.96 ppm). The alkyl protons from fluorinated products are integrated.

In an independent experiment, we left the C–H substrate out of the reaction and used $MeB(OH)_2$ as the limiting reagent with additional Cu catalyst in solution. These conditions led to a high 78% yield of the methylated sulfonimide.

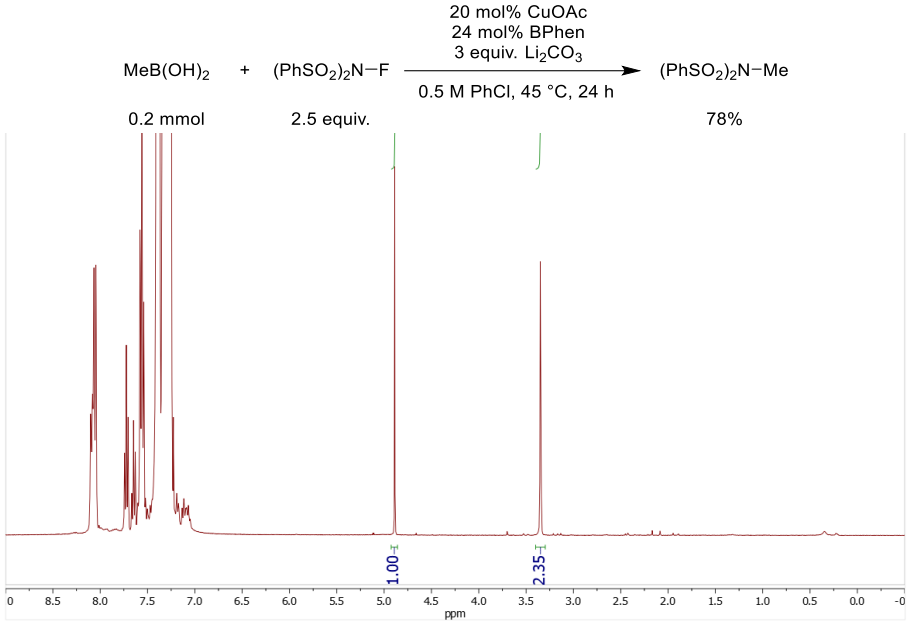

Figure 3B.3. ^1H NMR Spectrum ($CDCl_3$, 400 MHz, 25 °C) of the fluorination reaction with 0.1 mmol of CH_2Br_2 (7 µL) added as an internal standard (4.96 ppm). The Me peak from Me–NSI is integrated.

Based on these observations and on existing mechanistic studies of oxidative Chan-Lam coupling, it is possible that operative reduction pathways for Cu^{II} to Cu^{I} are via a disproportionation reaction and reductive elimination reaction.[2,3]

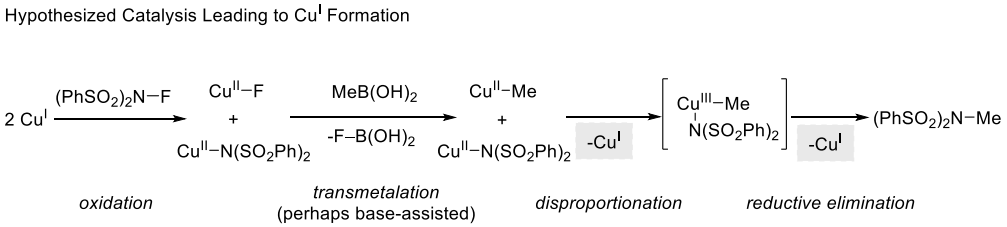

Figure 3B.4. A proposed reaction pathway allowing Cu^{II} reduction to Cu^{I} when using $MeB(OH)_2$ as the reductant. This suggested order of operations aligns with the proposed mechanism of Chan-Lam coupling reactions.

3B.IV.4. Time Course Data for Variations of the Optimized Reaction Conditions

A set of eighteen 1-bromo-4-ethylbenzene fluorination reactions were setup on a 0.3 mmol scale mostly in accord with the general procedure in section II. All of the reactions were placed in a pre-heated heating block (45 °C) on a stir plate set to 750 rpm. At the designated timepoints, reactions were removed from the plate, opened, diluted with 0.5 mL of PhCl and internal standards were added (21 µL CH_2Br_2 and 37 µL $PhCF_3$) via micro syringe. The reaction vials were then sealed, mixed vigorously, and a 50 µL aliquot was removed. This aliquot was filtered through a short (ca. 0.5 inch) celite plug with $CDCl_3$ (100 + 300 + 300 µL) directly into an NMR tube. ^1H and $^{19}F\{^1H\}$ NMR spectra were collected for each timepoint to track reaction speciation.

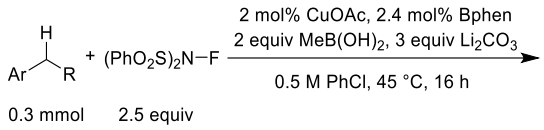

Table 3B.5. Time course data for optimized fluorination reaction conditions (*cf.* Figure 3.2C).

Time (h)	[C–H] (M)	[C–F] (M)	[C–F_2] (M)
0.08	0.49	0.02	0.00
0.25	0.46	0.03	0.00
0.50	0.44	0.04	0.00
0.75	0.43	0.06	0.00
1.0	0.40	0.06	0.00
1.5	0.39	0.10	0.00
2.0	0.36	0.14	0.00
2.5	0.32	0.16	0.00
3.0	0.31	0.17	0.00

Time (h)	[C–H] (M)	[C–F] (M)	[C–F_2] (M)
3.5	0.29	0.18	0.00
4.0	0.26	0.22	0.00
4.5	0.20	0.23	0.00
5.0	0.20	0.25	0.00
6.0	0.17	0.27	0.01
7.0	0.13	0.32	0.01
8.0	0.08	0.36	0.02
12.0	0.03	0.40	0.03
16.0	0.01	0.42	0.05

A second set of eighteen 1-bromo-4-ethylbenzene fluorination reactions were set up on a 0.3 mmol scale according to the general procedure in section II, except Li_2CO_3 was omitted. These vials were placed on a pre-heated block (45 °C) on a stir plate set to 750 rpm. The reactions were processed analogously to those described above (at the same time intervals), providing a kinetic profile for reactions run in the absence of Li_2CO_3 (Figure 3B.5).

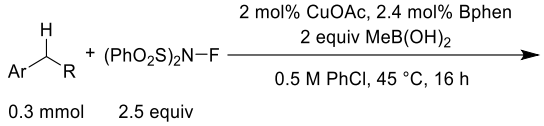

Table 3B.6. Time course data for an optimized fluorination reaction run in the absence of base (*cf.* Scheme 3.2A).

Time (h)	[C–H] (M)	[C–F] (M)	[C–OH] + [C=O] (M)	[C–N] (M)
0.08	0.50	0.01	0.00	0.00
0.25	0.49	0.02	0.01	0.01
0.50	0.45	0.02	0.01	0.01
0.75	0.44	0.03	0.01	0.02
1.0	0.43	0.03	0.02	0.02
1.5	0.40	0.05	0.02	0.03
2.0	0.36	0.05	0.04	0.03
2.5	0.34	0.07	0.05	0.04
3.0	0.29	0.07	0.06	0.05

Time (h)	[C–H] (M)	[C–F] (M)	[C–OH] + [C=O] (M)	[C–N] (M)
3.5	0.27	0.08	0.09	0.08
4.0	0.25	0.08	0.08	0.08
4.5	0.22	0.05	0.10	0.09
5.0	0.21	0.03	0.09	0.08
6.0	0.16	0.01	0.16	0.11
7.0	0.13	0.00	0.18	0.12
8.0	0.10	0.00	0.24	0.13
12.0	0.07	0.00	0.26	0.13
16.0	0.03	0.00	0.26	0.13

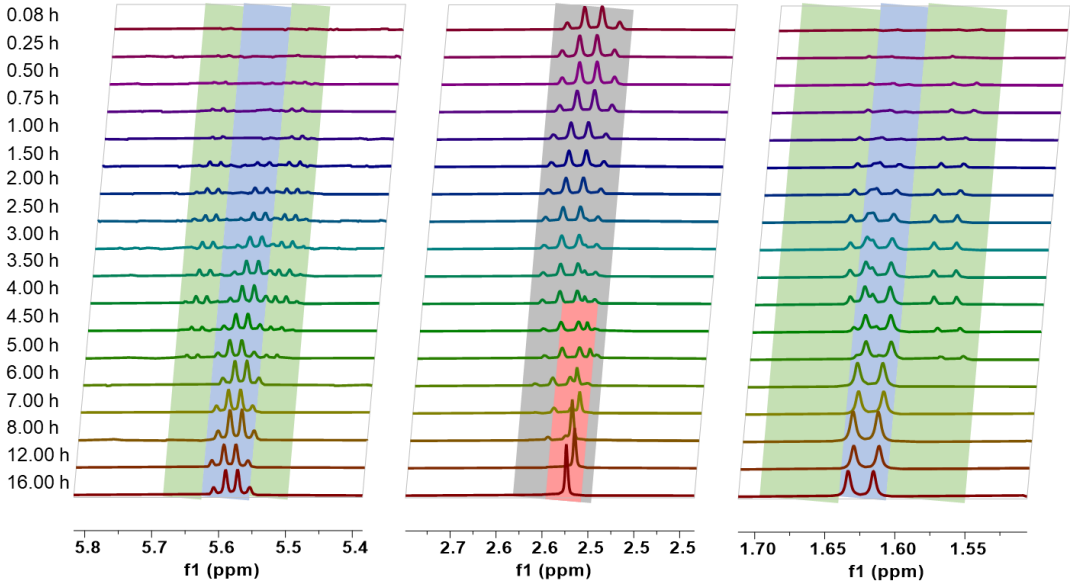

Figure 3B.5. Partial ^{1}H NMR spectrum (400 MHz, 25 °C) with representative time course data for an optimized fluorination reaction run in the absence of base. The shaded regions correspond to the resonances for the C–H starting material (; q, 2.61 ppm & t, 1.23 ppm) and C–F (; dq, 5.58 ppm & dd, 1.61 ppm), C–O (; s, 2.57 ppm [ketone] & d, 1.47 ppm [alcohol]), and C–N[4] (; q, 5.56 ppm & d, 1.62) products.

Discussion of Scheme 3.2B (related to Figure 3B.5):

The observation of fluorinated product forming (0 to 3.5 h) and later being consumed (4 to 7 h) under the base-free reaction conditions (Scheme 3.2A and Figure 3B.5) prompted exploration of NHSI-catalyzed acidolysis (Scheme 3.2B). Fluorination of ethyl benzene (following the general procedure in section II; 66% yield for this particular reaction), filtration through a silica plug (washed with DCE, 2 x 0.6 mL) and heating of the resulting solution of benzyl fluoride with added NHSI (89.2 mg, 0.3 mmol, 1 equiv) led to complete fluoride displacement in 10 minutes (70 °C). The benzyl fluoride was consumed quantitatively and afforded a 68% spectroscopic yield of sec-phenethyl alcohol relative to the benzyl fluoride product (corroborated by spiking the NMR sample with authentic alcohol).

A 4 mL scintillation vial was charged with Li_2CO_3 (201 mg, 2.7 mmol, 3 equiv), NFSI (711 mg, 2.25 mmol, 2.5 equiv), 1-bromo-4-ethylbenzene (126 µL, 0.9 mmol, 1 equiv), CH_2Br_2 (63 µL, 0.9 mmol, 1 equiv), $PhCF_3$ (111 µL, 0.9 mmol, 1 equiv), and a Teflon-coated magnetic stirbar on the bench top. The vial was sealed with a pierceable screw-on septum cap. Inside the glovebox, a BPhenCu^{I}(OAc) stock solution was prepared by dissolving Cu^{I}(OAc) (32.6 mg, 0.265 mmol) and BPhen (105.6 mg, 0.318 mmol) in PhCl (26.4 mL). 1.8 mL of this deep red stock solution (2% Cu^{I}(OAc)/2.4% BPhen) was added to the reaction vial, resulting in an immediate color change to light blue/green. The vial was placed in a pre-heated block (45 °C) atop a stir plate set to 750 rpm. 50 µL aliquots were removed via microsyringe at the appropriate time intervals and processed identically to those above.

Table 3B.7. Representative time course data for optimized fluorination reaction conditions run in the absence of $MeB(OH)_2$ (*cf.* Figure 3.2C).

Time (h)	[C–H] (M)	[C–F] (M)	[C–F_2] (M)
0.08	0.50	0.00	0.00
0.25	0.49	0.00	0.00
0.50	0.48	0.00	0.00
0.75	0.49	0.00	0.00
1.0	0.49	0.00	0.00
1.5	0.50	0.00	0.00
2.0	0.49	0.00	0.00
2.5	0.49	0.00	0.00
3.0	0.48	0.00	0.00

Time (h)	[C–H] (M)	[C–F] (M)	[C–F_2] (M)
3.5	0.49	0.00	0.00
4.0	0.49	0.00	0.00
4.5	0.49	0.00	0.00
5.0	0.49	0.00	0.00
6.0	0.50	0.00	0.00
7.0	0.50	0.00	0.00
8.0	0.50	0.00	0.00
12.0	0.50	0.00	0.00
16.0	0.52	0.00	0.00

3B.V. Reaction Protocol and Characterization Data for Benzylic Fluorination on 1 mmol Scale

The optimized fluorination conditions were evaluated with a small series of benzylic C–H substrates on 1 mmol scale, with more thorough assessment of the synthetic scope and utility reported elsewhere.[5]

Set-up: On the benchtop, a disposable 20 mL glass vial was charged with $MeB(OH)_2$ (2 mmol, 120 mg, 2 equiv), Li_2CO_3 (3 mmol, 222 mg, 3 equiv), NFSI (2.5 mmol, 788 mg, 2.5 equiv), and a Teflon stir bar. The vial was sealed by a PTFE-lined pierceable cap. BPhen (0.024 mmol, 8.0 mg, 0.024 equiv) was weighed into a secondary vial with a Teflon stir bar. Both vials were then transferred to a purging glovebox under N_2(g). In the glovebox, CuOAc (0.02 mmol, 2.5 mg, 0.02 equiv) was weighed into the vial containing BPhen. Chlorobenzene (2 mL) was added to this vial and the red solution was stirred for 3 minutes. The C–H substrate (1.0 mmol, 1 equiv) was weighed into the vial containing the rest of the reaction components, and then the copper catalyst solution was transferred to the reaction vial. This reaction vial was then sealed and removed from the glovebox and set to stir at 45 °C on a stir plate at 450 rpm for 16 h.

Work-up: The cap of the vial was loosened to vent the pressure build-up from the reaction. Dibromomethane (1 mmol, 70.2 µL, 1 equiv) and trifluorotoluene (1 mmol, 123 µL, 1 equiv) were then added as ^{1}H and ^{19}F NMR standards, respectively. The mixture was then diluted with $CDCl_3$ (0.6 mL), mixed, and a 30 µL aliquot was taken and filtered over a 1-inch celite plug directly into an NMR tube using 400 µL $CDCl_3$. The amount of benzyl fluoride product was then quantified relative to the two added internal standards. For purification, sodium dithionite (1 equiv with respect to the amount of NFSI used, ~150-250 mg) was added with 100 µL water directly to the reaction vial. The reaction was then stirred for 10 min to quench the remaining NFSI. The chunky mixture was then filtered over a 3-inch pad of silica into a disposable 24 mL glass vial using dichloromethane as the eluent. The vial was then carefully concentrated to prevent accidental evaporation of desired product and the remaining chlorobenzene solution was added directly to a silica gel column for separation of the product by column chromatography (0% pentane to 10% EtOAc, followed by ramping). Concentration of the product-containing fractions allows collection of the final product.

3B.VI. Summary of Cu/NFSI Benzylic C–H Fluorination Data

Product Isolations[6]:

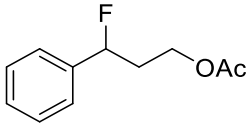

(1) 3-fluoro-3-phenylpropyl acetate: Prepared from 3-phenylpropyl acetate (1 mmol, 178 mg, 1 equiv) according to the reaction protocol in section V.
Isolated Yield: 38%, 73.6 mg of clear liquid (65% NMR yield).
Product Spectra Available in the Literature (CAS): Yes[7] (412026-80-3)
^{1}H NMR ($CDCl_3$, 500 MHz): δ 7.42 – 7.32 (m, 5H), 5.57 (ddd, J = 47.8, 8.7, 4.2 Hz, 1H), 4.26 (ddd, J = 11.2, 8.0, 5.6 Hz, 1H), 4.20 (dt, J = 11.3, 5.9 Hz, 1H), 2.30 (tdt, J = 14.6, 8.8, 5.6 Hz, 1H), 2.23 – 2.09 (m, 1H), 2.05 (s, 3H).
^{13}C NMR ($CDCl_3$, 126 MHz): δ 170.9, 139.5 (d, J = 19.5 Hz), 128.6, 128.5 (d, J = 2.0 Hz), 125.5 (d, J = 6.7 Hz), 91.4 (d, J = 170.9 Hz), 60.5 (d, J = 4.9 Hz), 36.2 (d, J = 24.1 Hz), 20.9.
^{19}F NMR ($CDCl_3$, 377 MHz): δ -177.42.

The chromatogram below is provided to show some of the characterized side products formed in the process of isolation, which resulted in a reduced isolated yield relative to the NMR yield.

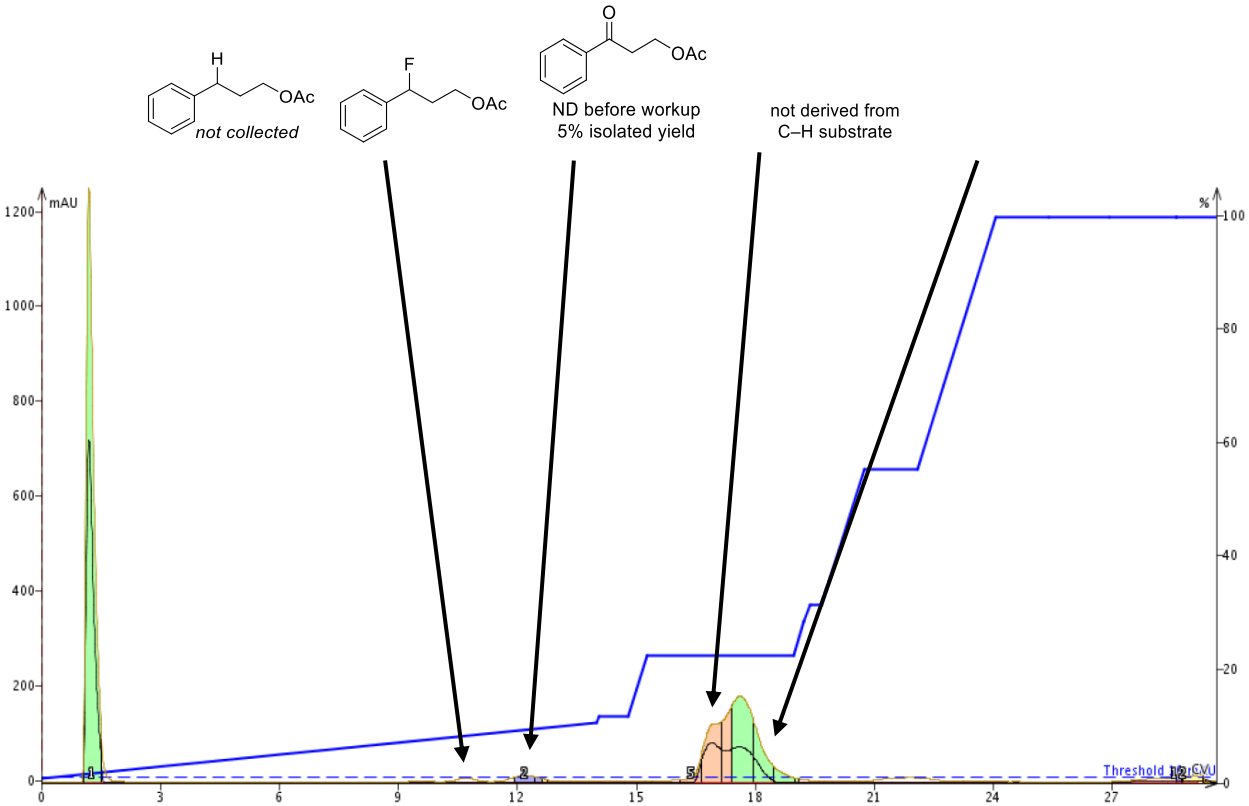

Figure 3B.6. Benzylic fluorination isolation breakdown for 3-phenyl propylacetate

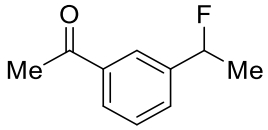

(2) 1-(3-(1-fluoroethyl)phenyl)ethan-1-one: Prepared from 1-(3-ethylphenyl)ethan-1-one (1 mmol, 148 mg, 1 equiv) according to the reaction protocol in section V.
Isolated Yield: 44%, 72.4 mg of clear liquid (66% NMR yield).
Product Spectra Available in the Literature (CAS): Yes (1550969-43-1)
^{1}H NMR ($CDCl_3$, 600 MHz): δ 7.95 – 7.88 (m, 2H), 7.59 – 7.54 (m, 1H), 7.48 (t, J = 7.7 Hz, 1H), 5.68 (dq, J = 47.5, 6.5 Hz, 1H), 2.62 (s, 3H), 1.66 (dd, J = 24.0, 6.5 Hz, 3H).
^{13}C NMR ($CDCl_3$, 150 MHz): δ 197.8, 142.2 (d, J = 19.9 Hz), 137.3, 129.8 (d, J = 6.8 Hz), 128.9, 128.2 (d, J = 1.8 Hz), 124.9 (d, J = 7.0 Hz), 90.4 (d, J = 168.9 Hz), 26.7, 23.0 (d, J = 24.9 Hz).
^{19}F NMR ($CDCl_3$, 377 MHz): δ -168.91.
HRMS (ESI) m/z: $[M+H]^+$ Calcd for $C_{10}H_{12}FO$ 167.0867; Found 167.0868.

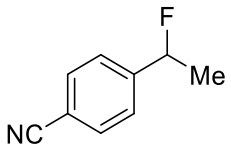

(3) 4-(1-fluoroethyl)benzonitrile: Prepared from 4-ethylbenzonitrile (1 mmol, 131 mg, 1 equiv) according to the reaction protocol in section V.
Isolated Yield: 12%, 18.6 mg of clear liquid (12% NMR yield).
Product Spectra Available in the Literature (CAS): Yes[7] (155671-14-0)
^{1}H NMR ($CDCl_3$, 500 MHz): δ 7.67 (d, J = 7.7 Hz, 2H), 7.45 (d, J = 8.7 Hz, 2H), 5.67 (dq, J = 47.4, 6.5 Hz, 1H), 1.64 (dd, J = 24.0, 6.5 Hz, 3H).
^{13}C NMR ($CDCl_3$, 126 MHz): δ 146.7 (d, J = 19.9 Hz), 132.4, 125.6 (d, J = 7.6 Hz), 118.5, 112.0 (d, J = 1.9 Hz), 89.8 (d, J = 171.3 Hz), 22.9 (d, J = 24.5 Hz).
^{19}F NMR ($CDCl_3$, 377 MHz): δ -172.70.

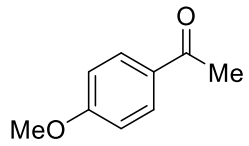

no C–F bond detected

(4) 1-(4-methoxyphenyl)ethan-1-one: Prepared from 4-ethylanisole (1 mmol, 136 mg, 1.0 equiv) according to the reaction protocol in section V.
Isolated Yield: 96%, 144.7 mg of colorless solid (97% NMR yield).
Product Spectra Available in the Literature (CAS): Yes[8] (100-06-1)
^{1}H NMR ($CDCl_3$, 500 MHz): δ 7.94 (d, J = 8.8 Hz, 1H), 6.93 (d, J = 8.8 Hz, 1H), 3.87 (s, 2H), 2.55 (s, 2H).
^{13}C NMR ($CDCl_3$, 126 MHz): δ 196.8, 163.5, 130.6, 113.7, 55.5, 26.3.

Products that were not successfully isolated:

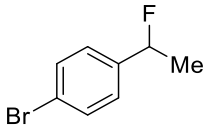

(5) 1-bromo-4-(1-fluoroethyl)benzene: Prepared from 1-bromo-4-ethylbenzene (1 mmol, 185 mg, 1 equiv) according to the reaction protocol in section V, but was not successfully isolated.
Product Spectra Available in the Literature (CAS): Yes[9] (159298-87-0)
Benzyl Fluoride C–H Shift: ^{1}H NMR ($CDCl_3$, 400 MHz): δ 5.59 (dq, J = 47.5, 6.4 Hz).
Calibrated ^{1}H NMR Yield from Benzyl Proton: 77%
Benzylic Fluoride Shift: ^{19}F NMR ($CDCl_3$, 377 MHz): δ -168.01.
Calibrated ^{19}F NMR Yield from Benzyl Fluoride: 75%
Benzyl Difluoride Fluorine Shift: ^{19}F NMR ($CDCl_3$, 377 MHz): δ -87.78.
Calibrated ^{19}F NMR Yield of Benzyl Difluoride: 3%

Purification: Normal phase silica gel chromatography was used with a gradient of 0%→10% EtOAc in pentane. The chromatogram below is provided to show what was obtained from attempted isolation. Significant acetophenone formation was observed after the NFSI quench and chromatography and the product was not readily separable from the starting material and chlorobenzene.

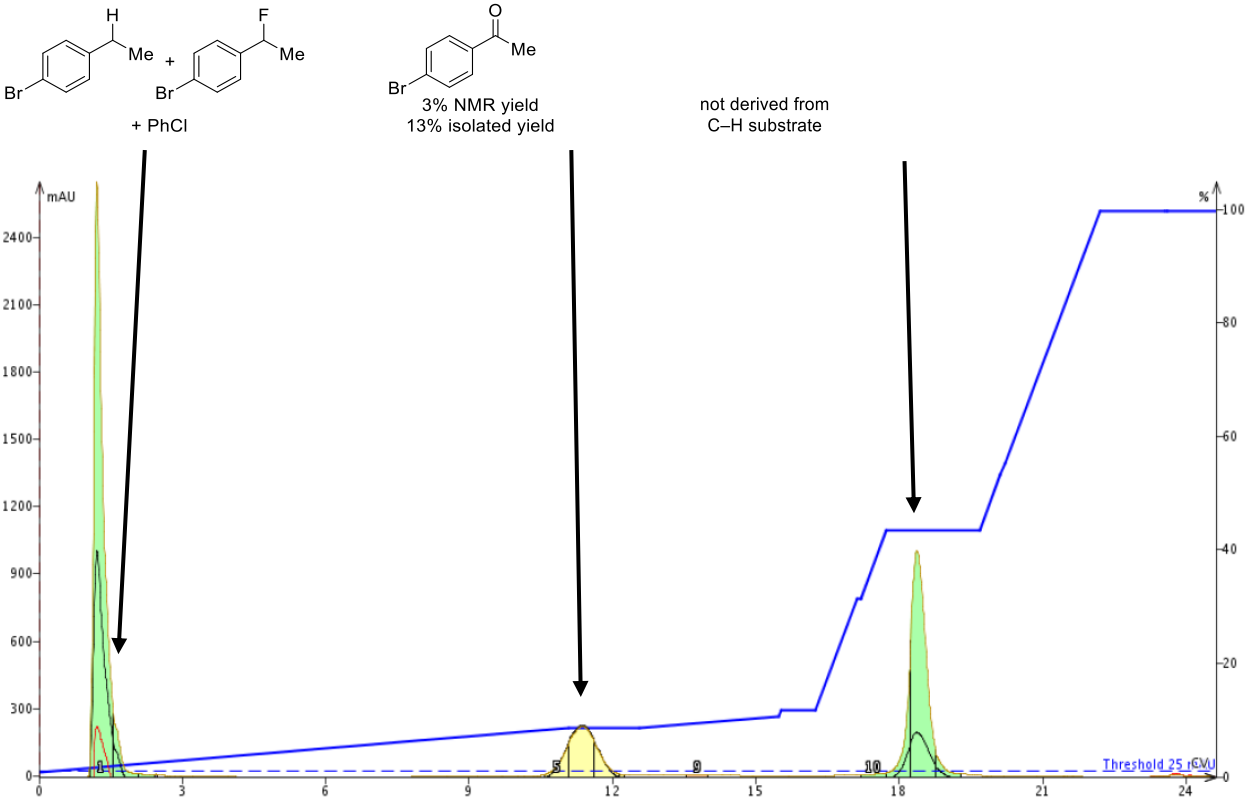

Figure 3B.7. Benzylic fluorination isolation breakdown for 4-Br ethylbenzene

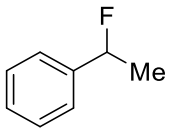

(6) (1-fluoroethyl)benzene: Prepared from ethylbenzene (1 mmol, 106 mg, 1.0 equiv) according to the reaction protocol in section V, but was not successfully isolated .
Product Spectra Available in the Literature (CAS): Yes[10] (7100-97-2)
Benzyl Fluoride C–H Shift: ^{1}H NMR ($CDCl_3$, 400 MHz): δ 5.63 (dq, J = 47.7, 6.5 Hz).
Calibrated ^{1}H NMR Yield from Benzyl Proton: 66%
Benzylic Fluoride Shift: ^{19}F NMR ($CDCl_3$, 377 MHz): δ -167.03.
Calibrated ^{19}F NMR Yield from Benzyl Fluoride: 67%
Benzyl Difluoride Fluorine Shift: ^{19}F NMR ($CDCl_3$, 377 MHz): δ -87.63.
Calibrated ^{19}F NMR Yield of Benzyl Difluoride: 6%

Purification: Normal phase silica gel chromatography was used with a gradient of 0%→10% EtOAc in pentane. The chromatogram below is provided to show what was obtained from attempted isolation. No desired product was observed in any column fractions, and numerous new side products were formed.

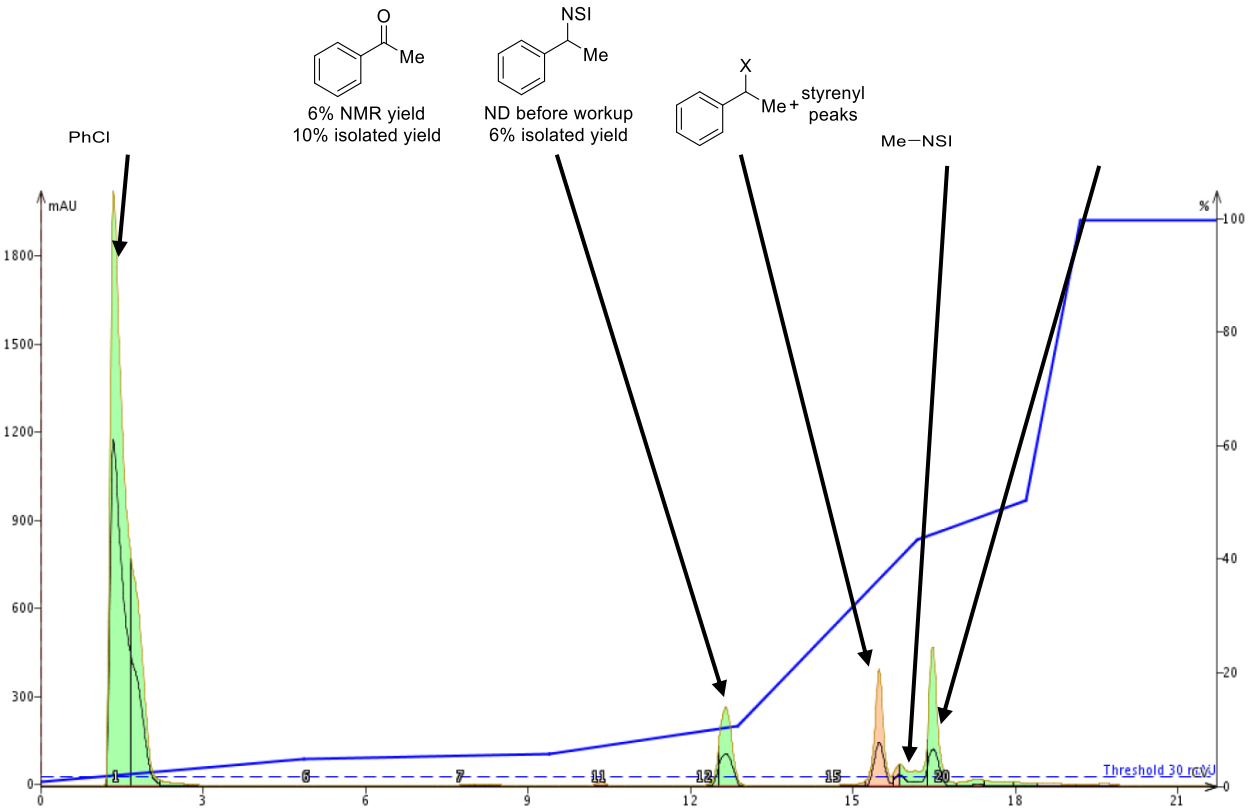

Figure 3B.8. Benzylic fluorination isolation breakdown for ethylbenzene

3B.VII. References

1. Chen, L.; Lang, H.; Fang, L.; Yu, J.; Wang, L. Nickel-Catalyzed Desulfitative Suzuki-Miyaura Cross-Coupling of *N*,*N*-Disulfonylmethylamines and Arylboronic Acids. *Eur. J. Org. Chem.* **2014**, *29*, 6385-6389.
2. Vantourout, J. C.; Miras, H. N.; Isidro-Llobet, A.; Sproules, S.; Watson, A. J. B. Spectroscopic Studies of the Chan-Lam Amination: A Mechanism-Inspired Solution to Boronic Ester Reactivity. *J. Am. Chem. Soc.* **2017**, *139*, 4769-4779.
3. Rossi, S. A.; Shimkin, K. W.; Xu, Q.; Mori-Quiroz, L. M.; Watson, D. A. Selective Formation of Secondary Amides via the Copper-Catalyzed Cross-Coupling of Alkylboronic Acids with Primary Amides. *Org. Lett.* **2013**, *15*, 2314-2317.
4. Ni, Z.; Zhang, Q.; Xiong, T.; Zheng, Y.; Li, Y.; Zhang, H.; Zhang, J.; Liu, Q. Highly Regioselective Copper-Catalyzed Benzylic C–H Amination by *N*-Fluorobenzenesulfonimide. *Angew. Chem. Int. Ed.* **2012**, *51*, 1244-1247.
5. Vasilopoulos, A.; Golden, D. L.; Buss, J. A.; Stahl, S. S. Copper-Catalyzed C–H Fluorination/Functionalization Sequence Enabling Benzylic C–H Cross Coupling with Diverse Nucleophiles. *Org. Lett.* **2020**, *22*, 5753-5757.
6. For NMR spectra, see: Buss, J. A.; Vasilopoulos, A.; Golden, D. L.; Stahl, S. S. Copper-Catalyzed Functionalization of Benzylic C–H Bonds with *N*-Fluorobenzenesulfonimide: Switch from C–N to C–F Bond Formation Promoted by a Redox Buffer and Brønsted Base. *Org. Lett.* **2020**, *22*, 5749-5752.
7. Xia, J.-B.; Zhu, C.; Chen, C. Visible Light-Promoted Metal-Free C–H Activation: Diarylketone-Catalyzed Selective Benzylic Mono- and Difluorination. *J. Am. Chem. Soc.* **2013**, *135*, 17494-17500.
8. SDBSWeb. https://sdbs.db.aist.go.jp/sdbs/cgi-bin/landingpage?sdbsno=1164 (accessed Jun 30, **2020**), National Institute of Advanced Industrial Science and Technology.
9. Liu, W.; Groves, J.T. Manganese-Catalyzed Oxidative Benzylic C–H Fluorination by Fluoride Ions. *Angew. Chem. Int. Ed.* **2013**, *52*, 6024-6027.
10. Bloom, S.; Pitts, C. R.; Woltornist, R.; Griswold, A.; Holl, M. G.; Lectka, T. Iron(II)-Catalyzed Benzylic Fluorination. *Org. Lett.* **2013**, *15*, 1722-1724.

Appendix C: Supporting Information Chapter 4

4C.I. General Considerations

All reagents were purchased from commercial sources and used as received. Nearly identical performance was observed when using reagents from different commercial sources. Cu salts were purchased from Strem Chemicals and Sigma-Aldrich. C–H substrates and nucleophiles were purchased from Oakwood, Combi-Blocks, Enamine, AK Scientific, TCI America, Ark-Pharm, Ambeed, or Sigma-Aldrich. Nosyl protected amines were synthesized from the corresponding primary amines according to a literature procedure.[1] 3-Phenylpropyl trifluoroacetamide was synthesized according to a literature procedure.[2] NFSI was purchased from Ark-Pharm and Oakwood. Bathophenanthroline and other ligands were purchased from Aldrich, Ambeed, or Strem. The boron reagents were purchased from Sigma-Aldrich, Oakwood, or Combi-Blocks.

All fluorination reaction solids were weighed out on the benchtop, while liquids were added in an inert atmosphere (N_2) glovebox. Retention in performance can be obtained by setting up the fluorination reaction on the benchtop with backfilling or sparging of the reaction vessel with N_2. The fluorine displacement reactions were all set-up on the benchtop under air. The displacement step can produce catalytic quantities of HF (quenches on the reaction vial), so it is recommended to have ready access to a tube of calcium gluconate in case of accidental exposure to the reaction mixture. ^{1}H, ^{13}C, and ^{19}F NMR spectra were recorded on a Bruker Avance III 400 spectrometer at 25 °C (^{1}H 400.1 MHz, ^{13}C 100.6 MHz, ^{19}F 376.5 MHz) or a Bruker Avance III 500 spectrometer at 25 °C (^{1}H 500.1 MHz, ^{13}C 125.7 MHz, ^{19}F 470.6 MHz), except where noted otherwise, and chemical shifts are reported in parts per million (ppm). NMR spectra were referenced to residual $CHCl_3$ at 7.26 ppm (^{1}H) and $CDCl_3$ at 77.16 ppm (^{13}C). All ^{19}F NMR spectra were absolutely referenced to their respective solvent peaks in the ^{1}H NMR spectrum. Chromatography was performed using an automated Biotage Isolera® with reusable 25 g Biotage® Sfär Silica HC D cartridges for normal phase or 60 g Biotage® SNAP Ultra C18 cartridges for reversed phase. High-resolution mass spectra were obtained using a Thermo Q Exactive™ Plus via (ASAP-MS) by the mass spectrometry facility at the University of Wisconsin.

4C.II. General Procedure for Benzylic C–H Fluorination and NMR Quantitation

Warning: This reaction evolves gas from protonation of Li_2CO_3, which is able to pressurize the reaction vial. Be sure to take appropriate safety precautions.

Set-up: On the benchtop, a disposable 4 mL glass vial was charged with $MeB(OH)_2$ (0.6 mmol, 35.9 mg, 2 equiv), Li_2CO_3 (0.9 mmol, 66.5 mg, 3 equiv), N-fluorobenzenesulfonimide (NFSI; 0.75 mmol, 236.5 mg, 2.5 equiv), and a Teflon stir bar. The vial was sealed by a PTFE-lined pierceable cap. Bathophenanthroline (BPhen, 0.0216 mmol, 7.2 mg, 0.072 equiv) was weighed into a secondary vial with a Teflon stir bar. Both vials were then transferred to a purging glovebox under N_2(g). In the glovebox, CuOAc (0.018 mmol, 2.2 mg, 0.06 equiv) was weighed into the vial containing BPhen. Chlorobenzene (1.8 mL) was added to this vial and the vial is stirred to form a deep red 0.01 M stock solution of copper catalyst. The C–H substrate (0.3 mmol, 1 equiv) was weighed into the vial containing the rest of the reaction components, and then 0.6 mL of the copper catalyst solution was transferred to the reaction vial to give a 0.5 M mixture with a 2 mol% catalyst loading. The solution color changes from red to blue/green. This reaction vial is then removed from the glovebox and set to stir at 45 °C on a stirring hotplate in an aluminum block at 600 rpm for 16 h.

Work-up: At the end of the reaction, the mixture often becomes a light blue paste. The cap of the vial is loosened to vent the pressure build-up from the reaction. Dibromomethane (0.3 mmol, 21 µL, 1 equiv) and trifluorotoluene (0.3 mmol, 37 µL, 1 equiv) are then added as ^{1}H and ^{19}F NMR standards, respectively. The mixture is then diluted with $CDCl_3$ (0.6 mL), mixed, and a 30 µL aliquot is taken and filtered over a 1-inch celite plug directly into an NMR tube using $CDCl_3$ (in a few cases, dilution was done with dichloromethane or $CHCl_3$). The amount of benzyl fluoride product is then quantified relative to the two added internal standards.

Reaction tip:

- The fluorination reaction is highly temperature sensitive, so it is recommended to use a hot plate with a thermocouple.
- For scale up reactions, it may be beneficial to use DCM or acetone as the solvent to improve homogeneity of the reaction.

4C.III. General Procedure for Catalyzed Benzyl Fluoride Displacement

Warning: This reaction gradually produces HF, which is seemingly quenched via etching of the inside of the borosilicate vial. This reaction could degrade glass reaction vessels.

Set-up: Following NMR quantitation of the benzyl fluoride product, sodium dithionite (1 equiv with respect to the amount of NFSI used, ~150-250 mg) is added with 100 µL water directly to the reaction vial. The reaction is then stirred for 15 min to quench the remaining NFSI (*warning*: dithionite oxidation results in protonation of remaining Li_2CO_3,[3] leading to further pressure build-up). This typically changes the reaction to a red color. The chunky mixture is then filtered over a 3-inch pad of silica or celite into a disposable 15 mL glass vial using dichloromethane as the eluent (silica is preferred if the benzyl fluoride tolerates it). After flushing to a filtrate volume of 5 mL, $MgSO_4$ (3-7 equiv, ~300 mg) is added to the vial and it is allowed to dry for 10 min. Meanwhile, the nucleophile (0.75 mmol, 2.5 equiv) is weighed into another disposable 15 mL glass vial with a Teflon coated stir bar. The benzyl fluoride-containing solution is filtered over a 1-inch celite plug into the 15 mL vial containing the nucleophile, and then 1 mL of additional dichloromethane is used to flush the plug and bring the final reaction volume to 6 mL (0.05 M). The vessel is then sealed with a PTFE-lined pierceable cap and hexafluoroisopropanol (HFIP; 3 mmol, 315 µL, 10 equiv) and/or BF_3•Et_2O (0.03 mmol, 3.7 µL, 0.1 equiv) is added to catalyze fluoride displacement. The reaction is stirred overnight. An aliquot of this reaction solution is then taken for ^{1}H NMR analysis to determine whether it is complete. Reactions showing incomplete fluoride conversion are subjected to harsher displacement conditions (i.e., heated to 45 °C in an aluminum block on a hotplate or additional BF_3•Et_2O is added). The final solution is concentrated on a rotovap and purified using automated flash column chromatography to yield the desired functionalization product.

Reaction tips:

- Lewis basic functional groups disrupt fluoride displacement. When using coupling partners with Lewis basic groups, it is typically required to use additional BF_3 to enact displacement (>0.25 equiv BF_3 is common, *cf.* Substrates **37** and **42**).
- Protonation of Lewis basic groups may also be helpful for enabling displacement reactivity (*cf.* Substrate **31**)

4C.IV. Procedure for 3 mmol Scale Fluorination/Functionalization Sequence to Prepare 46

Fluorination: On the benchtop, a disposable 20 mL glass vial was charged with $MeB(OH)_2$ (6 mmol, 359 mg, 2 equiv), Li_2CO_3 (9 mmol, 665 mg, 3 equiv), NFSI (7.5 mmol, 2.365 g, 2.5 equiv), and a Teflon stir bar. The vial was sealed by a PTFE-lined pierceable cap. Bathophenanthroline (BPhen, 0.072 mmol, 23.9 mg, 0.024 equiv) was weighed into a secondary vial with a Teflon stir bar. Both vials were then transferred to a purging glovebox under N_2(g). In the glovebox, CuOAc (0.06 mmol, 7.4 mg, 0.02 equiv) was weighed into the vial containing BPhen followed by addition of chlorobenzene (6 mL, 0.5 M). This solution was allowed to stir for 3 minutes to form a deep red solution. 1-chloro-3-phenylpropane (3 mmol, 429 µL, 1 equiv) was then weighed into the vial containing the rest of the reaction components and the copper catalyst solution was transferred to the reaction vial. The reaction vial was then sealed, removed from the glovebox, and set to stir at 45 °C in an aluminum block on a heated stir plate at 600 rpm for 16 h.

Functionalization: The cap was carefully opened to release built-up pressure (the septum may have been pierced with a needle instead). Dibromomethane was then added as an NMR standard (1 mmol, 70.2 µL, 0.33 equiv) and a 50 uL aliquot was taken and filtered over celite with 450 uL $CDCl_3$ directly into an NMR tube for NMR quantitation. To the reaction vial was added sodium dithionite (7.5 mmol, 1.305 g, 2.5 equiv) and water (500 uL) and this mixture was allowed to stir for 10 minutes uncapped. After quenching NFSI, the now chunky red-white mixture was filtered over a 3-inch pad of silica directly into a 250 mL round bottom flask using dichloromethane (54 mL, final concentration of 0.05 M). *p*-Cresol (7.5 mmol, 811 mg, 2.5 equiv) was added to the round bottom flask followed by HFIP (30 mmol, 3.159 mL, 10 equiv) and after initial agitation, the reaction was left to sit at room temperature for 16 h.

Work-up: A 100 µL aliquot was taken from the now light gold solution for NMR analysis to detect formation of product and consumption of benzyl fluoride (^{1}H and ^{19}F). If any residual fluoride were detected, the vessel would have been warmed to 40 °C on an aluminum block or catalytic BF_3•Et_2O would have been added. The reaction was concentrated on the rotovap at 40 °C to remove the solvent (chlorobenzene, dichloromethane, and HFIP) and the concentrated residue was purified by reverse phase chromatography using a 65%→100% MeOH in water gradient. The product fractions were collected and concentrated on the rotovap at 50 °C to yield 445 mg of the desired diarylalkane product **46**, corresponding to 57% yield with respect to the starting C–H substrate).

4C.V. Screening Tables

Table 4C.1. Control Experiments Table

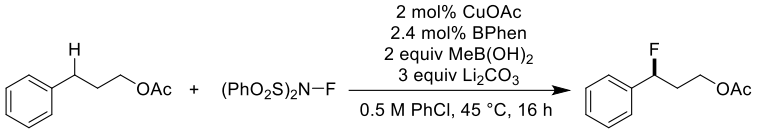

entry	control	MB	% SM	% C-N	% C-F(F_2)[a]
1	No CuOAc	102	102	--	--
2	No BPhen	101	77	--	24
3	No NFSI	102	102	--	--
4	No Li_2CO_3	70	70	--	--
5	No $MeB(OH)_2$	103	103	--	--
6	Under Air	66	42	--	24

[a]Reactions run at 0.2 mmol scale. Calibrated ^{1}H NMR yields using mesitylene as an internal standard.

Table 4C.2. Solvent Screening Table

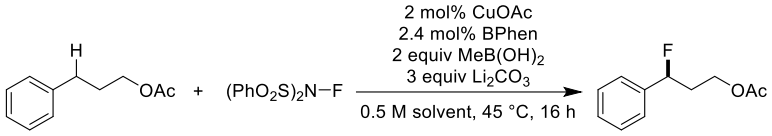

entry	solvent	MB	% SM	% C-N	% C-F(F_2)[a]
1	DCM	76	9	--	64(3)
2	DCE	87	16	--	69(2)
3	MeCN	25	2	--	23
4	EtOAc	80	26	--	53(1)
5	**acetone**	**71**	**--**	**--**	**68(3)**
6	PhF	94	38	--	55(1)
7	$PhCF_3$	89	38	--	50(1)
8	**PhCl**	**98**	**19**	**--**	**76(3)**
9	PhCl (0.4 M)	79	7	--	68(4)
10	PhCl (0.3 M)	85	9	--	72(4)
11	PhCl (0.2 M)	77	18	--	59
12	PhCl (0.1 M)	77	21	--	56

[a]Reactions run at 0.2 mmol scale. Calibrated ^{1}H NMR yields using mesitylene as an internal standard.

Table 4C.3. Cu Salt Screening Table

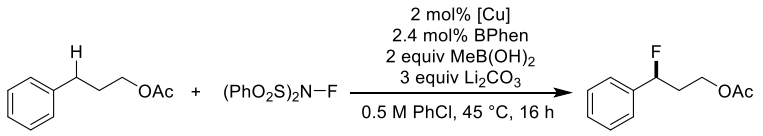

1 equiv 2.0 equiv

entry	Cu salt	MB	% SM	% C-N	% C-F(F_2)[a]
1	CuI•DMS	74	5	--	64(5)
2	CuBr•DMS	80	9	--	68(3)
3	CuCl	88	17	--	68(3)
4	**CuOAc**	**82**	**2**	**--**	**73(7)**
5	$Cu(MeCN)_4PF_6$	94	31	--	63
6	CuCN	102	92	--	10
7	$Cu(OAc)_2$	90	9	5	76
8	$Cu(OTf)_2$	100	100	--	--

[a]Reactions run at 0.2 mmol scale. Calibrated ^{1}H NMR yields using mesitylene as an internal standard.

Table 4C.4. Ligand Screening Table

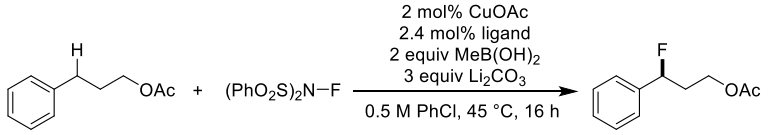

1 equiv 2.0 equiv

entry	ligand	MB	% SM	% C-N	% C-F(F_2)[a]
1	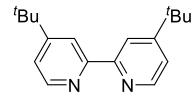	93	7	0	81(5)
2	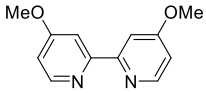	94	37	0	57
3*	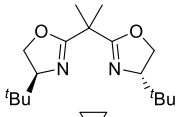	101	56	0	45
4*	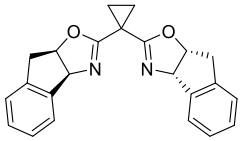	103	46	0	56(1)
5	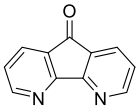	90	56	0	34
6	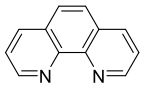	101	48	0	53
7*	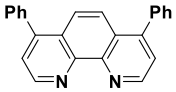	**101**	**19**	**0**	**78(4)**
8	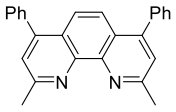	91	29	0	61(1)

[a]Reactions run at 0.2 mmol scale. Calibrated ^{1}H NMR yields using mesitylene as an internal standard. *In an experiment with 2-(S)-acetoxy-4-phenylbutane, these three ligands formed the fluorinated product with an identical d.r. of 2:1 (avg yield 50%). It is unlikely that enantioselectivity would be observed in fluorination of achiral benzylic substrates when using the chiral ligands in entries 3 or 4.

Table 4C.5. Base Screening Table

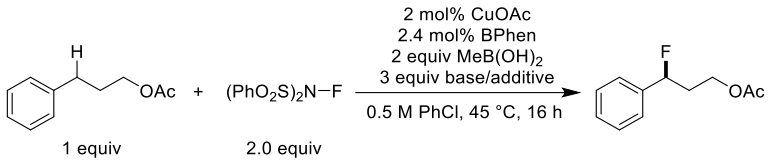

entry	base/additive	MB	% SM	% C-N	% C-F(F_2)[a]
1	K_2CO_3	92	75	--	17
2	Na_2CO_3	84	30	--	54
3	**Li_2CO_3**	**97**	**13**	**--**	**78(6)**
4	LiOAc	97	40	--	57
5	$NaHCO_3$	70	12	--	58
6	LiO^{t}Bu	100	100	--	--
7	LiOTf	82	82	--	--
8	K_3PO_4	99	99	--	--

[a]Reactions run at 0.2 mmol scale. Calibrated ^{1}H NMR yields using mesitylene as an internal standard.

Table 4C.6. Reductant Screening Table

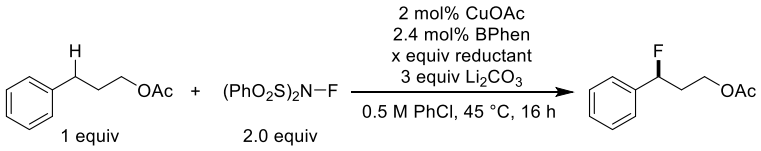

entry	reductant	equiv	MB	% SM	% C-N	% C-F(F_2)[a]
1		**2**	**88**	**5**	**--**	**77(6)**
2	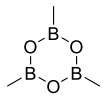	2	40	--	--	37(3)
3	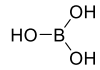	2	103	103	--	--
4	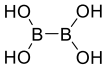	2	64	10	--	54
5	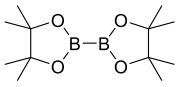	2	61	9	--	52

[a]Reactions run at 0.2 mmol scale. Calibrated ^{1}H NMR yields using mesitylene as an internal standard.

Table 4C.7. Reaction Stoichiometry Screening Table

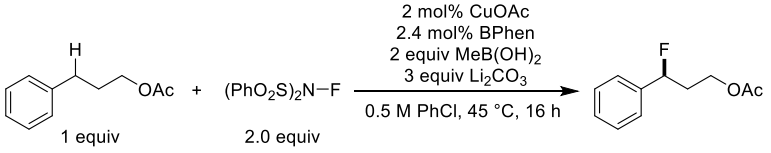

entry	variation	MB	% SM	% C-N	% C-F(F_2)[a]
1	standard cond.	95	2	--	80(5)
2	35 °C	93	44	--	48(1)
3	55 °C	92	3	--	74(10)
4	1 equiv. NFSI	90	34	--	52(2)
5	3 equiv. NFSI	98	7	--	89(5)
6	1 equiv. Li_2CO_3	95	13	--	78(4)
7	2 equiv. Li_2CO_3	93	5	--	82(6)
8	1 equiv. $MeB(OH)_2$	95	12	--	79(4)
9	2.5 equiv. $MeB(OH)_2$	97	3	--	87(7)
10	1 mol% BPhen	100	12	--	83(5)
11	4 mol% BPhen	103	103	--	0
12	1 mol% CuOAc/ 1 mol% BPhen	96	12	--	80(4)
13	10 mol% CuOAc/ 10 mol% BPhen	83	13	--	47(3)
14	10 mol% CuOAc/ 5 mol% BPhen	92	18	--	63(2)

[a]Reactions run at 0.2 mmol scale. Calibrated ^{1}H NMR yields using mesitylene as an internal standard. Mass balance in this table also accounts for formation of the benzyl ketone.

Table 4C.8. HFIP Loading Screening Table

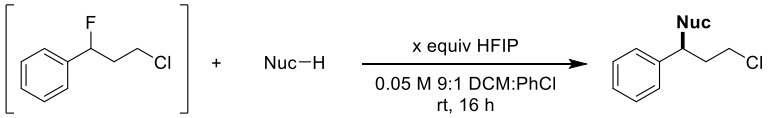

entry	Nuc–H	equiv HFIP	% SM	% C-Nuc[a]
1	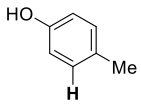	2	-	69
2		**10**	**-**	**100**
3		27	-	90
4		2	100	**-**
5		**10**	**-**	**96**
6		27	-	95
7		2	-	60
8		**10**	**-**	**90**
9		27	-	78

[a]Reactions run at 0.3 mmol scale. Calibrated ^{1}H NMR yields with respect to the benzyl fluoride using CH_2Br_2 as an internal standard. HFIP ether product is observed in reactions with 27 equiv HFIP.

4C.VI. Additional Experiments and Observations

Less Successful C–H Fluorination Substrates

Table 4C.9. Benzylic C–H fluorination results for substrates not included in Table 4.2.

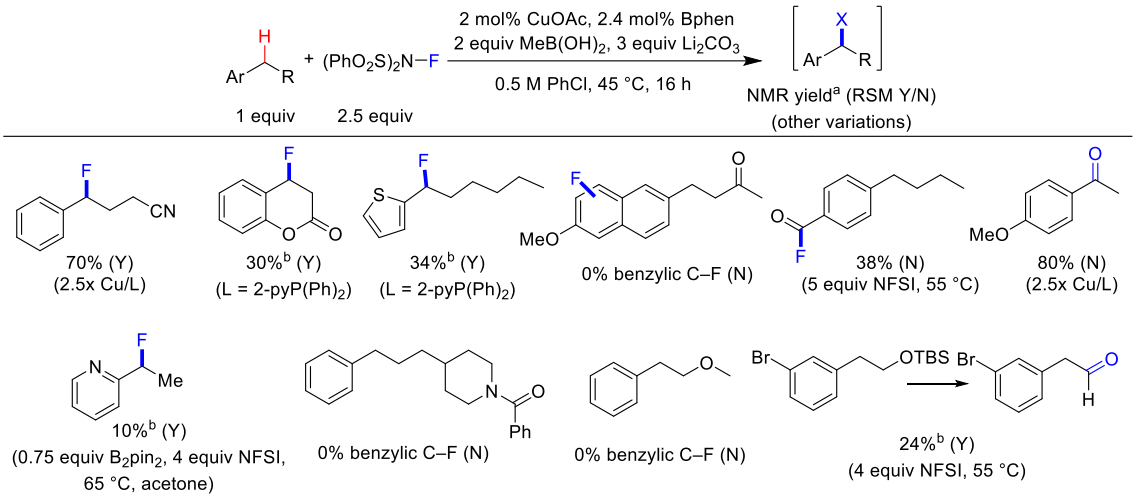

[a]Calibrated ^{1}H NMR yields using dibromomethane as the internal standard. Reactions with (Y) indicates that remaining starting material was the major remaining mass balance component. Reactions with (N) indicates that all starting material was consumed. [b]Half Cu/L loading, 1 equiv B_2pin_2 no $MeB(OH)_2$

Discussion:

The collection of molecules in Table 4C.9 includes products omitted from the manuscript, typically because of low yields and observed deleterious side-reactivity (except for the alkylcyanide substrate, which was omitted because propylbenzene analogs are well-represented in Table 4.2). The lactone substrate suffers from low yield because more forcing conditions result in a competitive dehydrogenation pathway to afford the α,β-unsaturated ester. The thiophene substrate showed very poor mass balance and no product was formed when BPhen was used as the ligand. Nabumetone (the ketone with a naphthalene ring) underwent complete conversion of starting material, but the only fluorination products observed were aryl fluorides. An aryl aldehyde substrate was tested for fluorination, but aldehydic C–H fluorination was observed, which agrees with a recently reported method for acyl fluoride generation.[4] 4-Ethyl anisole oxidation resulted in complete conversion to *p*-methoxy acetophenone. The origin of ketone products likely traces back to C–F displacement by water from Li_2CO_3 to form the benzyl alcohol, which is oxidized *in situ* to the ketone ($MeB(OH)_2$ can also serve as a hydroxide source). It is also possible that the more electron-rich substrate oxidizes directly from the benzyl radical to a carbocation in solution, which is trapped by water and oxidized.[5] 2-Ethyl pyridine fluorination resulted in a low yield of heterobenzylic fluoride. The nucleophilic pyridine likely coordinates to an electrophile *in situ*, which deactivates the C–H site to HAT. Ionic chemistries are typically more effective for fluorination of these types of heterobenzylic substrates.[6] Benzylic substrates bearing an amide or ether functionality were not successfully fluorinated despite complete conversion of starting material. It is likely that the weak α-hetero C–H bonds compete for oxidation with the benzylic C–H site under these mildly basic conditions. A benzylic substrate with a TBS-protected alcohol was also tested in the fluorination reaction (92% conversion), but the TBS group is removed *in situ*, leading to an alcohol that is oxidized to an aldehyde (major observed product).

Observations Regarding Nucleophilic Coupling Partners

Table 4C.10. Comparisons between ineffective and effective conditions for forming desired product.

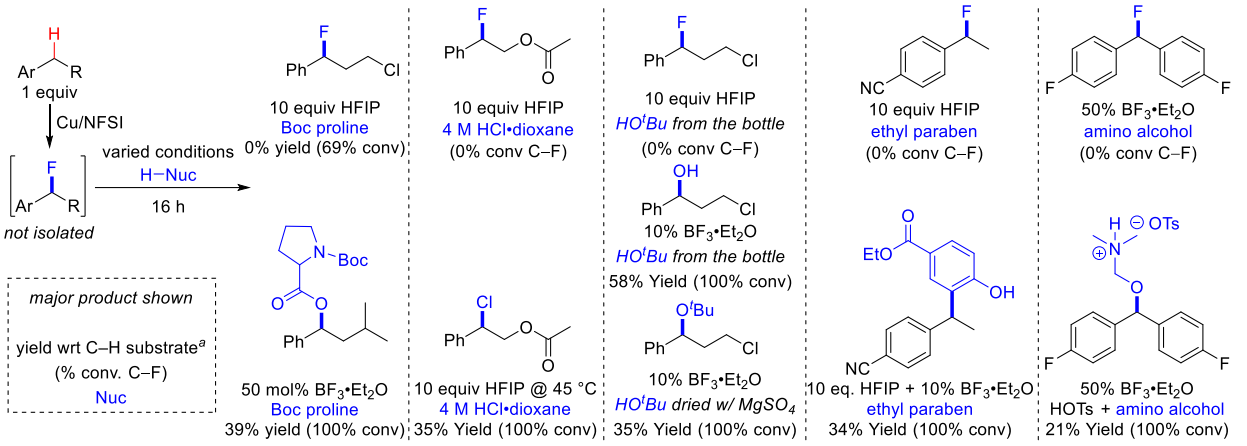

[a]Calibrated ^{1}H NMR yields using dibromomethane as the internal standard. Yield calculated based on the starting C–H substrate. 2.5 equiv H–Nuc used, solvent is 9:1 DCM:PhCl at 0.05 M, and reactions run at room temperature unless otherwise noted. Product formation and conversion of starting material is improved from top to bottom.

Discussion:

Table 4C.10 shows how changes in conditions could be used to make certain classes of nucleophiles effective for the functionalization reaction. When using Boc proline as the nucleophile, HFIP was not able to catalyze product formation. In general, Lewis basic functional groups like carbamates resulted in obstruction of C–F activation reactivity. For Boc proline, product formation could be enabled by using 50 mol% BF_3•Et_2O as the catalyst. 2-Phenethylacetate has a C–F bond that is relatively recalcitrant towards activation (likely due to having an electron withdrawing group at the homobenzylic position). In order to activate the C–F bond for substitution by chloride, the reaction needed to be heated to 45 °C in an aluminum block on a hotplate. If *tert*-butanol is used as the nucleophile for displacement, HFIP does not catalyze displacement and BF_3•Et_2O must be used. This may support an S_N2-like pathway for displacement under HFIP-catalyzed conditions.[7] If no precautions are taken to remove water when using *tert*-butanol as the nucleophile, the benzyl alcohol is formed as the product. If the reaction is dried with $MgSO_4$ and filtered before BF_3•Et_2O is added, the *tert*-butyl ether product is formed instead. In Table 4.3, benzyl fluorides can be displaced by phenols like ethyl paraben in excellent yields when using HFIP as the catalyst. The benzyl fluoride from 4-ethyl benzonitrile is not activated under these conditions. In order to displace this electronically deactivated fluoride, BF_3•Et_2O must also be added as a catalyst. This result suggests that electron-deficient aryl rings can stabilize benzyl fluorides. It is possible to protonate Lewis basic groups (like amines), so they do not interfere with C–F activation. This allows an amino alcohol to be used as an effective coupling partner (or a pyridine, cf. **31**). An acid with a DCM-soluble non-nucleophilic counterion should be used to avoid formation of side products (for example, TFA is able to compete for fluoride displacement, so TFA salts should not be used).

Table 4C.11. Benzylic C–F displacement results for less effective C–H substrate/nucleophile pairs.

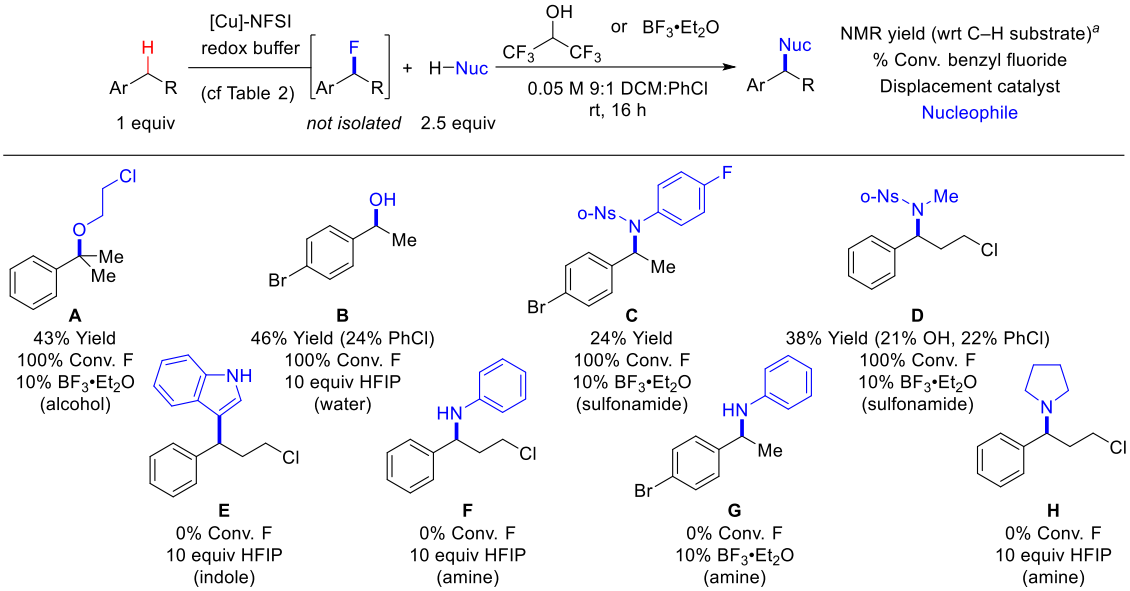

[a]Calibrated ^{1}H NMR yields using dibromomethane as the internal standard. Yield calculated based on the starting C–H substrate.

Discussion:

Tertiary fluorides can be activated with BF_3•Et_2O for trapping by nucleophilic species, albeit the resulting products may have stability issues (the tertiary ether, 4C-A, decomposed after 2 days in DCM). For poor nucleophiles like water, it is possible for chlorobenzene to compete in fluoride displacement (4C-B and D). To avoid this issue, the fluorination reaction can be run in DCM. Another issue observed when using water as a nucleophile is that the resulting benzyl alcohol can serve as a nucleophile to form ethereal dimers of the starting material (this led to the relatively low yield of the benzyl alcohol **27** from 6-bromochromane). Ortho-nitro sulfonamide protecting groups can be used to protect primary amines to make competent nucleophiles, but the ortho-nosyl amines tend to have worse reactivity than para-nosyl amines in this reaction (compare 4C-C to **43**). Nucleophiles with very Lewis basic groups like amines can completely shut down displacement of the benzyl fluoride (4C-E, F, G, H). It is possible that these groups compete with the fluoride for hydrogen-bond donors and for BF_3•Et_2O. Efforts to drive these reactions forward with heat (45 °C in an aluminum block on a hotplate) were unsuccessful (testing at higher temperature would need to be done in a different solvent).

Site Selectivity for Fluorination of Benzylic C–H Bonds

Fluorination reactions were set up under standard conditions (see the general procedure in section II) except 5 equiv of each C–H substrate was employed (160 µL PhMe, 1.5 mmol, 5 equiv; 185 µL PhEt, 1.5 mmol, 5 equiv; 210 µL cumene, 1.5 mmol, 5 equiv). Reactions were worked up in the standard fashion and analyzed via ^{1}H and $^{19}F\{^{1}H\}$ NMR spectroscopy. Product yields were determined relative to ^{1}H (CH_2Br_2, 21 µL, 0.3 mmol, 1 equiv) and ^{19}F ($PhCF_3$, 37 µL, 0.3 mmol, 1 equiv) internal standards.

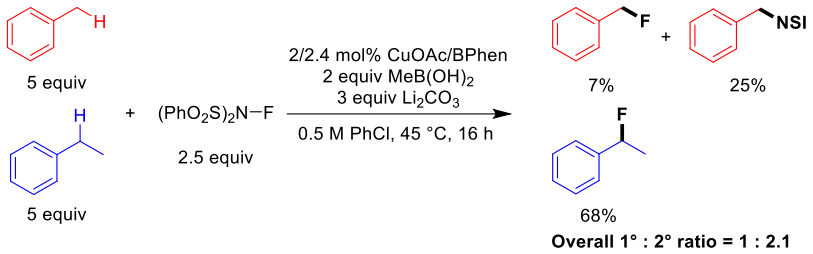

Figure 4C.1. Competition experiment for 1° vs. 2° benzylic C–H bond functionalization reactivity.

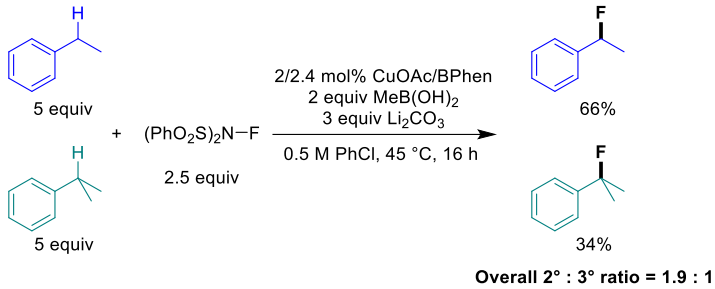

Figure 4C.2. Competition experiment for 2° vs. 3° benzylic C–H bond functionalization reactivity.

Similar selectivity preferences have been reported for photochemical benzylic fluorination reactions employing benzophenone and Selectfluor.[8]

4C.VII. Quantitative ^{1}H and ^{19}F NMR Spectra for Benzyl Fluoride Products

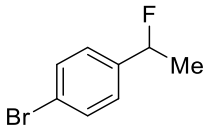

(1) 1-bromo-4-(1-fluoroethyl)benzene: Prepared from 1-bromo-4-ethylbenzene (0.3 mmol, 42 µL, 1.0 equiv) according to the general procedure in section II.
Spectra Available in the Literature (CAS): Yes[9] (159298-87-0)
Benzyl Fluoride C–H Shift: ^{1}H NMR ($CDCl_3$, 400 MHz): δ 5.59 (dq, $^{2}J_{(H,F)}$ = 47.4 Hz, $^{3}J_{(H,H)}$ = 6.4 Hz)
Calibrated ^{1}H NMR Yield from Benzylic Proton: 81%
Benzylic Fluoride Shift: ^{19}F NMR ($CDCl_3$, 377 MHz): δ -168.05 (dq, $^{2}J_{(H,F)}$ = 48.2 Hz, $^{3}J_{(H,F)}$ = 24.6 Hz)
Calibrated ^{19}F NMR Yields from Benzyl Fluorides: 86% (CF_2 – 11%)

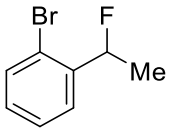

(2) 1-bromo-2-(1-fluoroethyl)benzene: Prepared from 1-bromo-2-ethylbenzene (0.3 mmol, 41 µL, 1.0 equiv) according to the general procedure in section II with the following variations: 1 mol% CuOAc, 1.2 mol% BPhen, 1 equiv B_2pin_2 (in place of 2 equiv $MeB(OH)_2$), and 4 equiv NFSI operating at 55 °C.
Spectra Available in the Literature (CAS): Yes[10] (1027513-77-4)
Benzyl Fluoride C–H Shift: ^{1}H NMR ($CDCl_3$, 400 MHz): δ 5.91 (dq, $^{2}J_{(H,F)}$ = 46.5 Hz, $^{3}J_{(H,H)}$ = 6.3 Hz)
Calibrated ^{1}H NMR Yield from Benzyl Fluoride Methyl Group: 50%
Benzylic Fluoride Shift: ^{19}F NMR ($CDCl_3$, 377 MHz): δ -173.76 (dq, $^{2}J_{(H,F)}$ = 48.3 Hz, $^{3}J_{(H,F)}$ = 24.4 Hz)
Calibrated ^{19}F NMR Yields from Benzyl Fluoride: 44%

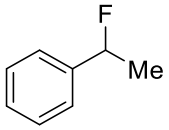

(3) (1-fluoroethyl)benzene: Prepared from ethylbenzene (0.3 mmol, 37 µL, 1.0 equiv) according to the general procedure in section II.
Spectra Available in the Literature (CAS): Yes[11] (7100-97-2)
Benzyl Fluoride C–H Shift: ^{1}H NMR ($CDCl_3$, 400 MHz): δ 5.62 (dq, $^{2}J_{(H,F)}$ = 47.8 Hz, $^{3}J_{(H,H)}$ = 6.5 Hz)
Calibrated ^{1}H NMR Yield from Benzylic Proton: 67%
Benzylic Fluoride Shift: ^{19}F NMR ($CDCl_3$, 377 MHz): δ -167.02 (dq, $^{2}J_{(H,F)}$ = 47.8 Hz, $^{3}J_{(H,F)}$ = 23.9 Hz)
Calibrated ^{19}F NMR Yields from Benzyl Fluoride: 64% (CF_2 – 11%)

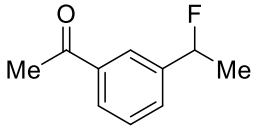

(4) 1-(3-(1-fluoroethyl)phenyl)ethan-1-one: Prepared from 1-(3-ethylphenyl)ethan-1-one (0.3 mmol, 49.9 mg, 1.0 equiv) according to the general procedure in section II with the following variations: 1 mol% CuOAc, 1.2 mol% BPhen, 1 equiv B_2pin_2 (in place of 2 equiv $MeB(OH)_2$), and 4 equiv NFSI operating at 55 °C.
Spectra Available in the Literature (CAS): See online publication[12] (1550969-43-1)
Benzyl Fluoride C–H Shift: ^{1}H NMR ($CDCl_3$, 400 MHz): δ 5.61 (dq, $^{2}J_{(H,F)}$ = 47.5 Hz, $^{3}J_{(H,H)}$ = 6.5 Hz)
Calibrated ^{1}H NMR Yield from Benzyl Fluoride Methyl Group: 83%
Decoupled Benzylic Fluoride Shift: ^{19}F NMR ($CDCl_3$, 377 MHz): δ -168.89 (s)
Calibrated ^{19}F NMR Yields from Benzyl Fluoride: 75% (CF_2 – 20%)

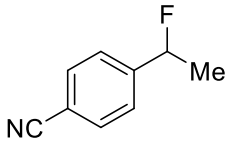

(5) 4-(1-fluoroethyl)benzonitrile: Prepared from 4-ethylbenzonitrile (0.3 mmol, 41 µL, 1.0 equiv) according to the general procedure in section II with the following variations: 1 mol% CuOAc, 1.2 mol% BPhen, 1 equiv B_2pin_2 (in place of 2 equiv $MeB(OH)_2$), and 4 equiv NFSI operating at 75 °C.
Spectra Available in the Literature (CAS): Yes[8] (155671-14-0)
Benzyl Fluoride C–H Shift: ^{1}H NMR ($CDCl_3$, 400 MHz): δ 5.70 (dq, $^2J_{(H,F)}$ = 47.4 Hz, $^3J_{(H,H)}$ = 6.5 Hz)
Calibrated ^{1}H NMR Yield from Benzyl Fluoride Methyl Group: 56%
Decoupled Benzylic Fluoride Shift: ^{19}F NMR ($CDCl_3$, 377 MHz): δ -172.67 (s)
Calibrated ^{19}F NMR Yield from Benzyl Fluoride: 64% (CF_2 – 8%)

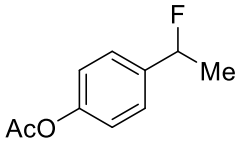

(6) 4-(1-fluoroethyl)phenyl acetate: Prepared from 4-ethylphenyl acetate (0.3 mmol, 48 µL, 1.0 equiv) according to the general procedure in section II with the following variations: 1 mol% CuOAc, 1.2 mol% BPhen, 1 equiv B_2pin_2 (in place of 2 equiv $MeB(OH)_2$), and 4 equiv NFSI operating at 55 °C.
Spectra Available in the Literature (CAS): Yes[13] (1487496-31-0)
Benzyl Fluoride C–H Shift: ^{1}H NMR ($CDCl_3$, 400 MHz): δ 5.62 (dq, $^2J_{(H,F)}$ = 47.5 Hz, $^3J_{(H,H)}$ = 6.4 Hz)
Calibrated ^{1}H NMR Yield from Benzyl Fluoride Methyl Group: 66%
Benzylic Fluoride Shift: ^{19}F NMR ($CDCl_3$, 377 MHz): δ -166.40 (dq, $^2J_{(H,F)}$ = 47.7 Hz, $^3J_{(H,F)}$ = 23.9 Hz)
Calibrated ^{19}F NMR Yields from Benzyl Fluoride: 63% (CF_2 – 7%)

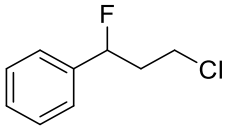

(7) (3-chloro-1-fluoropropyl)benzene: Prepared from (3-chloropropyl)benzene (0.3 mmol, 45 µL, 1.0 equiv) according to the general procedure in section II. When the reaction was repeated on 3 mmol scale, it was conducted in a 15 mL vial.
Spectra Available in the Literature (CAS): Yes[14] (1487496-36-5)
Benzyl Fluoride C–H Shift: ^{1}H NMR ($CDCl_3$, 400 MHz): δ 5.68 (ddd, $^{2}J_{(H,F)}$ = 47.8 Hz, $^{3}J_{(H,H)}$ = 8.9 & 3.8 Hz)
Calibrated ^{1}H NMR Yield from Benzyl Proton: 82% (0.3 mmol scale) or 68% (3 mmol scale)
Benzylic Fluoride Shift: ^{19}F NMR ($CDCl_3$, 377 MHz): δ -179.43 (ddd, $^{2}J_{(H,F)}$ = 46.9 Hz, $^{3}J_{(H,F)}$ = 31.3 & 14.0 Hz)
Calibrated ^{19}F NMR Yield from Benzyl Fluoride: 75% (CF_2 – 5%)

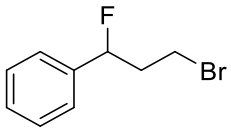

(8) (3-bromo-1-fluoropropyl)benzene: Prepared from (3-bromopropyl)benzene (0.3 mmol, 46 µL, 1.0 equiv) according to the general procedure in section II. When the reaction was repeated on 3 mmol scale, it was conducted in a 15 mL vial.
Spectra Available in the Literature (CAS): Yes[10] (1428331-73-0)
Benzyl Fluoride C–H Shift: ^{1}H NMR ($CDCl_3$, 400 MHz): δ 5.66 (ddd, $^{2}J_{(H,F)}$ = 47.7 Hz, $^{3}J_{(H,H)}$ = 8.8 & 3.9 Hz)
Calibrated ^{1}H NMR Yield from Benzyl Proton: 71% (0.3 mmol scale) or 67% (3 mmol scale)
Benzylic Fluoride Shift: ^{19}F NMR ($CDCl_3$, 377 MHz): δ -179.33 (ddd, $^{2}J_{(H,F)}$ = 46.9 Hz, $^{3}J_{(H,F)}$ = 31.3 & 14.0 Hz)
Calibrated ^{19}F NMR Yield from Benzyl Fluoride: 68%

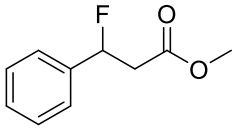

(9) Methyl 3-fluoro-3-phenylpropanoate: Prepared from methyl 3-phenylpropanoate (0.75 mmol, 47 µL, 1.0 equiv) that was formed according to the general procedure in section II with the following variations: 1 mol% CuOAc, 1.2 mol% BPhen, 1 equiv B_2pin_2 (in place of 2 equiv $MeB(OH)_2$), and 4 equiv NFSI operating at 55 °C.
Spectra Available in the Literature (CAS): Yes[8] (188941-05-1)
Benzyl Fluoride C–H Shift: ^{1}H NMR ($CDCl_3$, 400 MHz): δ 5.93 (ddd, $^2J_{(H,F)}$ = 46.9 Hz, $^3J_{(H,H)}$ = 9.2 & 4.1 Hz)
Calibrated ^{1}H NMR Yield from Benzyl Proton: 58%
Benzylic Fluoride Shift: ^{19}F NMR ($CDCl_3$, 377 MHz): δ -173.16 (ddd, $^2J_{(H,F)}$ = 46.4 Hz, $^3J_{(H,F)}$ = 32.6 & 13.4 Hz)
Calibrated ^{19}F NMR Yield from Benzyl Fluoride: 51% (CF_2 – 2%)

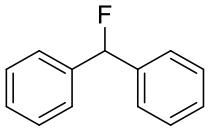

(10) (fluoromethylene)dibenzene: Prepared from diphenylmethane (0.3 mmol, 50.5 mg, 1.0 equiv) according to the general procedure in section II.
Spectra Available in the Literature (CAS): Yes[8] (579-55-5)
Benzyl Fluoride C–H Shift: ^{1}H NMR ($CDCl_3$, 400 MHz): δ 6.47 (d, $^2J_{(H,F)}$ = 47.4 Hz)
Calibrated ^{1}H NMR Yield from Benzyl Proton: 40%
Benzylic Fluoride Shift: ^{19}F NMR ($CDCl_3$, 377 MHz): δ -166.73 (d, $^2J_{(H,F)}$ = 47.5 Hz)
Calibrated ^{19}F NMR Yield from Benzyl Fluoride: 40%

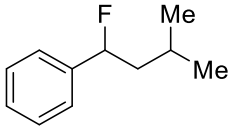

(11) (1-fluoro-3-methylbutyl)benzene: Prepared from isopentylbenzene (0.3 mmol, 52 µL, 1.0 equiv) according to the general procedure in section II.
Spectra Available in the Literature (CAS): See online publication[12] (N/A)
Benzyl Fluoride C–H Shift: ^{1}H NMR ($CDCl_3$, 400 MHz): δ 5.50 (ddd, $^{2}J_{(H,F)}$ = 48.2 Hz, $^{3}J_{(H,H)}$ = 9.2 & 4.3 Hz)
Calibrated ^{1}H NMR Yield from Benzyl Proton: 70%
Benzylic Fluoride Shift: ^{19}F NMR ($CDCl_3$, 377 MHz): δ -174.31 (ddd, $^{2}J_{(H,F)}$ = 48.4 Hz, $^{3}J_{(H,F)}$ = 33.6 & 14.6 Hz)
Calibrated ^{19}F NMR Yield from Benzyl Fluoride: 65% (CF_2 – 6%)

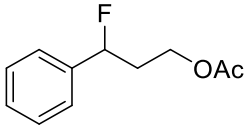

(12) 3-fluoro-3-phenylpropyl acetate: Prepared from 3-phenylpropyl acetate (0.3 mmol, 53 µL, 1.0 equiv) according to the general procedure in section II.
Spectra Available in the Literature (CAS): Yes[8] (412026-80-3)
Benzyl Fluoride C–H Shift: ^{1}H NMR ($CDCl_3$, 400 MHz): δ 5.57 (ddd, $^{2}J_{(H,F)}$ = 47.8 Hz, $^{3}J_{(H,H)}$ = 8.8 & 4.3 Hz)
Calibrated ^{1}H NMR Yield from Benzyl Proton: 79%
Benzylic Fluoride Shift: ^{19}F NMR ($CDCl_3$, 377 MHz): δ -177.40 (ddd, $^{2}J_{(H,F)}$ = 46.1 Hz, $^{3}J_{(H,F)}$ = 30.1 & 15.4 Hz)
Calibrated ^{19}F NMR Yield from Benzyl Fluoride: 74% (CF_2 – 3%)

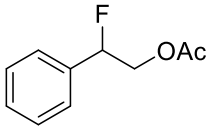

(13) 2-fluoro-2-phenylethyl acetate: Prepared from phenethyl acetate (0.3 mmol, 54.6 mg, 1.0 equiv) according to the general procedure in section II with the following variations: 1 mol% CuOAc, 1.2 mol% BPhen, 1 equiv B_2pin_2 (in place of 2 equiv $MeB(OH)_2$), and 4 equiv NFSI operating at 55 °C in acetone.
Spectra Available in the Literature (CAS): Yes[15] (33315-78-5)
Benzyl Fluoride C–H Shift: ^{1}H NMR ($CDCl_3$, 400 MHz): δ 5.58 (ddd, $^2J_{(H,F)}$ = 48.6 Hz, $^3J_{(H,H)}$ = 7.2 & 3.6 Hz)
Calibrated ^{1}H NMR Yield from Benzylic Proton: 53%
Decoupled Benzylic Fluoride Shift: ^{19}F NMR ($CDCl_3$, 377 MHz): δ -184.35 (s)
Calibrated ^{19}F NMR Yield from Benzyl Fluoride: 53%

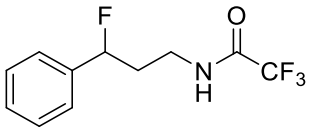

(14) 2,2,2-trifluoro-*N*-(3-fluoro-3-phenylpropyl)acetamide: Prepared from 2,2,2-trifluoro-*N*-(3-phenylpropyl)acetamide (0.3 mmol, 70 mg, 1.0 equiv) according to the general procedure in section II.
Spectra Available in the Literature (CAS): See online publication[12] (N/A)
Benzyl Fluoride C–H Shift: ^{1}H NMR ($CDCl_3$, 400 MHz): δ 5.60 (ddd, $^2J_{(H,F)}$ = 48.2 Hz, $^3J_{(H,H)}$ = 8.7 & 3.0 Hz)
Calibrated ^{1}H NMR Yield from Benzyl Proton: 63%
Benzylic Fluoride Shift: ^{19}F NMR ($CDCl_3$, 377 MHz): δ -183.75 (ddd, $^2J_{(H,F)}$ = 48.0 Hz, $^3J_{(H,F)}$ = 30.2 & 17.3 Hz)
Calibrated ^{19}F NMR Yield from Benzyl Fluoride: 63%

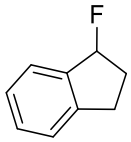

(15) 1-fluoro-2,3-dihydro-1*H*-indene: Prepared from indane (0.3 mmol, 37 µL, 1.0 equiv) according to the general procedure in section II with the following variations: 0.5 equiv $MeB(OH)_2$ operating at 35 °C.
Spectra Available in the Literature (CAS): Yes[16] (62393-01-5)
Benzyl Fluoride C–H Shift: ^{1}H NMR ($CDCl_3$, 400 MHz): δ 5.99 (ddd, $^2J_{(H,F)}$ = 58.1 Hz, $^3J_{(H,H)}$ = 6.1 & 2.8 Hz)
Calibrated ^{1}H NMR Yield from Benzyl Proton: 60%
Benzylic Fluoride Shift: ^{19}F NMR ($CDCl_3$, 377 MHz): δ -159.91 (dt, $^2J_{(H,F)}$ = 56.3 Hz, $^3J_{(H,F)}$ = 27.2 Hz)
Calibrated ^{19}F NMR Yield from Benzyl Fluoride: 49%

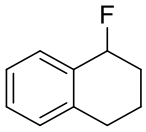

(16) 1-fluoro-1,2,3,4-tetrahydronaphthalene: Prepared from 1,2,3,4-tetrahydronaphthalene (0.3 mmol, 41 µL, 1.0 equiv) according to the general procedure in section II with the following variations: 0.5 equiv $MeB(OH)_2$ operating at 35 °C.
Spectra Available in the Literature (CAS): See online publication[12] (62462-11-7)
Benzyl Fluoride C–H Shift: ^{1}H NMR ($CDCl_3$, 400 MHz): δ 5.54 (dt, $^2J_{(H,F)}$ = 51.8 Hz, $^3J_{(H,H)}$ = 3.9 Hz)
Calibrated ^{1}H NMR Yield from Benzyl Proton: 61%
Benzylic Fluoride Shift: ^{19}F NMR ($CDCl_3$, 377 MHz): δ -155.88 (m)
Calibrated ^{19}F NMR Yield from Benzyl Fluoride: 57%

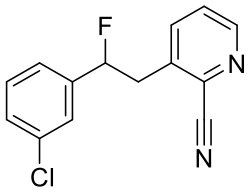

(17) 3-(2-(3-chlorophenyl)-2-fluoroethyl)picolinonitrile: Prepared from 3-(3-chlorophenethyl)picolinonitrile (0.3 mmol, 73 mg, 1.0 equiv) according to the general procedure in section II with the following variations: 1 mol% CuOAc, 1.2 mol% BPhen, 1 equiv B_2pin_2 (in place of 2 equiv $MeB(OH)_2$), and 4 equiv NFSI operating at 75 °C.
Spectra Available in the Literature (CAS): See online publication[12] (N/A)
Benzyl Fluoride C–H Shift: ^{1}H NMR ($CDCl_3$, 400 MHz): δ 5.71 (ddd, $^2J_{(H,F)}$ = 53.6 Hz, $^3J_{(H,H)}$ = 5.4 Hz)
Calibrated ^{1}H NMR Yield from Benzyl Proton: 45%
Benzylic Fluoride Shift: ^{19}F NMR ($CDCl_3$, 377 MHz): δ -178.75 (ddd, $^2J_{(H,F)}$ = 47.9 Hz, $^3J_{(H,F)}$ = 29.9 & 19.0 Hz)
Calibrated ^{19}F NMR Yield from Benzyl Fluoride: 39%

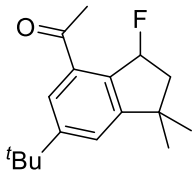

(18) 1-(6-(tert-butyl)-3-fluoro-1,1-dimethyl-2,3-dihydro-1H-inden-4-yl)ethan-1-one: Prepared from celestolide (0.3 mmol, 73 mg, 1.0 equiv) according to the general procedure in section II.
Spectra Available in the Literature (CAS): Yes[9] (1500096-10-5)
Benzyl Fluoride C–H Shift: ^{1}H NMR ($CDCl_3$, 400 MHz): δ 6.45 (dd, $^2J_{(H,F)}$ = 53.6 Hz, $^3J_{(H,H)}$ = 5.4 Hz)
Calibrated ^{1}H NMR Yield from Benzyl Proton: 86%
Benzylic Fluoride Shift: ^{19}F NMR ($CDCl_3$, 377 MHz): δ -158.62 (ddd, $^2J_{(H,F)}$ = 54.2 Hz, $^3J_{(H,F)}$ = 34.1 & 23.5 Hz)
Calibrated ^{19}F NMR Yield from Benzyl Fluoride: 90% (CF_2 – 6%)

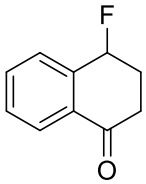

(19) 4-fluoro-3,4-dihydronaphthalen-1(*2H*)-one: Prepared from 1-tetralone (0.3 mmol, 41 µL, 1.0 equiv) formed according to the general procedure in section II with the following variations: 1 mol% CuOAc, 1.2 mol% BPhen, 1 equiv B_2pin_2 (in place of 2 equiv $MeB(OH)_2$), and 4 equiv NFSI operating at 75 °C in acetone.
Spectra Available in the Literature (CAS): Yes[17] (587853-65-4)
Benzyl Fluoride C–H Shift: ^{1}H NMR ($CDCl_3$, 400 MHz): δ 5.74 (dt, $^2J_{(H,F)}$ = 50.5 Hz, $^3J_{(H,H)}$ = 5.0 Hz)
Calibrated ^{1}H NMR Yield from Benzyl Proton: 38%
Benzylic Fluoride Shift: ^{19}F NMR ($CDCl_3$, 377 MHz): δ -170.59 (m)
Calibrated ^{19}F NMR Yield from Benzyl Fluoride: 44%

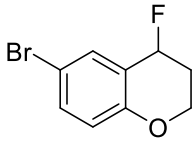

(20) 6-bromo-4-fluorochromane: Prepared from 6-bromochromane (0.3 mmol, 44 µL, 1.0 equiv) according to the general procedure in section II with the following variations: 0.5 equiv $MeB(OH)_2$ operating at 35 °C.
Spectra Available in the Literature (CAS): See online publication[12] (1780938-64-8)
Benzyl Fluoride C–H Shift: ^{1}H NMR ($CDCl_3$, 400 MHz): δ 5.43 (dt, $^2J_{(H,F)}$ = 52.4 Hz, $^3J_{(H,H)}$ = 3.4 Hz)
Calibrated ^{1}H NMR Yield from Benzylic Proton: 62%
Benzylic Fluoride Shift: ^{19}F NMR ($CDCl_3$, 377 MHz): δ -153.79 (ddd, $^2J_{(H,F)}$ = 50.6 Hz, $^3J_{(H,F)}$ = 34.3 & 16.4 Hz)
Calibrated ^{19}F NMR Yields from Benzyl Fluoride: 60%

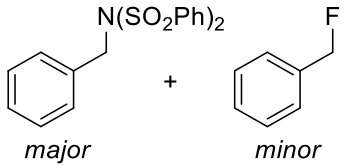

(21) (fluoromethyl)benzene: Prepared from toluene (0.3 mmol, 32 µL, 1.0 equiv) according to the general procedure in section II with the following variations: 1 mol% CuOAc, 1.2 mol% BPhen, 1 equiv B_2pin_2 (in place of 2 equiv $MeB(OH)_2$), and 4 equiv NFSI operating at 55 °C in acetone.
Spectra Available in the Literature (CAS): Yes[18] (70869-03-3), Yes[8] (350-50-5)
Benzyl Fluoride C–H Shift: ^{1}H NMR ($CDCl_3$, 400 MHz): δ 5.37 (d, $^2J_{(H,F)}$ = 47.9 Hz)
Calibrated ^{1}H NMR Yield from Benzylic Proton(s): 59% (C–N), 12% (C–F), 6% ($C–F_2$)
Benzylic Fluoride Shift: ^{19}F NMR ($CDCl_3$, 377 MHz): δ -206.64 (t, $^2J_{(H,F)}$ = 47.3 Hz)
Calibrated ^{19}F NMR Yields from Benzyl Fluoride(s): 8% (C–F), 8% ($C–F_2$)

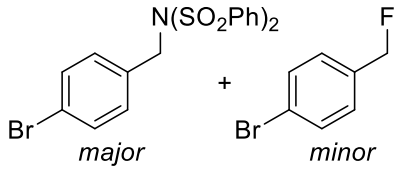

(22) 1-bromo-4-(fluoromethyl)benzene: Prepared from 4-bromotoluene (0.3 mmol, 37 µL, 1.0 equiv) according to the general procedure in section II with the following variations: 1 mol% CuOAc, 1.2 mol% BPhen, 1 equiv B_2pin_2 (in place of 2 equiv $MeB(OH)_2$), and 4 equiv NFSI operating at 55 °C.
Spectra Available in the Literature (CAS): Yes[18] (1361033-82-0), Yes[15] (459-49-4)
Benzyl Fluoride C–H Shift: ^{1}H NMR ($CDCl_3$, 400 MHz): δ 5.32 (d, $^2J_{(H,F)}$ = 47.7 Hz)
Calibrated ^{1}H NMR Yield from Benzylic Proton(s): 44% (C–N), 8% (C–F), 10% ($C–F_2$)
Benzylic Fluoride Shift: ^{19}F NMR ($CDCl_3$, 377 MHz): δ -208.09 (t, $^2J_{(H,F)}$ = 47.7 Hz)
Calibrated ^{19}F NMR Yields from Benzyl Fluoride: 7% (C–F), 10% ($C–F_2$)

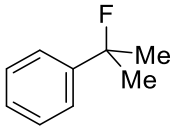

(23) (2-fluoropropan-2-yl)benzene: Prepared from cumene (0.3 mmol, 42 μL, 1.0 equiv) according to the general procedure in section II.
Spectra Available in the Literature (CAS): Yes[8] (74185-81-2)
Fluoride Product Methyl C–H Shift: ^{1}H NMR ($CDCl_3$, 400 MHz): δ 1.68 (d, $^{3}J_{(H,F)}$ = 21.9 Hz)
Calibrated ^{1}H NMR Yield from Benzyl Fluoride Methyl Protons: 92%
Benzylic Fluoride Shift: ^{19}F NMR ($CDCl_3$, 377 MHz): δ -137.39 (hept, $^{3}J_{(H,F)}$ = 21.8 Hz)
Calibrated ^{19}F NMR Yields from Benzyl Fluoride: 85%

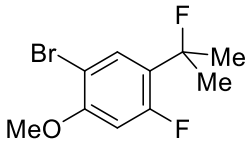

(24) 1-bromo-4-fluoro-5-(2-fluoropropan-2-yl)-2-methoxybenzene: Prepared from 1-bromo-4-fluoro-5-isopropyl-2-methoxybenzene (0.3 mmol, 74 mg, 1.0 equiv) according to the general procedure in section II.
Spectra Available in the Literature (CAS): See online publication[12] (N/A)
Fluoride Product Aromatic C–H Shift: ^{1}H NMR ($CDCl_3$, 400 MHz): δ 6.61 (d, $^{3}J_{(H,F)}$ = 12.8 Hz)
Calibrated ^{1}H NMR Yield from Benzyl Fluoride Aromatic Proton: 84%
Benzyl Fluoride Product Fluorine Shifts: ^{19}F NMR ($CDCl_3$, 377 MHz): δ -112.96 (dt, $^{3}J_{(H,F)}$ = 14.4 Hz, $^{4}J_{(H,F)}$ = 7.6 Hz), -135.16 (hd, $^{3}J_{(H,F)}$ = 22.8 Hz, $^{4}J_{(H,F)}$ = 6.7 Hz)
Calibrated ^{19}F NMR Yields from Benzyl Fluoride: 82%

4C.VIII. Characterization Data for Isolated Cross Coupling Products

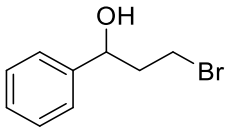

(25) 3-bromo-1-phenylpropan-1-ol: Prepared from benzyl fluoride **8** (0.3 mmol scale, 65% NMR yield) that was formed according to the general procedure in section II. The ensuing displacement step followed the general procedure in section III and used water (0.75 mmol, 13.5 µL, 2.5 equiv) as the nucleophile with HFIP (3.0 mmol, 315 µL, 10 equiv) as the displacement catalyst.
Purification: Normal phase silica gel chromatography was used with a gradient of 0%→10% EtOAc in pentane.
Isolated Yield from Benzyl Fluoride: 64%, 27.4 mg of yellow oil
Spectra Available in the Literature (CAS): Yes[19] (34052-63-6)
^{1}H NMR ($CDCl_3$, 500 MHz): δ 7.39 – 7.35 (m, 4H), 7.33 – 7.28 (m, 1H), 4.92 (dd, *J* = 8.4, 4.7 Hz, 1H), 3.59 (ddd, *J* = 10.0, 8.2, 6.0 Hz, 1H), 3.42 (dt, *J* = 10.0, 6.1 Hz, 1H), 2.32 (ddt, *J* = 14.3, 8.3, 5.9 Hz, 1H), 2.18 (dddd, *J* = 14.5, 8.2, 6.3, 4.6 Hz, 1H), 2.03 (bs, 1H).
^{13}C NMR ($CDCl_3$, 126 MHz): δ 143.6, 128.7, 127.9, 125.8, 72.3, 41.6, 30.2.

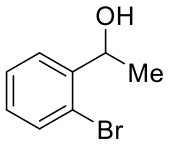

(26) 1-(2-bromophenyl)ethan-1-ol: Prepared from benzyl fluoride **2** (0.3 mmol scale, 44% NMR yield) that was formed according to the general procedure in section II with the following variations: 1 mol% CuOAc, 1.2 mol% BPhen, 1 equiv B_2pin_2 (in place of 2 equiv $MeB(OH)_2$), and 4 equiv NFSI operating at 75 °C. The ensuing displacement step followed the general procedure in section III and used water (0.75 mmol, 13.5 µL, 2.5 equiv) as the nucleophile with HFIP (3.0 mmol, 315 µL, 10 equiv) as the displacement catalyst.
Purification: Reverse phase silica gel chromatography was used with a gradient of 50%→85% MeOH in water. The product was extracted with 1:1 ether:pentane.
Isolated Yield from Benzyl Fluoride: 87%, 22.9 mg of colorless oil.
Spectra Available in the Literature (CAS): Yes[20] (5411-56-3)
^{1}H NMR ($CDCl_3$, 500 MHz): δ 7.60 (dd, *J* = 7.8, 1.7 Hz, 1H), 7.51 (dd, *J* = 7.9, 1.2 Hz, 1H), 7.35 (td, *J* = 7.6, 1.2 Hz, 1H), 7.13 (td, *J* = 7.7, 1.7 Hz, 1H), 5.24 (q, *J* = 6.4 Hz, 1H), 1.49 (d, *J* = 6.4 Hz, 3H).
^{13}C NMR ($CDCl_3$, 126 MHz): δ 144.6, 132.7, 128.8, 127.9, 126.7, 121.7, 69.2, 23.6.

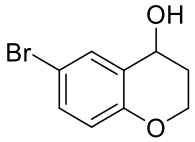

(27) 6-bromochroman-4-ol: Prepared from benzyl fluoride **20** (0.3 mmol scale, 57% NMR yield) that was formed according to the general procedure in section II with the following variations: 0.5 equiv $MeB(OH)_2$ operating at 35 °C. The ensuing displacement step followed the general procedure in section III and used water (0.75 mmol, 13.5 µL, 2.5 equiv) as the nucleophile with HFIP (3.0 mmol, 315 µL, 10 equiv) as the displacement catalyst.
Purification: Reverse phase silica gel chromatography was used with a gradient of 50%→85% MeOH in water. The product was extracted with 1:1 ether:pentane.
Isolated Yield from Benzyl Fluoride: 34%, 13.1 mg of colorless oil.
Spectra Available in the Literature (CAS): Yes[21] (18385-77-8)
^{1}H NMR ($CDCl_3$, 500 MHz): δ 7.45 (d, *J* = 2.5 Hz, 1H), 7.28 (dd, *J* = 8.7, 2.5 Hz, 1H), 6.73 (d, *J* = 8.7 Hz, 1H), 4.76 (t, *J* = 4.3 Hz, 1H), 4.31 – 4.21 (m, 2H), 2.18 – 1.98 (m, 2H), 1.87 (bs, 1H).
^{13}C NMR ($CDCl_3$, 126 MHz): δ 153.7, 132.5, 132.1, 126.3, 119.0, 112.4, 63.0, 62.2, 30.6.

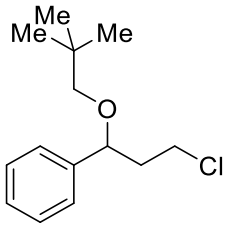

(28) (3-chloro-1-(neopentyloxy)propyl)benzene: Prepared from benzyl fluoride **7** (0.3 mmol scale, 76% NMR yield) that was formed according to the general procedure in section II. The ensuing displacement step followed the general procedure in section III and used neopentyl alcohol (0.75 mmol, 81.4 µL, 2.5 equiv) as the nucleophile with BF_3•Et_2O (0.03 mmol, 3.7 µL, 0.1 equiv) as the displacement catalyst. The nucleophile was dried in 1 mL DCM with $MgSO_4$ prior to use.
Purification: Reverse phase silica gel chromatography was used with a gradient of 70%→100% MeOH in water. The product was extracted with 1:1 ether:pentane.
Isolated Yield from Benzyl Fluoride: 51%, 28.2 mg of light yellow oil.
Spectra Available in the Literature (CAS):Yes (2173346-35-3)
^{1}H NMR ($CDCl_3$, 500 MHz): δ 7.35 (t, *J* = 7.5 Hz, 2H), 7.32 – 7.26 (m, 3H), 4.42 (dd, *J* = 9.2, 4.1 Hz, 1H), 3.78 (ddd, *J* = 10.6, 8.6, 5.8 Hz, 1H), 3.59 (ddd, *J* = 11.0, 6.4, 5.1 Hz, 1H), 3.03 (d, *J* = 8.5 Hz, 1H), 2.90 (d, *J* = 8.5 Hz, 1H), 2.21 (ddt, *J* = 14.5, 9.2, 5.5 Hz, 1H), 2.00 (dddd, *J* = 14.6, 8.6, 6.4, 4.1 Hz, 1H), 0.91 (s, 9H).
^{13}C NMR ($CDCl_3$, 126 MHz): δ 142.3, 128.4, 127.5, 126.4, 79.5, 78.9, 41.9, 41.6, 32.1, 26.7.
HRMS (ESI) m/z: $[M-H]^+$ Calcd for $C_{14}H_{20}ClO$ 239.1197; Found 239.1197.

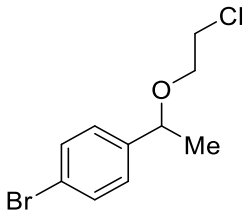

(29) 1-bromo-4-(1-(2-chloroethoxy)ethyl)benzene: Prepared from benzyl fluoride **1** (0.3 mmol scale, 74% NMR yield) that was formed according to the general procedure in section II. The ensuing displacement step followed the general procedure in section III and used 2-chloroethanol (0.75 mmol, 50.3 µL, 2.5 equiv) as the nucleophile with HFIP (3.0 mmol, 315 µL, 10 equiv) as the displacement catalyst.
Purification: Normal phase silica gel chromatography was used with a gradient of 0%→20% EtOAc in pentane.
Isolated Yield from Benzyl Fluoride: 60%, 35.3 mg of colorless amorphous solid.
Spectra Available in the Literature (CAS):Yes (N/A)
^{1}H NMR ($CDCl_3$, 500 MHz): δ 7.48 (d, *J* = 8.4 Hz, 2H), 7.21 (d, *J* = 8.4 Hz, 2H), 4.43 (q, *J* = 6.5 Hz, 1H), 3.62 – 3.53 (m, 4H), 1.44 (d, *J* = 6.5 Hz, 3H).
^{13}C NMR ($CDCl_3$, 126 MHz): δ 142.4, 131.7, 127.9, 121.4, 77.9, 68.7, 43.0, 23.9.
HRMS (ESI) m/z: $[M+NH_4]^+$ Calcd for $C_{10}H_{16}BrClNO$ 280.0098; Found 280.0100.

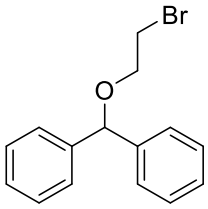

(30) ((2-bromoethoxy)methylene)dibenzene: Prepared from benzyl fluoride **10** (0.3 mmol scale, 46% NMR yield) that was formed according to the general procedure in section II. The ensuing displacement step followed the general procedure in section III and used 2-bromoethanol (0.75 mmol, 53.2 µL, 2.5 equiv) as the nucleophile with HFIP (3.0 mmol, 315 µL, 10 equiv) as the displacement catalyst.
Purification: Reverse phase silica gel chromatography was used with a gradient of 50%→85% MeOH in water. The product was extracted with 1:1 ether:pentane.
Isolated Yield from Benzyl Fluoride: 80%, 32.3 mg of white solid.
Spectra Available in the Literature (CAS): Yes[22] (91-01-0)
^{1}H NMR ($CDCl_3$, 500 MHz): δ 7.40 – 7.31 (m, 8H), 7.30 – 7.24 (m, 2H), 5.44 (s, 1H), 3.79 (t, *J* = 6.3 Hz, 2H), 3.53 (t, *J* = 6.2 Hz, 2H).
^{13}C NMR ($CDCl_3$, 126 MHz): δ 141.7, 128.4, 127.7, 127.0, 83.9, 68.9, 30.6.

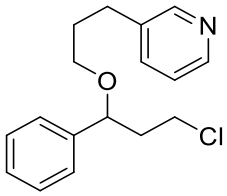

(31) 3-(3-(3-chloro-1-phenylpropoxy)propyl)pyridine: Prepared from benzyl fluoride **7** (0.3 mmol scale, 78% NMR yield) that was formed according to the general procedure in section II. The ensuing displacement step followed the general procedure in section III and used 3-(3-pyridyl)-1-propanol (0.75 mmol, 43 µL, 2.5 equiv) that was protonated with methanesulfonic acid (0.75 mmol, 48.7 µL, 2.5 equiv) as the nucleophile with both HFIP (3.0 mmol, 315 µL, 10 equiv) and BF_3•Et_2O (0.15 mmol, 18.5 µL, 0.5 equiv) as the displacement catalysts. The nucleophile was dried in 1 mL DCM with $MgSO_4$
Purification: An extraction with DCM and sodium bicarbonate was used to remove MsOH and BF_3 from pyridine. The organic phase was collected, dried with $MgSO_4$, concentrated on the rotovap and then subjected to chromatography with a gradient of 20%→60% EtOAc in pentane.
Isolated Yield from Benzyl Fluoride: 36%, 24.1 mg of slightly yellow oil.
Spectra Available in the Literature (CAS):Yes (N/A)
^{1}H NMR ($CDCl_3$, 500 MHz): δ 8.44 (t, *J* = 2.1 Hz, 2H), 7.47 (dt, *J* = 7.8, 2.0 Hz, 1H), 7.38 – 7.33 (m, 2H), 7.33 – 7.28 (m, 3H), 7.19 (dd, *J* = 7.8, 4.8 Hz, 1H), 4.47 (dd, *J* = 8.7, 4.6 Hz, 1H), 3.75 (ddd, *J* = 10.7, 8.5, 5.4 Hz, 1H), 3.54 (dt, *J* = 11.0, 5.7 Hz, 1H), 3.38 (dt, *J* = 9.5, 6.1 Hz, 1H), 3.30 (dt, *J* = 9.5, 6.1 Hz, 1H), 2.76 – 2.61 (m, 2H), 2.25 (ddt, *J* = 14.3, 8.8, 5.5 Hz, 1H), 2.02 (dddd, *J* = 14.4, 8.5, 5.9, 4.6 Hz, 1H), 1.87 (tt, *J* = 8.0, 6.2 Hz, 2H).
^{13}C NMR ($CDCl_3$, 126 MHz): δ 149.9, 147.3, 141.7, 137.2, 135.9, 128.6, 127.8, 126.5, 123.3, 78.7, 67.7, 41.7, 41.0, 31.2, 29.6.
HRMS (ESI) m/z: $[M+H]^+$ Calcd for $C_{17}H_{21}ClNO$ 290.1306; Found 290.1302.

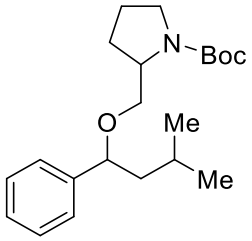

(32) *tert*-butyl (2R)-2-((3-methyl-1-phenylbutoxy)methyl)pyrrolidine-1-carboxylate:
Prepared from benzyl fluoride **11** (0.3 mmol scale, 76% NMR yield) that was formed according to the general procedure in section II. The ensuing displacement step followed the general procedure in section III and used N-Boc-DL-prolinol (0.75 mmol, 151 mg, 2.5 equiv) as the nucleophile with BF_3•Et_2O (0.15 mmol, 18.5 µL, 0.5 equiv) as the displacement catalyst.
Purification: Silica gel chromatography was used with a gradient of 0%→20% EtOAc in pentane.
Isolated Yield from Benzyl Fluoride: 49%, 38.8 mg of colorless oil.
Spectra Available in the Literature (CAS):Yes (N/A)
^{1}H NMR ($CDCl_3$, 500 MHz): δ 7.34 – 7.29 (m, 2H), 7.28 – 7.23 (m, 3H), 4.34 – 4.16 (m, 1H), 4.04 – 3.73 (m, 1H), 3.43 – 3.01 (m, 4H), 2.06 – 1.85 (m, 3H), 1.86 – 1.65 (m, 4H), 1.47 – 1.42 (m, 2H), 1.44 – 1.31 (m, 9H), 0.96 – 0.85 (m, 6H).
^{13}C NMR ($CDCl_3$, 126 MHz): δ 154.4, 143.3, 128.3, 127.3, 126.4, 81.2, 80.6, 79.1, 70.0, 69.6, 68.8, 56.8, 56.5, 47.9, 47.8, 46.7, 46.4, 29.1, 28.5, 24.8, 24.8, 23.2, 23.0, 22.2.
HRMS (ESI) m/z: $[M+Na]^+$ Calcd for $C_{21}H_{33}NNaO_3$ 370.2353; Found 370.2348.

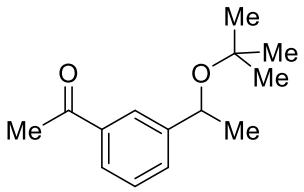

(33) 1-(3-(1-(*tert*-butoxy)ethyl)phenyl)ethan-1-one: Prepared from benzyl fluoride **4** (0.3 mmol scale, 80% NMR yield) that was formed according to the general procedure in section II with the following variations: 1 mol% CuOAc, 1.2 mol% BPhen, 1 equiv B_2pin_2 (in place of 2 equiv $MeB(OH)_2$), and 4 equiv NFSI operating at 55 °C. The ensuing displacement step followed the general procedure in section III and used *tert*-butanol (0.75 mmol, 71.7 µL, 2.5 equiv) as the nucleophile with BF_3•Et_2O (0.03 mmol, 3.7 µL, 0.1 equiv) as the displacement catalyst. The nucleophile was dried in 1 mL DCM with $MgSO_4$ prior to use.
Purification: Reverse phase silica gel chromatography was used with a gradient of 70%→100% MeOH in water. The product was extracted with 1:1 ether:pentane.
Isolated Yield from Benzyl Fluoride: 66%, 35.5 mg of colorless oil.
Spectra Available in the Literature (CAS):Yes (N/A)
^{1}H NMR ($CDCl_3$, 500 MHz): δ 7.93 (s, 1H), 7.80 (d, *J* = 7.8 Hz, 1H), 7.59 (d, *J* = 7.6 Hz, 1H), 7.41 (t, *J* = 7.7 Hz, 1H), 4.72 (q, *J* = 6.5 Hz, 1H), 2.61 (s, 3H), 1.38 (d, *J* = 6.5 Hz, 3H), 1.16 (s, 9H).
^{13}C NMR ($CDCl_3$, 126 MHz): δ 198.3, 148.2, 137.1, 130.4, 128.4, 126.7, 125.3, 83.5, 74.4, 69.5, 28.5, 26.7, 26.6, 25.0.
HRMS (ESI) m/z: $[M+Na]^+$ Calcd for $C_{14}H_{20}NaO_2$ 243.1356; Found 243.1353.

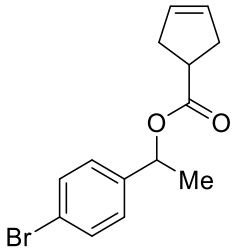

(34) 1-(4-bromophenyl)ethyl cyclopent-3-ene-1-carboxylate: Prepared from benzyl fluoride **1** (0.3 mmol scale, 72% NMR yield) that was formed according to the general procedure in section II. The ensuing displacement step followed the general procedure in section III and used cyclopent-3-ene-1-carboxylic acid (0.75 mmol, 77.6 µL, 2.5 equiv) as the nucleophile with BF_3•Et_2O (0.03 mmol, 3.7 µL, 0.1 equiv) as the displacement catalyst.
Purification: Normal phase silica gel chromatography was used with a gradient of 0%→20% EtOAc in pentane.
Isolated Yield from Benzyl Fluoride: 57%, 36.1 mg of clear, colorless liquid.
Spectra Available in the Literature (CAS):Yes (N/A)
^{1}H NMR ($CDCl_3$, 500 MHz): δ 7.47 (d, *J* = 8.5 Hz, 2H), 7.22 (d, *J* = 8.4 Hz, 2H), 5.84 (q, *J* = 6.6 Hz, 1H), 5.69 – 5.60 (m, 2H), 3.13 (tt, *J* = 9.0, 7.5 Hz, 1H), 2.73 – 2.54 (m, 4H), 1.51 (d, *J* = 6.7 Hz, 3H).
^{13}C NMR ($CDCl_3$, 126 MHz): δ 175.2, 140.9, 131.6, 128.9, 127.8, 121.7, 71.5, 41.6, 36.2, 22.1.
HRMS (ESI) m/z: $[M+Na]^+$ Calcd for $C_{14}H_{15}BrNaO_2$ 317.0148; Found 317.0147.

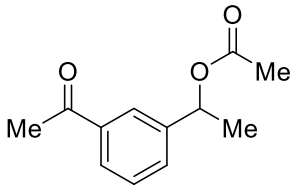

(35) 1-(3-acetylphenyl)ethyl acetate: Prepared from benzyl fluoride **4** (0.3 mmol scale, 76% NMR yield) that was formed according to the general procedure in section II with the following variations: 1 mol% CuOAc, 1.2 mol% BPhen, 1 equiv B_2pin_2 (in place of 2 equiv $MeB(OH)_2$), and 4 equiv NFSI operating at 55 °C. The ensuing displacement step followed the general procedure in section III and used acetic acid (0.75 mmol, 43 µL, 2.5 equiv) as the nucleophile with HFIP (3.0 mmol, 315 µL, 10 equiv) as the displacement catalyst.
Purification: Normal phase silica gel chromatography was used with a gradient of 0%→20% EtOAc in pentane.
Isolated Yield from Benzyl Fluoride: 80%, 37.8 mg of colorless oil.
Spectra Available in the Literature (CAS):Yes (N/A)
^{1}H NMR ($CDCl_3$, 500 MHz): δ 7.95 (s, 1H), 7.88 (dd, *J* = 7.7, 1.4 Hz, 1H), 7.55 (d, *J* = 7.6 Hz, 1H), 7.45 (t, *J* = 7.7 Hz, 1H), 5.92 (q, *J* = 6.7 Hz, 1H), 2.62 (s, 3H), 2.09 (s, 3H), 1.56 (d, *J* = 6.7 Hz, 3H).
^{13}C NMR ($CDCl_3$, 126 MHz): δ 197.8, 170.2, 142.4, 137.4, 130.8, 128.8, 127.9, 125.8, 71.9, 26.7, 22.2, 21.3.
HRMS (ESI) m/z: $[M+Na]^+$ Calcd for $C_{12}H_{14}NaO_3$ 229.0835; Found 229.0832.

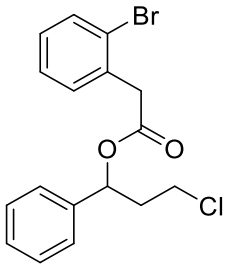

(36) 3-chloro-1-phenylpropyl 2-(2-bromophenyl)acetate: Prepared from benzyl fluoride **7** (0.3 mmol scale, 72% NMR yield) that was formed according to the general procedure in section II. The ensuing displacement step followed the general procedure in section III and used 2-(2-bromophenyl)acetic acid (0.75 mmol, 161.3 mg, 2.5 equiv) as the nucleophile with HFIP (3.0 mmol, 315 µL, 10 equiv) as the displacement catalyst.
Purification: Normal phase silica gel chromatography was used with a gradient of 0%→20% EtOAc in pentane.
Isolated Yield from Benzyl Fluoride: 64%, 50.5 mg of yellow solid.
Spectra Available in the Literature (CAS):Yes (N/A)
^{1}H NMR ($CDCl_3$, 500 MHz): δ 7.58 (d, *J* = 7.9 Hz, 1H), 7.38 – 7.23 (m, 7H), 7.15 (ddd, *J* = 8.8, 6.0, 3.0 Hz, 1H), 5.98 (dd, *J* = 8.4, 5.3 Hz, 1H), 3.89 – 3.78 (m, 2H), 3.52 (dt, *J* = 10.9, 7.0 Hz, 1H), 3.43 (dt, *J* = 10.9, 6.4 Hz, 1H), 2.38 (ddt, *J* = 14.5, 8.3, 6.2 Hz, 1H), 2.18 (dtd, *J* = 14.3, 7.1, 5.3 Hz, 1H).
^{13}C NMR ($CDCl_3$, 126 MHz): δ 169.5, 139.3, 134.1, 132.8, 131.4, 129.0, 128.6, 128.3, 127.6, 126.4, 125.0, 73.8, 41.9, 40.6, 39.1.
HRMS (ESI) m/z: $[M+Na]^+$ Calcd for $C_{17}H_{16}BrClNaO_2$ 390.9893; Found 390.9886.

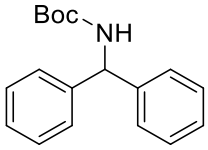

(37) *tert*-butyl benzhydrylcarbamate: Prepared from benzyl fluoride **10** (0.3 mmol scale, 44% NMR yield) that was formed according to the general procedure in section II. The ensuing displacement step followed the general procedure in section III and used Boc carbamate (0.75 mmol, 87.9 mg, 2.5 equiv) as the nucleophile with BF_3•Et_2O (0.15 mmol, 18.5 µL, 0.5 equiv) as the displacement catalyst.
Purification: Normal phase silica gel chromatography was used with a gradient of 0%→20% EtOAc in pentane.
Isolated Yield from Benzyl Fluoride: 70%, 26.2 mg of white solid.
Spectra Available in the Literature (CAS): Yes[23] (21420-61-1)
^{1}H NMR ($CDCl_3$, 500 MHz): δ 7.35 – 7.30 (m, 4H), 7.29 – 7.22 (m, 6H), 5.92 (bs, 1H), 5.15 (bs, 1H), 1.44 (bs, 9H).
^{13}C NMR ($CDCl_3$, 126 MHz): δ 155.0, 142.1, 128.6, 127.3, 127.2, 79.8, 58.4, 28.4.

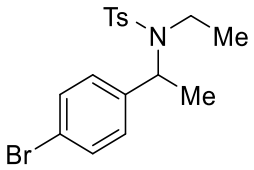

(38) N-(1-(4-bromophenyl)ethyl)-N-ethyl-4-methylbenzenesulfonamide: Prepared from benzyl fluoride **1** (0.3 mmol scale, 56% NMR yield) that was formed according to the general procedure in section II with the following variations: 1 mol% CuOAc, 1.2 mol% BPhen, 1 equiv B_2pin_2 (in place of 2 equiv $MeB(OH)_2$), and 4 equiv NFSI operating at 45 °C with DCM as the solvent instead of PhCl. The ensuing displacement step followed the general procedure in section III and used N-ethyl-4-methylbenzenesulfonamide (0.75 mmol, 149.4 mg, 2.5 equiv) as the nucleophile with BF_3.Et_2O (0.03 mmol, 3.7 µL, 0.1 equiv) as the displacement catalyst.
Purification: Reverse phase chromatography was used with a gradient of 65%→100% MeOH in water. Solvent was removed directly on the rotovap at elevated temperatures.
Isolated Yield from Benzyl Fluoride: 78%, 50 mg of white solid.
Spectra Available in the Literature (CAS):Yes (N/A)
^{1}H NMR ($CDCl_3$, 500 MHz): δ 7.73 (d, *J* = 8.3 Hz, 2H), 7.41 (d, *J* = 8.5 Hz, 2H), 7.30 (d, *J* = 8.0 Hz, 2H), 7.16 (d, *J* = 8.5 Hz, 2H), 5.14 (q, *J* = 7.1 Hz, 1H), 3.20 – 3.02 (m, *J* = 7.3 Hz, 2H), 2.44 (s, 3H), 1.37 (d, *J* = 7.1 Hz, 3H), 0.93 (t, *J* = 7.1 Hz, 3H).
^{13}C NMR ($CDCl_3$, 126 MHz): δ 143.1, 139.7, 138.4, 131.4, 129.7, 129.2, 127.1, 121.5, 54.7, 38.9, 21.5, 16.7, 16.6.
HRMS (ESI) m/z: $[M+Na]^+$ Calcd for $C_{17}H_{20}BrNNaO_2S$ 404.0290; Found 404.0287.

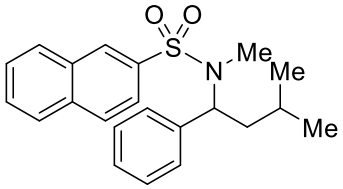

(39) N-methyl-N-(3-methyl-1-phenylbutyl)naphthalene-2-sulfonamide: Prepared from benzyl fluoride **11** (0.3 mmol scale, 70% NMR yield) that was formed according to the general procedure in section II. The ensuing displacement step followed the general procedure in section III and used N-methyl-2-naphthylsulfonamide (0.75 mmol, 166 mg, 2.5 equiv) as the nucleophile with $BF_3.Et_2O$ (0.03 mmol, 3.7 µL, 0.1 equiv) as the displacement catalyst.
Purification: Normal phase silica gel chromatography was used with a gradient of 0%→20% EtOAc in pentane.
Isolated Yield from Benzyl Fluoride: 82%, 63.1 mg of white solid.
Spectra Available in the Literature (CAS):Yes (N/A)
^{1}H NMR ($CDCl_3$, 500 MHz): δ 8.32 (s, 1H), 7.89 (t, *J* = 8.4 Hz, 3H), 7.71 (dd, *J* = 8.7, 1.9 Hz, 1H), 7.66 – 7.55 (m, 2H), 7.28 – 7.21 (m, 5H), 5.29 (dd, *J* = 8.4, 7.0 Hz, 1H), 2.69 (s, 3H), 1.84 – 1.74 (m, 1H), 1.56 – 1.43 (m, 2H), 0.90 (dd, *J* = 13.0, 6.3 Hz, 6H).
^{13}C NMR ($CDCl_3$, 126 MHz): δ 138.5, 137.1, 134.6, 132.1, 129.1, 129.1, 128.5, 128.4, 128.4, 128.1, 127.8, 127.7, 127.4, 122.7, 58.2, 39.6, 28.8, 24.8, 22.7, 22.4.
HRMS (ESI) m/z: $[M+Na]^+$ Calcd for $C_{22}H_{25}NNaO_2S$ 390.1498; Found 390.1495.

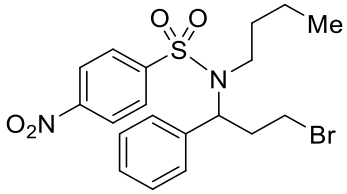

(40) N-(3-bromo-1-phenylpropyl)-N-butyl-4-nitrobenzenesulfonamide: Prepared from benzyl fluoride **8** (0.3 mmol scale, 67% NMR yield) that was formed according to the general procedure in section II with DCM as the solvent instead of PhCl. The ensuing displacement step followed the general procedure in section III and used N-butyl-4-nitrobenzenesulfonamide (0.75 mmol, 193.7 mg, 2.5 equiv) as the nucleophile with $BF_3.Et_2O$ (0.03 mmol, 3.7 µL, 0.1 equiv) as the displacement catalyst. The nucleophile was dried in 1 mL DCM with $MgSO_4$ prior to use.
Purification: Reverse phase chromatography was used with 65%→100% MeOH in water. Solvent was removed directly on the rotovap at elevated temperatures.
Isolated Yield from Benzyl Fluoride: 62%, 56.3 mg of colorless oil.
Spectra Available in the Literature (CAS):Yes (N/A)
^{1}H NMR ($CDCl_3$, 500 MHz): δ 8.26 (d, *J* = 8.7 Hz, 2H), 7.88 (d, *J* = 8.7 Hz, 2H), 7.31 – 7.25 (m, 3H), 7.20 – 7.14 (m, 2H), 5.15 (dd, *J* = 8.9, 6.3 Hz, 1H), 3.43 (dt, *J* = 10.3, 6.0 Hz, 1H), 3.26 (ddd, *J* = 10.4, 8.4, 5.9 Hz, 1H), 3.14 (ddd, *J* = 9.8, 6.0, 3.7 Hz, 2H), 2.67 (ddt, *J* = 14.6, 8.9, 5.8 Hz, 1H), 2.37 (dt, *J* = 14.7, 7.3 Hz, 1H), 1.56 – 1.45 (m, 1H), 1.41 – 1.29 (m, 1H), 1.18 (h, *J* = 7.4 Hz, 2H), 0.83 (t, *J* = 7.4 Hz, 3H).
^{13}C NMR ($CDCl_3$, 126 MHz): δ 149.7, 146.8, 136.3, 128.9, 128.7, 128.3, 128.2, 124.1, 60.1, 46.1, 35.3, 32.7, 29.7, 20.1, 13.6.
HRMS (ESI) m/z: $[M+Na]^+$ Calcd for $C_{19}H_{23}BrN_2NaO_4S$ 477.0454; Found 477.0448.

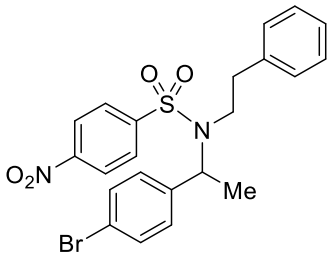

(41) N-(1-(4-bromophenyl)ethyl)-4-nitro-N-phenethylbenzenesulfonamide: Prepared from benzyl fluoride **1** (0.3 mmol scale, 83% NMR yield) that was formed according to the general procedure in section II with DCM as the solvent instead of PhCl. The ensuing displacement step followed the general procedure in section III and used N-phenethyl-4-nitrobenzenesulfonamide (0.75 mmol, 229.8 mg, 2.5 equiv) as the nucleophile with $BF_3.Et_2O$ (0.03 mmol, 3.7 µL, 0.1 equiv) as the displacement catalyst. The nucleophile was dried in 1 mL DCM with $MgSO_4$ prior to use.
Purification: Reverse phase chromatography was used with 65%→100% MeOH in water. Solvent was removed directly on the rotovap at elevated temperatures.
Isolated Yield from Benzyl Fluoride: 42%, 51.4 mg of white solid.
Spectra Available in the Literature (CAS):Yes (N/A)
^{1}H NMR ($CDCl_3$, 500 MHz): δ 8.34 (d, *J* = 8.8 Hz, 2H), 8.02 (d, *J* = 8.9 Hz, 2H), 7.46 (d, *J* = 8.5 Hz, 2H), 7.27 – 7.22 (m, 2H), 7.22 – 7.16 (m, 3H), 6.96 (d, *J* = 7.0 Hz, 2H), 5.22 (q, *J* = 7.1 Hz, 1H), 3.31 (ddd, *J* = 14.8, 11.4, 5.5 Hz, 1H), 3.19 (ddd, *J* = 14.8, 11.3, 5.2 Hz, 1H), 2.80 (td, *J* = 12.8, 11.3, 5.5 Hz, 1H), 2.38 (td, *J* = 12.8, 11.3, 5.5 Hz, 1H), 1.39 (d, *J* = 7.1 Hz, 3H).
^{13}C NMR ($CDCl_3$, 126 MHz): δ 149.9, 146.7, 138.5, 138.1, 131.8, 129.2, 128.7, 128.6, 128.2, 126.7, 124.4, 122.3, 55.6, 46.4, 37.6, 16.8.
HRMS (ESI) m/z: $[M+Na]^+$ Calcd for $C_{22}H_{21}BrN_2NaO_4S$ 511.0298; Found 511.0295.

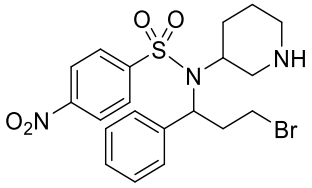

Boc from the Nuc–H piperidine
was removed under displacement conditions

(42) *tert*-butyl 3-((N-(3-bromo-1-phenylpropyl)-4-nitrophenyl)sulfonamido)piperidine-1-carboxylate: Prepared from benzyl fluoride **8** (0.3 mmol scale, 63% NMR yield) that was formed according to the general procedure in section II with DCM as the solvent instead of PhCl. The ensuing displacement step followed the general procedure in section III and used 3-((4-nitrophenyl)sulfonamido)-N-Boc-piperidine (0.75 mmol, 289.1 mg, 2.5 equiv) as the nucleophile with $BF_3.Et_2O$ (0.45 mmol, 55.5 µL, 1.5 equiv) as the displacement catalyst.
Purification: Reverse phase chromatography was used with 65%→100% MeOH in water. Solvent was removed directly on the rotovap at elevated temperatures.
Isolated Yield from Benzyl Fluoride: 23%, 21.0 mg of yellow oil.
Spectra Available in the Literature (CAS):Yes (N/A)
^{1}H NMR ($CDCl_3$, 500 MHz): δ 8.43 – 8.25 (m, 2H), 8.12 – 7.96 (m, 2H), 7.40 – 7.28 (m, 5H), 5.82 (t, *J* = 6.6 Hz, 1H), 4.90 (bs, 1H), 3.56 – 3.18 (m, 7H), 2.55 – 2.44 (m, 1H), 2.39 – 2.20 (m, 1H), 1.86 – 1.70 (m, 1H), 1.70 – 1.62 (m, 1H), 1.53 – 1.43 (m, 2H).
^{13}C NMR ($CDCl_3$, 126 MHz): δ 150.1, 146.5, 139.7, 139.7, 128.8, 128.4, 128.4, 128.3, 126.2, 124.6, 124.6, 75.8, 49.6, 39.6, 39.5, 30.9, 28.7, 28.6, 22.4.
HRMS (ESI) m/z: $[M+CO_2+Na]^+$ Calcd for $C_{21}H_{24}BrN_3NaO_6S$ 548.0461; Found 548.0462.

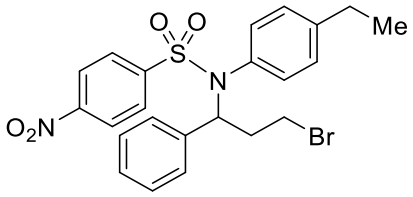

(43) N-(3-bromo-1-phenylpropyl)-N-(4-ethylphenyl)-4-nitrobenzenesulfonamide: Prepared from benzyl fluoride **8** (0.3 mmol scale, 68% NMR yield) that was formed according to the general procedure in section II with DCM as the solvent instead of PhCl. The ensuing displacement step followed the general procedure in section III and used N-4-ethylphenyl-4-nitrobenzenesulfonamide (0.75 mmol, 229.8 mg, 2.5 equiv) as the nucleophile with BF_3•Et_2O (0.15 mmol, 18.5 µL, 0.5 equiv) as the displacement catalyst. The nucleophile was dried in 1 mL DCM with $MgSO_4$ prior to use.
Purification: Reverse phase chromatography was used with 65%→100% MeOH in water.
Isolated Yield from Benzyl Fluoride: 70%, 72 mg of yellow oil.
Spectra Available in the Literature (CAS):Yes (N/A)
^{1}H NMR ($CDCl_3$, 500 MHz): δ 8.25 (d, *J* = 8.8 Hz, 2H), 7.84 (d, *J* = 8.8 Hz, 2H), 7.29 (t, *J* = 7.3 Hz, 1H), 7.24 (t, *J* = 7.4 Hz, 2H), 7.03 (t, *J* = 7.0 Hz, 4H), 6.48 (d, *J* = 7.9 Hz, 2H), 5.74 (t, *J* = 7.6 Hz, 1H), 3.38 (dt, *J* = 10.3, 6.2 Hz, 1H), 3.23 (dt, *J* = 10.3, 7.1 Hz, 1H), 2.63 (q, *J* = 7.6 Hz, 2H), 2.43 – 2.27 (m, 2H), 1.22 (t, *J* = 7.6 Hz, 3H).
^{13}C NMR ($CDCl_3$, 126 MHz): δ 149.8, 146.5, 145.7, 136.9, 132.3, 131.5, 128.8, 128.7, 128.7, 128.5, 128.4, 123.9, 61.7, 35.7, 29.4, 28.4, 15.1.
HRMS (ESI) m/z: $[M+Na]^+$ Calcd for $C_{23}H_{23}BrN_2NaO_4S$ 525.0454; Found 525.0452.

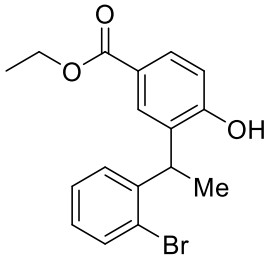

(44) 3-(1-(2-bromophenyl)ethyl)-4-hydroxy-ethylbenzoate: Prepared from benzyl fluoride **2** (0.3 mmol scale, 48% NMR yield) that was formed according to the general procedure in section II with the following variations: 1 mol% CuOAc, 1.2 mol% BPhen, 1 equiv B_2pin_2 (in place of 2 equiv $MeB(OH)_2$), and 4 equiv NFSI operating at 75 °C. The ensuing displacement step followed the general procedure in section III and used ethyl paraben (0.75 mmol, 124.7 mg, 2.5 equiv) as the nucleophile with HFIP (3.0 mmol, 315 µL, 10 equiv) as the displacement catalyst.
Purification: Reverse phase silica gel chromatography was used with a gradient of 50%→85% MeOH in water. The product was extracted with 1:1 ether:pentane.
Isolated Yield from Benzyl Fluoride: 75%, 37.5 mg of colorless oil.
Spectra Available in the Literature (CAS):Yes (N/A)
^{1}H NMR ($CDCl_3$, 500 MHz): δ 7.90 (d, *J* = 8.9 Hz, 2H), 7.55 (dd, *J* = 8.0, 1.2 Hz, 1H), 7.41 (dd, *J* = 7.8, 1.7 Hz, 1H), 7.25 (t, *J* = 7.6 Hz, 1H), 7.11 (td, *J* = 7.7, 1.7 Hz, 1H), 6.80 (d, *J* = 8.9 Hz, 2H), 5.69 (q, *J* = 6.3 Hz, 1H), 4.30 (q, *J* = 7.1 Hz, 2H), 1.64 (d, *J* = 6.3 Hz, 3H), 1.34 (t, *J* = 7.1 Hz, 3H).
^{13}C NMR ($CDCl_3$, 126 MHz): δ 166.3, 161.2, 141.4, 132.8, 132.8, 131.5, 129.1, 129.1 128.2, 126.8, 123.0, 121.5, 115.1, 74.9, 60.5, 22.6, 14.3.
HRMS (ESI) m/z: $[M+Na]^+$ Calcd for $C_{17}H_{17}BrNaO_3$ 371.0253; Found 371.0251.

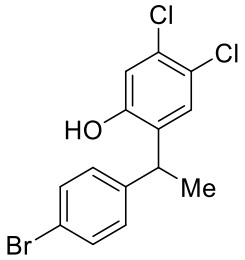

(45) 2-(1-(4-bromophenyl)ethyl)-4,5-dichlorophenol: Prepared from benzyl fluoride **1** (0.3 mmol scale, 75% NMR yield) that was formed according to the general procedure in section II. The ensuing displacement step followed the general procedure in section III and used 3,4-dichlorophenol (0.75 mmol, 122.3 mg, 2.5 equiv) as the nucleophile with HFIP (3.0 mmol, 315 µL, 10 equiv) as the displacement catalyst.
Purification: Reverse phase chromatography was used with a gradient of 65%→100% MeOH in water.
Isolated Yield from Benzyl Fluoride: 83%, 64.3 mg of yellow solid.
Spectra Available in the Literature (CAS):Yes (N/A)
^{1}H NMR ($CDCl_3$, 500 MHz): δ 7.42 (d, *J* = 8.7 Hz, 2H), 7.24 (s, 1H), 7.09 (d, *J* = 8.6 Hz, 2H), 6.84 (s, 1H), 4.97 (s, 1H), 4.29 (q, *J* = 7.2 Hz, 1H), 1.57 (d, *J* = 7.3 Hz, 3H).
^{13}C NMR ($CDCl_3$, 126 MHz): δ 152.1, 143.4, 132.4, 132.4 131.8, 130.5, 129.2, 124.2, 120.5, 117.6, 37.7, 20.6.
HRMS (ESI) m/z: $[M-H]^-$ Calcd for $C_{14}H_{10}BrCl_2O$ 342.9298; Found 342.9300.

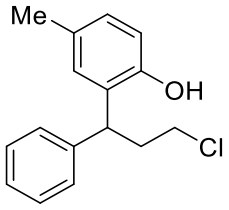

(46) 2-(3-chloro-1-phenylpropyl)-4-methylphenol: Prepared from benzyl fluoride **7** (0.3 mmol scale, 77% NMR yield) that was formed according to the general procedure in section II. The ensuing displacement step followed the general procedure in section III and used *p*-cresol (0.75 mmol, 81 mg, 2.5 equiv) as the nucleophile with HFIP (3.0 mmol, 315 µL, 10 equiv) as the displacement catalyst.
Purification: Reverse phase silica gel chromatography was used with a gradient of 70%→100% MeOH in water. The product was extracted with 1:1 ether:pentane.
Isolated Yield from Benzyl Fluoride: 87%, 52.6 mg of off-white oil.
Isolated Yield from Benzyl Fluoride on 3 mmol Scale (see section IV): 84%, 445 mg of gold oil.
Spectra Available in the Literature (CAS):Yes (926890-10-0)
^{1}H NMR ($CDCl_3$, 500 MHz): δ 7.33 – 7.27 (m, 4H), 7.21 (tt, *J* = 5.5, 2.5 Hz, 1H), 7.02 (d, *J* = 2.1 Hz, 1H), 6.91 (dd, *J* = 8.1, 2.2 Hz, 1H), 6.64 (d, *J* = 8.1 Hz, 1H), 4.48 (s, 1H), 4.46 (t, *J* = 7.8 Hz, 1H), 3.54 – 3.44 (m, 2H), 2.60 – 2.44 (m, 2H), 2.28 (s, 3H).
^{13}C NMR ($CDCl_3$, 126 MHz): δ 151.1, 142.8, 130.2, 129.4, 128.7, 128.6, 128.2, 128.0, 126.7, 116.0, 43.3, 41.4, 37.2, 20.7.
HRMS (ESI) m/z: $[M-Cl]^+$ Calcd for $C_{16}H_{17}O$ 225.1274; Found 225.1271.

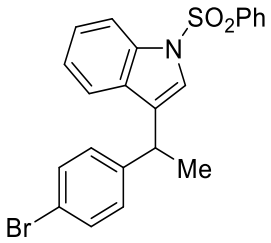

(47) 3-(1-(4-bromophenyl)ethyl)-1-(phenylsulfonyl)-1H-indole: Prepared from benzyl fluoride **1** (0.3 mmol scale, 78% NMR yield) that was formed according to the general procedure in section II. The ensuing displacement step followed the general procedure in section III and used 1-(phenylsulfonyl)indole (0.75 mmol, 193 mg, 2.5 equiv) as the nucleophile with HFIP (3.0 mmol, 315 µL, 10 equiv) as the displacement catalyst.
Purification: Reverse phase silica gel chromatography was used with a gradient of 70%→100% MeOH in water. The product was extracted with 1:1 ether:pentane.
Isolated Yield from Benzyl Fluoride: 78%, 80.4 mg of white solid.
Spectra Available in the Literature (CAS):Yes (N/A)
^{1}H NMR ($CDCl_3$, 500 MHz): δ 7.97 (d, *J* = 8.4 Hz, 1H), 7.87 (d, *J* = 7.2 Hz, 2H), 7.55 (t, *J* = 7.5 Hz, 1H), 7.45 (t, *J* = 7.9 Hz, 2H), 7.42 (d, *J* = 1.3 Hz, 1H), 7.36 (d, *J* = 8.5 Hz, 2H), 7.27 (ddd, *J* = 8.5, 6.9, 1.5 Hz, 1H), 7.15 – 7.07 (m, 2H), 7.02 (d, *J* = 8.5 Hz, 2H), 4.18 (q, *J* = 7.6 Hz, 1H), 1.64 (d, *J* = 7.1 Hz, 3H).
^{13}C NMR ($CDCl_3$, 126 MHz): δ 143.9, 138.2, 135.7, 133.7, 131.6, 130.1, 129.2, 129.0, 127.2, 126.7, 124.8, 123.2, 122.9, 120.2, 120.2, 113.8, 36.4, 21.8.
HRMS (ESI) m/z: $[M+Na]^+$ Calcd for $C_{22}H_{18}BrNNaO_2S$ 462.0134; Found 462.0131.

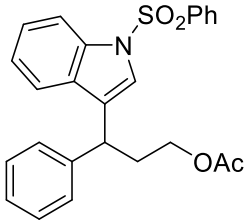

(48) 3-phenyl-3-(1-(phenylsulfonyl)-1H-indol-3-yl)propylacetate: Prepared from benzyl fluoride **12** (0.3 mmol scale, 76% NMR yield) that was formed according to the general procedure in section II. The ensuing displacement step followed the general procedure in section III and used 1-(phenylsulfonyl)indole (0.75 mmol, 193 mg, 2.5 equiv) as the nucleophile with HFIP (3.0 mmol, 315 µL, 10 equiv) as the displacement catalyst.
Purification: Reverse phase silica gel chromatography was used with a gradient of 70%→100% MeOH in water. The product was extracted with 1:1 ether:pentane.
Isolated Yield from Benzyl Fluoride: 50%, 49.5 mg of white solid.
Spectra Available in the Literature (CAS):Yes (N/A)
^{1}H NMR ($CDCl_3$, 500 MHz): δ 7.96 (d, *J* = 8.3 Hz, 1H), 7.86 (d, *J* = 7.3 Hz, 2H), 7.53 (t, *J* = 7.5 Hz, 1H), 7.49 (d, *J* = 1.1 Hz, 1H), 7.44 (t, *J* = 7.9 Hz, 2H), 7.29 – 7.21 (m, 4H), 7.22 – 7.16 (m, 3H), 7.10 (td, *J* = 7.6, 7.1, 1.0 Hz, 1H), 4.21 – 4.16 (m, 1H), 4.10 – 3.97 (m, 2H), 2.48 (dq, *J* = 13.6, 6.8 Hz, 1H), 2.29 (ddt, *J* = 13.7, 9.0, 6.0 Hz, 1H), 2.03 (s, 3H).
^{13}C NMR ($CDCl_3$, 126 MHz): δ 170.9, 142.0, 138.1, 135.6, 133.7, 130.3, 129.2, 128.7, 127.7, 126.9, 126.7, 126.1, 124.9, 123.2, 122.7, 120.1, 113.8, 62.4, 39.2, 34.1, 20.9.
HRMS (ESI) m/z: $[M+Na]^+$ Calcd for $C_{25}H_{23}NNaO_4S$ 456.1240; Found 456.1234.

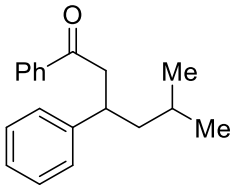

(49) 5-methyl-1,3-diphenylhexan-1-one: Prepared from benzyl fluoride **11** (0.3 mmol scale, 70% NMR yield) that was formed according to the general procedure in section II. The ensuing displacement step followed the general procedure in section III and used 1-phenyl-1-trimethylsiloxyethylene (0.75 mmol, 153.8 µL, 2.5 equiv) as the nucleophile with BF_3•Et_2O (0.03 mmol, 3.7 µL, 0.1 equiv) as the displacement catalyst.
Purification: Normal phase silica gel chromatography was used with a gradient of 0%→20% EtOAc in pentane.
Isolated Yield from Benzyl Fluoride: 68%, 38.3 mg of colorless oil.
Spectra Available in the Literature (CAS):Yes (N/A)
^{1}H NMR ($CDCl_3$, 500 MHz): δ 7.89 (dd, *J* = 8.4, 1.4 Hz, 2H), 7.53 (t, *J* = 7.4 Hz, 1H), 7.42 (t, *J* = 7.8 Hz, 2H), 7.31 – 7.22 (m, 4H), 7.17 (t, *J* = 7.0 Hz, 1H), 3.45 (dtd, *J* = 10.3, 6.9, 4.9 Hz, 1H), 3.31 – 3.13 (m, 2H), 1.66 (ddd, *J* = 13.4, 10.3, 4.7 Hz, 1H), 1.50 (ddd, *J* = 13.7, 9.3, 5.0 Hz, 1H), 1.36 (dpd, *J* = 9.3, 6.6, 4.8 Hz, 1H), 0.91 (d, *J* = 6.5 Hz, 3H), 0.83 (d, *J* = 6.7 Hz, 3H).
^{13}C NMR ($CDCl_3$, 126 MHz): δ 199.1, 144.9, 137.3, 132.8, 128.5, 128.4, 128.0, 127.6, 126.2, 46.5, 45.5, 39.1, 25.4, 23.6, 21.6.
HRMS (ESI) m/z: $[M+H]^+$ Calcd for $C_{19}H_{23}O$ 267.1743; Found 267.1740.

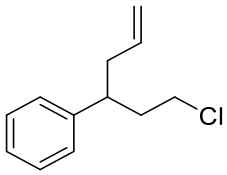

(50) (1-chlorohex-5-en-3-yl)benzene: Prepared from benzyl fluoride **7** (0.3 mmol scale, 77% NMR yield) that was formed according to the general procedure in section II. The ensuing displacement step followed the general procedure in section III and used allyltrimethylsilane (0.75 mmol, 119.2 µL, 2.5 equiv) as the nucleophile with both HFIP (3.0 mmol, 315 µL, 10 equiv) and BF_3•Et_2O (0.03 mmol, 3.7 µL, 0.1 equiv) as the displacement catalysts.
Purification: Reverse phase silica gel chromatography was used with a gradient of 70%→100% MeOH in water. The product was extracted with 1:1 ether:pentane.
Isolated Yield from Benzyl Fluoride: 43%, 19.2 mg of colorless oil.
Spectra Available in the Literature (CAS): Yes[24] (276254-98-9)
^{1}H NMR ($CDCl_3$, 500 MHz): δ 7.31 (t, *J* = 7.5 Hz, 2H), 7.22 (t, *J* = 7.4 Hz, 1H), 7.17 (d, *J* = 6.7 Hz, 2H), 5.67 (ddt, *J* = 17.1, 10.1, 7.0 Hz, 1H), 5.06 – 4.88 (m, 2H), 3.42 (ddd, *J* = 10.8, 7.1, 4.8 Hz, 1H), 3.26 (ddd, *J* = 10.8, 8.7, 6.5 Hz, 1H), 2.96 – 2.81 (m, 1H), 2.50 – 2.32 (m, 2H), 2.16 (dddd, *J* = 13.4, 8.7, 7.1, 4.4 Hz, 1H), 2.06 – 1.93 (m, 1H).
^{13}C NMR ($CDCl_3$, 126 MHz): δ 143.3, 136.3, 128.5, 127.6, 126.5, 116.4, 43.1, 42.8, 40.9, 38.6.

4C.IX. References

1. Gonçalves, C. R.; Lemmerer, M.; Teskey, C. J.; Adler, P.; Kaiser, D.; Maryasin, B.; González, L.; Maulide, N. A Unified Approach to the Chemoselective α-Functionalization of Amides with Heteroatom Nucleophiles. *J. Am. Chem. Soc.* **2019**, *46*, 18437-18443.
2. Piszel, P. E.; Vasilopoulos, A.; Stahl, S. S. Oxidative Amide Coupling from Functionally Diverse Alcohols and Amines using Aerobic Copper/Nitroxyl Catalysis. *Angew. Chem. Int. Ed.* **2019**, *58*, 12211-12215.
3. Mayhew, S. G. The Redox Potential of Dithionite and SO; from Equilibrium Reactions with Flavodoxins, Methyl Viologen and Hydrogen Plus Hydrogenase. *Eur. J. Biochem.* **1978**, *85*, 535-547.
4. Meanwell, M.; Lehmann, J.; Eichenberger, M.; Martin, R. E.; Britton, R. Synthesis of Acyl Fluorides *via* Photocatalytic Fluorination of Aldehydic C–H Bonds. *Chem. Commun.* **2018**, *54*, 9985-9988.
5. Lee, B. J.; DeGlopper, K. S.; Yoon, T. P. Site-Selective Alkoxylation of Benzylic C–H Bonds by Photoredox Catalysis. *Angew. Chem. Int. Ed.* **2020**, *59*, 197-202.
6. Meanwell, M.; Adluri, B. S.; Yuan, Z.; Newton, J.; Prevost, P.; Nodwell, M. B.; Friesen, C. M.; Schaffer, P.; Martin, R. E.; Britton, R. Direct Heterobenzylic Fluorination, Difluorination and Trifluoromethylthiolation with Dibenzenesulfonamide Derivatives. *Chem. Sci.* **2018**, *9*, 5608-5613.
7. Champagne, P. A.; Pomarole, J.; Thérien, M.-E.; Benhassine, Y.; Beaulieu, S.; Legault, C. Y.; Paquin, J.-F. Enabling Nucleophilic Substitution Reactions of Activated Alkyl Fluorides Through Hydrogen Bonding. *Org. Lett.* **2013**, *15*, 2210-2213.
8. Xia, J.-B.; Zhu, C.; Chen, C. Visible Light-Promoted Metal-Free C–H Activation: Diarylketone-Catalyzed Selective Benzylic Mono- and Difluorination. *J. Am. Chem. Soc.* **2013**, *135*, 17494-17500.
9. Liu, W.; Groves, J.T. Manganese-Catalyzed Oxidative Benzylic C–H Fluorination by Fluoride Ions. *Angew. Chem. Int. Ed.* **2013**, *52*, 6024-6027.
10. Huang, X.; Liu, W.; Ren, H.; Neelamegam, R.; Hooker, J. M.; Groves, J. T. Late Stage Benzylic C–H Fluorination with [^{18}F]Fluoride for PET Imaging. *J. Am. Chem. Soc.* **2014**, *136*, 6842-6845.
11. Bloom, S.; Pitts, C. R.; Woltornist, R.; Griswold, A.; Holl, M. G.; Lectka, T. Iron(II)-Catalyzed Benzylic Fluorination. *Org. Lett.* **2013**, *15*, 1722-1724.
12. Vasilopoulos, A.; Golden, D. L.; Buss, J. A.; Stahl, S. S. Copper-Catalyzed C–H Fluorination/Functionalization Sequence Enabling Benzylic C–H Cross Coupling with Diverse Nucleophiles. *Org. Lett.* **2020**, *22*, 5753-5757.
13. Nodwell, M. B.; Bagai, A.; Halperin, S. D.; Matin, R. E.; Knust, H.; Britton, R. Direct Photocatalytic Fluorination of Benzylic C–H Bonds with *N*-Fluorobenzenesulfonimide. *Chem. Commun.* **2015**, *51*, 11783-11786.
14. Cantillo, D.; de Frutos, O.; Rincón, J. A.; Mateos, C.; Kappe, C. O. A Continuous-Flow Protocol for Light-Induced Benzylic Fluorinations. *J. Org. Chem.* **2014**, *79*, 8486-8490.
15. Bloom, S.; McCann, M.; Lectka, T. Photocatalyzed Benzylic Fluorination: Shedding "Light" on the Involvement of Electron Transfer. *Org. Lett.* **2014**, *16*, 6338-6341.
16. Sood, D. E.; Champion, S.; Dawson, D. M.; Chabbra, S.; Bode, B. E.; Sutherland, A.; Watson, A. J. B. Deoxyfluorination with CuF_2: Enabled by Using a Lewis Base Activating Group. *Angew. Chem. Int. Ed.* **2020**, *59*, 8460-8463.

17. Dinoiu, V.; Fukuhara, T.; Miura, K.; Yoneda, N. Electrochemical Partial Fluorination of Phenylacetic Acids Esters and 1-Tetralone. *J. Fluor. Chem.* **2003**, *121*, 227-231.
18. Ni, Z.; Zhang, Q.; Xiong, T.; Zheng, Y.; Li, Y.; Zhang, H.; Zhang, J.; Liu, Q. Highly Regioselective Copper-Catalyzed Benzylic C–H Amination by *N*-Fluorobenzenesulfonimide. *Angew. Chem. Int. Ed.* **2012**, *51*, 1244-1247.
19. Trahanovsky, W. S.; Fox, N. S. Oxidation of Organic Compounds with Cerium(IV). XIX. Effect of Alkyl Substitution on the Oxidative Cleavage of Alkylphenylmethanols. *J. Am. Chem. Soc.* **1974**, *96*, 7968-7974.
20. Bosson, J.; Nolan, S. P. N-Heterocyclic Carbene–Ruthenium Complexes for the Racemization of Chiral Alcohols. *J. Org. Chem.* **2010**, *75*, 2039-2043.
21. Ramadas, S.; Krupadanam, G. L. D. Enantioselective Acylation of Chroman-4-ols Catalyzed by Lipase from *Pseudomonas Cepecia* (Amano PS). *Tetrahedron: Asymmetry* **1997**, *8*, 3059-3066.
22. Darwish, K. M.; Salama, I.; Mostafa, S.; Gomaa, M. S.; Khafagy, E.-S.; Helal, M. A. Synthesis, Biological Evaluation, and Molecular Docking Investigation of Benzhydrol- and Indole-Based Dual PPAR-γ/FFAR1 Agonists. *Bioorg. Med. Chem. Lett.* **2018**, *28*, 1595-1602.
23. Dastbaravardeh, N.; Schnürch, M.; Mihovilovic, M. D. Ruthenium(0)-Catalyzed sp^3 C–H Bond Arylation of Benzylic Amines Using Arylboronates. *Org. Lett.* **2012**, *14*, 1930-1933.
24. Yasuda, M.; Saito, T.; Ueba, M.; Baba, A. Direct Substitution of the Hydroxy Group in Alcohols with Silyl Nucleophiles Catalyzed by Indium Trichloride. *Angew. Chem. Int. Ed.* **2004**, *43*, 1414-1416.

Appendix D: Supporting Information Chapter 5

5D.I. General Considerations

All reagents were purchased from commercial sources and used as received. Ni salts and photocatalysts were purchased from Strem Chemicals, Sigma-Aldrich, and Oakwood. C–H substrates were purchased from Oakwood, Combi-Blocks, TCI America, Chem-Impex, Ambeed, Enamine, AK Scientific, and Sigma-Aldrich. Ligands were purchased from Sigma-Aldrich, Oakwood, Strem Chemicals, and Combi-Blocks. Peroxides were purchased from Sigma-Aldrich and TCI America. Trifluoroethanol was purchased from Sigma-Aldrich and TCI America. 3-Phenyl-propylphthalimide was synthesized according to a known literature procedure (15 mmol scale).[1] Benzoate substrates were synthesized via alcohol benzoylation with benzoyl chloride (2-3 mmol scale).[2] Some *N*-Boc substrates were synthesized via Boc protection of the corresponding amine with Boc anhydride in dichloromethane (2-4 mmol scale). *N*-Boc mafenide was synthesized according to a known procedure from the amine HCl salt (3 mmol scale).[3] TBS protection was performed according to a known literature procedure using TBSCl.[4] 4-CzIPN was synthesized according to a known literature procedure (2.5 mmol scale).[5] BPI ligand was synthesized according to a known literature procedure (3 mmol scale).[6]

All methylation reaction solids were weighed out on the benchtop, while liquids were added in an LC Technology Solutions nitrogen-filled glovebox or a nitrogen purgebox. Retention in performance can be obtained by setting up the methylation reaction on the benchtop with backfilling of the reaction vessel with N_2. An ABI Tuna Blue light was used for all reactions at ambient temperature (22 to 27 °C), except where noted otherwise. LC-MS data were collected using a Waters ACQUITY UPLC I-Class PLUS equipped with an ACQUITY PDA detector and QDa Detector. ACQUITY UPLC BEH C18 columns were used for the UPLC separations. In section VIII, [M] is equal to the ionization weight of the given starting material (C–H substrate). SFC analyses were collected on a Waters ACQUITY UPC2 equipped with an ACQUITY UPC2 PDA and ACQUITY QDa detector. For SFC separations, a Daicel DCpack SFC-A column was used with an eluent of 97:3 CO_2:MeOH with a flow rate of 2 mL/min at 40 °C with a ABPR at 1500 psi. ^{1}H, ^{13}C, and ^{19}F NMR spectra were recorded on a Bruker Avance III 400 spectrometer at 25 °C (^{1}H 400.1 MHz, ^{13}C 100.6 MHz, ^{19}F 376.5 MHz) or a Bruker Avance III 500 spectrometer at 25 °C (^{1}H 500.1 MHz, ^{13}C 125.7 MHz, ^{19}F 470.6 MHz), except where noted otherwise, and chemical shifts are reported in parts per million (ppm) (NSF - CHE-1048642). NMR spectra were absolutely referenced to $CHCl_3$ at 7.26 ppm (^{1}H) and $CDCl_3$ at 77.16 ppm (^{13}C). Chromatography was performed using an automated Biotage Isolera® with reusable 25 g Biotage® Sfär Silica HC D cartridges for normal phase or 60 g Biotage® SNAP Ultra C18 cartridges for reverse-phase. High-resolution mass spectra were obtained using a Thermo Q Exactive™ Plus via ASAP-MS by the mass spectrometry facility at the University of Wisconsin (NIH - 1S10OD020022-1).

Lighting and cooling for general reaction conditions:
Amazon:
B073V5V5JP (ABI Tuna Blue 23W LED lamp) – Primary lighting source
B00QHC6D7O (Kessil Tuna Blue A160WE LED lamp)
B0749JNZXV (Kingbo 400 nm LED violet lamp)
B002P4TYVK (Sunlite 365 nm CFL blacklight bulb)
B012BKZC86 (clip fan)

Equipment for 24-well plate screening:
V&P Scientific, Inc.:
VP 710C5 (tumble stirrer)
VP 711D (stir bars)

Analytical Sales & Services, Inc.:
24253 (24-well plate)
84001-Case (1 mL vials)
964PP45 (filter plates)
96355 (collection plates)
961802 (scored Teflon film)
96844 (vacuum manifold filtration system)

Materials for constructing LED photoboxes:
Misumi:
1x TWF7-2-11D (enclosure)
Note: All holes were drilled manually in a machine shop (sized to fit the LED collars and a grommet for the power cable)

superbrightleds:
24x BC-5 (LED Collars)
5’ WP18-2 (Wire)
5x DWS-125 (Heat Shrink)

LEDSupply:
24x L1-0-B5TH15-1 (470 nm blue LED) or 24x L3-0-U5TH15-1 (400 nm violet LED)
4x 04006-020 (20 mA resistor)
1x APV-12-24 (24V power supply)

Mouser:
1x 562-221001-01 (power cable)
A grommet for the power cable was obtained from an electronics shop.

Reaction set-up photos:

Figure 5D.1. General procedure reaction set-up (sections II & III)

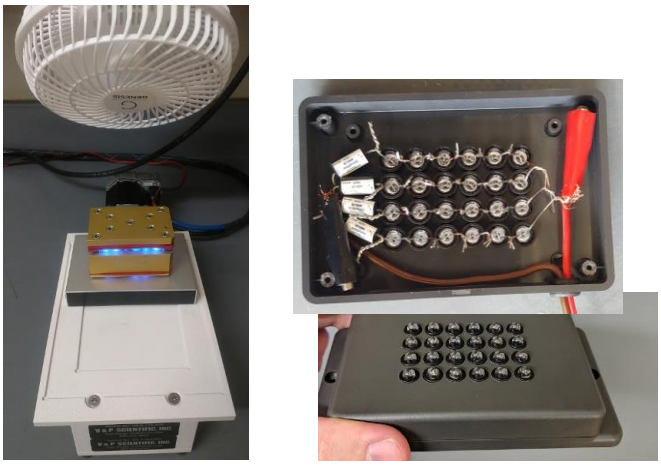

Figure 5D.2. Microscale photobox reaction set-up (section IV)

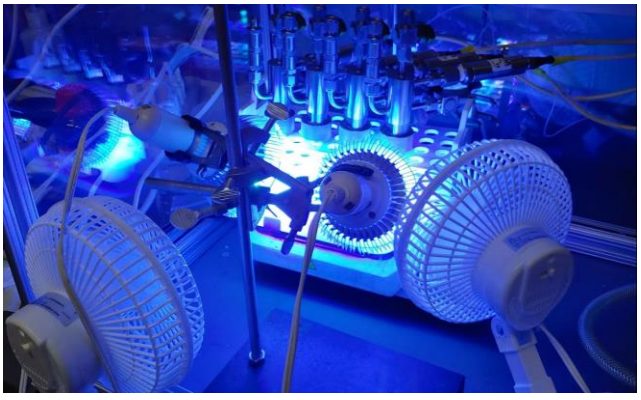

Figure 5D.3. Gas evolution reaction set-up (section VI)

5D.II. General procedure for C(sp^3)–H methylation with di-*tert*-butyl peroxide (DTBP)

Warning: Productive reactions may pressurize the vessel as the reaction progresses.

Set-up: $NiCl_2$•glyme (0.04 equiv, 0.012 mmol, 2.6 mg), $Ir[dF(CF_3)ppy]_2{}^{tBu}bpyPF_6$ (0.01 equiv, 0.003 mmol, 3.4 mg), and 4-*tert*-Butyl terpyridine (0.04 equiv, 0.012 mmol, 4.8 mg) are weighed into a 4 mL vial with a Teflon magnetic stir bar. If the C–H substrate (1 equiv, 0.3 mmol) or acid (0.5 equiv) is a solid, it is also weighed out into the vial on the benchtop in this step. The vial is then sealed with a PTFE-lined pierceable cap and moved into an inert atmosphere glovebox. In the glovebox, the vial is opened and 2,2,2-trifluoroethanol (0.3 M, 0.3 mmol scale, 1000 µL) is added followed by di-*tert*-butyl peroxide (6 equiv, 1.8 mmol, 330 µL). If the C–H substrate (1 equiv, 0.3 mmol) or acid (0.5 equiv) is a liquid, it is also weighed out into the vial in the glovebox in this step. The vial is then sealed, removed from the glovebox, and mounted to a stir plate with a piece of double-sided tape. A clip fan and LED light are mounted 8 inches away from the vial, and the vial is illuminated at room temperature (22-27 °C) for 16 hours.

Work-up: The vial is removed from the stir plate and a 3 µL aliquot is taken for LC-MS analysis. If a precipitate forms, the remaining reaction mixture is diluted with 1 mL $CHCl_3$ or CH_2Cl_2 and filtered over a 0.2 µm syringe filter or celite plug into a 15 mL vial (use additional solvent as needed to complete the transfer). The contents of the 15 mL vial are then concentrated on the rotovap. A column is run to separate the product; dichloromethane is used to load the column. Elution of the product is predicted based on the collected LC-MS trace. For some reactions, the product is extracted from the column fractions 2x using 1:1 pentane:Et_2O and brine (additional water is added if NaCl precipitates during the extraction). The organic layers are combined, dried over $MgSO_4$, filtered over cotton, and then concentrated to give the purified methylated product. For other products, the column fractions are collected and concentrated directly at 55 °C on a rotary evaporator.

5D.III. General procedure for C(sp^3)–H methylation with dicumyl peroxide (DCP)

Warning: Productive reactions typically pressurize the vessel as the reaction progresses.

Set-up: $NiCl_2$•glyme (0.04 equiv, 0.012 mmol, 2.6 mg), $Ir[dF(CF_3)ppy]_2{}^{t\text{Bu}}bpyPF_6$ (0.01 equiv, 0.003 mmol, 3.4 mg), 4-*tert*-Butyl terpyridine (0.04 equiv, 0.012 mmol, 4.8 mg), acid (0.5 equiv), and dicumyl peroxide (6 equiv, 1.8 mmol, 486.7 mg) are weighed into a 4 mL vial with a Teflon magnetic stir bar on the benchtop. If the C–H substrate (1 equiv, 0.3 mmol) is a solid, it is also weighed out into the vial on the benchtop in this step. The vial is then sealed with a PTFE-lined pierceable cap and moved into an inert atmosphere glovebox. In the glovebox, the vial is opened and acetonitrile (0.3 M, 0.3 mmol scale, 1000 µL) is added. If the C–H substrate (1 equiv, 0.3 mmol) is a liquid, it is also weighed out into the vial in the glovebox in this step. The vial is then sealed, removed from the glovebox, and mounted to a stir plate with a piece of double-sided tape. A clip fan and LED light are mounted 8 inches away from the vial, and the vial is illuminated at room temperature (22-27 °C) for 16 hours.

Work-up: The vial is removed from the stir plate and a 3 µL aliquot is taken for LC-MS analysis. If a precipitate forms, the remaining reaction mixture is diluted with 1 mL $CHCl_3$ or CH_2Cl_2 and filtered over a 0.2 µm syringe filter or celite plug into a 15 mL vial (use additional solvent as needed to complete the transfer). The contents of the 15 mL vial are then concentrated on the rotovap. A column is run to separate the product; dichloromethane is used to load the column. Elution of the product is predicted based on the collected LC-MS trace. For some reactions, the product is extracted from the column fractions 2x using 1:1 pentane:Et_2O and brine (additional water is added if NaCl precipitates during the extraction). The organic layers are combined, dried over $MgSO_4$, filtered over cotton, and then concentrated to give the purified methylated product. For other products, the column fractions are collected and concentrated directly at 55 °C on a rotary evaporator.

5D.IV. General procedure for microscale scouting reactions

Well plate reaction scouting example (microscale variant of metal screening Table 5D.4): For 30 µmol scale reactions, four doses of each metal salt (1 dose = 0.04 equiv, 1.2 µmol; 4 doses = 4.8 µmol) were weighed into 4 mL vials (one salt per vial). Four doses of 4-*tert*-Butyl terpyridine (1 dose = 0.04 equiv, 1.2 µmol; 4 doses = 4.8 µmol, 1.9 mg) were then added to each of the vials. 200 uL of acetone was added to the vials and they were sealed and agitated to allow binding of the ligand to the metal. 50 uL of each stock solution was dispensed into a 1 ml vial in a sealable 24-well plate and a 5 mm stainless steel stir bar was added to each (10 different metal salt stock solutions were used for the variant of Table 5D.4). A fan was aimed at the uncovered well plate, which was left to sit for 1 hour to remove acetone, leaving the dried metal and ligand. The well plate was then sealed and moved into an inert atmosphere glovebox.

Set-up: Fourteen doses of $Ir[dF(CF_3)ppy]_2{}^{t\text{Bu}}bpyPF_6$ (1 dose = 0.01 equiv, 0.3 µmol; 14 doses = 4.2 µmol, 4.7 mg) and 3-phenyl-propylphthalimide (1 dose = 1 equiv, 30 µmol; 14 doses = 420 µmol, 111.4 mg) were weighed into a 4 mL vial with a PTFE-lined pierceable cap on the benchtop. The vial was then sealed and moved into the inert atmosphere glovebox. In the glovebox, the vial was opened and fourteen doses of 2,2,2-trifluoroethanol (0.3 M, 30 µmol scale, 1 dose = 100 µL; 14 doses = 1400 µL) was added followed by fourteen doses of di-*tert*-butyl peroxide (1 dose = 6 equiv, 180 µmol; 14 doses = 2520 µmol, 462.9 µL) and fourteen doses of trifluoroacetic acid (1 dose = 0.5 equiv, 15 µmol; 14 doses = 210 µmol, 16.1 µL). Inside the glovebox, the plated well plate was opened and 142 µL of the C–H substrate stock solution was added to each well with a metal salt using a pipettor. The well plate was then sealed, removed from the glovebox, and placed on top of an LED light plate on a magnetic tumble stirrer with a clip fan aimed at it to maintain ~27 °C temperature. The plate was stirred and illuminated for 16 hours.

Work-up: The well plate was opened and the wells were diluted with 75 µL of THF with 0.02 M concentration of 4,4’-di-*tert*-butylbiphenyl using a multi-channel pipettor. If solids in the reaction vial were not dissolved, 100 µL 3:1 MeCN:DMSO was also added at this stage. 10 uL aliquots from each well were then transferred to a filter plate and diluted with 190 µL of 3:1 MeCN:DMSO. The 200 µL wells were filtered into a 300 µL collection plate, sealed with a scored Teflon sheet, and then submitted for a 2-minute LC-MS analysis using a 10%→95% gradient of MeCN/H_2O with 0.1% formic acid by volume (95% MeCN @ 1.3 minutes).

5D.V. Screening tables

Table 5D.1. Control experiments

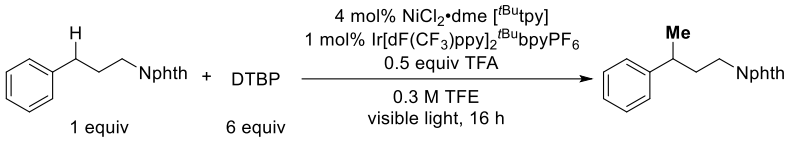

entry	variation	% conversion	% dimethylation	% yield[a]
1	standard	80	18	60
2	no light	-	-	-
3	no photocatalyst	6	-	6
4	no Ni and no ligand	45	-	9
5	no acid	44	-	17
6	under air	78	13	52
7	sparged with N_2	79	15	52
8	Kessil lamp	81	17	61

[a]Reactions run on 0.1 mmol scale and yields analyzed by LC-MS @ 275 nm with 0.05 equiv di-*t*Bu-biphenyl added as an internal standard and/or ^{1}H NMR with 1 equiv mesitylene added as an internal standard.

Table 5D.2. Additive screening table

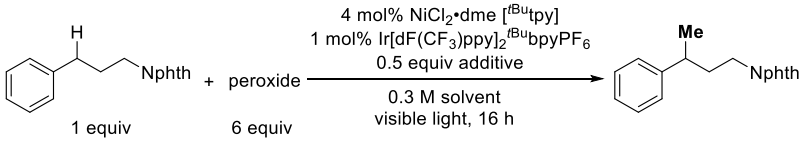

entry	peroxide - solvent	additive	% conversion	% dimethylation	% yield[a]
1	DTBP - TFE	none	39	-	15
2	DTBP - TFE	TFA	80	18	60
3	DTBP - TFE	$B(OH)_3$	60	7	47
4	DTBP - TFE	$MeB(OH)_2$	45	<5	32
5	DTBP - TFE	benzoic acid	50	5	32
6	DTBP - TFE	guanidinium chloride	55	6	43
7	DTBP - TFE	H_2O	33	-	15
8	DTBP - TFE	Li_2CO_3	40	-	18
9	DCP - MeCN	none	53	7	35
10	DCP - MeCN	TFA	70	11	41
11	DCP - MeCN	$B(OH)_3$	71	15	47
12	DCP - MeCN	$MeB(OH)_2$	75	16	48

[a]Reactions run on 0.1 mmol scale and yields analyzed by LC-MS @ 275 nm with 0.05 equiv di-*t*Bu-biphenyl added as an internal standard and/or ^{1}H NMR with 1 equiv mesitylene added as an internal standard.

Table 5D.3. Solvent screening table

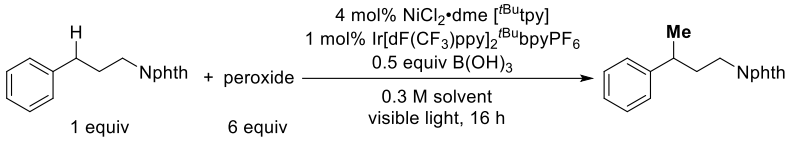

entry	peroxide - solvent	% conversion	% dimer*2	% dimethylation	% yield[a]
1	DTBP - MeCN	95	20	5	17
2	DTBP - acetone	93	17	-	<5
3	DTBP - PhCl	88	43	-	<5
4	DTBP - TFE	64	-	8	44
5	DTBP - DMSO	82	21	-	16
6	DTBP - 1:1 MeCN:DMSO	89	22	<5	17
7	DCP - MeCN	75	<5	11	49
8	DCP - acetone	74	11	7	33
9	DCP - PhCl	45	19	-	8
10	DCP - TFE	41	-	<5	29
11	DCP - DMSO	73	8	7	32
12	DCP - 1:1 MeCN:DMSO	78	8	10	36

[a]Reactions run on 0.1 mmol scale and yields analyzed by LC-MS @ 275 nm with 0.05 equiv di-*t*Bu-biphenyl added as an internal standard and/or ^{1}H NMR with 1 equiv mesitylene added as an internal standard. Dimer refers to the bibenzyl dimer from coupling two benzylic sites.

Table 5D.4. Metal screening table

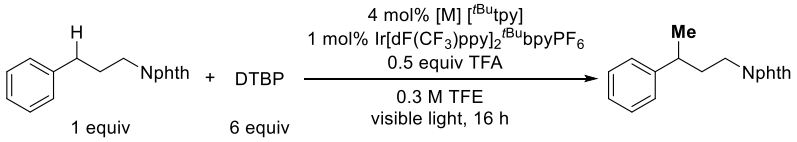

entry	metal salt	% conversion	% dimethylation	% yield[a]
1	$NiCl_2$•dme	79	18	58
2	$NiCl_2$•$6H_2O$	79	18	58
3	$NiBr_2$•dme	83	23	56
4	$NiBr_2$	79	20	52
5	NiI_2	74	<5	10
6	$Ni(acac)_2$	81	19	58
7	$Ni(OAc)_2$•$4H_2O$	81	18	56
8	$Ni(NO_3)_2$•$6H_2O$	82	17	52
9	CuCl	65	6	28
10	$Pd(OAc)_2$	69	<5	<5

[a]Reactions run on 0.1 mmol scale and yields analyzed by LC-MS @ 275 nm with 0.05 equiv di-*t*Bu-biphenyl added as an internal standard.

Table 5D.5. Photocatalyst and light screening table for C–H activation[5,7,8,9]

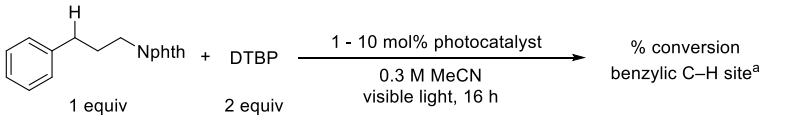

entry	photocatalyst	light source (wavelength)	excited reduction potential (V, SCE)	triplet energy level (kcal/mol)	% conv
1	$Ir[dF(CF_3)ppy]_2{}^{tBu}bpyPF_6$	Blue (470 nm)	-0.89 (MeCN)	61	64
2	none		-	-	0
3	$Ir[dF(CF_3)ppy]_2{}^{tBu}bpyPF_6$		-0.89 (MeCN)	61	79
4	$Ir[dF(H)ppy]_2{}^{tBu}bpyPF_6$		-0.93 (MeCN)	56	78
5[d]	benzil		NR	54	28
6[d]	fluorenone		-0.61 (MeCN)	53	22
7	1,2,3,5-tetrakis(carbazolyl)-4, 6-dicyanobenzene (4-CzIPN)		-1.04 (MeCN)	53	13
8[b]	4-CzIPN		-1.04 (MeCN)	53	19
9	triphenyl pyrylium BF_4	"Tuna Blue" (400 nm-470 nm)	NR	53	10
10[c]	triphenyl pyrylium BF_4		NR	53	22
11	$Ir(ppy)_2{}^{tBu}bpyPF_6$		-0.96 (MeCN)	49	17
12[b]	$Ru(bpy)_3Cl_2$		-0.81 (MeCN)	47	0
13[c]	9-Mes-10-Me-acridinium ClO_4		NR	45	0
14	Eosin Y		-1.15 (MeOH)	44	10
15[c]	Eosin Y		-1.15 (MeOH)	44	3
16	none		-	-	12
17[d]	thioxanthone		-1.11 (MeCN)	65	82
18[d]	2-CF_3 thioxanthone	Violet (395 nm)	NR	NR	90
19	none		-	-	37
20[d]	xanthone		-1.42 (MeCN)	74	46
21[d]	benzophenone	Household CFL Blacklight (365 nm)	-0.61 (MeCN)	69	44
22	none		-	-	32

[a]Reactions run on 0.1 mmol scale and conversion analyzed by ^1H NMR with 1 equiv mesitylene added as an internal standard. Used 1 mol% photocatalyst. [b]Used 3 mol% photocatalyst. [c]Used 5 mol% photocatalyst. [d]Used 10 mol% photocatalyst.

Table 5D.6. Photocatalyst screening table

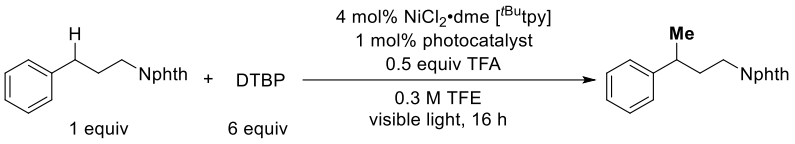

entry	photocatalyst	triplet energy level (kcal/mol)	% conversion	% dimethylation	% yield[a]
1	$Ir[dF(CF_3)ppy]_2{}^{tBu}bpyPF_6$	61	80	18	60
2	$Ir[dF(H)ppy]_2{}^{tBu}bpyPF_6$	56	66	-	50
3	4-CzIPN	53	<5	-	<5
4	triphenyl pyrylium BF_4	53	12	-	8
5	$Ir(ppy)_2{}^{tBu}bpyPF_6$	49	6	-	<5
6	Eosin Y	44	17	-	14
7	none	-	6	-	6

[a]Reactions run on 0.1 mmol scale and yields analyzed by LC-MS @ 275 nm with 0.05 equiv di-*t*Bu-biphenyl added as an internal standard and/or ^{1}H NMR with 1 equiv mesitylene added as an internal standard.

Table 5D.7. Oxidant screening table

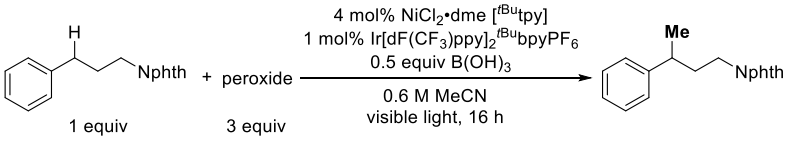

entry	peroxide	% conversion	% dimer*2	% dimethylation	% yield[a]
1	$^tBuO-O^tBu$	94	25	5	18
2	CumylO−OCumyl	74	<5	16	49
3	$^tBuO-OH$ (6 M hexane)	28	-	-	-
4	$^tBuO-OBz$	60	7	-	8
5	$^tBuO-OAc$ (75% in oil)	40	<5	-	10

[a]Reactions run on 0.1 mmol scale and yields analyzed by LC-MS @ 275 nm with 0.05 equiv di-*t*Bu-biphenyl added as an internal standard and/or ^{1}H NMR with 1 equiv mesitylene added as an internal standard. Dimer refers to the bibenzyl dimer from coupling two benzylic sites.

Table 5D.8. Ligand screening table (benzylic)

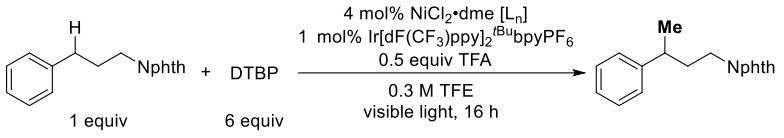

entry	ligand	% diMe	% yield	entry	ligand	% diMe	% yield
1	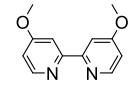	14	48	7	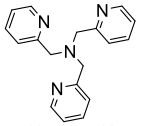	12	40
2	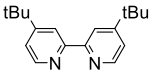	7	29	8	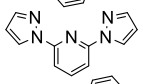	16	51
3	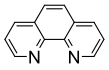	11	42	9	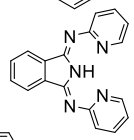	17	50
4	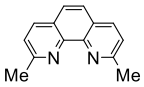	20	44	10	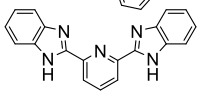	14	48
5	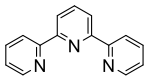	13	45	11	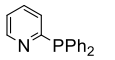	8	33
6	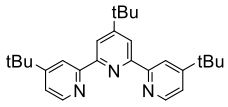	18	55	12	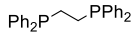	<5	20

[a]Reactions run on 0.1 mmol scale and yields analyzed by LC-MS @ 275 nm with 0.05 equiv di-*t*Bu-biphenyl added as an internal standard. The Ni and ligand were pre-plated into vials for this set of reactions.

Table 5D.9. Ligand screening table (α-amino)

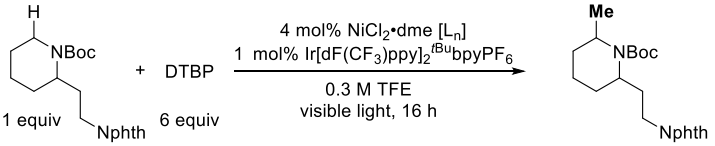

entry	ligand	% conv	% yield	entry	ligand	% conv	% yield
1	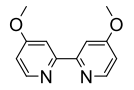	50	29	7	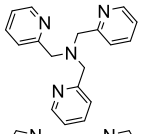	71	48 (15 diMe)
2	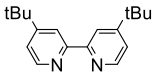	48	12	8	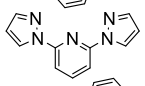	56	15
3	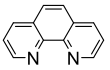	56	21	9	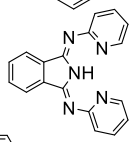	55	23
4	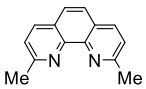	49	14	10	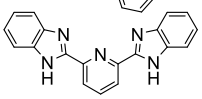	43	15
5	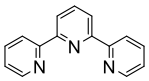	49	15	11	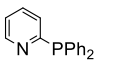	50	15
6	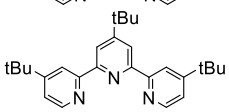	43	16	12	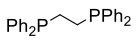	33	14

[a]Reactions run on 0.1 mmol scale and yields analyzed by LC-MS @ 275 nm with 0.05 equiv di-*t*Bu-biphenyl added as an internal standard. The Ni and ligand were pre-plated into vials for this set of reactions.

5D.VI. Additional experiments and observations

5D.VI.1. HAT vs β-scission data when using limiting peroxide

Reactions were set up according to the general procedure in sections II and III except on a 0.1 mmol reaction scale using the reagent combinations denoted in the reaction equation (and using variations shown throughout figures 5D.4-6). Hydrogen atom transfer was quantified by monitoring conversion of the benzylic C–H bond peak, while β-scission was quantified by monitoring acetone formation both using ^{1}H NMR with 1 equiv mesitylene added as an internal standard.

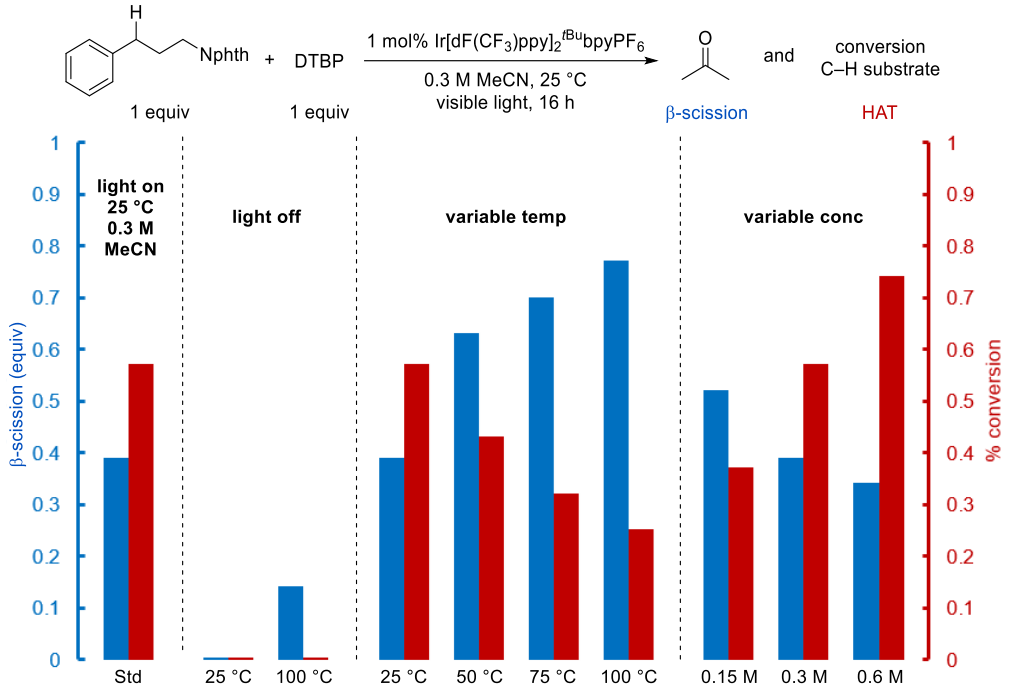

Figure 5D.4. β-Scission vs hydrogen atom transfer using di-*tert*-butyl peroxide as the oxidant as a function of light, temperature, and concentration.

Discussion:

Several noteworthy reaction characteristics were determined by the experiments shown in Figure 5D.4. When the light is turned off, no conversion of the peroxide or C–H substrate is observed at room temperature. If the same reaction is conducted at 100 °C, still no substrate conversion is observed and there is now a relatively minor amount of peroxide conversion to acetone. This highlights the importance of light towards enabling catalysis and the importance of low reaction temperatures for enabling HAT reactivity. As described in the main text, changes in the reaction temperature greatly affects the relationship between HAT and β-scission. At high temperatures, β-scission is increasingly favored whereas HAT can be promoted by reducing the reaction temperatures. Another reaction parameter that allows tuning of HAT vs β-scission is the reaction concentration. At high concentrations, HAT is favored, while at low concentrations β-scission is favored. This can be rationalized by the first-order reaction rate of the HAT reaction vs the zero-order reaction rate of the β-scission reaction. Understanding and applying these trends was essential for development of the C–H methylation reaction.

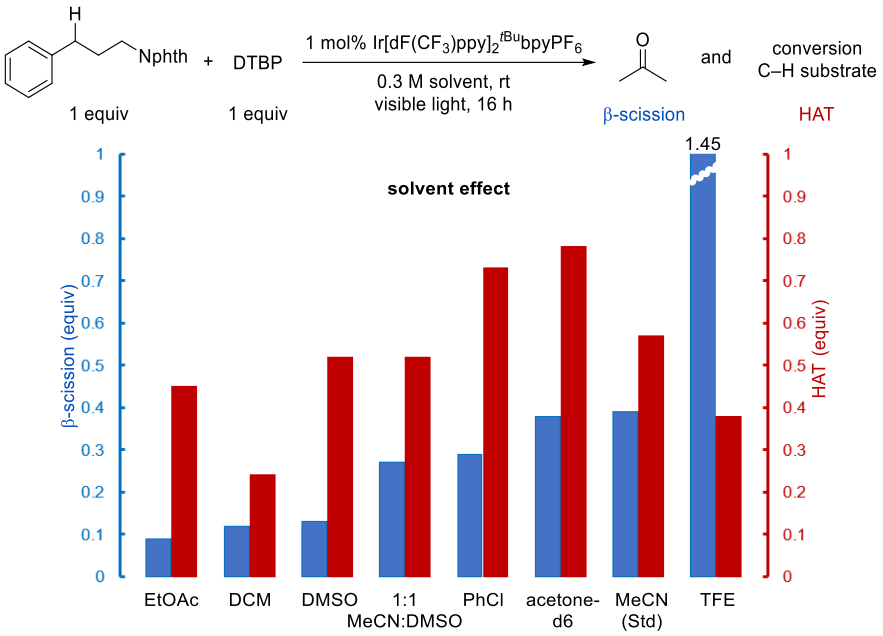

Figure 5D.5. β-Scission vs hydrogen atom transfer using di-*tert*-butyl peroxide as the oxidant as a function of reaction solvent.

Discussion:

In Figure 5D.5, the effects of different solvents on β-scission vs HAT were examined. In general, more polar solvents led to higher amounts of β-scission, while non-polar solvents promoted conversion of the substrate. For development of the C(sp^3)–H methylation reaction, both HAT and β-scission needed to be efficient processes, so use of trifluoroethanol was advantageous in reaction optimization. By increasing the reaction concentration of the TFE reaction and/or by using additional equivalents of peroxide we were able to increase the relative rate of HAT enough to catalyze C–H methylation in good yields, even with limiting C–H substrate. The other reaction solvents here may be more suitable for pursuit of alternative C–H functionalization reactions.

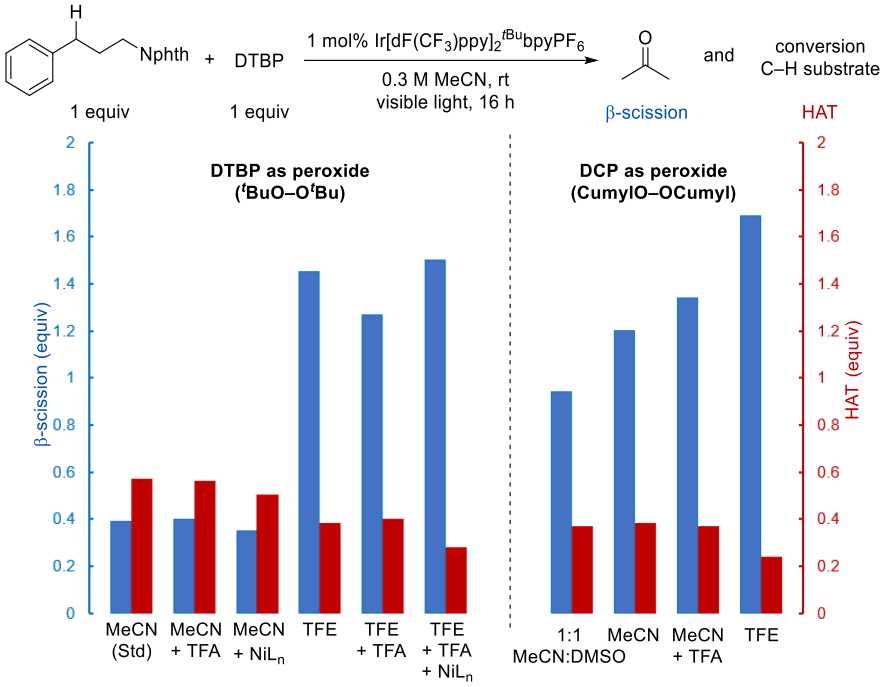

Figure 5D.6. Comparison of β-scission vs hydrogen atom transfer when using either di-*tert*-butyl peroxide or dicumyl peroxide as the oxidant when adding different reagents and solvents.

Discussion:

In Figure 5D.6, we explored the effects of acid, Ni, and peroxide on HAT vs β-scission. If we add TFA or $NiCl_2$•dme + ^{tBu}tpy to the "standard" MeCN reaction conditions, we observe almost no change in HAT vs β-scission reactivity. When using trifluoroethanol as the solvent with DTBP, we again observe only minute changes in the amount of HAT vs β-scission by adding these reagents. When the oxidant is switched to dicumyl peroxide, β-scission is significantly more favored. The inherently high reactivity of DCP towards undergoing β-scission allowed MeCN and DMSO to be used as solvents in the optimized methylation reaction. Like with DTBP, addition of acid showed only a minor change in β-scission reactivity. The most efficient β-scission reactivity of all the experiments tested was obtained by activating DCP in TFE. Unfortunately, the poor solubility of DCP in TFE and sluggish HAT reactivity makes this pairing impractical for application in the C(sp^3)–H methylation reaction.

5D.VI.2. Examining the effect of acid on catalyst speciation

Methylation reactions were set up and worked up according to the general procedure in section II except using 2 equiv of DTBP, boric acid as the acid, and acetonitrile-d3 as the solvent. Table 5D.10 shows the effect of adding acid and Ni catalyst on conversion of peroxide and C–H substrate and yield in the methylation reaction at room temperature.

Table 5D.10. Effects of the addition of acid and Ni to the C–H methylation reaction.

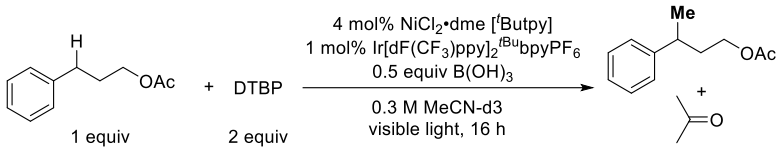

entry	[Ni]	$B(OH)_3$	% peroxide conversion	equiv acetone	% C–H conversion	% yield[a]
1	X	X	42	0.66	58	<5
2	X	✓	41	0.72	57	<5
3	✓	X	60	0.90	67	30
4	✓	✓	85	1.43	82	39

[a]Reactions run on 0.2 mmol scale and yields analyzed by ^{1}H NMR using 1 equiv CH_2Br_2 as an external standard.

Discussion:

Table 5D.10 shows that the addition of acid has minimal effect on catalysis when Ni is absent. LC-MS traces were used to analyze differences in catalyst speciation caused by adding acid to the peroxide photosensitization reaction in the absence of Ni (Fig. 5D.7).

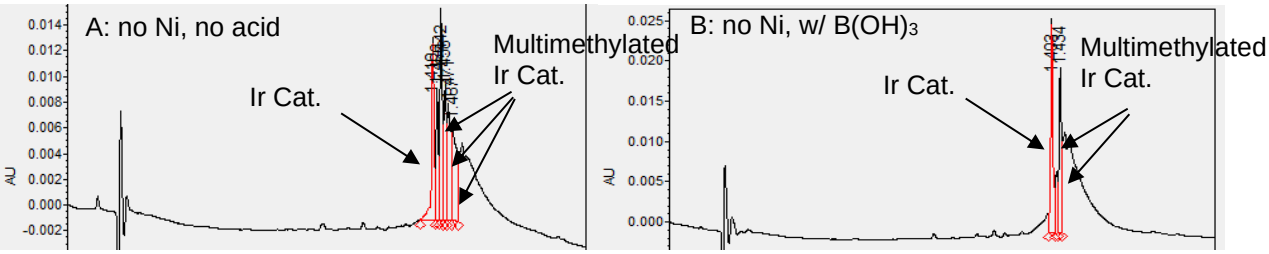

Figure 5D.7. UV-Vis traces from LC-MS chromatograms at 303.7 nm of the methylation reaction without Ni. (A) Table 5D.10, entry 1 (B) Table 5D.10, entry 2

The absence or presence of an acid under Ni-free conditions shows no noteworthy effect on photocatalyst speciation. In both cases, the Ir photocatalyst is methylated, presumably via Me radical addition to the ligands. Based on the incomplete conversion of peroxide in these reactions, this methylation process leads to photocatalyst deactivation. Photocatalyst methylation is accompanied by a visual change in color from bright yellow to orange-red. A similar comparison of reactions was then tested, but now with the Ni catalyst added (Fig. 5D.8).

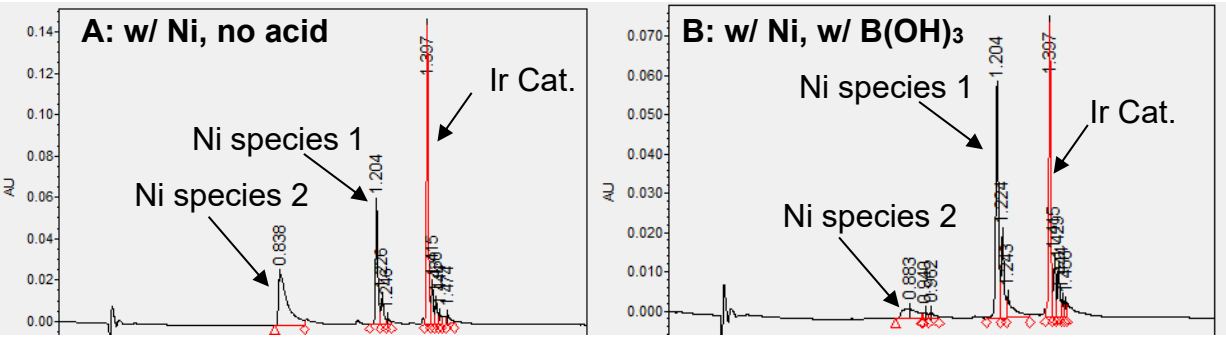

Figure 5D.8. UV-Vis traces from LC-MS chromatograms at 303.7 nm of the methylation reaction with Ni (A) Table 5D.10, entry 3 (B) Table 5D.10, entry 4

Discussion:

A comparison between Fig. 5D.7 and Fig. 5D.8 shows that the introduction of a Ni catalyst greatly inhibits methylation of the photocatalyst and thus promotes activation of the peroxide (Table 5D.10 entry 1 vs entries 3 and 4). Also, in Figure 5D.8 the addition of an acid exhibits a significant effect on the Ni catalyst speciation, as more of the peak at retention time 1.204 minutes is observed over the peak at 0.838 when acid was present. The change in speciation aligns with a significant increase in peroxide conversion and a corresponding increase in C–H conversion and yield (Table 5D.10 entry 3 vs entry 4). The evidence suggests that the role of the acid is related to a Ni-based interaction that promotes peroxide activation and methylation reactivity.

5D.VI.3. Gas evolution experiments

In the optimized C(sp^3)–H methylation reaction, a substantial amount of gas is formed in productive reactions. Gas evolution studies were conducted using pressurized reaction vessels monitored by pressure transducers to evaluate the rate of gas formation. The reaction vessel is pictured below (Fig. 5D.9).

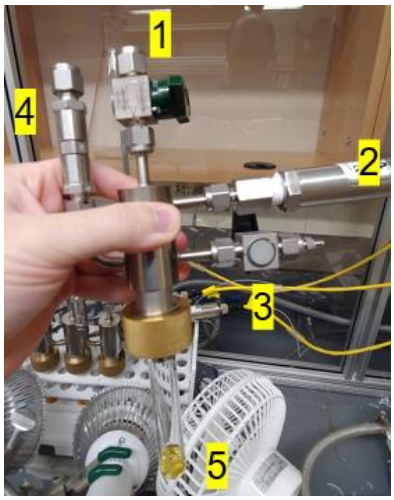

Figure 5D.9. Gas evolution reaction vessel. (1) Injection port (2) Pressure transducer (3) Gas inlet/outlet (4) Pressure release valve (5) Microwave tube vessel.

Gas evolution experiments were set up akin to the general procedure in section II except using microwave tubes as the reaction vessels and a different lighting setup. Solids and stir bars were added to the microwave tubes, and the tubes as well as the pressure reactor assemblies were then moved into a N_2 purge box. Liquids were added to the tubes and the pressure reactor components were fitted to the tube and sealed under N_2 atmosphere. Once the experiments were sealed, they were removed from the purge box and lined up in a secured test tube rack on a stir plate where they stirred for 5 minutes. The transducers were then plugged into cables from a computer equipped to continuously monitor the pressure of each reactor. After collecting a baseline pressure for 5 minutes, two LED lights and two fans were pointed at the reaction vessels and turned on and allowed to operate for 18 hours. The thousands of data points collected from each transducer during the runs were aggregated into the points seen in the following figures (Fig. 5D.11-14).

Figure 5D.10. Photo of the gas evolution reaction tubes (see Fig. 5D.3 for another set up picture).

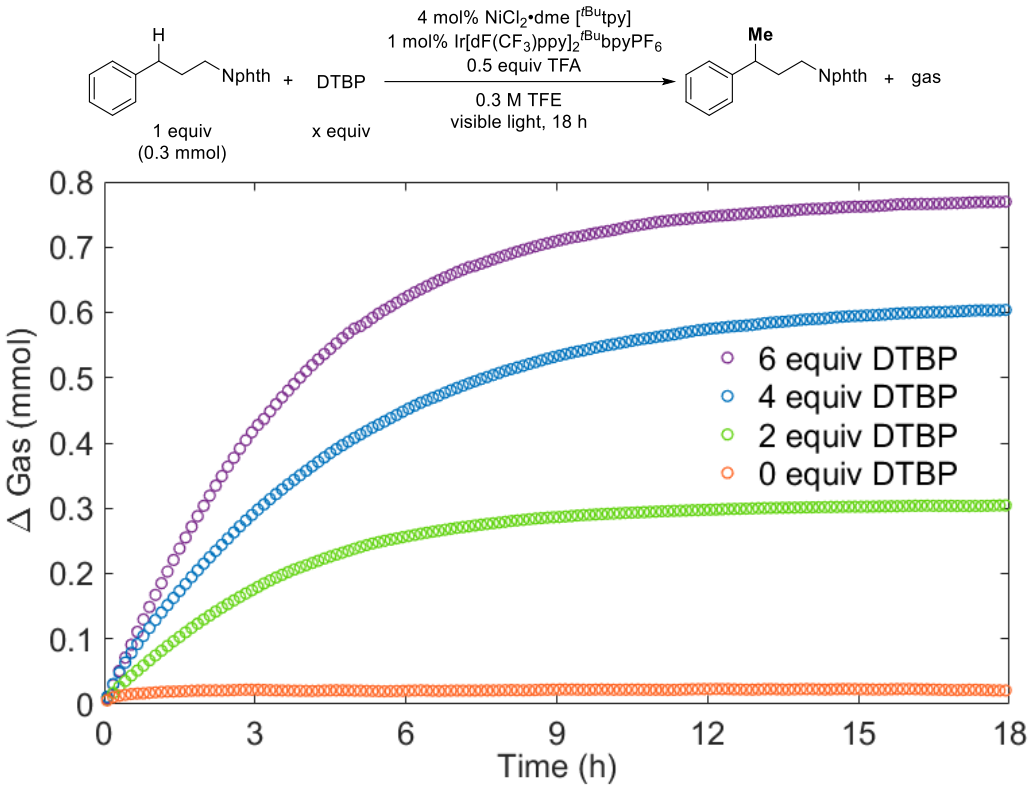

Figure 5D.11. Comparison of total gas pressure as a function of peroxide equivalents.

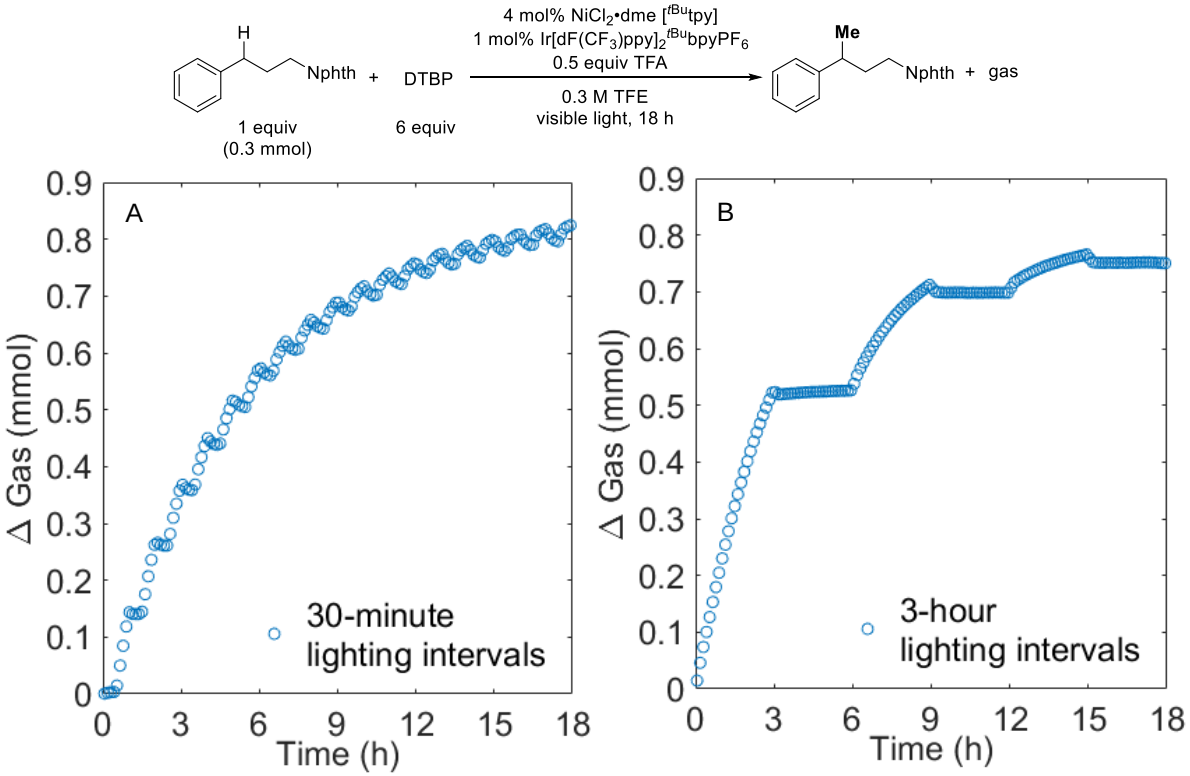

Figure 5D.12. Lighting on-off experiments with power cycling at 30-minute (A) and 3-hour (B) time intervals.

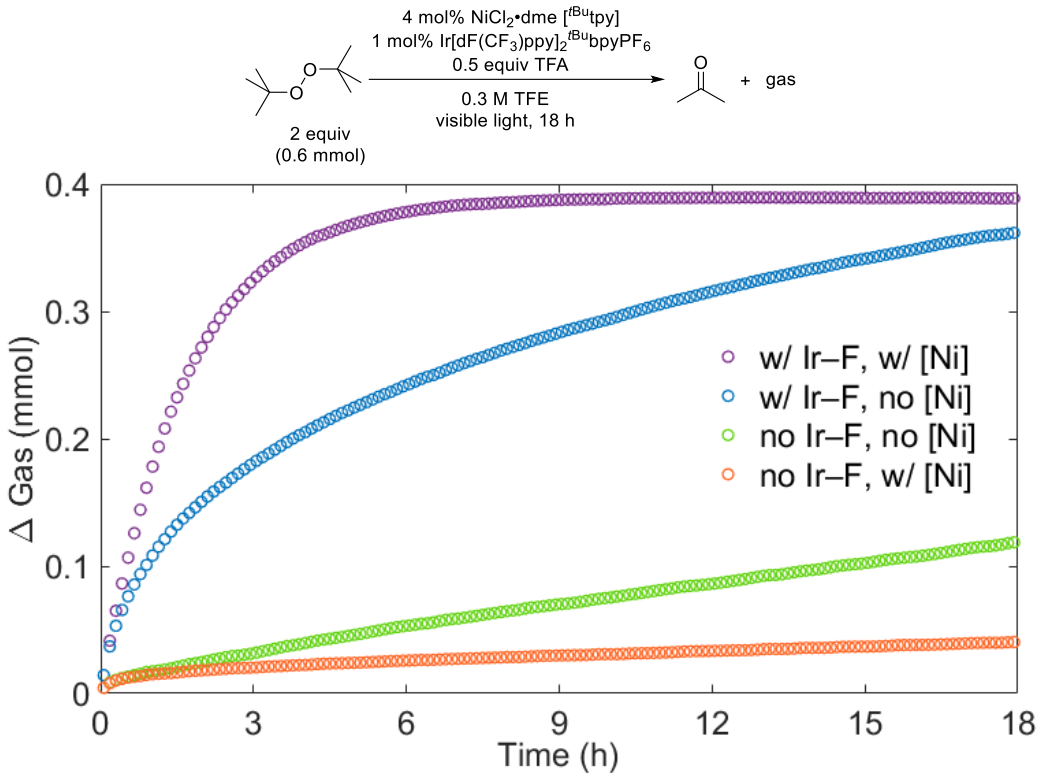

Figure 5D.13. Analysis of gas formation in the presence and absence of the photocatalyst and Ni catalyst.

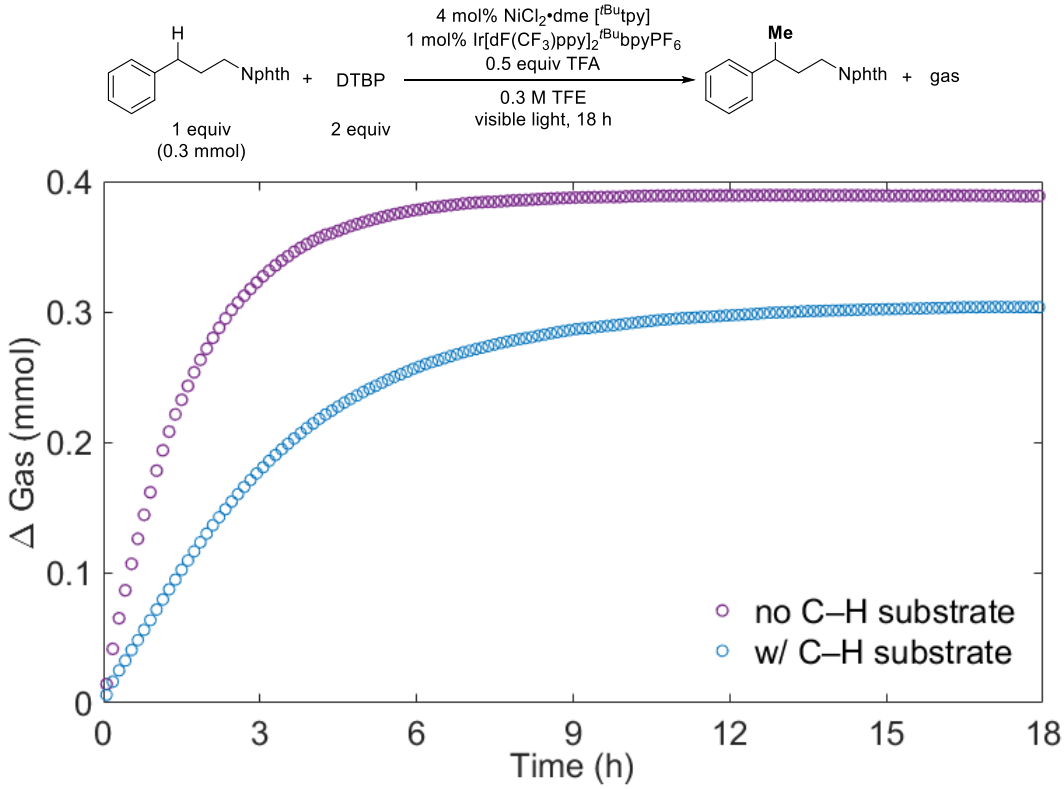

Figure 5D.14. Comparison of gas formed with and without the C–H substrate present.

Discussion:

In Fig. 5D.11, the stoichiometry of peroxide added to the reaction was varied. In the reaction without peroxide, almost no pressure build-up was detected in the time course (there is a small increase at the beginning, which is due to the slight temperature increase from the lamp). In the reaction with 0.6 mmol of peroxide added, 0.3 mmol of gas was formed. Each time the amount of peroxide in the reaction was increased, there was an increase in both the rate and quantity of gas formed. This phenomenon indicates that the gas forming reaction has a dependence on peroxide concentration.

In Fig. 5D.12, an optimized methylation reaction was setup using an LED lamp that was programmed to cycle on and off for the duration of the time course. In Fig. 5D.12 A, the lighting cycled on and off every 30 minutes, while in Fig. 5D.12 B, the lighting was cycled on and off every 3 hours. The small irregularities in pressure are a result of the reaction vessel cooling down a few °C each time the lamps are powered off (from around 27 °C to 22 °C). These experiments suggest that the gas-forming reaction only proceeds with the lights on and has no significant background dark cycle.

In Fig 5D.13, the effects of the various catalysts on gas formation were examined without the C–H substrate present. In the reaction with both the Ir photocatalyst and Ni catalyst present, nearly 0.4 mmol of gas was formed. Removal of the Ni catalyst resulted in a significant change in reaction rate and slight decrease in the amount of gas formed. Based on the information presented in experiment 5D.VI.2, it is reasonable to expect that in the absence of Ni, the Ir photocatalyst is methylated and deactivated in the first 9 hours of this reaction and ensuing gas formation is from direct photolysis of the peroxide. Indeed, if both the Ir photocatalyst and Ni catalyst are excluded, there is a comparable rate of gas formation as to the reaction with only Ir photocatalyst after 9 hours (compare 9-18 hours for the blue and green traces). The Ni catalyst suppresses background activation of the peroxide, which is evident from the orange trace where the Ni catalyst is added without the photocatalyst. This can likely be explained by the strong absorption bands of the Ni catalyst in the 350-420 nm range, which compete for light absorption with the peroxide and deactivate the direct photolysis pathway.

In Fig. 5D.14, the amount of gas formed in the methylation reaction without the C–H substrate was compared to the amount of gas formed with the C–H substrate present. Adding the C–H substrate to the reaction mixture caused the starting material to be methylated in 36% yield (0.11 mmol product), while the amount of gas formed decreased by 0.09 mmol. This indicates that activation of the C–H substrate and/or coupling of the substrate radical to a Me group can cause a decrease in gas formation.

The data in Figure 5D.13 revealed an interesting phenomenon. Despite the similarity in equivalents of gas formed, the experiment with Ni present generated nearly twice as much acetone (purple, 0.97 mmol acetone by NMR) as the one without Ni (blue, 0.54 mmol acetone by NMR). This result led us to question the composition of the gasses formed in these reactions, since more acetone is expected to result in more Me radicals and therefore more gas.

To evaluate the reaction head space, we used the built-in gas outlet on the pressure vessel to vent directly into a GC that is specialized for separating light alkane gasses (Inficon Micro GC Fusion Gas Analyzer with micro thermal conductivity detectors). In this GC, gasses like methane and ethane are separated by diverting the gas sample to columns with unique pore sizes and binding affinities (Rt-Molsieve 5A column and Rt-Alumina bond/Na_2SO_4 column, respectively).

After a gas evolution experiment was completed, the vessel was removed from the test tube rack and disconnected from the computer. It was then brought to the GC and the reaction tube was submerged in a dry ice acetone bath (to reduce vapor pressure) while the other portion was secured with a clamp. Once the solution was chilled, the gas outlet was attached to the GC using tygon tubing. The gas outlet was opened to fill the tubing with the gas from the reaction headspace, which was then sampled by the GC. In between each run, air was sampled to ensure the column was purged of residual gasses from prior runs.

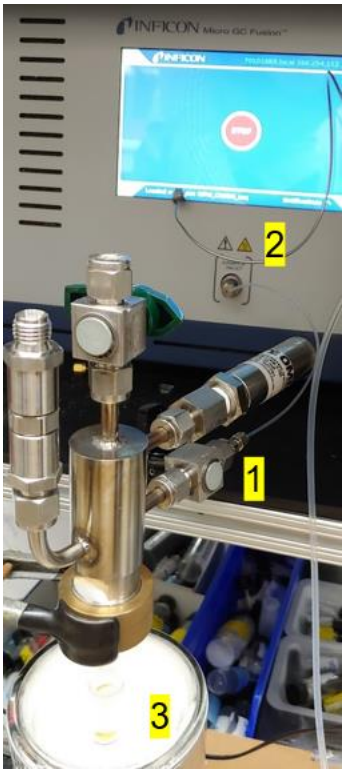

Figure 5D.15. GC headspace analysis setup. (1) Gas inlet/outlet (2) GC sampler (3) Dry ice acetone bath.

To quantify the concentration of each gas present, the GC traces were evaluated by comparing them to a calibration gas trace of 68.58% nitrogen, 27% propane, 3% propylene, 0.5% ethylene, 0.5% carbon monoxide, **0.1% methane**, 0.1% carbon dioxide, **0.05% ethane**, and 0.175% of various 4-carbon hydrocarbons. Data collected from the calibration gas were used to assist in determining the ratio of ethane to methane in the reaction headspaces.

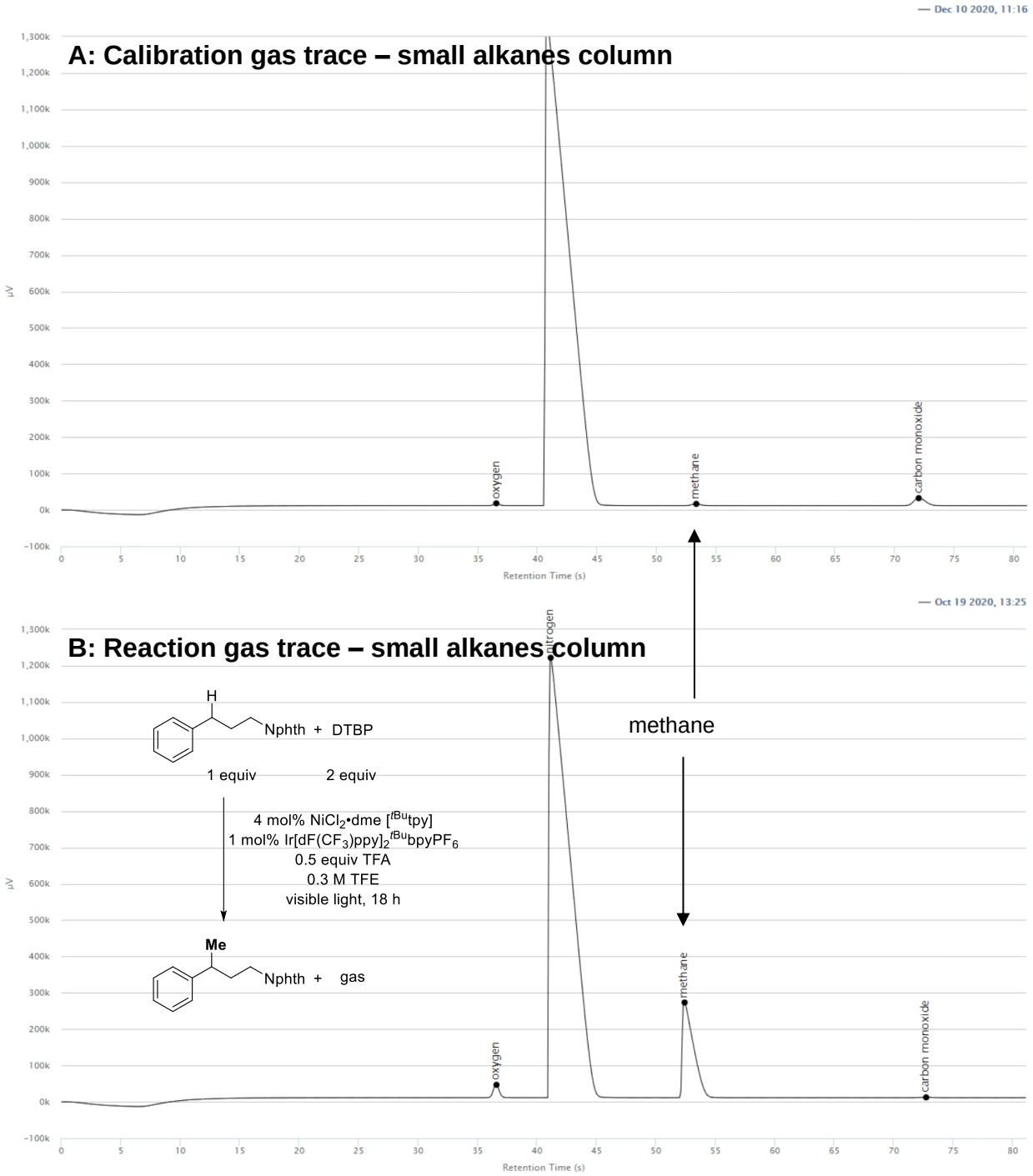

Figure 5D.16. Example GC headspace analysis for methane. (A) Calibration gas trace from the small alkane gas column (B) Reaction headspace trace from the small alkane gas column (Fig. 5D.14, blue)

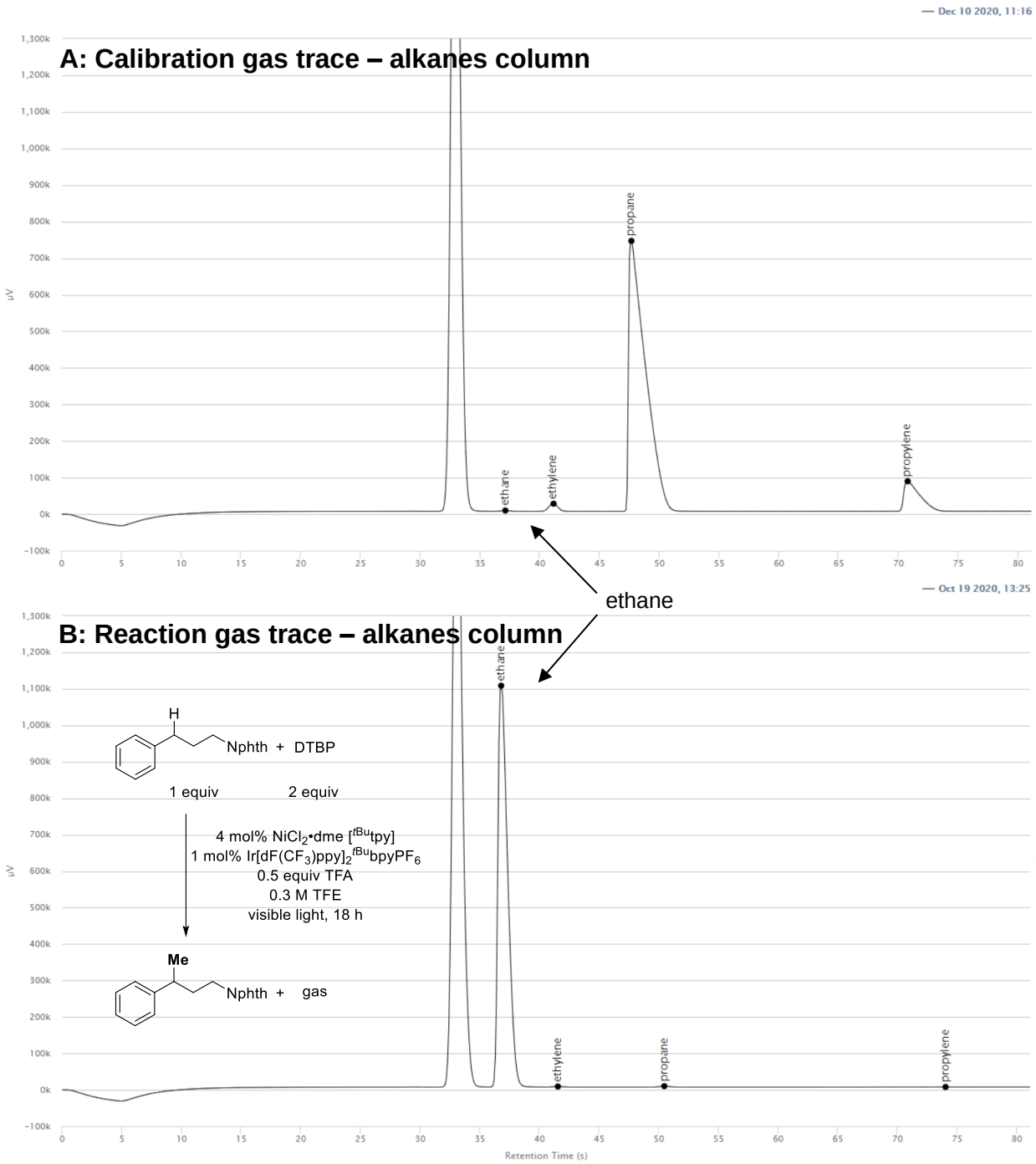

Figure 5D.17. Example GC headspace analysis for ethane. (A) Calibration gas trace from the large alkane gas column (B) Reaction headspace trace from the large alkane gas column (Fig. 5D.14, blue)

Table 5D.11. Concentration and quantity of non-N_2 gasses

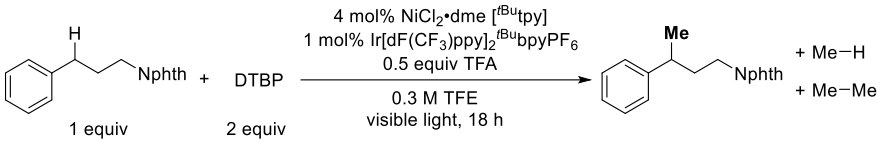

Variation	% O_2	% CO	% CO_2	% propane	% ethane	% methane	ethane: methane	total mmol gas	mmol ethane	mmol methane
No [Ni] No alkylarene (Fig. 5D.13, blue)	0.2	0.2	-	-	0.7%	30.0%	0.02	0.35	<0.01	0.34
With [Ni] No alkylarene (Fig. 5D.14, purple)	0.2	-	-	0.1	36.7%	3.5%	10.5	0.39	0.36	0.03
With [Ni] With alkylarene (Fig. 5D.14, blue)	0.3	-	0.1	0.1	27.5%	5.8%	4.7	0.30	0.25	0.05

[a]The total mmol gas column is based on data from the gas evolution experiments (see Fig. 5D.13 and 5D.14) and the mmol ethane and mmol methane data are calculated based on the % of each gas present according to calibrated GC analysis.

Discussion:

These experiments revealed that Ni catalyzes coupling of methyl radicals to form ethane in the methylation reaction, whereas methyl radical to methane formation is the predominant pathway in the absence of the metal. It is noteworthy that some propane can also be observed in reactions with the Ni catalyst, which is perhaps indicative of some solvated ethane that is able to engage as a substrate in HAT and ensuing methylation. The results here also rationalize the observed disparity in acetone formation for the experiments in Fig. 5D.13, where despite nearly equivalent gas formation the reaction with Ni produced nearly twice as much acetone as the one without. The reaction with Ni was producing primarily ethane gas, which uses 2 equiv of methyl radical, while the reaction without Ni was producing methane gas.

5D.VI.4. Time course of the methylation reaction

Figure 5D.18 and 5D.19 shows methylation time courses of an alkylarene substrate with $^{t\text{Bu}}$tpy as the ligand and an NBoc piperidine substrate with TPA as the ligand. In both cases, the reaction yield of the monomethylated product peaks at around 6 hours into the time course. Yields were evaluated by LC-MS @ 275 nm with 0.05 equiv di-*t*Bu-biphenyl added as an internal standard for the alkylarene and LC-area percent (LC-AP) of substrate-related ions for the NBoc piperidine methylation reaction.

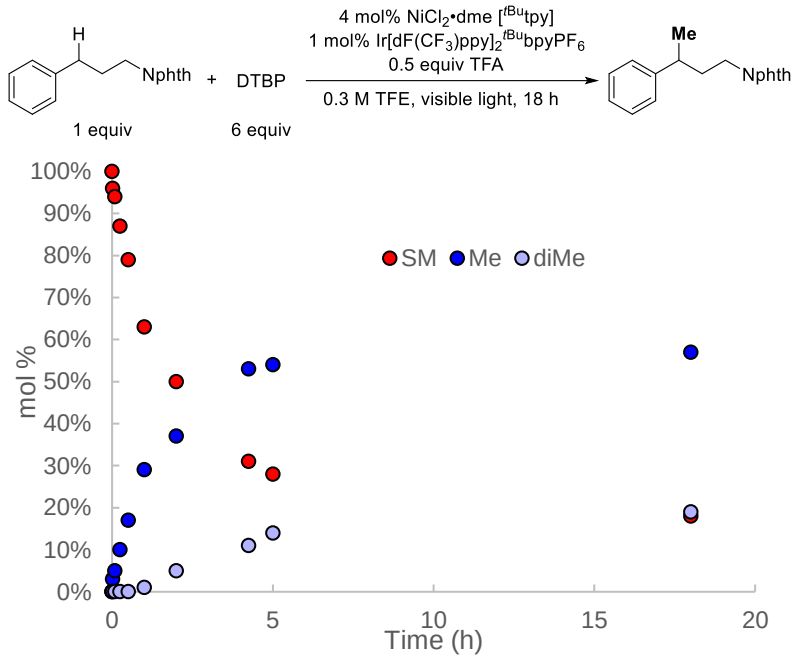

Figure 5D.18. Reaction time course for methylation of an alkylarene substrate

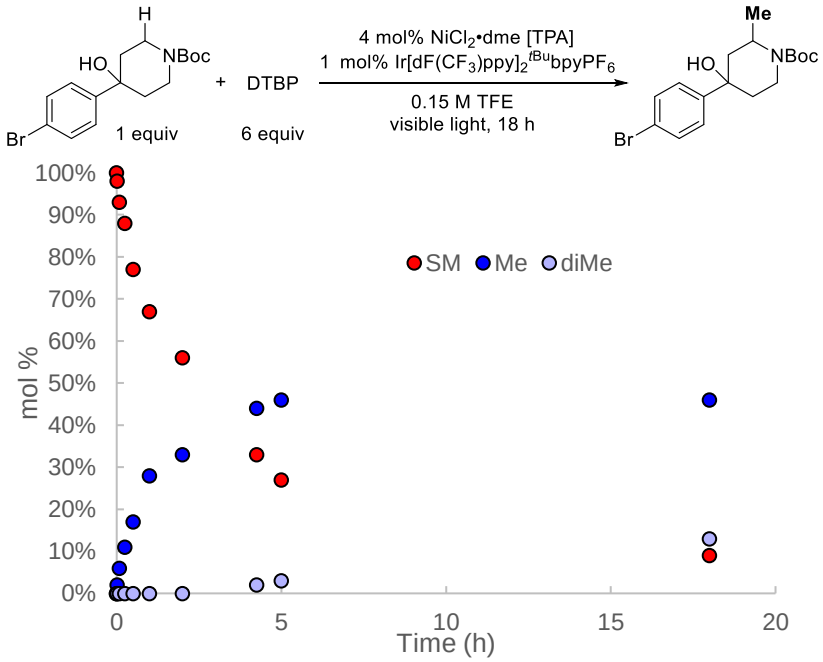

Figure 5D.19. Reaction time course for methylation of an NBoc amine substrate

5D.VI.5. Testing for enantioselective methylation

Tables 5D.12 and 5D.13 show the yield and selectivity observed when using compatible chiral ligands.

Table 5D.12. Enantioselectivity results using DCP/MeCN

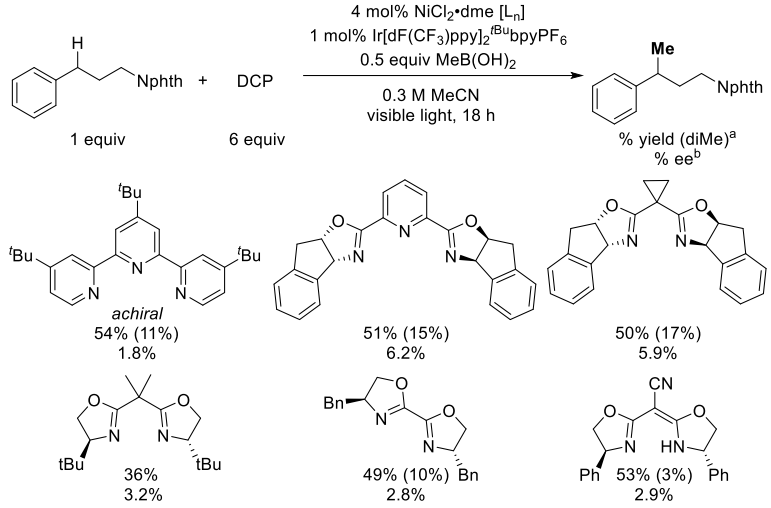

[a]Reactions run on 0.2 mmol scale and reported yields based on LC-AP at 273 nm (first result was confirmed by ^{1}H NMR). [b]Chiral SFC was used for separation and the reported enantioselectivities are those resulting from averaging the ee determined by manual integration of the max absorption spectrum with an automated integration of the 273 nm spectrum.

Table 5D.13. Enantioselectivity results using DTBP/TFE

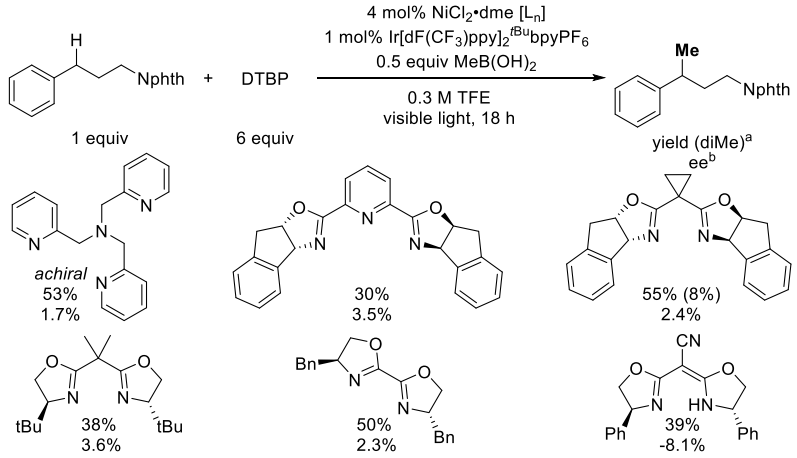

[a]Reactions run on 0.2 mmol scale and reported yields based on LC-AP at 273 nm (first result was confirmed by ^{1}H NMR). [b]Chiral SFC was used for separation and the reported enantioselectivities are those resulting from averaging the ee determined by manual integration of the max absorption spectrum with an automated integration of the 273 nm spectrum.

Discussion:

The lack of enantiomeric excess over 10% in any experiments from tables 5D.12 and 5D.13 suggest that further reaction develop would be needed to enable an enantioselective variant of the methylation chemistry.

5D.VI.6. Resubjection of monomethylation product to the reaction conditions

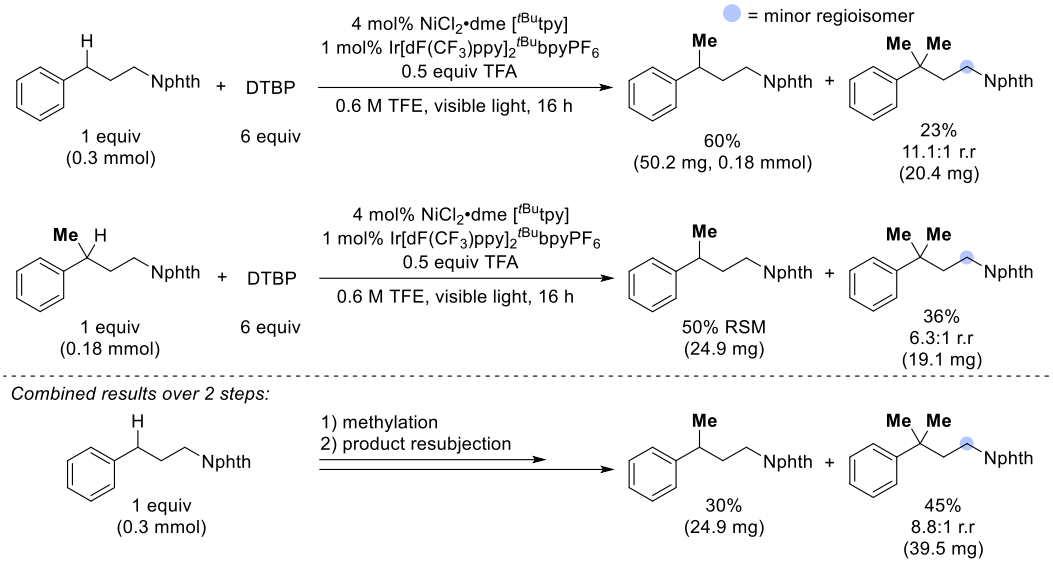

Discussion:

In the optimized C–H methylation reaction, it is common to observe starting material, monomethylated, and dimethylated products as the primary components at the end of the reaction. For some applications, it could be advantageous to selectively access the dimethylated product from a methylene site of a substrate. To test whether this could be done with the C(sp^3)–H methylation reaction, the substrate 3-phenyl-propylphthalimide (0.3 mmol, 79.6 mg) was subjected to the reaction conditions in section II with 0.5 equiv TFA (11.5 µL) at 0.6 M concentration (500 µL TFE). The elevated concentration of 0.6 M was chosen in an effort to induce dimethylation reactivity. Under these reaction conditions, >90% conversion of the C–H substrate was observed and a 60% yield of monomethylated product was isolated as well as a 23% yield of the dimethylated product. The monomethylated product was then resubjected to the same reaction conditions, allowing a 36% yield of the dimethylated product to be obtained from the now 0.18 mmol scale reaction. Overall, a combined 45% yield of dimethylated product could be obtained from the starting C–H substrate over 2 steps.

5D.VI.7. Additional substrates and reactivity discussion

The results in Table 5D.14 were collected by conducting reactions on micro scale using a reaction procedure like that outlined in section IV. Each substrate was subjected to the four sets of reaction conditions from the main text, and a fifth reaction that uses conditions B with DMSO as a co-solvent. The results of these experiments were determined using LC-AP integrations on the UPLC-MS to give an estimation for reaction performance. In general, this method has been reliable across varied substrates for the methylation reaction when compared with calibrated NMR data. These substrates were not scaled up or isolated.

Table 5D.14. Microscale C(sp^3)–H methylation testing results

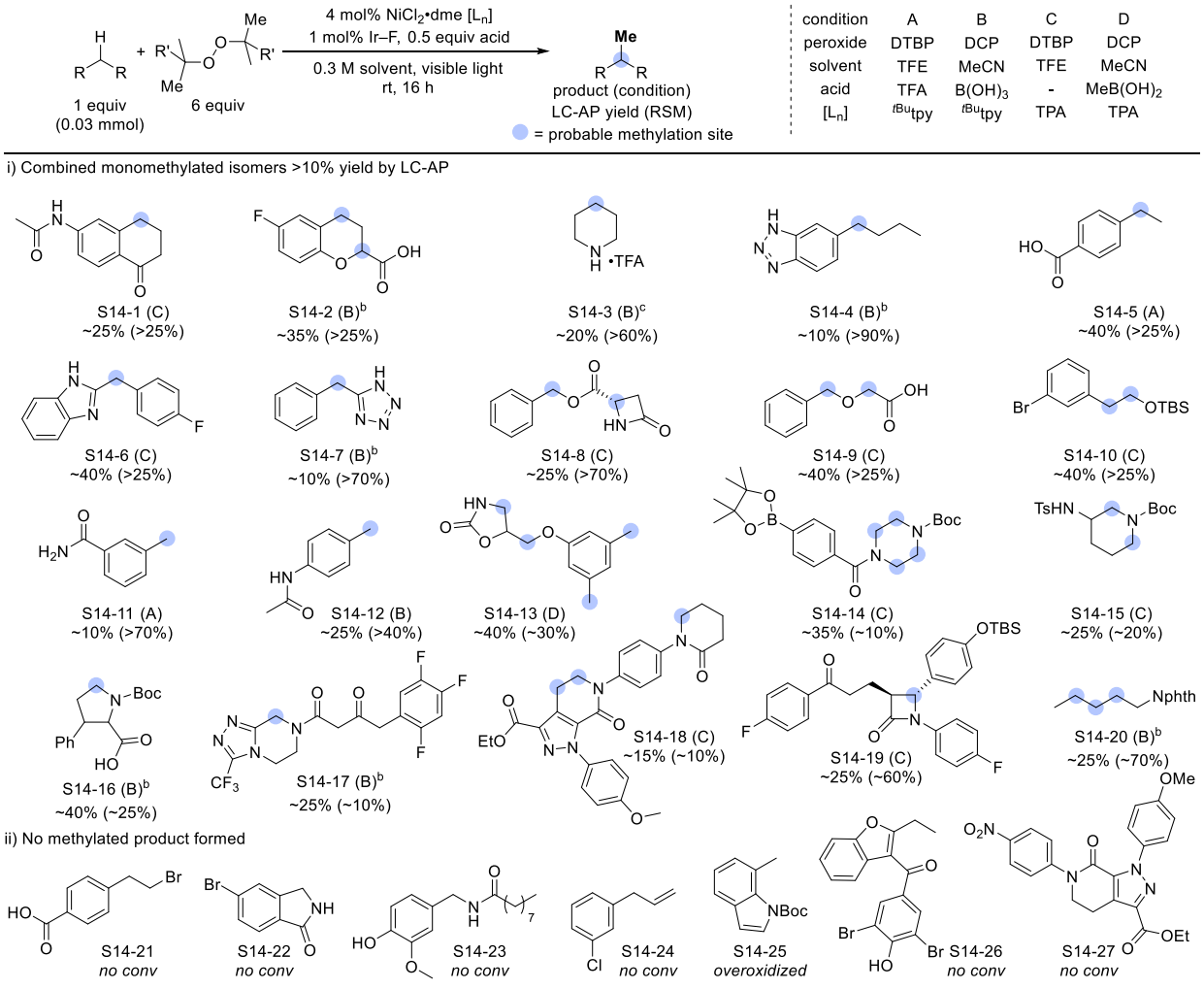

[a]Reactions run on 0.03 mmol scale and yield and remaining starting material (RSM) is based on LC-AP at a wavelength where max absorption of the starting material-derived products are less than 1.0 absorption units. Methylation products are identified as peaks with retention times later than the starting material with an ionization mass equal to ionization mass of SM+14. [b]1:1 MeCN:DMSO used as the solvent. [c]1.5 equiv TFA used as the acid and product observed by UPLC after an Fmoc protection.

Discussion:

The substrates in Table 5D.14 represent a variety of substrate classes that differ from those in the main substrate tables with varying functional groups and selectivity challenges. Some functional groups that are tolerated but give lower yields include acidic heterocycles like benzotriazole, benzimidazole, and tetrazole (5D.14-4, 6, and 7). Methyl arenes are able to be

methylated under the reaction conditions, but the ethylarene products are more reactive than the starting materials and readily undergo further methylation to isopropyl and beyond when run at higher concentrations (5D.14-11, 12, and 13). Some relatively complex structures could be successfully methylated under the reaction conditions but competing weak C–H sites allowed for overoxidation and formation of complex regioisomeric mixtures (5D.14-8, 9, 10, 13, 14, 18). In the case of 5D.14-14, the LC-MS trace revealed mono-, di-, tri-, and tetra-methylation and beyond of the starting material. The methylation reaction is also capable of methylating unactivated C–H bonds, such as those in 5D.14-3 and 20. The challenge with this substrate class is that the starting material conversion is typically low (> 20 %) and in the case of 5D.14-20, three methylation isomers were detected as products. In general, when all five sets of conditions are tested on a given substrate, it is likely that a yield of 5% or more of the monomethylated product will be formed in at least one reaction. However, there are a few functional groups that prevented any methylation reactivity including homobenzyl-bromide, allylbenzene, phenol, and nitroarene. It is possible that these functionalities can initiate redox or energy transfer processes with the Ir photocatalyst that bring it off-cycle and prevent peroxide activation and methylation reactivity.

5D.VII. Starting material syntheses

(21a) *tert*-Butyl 2-(2-phthalimidyl-ethyl)piperidine-1-carboxylate

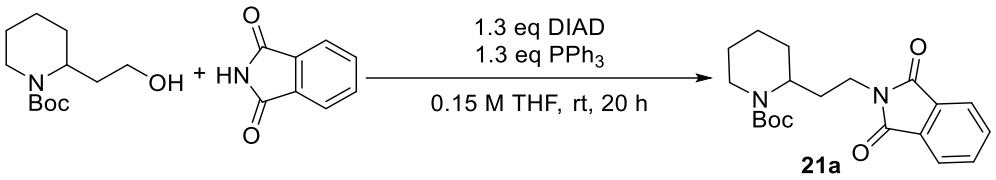

Set-up[10]: The NBoc 2-ethanol piperidine substrate (1 equiv, 10 mmol, 2.22 mL), phthalimide (1.3 equiv, 13 mmol, 1.91 g), and triphenylphosphine (1.3 equiv, 13 mmol, 3.41 g), were added to an oven-dried 250 mL round bottom flask with a Teflon stir bar and then sealed with a rubber septum. The vessel was backfilled with N_2. Tetrahydrofuran from a solvent purification system (0.15 M, 10 mmol scale, 67 mL) was added via syringe under N_2 and the solution was set to stir. Diisopropyl azodicarboxylate (1.3 equiv, 13 mmol, 2.56 mL) was added dropwise over 5 minutes. The solution was left to stir overnight.

Work-up: Tetrahydrofuran was removed by rotary evaporation. The flask was rinsed with 150 mL of water into a separatory funnel, followed by rinsing 3x with 50 mL of hexane into the same separatory funnel. Several grams of sticky insoluble yellow material formed. The organic phase was collected, and the aqueous phase was diluted with 50 mL brine then extracted with 50 mL of hexane. The organic phases were combined, and the aqueous phase and yellow residue were discarded. The organic phase was washed 3x with 50 mL brine. Yellow residue was also removed in this step. The organic phase was collected, dried with $MgSO_4$, filtered, and then concentrated on the rotovap. A normal phase column was run with a 20%→35% gradient of EtOAc in pentane to isolate the desired product. An oversized round bottom flask (1 L) was used to remove solvent, since the purified product foams vigorously when removing EtOAc. 69%, 2.47 g of white solid was isolated.

Spectra available in the literature (CAS): No (N/A)

^{1}H NMR ($CDCl_3$, 500 MHz): δ 7.83 (dd, J = 5.4, 3.0 Hz, 2H), 7.70 (dd, J = 5.4, 3.0 Hz, 2H), 4.31 (s, 1H), 4.03 (s, 1H), 3.71 (ddd, J = 13.6, 10.4, 5.2 Hz, 1H), 3.59 (ddd, J = 13.6, 10.4, 5.8 Hz, 1H), 2.86 (t, J = 13.4 Hz, 1H), 2.10 (dtd, J = 13.5, 10.0, 5.9 Hz, 1H), 1.78 (ddt, J = 13.5, 10.9, 5.6 Hz, 1H), 1.71 – 1.36 (m, 6H), 1.42 (s, 9H).

^{13}C NMR ($CDCl_3$, 126 MHz): δ 168.2, 154.9, 133.9, 132.2, 123.1, 79.4, 48.4, 38.6, 35.5, 28.6, 28.5, 28.4, 25.5, 19.0.

HRMS (ESI) m/z: $[M+H]^+$ Calcd for $C_{20}H_{27}N_2O_4$ 359.1965; Found 359.1958.

(28a) (*R*)-2,2,2-Trifluoro-*N*-(4-oxo-4-(3-(trifluoromethyl)-5,6-dihydro-[1,2,4]triazolo[4,3-a]pyrazin-7(8H)-yl)-1-(2,4,5-trifluorophenyl)butan-2-yl)acetamide

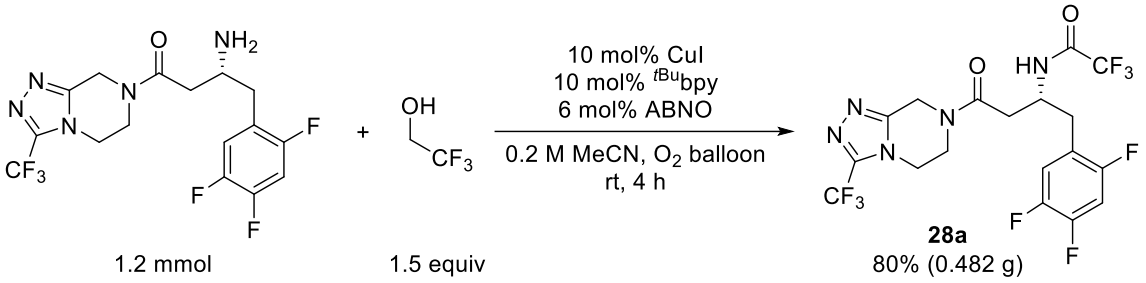

Set-up[11]: On the benchtop, a disposable 15 mL glass vial was charged with CuI (0.1 equiv, 0.12 mmol, 22.8 mg), 4,4'-di-*tert*-butyl-2,2'-bipyridine (0.1 equiv, 0.12 mmol, 32.2 mg), 9-azabicyclo[3.3.1]nonane *N*-oxyl (0.06 equiv, 0.072 mmol, 10.0 mg), acetonitrile (0.2 M, 1.2 mmol scale, 5 mL out of 6 mL – see below), and a Teflon stir bar. The vial was sealed by a PTFE-lined pierceable cap, placed on a stir plate, and allowed to stir for approximately 3 minutes. An O_2 balloon (1 atm) with a needle was added to the reaction by piercing through the cap. The amine (1 equiv, 1.2 mmol, 488.8 mg – dissolved in 1 mL MeCN) and alcohol (1.5 equiv, 1.8 mmol, 135.9 µL) were injected via Hamilton syringes simultaneously through the pierceable septum. The reaction was allowed to stir at room temperature for 4 hours.

Work-up: The balloon and stir bar were removed and the reaction mixture was concentrated by rotary evaporation then purified using automated normal phase column chromatography with a 50%→85% gradient of EtOAc in pentane to yield the desired product. 80%, 0.482 g of white solid was isolated.

Spectra available in the literature (CAS): No (1883288-76-3)

^{1}H NMR (MeCN-d3, 500 MHz): δ 7.79 (t, J = 10.6 Hz, 1H), 7.22 (ddd, J = 11.4, 8.9, 6.8 Hz, 1H), 7.08 (ddt, J = 11.6, 9.8, 6.1 Hz, 1H), 4.90 (s, 1H), 4.87 (s, 1H), 4.52 (ddq, J = 14.2, 9.4, 5.0, 4.6 Hz, 1H), 4.16 (q, J = 5.1 Hz, 1H), 4.09 (t, J = 5.6 Hz, 1H), 3.98 (qt, J = 14.0, 5.5 Hz, 1H), 3.88 (t, J = 5.5 Hz, 1H), 2.98 (dt, J = 12.1, 5.8 Hz, 1H), 2.98 – 2.73 (m, 3H).

^{13}C NMR (MeCN-d3, 126 MHz): δ 170.2 (d, J = 5.2 Hz), 158.4 (d, J = 9.9 Hz), 157.1 (q, J = 36.5 Hz), 156.5 (d, J = 9.1 Hz), 151.9, 151.5, 151.0 – 150.4 (m), 149.0 – 148.5 (m), 148.3 (dd, J = 12.6, 3.7 Hz), 146.4 (d, J = 12.5 Hz), 144.9 – 143.3 (m), 123.8 – 122.0 (m), 120.2 (dd, J = 19.2, 6.1 Hz), 115.7, 106.3 (dd, J = 29.1, 21.1 Hz), 48.4, 44.5, 44.0, 43.1, 42.1, 39.6, 38.5, 36.9, 36.5, 33.3.

^{19}F NMR (MeCN-d3, 471 MHz): δ -64.64, -77.74 (d, J = 8.6 Hz), -120.98 (ddp, J = 15.5, 11.0, 5.7, 4.6 Hz), -138.82 (dtd, J = 20.5, 10.6, 10.0, 3.3 Hz), -146.20 (dddd, J = 27.2, 15.3, 11.3, 6.8 Hz).

HRMS (ESI) m/z: $[M+H]^+$ Calcd for $C_{18}H_{15}F_9N_5O_2$ 504.1077; Found 504.1071.

5D.VIII. Experimental data for C(sp^3)–H methylation products (compounds 1-36)

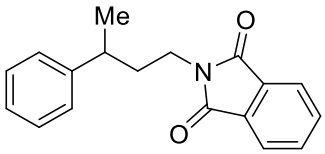

(1) 3-Phenyl-butylphthalimide: Prepared from 3-phenyl-propylphthalimide (0.3 mmol, 79.6 mg) according to the general procedure in section II using the following variation: added trifluoroacetic acid (0.5 equiv, 0.15 mmol, 11.5 µL).
Purification: Reverse phase silica gel chromatography was used with a gradient of 65%→90% MeOH in H_2O, both w/ 0.1% TFA. The product was extracted with 1:1 ether:pentane.
Isolated yield: 59%, 48.9 mg of colorless semisolid.
Spectra available in the literature (CAS): Yes (1383435-90-2)[12]
^{1}H NMR – *mono-methylated* – ($CDCl_3$, 500 MHz): δ 7.78 (dd, J = 5.4, 3.1 Hz, 2H), 7.68 (dd, J = 5.4, 3.0 Hz, 2H), 7.25 – 7.19 (m, 4H), 7.10 (tt, J = 7.5, 1.6 Hz, 1H), 3.68 – 3.56 (m, 2H), 2.78 (dp, J = 8.9, 6.9 Hz, 1H), 2.09 (dtd, J = 13.6, 8.6, 6.9 Hz, 1H), 1.92 (ddt, J = 14.1, 8.3, 5.9 Hz, 1H), 1.29 (d, J = 7.0 Hz, 3H).
^{13}C NMR – *mono-methylated* – ($CDCl_3$, 126 MHz): δ 168.3, 146.1, 133.7, 132.1, 128.4, 126.8, 126.1, 123.0, 38.0, 36.8, 36.1, 22.8.
HRMS (ESI) m/z – *mono-methyl* – **:** $[M+H]^+$ Calcd for $C_{18}H_{18}NO_2$ 280.1332; Found 280.1327.

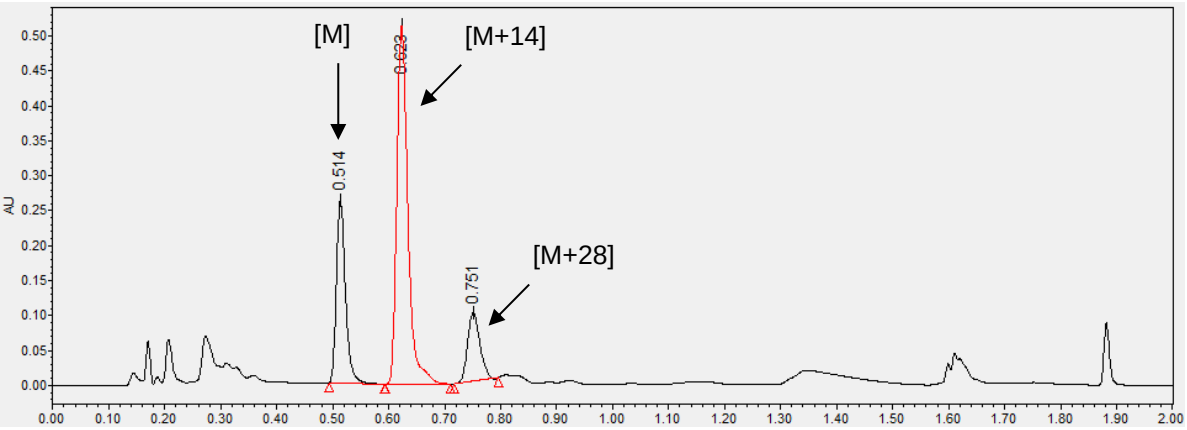

Figure 5D.20. 1 crude reaction LC-MS @ 294 nm (62%→58% MeCN/H_2O, w/ 0.1% HCOOH)

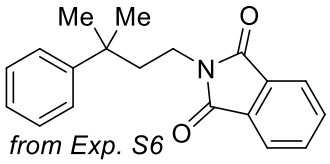

^{1}H NMR – *di-methylated (major)* – ($CDCl_3$, 500 MHz): δ 7.73 (dd, J = 5.4, 3.1 Hz, 2H), 7.64 (dd, J = 5.5, 3.0 Hz, 2H), 7.38 – 7.33 (m, 2H), 7.21 (t, J = 7.9 Hz, 2H), 7.01 (tt, J = 7.2, 1.2 Hz, 1H), 3.58 – 3.43 (m, 2H), 2.13 – 2.03 (m, 2H), 1.40 (s, 6H).
^{13}C NMR – *di-methylated* – ($CDCl_3$, 126 MHz): δ 168.4, 168.2, 147.7, 147.1, 146.1, 133.8, 133.6, 133.1, 132.1, 132.0, 131.8, 128.4, 128.1, 127.6, 127.0, 126.2, 125.6, 125.5, 125.5, 124.6, 123.0, 122.9, 122.4, 46.7, 45.5, 43.7, 41.7, 41.5, 37.4, 36.9, 36.8, 34.7, 32.8, 29.1, 26.1, 22.5, 20.5, 19.3.
HRMS (ESI) m/z – *di-methyl* – **:** $[M+Na]^+$ Calcd for $C_{19}H_{19}NO_2Na$ 316.1308; Found 316.1305.

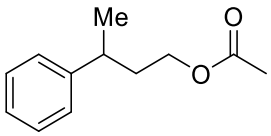

(2) 3-Phenyl-butylacetate: Prepared from 3-phenyl-propylacetate (0.3 mmol, 53.5 mg) according to the general procedure in section II using the following variations: added trifluoroacetic acid (0.5 equiv, 0.15 mmol, 11.5 µL) and used 0.6 M concentration (500 µL TFE). Purification: Reverse phase silica gel chromatography was used with a gradient of 70%→90% MeOH in H_2O, both w/ 0.1% TFA. The product was extracted with 1:1 ether:pentane.
Isolated yield: 59%, 34.2 mg of colorless oil.
Spectra available in the literature (CAS): No (46319-71-5)
^{1}H NMR ($CDCl_3$, 500 MHz): δ 7.32 – 7.27 (m, 2H), 7.22 – 7.16 (m, 3H), 4.05 – 3.89 (m, 2H), 2.84 (h, J = 7.1 Hz, 1H), 2.01 (s, 3H), 1.92 (q, J = 7.0 Hz, 2H), 1.28 (d, J = 6.9 Hz, 3H).
^{13}C NMR ($CDCl_3$, 126 MHz): δ 171.3, 146.2, 128.5, 126.9, 126.2, 63.1, 36.8, 36.7, 22.3, 21.0.
HRMS (ESI) m/z: $[M+NH_4]^+$ Calcd for $C_{12}H_{20}NO_2$ 210.1489; Found 210.1486.

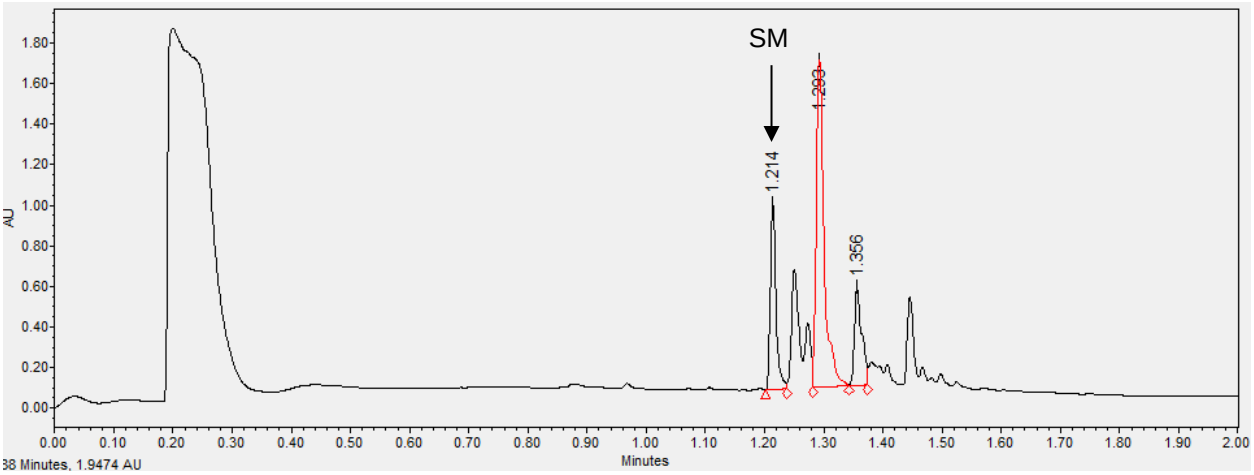

Figure 5D.21. 2 crude reaction LC-MS @ 210 nm (10%→95% MeCN/H_2O, w/ 0.1% HCOOH)

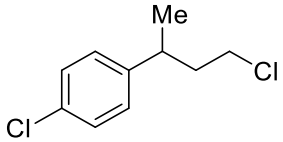

(3) 3-(4-Chlorophenyl)-butylchloride: Prepared from 3-(4-chlorophenyl)-propylchloride (0.3 mmol, 56.7 mg) according to the general procedure in section III using the following variations: added $B(OH)_3$ (0.5 equiv, 0.15 mmol, 9.3 mg) and used 0.6 M concentration (500 µL MeCN). Purification: Reverse phase silica gel chromatography was used with a gradient of 75%→90% MeOH in H_2O, both w/ 0.1% TFA. The product was extracted with 1:1 ether:pentane.
Isolated yield: 46%, 27.7 mg of light yellow oil.
Spectra available in the literature (CAS): No (1225886-34-9)
^{1}H NMR ($CDCl_3$, 500 MHz): δ 7.28 (d, J = 8.5 Hz, 2H), 7.14 (d, J = 8.4 Hz, 2H), 3.49 – 3.41 (m, 1H), 3.30 (ddd, J = 10.8, 8.0, 6.5 Hz, 1H), 2.98 (dp, J = 8.9, 6.9 Hz, 1H), 2.09 – 1.92 (m, 2H), 1.27 (d, J = 7.0 Hz, 3H).
^{13}C NMR ($CDCl_3$, 126 MHz): δ 144.0, 132.7, 128.7, 127.8, 43.0, 40.2, 36.4, 21.8.
HRMS (ESI) m/z: $[M-H]^+$ Calcd for $C_{10}H_{11}Cl_2$ 201.0232; Found 201.0230.

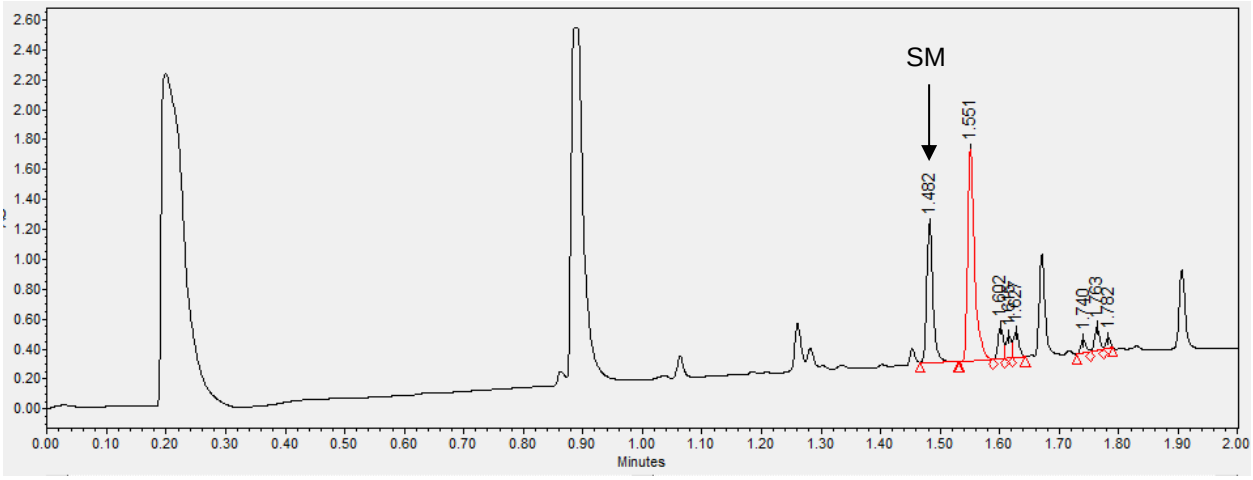

Figure 5D.22. 3 crude reaction LC-MS @ 223 nm (10%→95% MeCN/H_2O, w/ 0.1% HCOOH)

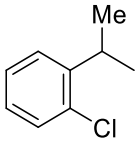

(4) 2-Isopropyl-chlorobenzene: Prepared from 2-ethyl-chlorobenzene (0.3 mmol, 42.1 mg) according to the general procedure in section II using the following variations: added trifluoroacetic acid (0.5 equiv, 0.15 mmol, 11.5 µL) and used 0.6 M concentration (500 µL TFE). Purification: Reverse phase silica gel chromatography was used with a gradient of 80%→85% MeOH in H_2O. The product was extracted with 1:1 ether:pentane. Note: The compound is volatile on the rotovap, so caution should be taken when removing pentane:Et_2O.
Isolated yield: 54%, 25.2 mg of colorless oil.
Spectra available in the literature (CAS): Yes (2077-13-6)[13]
^{1}H NMR ($CDCl_3$, 500 MHz): δ 7.34 (dd, J = 7.9, 1.4 Hz, 1H), 7.30 (dd, J = 7.8, 1.7 Hz, 1H), 7.23 (td, J = 7.5, 1.3 Hz, 1H), 7.15 – 7.08 (m, 1H), 3.42 (hept, J = 6.9 Hz, 1H), 1.25 (d, J = 6.9 Hz, 6H).
^{13}C NMR ($CDCl_3$, 126 MHz): δ 146.5, 133.9, 129.4, 126.9, 126.8, 126.6, 30.1, 22.6.
HRMS (ESI) m/z: $[M\text{-}CH_3]^+$ Calcd for C_8H_8Cl 139.0309; Found 139.0307.

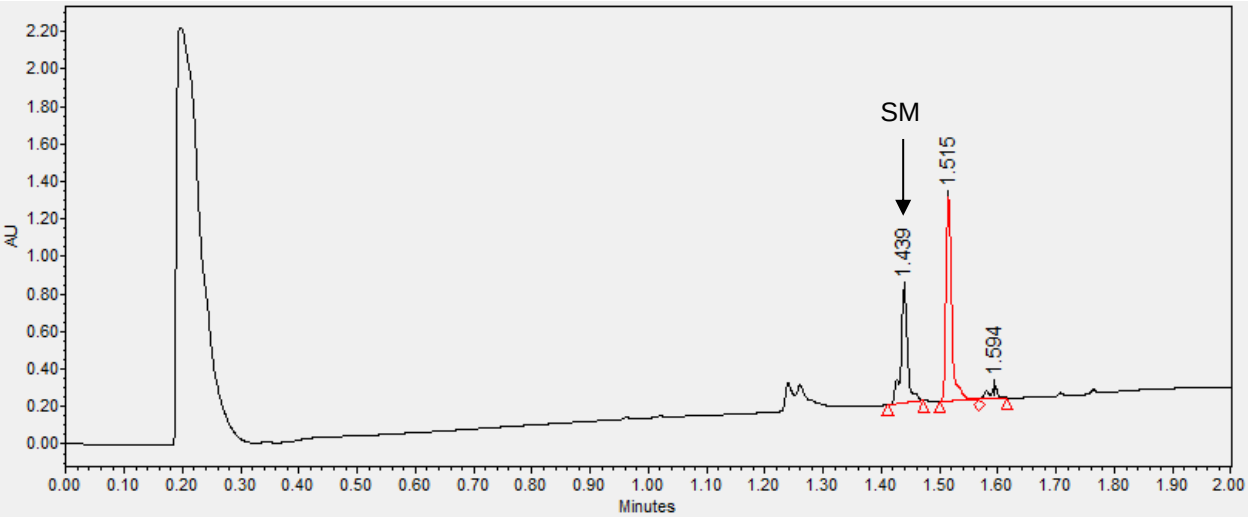

Figure 5D.23. 4 crude reaction LC-MS @ 221 nm (10%→95% MeCN/H_2O, w/ 0.1% HCOOH)

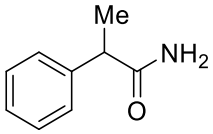

(5) 2-Phenylpropanamide: Prepared from 2-phenylacetamide (0.3 mmol, 40.6 mg) according to the general procedure in section III using the following variations: added $B(OH)_3$ (0.5 equiv, 0.15 mmol, 9.3 mg) and used 0.6 M concentration (500 µL MeCN).
Purification: Reverse phase silica gel chromatography was used with a gradient of 40%→45% MeOH in H_2O. The product was collected by removing MeOH and H_2O using a rotovap.
Isolated yield: 38%, 17.1 mg of white solid.
Spectra available in the literature (CAS): Yes (1125-70-8)[14]
^{1}H NMR ($CDCl_3$, 500 MHz): δ 7.48 – 7.15 (m, 5H), 5.60 (bs, 1H), 5.33 (bs, 1H), 3.60 (q, J = 7.2 Hz, 1H), 1.53 (d, J = 7.2 Hz, 3H).
^{13}C NMR ($CDCl_3$, 126 MHz): δ 176.7, 141.3, 129.0, 127.6, 127.4, 46.7, 18.3.
HRMS (ESI) m/z: $[M+H]^+$ Calcd for $C_9H_{12}NO$ 150.0913; Found 150.0913.

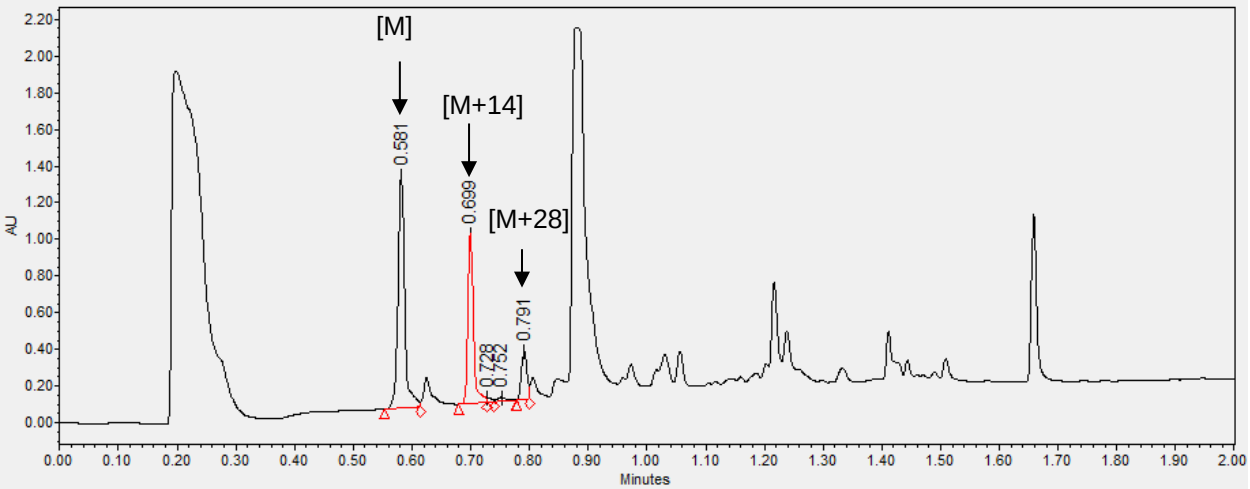

Figure 5D.24. 5 crude reaction LC-MS @ 217 nm (10%→95% MeCN/H_2O, w/ 0.1% HCOOH)

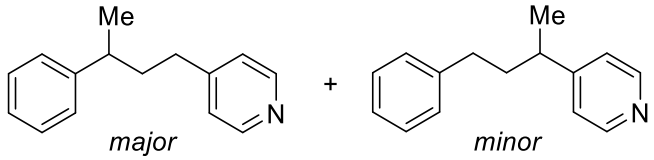

(6) 4-(3-Phenylbutyl)pyridine: Prepared from 4-(3-phenylpropyl)pyridine (0.3 mmol, 59.2 mg) according to the general procedure in section III using the following variation: added $MeB(OH)_2$ (0.5 equiv, 0.15 mmol, 9.0 mg).
Purification: Extracted away acetophenone and dicumyl peroxide with pentane. Concentrated and subjected to reverse phase silica gel chromatography with a gradient of 40%→45% MeOH in H_2O. The product was collected by removing MeOH and H_2O using a rotovap.
Purification yield: 52% as a 2.8:1 mixture of two regioisomers, 33.0 mg of light yellow oil.
Spectra available in the literature (CAS): Yes (19991-13-0)[15]
Enough unique NMR peaks were resolved to allow individual assignments for each isomer:
^{1}H NMR - *major isomer* - ($CDCl_3$, 500 MHz): δ 8.69 (d, J = 6.7 Hz, 2H), 7.54 (d, J = 6.7 Hz, 2H), 7.36 – 7.07 (m, 5H), 2.83 – 2.67 (m, 3H), 2.07 – 1.96 (m, 2H), 1.32 (d, J = 6.9 Hz, 3H).
^{13}C NMR - *major isomer* - ($CDCl_3$, 126 MHz): δ 162.4, 145.3, 141.6, 128.8, 126.9, 126.7, 126.4, 39.7, 38.1, 34.3, 22.5.
^{1}H NMR - *minor isomer* - ($CDCl_3$, 500 MHz): δ 8.75 (d, J = 6.6 Hz, 2H), 7.63 (d, J = 6.6 Hz, 2H), 7.35 – 7.06 (m, 5H), 2.97 (h, J = 7.2 Hz, 1H), 2.64 – 2.51 (m, 2H), 2.08 – 1.95 (m, 2H), 1.38 (d, J = 6.9 Hz, 3H).
^{13}C NMR - *minor isomer* - ($CDCl_3$, 126 MHz): δ 166.9, 142.0, 140.4, 128.6, 128.2, 126.4, 125.2, 39.7, 38.6, 33.4, 21.0.
HRMS (ESI) m/z: $[M+H]^+$ Calcd for $C_{15}H_{18}N$ 212.1434; Found 212.1431.

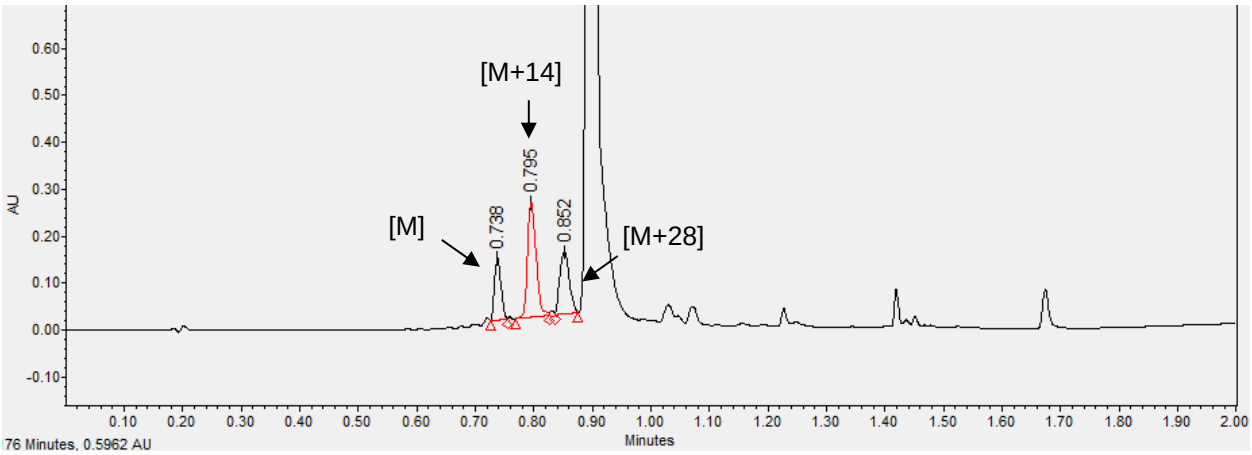

Figure 5D.25. 6 crude reaction LC-MS @ 259 nm (10%→95% MeCN/H_2O, w/ 0.1% HCOOH)

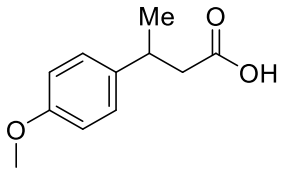

(7) 3-(4-Methoxyphenyl)-butanoic acid: Prepared from 3-(4-methoxyphenyl)-propanoic acid (0.3 mmol, 54.1 mg) according to the general procedure in section II using the following variation: added trifluoroacetic acid (0.5 equiv, 0.15 mmol, 11.5 µL).
Purification: Reverse phase silica gel chromatography was used with a gradient of 40%→70% MeOH in H_2O. The product was collected by removing MeOH and H_2O using a rotovap.
Isolated yield: 33%, 18.9 mg of white solid.
Spectra available in the literature (CAS): Yes (6555-30-2)[16]
^{1}H NMR ($CDCl_3$, 500 MHz): δ 7.15 (d, J = 8.6 Hz, 2H), 6.85 (d, J = 8.6 Hz, 2H), 3.79 (s, 3H), 3.23 (h, J = 7.1 Hz, 1H), 2.69 – 2.50 (m, 2H), 1.30 (d, J = 6.9 Hz, 3H).
^{13}C NMR ($CDCl_3$, 126 MHz): δ 178.4, 158.1, 137.5, 127.6, 113.9, 55.2, 42.9, 35.4, 22.0.
HRMS (ESI) m/z: $[M-H]^-$ Calcd for $C_{11}H_{13}O_3$ 193.0870; Found 193.0869.

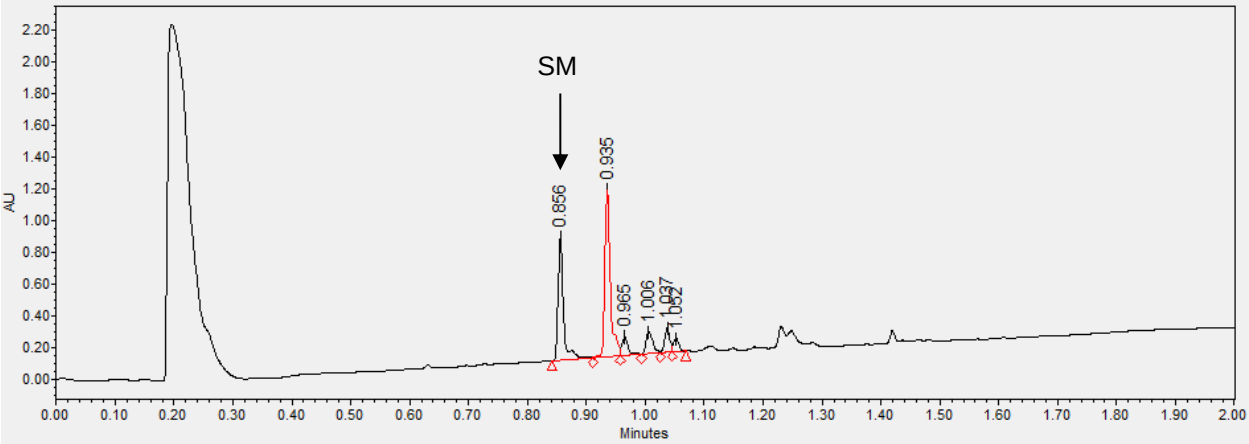

Figure 5D.26. 7 crude reaction LC-MS @ 224 nm (10%→95% MeCN/H_2O, w/ 0.1% HCOOH)

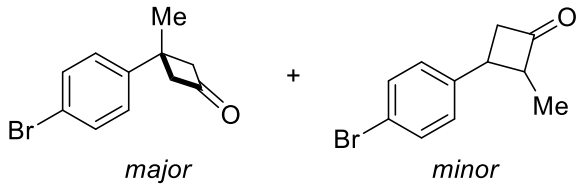

(8) 3-(4-Bromophenyl)-3-methylcyclobutan-1-one: Prepared from 3-(4-bromophenyl)cyclobutan-1-one (0.3 mmol, 67.5 mg) according to the general procedure in section II using the following variations: added trifluoroacetic acid (0.5 equiv, 0.15 mmol, 11.5 µL) and used 0.6 M concentration (500 µL TFE).

Purification: Reverse phase silica gel chromatography was used with a gradient of 60%→75% MeOH in H_2O, both w/ 0.1% TFA. The product was extracted with 1:1 ether:pentane.

Purification yield: 28% as a 6.7:1 mixture of two regioisomers, 20.4 mg of beige semisolid.

Spectra available in the literature (CAS): No (N/A)

Enough unique NMR peaks were resolved to allow individual assignments for each isomer:

^{1}H NMR - *major isomer* - ($CDCl_3$, 500 MHz): δ 7.49 (d, J = 8.5 Hz, 2H), 7.19 (d, J = 8.5 Hz, 2H), 3.51 – 3.37 (m, 2H), 3.17 – 3.05 (m, 2H), 1.59 (s, 3H).

^{13}C NMR - *major isomer* - ($CDCl_3$, 126 MHz): δ 205.8, 147.2, 131.7, 127.5, 120.2, 59.2, 33.7, 30.9.

^{1}H NMR - *minor isomer* - ($CDCl_3$, 500 MHz): δ 7.49 (d, J = 8.5 Hz, 2H), 7.19 (d, J = 8.5 Hz, 2H), 3.38 – 3.30 (m, 2H), 3.25 – 3.16 (m, 2H), 1.29 (d, J = 7.0 Hz, 3H).

^{13}C NMR - *minor isomer* - ($CDCl_3$, 126 MHz): δ 208.4, 141.9, 131.8, 128.2, 120.5, 62.8, 54.7, 51.5, 37.3, 14.1, 13.2.

HRMS (ESI) m/z: $[M+H]^+$ Calcd for $C_{11}H_{12}BrO$ 239.0066; Found 239.0063.

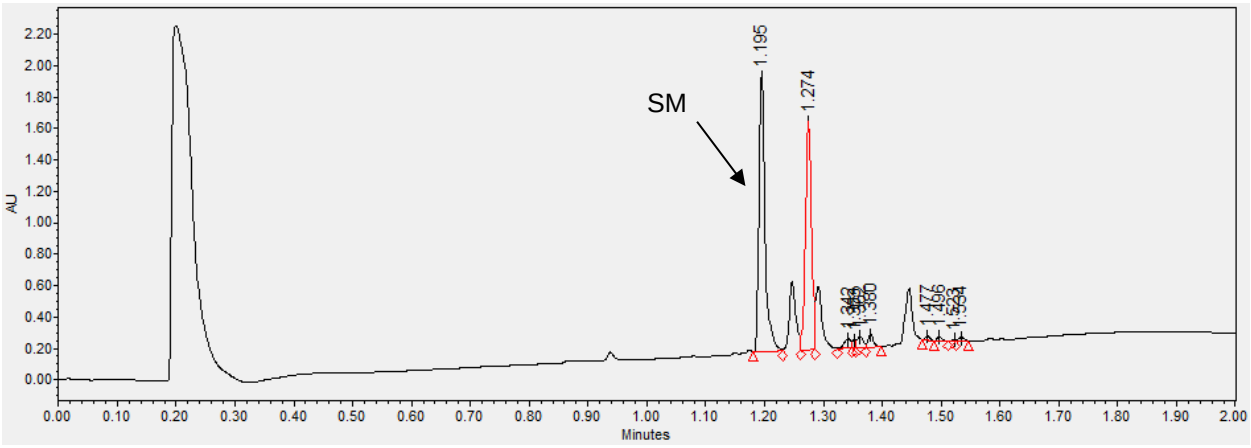

Figure 5D.27. 8 crude reaction LC-MS @ 224 nm (10%→95% MeCN/H_2O, w/ 0.1% HCOOH)

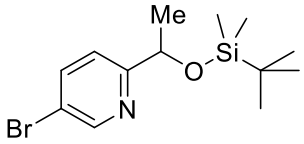

(9) 5-Bromo-2-(1-((tert-butyldimethylsilyl)oxy)ethyl)pyridine: Prepared from 5-bromo-2-(((tert-butyldimethylsilyl)oxy)methyl)pyridine (0.3 mmol, 90.7 mg) according to the general procedure in section II using the following variations: employed tripicolylamine as the ligand (0.04 equiv, 0.012 mmol, 3.5 mg) and used 0.15 M concentration (2000 µL TFE).
Purification: Reverse phase silica gel chromatography was used with a gradient of 80%→100% MeCN in H_2O. The product was collected by removing MeCN and H_2O using a rotovap.
Isolated yield: 58%, 55.0 mg of colorless oil.
Spectra available in the literature (CAS): No (N/A)
^{1}H NMR ($CDCl_3$, 500 MHz): δ 8.54 (d, J = 2.3 Hz, 1H), 7.80 (dd, J = 8.4, 2.4 Hz, 1H), 7.44 (d, J = 8.4 Hz, 1H), 4.90 (q, J = 6.5 Hz, 1H), 1.43 (d, J = 6.4 Hz, 3H), 0.91 (s, 9H), 0.08 (s, 3H), 0.01 (s, 3H).
^{13}C NMR ($CDCl_3$, 126 MHz): δ 164.5, 149.3, 139.2, 120.9, 118.4, 71.7, 25.8, 25.4, 18.2, -4.8, -5.0.
HRMS (ESI) m/z: $[M+H]^+$ Calcd for $C_{13}H_{23}BrNOSi$ 316.0727; Found 316.0726.

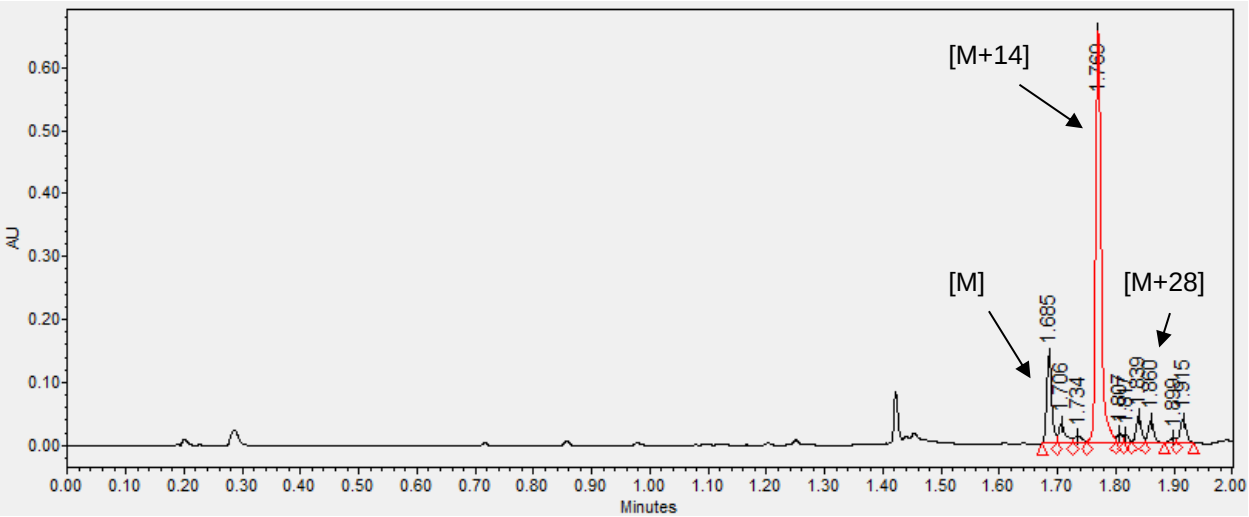

Figure 5D.28. 9 crude reaction LC-MS @ 272 nm (10%→95% MeCN/H_2O, w/ 0.1% HCOOH)

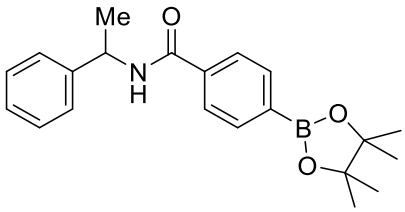

(10) 4-(α-Methyl-benzylaminocarbonyl)benzeneboronic acid pinacol ester: Prepared from 4-(benzylaminocarbonyl)benzeneboronic acid pinacol ester (0.3 mmol, 101.2 mg) according to the general procedure in section III using the following variation: added $B(OH)_3$ (0.5 equiv, 0.15 mmol, 9.3 mg) and used 1:1 MeCN:DMSO as the solvent.
Purification: Reverse phase silica gel chromatography was used with a gradient of 70%→72% MeOH in H_2O. The product was extracted with 1:1 ether:pentane.
Isolated yield: 60%, 62.9 mg of white solid.
Spectra available in the literature (CAS): No (N/A)
^{1}H NMR ($CDCl_3$, 500 MHz): δ 7.85 (d, J = 8.1 Hz, 2H), 7.75 (d, J = 8.2 Hz, 2H), 7.42 – 7.32 (m, 4H), 7.31 – 7.26 (m, 1H), 6.40 (d, J = 7.6 Hz, 1H), 5.34 (p, J = 7.1 Hz, 1H), 1.61 (d, J = 6.9 Hz, 3H), 1.35 (s, 12H).
^{13}C NMR ($CDCl_3$, 126 MHz): δ 166.5, 143.0, 136.7, 134.9, 128.7, 127.5, 126.3, 126.0, 84.1, 49.2, 30.3, 24.9, 21.7.
HRMS (ESI) m/z: $[M+H]^+$ Calcd for $C_{21}H_{27}BNO_3$ 352.2079; Found 352.2073.

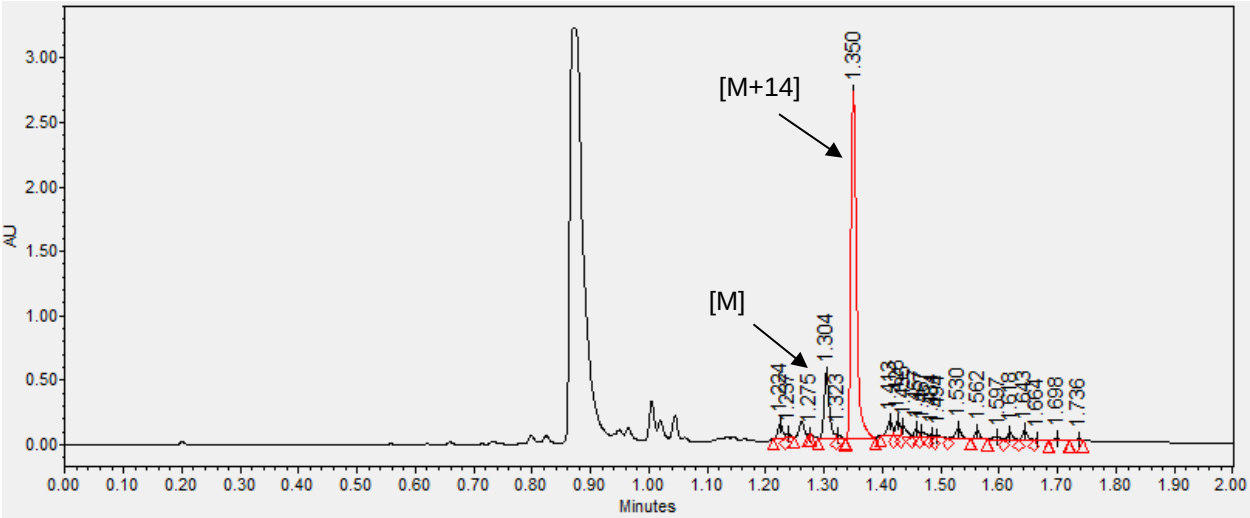

Figure 5D.29. 10 crude reaction LC-MS @ 255 nm (10%→95% MeCN/H_2O, w/ 0.1% HCOOH)

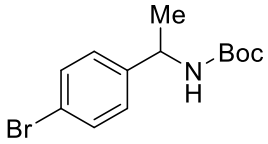

(11) *tert*-Butyl (1-(4-bromophenyl)ethyl)carbamate: Prepared from *tert*-butyl (4-bromobenzyl)
carbamate (0.3 mmol, 85.9 mg) according to the general procedure in section II using the following variation: employed tripicolylamine as the ligand (0.04 equiv, 0.012 mmol, 3.5 mg). Purification: Reverse phase silica gel chromatography was used with a gradient of 60%→75% MeOH in H_2O, both w/ 0.1% TFA. The product was extracted with 1:1 ether:pentane.
Isolated yield: 61%, 54.8 mg of white solid.
Spectra available in the literature (CAS): Yes (850363-42-7)[17]
^{1}H NMR ($CDCl_3$, 500 MHz): δ 7.44 (d, J = 8.4 Hz, 2H), 7.17 (d, J = 8.0 Hz, 2H), 4.81 – 4.61 (m, 2H), 1.44 – 1.37 (m, 12H).
^{13}C NMR ($CDCl_3$, 126 MHz): δ 155.0, 143.3, 131.6, 127.6, 120.8, 79.6, 49.7, 28.3, 22.6.
HRMS (ESI) m/z: $[M+H]^+$ Calcd for $C_{13}H_{19}BrNO_2$ 300.0594; Found 300.0592.

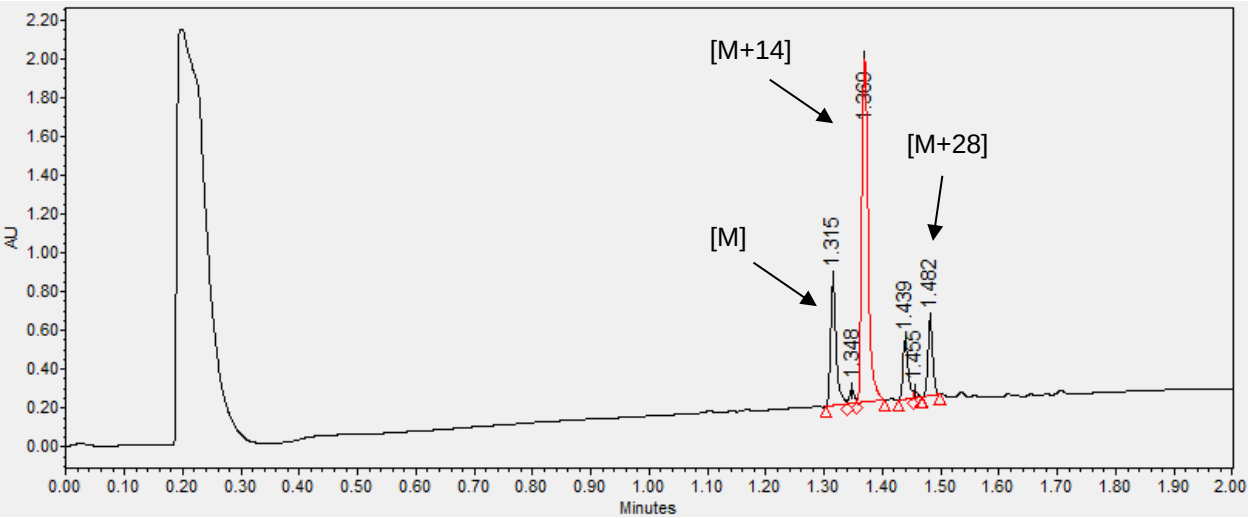

Figure 5D.30. 11 crude reaction LC-MS @ 219 nm (10%→95% MeCN/H_2O, w/ 0.1% HCOOH)

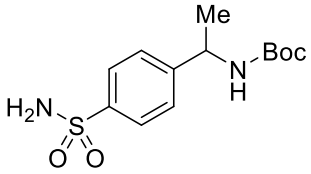

(12) *tert*-Butyl (1-(4-sulfamoylphenyl)ethyl)carbamate: Prepared from *tert*-butyl (4-sulfamoylbenzyl)carbamate (0.3 mmol, 85.9 mg) according to the general procedure in section II using the following variations: employed tripicolylamine as the ligand (0.04 equiv, 0.012 mmol, 3.5 mg) and added $MeB(OH)_2$ (0.5 equiv, 0.15 mmol, 9.0 mg).

Purification: Reverse phase silica gel chromatography was used with a gradient of 45%→57% MeOH in H_2O. The product was collected by removing MeOH and H_2O using a rotovap.

Isolated yield: 50%, 45.0 mg of white solid.

Spectra available in the literature (CAS): No (1484603-81-7)

^{1}H NMR (acetone-d6, 500 MHz): δ 7.84 (d, J = 8.5 Hz, 2H), 7.53 (d, J = 8.3 Hz, 2H), 6.56 (bs, 1H), 6.51 (bs, 2H), 4.87 – 4.72 (m, 1H), 1.44 (d, J = 7.1 Hz, 3H), 1.38 (bs, 9H).

^{13}C NMR (DMSO-d6, 126 MHz): δ 154.8, 149.6, 142.3, 126.2, 125.7, 77.9, 49.5, 28.2, 22.6.

HRMS (ESI) m/z: $[M+Na]^+$ Calcd for $C_{13}H_{20}N_2O_4SNa$ 323.1036; Found 323.1030.

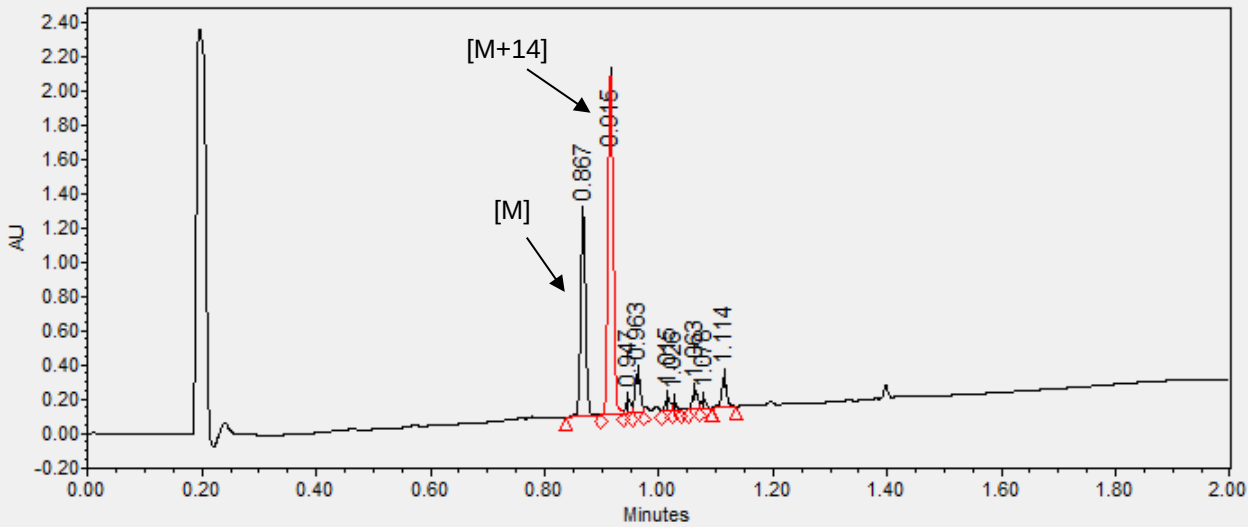

Figure 5D.31. 12 crude reaction LC-MS @ 230 nm (10%→95% MeCN/H_2O, w/ 0.1% HCOOH)

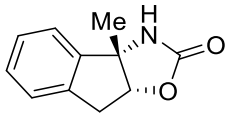

(13) (3a*S*,8a*R*)-3-Methyl-3a,8,8a-trihydro-2*H*-indeno[1,2-*d*]oxazol-2-one: Prepared from (3a*S*,8a*R*)-3,3a,8,8a-Tetrahydro-2*H*-indeno[1,2-*d*]oxazol-2-one (0.3 mmol, 52.6 mg) according to the general procedure in section III using the following variations: employed tripicolylamine as the ligand (0.04 equiv, 0.012 mmol, 3.5 mg), added $MeB(OH)_2$ (0.5 equiv, 0.15 mmol, 9.0 mg), and used 0.6 M concentration (500 µL MeCN).
Purification: Reverse phase silica gel chromatography was used with a gradient of 40%→45% MeOH in H_2O. The product was collected by removing MeOH and H_2O using a rotovap.
Isolated yield: 46%, 26.3 mg of white solid.
Spectra available in the literature (CAS): No (N/A)
^{1}H NMR (methanol-d4, 400 MHz): δ 7.37 – 7.25 (m, 4H), 4.98 (dd, J = 6.3, 1.3 Hz, 1H), 3.44 (dd, J = 18.0, 6.2 Hz, 1H), 3.18 (dd, J = 17.9, 1.3 Hz, 1H), 1.61 (s, 3H).
^{1}H NMR (methanol-d4, 126 MHz): δ 158.8, 143.9, 137.9, 127.9, 126.8, 124.4, 122.0, 86.3, 67.8, 36.2, 22.6.
HRMS (ESI) m/z: $[M+H]^+$ Calcd for $C_{11}H_{12}O_2N$ 190.0863; Found 190.0863.

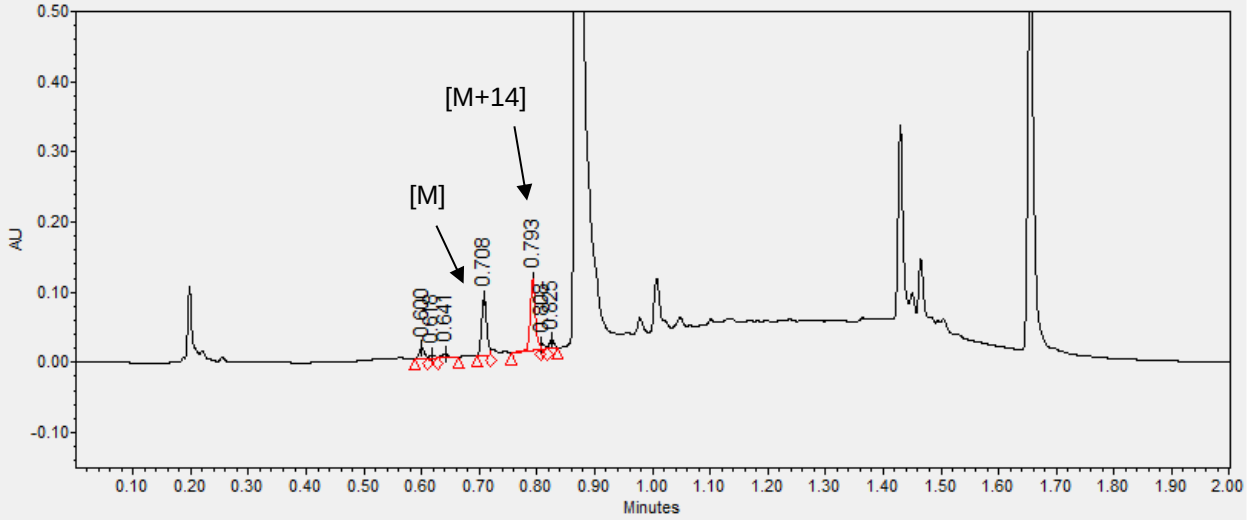

Figure 5D.32. 13 crude reaction LC-MS @ 266 nm (10%→95% MeCN/H_2O, w/ 0.1% HCOOH)

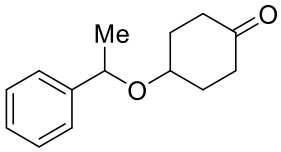

(14) 4-(1-Phenylethoxy)cyclohexan-1-one: Prepared from 4-(benzyloxy)cyclohexan-1-one (0.3 mmol, 61.3 mg) according to the general procedure in section II using the following variation: employed tripicolylamine as the ligand (0.04 equiv, 0.012 mmol, 3.5 mg) and used 0.15 M concentration (2000 µL TFE).
Purification: Reverse phase silica gel chromatography was used with a gradient of 60%→70% MeOH in H_2O. The product was extracted with 1:1 ether:pentane. Note: The compound is volatile on the rotovap, so caution should be taken when removing pentane:Et_2O.
Isolated yield: 42%, 27.4 mg of colorless oil.
Spectra available in the literature (CAS): No (1564713-98-9)
^{1}H NMR ($CDCl_3$, 500 MHz): δ 7.39 – 7.33 (m, 4H), 7.32 – 7.26 (m, 1H), 4.60 (q, J = 6.5 Hz, 1H), 3.65 (tt, J = 6.0, 3.0 Hz, 1H), 2.71 – 2.50 (m, 2H), 2.30 – 2.16 (m, 2H), 2.10 (dddd, J = 13.9, 5.9, 4.6, 2.1 Hz, 1H), 2.01 – 1.87 (m, 2H), 1.87 – 1.77 (m, 1H), 1.46 (d, J = 6.4 Hz, 3H).
^{13}C NMR ($CDCl_3$, 126 MHz): δ 211.5, 144.2, 128.5, 127.5, 126.0, 75.1, 70.0, 37.5, 37.2, 31.9, 29.8, 24.7.
HRMS (ESI) m/z: $[M+H]^+$ Calcd for $C_{14}H_{19}O_2$ 219.1380; Found 219.1380.

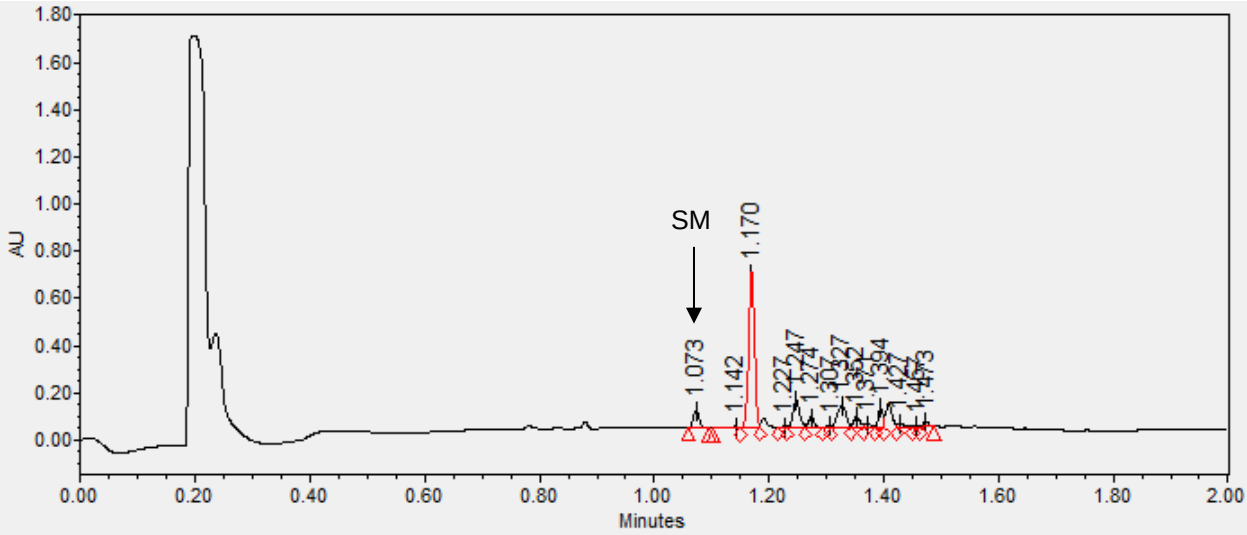

Figure 5D.33. 14 crude reaction LC-MS @ 210 nm (10%→95% MeCN/H_2O, w/ 0.1% HCOOH)

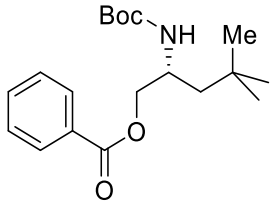

(15) (*R*)-2-((*tert*-Butoxycarbonyl)amino)-4,4-dimethylpentyl benzoate: Prepared from (*R*)-2-((*tert*-butoxycarbonyl)amino)-4-methylpentyl benzoate (0.3 mmol, 96.4 mg) according to the general procedure in section II using the following variations: employed tripicolylamine as the ligand (0.04 equiv, 0.012 mmol, 3.5 mg) and used 0.6 M concentration (500 µL TFE).
Purification: Reverse phase silica gel chromatography was used with a gradient of 75%→80% MeOH in H_2O. The product was collected by removing MeOH and H_2O using a rotovap.
Isolated yield: 53%, 53.3 mg of white solid.
Spectra available in the literature (CAS): No (N/A)
^{1}H NMR ($CDCl_3$, 500 MHz): δ 8.05 (d, J = 8.4 Hz, 2H), 7.56 (t, J = 7.4 Hz, 1H), 7.44 (t, J = 7.7 Hz, 2H), 4.45 (d, J = 9.3 Hz, 1H), 4.21 (d, J = 5.6 Hz, 2H), 4.18 – 4.08 (m, 1H), 1.51 – 1.45 (m, 1H), 1.40 (s, 9H), 1.37 – 1.31 (m, 1H), 0.98 (s, 9H).
^{13}C NMR ($CDCl_3$, 126 MHz): δ 166.5, 155.0, 133.0, 130.0, 129.7, 128.3, 79.4, 68.4, 46.9, 45.7, 30.4, 29.7, 28.3.
HRMS (ESI) m/z: $[M+Na]^+$ Calcd for $C_{19}H_{29}NO_4Na$ 358.1989; Found 358.1984.

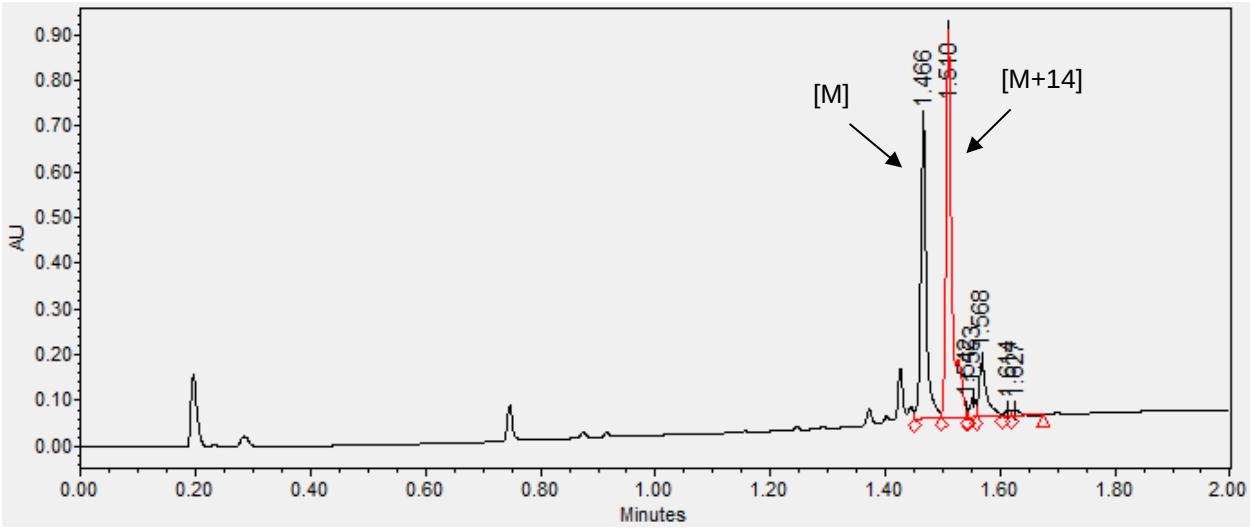

Figure 5D.34. 15 crude reaction LC-MS @ 210 nm (10%→95% MeCN/H_2O, w/ 0.1% HCOOH)

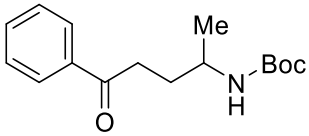

(16) *tert*-Butyl (5-oxo-5-phenylpentan-2-yl)carbamate: Prepared from *tert*-butyl (4-oxo-4-phenylbutyl)carbamate (0.3 mmol, 79.0 mg) according to the general procedure in section II using the following variations: employed tripicolylamine as the ligand (0.04 equiv, 0.012 mmol, 3.5 mg), added $MeB(OH)_2$ (0.5 equiv, 0.15 mmol, 9.0 mg), and used 0.6 M concentration (500 µL TFE).
Purification: Reverse phase silica gel chromatography was used with a gradient of 65%→75% MeOH in H_2O, both w/ 0.1% TFA. The product was extracted with 1:1 ether:pentane.
Isolated yield: 40%, 33.5 mg of white solid. This product decomposes to a red solid over time at rt.
Spectra available in the literature (CAS): Yes (2029483-34-7)[18]
^{1}H NMR ($CDCl_3$, 500 MHz): δ 7.95 (d, J = 7.0 Hz, 2H), 7.55 (t, J = 7.4 Hz, 1H), 7.45 (t, J = 7.7 Hz, 2H), 4.39 (bs, 1H), 3.74 (bs, 1H), 3.04 (t, J = 7.4 Hz, 2H), 1.96 – 1.74 (m, 2H), 1.39 (s, 9H), 1.18 (d, J = 6.6 Hz, 3H).
^{13}C NMR ($CDCl_3$, 126 MHz): δ 200.0, 155.5, 136.9, 133.0, 128.5, 128.0, 79.1, 46.5, 35.5, 31.4, 28.3, 21.7.
HRMS (ESI) m/z: $[M+H]^+$ Calcd for $C_{16}H_{24}NO_3$ 278.1751; Found 278.1745.

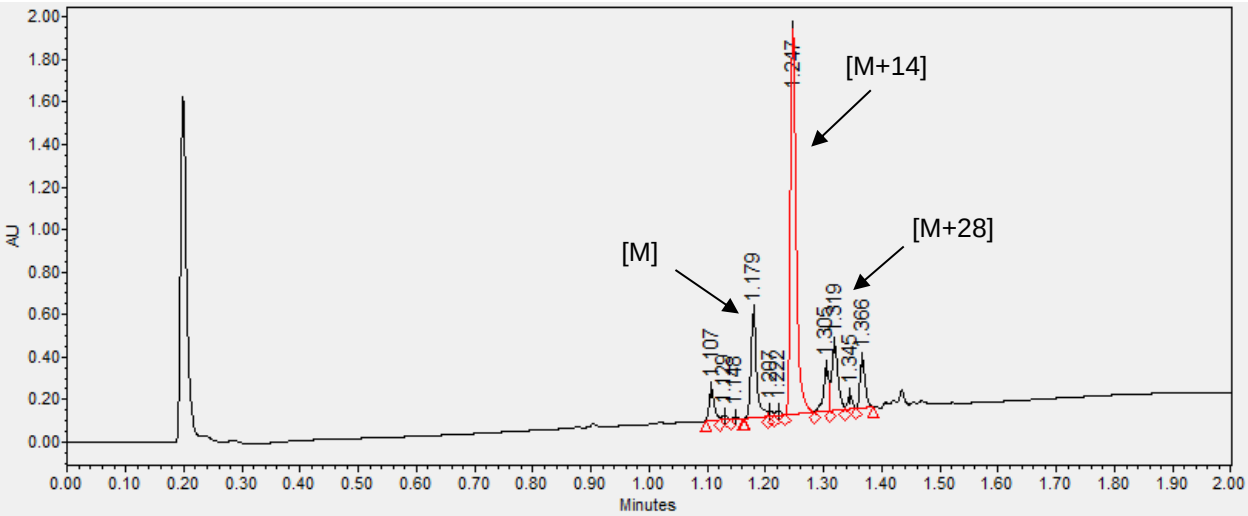

Figure 5D.35. 16 crude reaction LC-MS @ 235 nm (10%→95% MeCN/H_2O, w/ 0.1% HCOOH)

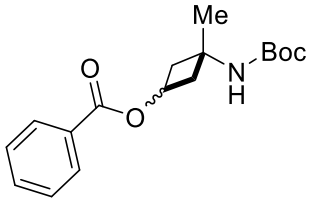

(17) 3-((*tert*-Butoxycarbonyl)amino)-3-methylcyclobutyl benzoate: Prepared from 3-((*tert*-butoxycarbonyl)amino)cyclobutyl benzoate (0.3 mmol, 87.4 mg) according to the general procedure in section II using the following variations: employed tripicolylamine as the ligand (0.04 equiv, 0.012 mmol, 3.5 mg) and used 0.6 M concentration (500 µL TFE).
Purification: Reverse phase silica gel chromatography was used with a gradient of 70%→72% MeOH in H_2O. The product was extracted with 1:1 ether:pentane.
Isolated yield: 44% as a 1.3:1 mixture of diastereomers, 40.2 mg of white solid.
Spectra available in the literature (CAS): No (N/A)
^{1}H NMR ($CDCl_3$, 500 MHz): δ 8.04 (d, J = 7.8 Hz, 2H), 7.55 (td, J = 7.5, 2.8 Hz, 1H), 7.48 – 7.39 (m, 2H), 5.33 (p, J = 6.7 Hz, 0.43H), 5.10 (p, J = 7.3 Hz, 0.55H), 4.73 (bs, 0.55H), 4.67 (bs, 0.43H), 2.93 – 2.80 (m, 0.84H), 2.74 – 2.56 (m, 1.19H), 2.58 – 2.49 (m, 1.15H), 2.28 – 2.12 (m, 0.87H), 1.52 (s, 1.30H), 1.50 – 1.40 (m, 10.71H).
^{13}C NMR ($CDCl_3$, 126 MHz): δ 166.1, 166.1, 154.5, 154.2, 133.0, 133.0, 130.2, 130.0, 129.6, 129.5, 128.3, 128.3, 79.3, 65.9, 64.4, 54.8, 50.0, 46.9, 42.5, 41.7, 28.4, 28.2, 27.9, 26.9.
HRMS (ESI) m/z: $[M+Na]^+$ Calcd for $C_{17}H_{23}NO_4Na$ 328.1519; Found 328.1515.

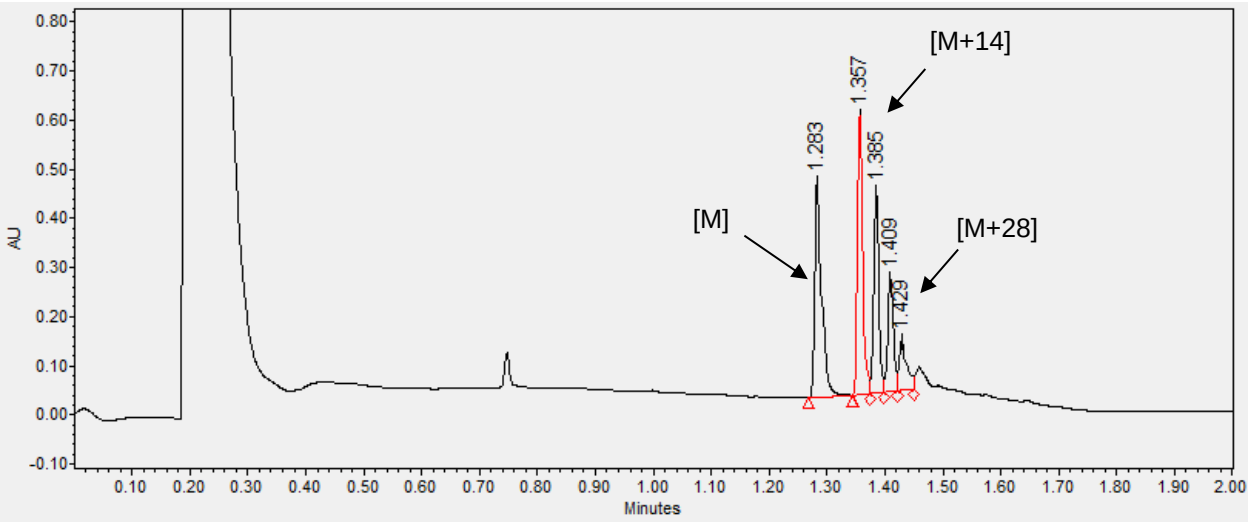

Figure 5D.36. 17 crude reaction LC-MS @ 210 nm (10%→95% MeCN/H_2O, w/ 0.1% HCOOH)

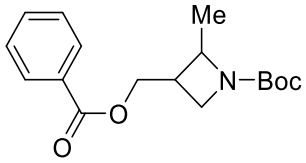

(18) *tert*-Butyl 3-((benzoyloxy)methyl)-2-methylazetidine-1-carboxylate: Prepared from *tert*-butyl 3-((benzoyloxy)methyl)azetidine-1-carboxylate (0.3 mmol, 87.4 mg) according to the general procedure in section II using the following variations: employed tripicolylamine as the ligand (0.04 equiv, 0.012 mmol, 3.5 mg) and used 0.15 M concentration (2000 µL TFE).
Purification: Reverse phase silica gel chromatography was used with a gradient of 68%→75% MeOH in H_2O. The product was extracted with 1:1 ether:pentane.
Isolated yield: 31% as a 3.8:1 mixture of diastereomers, 28.0 mg of colorless oil.
Spectra available in the literature (CAS): No (N/A)
^{1}H NMR ($CDCl_3$, 500 MHz): δ 8.02 (d, J = 6.8 Hz, 2H), 7.56 (t, J = 7.4 Hz, 1H), 7.44 (t, J = 7.7 Hz, 2H), 4.59 – 4.35 (m, 2.27H), 4.21 – 4.10 (m, 0.80H), 4.04 – 3.94 (m, 1H), 3.70 (dd, J = 8.7, 6.1 Hz, 0.80H), 3.64 (dd, J = 8.8, 5.0 Hz, 0.24H), 3.02 – 2.90 (m, 0.21H), 2.53 (dp, J = 8.4, 6.1 Hz, 0.80H), 1.46 – 1.42 (m, 12H).
^{13}C NMR ($CDCl_3$, 126 MHz): δ 166.4, 156.5, 133.2, 129.9, 129.6, 128.5, 79.4, 65.4, 63.6, 60.9, 47.9, 36.3, 31.1, 28.4, 20.9, 15.6.
HRMS (ESI) m/z: $[M+Na]^+$ Calcd for $C_{17}H_{23}NO_4Na$ 328.1519; Found 328.1515.

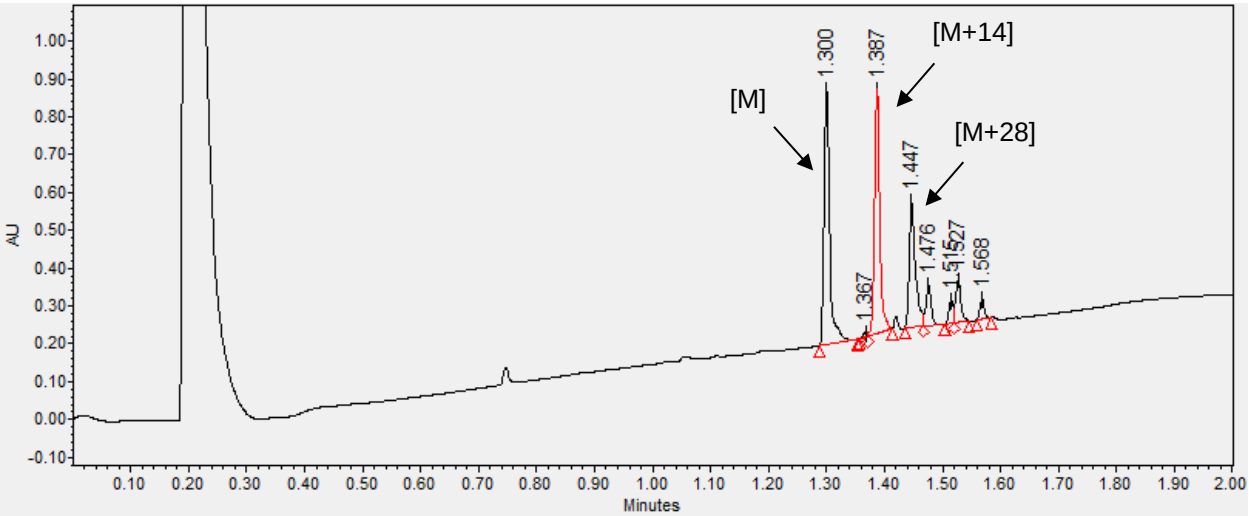

Figure 5D.37. 18 crude reaction LC-MS @ 224 nm (10%→95% MeCN/H_2O, w/ 0.1% HCOOH)

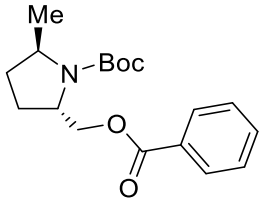

(19) *tert*-Butyl (2*S*)-2-((benzoyloxy)methyl)-5-methylpyrrolidine-1-carboxylate: Prepared from *tert*-butyl (*S*)-2-((benzoyloxy)methyl)pyrrolidine-1-carboxylate (0.3 mmol, 91.6 mg) according to the general procedure in section II using the following variations: employed tripicolylamine as the ligand (0.04 equiv, 0.012 mmol, 3.5 mg), added $MeB(OH)_2$ (0.5 equiv, 0.15 mmol, 9.0 mg), and used 0.15 M concentration (2000 µL TFE).
Purification: Reverse phase silica gel chromatography was used with a gradient of 70%→85% MeOH in H_2O, both w/ 0.1% TFA. The product was extracted with 1:1 ether:pentane.
Isolated yield: 44% as a 5.4:1 mixture of diastereomers, 42.1 mg of colorless oil.
Spectra available in the literature (CAS): No (N/A)
^{1}H NMR ($CDCl_3$, 500 MHz): δ 8.11 – 8.00 (m, 2H), 7.62 – 7.52 (m, 1H), 7.49 – 7.39 (m, 2H), 4.53 – 3.79 (m, 4H), 2.26 – 1.77 (m, 3H), 1.70 – 1.52 (m, 1H), 1.52 – 1.38 (m, 9H), 1.31 – 1.10 (m, 3H).
^{13}C NMR ($CDCl_3$, 126 MHz): δ 166.5, 166.3, 154.1, 153.6, 133.1, 132.9, 130.3, 130.1, 129.7, 129.6, 128.4, 128.3, 79.7, 79.4, 64.8, 64.2, 57.1, 55.9, 53.5, 53.4, 30.8, 29.8, 29.7, 28.5, 28.5, 26.5, 25.5, 20.4, 19.4.
HRMS (ESI) m/z: $[M+H]^+$ Calcd for $C_{18}H_{26}NO_4$ 320.1856; Found 320.1852.

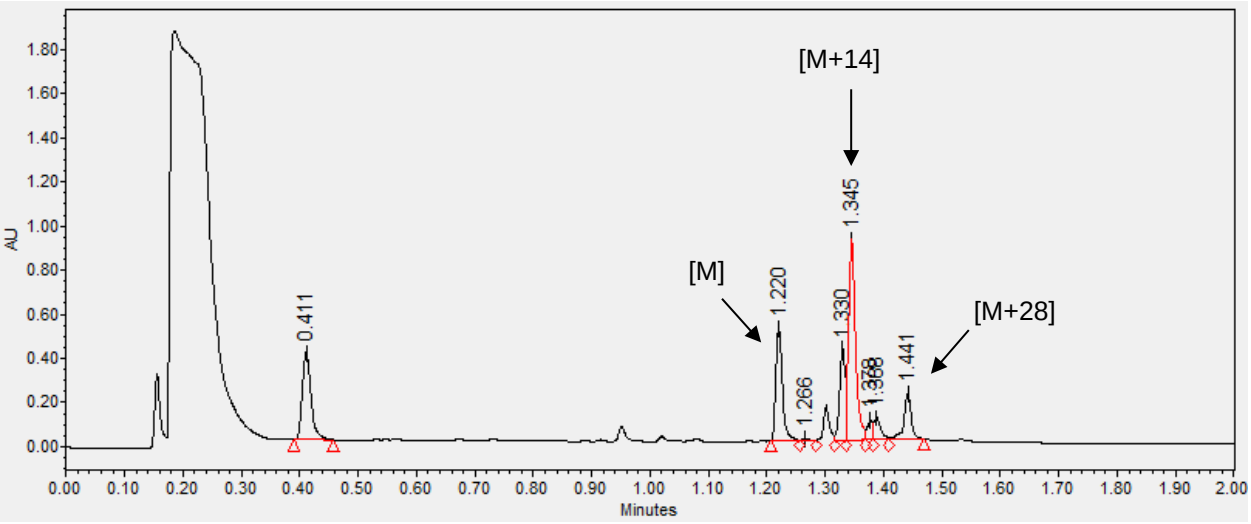

Figure 5D.38. 19 crude reaction LC-MS @210 nm (10%→95% MeCN/H_2O, w/ 0.1% HCOOH)

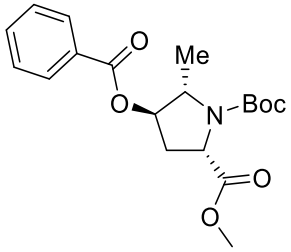

(20) 1-*tert*-Butyl 2-methyl-(2*S*,4*R*,5*S*)-4-(benzoyloxy)-5-methylpyrrolidine-1,2-dicarboxylate: Prepared from 1-*tert*-butyl 2-methyl (2*S*,4*R*)-4-(benzoyloxy)pyrrolidine-1,2-dicarboxylate (0.3 mmol, 104.8 mg) according to the general procedure in section III using the following variations: employed tripicolylamine as the ligand (0.04 equiv, 0.012 mmol, 3.5 mg), added $MeB(OH)_2$ (0.5 equiv, 0.15 mmol, 9.0 mg), and used 0.15 M concentration (2000 µL MeCN).

Purification: Reverse phase silica gel chromatography was used with a gradient of 70%→75% MeOH in H_2O, both w/ 0.1% TFA. The product was extracted with 1:1 ether:pentane.

Isolated yield: 42% as an 8.4:1 mixture of diastereomers, 45.6 mg of colorless semisolid.

Spectra available in the literature (CAS): No (N/A)

^{1}H NMR ($CDCl_3$, 500 MHz): δ 8.00 (d, J = 7.7 Hz, 2H), 7.58 (t, J = 7.5 Hz, 1H), 7.45 (t, J = 7.7 Hz, 2H), 5.53 (s, 0.1H), 5.28 – 5.10 (m, 0.85H), 5.05 (s, 0.11H), 4.53 (t, J = 8.6 Hz, 0.38H), 4.43 (d, J = 9.3 Hz, 0.49H), 4.20 (q, J = 6.8 Hz, 0.52H), 4.05 (q, J = 6.9 Hz, 0.39H), 3.80 – 3.75 (m, 2.67H), 3.67 – 3.61 (m, 0.35H), 2.62 – 2.43 (m, 1H), 2.41 – 2.23 (m, 1H), 1.51 – 1.41 (m, 9H), 1.41 – 1.27 (m, 3H).

^{13}C NMR ($CDCl_3$, 126 MHz): δ 173.4, 173.1, 165.9, 165.9, 154.2, 153.3, 133.4, 133.3, 129.7, 129.7, 128.5, 128.4, 128.3, 80.4, 79.1, 78.3, 61.8, 61.7, 60.4, 60.2, 58.7, 58.4, 52.4, 52.2, 34.6, 33.7, 30.9, 28.4, 28.3, 18.4, 18.0.

HRMS (ESI) m/z: $[M+Na]^+$ Calcd for $C_{19}H_{25}NO_6Na$ 386.1574; Found 386.1569.

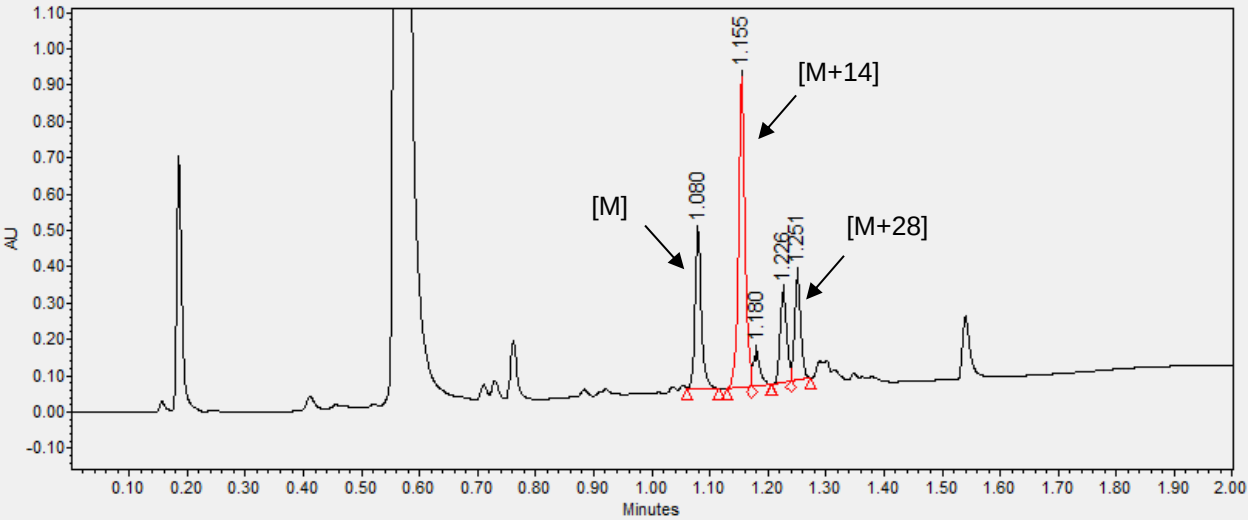

Figure 5D.39. 20 crude reaction LC-MS @ 239 nm (10%→95% MeCN/H_2O, w/ 0.1% HCOOH)

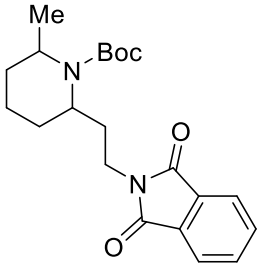

(21) *tert*-Butyl 2-(2-(phthalimidyl)ethyl)-6-methylpiperidine-1-carboxylate: Prepared from *tert*-butyl 2-(2-(phthalimidyl)ethyl)piperidine-1-carboxylate (0.3 mmol, 107.5 mg) according to the general procedure in section III using the following variations: employed tripicolylamine as the ligand (0.04 equiv, 0.012 mmol, 3.5 mg), added $MeB(OH)_2$ (0.5 equiv, 0.15 mmol, 9.0 mg), and used 0.15 M concentration (2000 µL MeCN).
Purification: Reverse phase silica gel chromatography was used with a gradient of 75%→85% MeOH in H_2O, both w/ 0.1% TFA. The product was extracted with 1:1 ether:pentane.
Isolated yield: 55% as a 4.1:1 mixture of diastereomers, 61.4 mg of colorless semisolid.
Spectra available in the literature (CAS): No (N/A)
^{1}H NMR ($CDCl_3$, 500 MHz): δ 7.82 (dd, J = 5.4, 3.0 Hz, 2H), 7.69 (dd, J = 5.5, 3.0 Hz, 2H), 4.33 (h, J = 7.1, 6.4 Hz, 0.84H), 4.23 – 4.13 (m, 0.82H), 3.95 (dt, J = 6.8, 4.3 Hz, 0.20H), 3.92 – 3.86 (m, 0.19H), 3.68 (dddt, J = 20.5, 13.6, 9.5, 6.3 Hz, 2H), 2.09 – 1.55 (m, 8H), 1.42 (s, 9H), 1.24 (d, J = 7.1 Hz, 0.63H), 1.21 (d, J = 7.1 Hz, 2.4H).
^{13}C NMR ($CDCl_3$, 126 MHz): δ 168.3, 168.3, 155.2, 155.1, 133.8, 132.2, 123.1, 79.3, 79.2, 49.4, 47.9, 47.2, 45.5, 36.2, 35.9, 34.1, 33.3, 30.1, 28.4, 28.4, 27.9, 26.9, 24.1, 20.6, 20.4, 14.1, 14.1.
HRMS (ESI) m/z: $[M+Na]^+$ Calcd for $C_{21}H_{28}N_2O_4Na$ 395.1935; Found 395.1941.

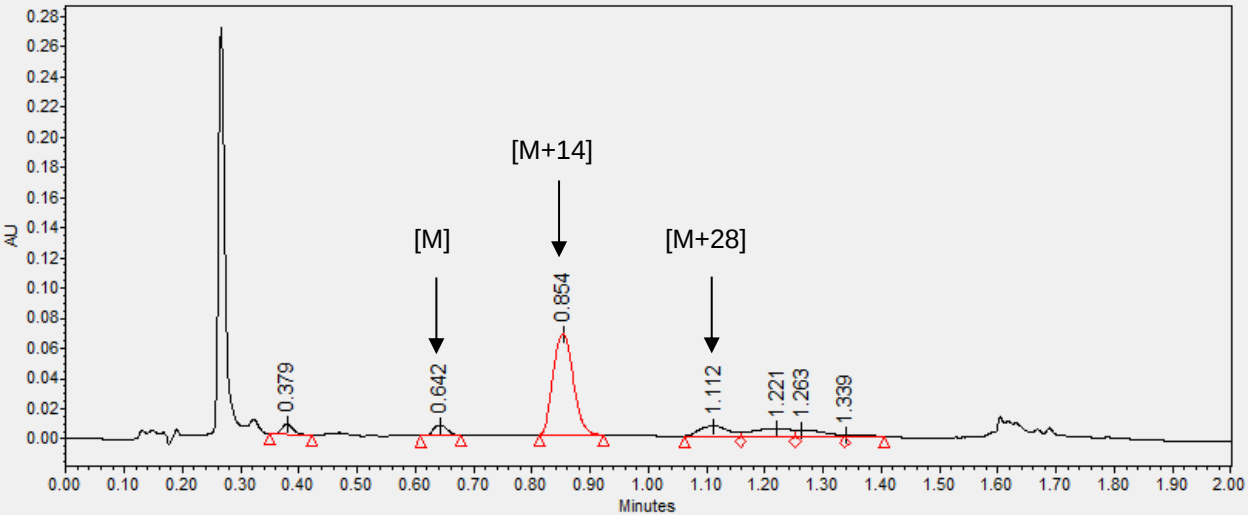

Figure 5D.40. 21 crude reaction LC-MS @ 299 nm (62%→58% MeCN/H_2O, w/ 0.1% HCOOH)

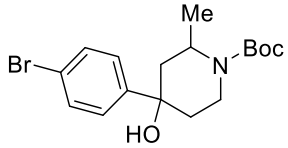

(22) *tert*-Butyl 4-(4-bromophenyl)-4-hydroxy-2-methylpiperidine-1-carboxylate: Prepared from *tert*-butyl 4-(4-bromophenyl)-4-hydroxypiperidine-1-carboxylate (0.3 mmol, 106.9 mg) according to the general procedure in section II using the following variations: employed TPA as the ligand (0.04 equiv, 0.012 mmol, 3.5 mg) and used 0.15 M concentration (2000 µL TFE). Purification: Preparative LC with a C18 column was used with a gradient of 50%→75% MeCN in H_2O w/ 0.1% TFA added. The product was collected by removing solvent in vacuo.
Isolated yield: monomethyl - 28% in a 1.6:1 ratio of isolated diastereomers, 30.5 mg total, and dimethyl - 24% as three diastereomers (one isolated), 27.1 mg total, all as off-white solids.
Spectra available in the literature (CAS): No

The following were all collected from the reaction described above:

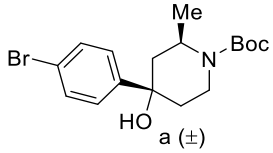

(a) 11.8 mg
^{1}H NMR ($CDCl_3$, 500 MHz): δ 7.48 (d, J = 8.4 Hz, 2H), 7.35 (d, J = 8.6 Hz, 2H), 4.20 (h, J = 6.7 Hz, 1H), 3.98 – 3.86 (m, 1H), 3.33 – 3.21 (m, 1H), 2.16 (dt, J = 14.3, 4.1 Hz, 1H), 2.07 – 1.86 (m, 3H), 1.48 (s, 9H), 1.07 (d, J = 6.7 Hz, 3H).
^{13}C NMR ($CDCl_3$, 126 MHz): δ 155.1, 146.4, 131.5, 126.7, 121.2, 79.6, 71.9, 46.8, 43.3, 38.3, 38.0, 28.5, 19.1.
HRMS (ESI) m/z: $[M+Na]^+$ Calcd for $C_{17}H_{24}BrNO_3Na$ 392.0832; Found 392.0826.

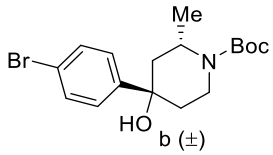

(b) 18.7 mg
^{1}H NMR ($CDCl_3$, 500 MHz): δ 7.47 (d, J = 8.6 Hz, 2H), 7.34 (d, J = 8.4 Hz, 2H), 4.44 (bs, 1H), 4.02 (bs, 1H), 3.36 (t, J = 13.4 Hz, 1H), 2.06 (dd, J = 14.5, 6.7 Hz, 1H), 2.01 – 1.93 (m, 1H), 1.77 – 1.62 (m, 2H), 1.48 (s, 9H), 1.40 (d, J = 7.1 Hz, 3H).
^{13}C NMR ($CDCl_3$, 126 MHz): δ 154.8, 147.8, 131.4, 126.3, 121.1, 79.5, 72.5, 45.9, 42.0, 37.9, 34.4, 28.5, 18.5.
HRMS (ESI) m/z: $[M+Na]^+$ Calcd for $C_{17}H_{24}BrNO_3Na$ 392.0832; Found 392.0825.

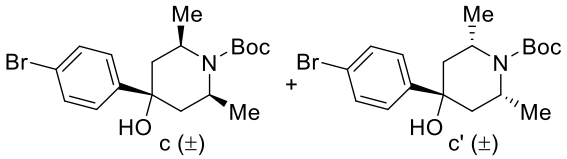

(c and c') 15.4 mg

^{1}H NMR ($CDCl_3$, 500 MHz): δ 7.50 – 7.44 (m, 2H), 7.37 – 7.32 (m, 2H), 4.42 (dt, J = 8.3, 6.6 Hz, 0.75H), 4.33 – 4.23 (m, 0.64H), 4.11 – 3.96 (m, 0.61H), 2.27 – 2.04 (m, 2H), 1.96 – 1.76 (m, 2H), 1.51 – 1.46 (m, 11H), 1.38 – 1.29 (m, 4H).

^{13}C NMR ($CDCl_3$, 126 MHz): δ 155.8, 155.1, 147.8, 147.1, 131.5, 131.3, 126.5, 126.4, 121.1, 120.8, 79.7, 79.4, 73.1, 71.8, 48.0, 45.0, 44.9, 44.3, 42.7, 42.4, 28.6, 28.5, 24.1, 21.1, 19.7.

HRMS (ESI) m/z: $[M+Na]^+$ Calcd for $C_{18}H_{26}BrNO_3Na$ 406.0988; Found 406.0982.

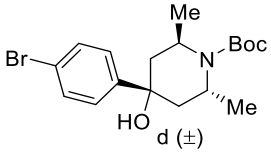

(d) 11.7 mg

^{1}H NMR ($CDCl_3$, 500 MHz): δ 7.46 (d, J = 8.6 Hz, 2H), 7.33 (d, J = 8.6 Hz, 2H), 4.36 (pd, J = 7.2, 2.4 Hz, 2H), 2.21 (dd, J = 14.0, 7.7 Hz, 2H), 1.82 (d, J = 15.0 Hz, 2H), 1.49 – 1.44 (m, 15H).

^{13}C NMR ($CDCl_3$, 126 MHz): δ 154.8, 147.5, 131.4, 126.5, 121.1, 79.3, 72.8, 45.6, 41.7, 28.5, 22.8.

HRMS (ESI) m/z: $[M+Na]^+$ Calcd for $C_{17}H_{24}BrNO_3Na$ 406.0988; Found 406.0984.

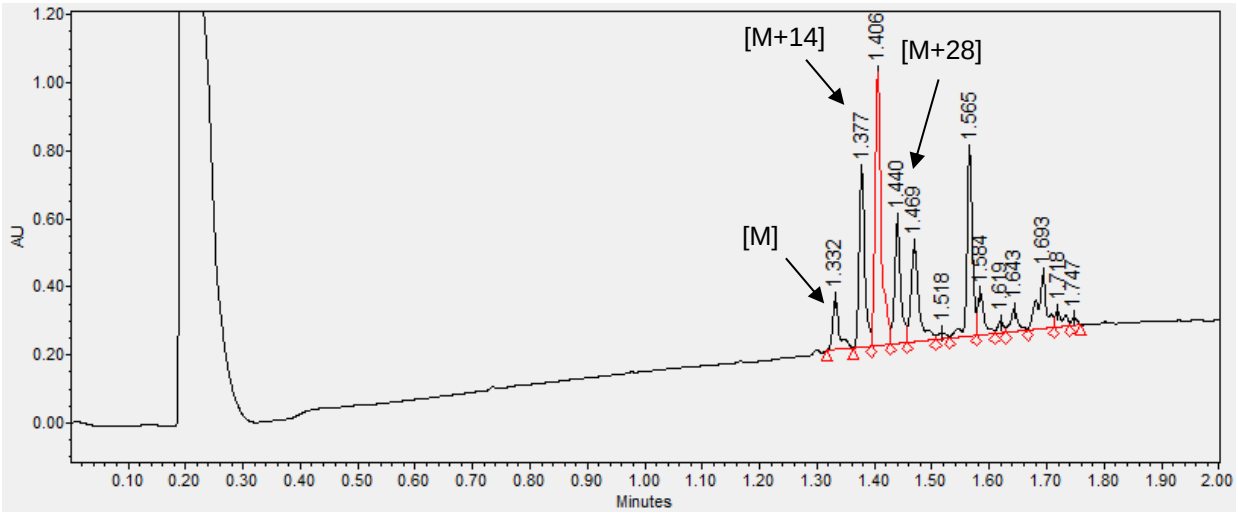

Figure 5D.41. 22 crude reaction LC-MS @ 219 nm (10%→95% MeCN/H_2O, w/ 0.1% HCOOH)

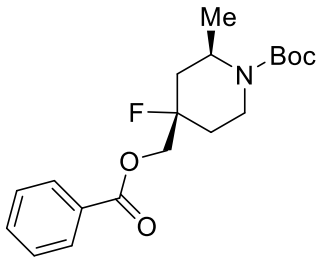

(23) *tert*-Butyl 4-((benzoyloxy)methyl)-4-fluoro-2-methylpiperidine-1-carboxylate: Prepared from *tert*-butyl 4-((benzoyloxy)methyl)-4-fluoropiperidine-1-carboxylate (0.3 mmol, 101.2 mg) according to the general procedure in section II using the following variations: employed tripicolylamine as the ligand (0.04 equiv, 0.012 mmol, 3.5 mg) and added $MeB(OH)_2$ (0.5 equiv, 0.15 mmol, 9.0 mg).
Purification: Reverse phase silica gel chromatography was used with a gradient of 75%→85% MeOH in H_2O. The product was collected by removing MeOH and H_2O using a rotovap.
Isolated yield: 38% as a > 10:1 mixture of diastereomers, 40.0 mg of colorless semisolid.
Spectra available in the literature (CAS): No (N/A)
^{1}H NMR ($CDCl_3$, 500 MHz): δ 8.06 (d, J = 6.9 Hz, 2H), 7.58 (t, J = 7.5 Hz, 1H), 7.46 (t, J = 7.8 Hz, 2H), 4.48 (s, 1H), 4.42 – 4.17 (m, 2H), 4.08 – 3.93 (m, 1H), 3.28 – 3.15 (m, 1H), 1.98 (t, J = 11.7 Hz, 1H), 1.93 – 1.63 (m, 3H), 1.47 (s, 9H), 1.29 (dd, J = 7.1, 2.2 Hz, 3H).
^{13}C NMR ($CDCl_3$, 126 MHz): δ 166.0, 154.6, 133.3, 129.7, 129.6, 128.5, 93.8, 92.4, 79.7, 69.3 (d, J = 25.7 Hz), 44.7, 43.7, 35.7 (d, J = 22.8 Hz), 35.3 (d, J = 19.9 Hz), 33.5, 31.5 (d, J = 21.8 Hz), 28.5, 28.4, 23.7, 18.0, 18.0.
^{19}F NMR ($CDCl_3$, 377 MHz): δ -151.8, -161.7.
HRMS (ESI) m/z: $[M+Na]^+$ Calcd for $C_{19}H_{26}FNO_4Na$ 374.1738; Found 374.1733.

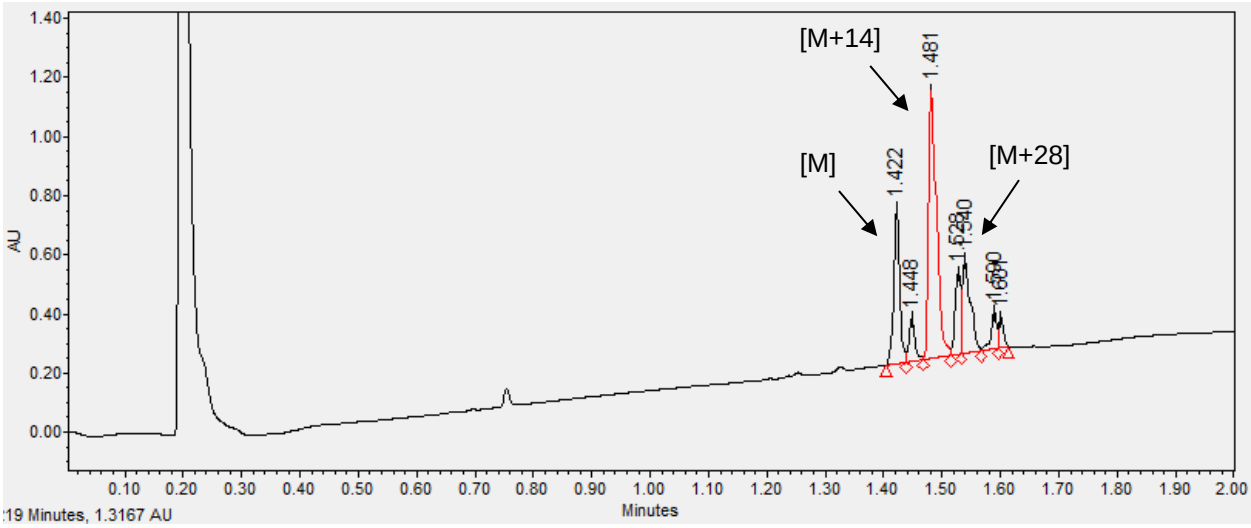

Figure 5D.42. 23 crude reaction LC-MS @ 226 nm (10%→95% MeCN/H_2O, w/ 0.1% HCOOH)

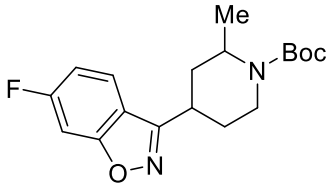

(24) *tert*-Butyl 4-(6-fluorobenzo[*d*]isoxazol-3-yl)-2-methylpiperidine-1-carboxylate: Prepared from *tert*-butyl 4-(6-fluorobenzo[*d*]isoxazol-3-yl)piperidine-1-carboxylate (0.3 mmol, 96.1 mg) according to the general procedure in section II using the following variation: employed tripicolylamine as the ligand (0.04 equiv, 0.012 mmol, 3.5 mg).

Purification: Reverse phase silica gel chromatography was used with a gradient of 68%→75% MeOH in H_2O. The product was collected by removing MeOH and H_2O using a rotovap.

Isolated yield: 29% as a 3.2:1 mixture of diastereomers, 29.1 mg of colorless semisolid.

Spectra available in the literature (CAS): No (N/A)

^{1}H NMR ($CDCl_3$, 500 MHz): δ 7.65 (dd, J = 8.7, 5.1 Hz, 0.75H), 7.61 (dd, J = 8.7, 5.1 Hz, 0.24H), 7.25 (dd, J = 8.7, 2.4 Hz, 1H), 7.06 (tt, J = 8.8, 2.3 Hz, 1H), 4.60 (s, 0.72H), 4.16 (dp, J = 8.4, 6.4 Hz, 1H), 3.95 (ddd, J = 14.0, 6.9, 2.8 Hz, 0.24H), 3.44 (tt, J = 12.8, 3.6 Hz, 0.76H), 3.39 – 3.26 (m, 0.48H), 3.05 (s, 0.74H), 2.27 – 2.19 (m, 0.51H), 2.17 – 2.01 (m, 2H), 1.99 – 1.76 (m, 2H), 1.49 (s, 9H), 1.28 (d, J = 6.9 Hz, 2.37H), 1.11 (d, J = 6.6 Hz, 0.73H).

^{13}C NMR ($CDCl_3$, 126 MHz): δ 165.2, 165.2, 164.0, 163.9, 163.8, 163.2, 163.2, 161.1, 160.9, 155.2, 154.8, 122.4 (d, J = 11.1 Hz), 122.3 (d, J = 11.1 Hz), 117.5, 117.1, 112.5 (d, J = 25.3 Hz), 112.5 (d, J = 25.4 Hz), 97.6 (d, J = 26.7 Hz), 97.5 (d, J = 26.8 Hz), 79.7, 79.5, 48.5, 45.8, 38.2, 36.4, 35.0, 33.5, 30.5, 29.7, 29.4, 28.5, 28.5, 27.6, 19.0, 15.9.

^{19}F NMR ($CDCl_3$, 377 MHz): δ -104.97 – -115.55 (m).

HRMS (ESI) m/z: $[M+Na]^+$ Calcd for $C_{18}H_{23}FN_2O_3Na$ 357.1585; Found 357.1580.

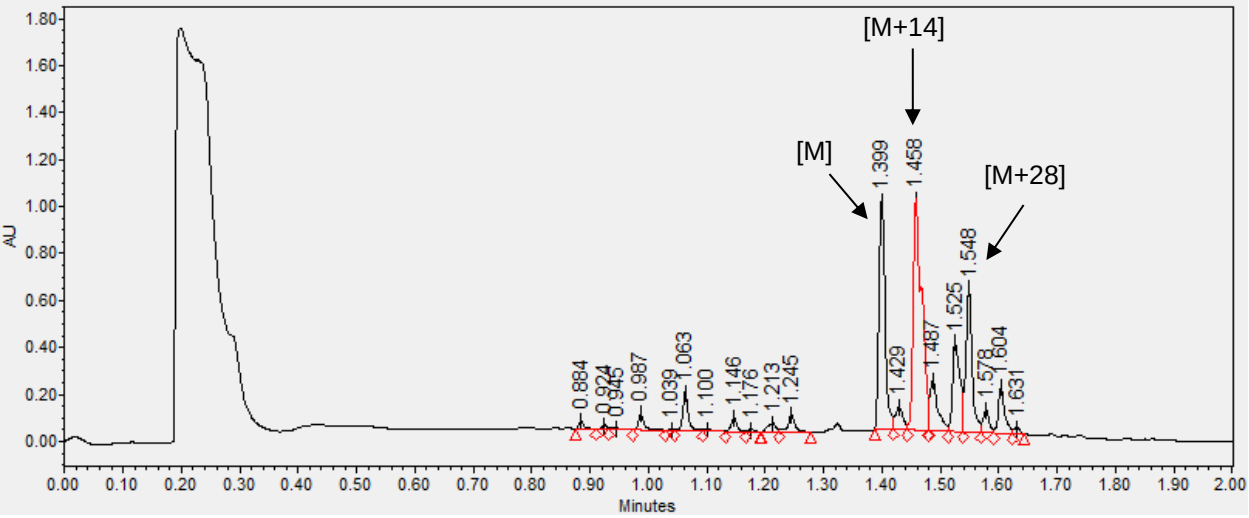

Figure 5D.43. 24 crude reaction LC-MS @ 210 nm (10%→95% MeCN/H_2O, w/ 0.1% HCOOH)

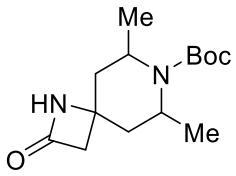

(25) *tert*-Butyl 6,8-dimethyl-2-oxo-1,7-diazaspiro[3.5]nonane-7-carboxylate: Prepared from *tert*-butyl 2-oxo-1,7-diazaspiro[3.5]nonane-7-carboxylate (0.3 mmol, 72.1 mg) according to the general procedure in section II using the following variation: employed tripicolylamine as the ligand (0.04 equiv, 0.012 mmol, 3.5 mg).

Purification: Reverse phase silica gel chromatography was used with a gradient of 45%→60% MeOH in H_2O. The product was collected by removing MeOH and H_2O using a rotovap.

Isolated yield: 53% as a mixture of three diastereomers, 42.6 mg of white solid.

Spectra available in the literature (CAS): No (N/A)

^{1}H NMR ($CDCl_3$, 500 MHz): δ 6.52 – 6.26 (m, 0.42H), 6.17 – 6.01 (m, 0.27H), 6.01 – 5.77 (m, 0.26H), 4.43 (dqd, J = 17.6, 7.2, 2.9 Hz, 1.46H), 4.22 – 4.09 (m, 0.29H), 4.03 (dtd, J = 11.4, 6.9, 4.4 Hz, 0.29H), 2.97 – 2.73 (m, 2H), 2.38 (dd, J = 14.9, 4.9 Hz, 0.31H), 2.29 (dd, J = 14.5, 5.2 Hz, 0.30H), 2.10 (dd, J = 13.8, 7.7 Hz, 1H), 2.03 (dd, J = 13.6, 7.5 Hz, 0.61H), 2.00 – 1.92 (m, 0.60H), 1.82 (dd, J = 13.4, 3.0 Hz, 1.48H), 1.46 (s, 9H), 1.27 (d, J = 7.2 Hz, 5.15H), 1.21 (d, J = 6.9 Hz, 0.85H).

^{13}C NMR ($CDCl_3$, 126 MHz): δ 167.1, 167.1, 166.6, 154.7, 154.7, 154.6, 79.7, 79.7, 79.5, 53.4, 51.9, 51.4, 50.9, 50.5, 49.0, 46.5, 46.5, 46.1, 45.7, 40.0, 39.8, 39.8, 39.5, 28.4, 28.4, 28.2, 22.4, 22.4, 21.7, 21.0, 20.3.

HRMS (ESI) m/z: $[M+Na]^+$ Calcd for $C_{14}H_{24}N_2O_3Na$ 291.1679; Found 291.1675.

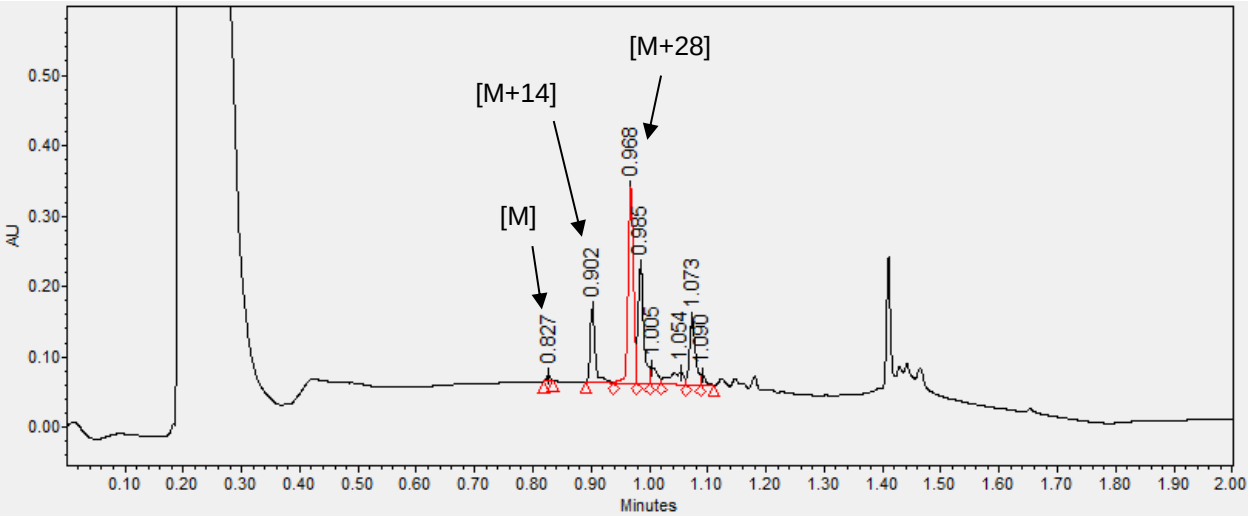

Figure 5D.44. 25 crude reaction LC-MS @ 210 nm (10%→95% MeCN/H_2O, w/ 0.1% HCOOH)

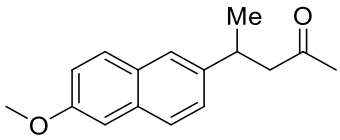

(26) 4-(6-Methoxynaphthalen-2-yl)pentan-2-one: Prepared from 4-(6-methoxynaphthalen-2-yl)butan-2-one (0.3 mmol, 68.5 mg) according to the general procedure in section III using the following variations: added $MeB(OH)_2$ (0.5 equiv, 0.15 mmol, 9.0 mg) and used 1:1 MeCN:DMSO as the solvent at 0.6 M (500 µL).

Purification: Reverse phase silica gel chromatography was used with a gradient of 65%→70% MeOH in H_2O. The product was collected by removing MeOH and H_2O using a rotovap.

Isolated yield: 35%, 25.4 mg of beige oil.

Spectra available in the literature (CAS): Yes (56600-70-5)[19]

^{1}H NMR ($CDCl_3$, 500 MHz): δ 7.68 (d, J = 9.3 Hz, 2H), 7.56 (s, 1H), 7.33 (dd, J = 8.4, 1.9 Hz, 1H), 7.16 – 7.03 (m, 2H), 3.91 (s, 3H), 3.44 (h, J = 7.0 Hz, 1H), 2.84 (dd, J = 16.2, 6.6 Hz, 1H), 2.73 (dd, J = 16.2, 7.8 Hz, 1H), 2.07 (s, 3H), 1.34 (d, J = 6.9 Hz, 3H).

^{13}C NMR ($CDCl_3$, 126 MHz): δ 208.0, 157.3, 141.3, 133.3, 129.1, 129.0, 127.1, 126.0, 124.8, 118.8, 105.6, 55.3, 52.0, 35.4, 30.6, 22.0.

HRMS (ESI) m/z: $[M+H]^+$ Calcd for $C_{16}H_{19}O_2$ 243.1380; Found 243.1375.

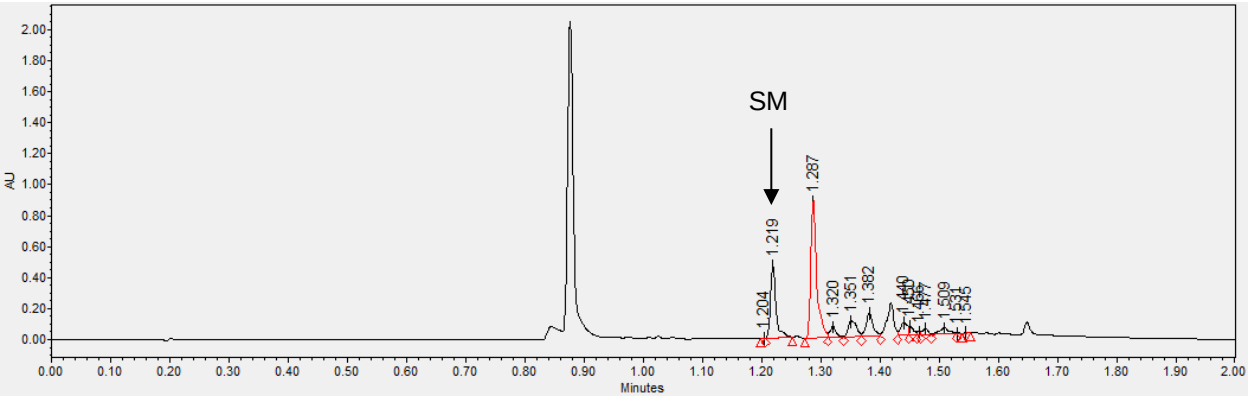

Figure 5D.45. 26 crude reaction LC-MS @ 273 nm (10%→95% MeCN/H_2O, w/ 0.1% HCOOH)

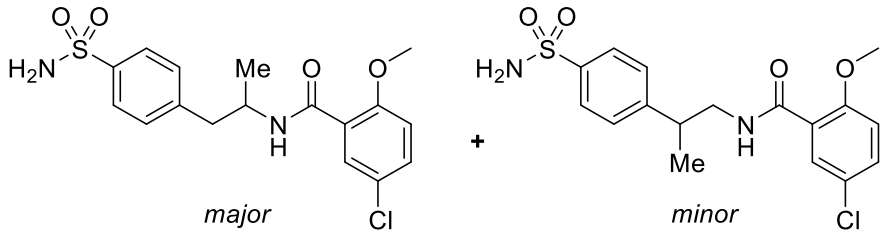

(27) 5-Chloro-2-methoxy-*N*-(1-(4-sulfamoylphenyl)propan-2-yl)benzamide: Prepared from 5-chloro-2-methoxy-*N*-(4-sulfamoylphenethyl)benzamide (0.3 mmol, 110.6 mg) according to the general procedure in section III using the following variations: added $B(OH)_3$ (0.5 equiv, 0.15 mmol, 9.3 mg) and used 1:1 MeCN:DMSO as the solvent.
Purification: Reverse phase silica gel chromatography was used with a gradient of 50%→55% MeOH in H_2O. The product was collected by removing MeOH and H_2O using a rotovap.
Isolated yield: 43% as a 6.7:1 mixture of two regioisomers, 49.3 mg of white solid.
Spectra available in the literature (CAS): No (N/A)
^{1}H NMR - *major isomer* - (acetone-d6, 500 MHz): δ 7.93 (d, J = 2.9 Hz, 1H), 7.88 (d, J = 8.3 Hz, 1H), 7.83 (d, J = 8.4 Hz, 2H), 7.51 – 7.43 (m, 3H), 7.17 (d, J = 8.8 Hz, 1H), 6.52 (bs, 2H), 4.41 (hept, J = 6.6 Hz, 1H), 3.96 (s, 3H), 3.04 (dd, J = 13.5, 7.2 Hz, 1H), 2.97 (dd, J = 13.5, 6.7 Hz, 1H), 1.24 (d, J = 6.6 Hz, 3H).
^{13}C NMR (acetone-d6, 126 MHz): δ 163.5, 157.2, 144.3, 143.2, 132.7, 131.7, 130.7, 129.2, 128.8, 127.2, 126.9, 126.3, 124.9, 114.7, 56.9, 56.8, 47.6, 47.5, 42.5, 42.5, 30.6, 30.4, 20.5, 20.5.
HRMS (ESI) m/z: $[M+H]^+$ Calcd for $C_{17}H_{20}ClN_2O_4S$ 383.0827; Found 383.0820.

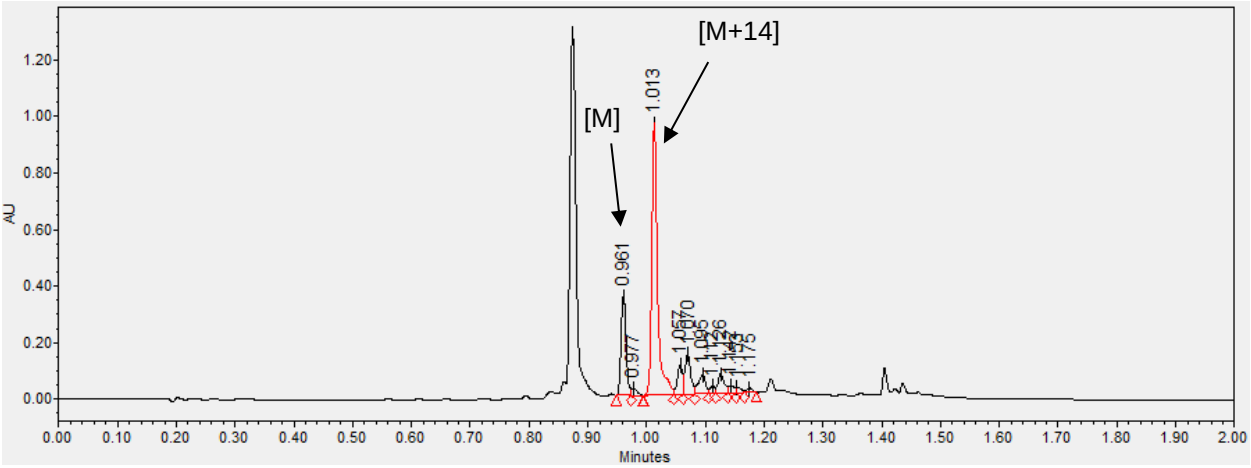

Figure 5D.46. 27 crude reaction LC-MS @ 297 nm (10%→95% MeCN/H_2O, w/ 0.1% HCOOH)

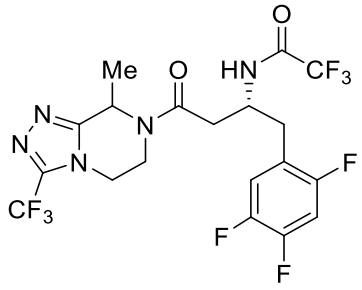

(28) 2,2,2-Trifluoro-*N*-((2*S*)-4-(8-methyl-3-(trifluoromethyl)-5,6-dihydro-[1,2,4]triazolo[4,3-*a*]pyrazin-7(8*H*)-yl)-4-oxo-1-(2,4,5-trifluorophenyl)butan-2-yl)acetamide: Prepared from (*S*)-2,2,2-trifluoro-*N*-(4-oxo-4-(3-(trifluoromethyl)-5,6-dihydro-[1,2,4]triazolo[4,3-*a*]pyrazin-7(8*H*)-yl)-1-(2,4,5-trifluorophenyl)butan-2-yl)acetamide (0.3 mmol, 151.0 mg) according to the general procedure in section II using the following variation: employed tripicolylamine as the ligand (0.04 equiv, 0.012 mmol, 3.5 mg).
Purification: Reverse phase silica gel chromatography was used with a gradient of 55%→70% MeOH in H_2O. The product was collected by removing MeOH and H_2O using a rotovap.
Isolated yield: 61% as a 1.6:1 mixture of diastereomers, 94.6 mg of white solid.
Spectra available in the literature (CAS): No (N/A)
^{1}H NMR ($CDCl_3$, 500 MHz): δ 8.02 – 7.66 (m, 1H), 7.13 – 7.00 (m, 1H), 6.98 – 6.70 (m, 1H), 6.07 (dq, J = 13.8, 7.0 Hz, 0.35H), 5.37 (p, J = 6.3, 5.7 Hz, 0.58H), 5.13 – 5.01 (m, 0.60H), 4.61 – 4.41 (m, 1H), 4.33 – 4.22 (m, 1H), 4.13 – 3.92 (m, 1.43H), 3.74 – 3.58 (m, 0.38H), 3.28 – 3.17 (m, 0.60H), 3.12 – 2.97 (m, 2H), 2.96 – 2.55 (m, 2H), 1.77 – 1.56 (m, 3H).
^{13}C NMR ($CDCl_3$, 126 MHz): δ 169.4, 169.2, 168.6, 168.6, 157.2 – 157.0 (m), 156.7 (q, J = 38.3, 37.8 Hz), 155.3 – 155.0 (m), 154.2, 153.3, 151.0 – 150.0 (m), 148.4 – 148.2 (m), 148.1 – 147.7 (m), 146.3 – 145.2 (m), 144.3 – 142.5 (m), 120.6 – 119.8 (m), 119.4 – 118.5 (m), 117.4 – 116.7 (m), 114.5 (m), 105.70 (dd, J = 28.4, 20.9 Hz), 48.4, 48.1, 47.7, 47.4, 45.3, 45.2, 43.6, 43.6, 43.5, 43.4, 38.3, 38.0, 34.7, 34.5, 34.4, 33.9, 33.7, 32.2, 32.1, 20.1, 19.9, 18.6, 18.5.
^{19}F NMR ($CDCl_3$, 471 MHz): δ -62.84 – -63.41 (m), -75.99 – -76.51 (m), -118.59 – -120.91 (m), -133.25 – -135.06 (m), -141.45 – -142.26 (m).
HRMS (ESI) m/z: $[M+H]^+$ Calcd for $C_{19}H_{17}F_9N_5O_2$ 518.1233; Found 518.1230.

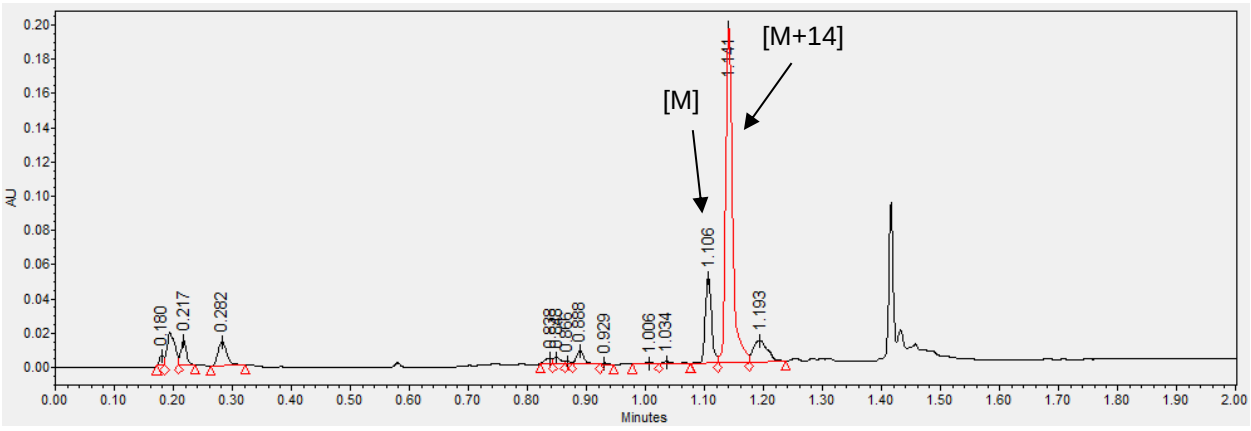

Figure 5D.47. 28 crude reaction LC-MS @ 257 nm (10%→95% MeCN/H_2O, w/ 0.1% HCOOH)

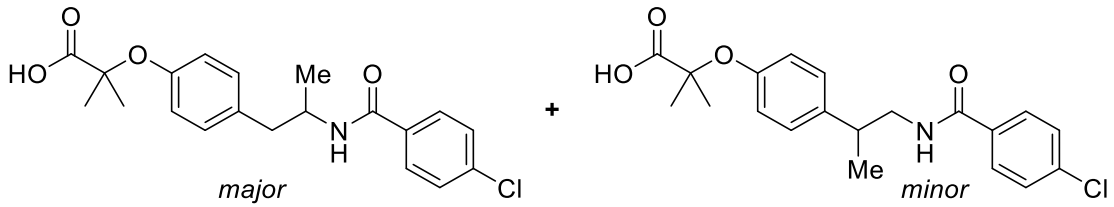

(29) 2-(4-(2-(4-Chlorobenzamido)propyl)phenoxy)-2-methylpropanoic acid: Prepared from 2-(4-(2-(4-chlorobenzamido)ethyl)phenoxy)-2-methylpropanoic acid (0.3 mmol, 108.5 mg) according to the general procedure in section III using the following variations: added $B(OH)_3$ (0.5 equiv, 0.15 mmol, 9.3 mg) and used 1:1 MeCN:DMSO as the solvent.
Purification: Reverse phase silica gel chromatography was used with a gradient of 55%→70% MeOH in H_2O. The product was collected by removing MeOH and H_2O using a rotovap.
Isolated yield: 38% as a 5.9:1 mixture of two regioisomers, 42.8 mg of white solid.
Spectra available in the literature (CAS): No (N/A)
^{1}H NMR - *major isomer* - ($CDCl_3$, 500 MHz): δ 7.61 (d, J = 8.5 Hz, 2H), 7.38 (d, J = 8.5 Hz, 2H), 7.12 (d, J = 7.5 Hz, 2H), 6.88 (d, J = 8.2 Hz, 2H), 5.86 (d, J = 8.1 Hz, 1H), 4.41 (p, J = 6.9 Hz, 1H), 2.88 (dd, J = 13.6, 5.8 Hz, 1H), 2.81 (dd, J = 13.6, 7.0 Hz, 1H), 1.61 (s, 6H), 1.22 (d, J = 6.7 Hz, 3H).
^{13}C NMR ($CDCl_3$, 126 MHz): δ 165.8, 152.8, 137.7, 133.1, 133.0, 130.3, 128.8, 128.8, 128.7, 128.2, 128.1, 120.9, 46.7, 44.3, 41.6, 39.0, 25.2, 20.0.
HRMS (ESI) m/z: $[M+H]^+$ Calcd for $C_{20}H_{23}ClNO_4$ 376.1310; Found 376.1304.

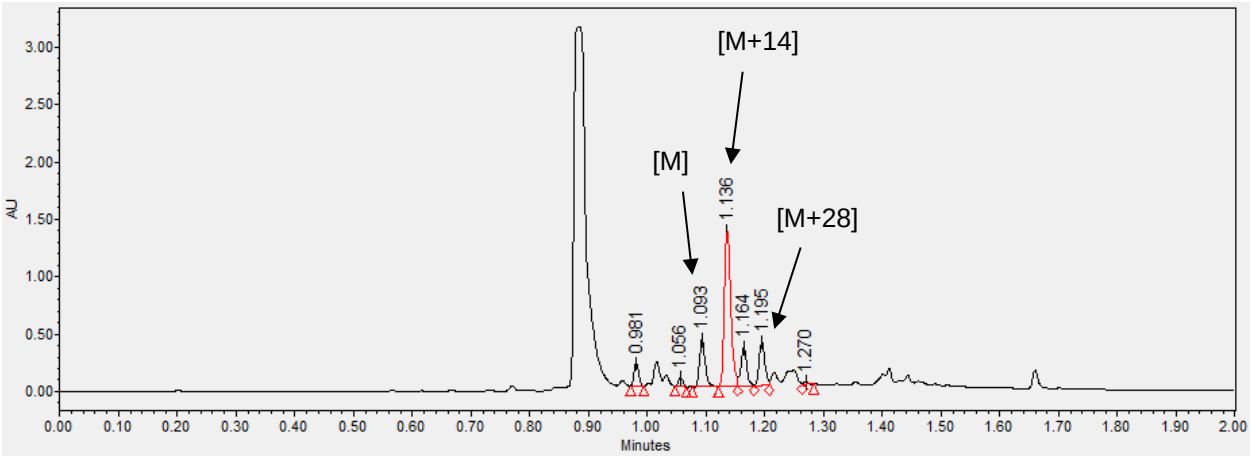

Figure 5D.48. 29 crude reaction LC-MS @ 257 nm (10%→95% MeCN/H_2O, w/ 0.1% HCOOH)

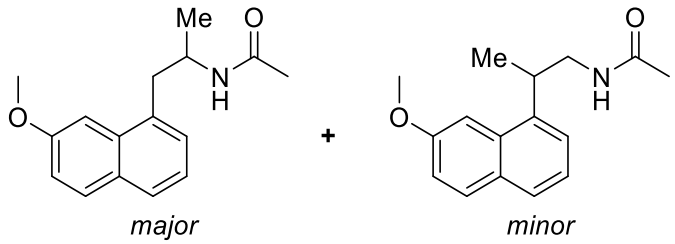

major *minor*

(30) *N*-(1-(7-Methoxynaphthalen-1-yl)propan-2-yl)acetamide: Prepared from *N*-(2-(7-methoxynaphthalen-1-yl)ethyl)acetamide (0.3 mmol, 73.0 mg) according to the general procedure in section III using the following variations: added $B(OH)_3$ (0.5 equiv, 0.15 mmol, 9.3 mg) and used 1:1 MeCN:DMSO as the solvent.

Purification: Reverse phase silica gel chromatography was used with a gradient of 60%→70% MeOH in H_2O. The product was collected by removing MeOH and H_2O using a rotovap.

Isolated yield: 49% as a 2.5:1 mixture of regioisomers, 38.0 mg of beige solid. This product decomposes at rt over time.

Spectra available in the literature (CAS): No (N/A)

^{1}H NMR - *major isomer* - ($CDCl_3$, 500 MHz): δ 7.82 – 7.77 (m, 1H), 7.78 – 7.54 (m, 2H), 7.46 – 7.27 (m, 2H), 7.18 (dd, J = 8.9, 2.5 Hz, 1H), 5.46 (bs, 1H), 4.50 – 4.30 (m, 1H), 4.07 (s, 3H), 3.67 (dd, J = 13.4, 4.2 Hz, 1H), 2.78 (dd, J = 13.4, 9.5 Hz, 1H), 2.01 (s, 3H), 1.12 (d, J = 6.6 Hz, 3H).

^{13}C NMR ($CDCl_3$, 126 MHz): δ 170.3, 169.6, 158.0, 157.3, 138.7, 133.5, 133.2, 133.2, 130.4, 130.0, 129.4, 129.3, 128.1, 127.1, 126.9, 123.2, 123.0, 122.8, 118.6, 118.3, 103.0, 101.9, 55.8, 55.5, 53.4, 46.2, 45.6, 40.9, 40.0, 33.6, 33.1, 23.6, 23.4, 19.7, 18.7.

HRMS (ESI) m/z: $[M+H]^+$ Calcd for $C_{16}H_{20}NO_2$ 258.1489; Found 258.1484.

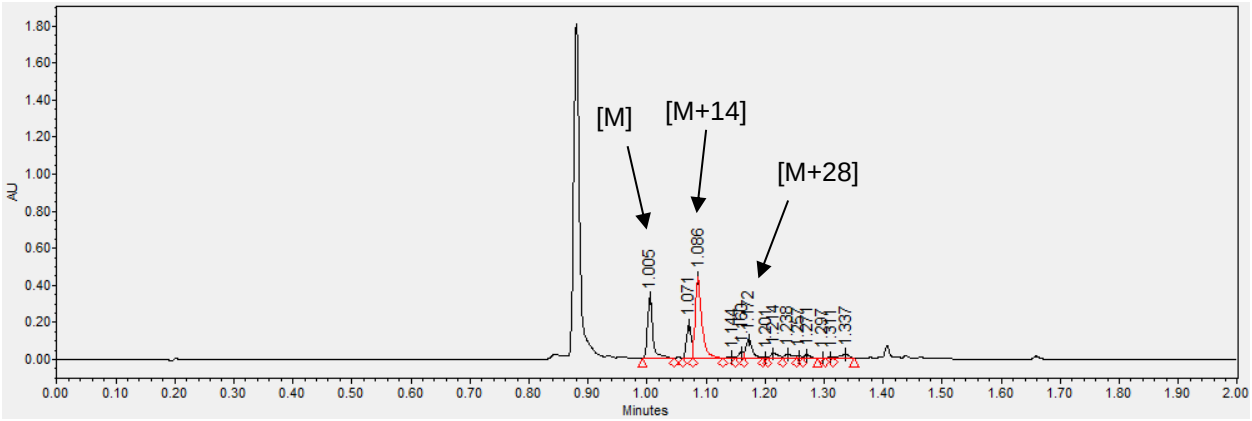

Figure 5D.49. 30 crude reaction LC-MS @ 284 nm (10%→95% MeCN/H_2O, w/ 0.1% HCOOH)

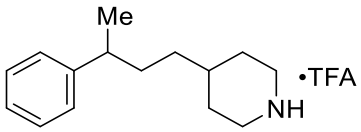

(31) 4-(3-Phenylbutyl)piperidine: Prepared from 4-(3-phenylpropyl)piperidine (0.3 mmol, 61.0 mg) according to the general procedure in section II using the following variation: added trifluoroacetic acid (1.5 equiv, 0.45 mmol, 34.5 µL).
Purification: Reverse phase silica gel chromatography was used with a gradient of 45%→55% MeOH in H_2O. The product was collected by removing MeOH and H_2O using a rotovap.
Isolated yield: 48%, 47.6 mg of colorless semisolid.
Spectra available in the literature (CAS): No (1857465-42-9)
^{1}H NMR ($CDCl_3$, 500 MHz): δ 8.95 (bs, 1.15H), 8.42 (bs, 0.73H), 7.29 (t, J = 7.4 Hz, 2H), 7.22 – 7.11 (m, 3H), 3.36 (bs, 2H), 2.82 (bs, 2H), 2.63 (h, J = 6.9 Hz, 1H), 1.90 – 1.76 (m, 2H), 1.57 (q, J = 7.8 Hz, 2H), 1.46 – 1.37 (m, 3H), 1.32 – 1.25 (m, 1H), 1.25 (d, J = 6.9 Hz, 3H), 1.21 – 1.09 (m, 1H).
^{13}C NMR ($CDCl_3$, 126 MHz): δ 161.9, 147.1, 128.4, 128.3 (q, J = 6.8 Hz), 126.9, 126.1, 44.3, 40.0, 35.0, 34.1, 33.7, 28.8, 28.7, 22.4.
^{19}F NMR ($CDCl_3$, 377 MHz): δ -75.9.
HRMS (ESI) m/z: $[M+H]^+$ Calcd for $C_{15}H_{24}N$ 218.1903; Found 218.1902.

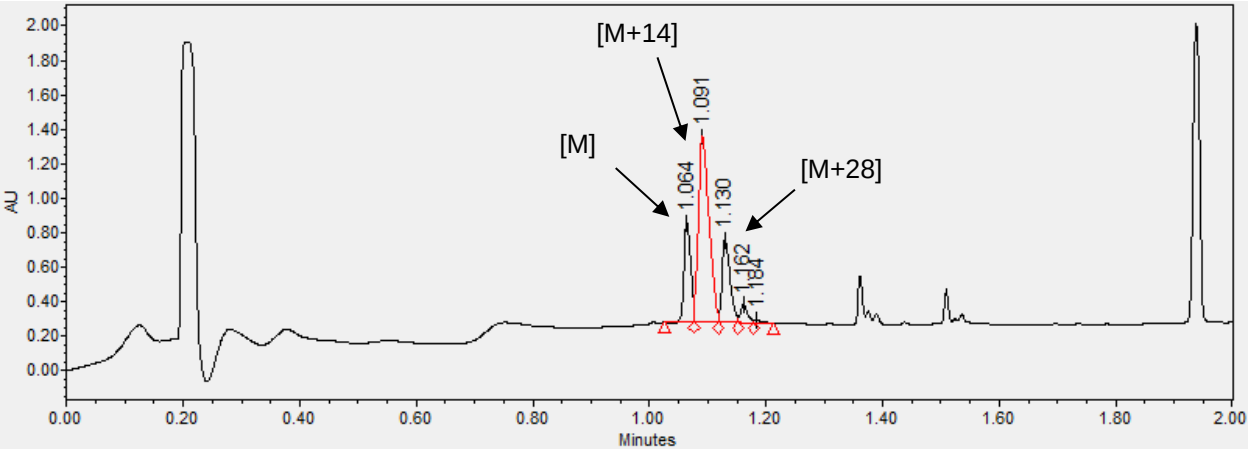

Figure 5D.50. 31 crude reaction LC-MS @ 210 nm (5%→95% MeCN/H_2O, w/ 0.1% HCOOH)

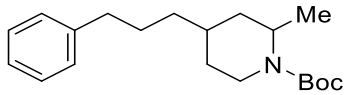

(32) *tert*-Butyl 2-methyl-4-(3-phenylpropyl)piperidine-1-carboxylate: Prepared from *tert*-butyl 4-(3-phenylpropyl)piperidine-1-carboxylate (0.3 mmol, 91.0 mg) according to the general procedure in section III using the following variations: employed tripicolylamine as the ligand (0.04 equiv, 0.012 mmol, 3.5 mg), used 3 equiv DCP (243.3 mg), did not add acid, and used 0.15 M concentration (2000 µL MeCN).

Purification: Reverse phase silica gel chromatography was used with a gradient of 88%→93% MeOH in H_2O. The product was collected by removing MeOH and H_2O using a rotovap.

Isolated yield: 21% as a 4.8:1 mixture of diastereomers, 19.9 mg of colorless semisolid.

Spectra available in the literature (CAS): No (N/A)

^{1}H NMR ($CDCl_3$, 500 MHz): δ 7.30 – 7.25 (m, 2H), 7.22 – 7.12 (m, 3H), 4.57 – 3.61 (m, 2H), 3.01 (m, 0.17H), 2.81 (m, 0.82H), 2.59 (t, J = 7.7 Hz, 2H), 1.96 – 1.49 (m, 7H), 1.45 (s, 9H), 1.33 – 1.20 (m, 2H), 1.10 (d, J = 7.0 Hz, 3H).

^{13}C NMR ($CDCl_3$, 126 MHz): δ 154.9, 142.6, 128.3, 128.3, 125.7, 79.0, 78.9, 49.3, 37.1, 36.8, 36.5, 36.1, 36.1, 35.9, 35.9, 32.3, 31.4, 29.9, 29.7, 29.5, 29.0, 28.6, 28.5, 28.5, 19.9, 16.3.

HRMS (ESI) m/z: $[M+Na]^+$ Calcd for $C_{20}H_{31}NO_2Na$ 340.2247; Found 340.2241.

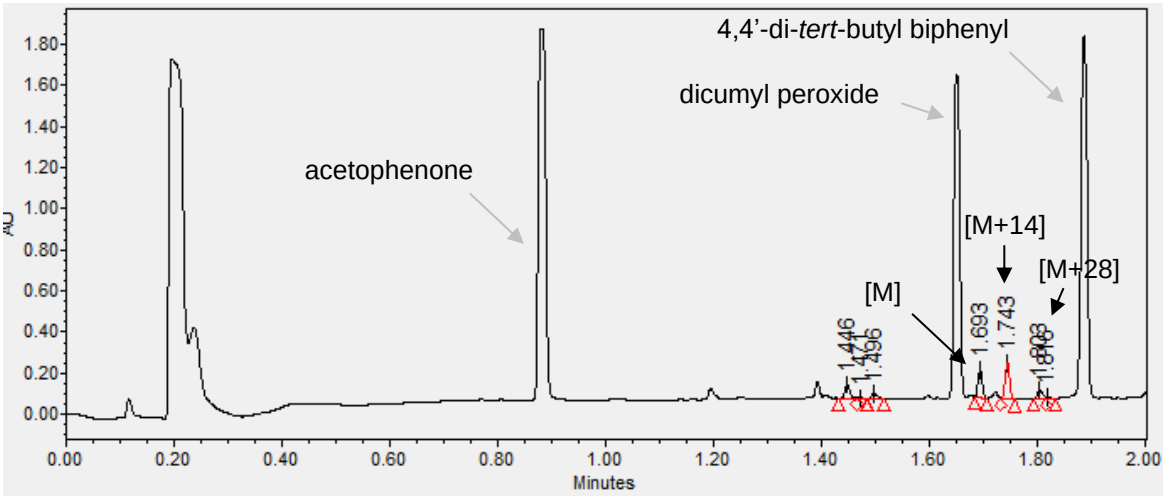

Figure 5D.51. 32 crude reaction LC-MS @ 210 nm (10%→95% MeCN/H_2O, w/ 0.1% HCOOH)

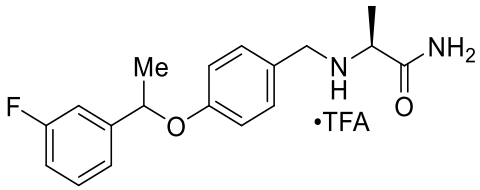

(33) (2*S*)-2-((4-(1-(3-Fluorophenyl)ethoxy)benzyl)amino)propanamide: Prepared from (S)-2-((4-((3-fluorobenzyl)oxy)benzyl)amino)propanamide (0.3 mmol, 90.7 mg) according to the general procedure in section III using the following variations: added trifluoroacetic acid (1.5 equiv, 0.45 mmol, 34.5 µL) and used 4 equiv DCP (324.4 mg).
Purification: Reverse phase silica gel chromatography was used with a gradient of 42%→52% MeOH in H_2O. The product was collected by removing MeOH and H_2O using a rotovap.
Isolated yield: 51%, 65.9 mg of white solid.
Spectra available in the literature (CAS): No (N/A)
^{1}H NMR (DMSO-d6, 400 MHz): δ 9.06 (bs, 1H), 8.96 (bs, 1H), 7.90 (s, 1H), 7.61 (s, 1H), 7.38 (td, J = 8.0, 6.1 Hz, 1H), 7.30 (d, J = 8.6 Hz, 2H), 7.27 – 7.17 (m, 2H), 7.07 (td, J = 8.6, 3.7 Hz, 1H), 6.96 (d, J = 8.7 Hz, 2H), 5.57 (q, J = 6.3 Hz, 1H), 4.04 – 3.87 (m, 2H), 3.81 – 3.53 (m, 1H), 1.54 (d, J = 6.3 Hz, 3H), 1.37 (d, J = 6.9 Hz, 3H).
^{13}C NMR (DMSO-d6, 126 MHz): δ 170.3, 163.1, 161.2, 157.9 (q, J = 32.6 Hz), 157.6, 145.7 (d, J = 6.9 Hz), 131.5 (d, J = 2.5 Hz), 130.5 (d, J = 8.3 Hz), 123.6, 121.7 (d, J = 2.7 Hz), 115.7, 114.2 (d, J = 21.0 Hz), 112.5 (d, J = 21.8 Hz), 73.9, 54.1, 54.1, 47.8, 26.3, 23.8, 15.8, 15.8.
^{19}F NMR ($CDCl_3$, 377 MHz): δ -74.10, -113.38.
HRMS (ESI) m/z: $[M+H]^+$ Calcd for $C_{18}H_{22}FN_2O_2$ 317.1660; Found 317.1656.

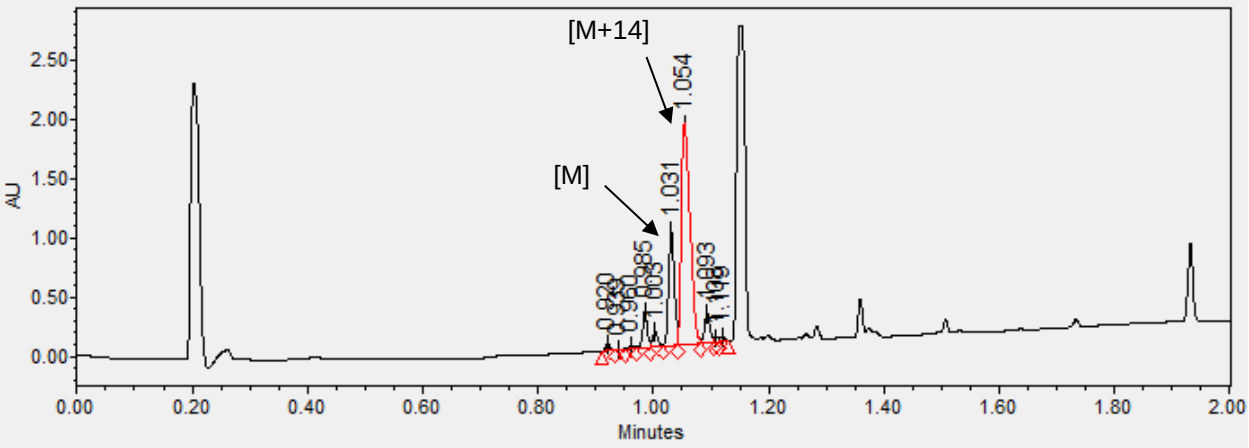

Figure 5D.52. 33 crude reaction LC-MS @ 231 nm (5%→95% MeCN/H_2O, w/ 0.1% HCOOH)

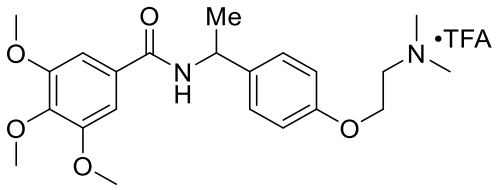

(34) *N*-(1-(4-(2-(Dimethylamino)ethoxy)phenyl)ethyl)-3,4,5-trimethoxybenzamide: Prepared from *N*-(4-(2-(dimethylamino)ethoxy)benzyl)-3,4,5-trimethoxybenzamide (0.3 mmol, 116.6 mg) according to the general procedure in section III using the following variations: added trifluoroacetic acid (1.5 equiv, 0.45 mmol, 34.5 µL) and used 4 equiv DCP (324.4 mg).
Purification: Reverse phase silica gel chromatography was used with a gradient of 39%→49% MeOH in H_2O. The product was collected by removing MeOH and H_2O using a rotovap.
Isolated yield: 44%, 68.0 mg of white solid.
Spectra available in the literature (CAS): No (N/A)
^{1}H NMR ($CDCl_3$, 500 MHz): δ 10.11 (bs, 1H), 7.30 (d, J = 8.7 Hz, 2H), 6.99 (s, 2H), 6.83 (d, J = 6.8 Hz, 2H), 6.63 – 6.49 (m, 1H), 5.23 (p, J = 7.0 Hz, 1H), 4.35 – 4.20 (m, 2H), 3.85 (s, 9H), 3.50 – 3.42 (m, 2H), 2.92 (s, 6H), 1.56 (d, J = 6.9 Hz, 3H).
^{13}C NMR ($CDCl_3$, 126 MHz): δ 166.7, 161.4 (q, J = 37.2 Hz), 156.4, 153.2, 141.1, 136.9, 129.6, 129.6 (q, J = 9.9 Hz), 127.8, 114.6, 104.6, 62.5, 60.9, 56.6, 56.3, 48.9, 43.8, 21.5.
^{19}F NMR ($CDCl_3$, 377 MHz): δ -75.76.
HRMS (ESI) m/z: $[M+H]^+$ Calcd for $C_{22}H_{31}N_2O_5$ 403.2228; Found 403.2222.

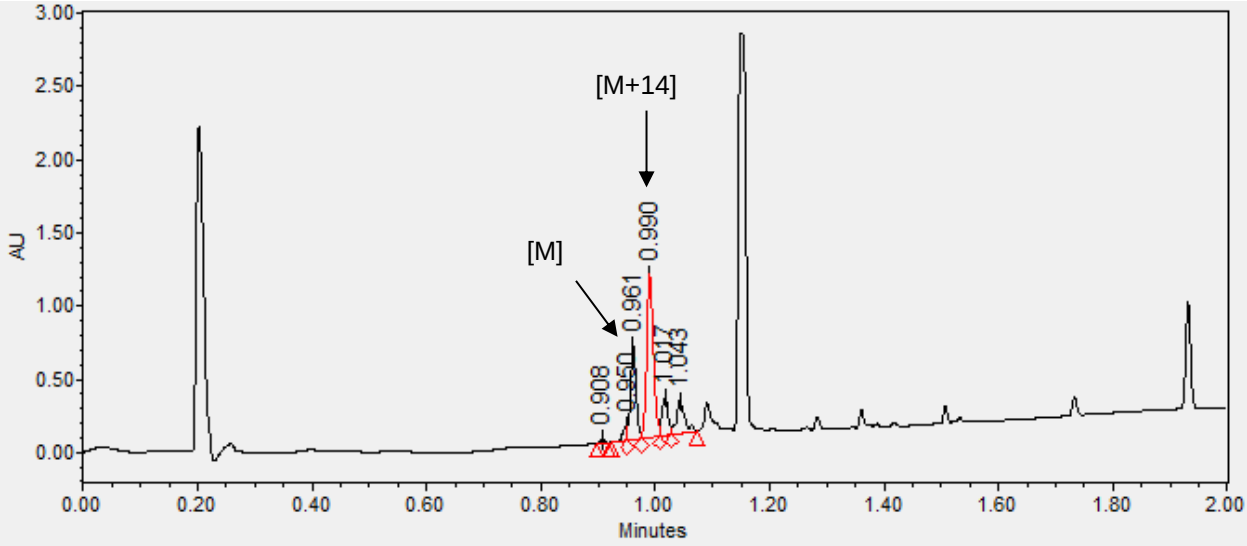

Figure 5D.53. 34 crude reaction LC-MS @ 232 nm (5%→95% MeCN/H_2O, w/ 0.1% HCOOH)

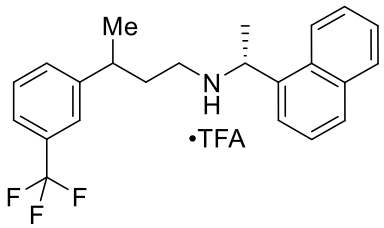

(35) *N*-((*R*)-1-(Naphthalen-1-yl)ethyl)-3-(3-(trifluoromethyl)phenyl)butan-1-amine:
Prepared from (*R*)-*N*-(1-(naphthalen-1-yl)ethyl)-3-(3-(trifluoromethyl)phenyl)propan-1-amine (0.3 mmol, 107.2 mg) according to the general procedure in section II using the following variations: added trifluoroacetic acid (1.5 equiv, 0.45 mmol, 34.5 µL) and used 0.6 M concentration (500 µL TFE).
Purification: Reverse phase silica gel chromatography was used with a gradient of 55%→65% MeOH in H_2O. The product was collected by removing MeOH and H_2O using a rotovap.
Isolated yield: 27% as a 1.2:1 mixture of diastereomers, 39.3 mg of white solid.
Spectra available in the literature (CAS): No (N/A)
^{1}H NMR ($CDCl_3$, 500 MHz): δ 10.05 (d, J = 33.7 Hz, 1H), 9.44 (s, 1H), 8.02 – 7.75 (m, 4H), 7.72 – 7.46 (m, 3H), 7.35 (t, J = 8.2 Hz, 1H), 7.29 – 7.07 (m, 3H), 5.22 – 4.98 (m, 1H), 2.98 – 2.40 (m, 3H), 1.98 (qd, J = 6.6, 3.0 Hz, 2H), 1.68 (t, J = 6.5 Hz, 3H), 1.08 (dd, J = 10.3, 6.9 Hz, 3H).
^{13}C NMR ($CDCl_3$, 126 MHz): δ 162.2, 161.9, 145.9, 145.6, 133.8, 133.8, 132.0, 131.0, 130.8, 130.6, 130.6, 130.5, 129.8, 129.7, 129.6, 129.4, 129.1, 129.1, 127.3, 127.3, 126.3, 126.3, 125.8, 125.8, 125.0, 124.0, 123.6 – 123.3 (m), 123.3 (q, J = 3.8 Hz), 122.9, 121.3, 53.1, 44.4, 44.3, 37.2, 37.1, 33.7, 22.0, 21.5, 20.6, 20.5.
^{19}F NMR ($CDCl_3$, 471 MHz): δ -62.69, -62.71, -75.71.
HRMS (ESI) m/z: $[M+H]^+$ Calcd for $C_{23}H_{25}F_3N$ 372.1934; Found 372.1930.

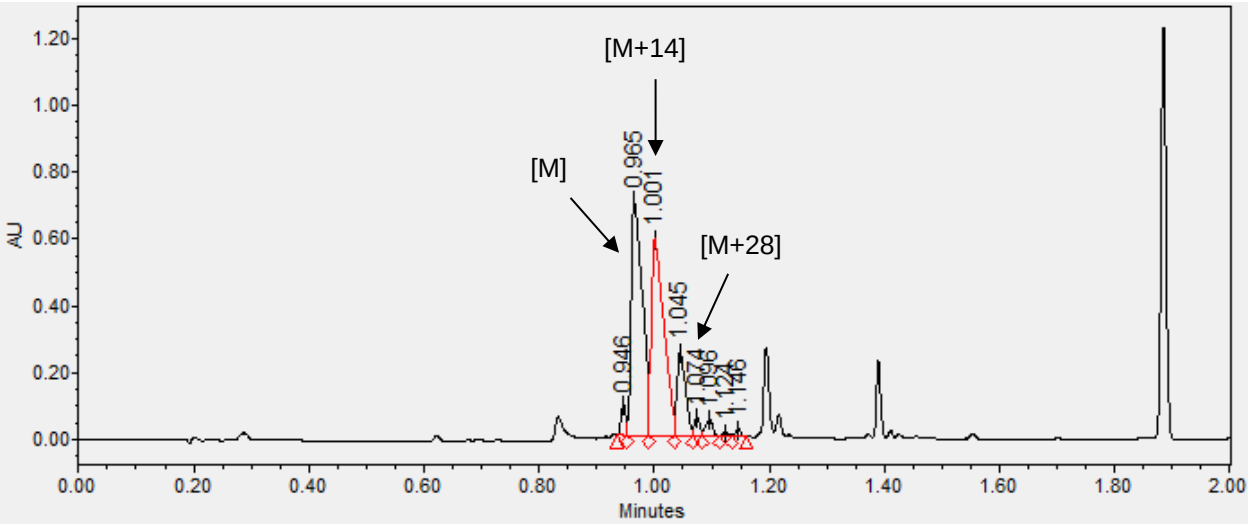

Figure 5D.54. 35 crude reaction LC-MS @ 278 nm (5%→95% MeCN/H_2O, w/ 0.1% HCOOH)

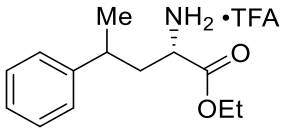

(36) Ethyl (2*S*)-2-amino-4-phenylpentanoate: Prepared from ethyl (*S*)-2-amino-4-phenylbutanoate (0.3 mmol, 62.2 mg) according to the general procedure in section II using the following variation: added trifluoroacetic acid (1.5 equiv, 0.45 mmol, 34.5 µL).
Purification: Reverse phase silica gel chromatography was used with a gradient of 35%→45% MeOH in H_2O. The product was collected by removing MeOH and H_2O using a rotovap.
Isolated yield: 39% as a 1.2:1 mixture of diastereomers, 38.8 mg of colorless semisolid.
Spectra available in the literature (CAS): No (1250247-91-6)
^{1}H NMR (DMSO-d6, 500 MHz): δ 8.51 (s, 3H), 7.37 – 7.29 (m, 2H), 7.28 – 7.18 (m, 3H), 4.17 – 3.98 (m, 2H), 3.68 (ddd, J = 10.3, 7.6, 6.1 Hz, 1H), 2.94 (ddt, J = 17.8, 8.5, 6.6 Hz, 1H), 2.15 – 1.92 (m, 2H), 1.29 – 1.11 (m, 6H).
^{13}C NMR (DMSO-d6, 126 MHz): δ 170.0, 169.8, 158.6 (q, J = 30.9 Hz), 145.6, 145.5, 129.1, 128.9, 127.5, 127.4, 127.0, 126.9, 117.7 (q, J = 299.9 Hz), 62.3, 62.2, 51.3, 51.0, 38.9, 38.6, 35.6, 35.3, 22.9, 22.4, 14.3, 14.3.
^{19}F NMR ($CDCl_3$, 377 MHz): δ -74.17.
HRMS (ESI) m/z: $[M+H]^+$ Calcd for $C_{13}H_{20}NO_2$ 222.1494; Found 222.1486.

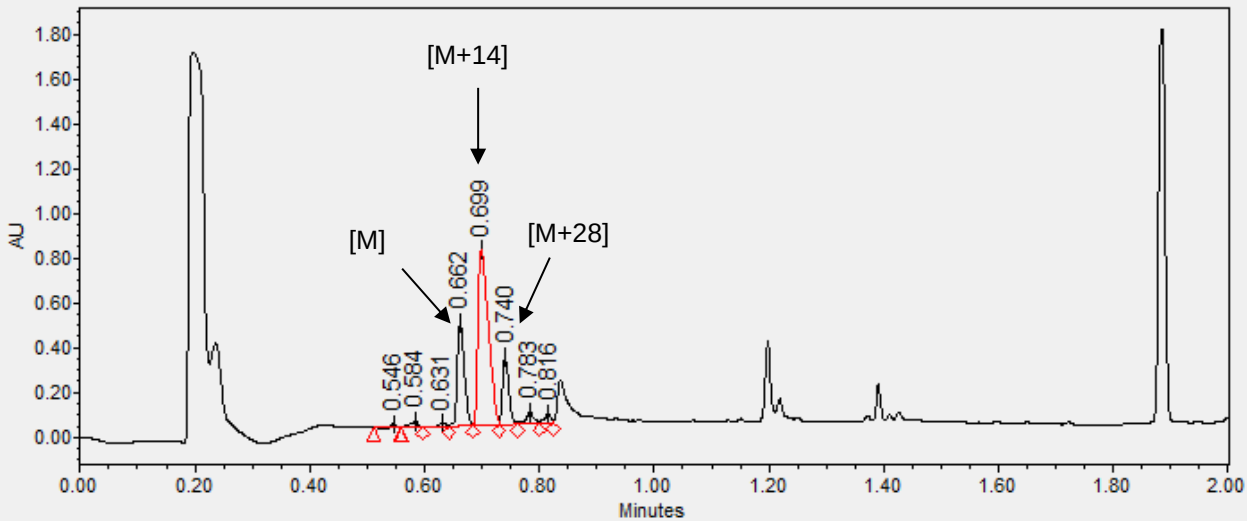

Figure 5D.55. 36 crude reaction LC-MS @ 210 nm (5%→95% MeCN/H_2O, w/ 0.1% HCOOH)

5D.IX. ^{1}H, ^{13}C, and ^{19}F NMR spectra

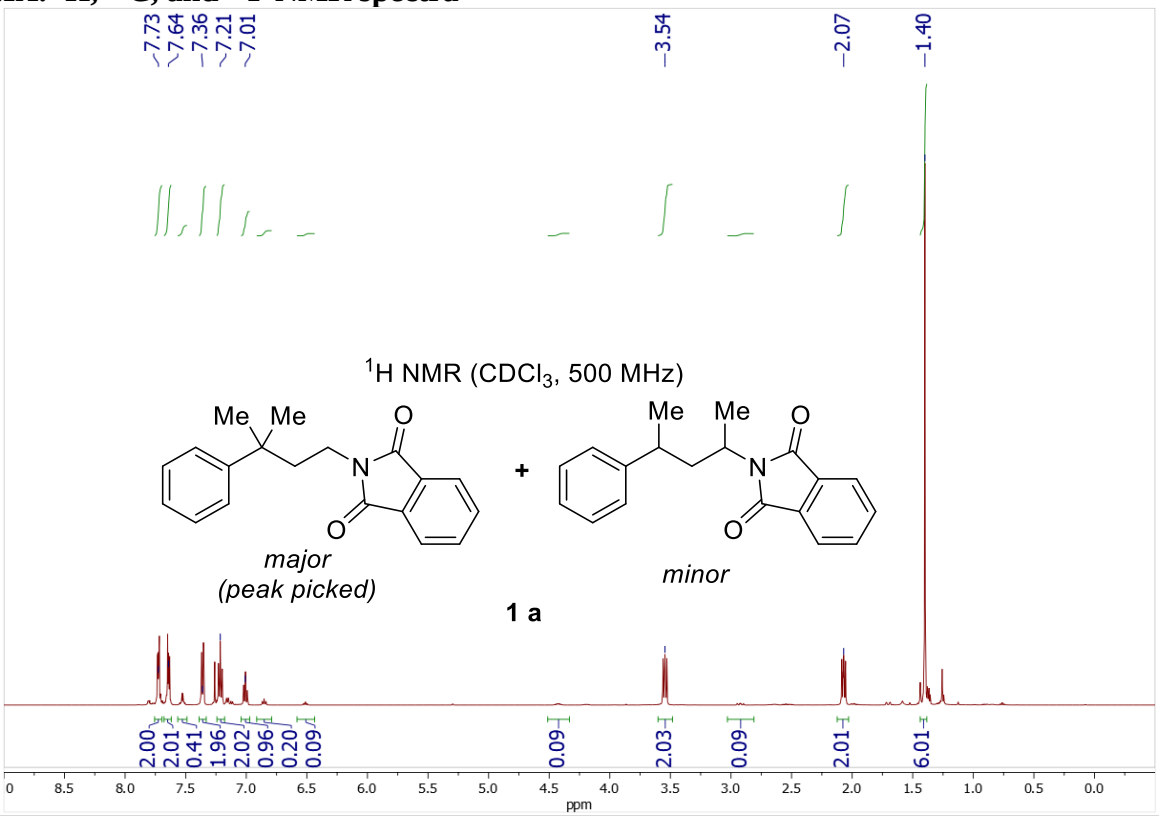

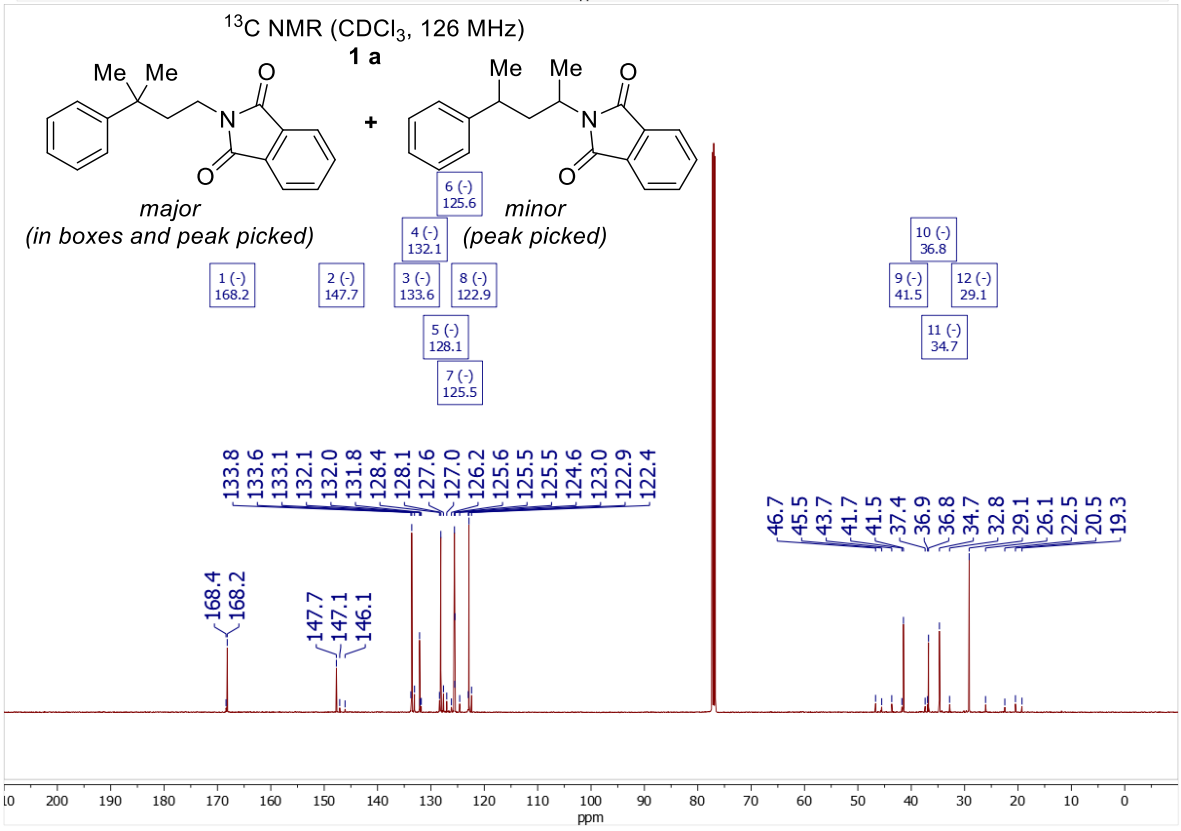

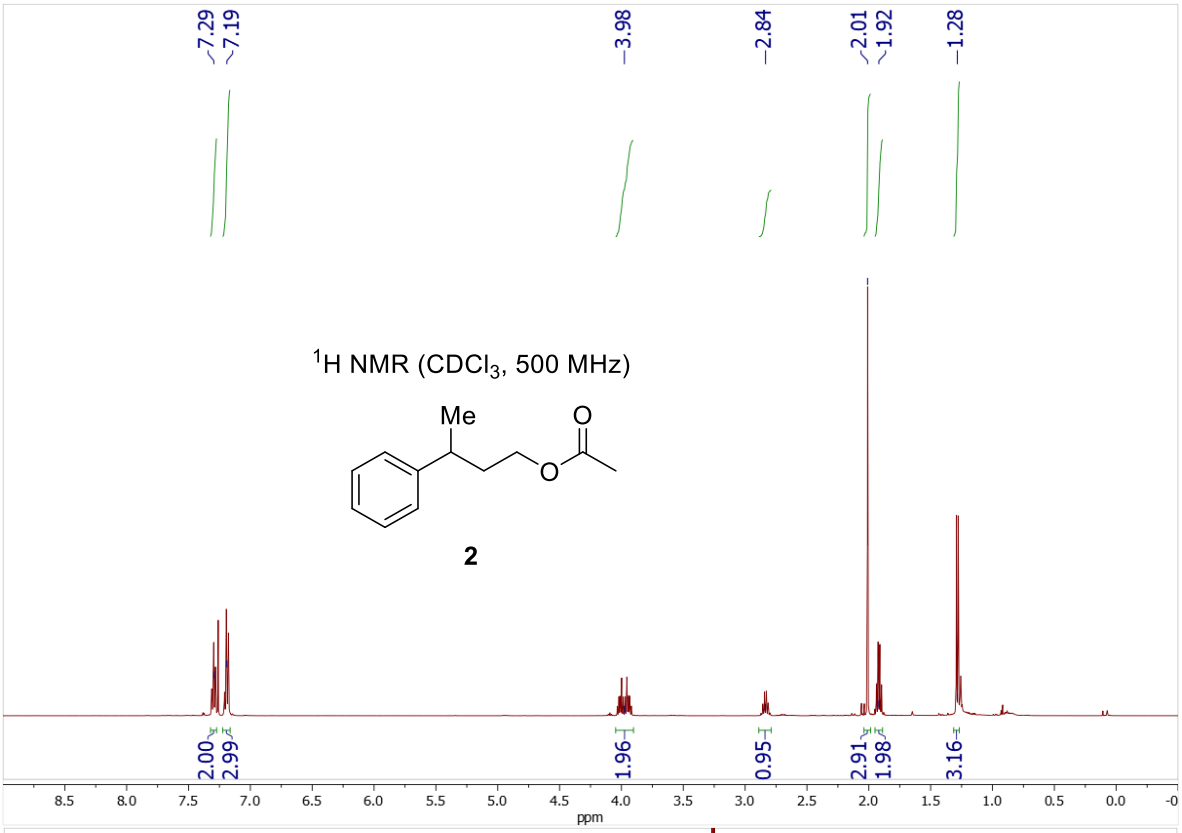
7.29
7.19
3.98
2.84
2.01
1.92
1.28
^{1}H NMR ($CDCl_3$, 500 MHz)
Me
O
O
2
2.00
2.99
1.96
0.95
2.91
1.98
3.16
ppm

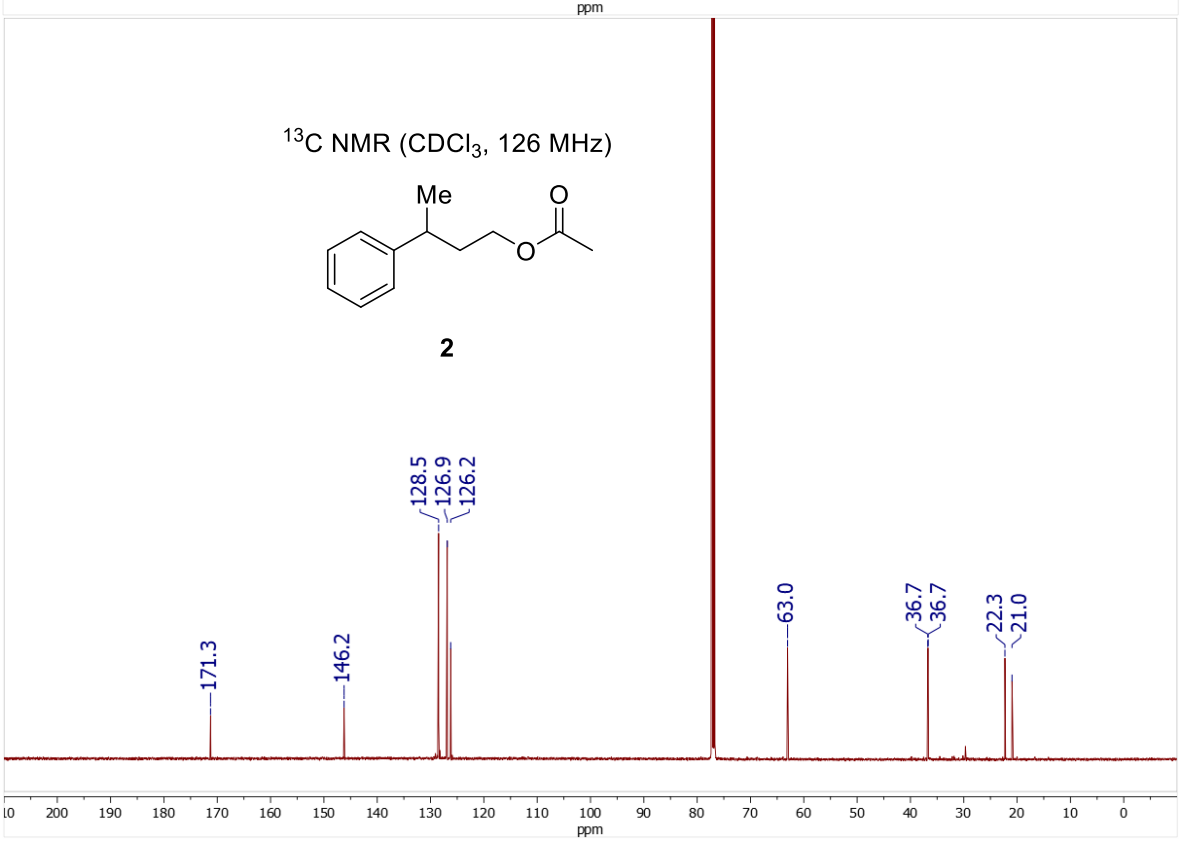
^{13}C NMR ($CDCl_3$, 126 MHz)
Me
O
O
2
128.5
126.9
126.2
171.3
146.2
63.0
36.7
36.7
22.3
21.0
ppm

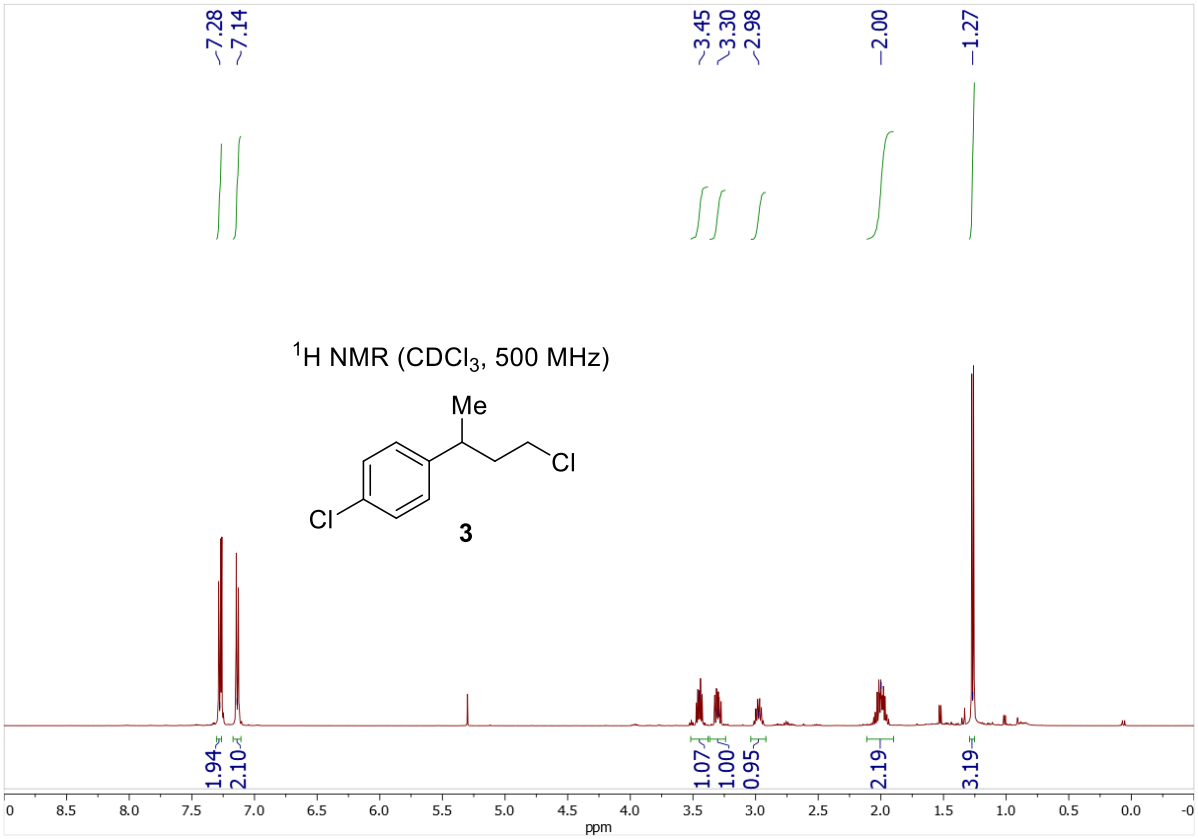
7.28
7.14
3.45
3.30
2.98
2.00
1.27
^{1}H NMR ($CDCl_3$, 500 MHz)
Me
Cl
Cl
3
1.94
2.10
1.07
1.00
0.95
2.19
3.19
ppm

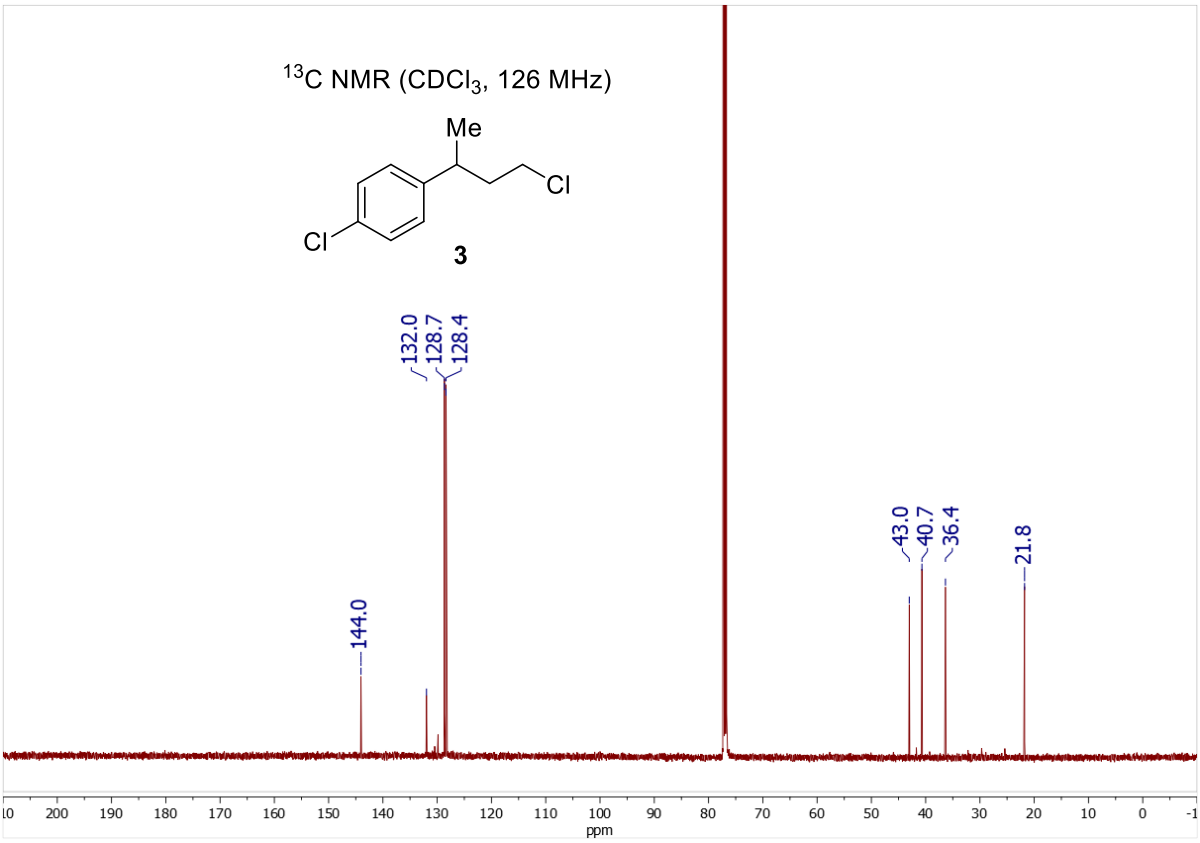
^{13}C NMR ($CDCl_3$, 126 MHz)
Me
Cl
Cl
3
132.0
128.7
128.4
144.0
43.0
40.7
36.4
21.8
ppm

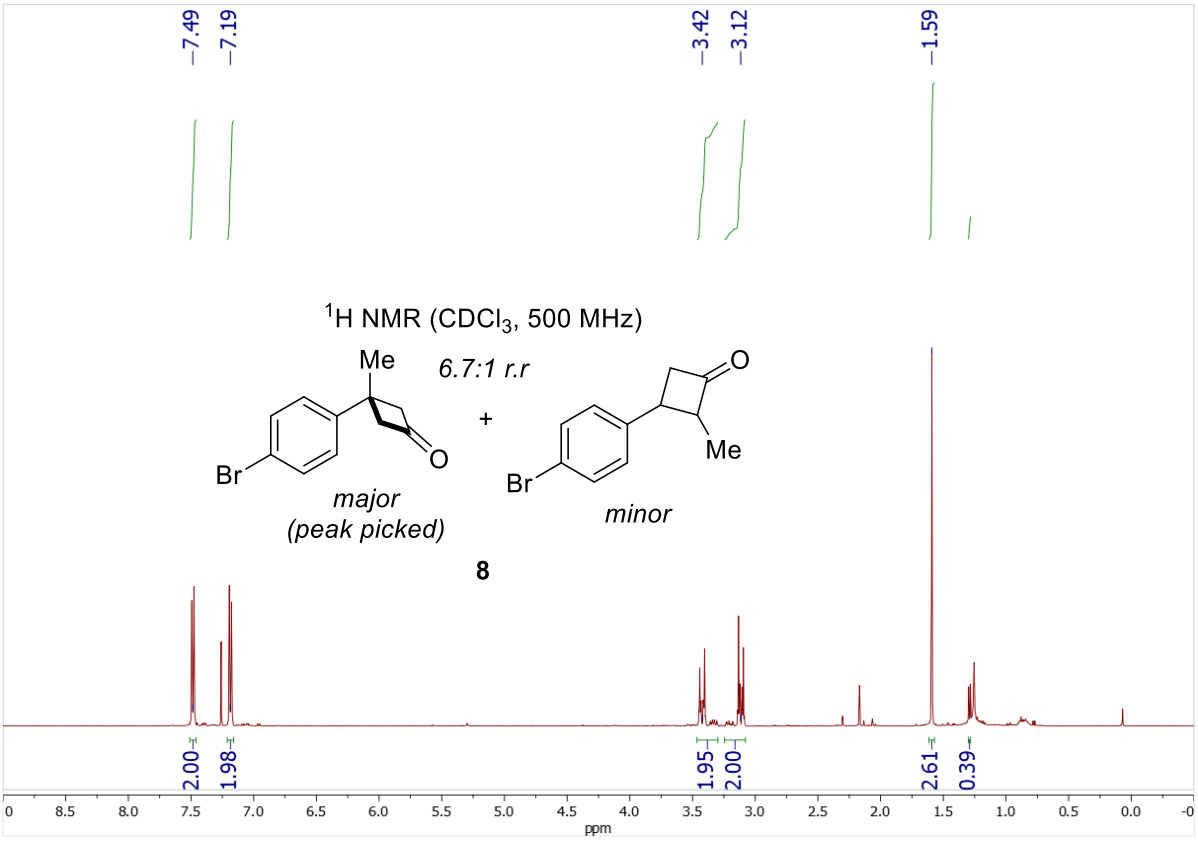

Assignment of ^{13}C peaks to isomers was aided with prediction software. Major isomer ^{13}C peaks are shown twice (in peak picking and again in the boxes). The minor isomer has diastereotopic peaks.

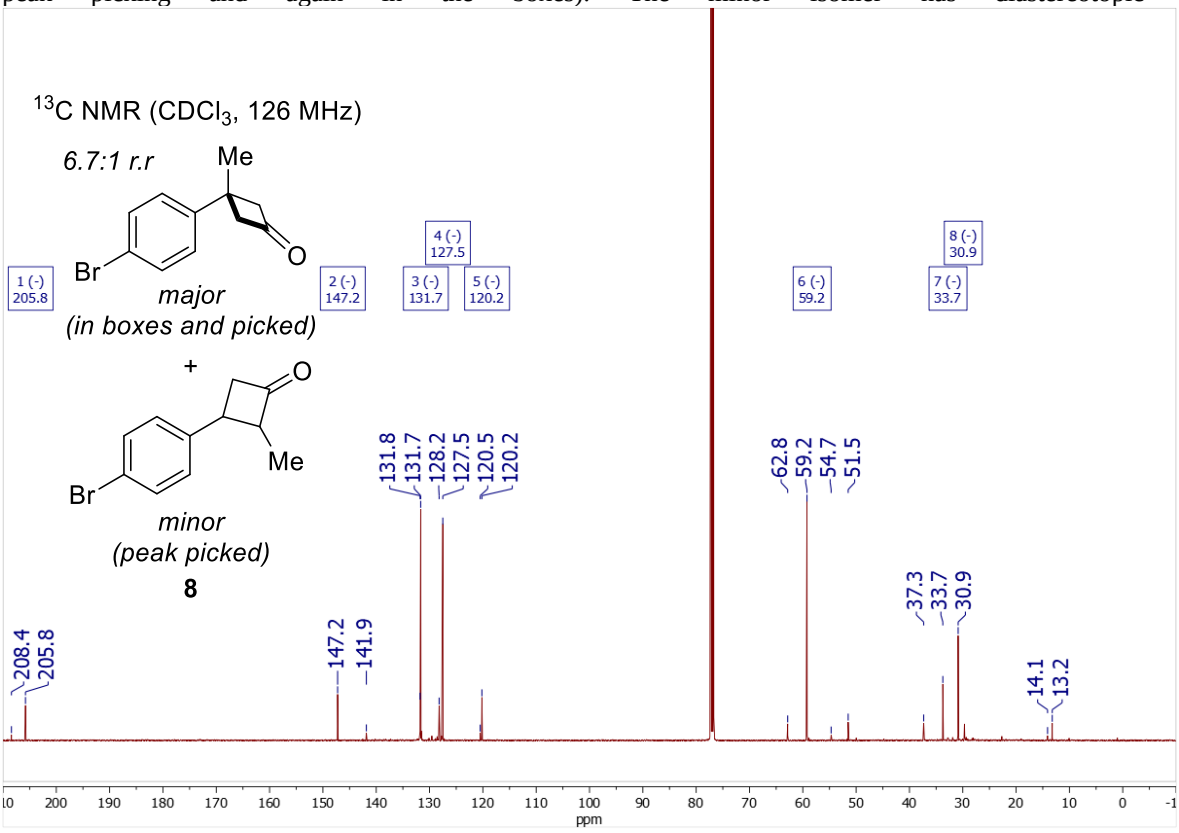

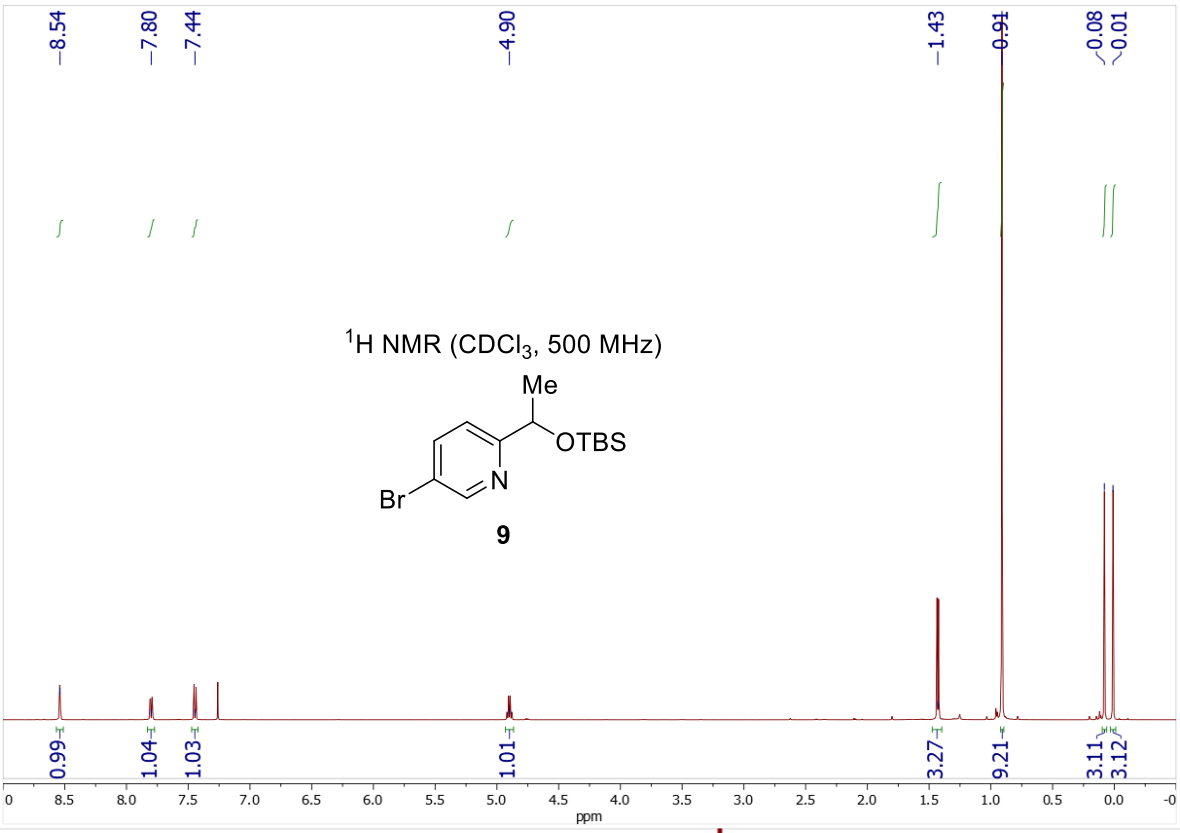
8.54
7.80
7.44
4.90
1.43
0.91
0.08
0.01
^{1}H NMR ($CDCl_3$, 500 MHz)
Me
OTBS
N
Br
9
0.99
1.04
1.03
1.01
3.27
9.21
3.11
3.12
ppm

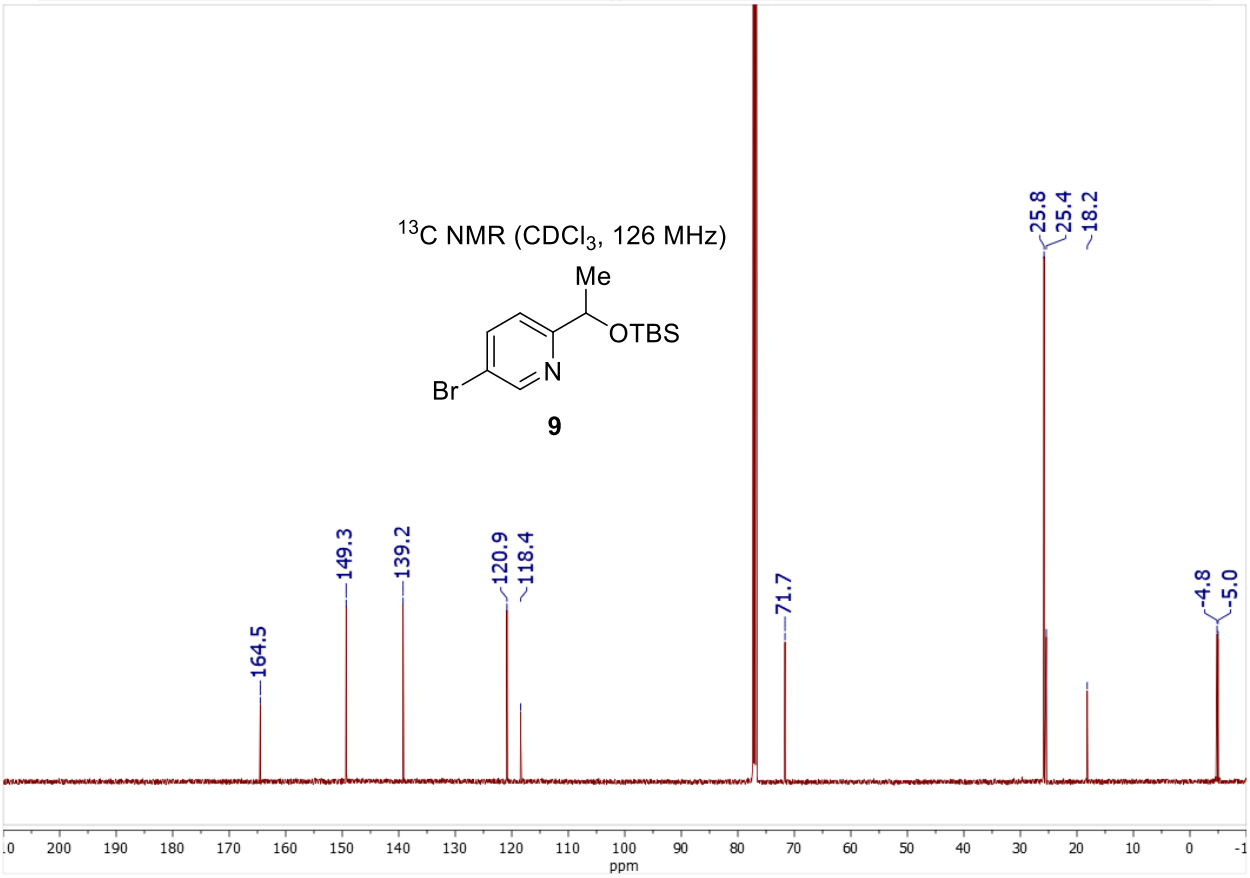
^{13}C NMR ($CDCl_3$, 126 MHz)
Me
OTBS
N
Br
9
164.5
149.3
139.2
120.9
118.4
71.7
25.8
25.4
18.2
-4.8
-5.0
ppm

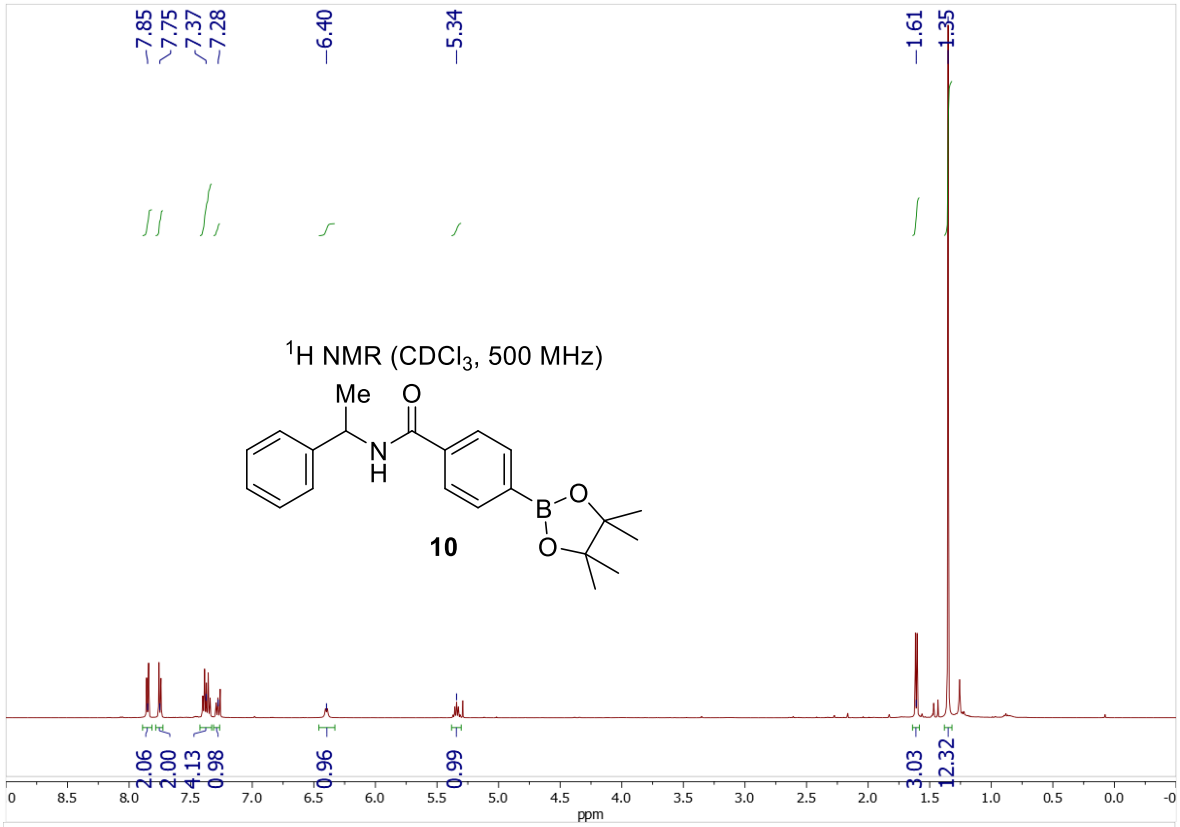
7.85
7.75
7.37
7.28
6.40
5.34
1.61
1.35
^{1}H NMR ($CDCl_3$, 500 MHz)
Me
O
N
H
B
O
O
10
2.06
2.00
4.13
0.98
0.96
0.99
3.03
12.32
ppm

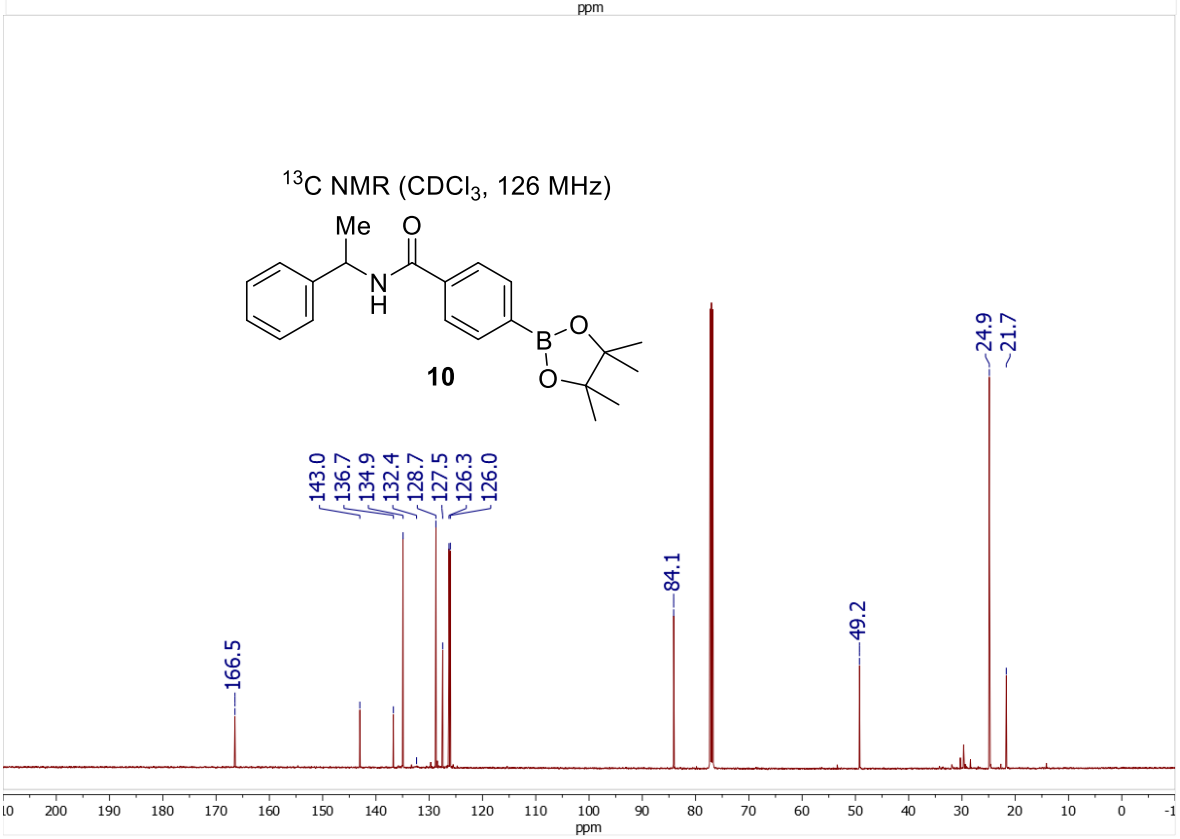
^{13}C NMR ($CDCl_3$, 126 MHz)
Me
O
N
H
B
O
O
10
143.0
136.7
134.9
132.4
128.7
127.5
126.3
126.0
84.1
49.2
24.9
21.7
166.5
ppm

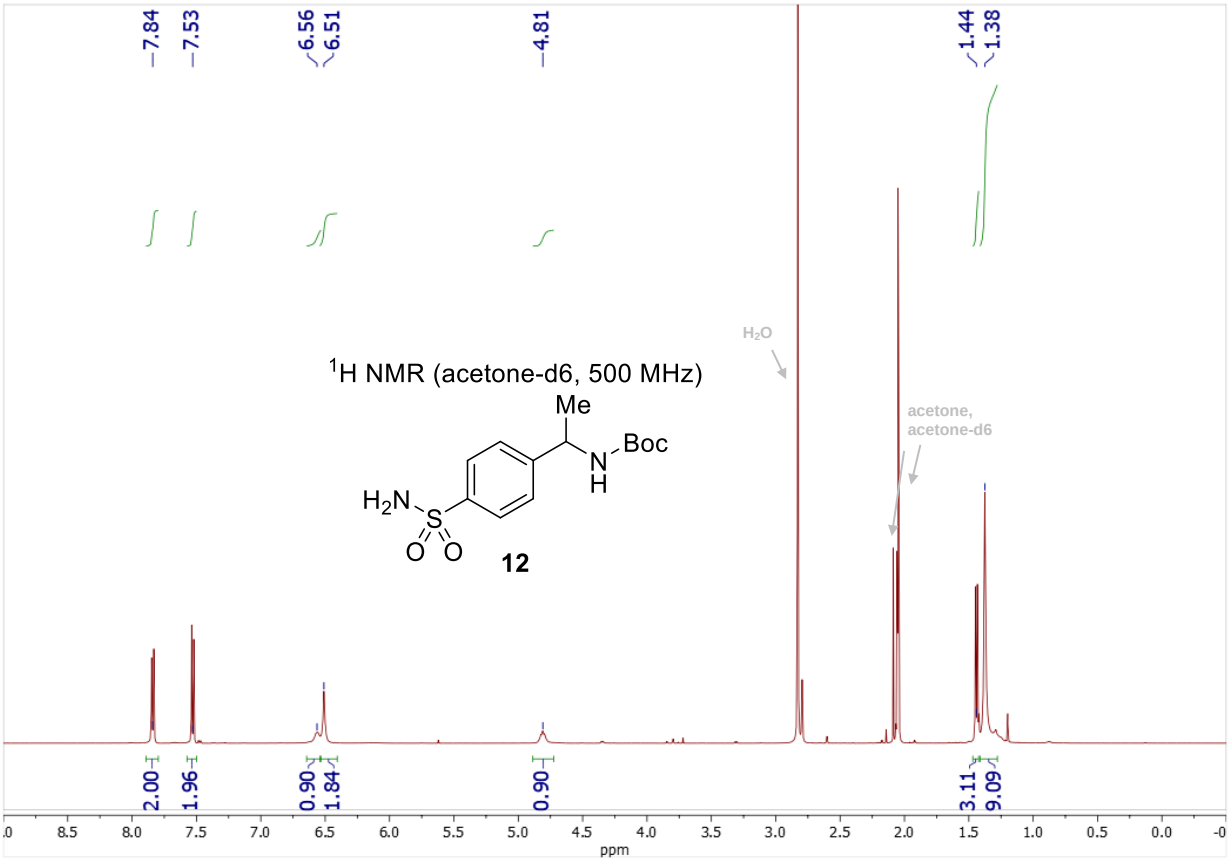
7.84
7.53
6.56
6.51
4.81
1.44
1.38
H2O
acetone,
acetone-d6
1H NMR (acetone-d6, 500 MHz)
Me
Boc
N
H
H2N
S
O
O
12
2.00
1.96
0.90
1.84
0.90
3.11
9.09
ppm

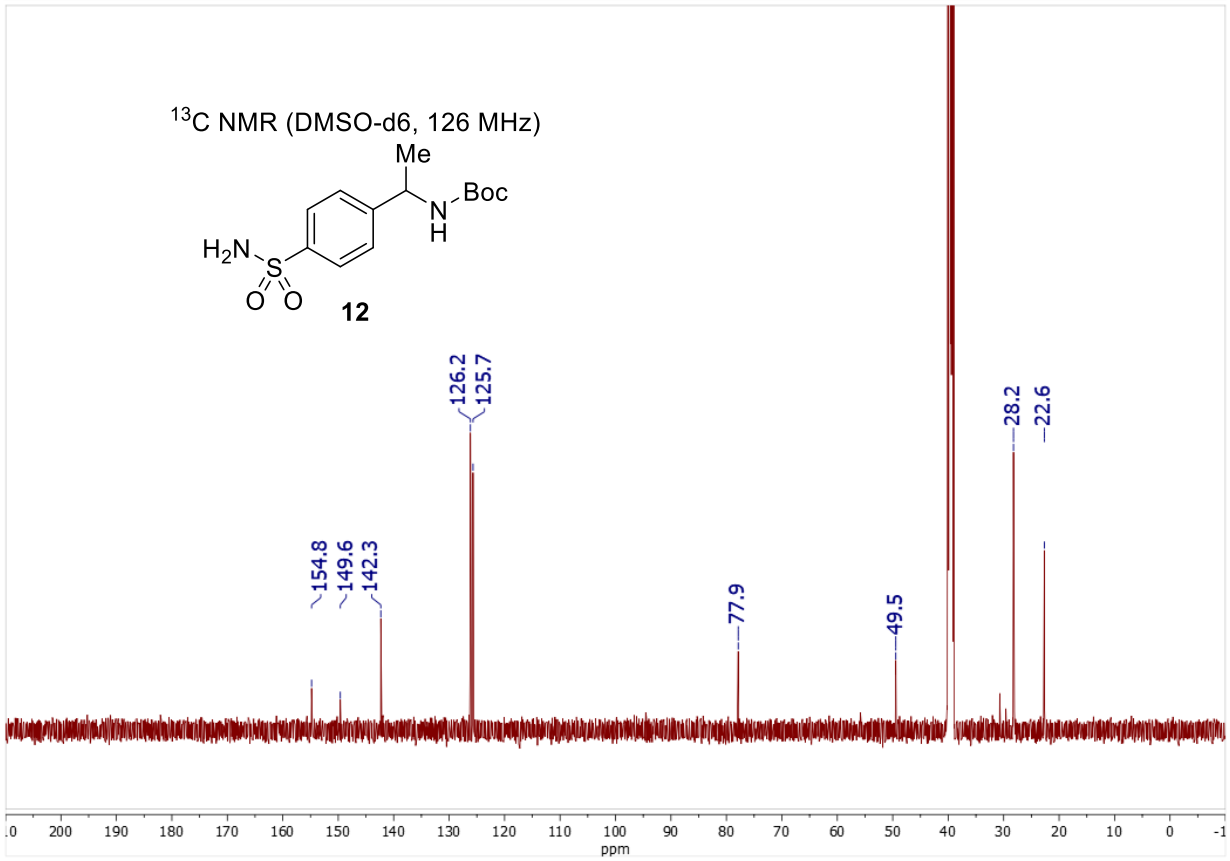
13C NMR (DMSO-d6, 126 MHz)
Me
Boc
N
H
H2N
S
O
O
12
126.2
125.7
28.2
22.6
154.8
149.6
142.3
77.9
49.5
ppm

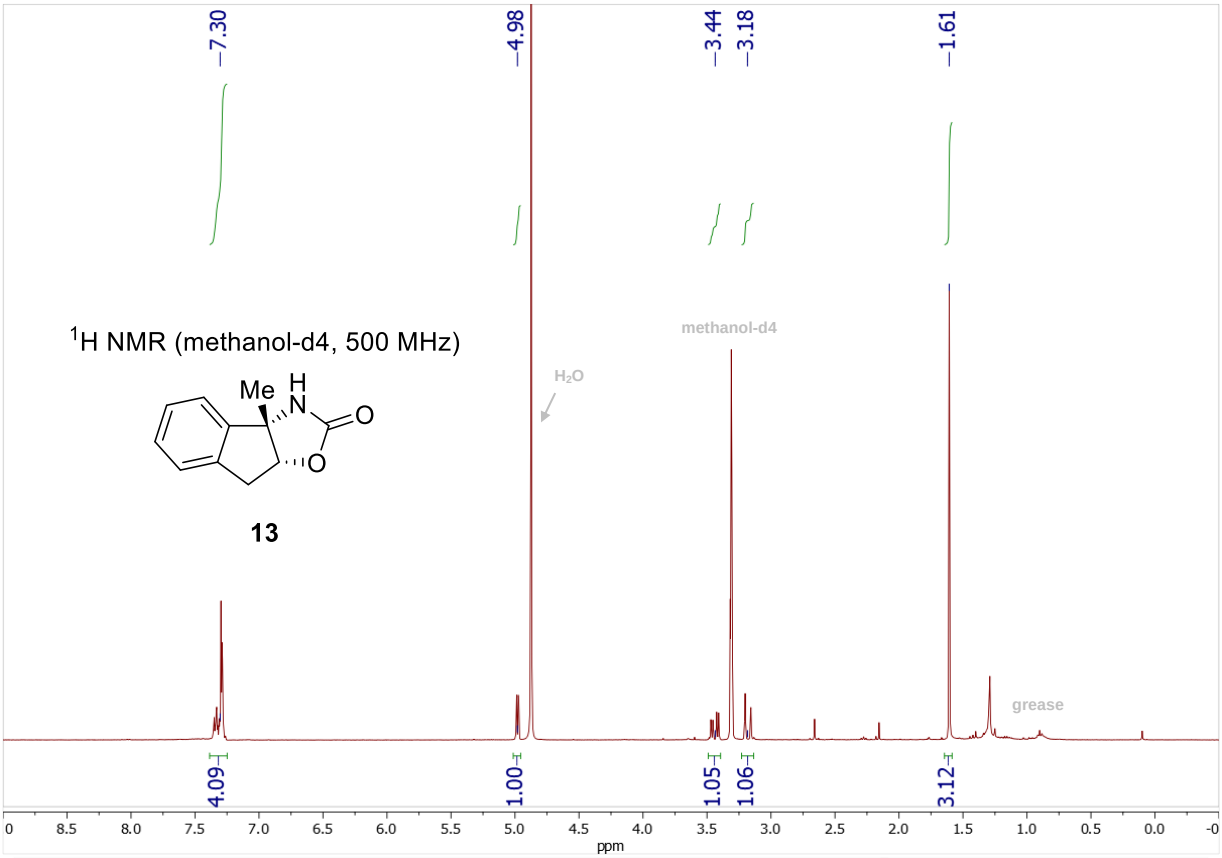
7.30
4.98
3.44
3.18
1.61
^{1}H NMR (methanol-d4, 500 MHz)
Me
H
N
O
O
13
methanol-d4
H$_2$O
grease
4.09
1.00
1.05
1.06
3.12
ppm

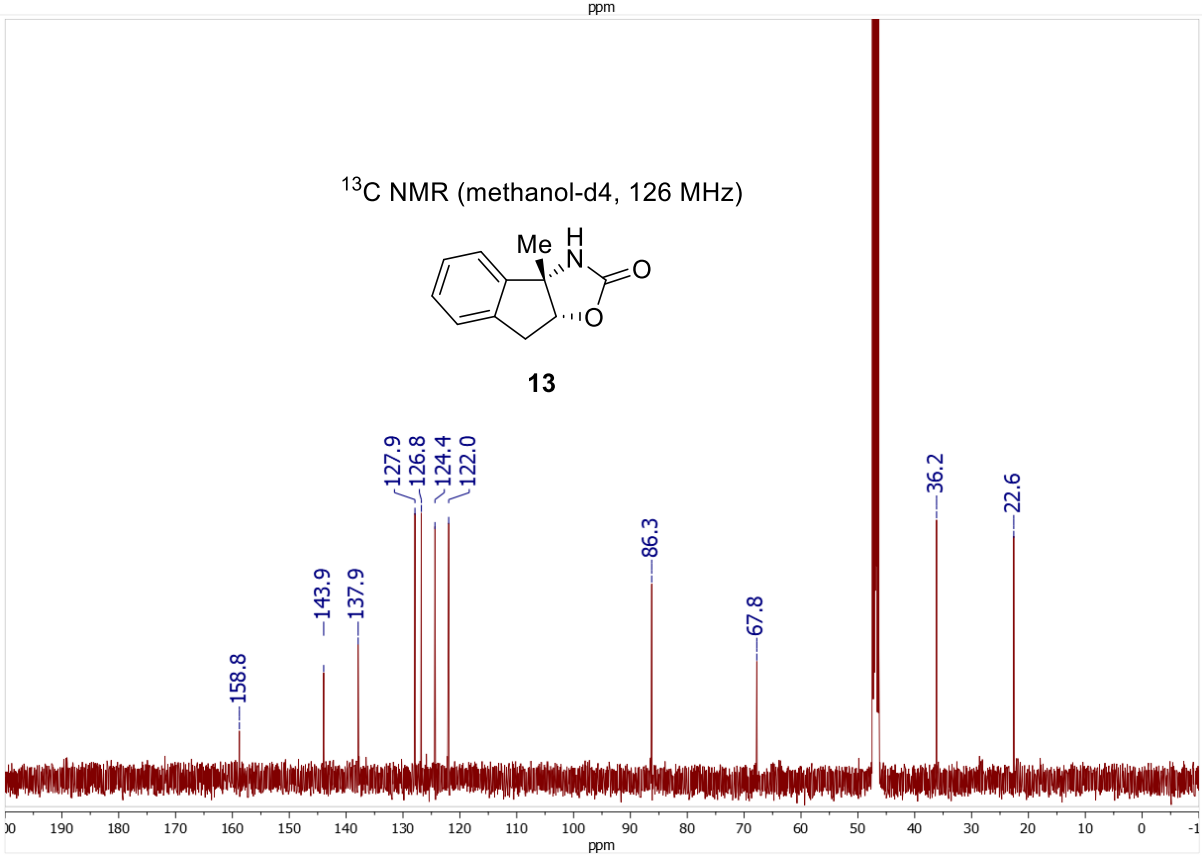
^{13}C NMR (methanol-d4, 126 MHz)
Me
H
N
O
O
13
127.9
126.8
124.4
122.0
143.9
137.9
158.8
86.3
67.8
36.2
22.6
ppm

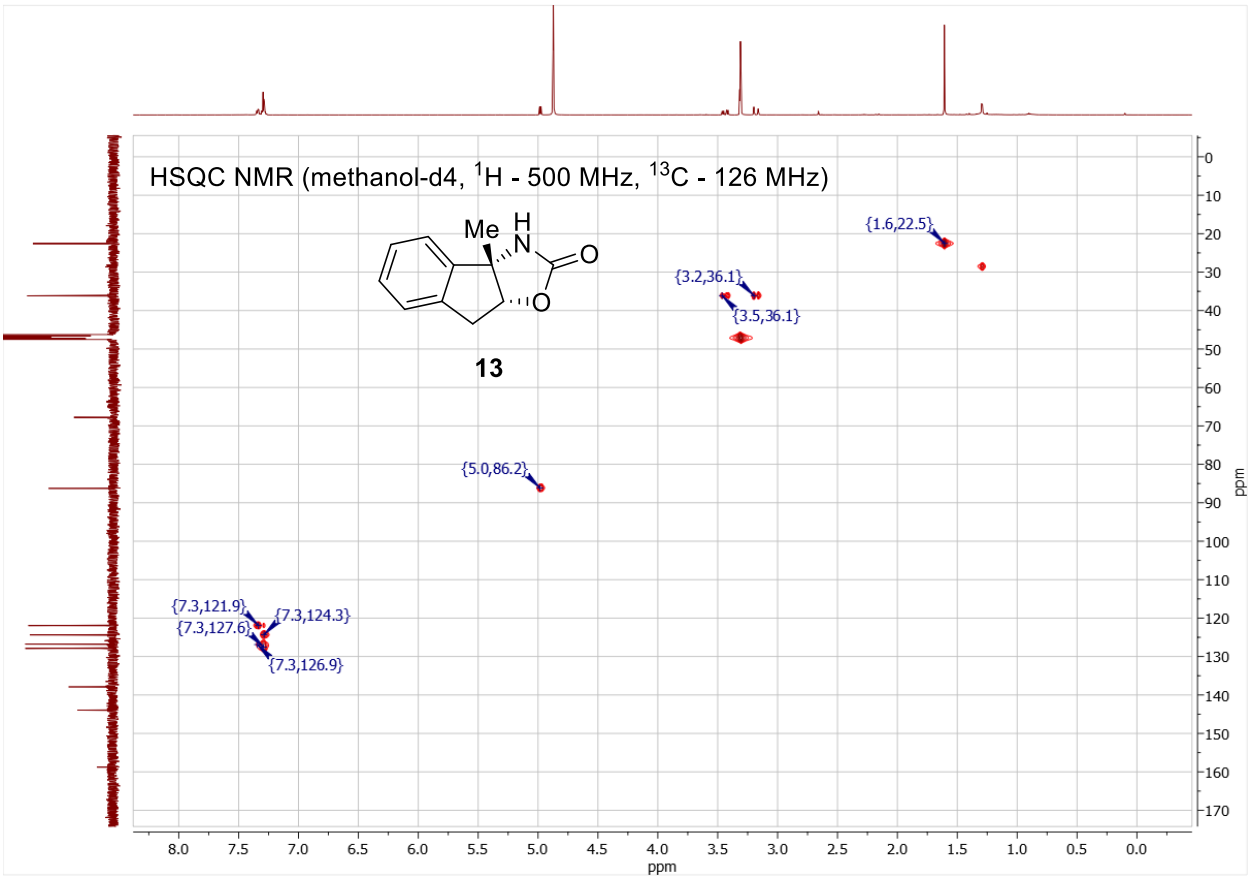
HSQC NMR (methanol-d4, 1H - 500 MHz, 13C - 126 MHz)
Me
H
N
O
O
13
{1.6,22.5}
{3.2,36.1}
{3.5,36.1}
{5.0,86.2}
{7.3,121.9}
{7.3,124.3}
{7.3,127.6}
{7.3,126.9}
ppm
ppm

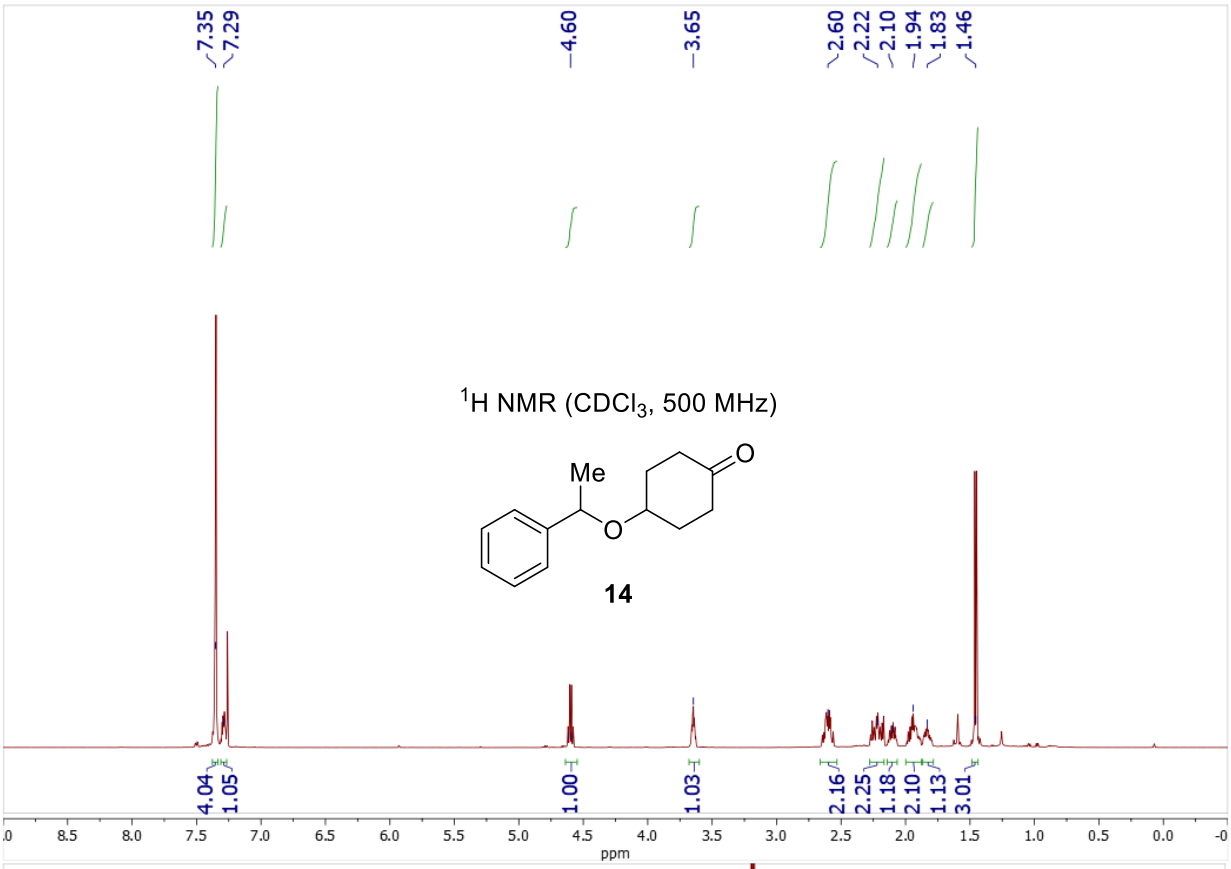
7.35
7.29
4.60
3.65
2.60
2.22
2.10
1.94
1.83
1.46
^{1}H NMR ($CDCl_3$, 500 MHz)
Me
O
O
14
4.04
1.05
1.00
1.03
2.16
2.25
1.18
2.10
1.13
3.01
ppm

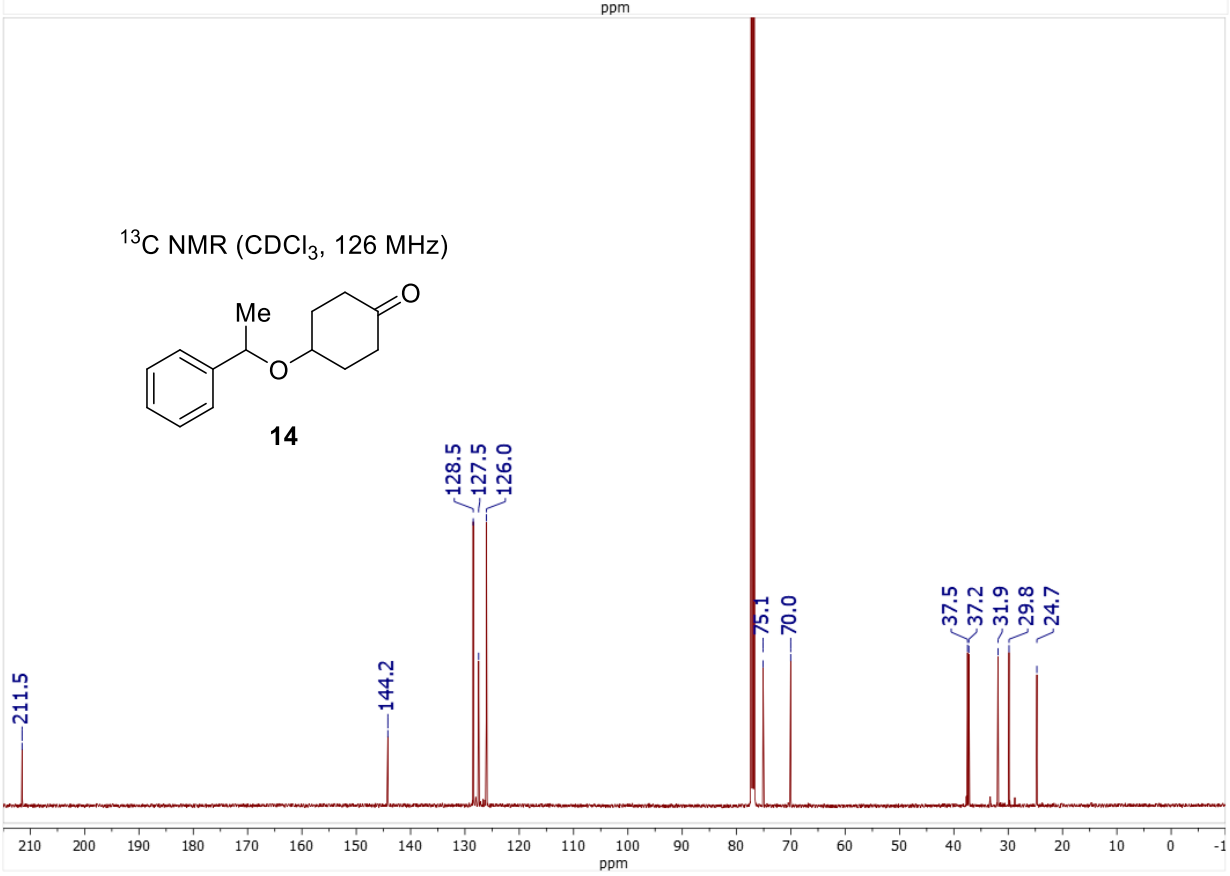
^{13}C NMR ($CDCl_3$, 126 MHz)
Me
O
O
14
128.5
127.5
126.0
211.5
144.2
75.1
70.0
37.5
37.2
31.9
29.8
24.7
ppm

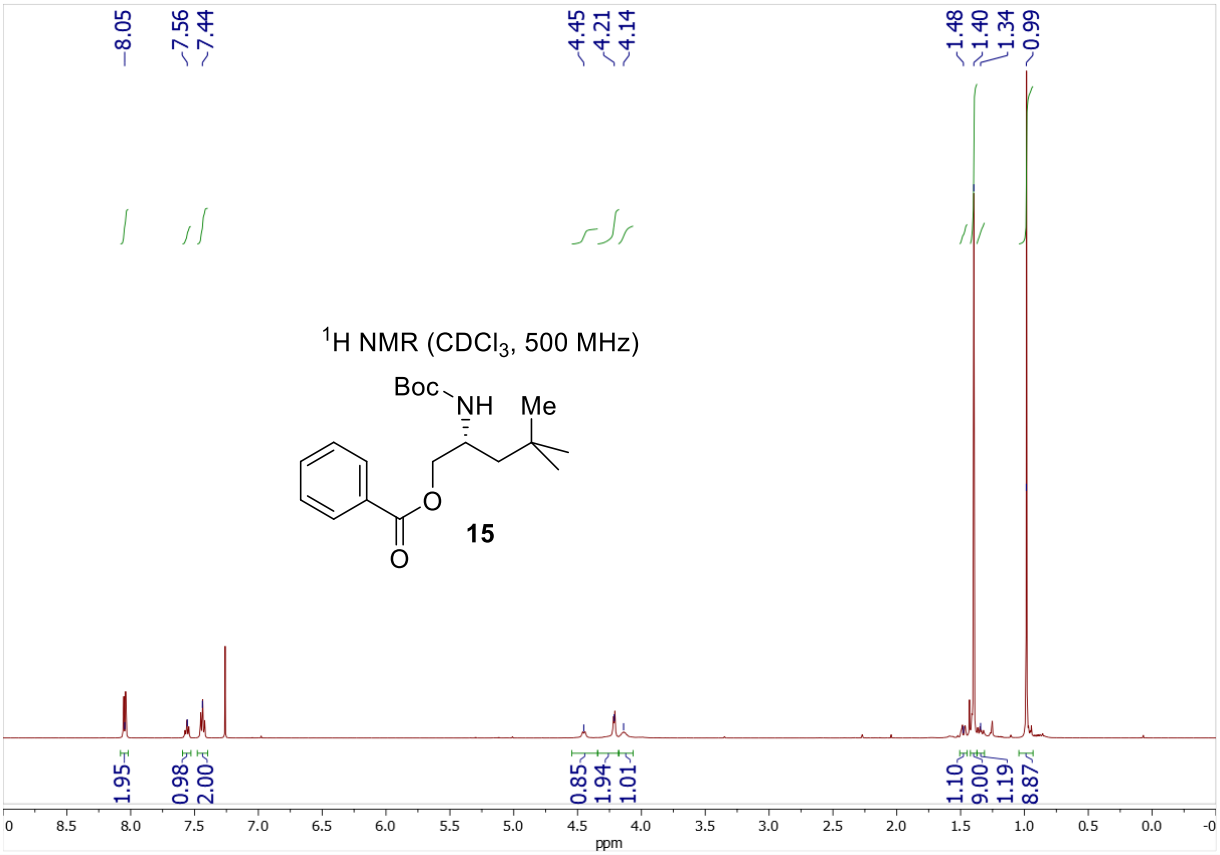
8.05
7.56
7.44
4.45
4.21
4.14
1.48
1.40
1.34
0.99
^{1}H NMR ($CDCl_3$, 500 MHz)
Boc
NH
Me
O
O
15
1.95
0.98
2.00
0.85
1.94
1.01
1.10
9.00
1.19
8.87
ppm

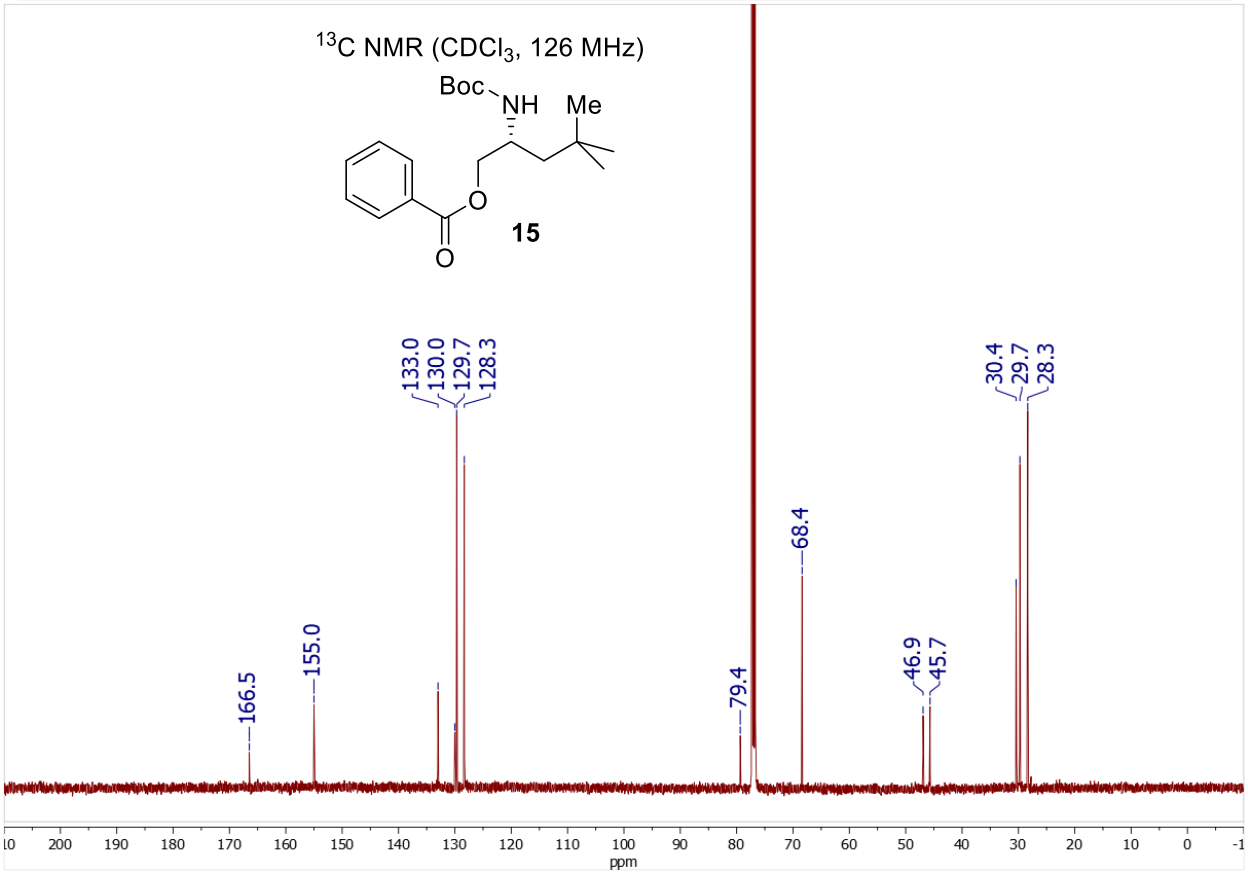
^{13}C NMR ($CDCl_3$, 126 MHz)
Boc
NH
Me
O
O
15
133.0
130.0
129.7
128.3
30.4
29.7
28.3
68.4
166.5
155.0
79.4
46.9
45.7
ppm

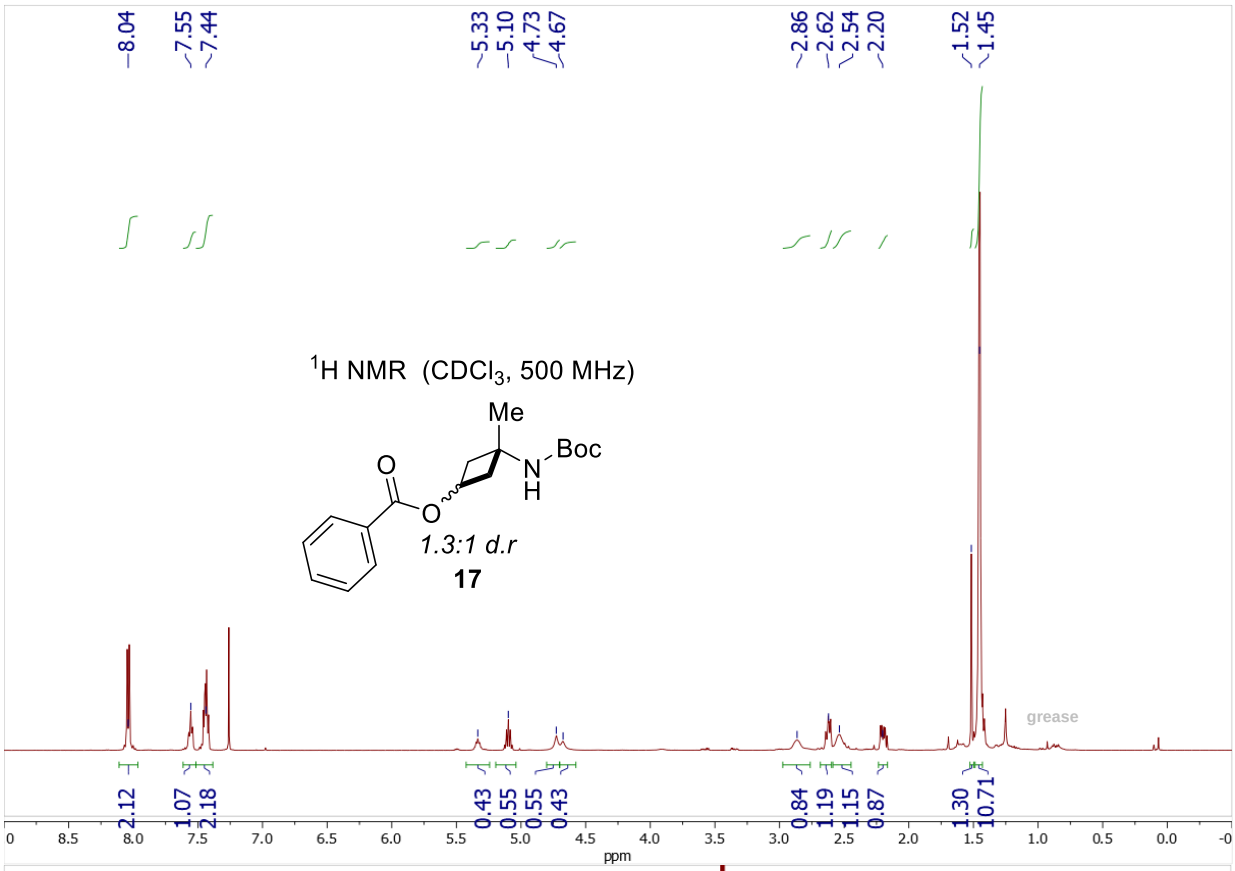

^{1}H NMR ($CDCl_3$, 500 MHz)

1.3:1 d.r

17

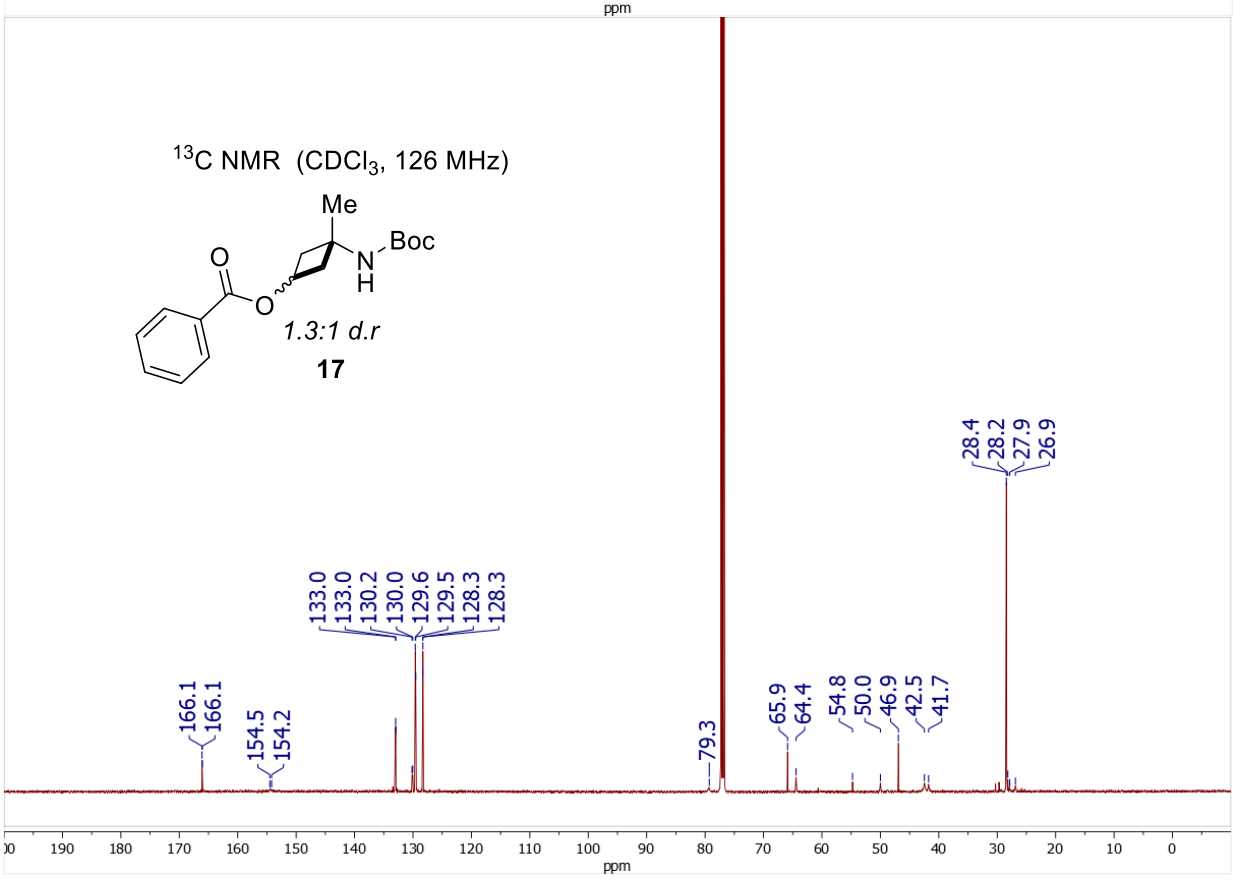

^{13}C NMR ($CDCl_3$, 126 MHz)

1.3:1 d.r

17

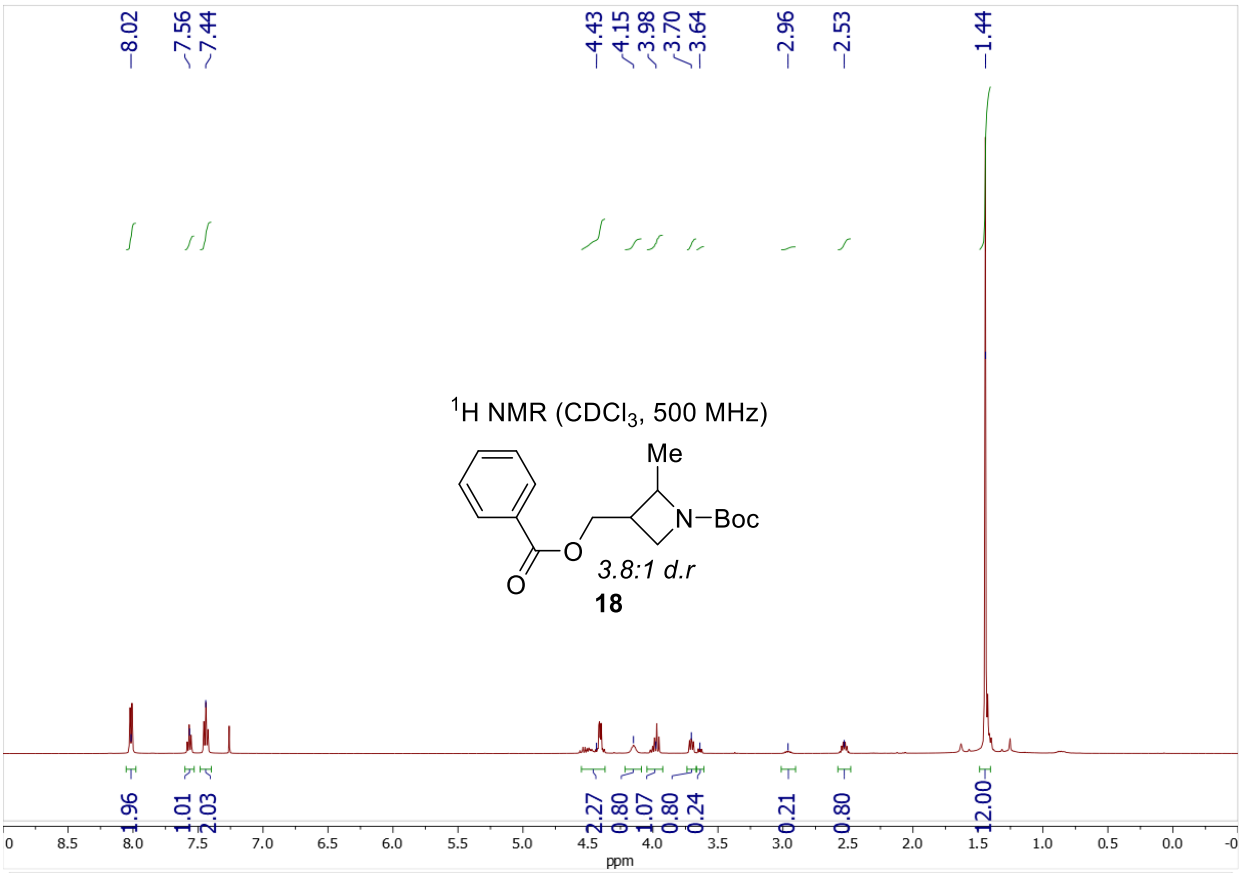
8.02
7.56
7.44
4.43
4.15
3.98
3.70
3.64
2.96
2.53
1.44
1H NMR (CDCl3, 500 MHz)
Me
N–Boc
O
O
3.8:1 d.r
18
1.96
1.01
2.03
2.27
0.80
1.07
0.80
0.24
0.21
0.80
12.00
ppm

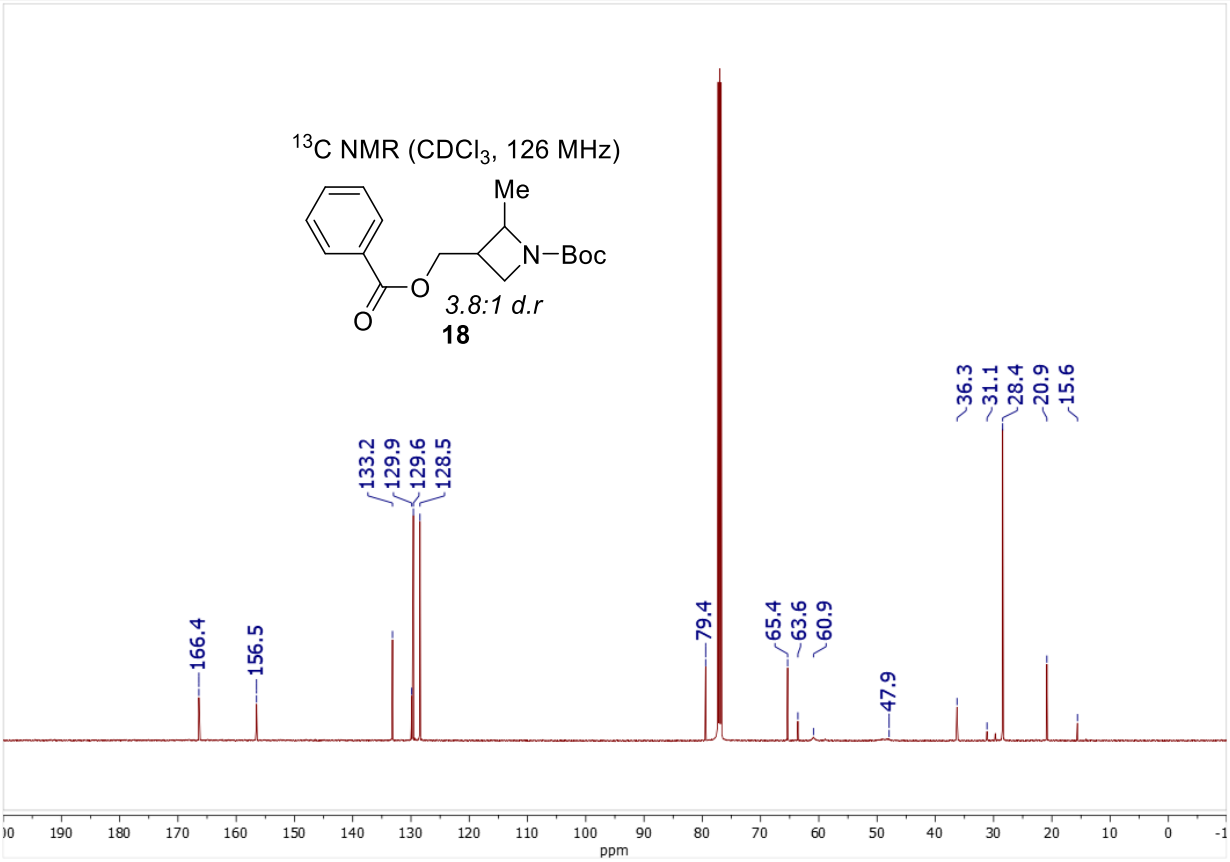
13C NMR (CDCl3, 126 MHz)
Me
N–Boc
O
O
3.8:1 d.r
18
166.4
156.5
133.2
129.9
129.6
128.5
79.4
65.4
63.6
60.9
47.9
36.3
31.1
28.4
20.9
15.6
ppm

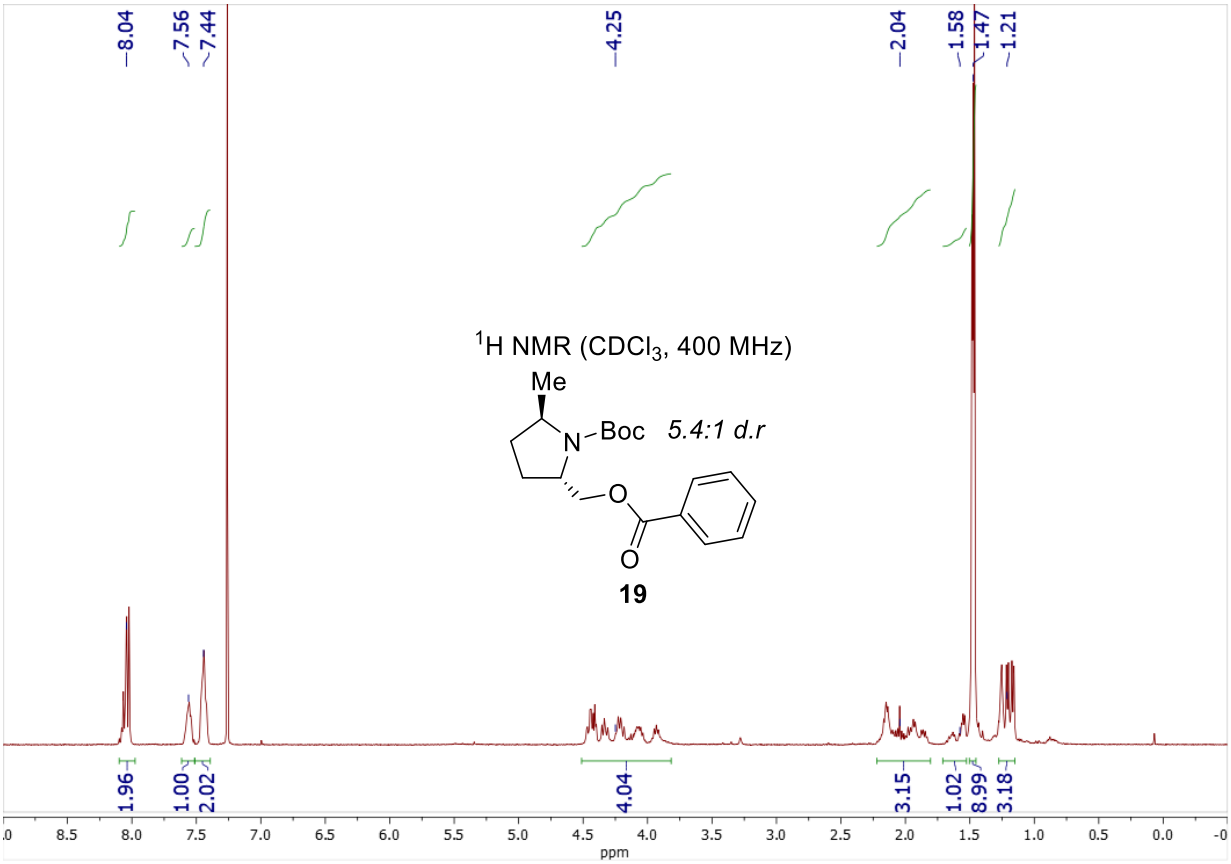

A combination of diastereomers and Boc rotamers make these spectra complex (tert-butyl peak above is >3 peaks).

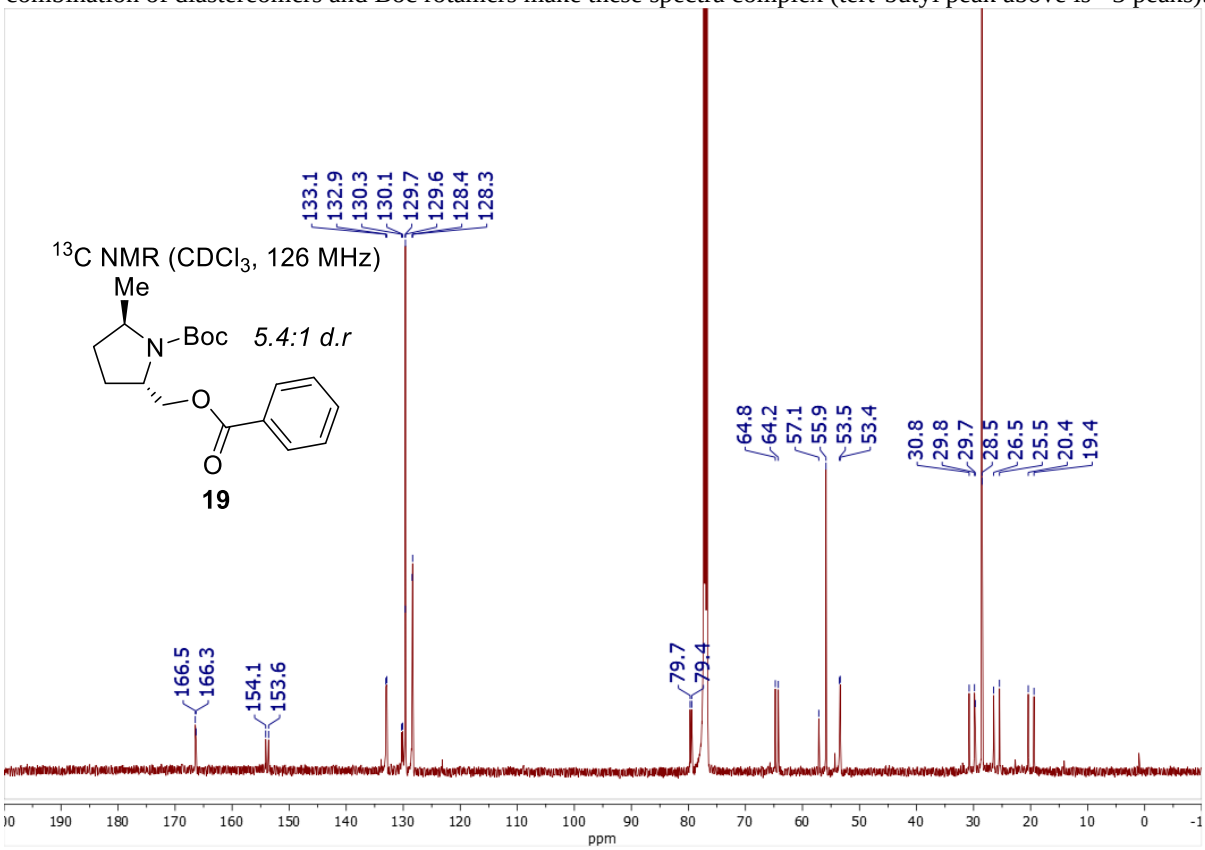

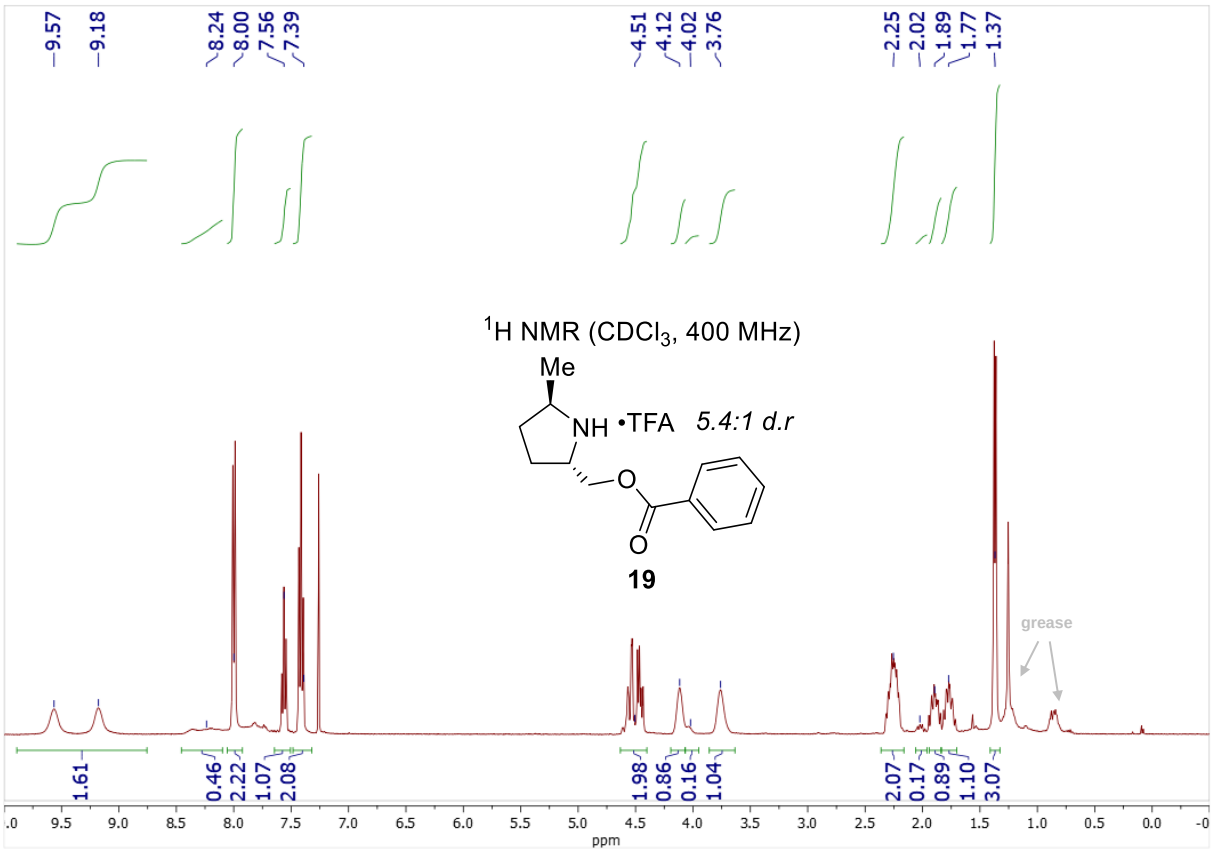

Boc from **19** was removed with TFAH, which eliminated rotameric peaks.

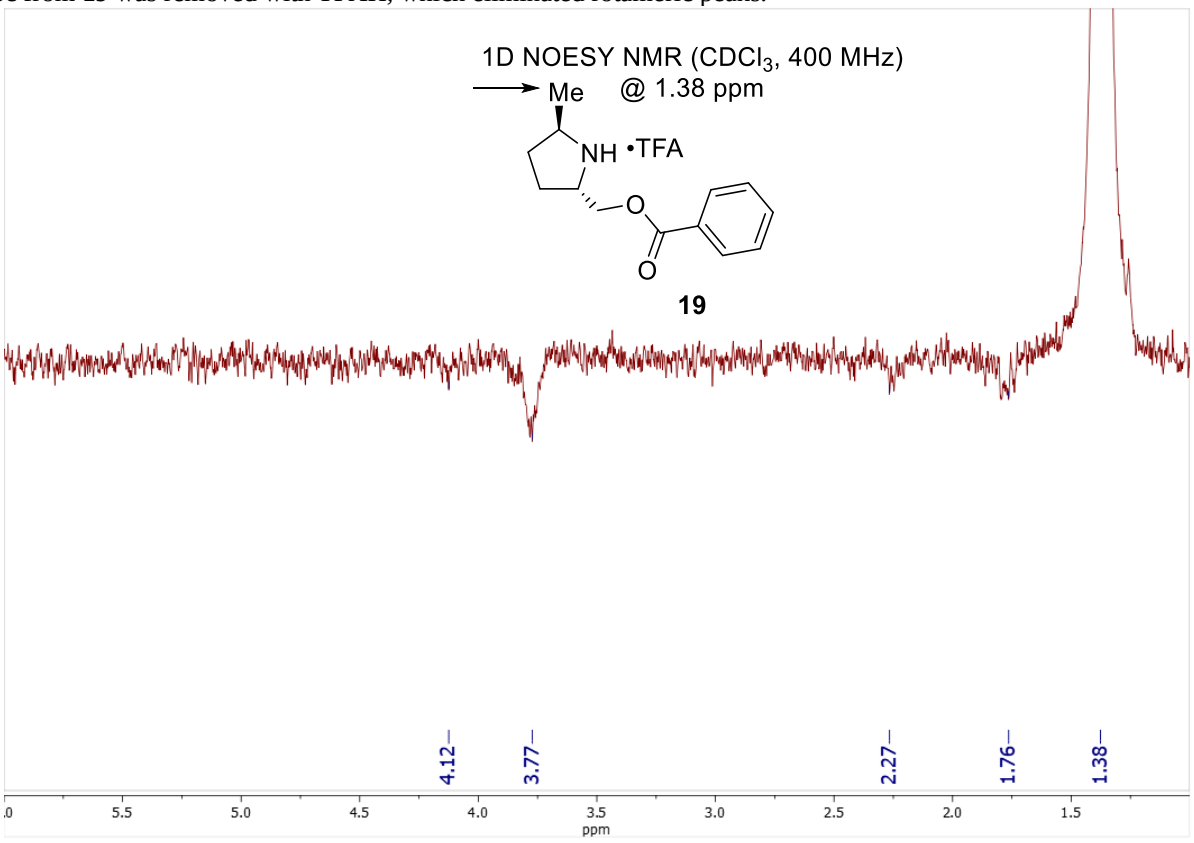

The Me group at 1.38 ppm interacts with the hydrogen across nitrogen, while the two α-amino hydrogens do not interact with one another. This suggests trans configuration.

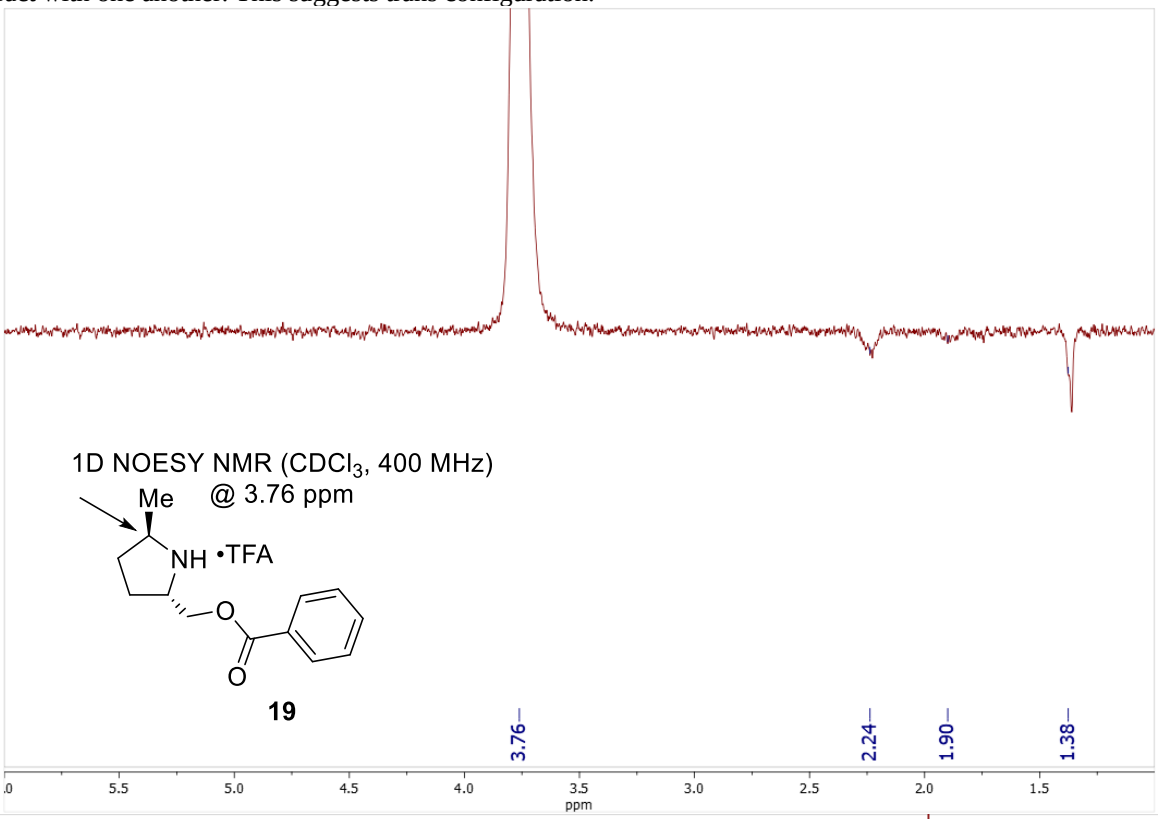

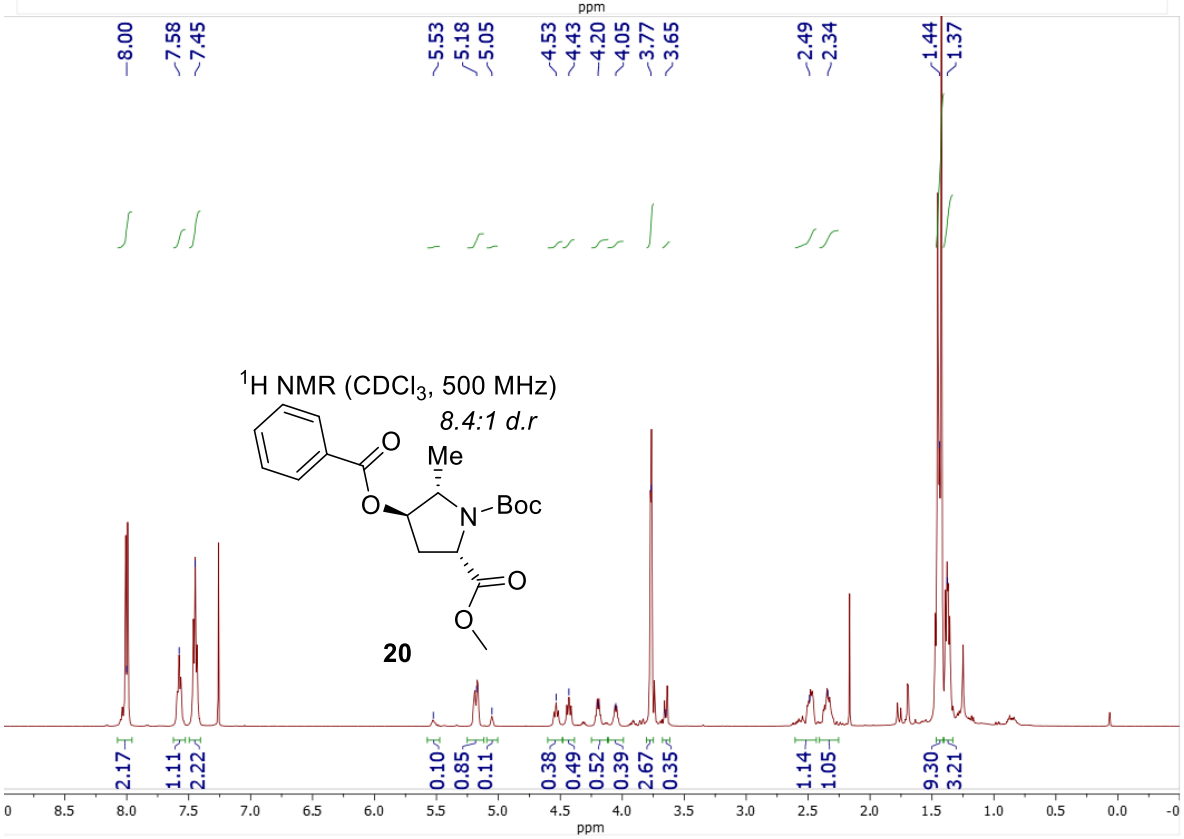

A combination of diastereomers and Boc rotamers make these spectra complex (tert-butyl peak above is >3 peaks).

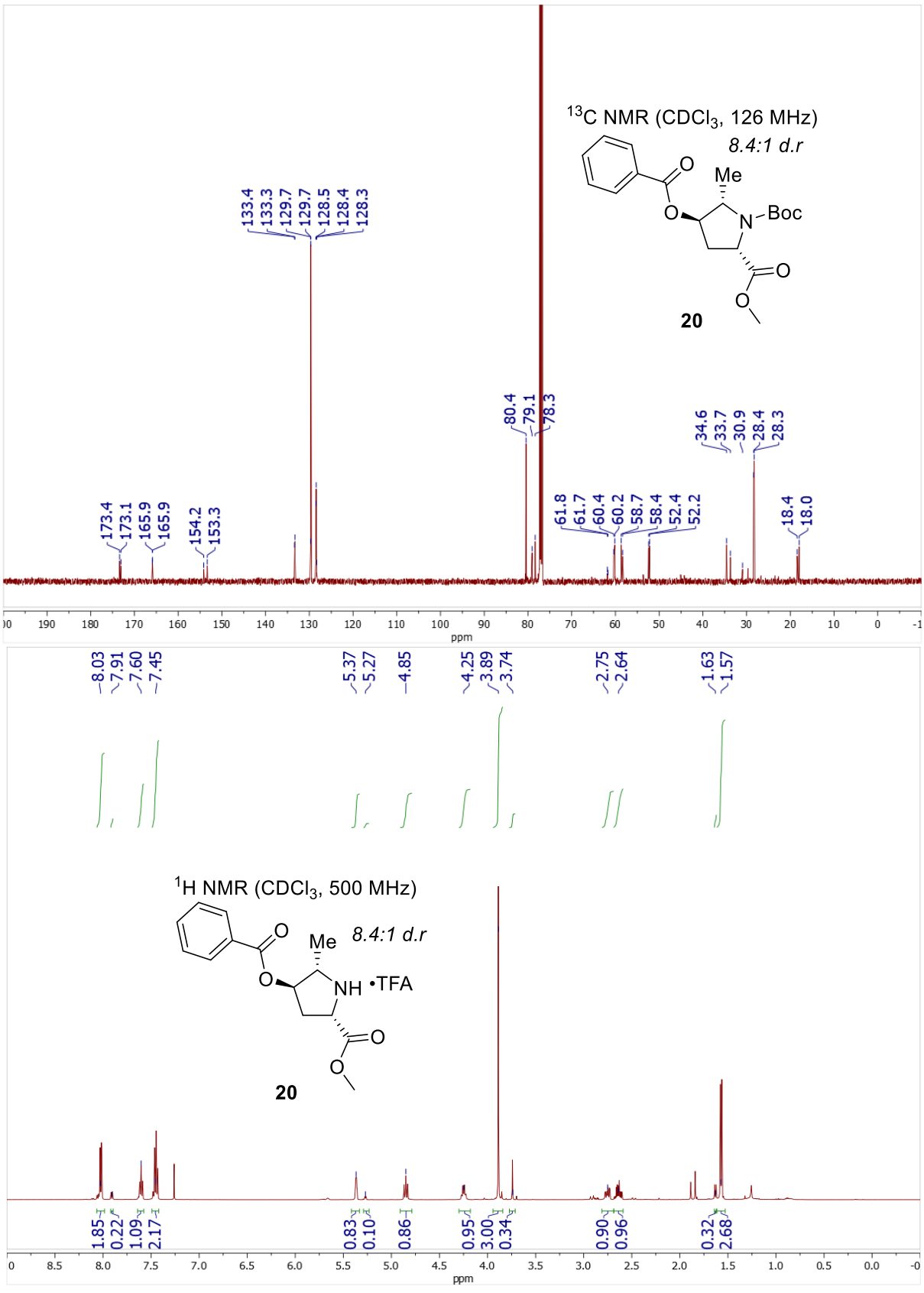

Boc from **20** was removed with TFAH, which eliminated rotameric peaks.

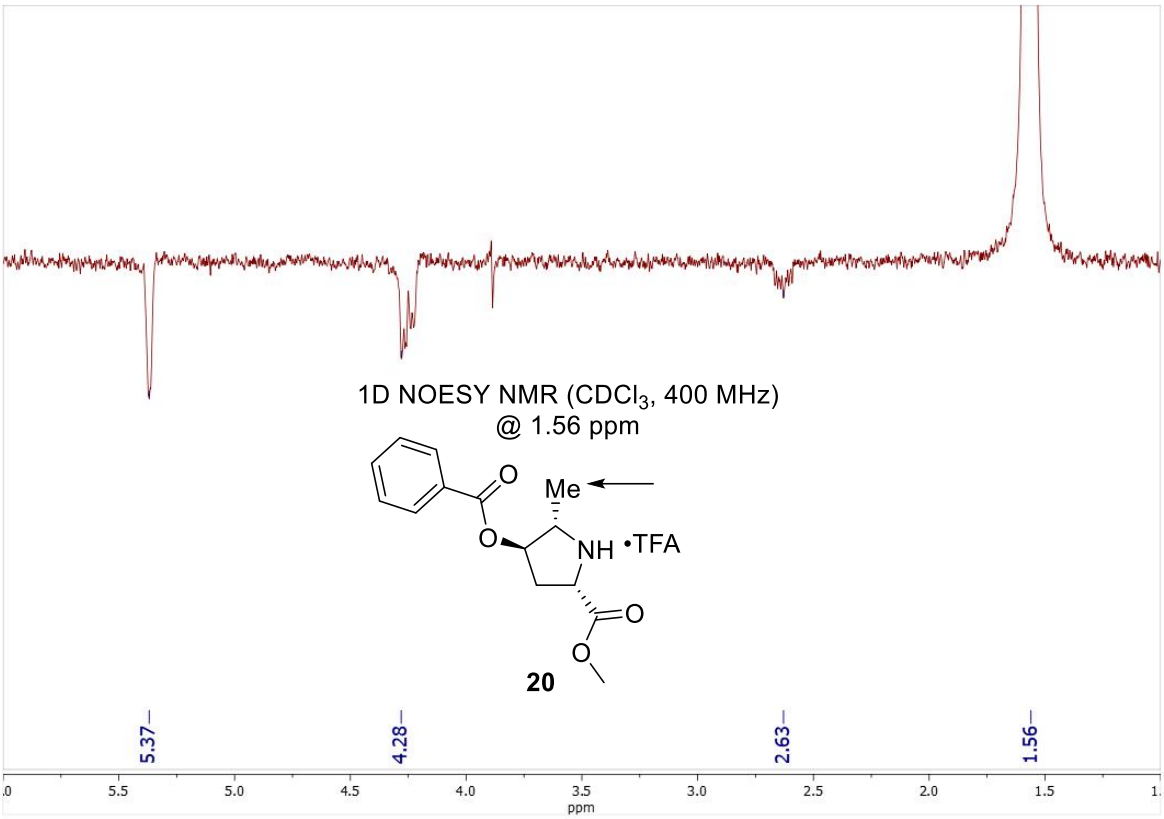

The Me group at 1.56 ppm does not interact with the hydrogen across nitrogen, but it does interact with the neighboring α-oxy C–H. The C2 C–H interacts with the C5 C–H. Taken together, these data suggest the shown major stereoconfiguration.

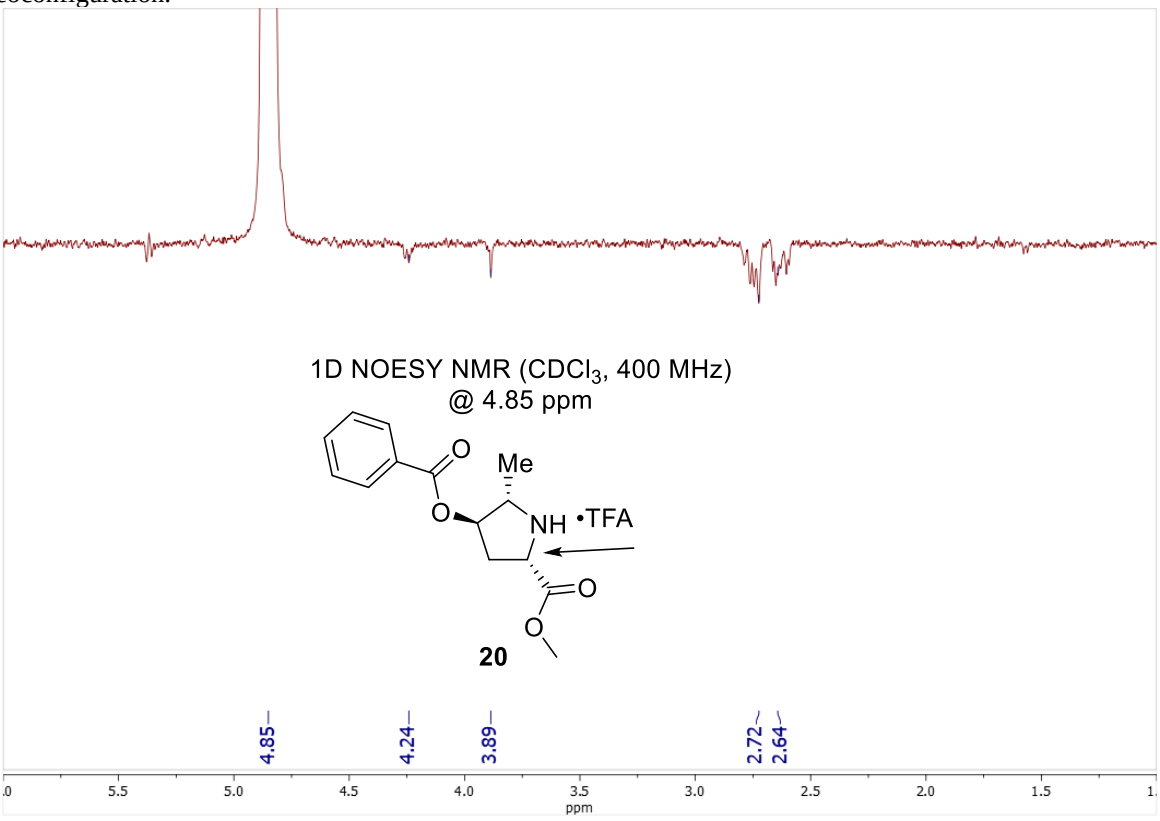

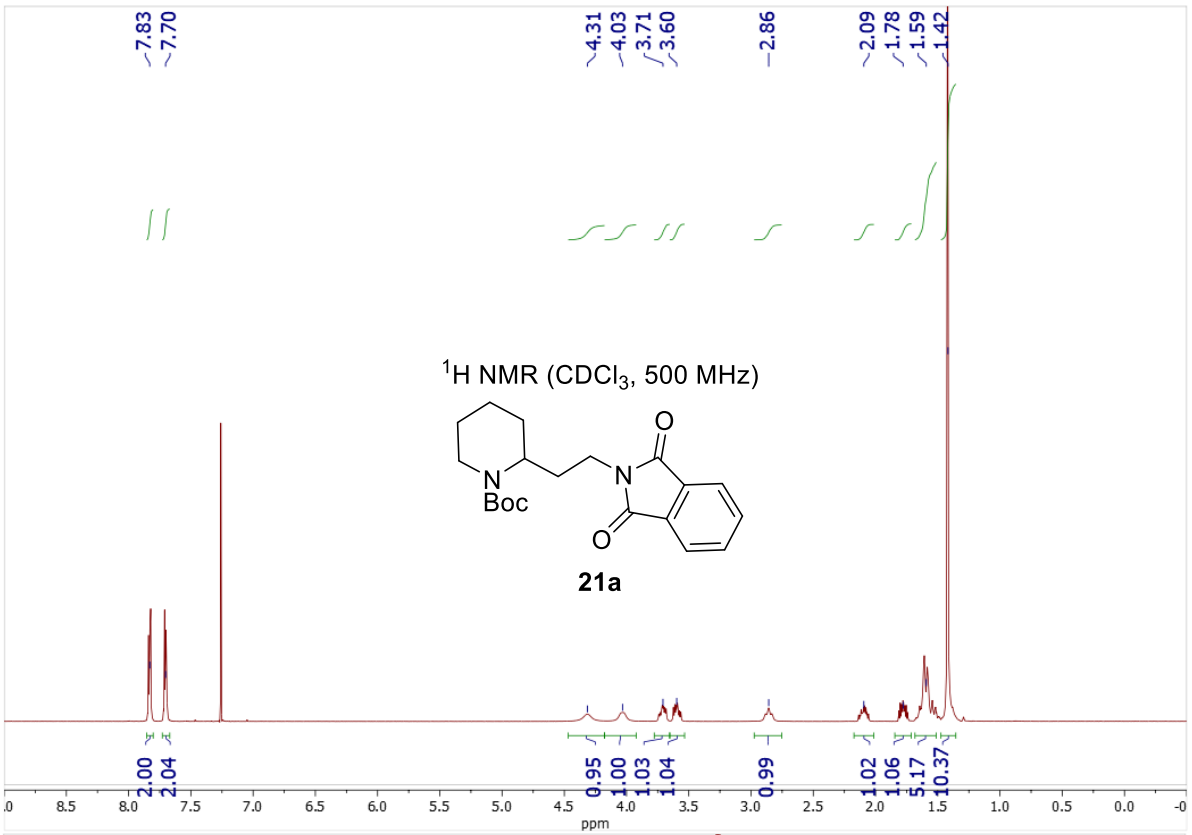
7.83
7.70
4.31
4.03
3.71
3.60
2.86
2.09
1.78
1.59
1.42
^{1}H NMR ($CDCl_3$, 500 MHz)
N
Boc
N
O
O
21a
2.00
2.04
0.95
1.00
1.03
1.04
0.99
1.02
1.06
5.17
10.37
ppm

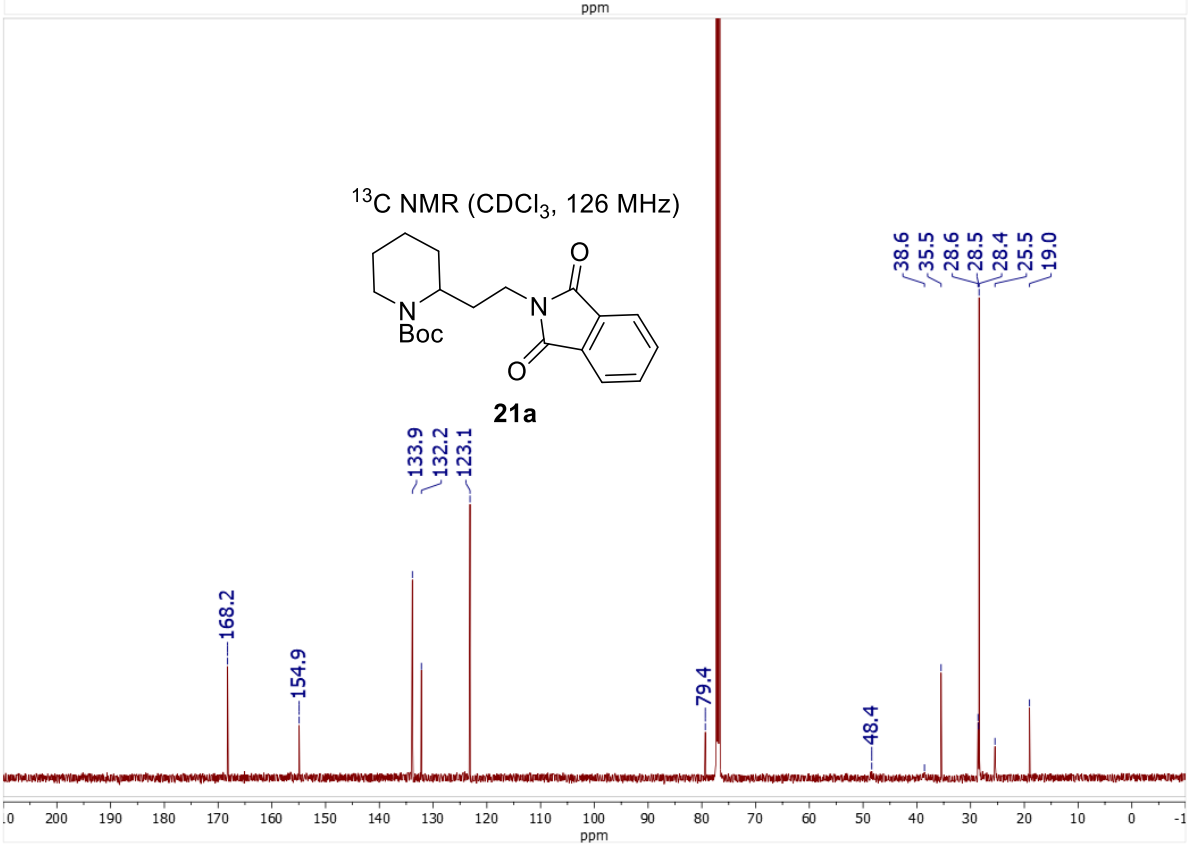
^{13}C NMR ($CDCl_3$, 126 MHz)
N
Boc
N
O
O
21a
38.6
35.5
28.6
28.5
28.4
25.5
19.0
133.9
132.2
123.1
168.2
154.9
79.4
48.4
ppm

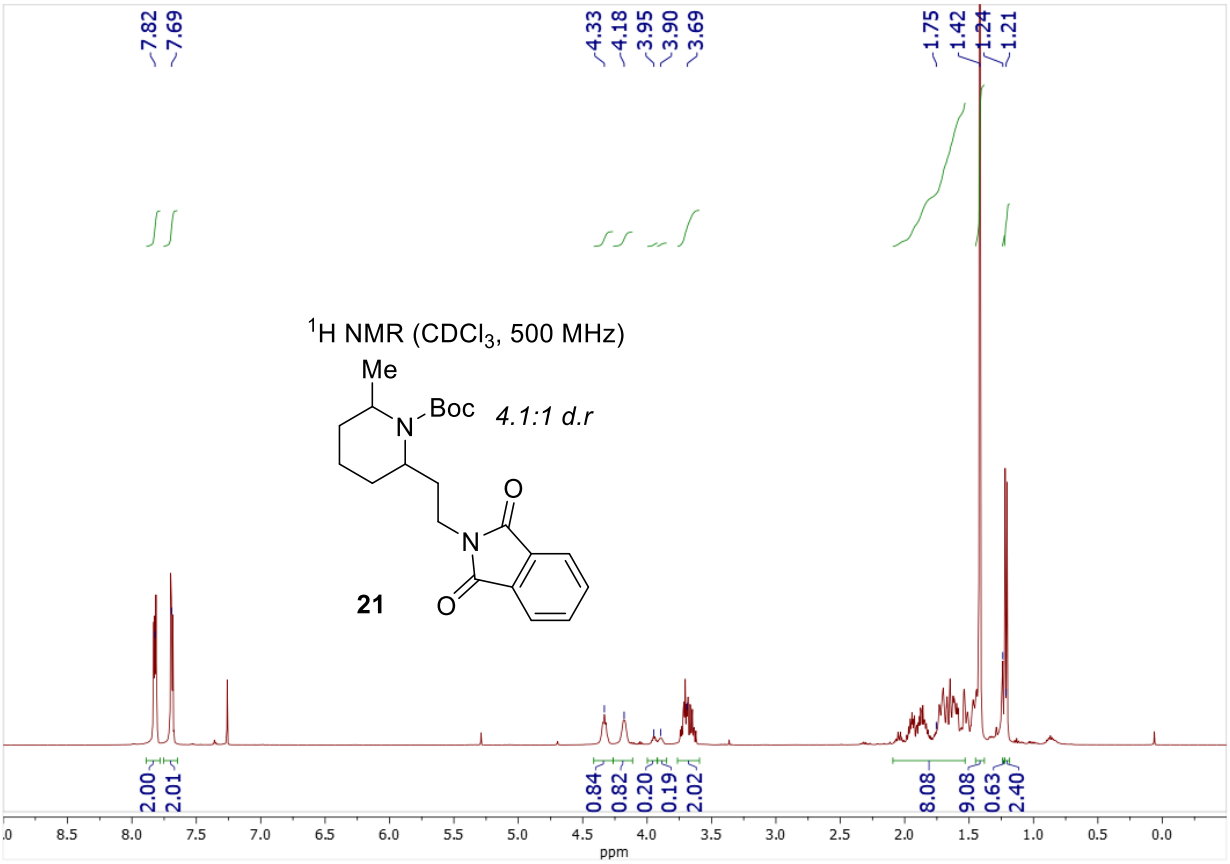
7.82
7.69
4.33
4.18
3.95
3.90
3.69
1.75
1.42
1.24
1.21
^{1}H NMR ($CDCl_3$, 500 MHz)
Me
Boc
N
4.1:1 d.r
O
N
O
21
2.00
2.01
0.84
0.82
0.20
0.19
2.02
8.08
9.08
0.63
2.40
ppm

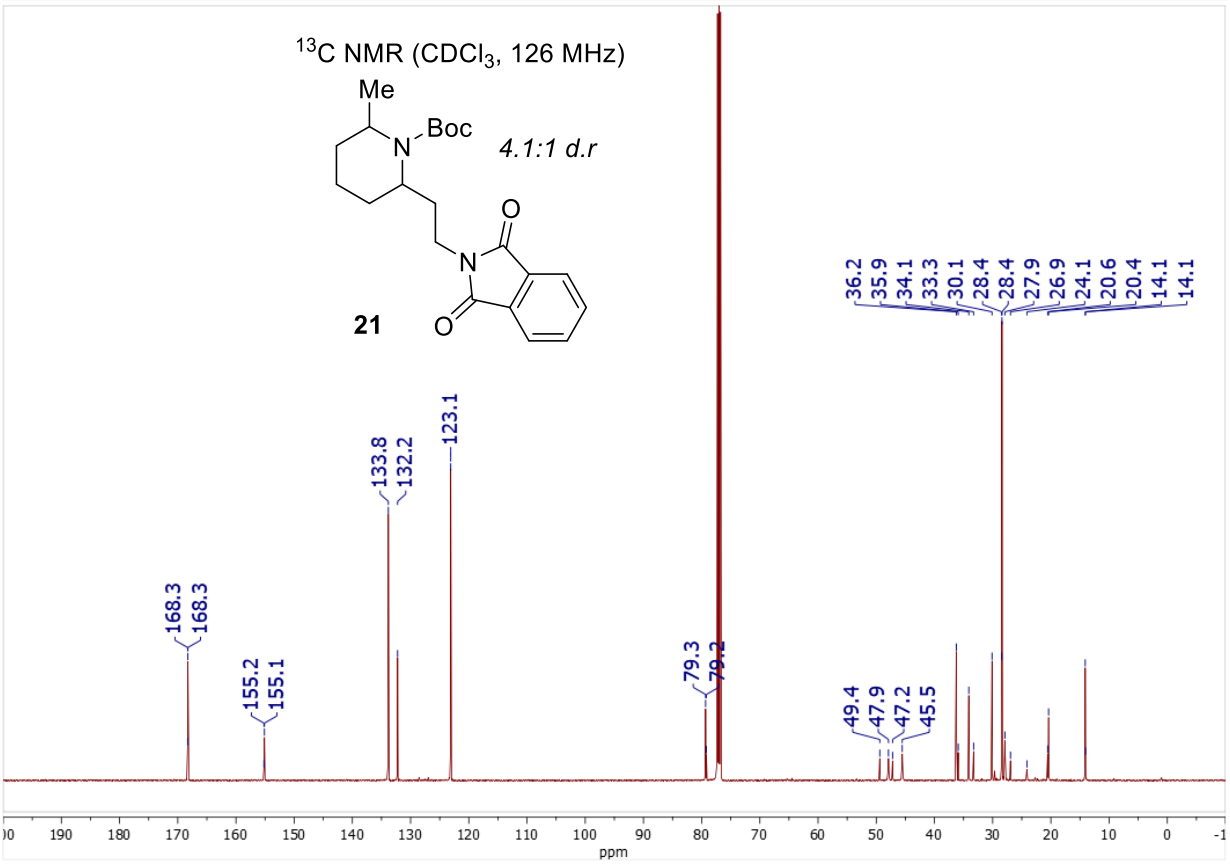
^{13}C NMR ($CDCl_3$, 126 MHz)
Me
Boc
N
4.1:1 d.r
O
N
O
21
36.2
35.9
34.1
33.3
30.1
28.4
28.4
27.9
26.9
24.1
20.6
20.4
14.1
14.1
133.8
132.2
123.1
168.3
168.3
155.2
155.1
79.3
79.2
49.4
47.9
47.2
45.5
ppm

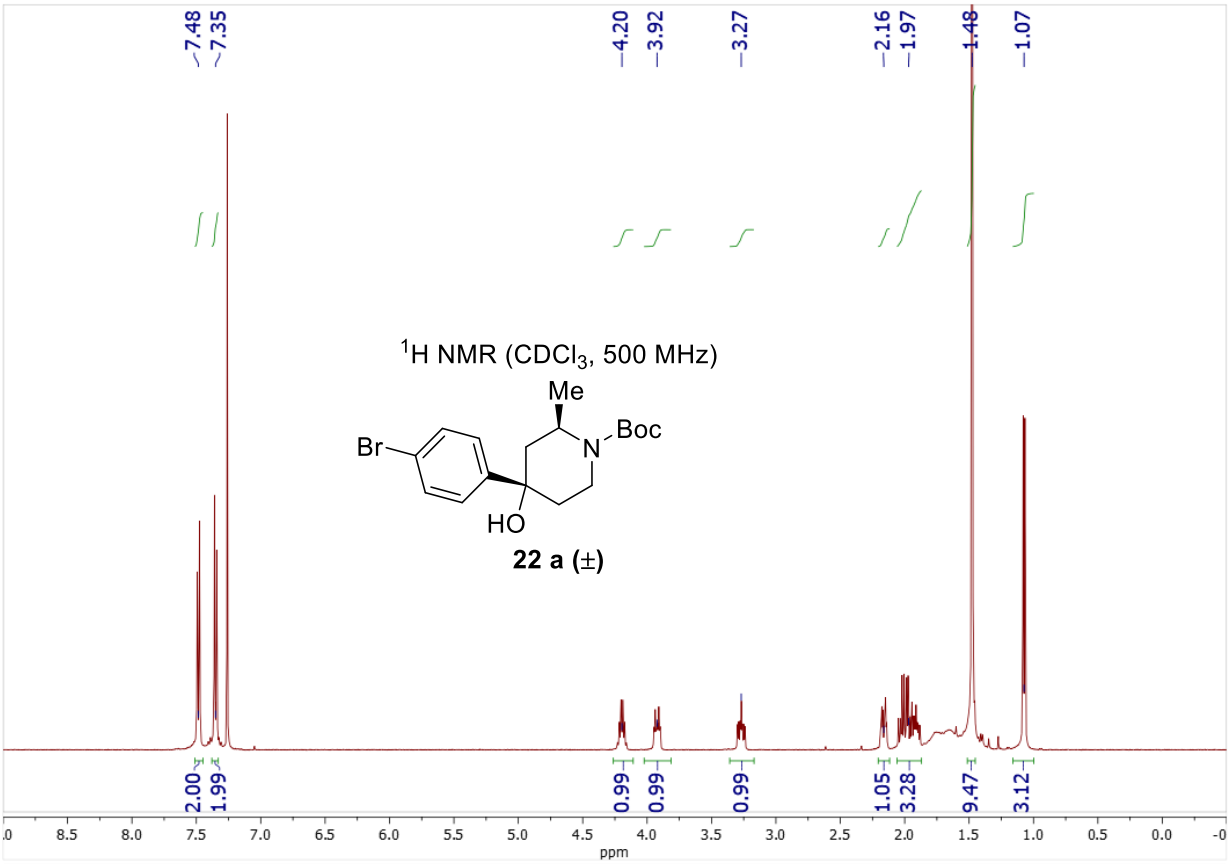

^{1}H NMR ($CDCl_3$, 500 MHz)

22 a (±)

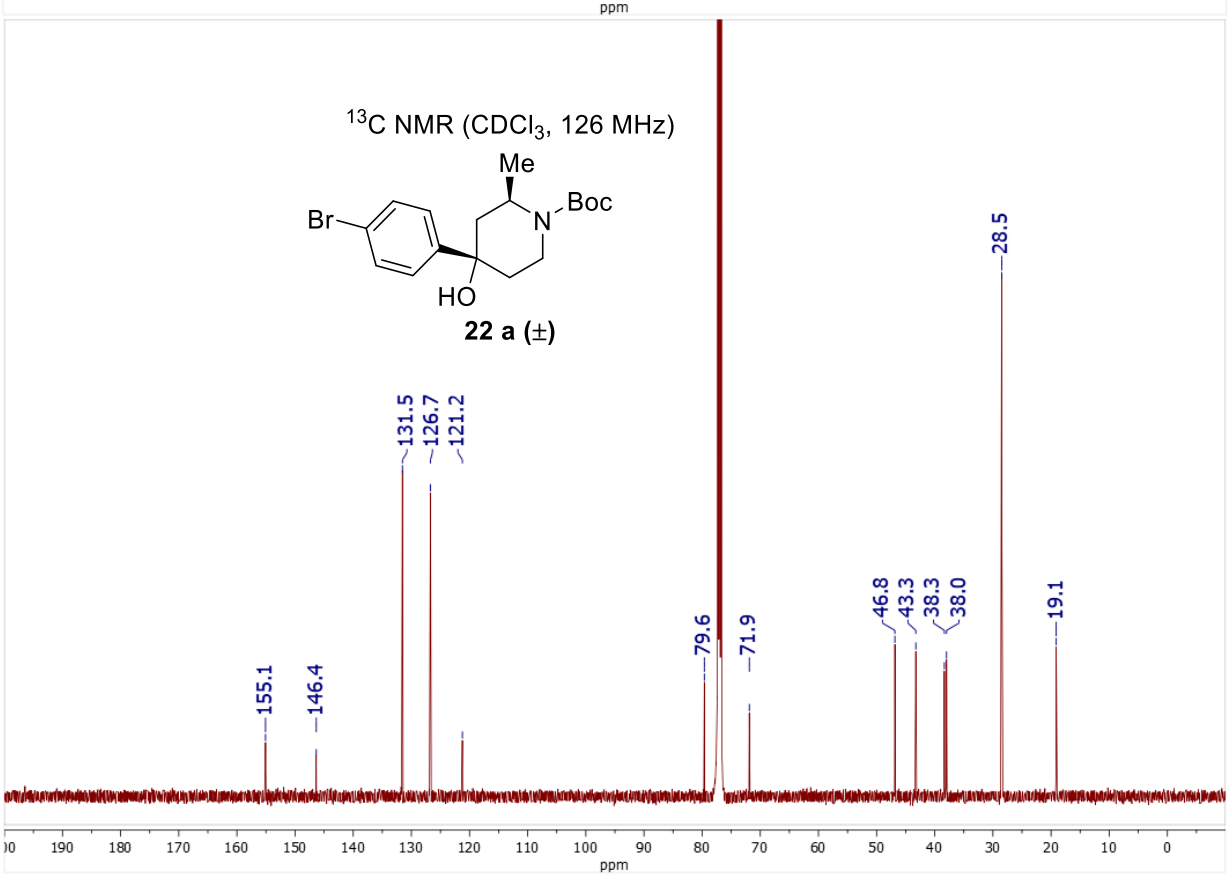

^{13}C NMR ($CDCl_3$, 126 MHz)

22 a (±)

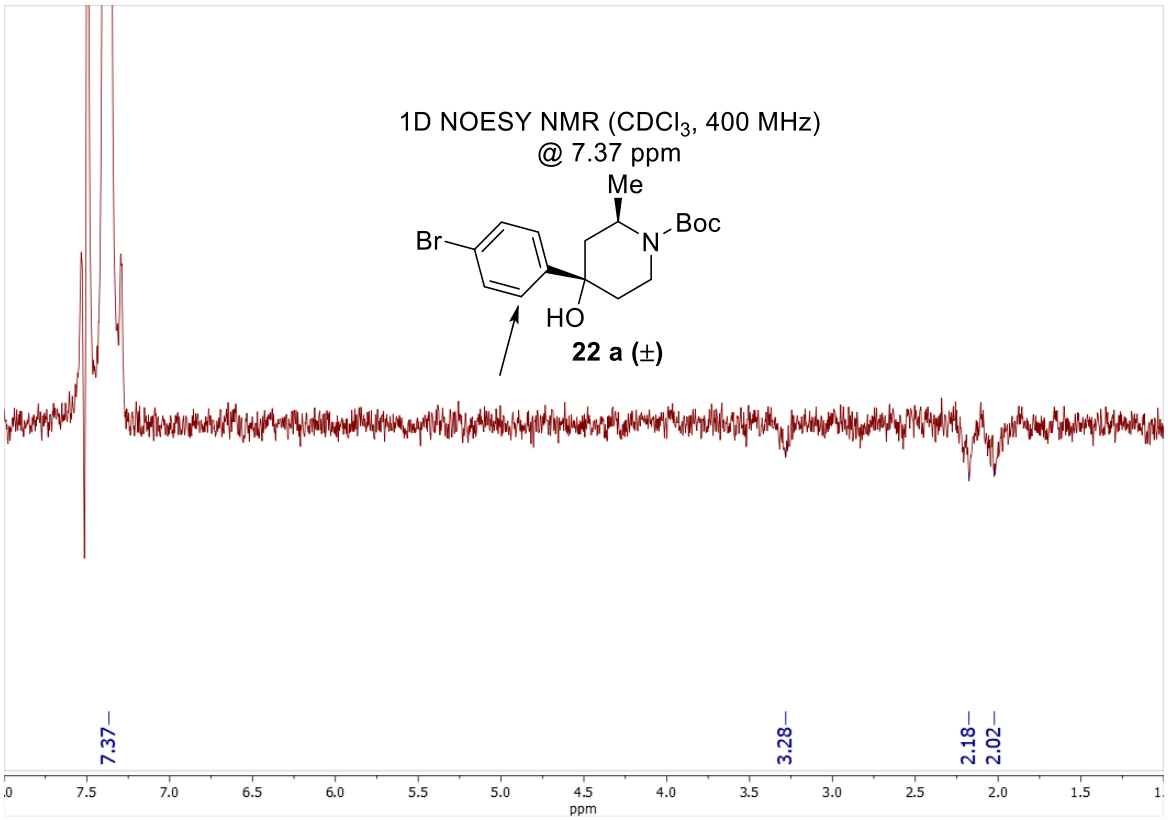

The aryl H atoms near the piperdine ring (7.37 ppm) interact with the same H atoms of the piperidine ring as the Me group at 1.10 ppm. This suggests that the two groups reside on the same face of the ring.

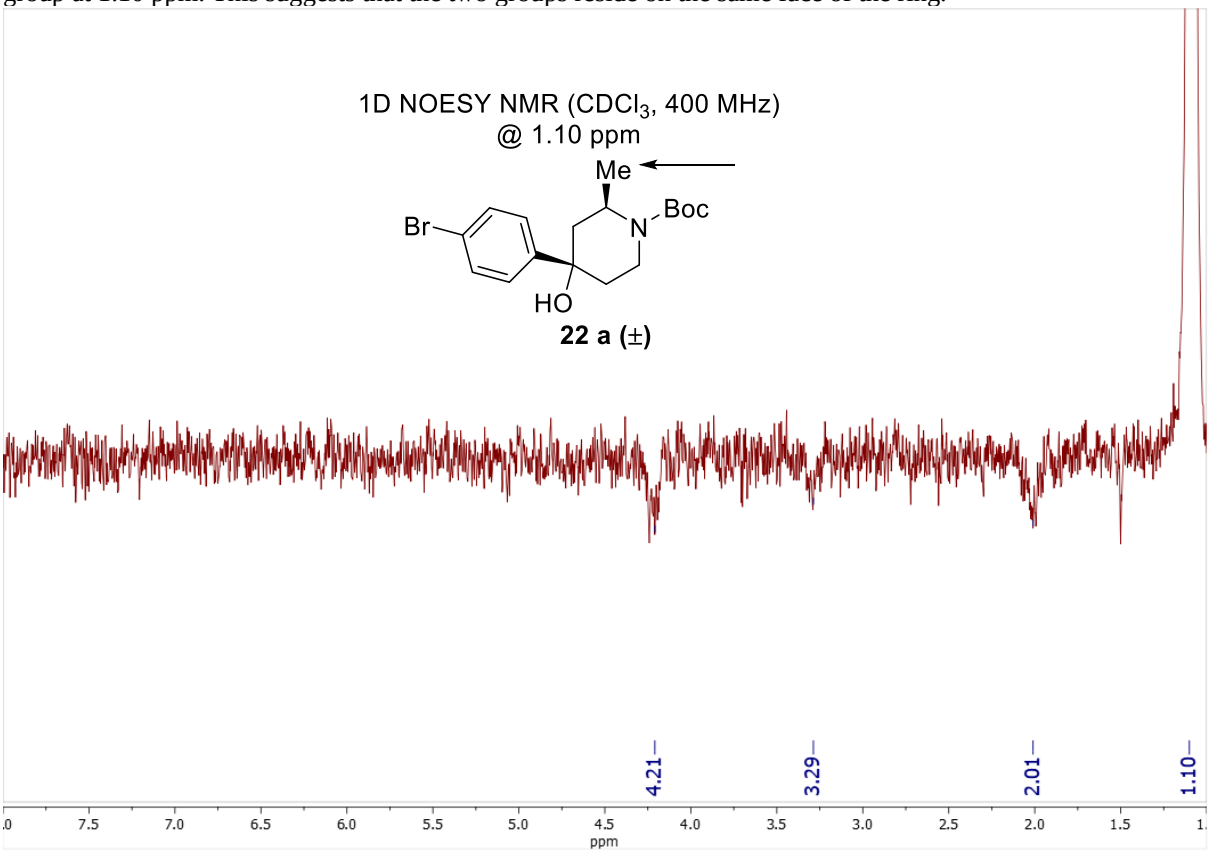

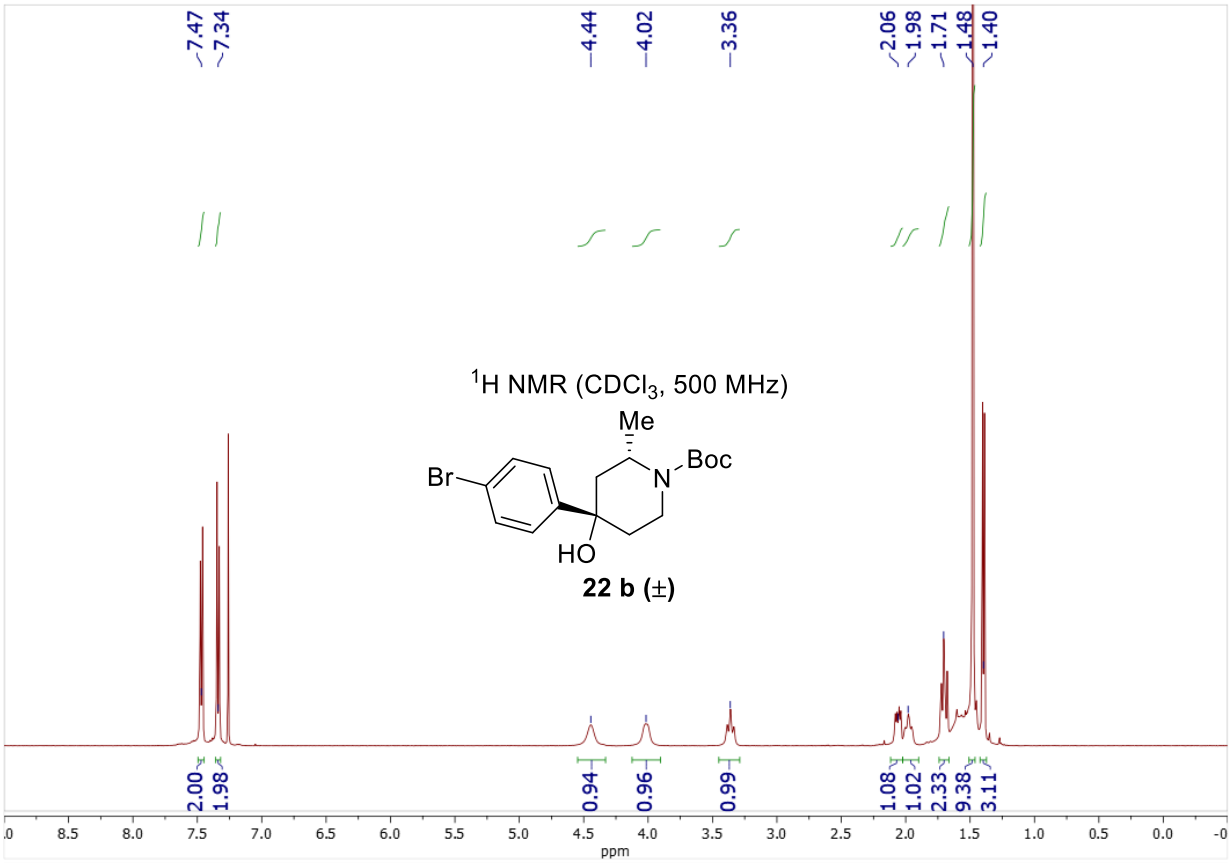
7.47
7.34
4.44
4.02
3.36
2.06
1.98
1.71
1.48
1.40
^{1}H NMR ($CDCl_3$, 500 MHz)
Me
Br
N
Boc
HO
22 b (±)
2.00
1.98
0.94
0.96
0.99
1.08
1.02
2.33
9.38
3.11
ppm

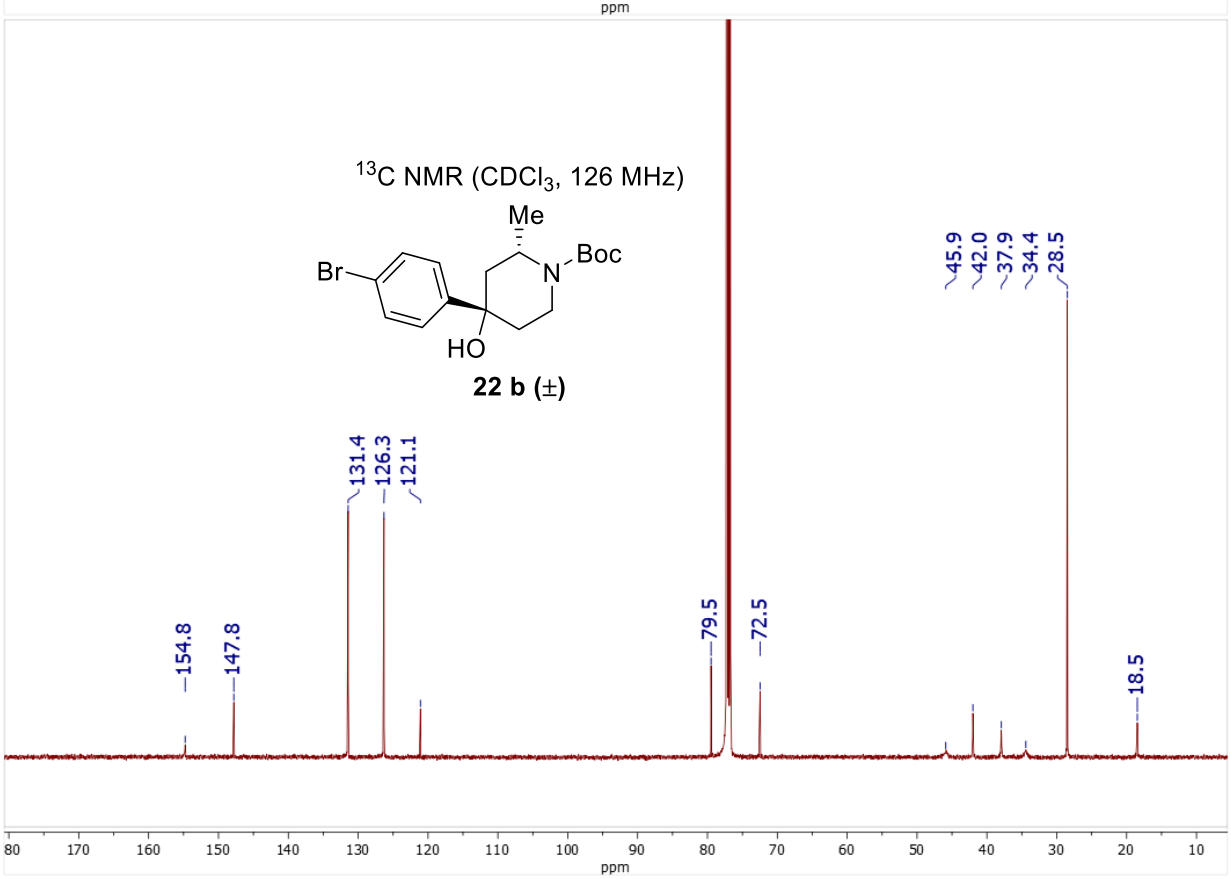
^{13}C NMR ($CDCl_3$, 126 MHz)
Me
Br
N
Boc
HO
22 b (±)
45.9
42.0
37.9
34.4
28.5
131.4
126.3
121.1
154.8
147.8
79.5
72.5
18.5
ppm

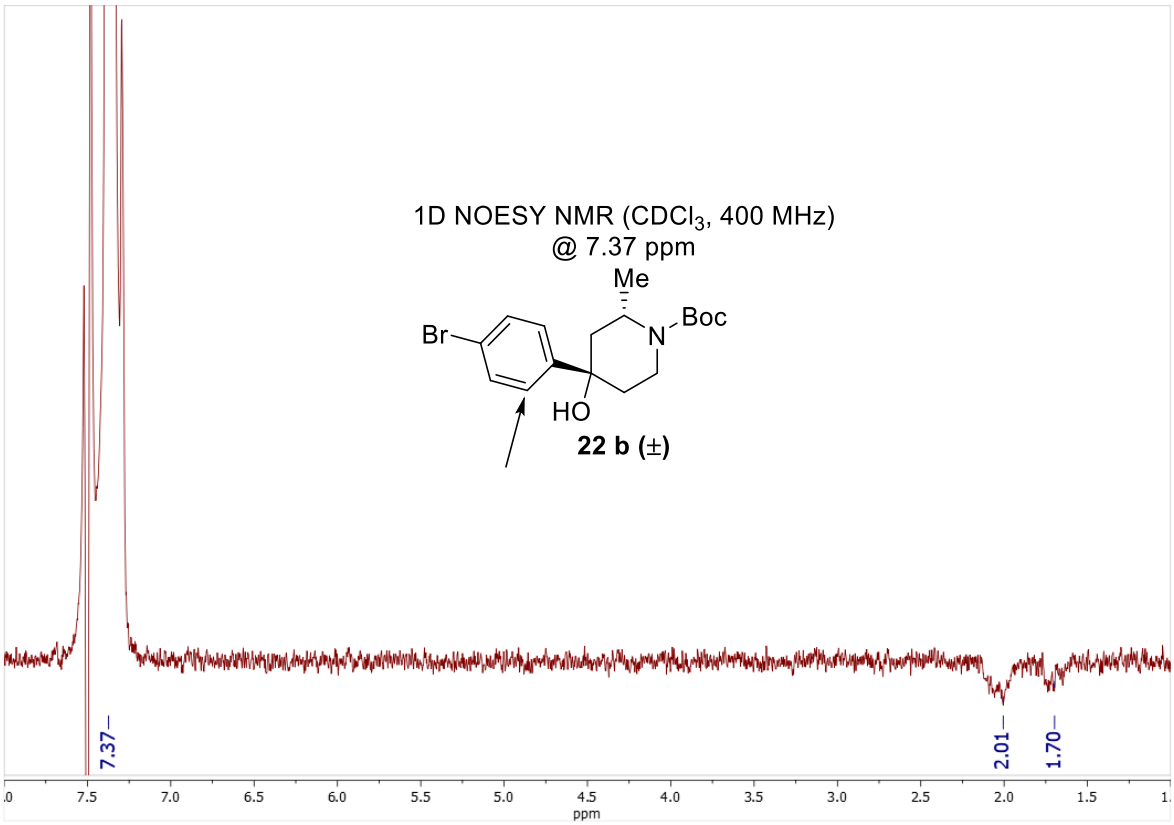

The aryl H atoms near the piperdine ring (7.37 ppm) interact with different H atoms of the piperidine ring than the Me group at 1.43 ppm. This suggests that the two groups reside on different faces of the ring.

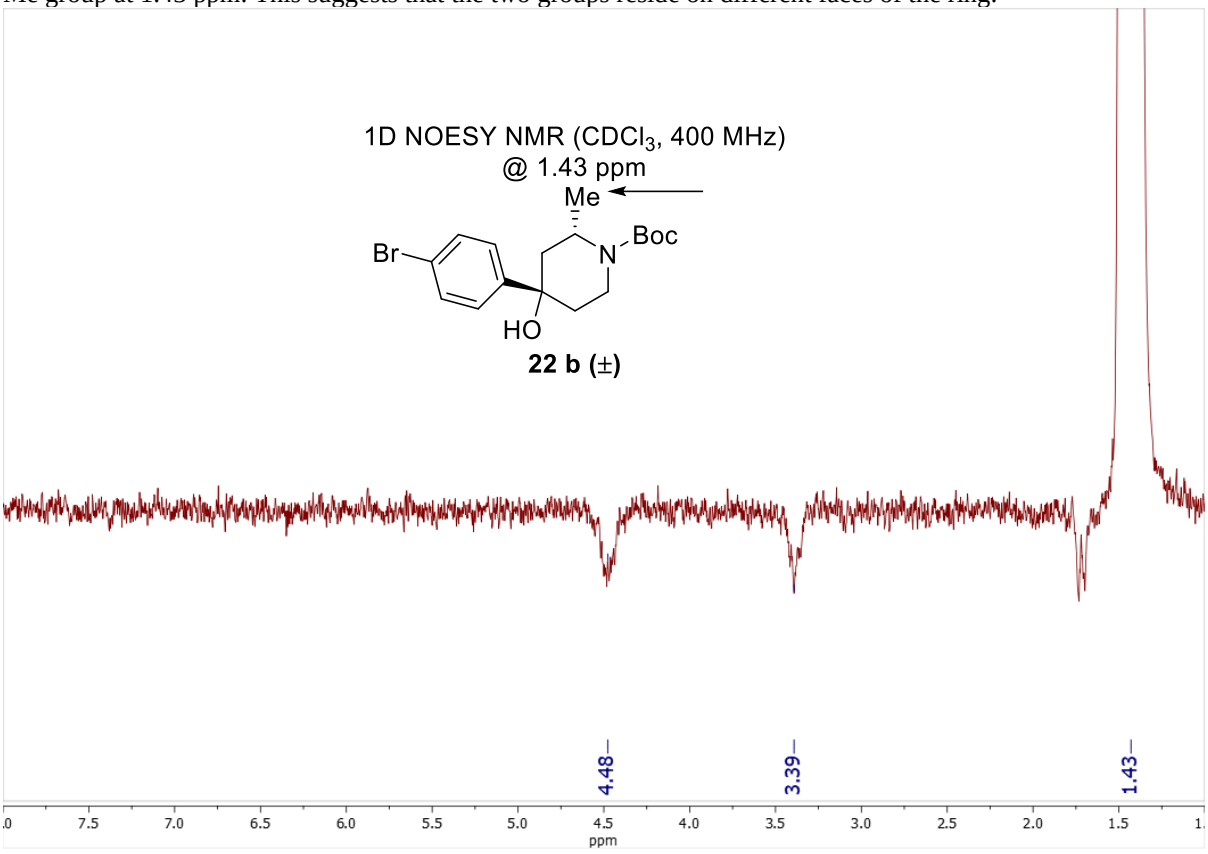

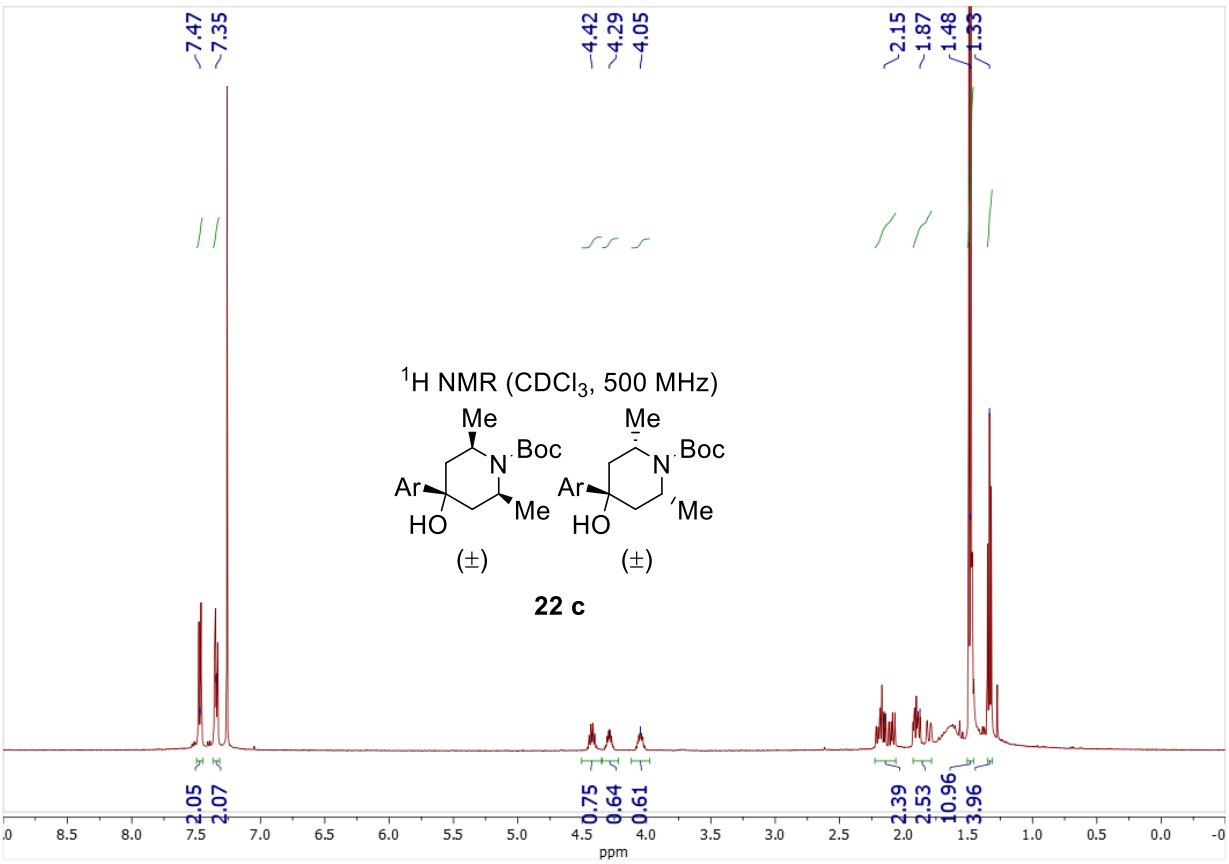

^{1}H NMR ($CDCl_3$, 500 MHz)

22 c

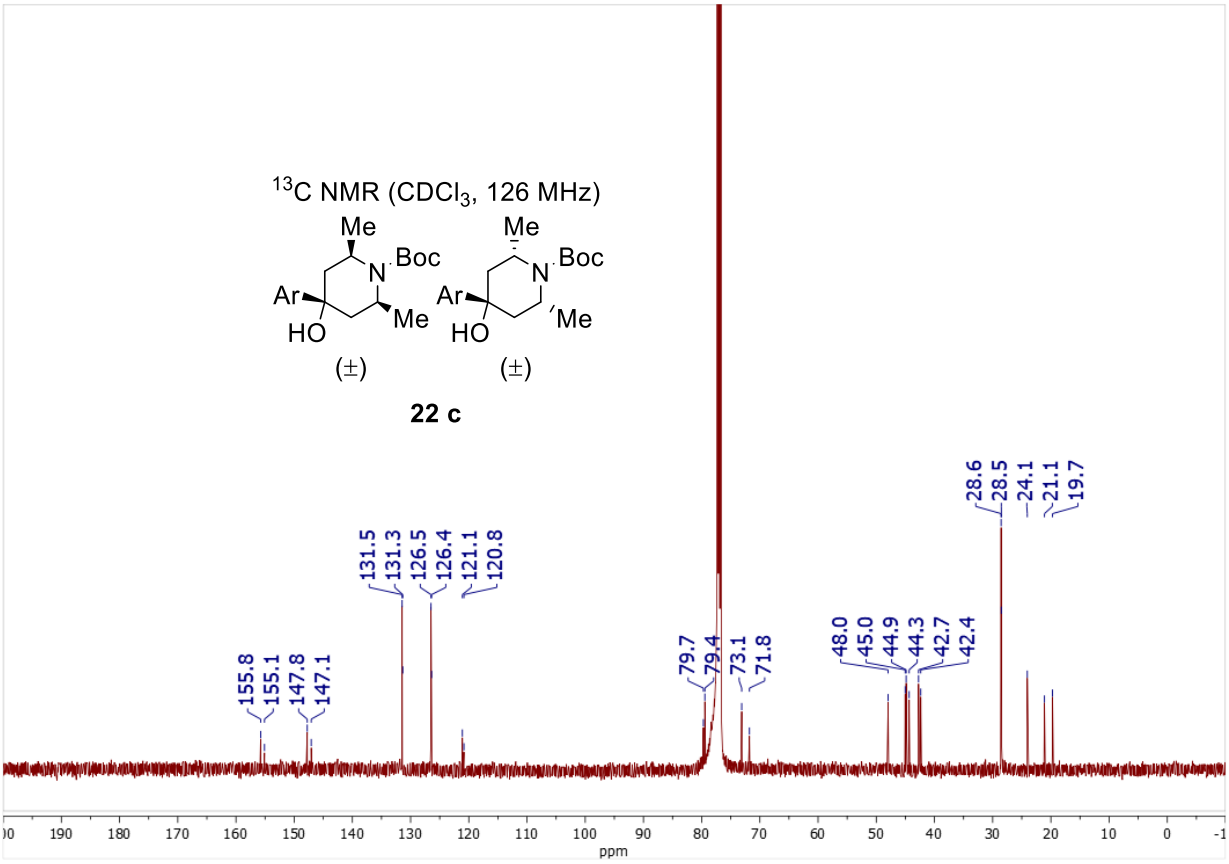

^{13}C NMR ($CDCl_3$, 126 MHz)

22 c

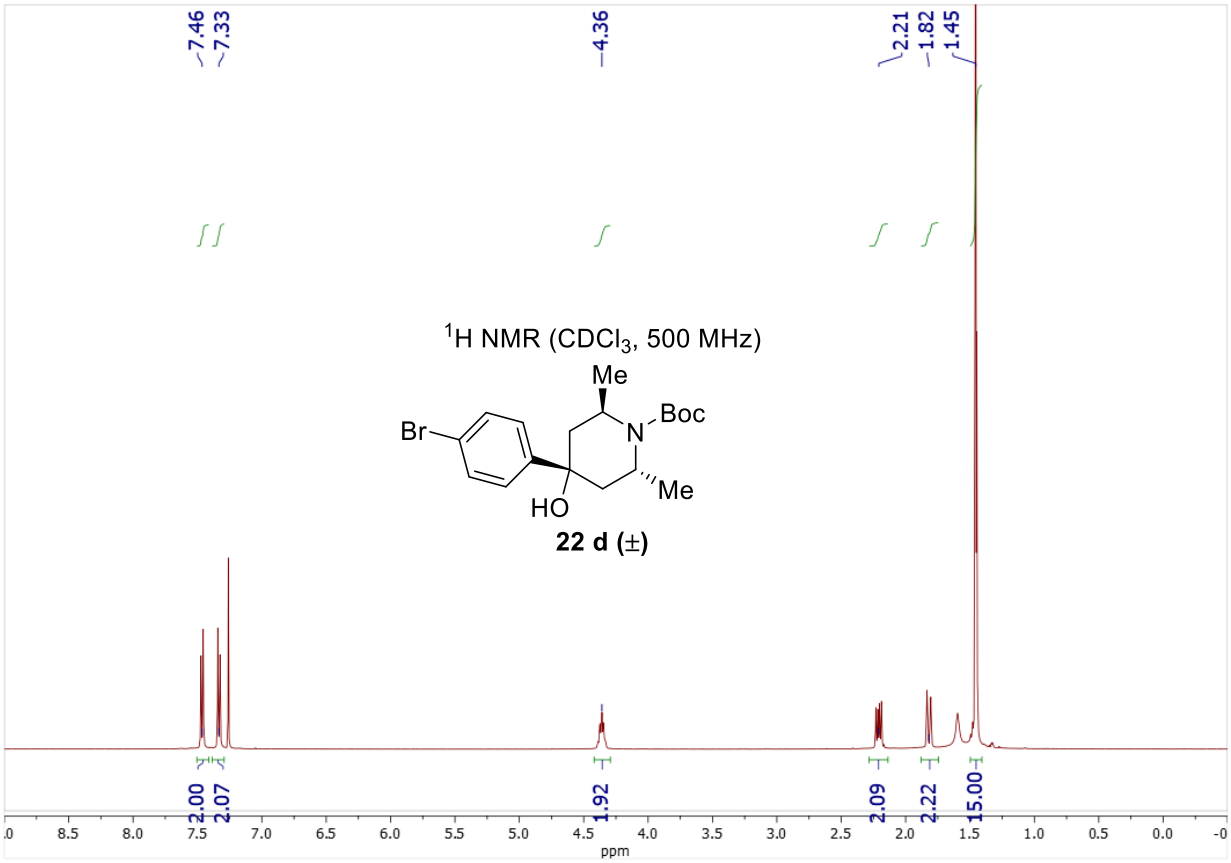
7.46
7.33
4.36
2.21
1.82
1.45
^{1}H NMR (CDCl$_3$, 500 MHz)
Me
Br
N
Boc
Me
HO
22 d (±)
2.00
2.07
1.92
2.09
2.22
15.00
ppm

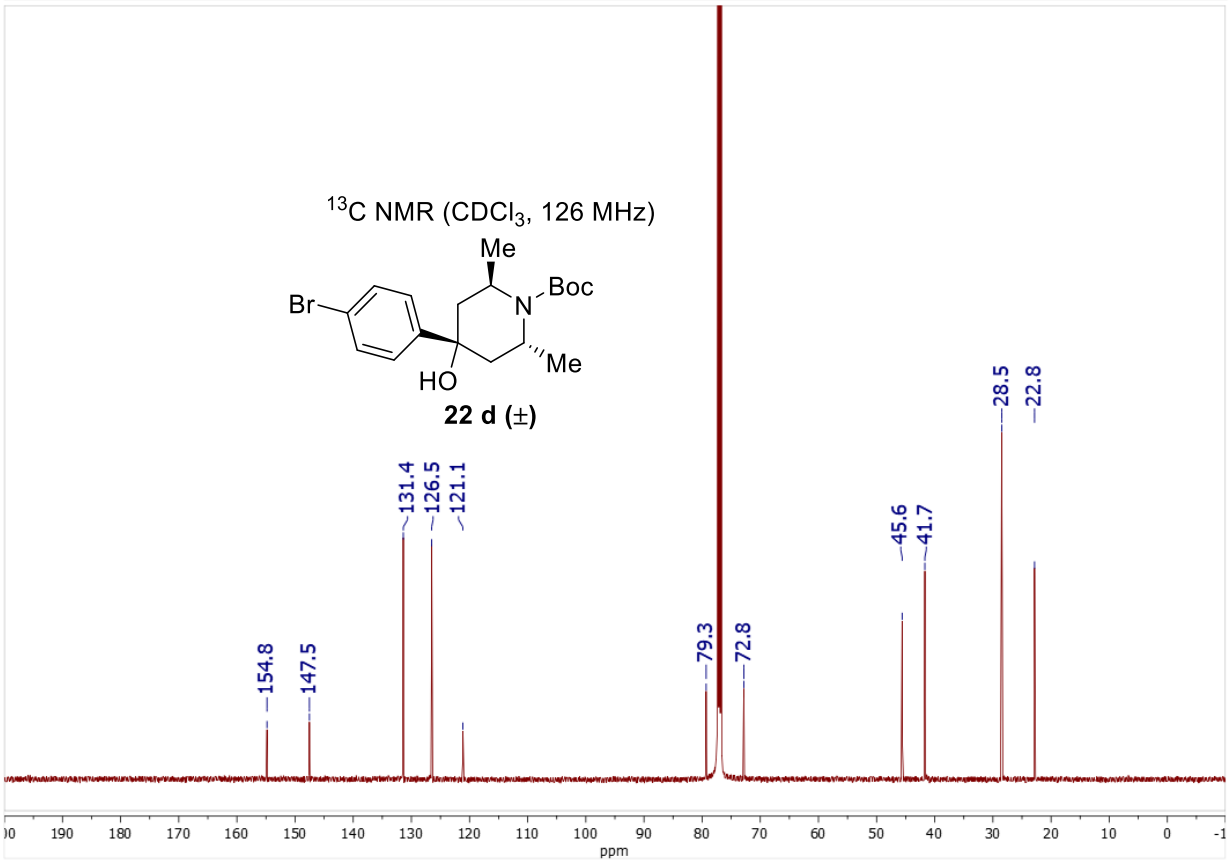
^{13}C NMR (CDCl$_3$, 126 MHz)
Me
Br
N
Boc
Me
HO
22 d (±)
154.8
147.5
131.4
126.5
121.1
79.3
72.8
45.6
41.7
28.5
22.8
ppm

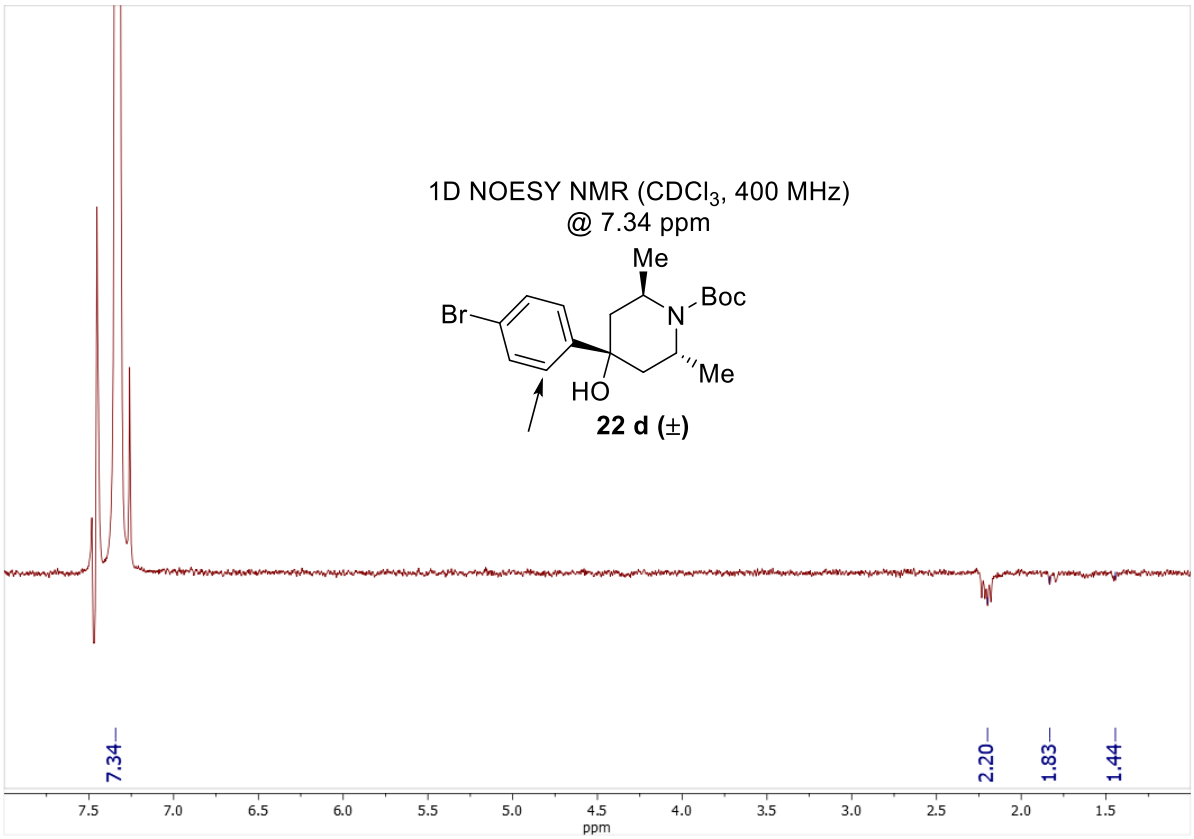

The aryl and Me hydrogen atoms interact with the same hydrogen atoms on the piperidine ring. This information combined with the 6-peak ^{1}H NMR spectrum are suggestive of the proposed symmetric structure.

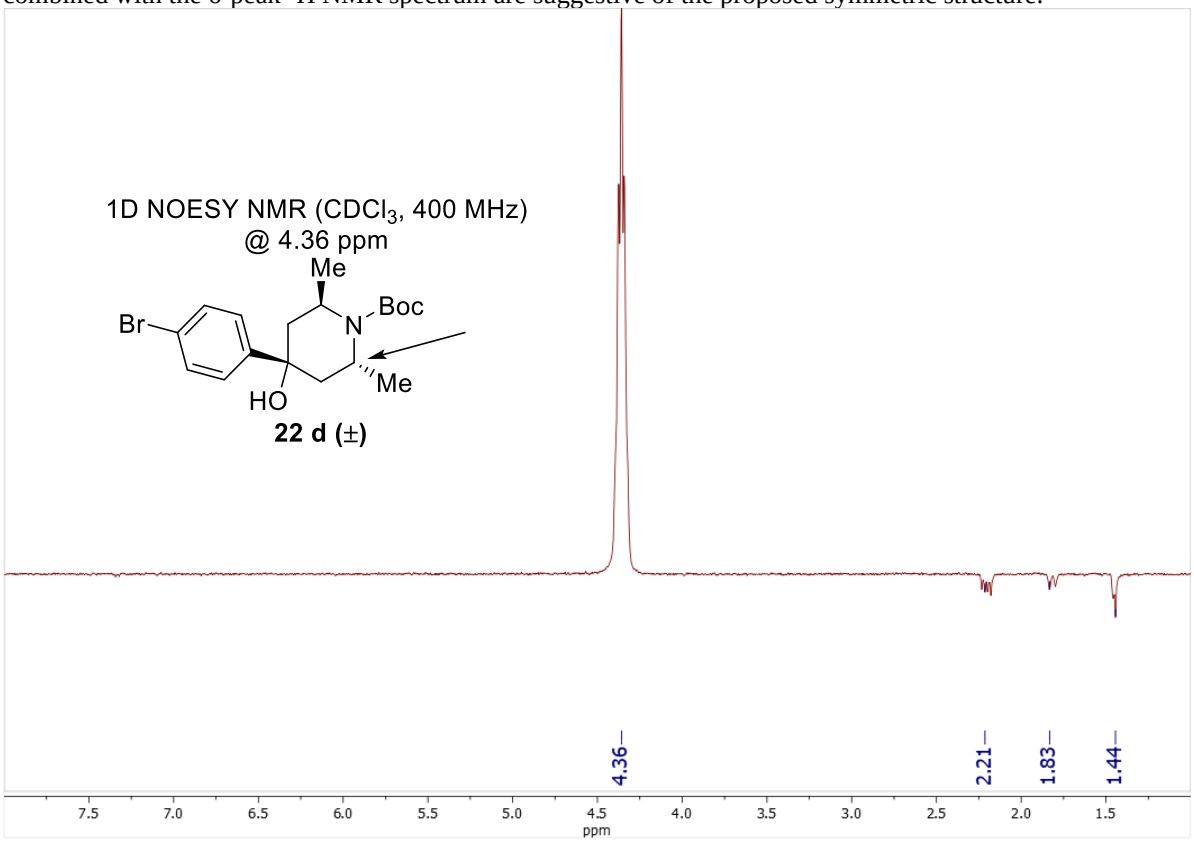

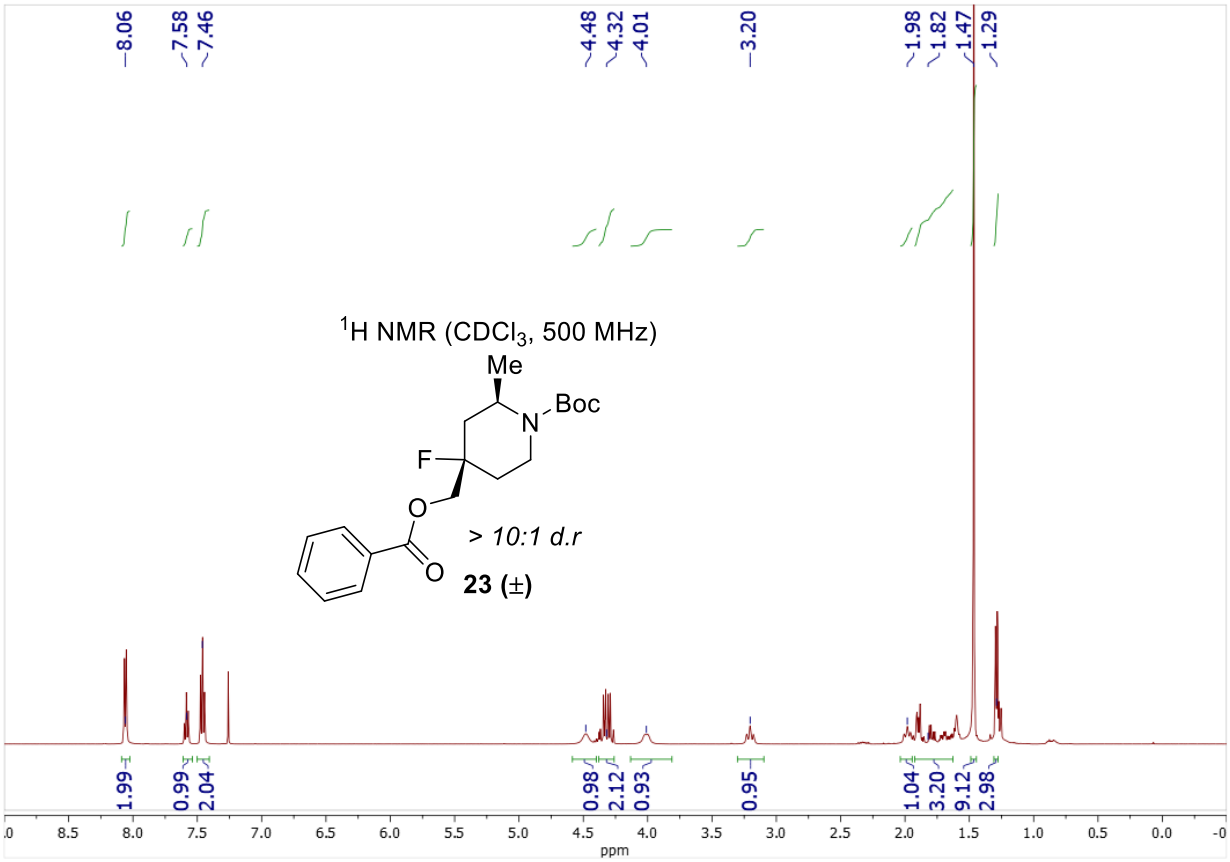
8.06
7.58
7.46
4.48
4.32
4.01
3.20
1.98
1.82
1.47
1.29
1H NMR (CDCl3, 500 MHz)
Me
Boc
N
F
O
O
> 10:1 d.r
23 (±)
1.99
0.99
2.04
0.98
2.12
0.93
0.95
1.04
3.20
9.12
2.98
ppm

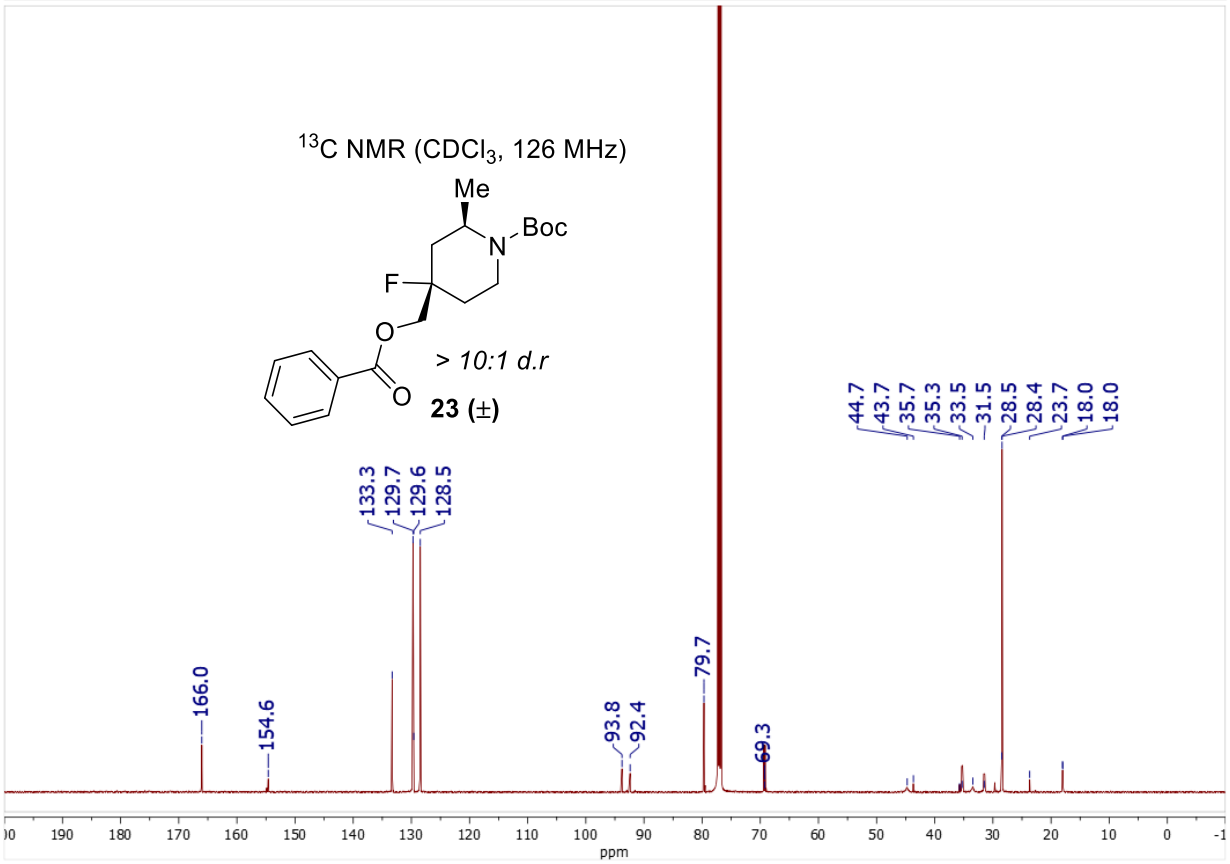
13C NMR (CDCl3, 126 MHz)
Me
Boc
N
F
O
O
> 10:1 d.r
23 (±)
166.0
154.6
133.3
129.7
129.6
128.5
93.8
92.4
79.7
69.3
44.7
43.7
35.7
35.3
33.5
31.5
28.5
28.4
23.7
18.0
18.0
ppm

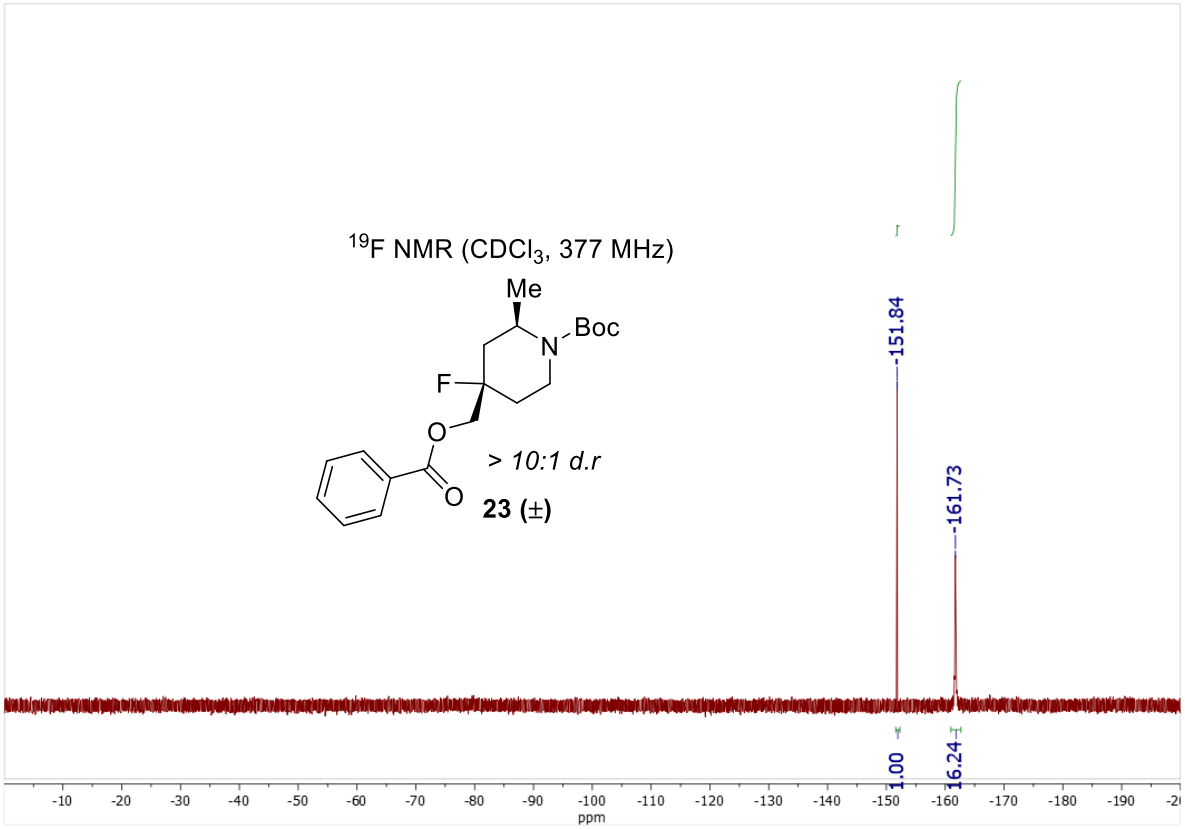
^{19}F NMR ($CDCl_3$, 377 MHz)
Me
N
Boc
F
O
O
> 10:1 d.r
23 (±)
-151.84
-161.73
1.00
16.24
-10 -20 -30 -40 -50 -60 -70 -80 -90 -100 -110 -120 -130 -140 -150 -160 -170 -180 -190
ppm

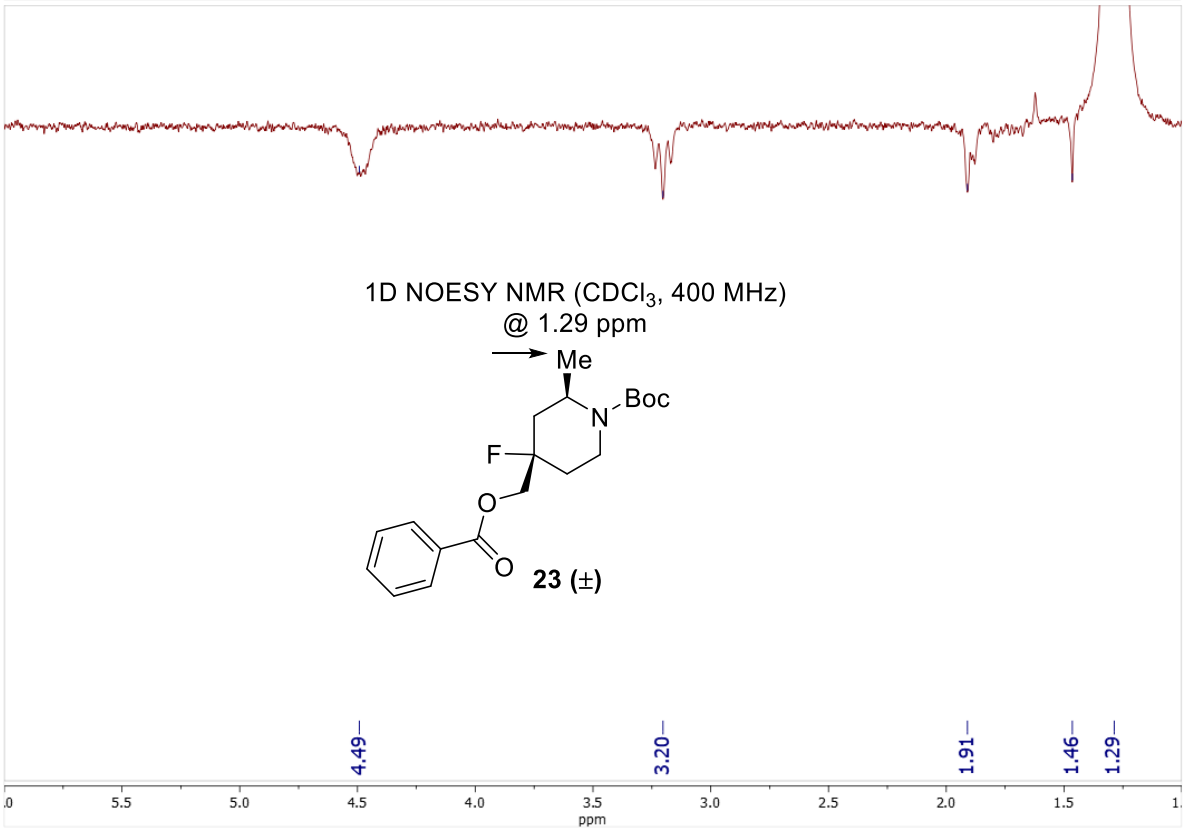
1D NOESY NMR ($CDCl_3$, 400 MHz)
@ 1.29 ppm
Me
N
Boc
F
O
O
23 (±)
4.49
3.20
1.91
1.46
1.29
5.5 5.0 4.5 4.0 3.5 3.0 2.5 2.0 1.5
ppm

The Me hydrogen atoms (1.29 ppm) interact with the H atoms on the methylene next to the benzoyloxy group (4.32 ppm). The two groups also interact with piperidine C–H bonds on the same face, which indicates they are cis.

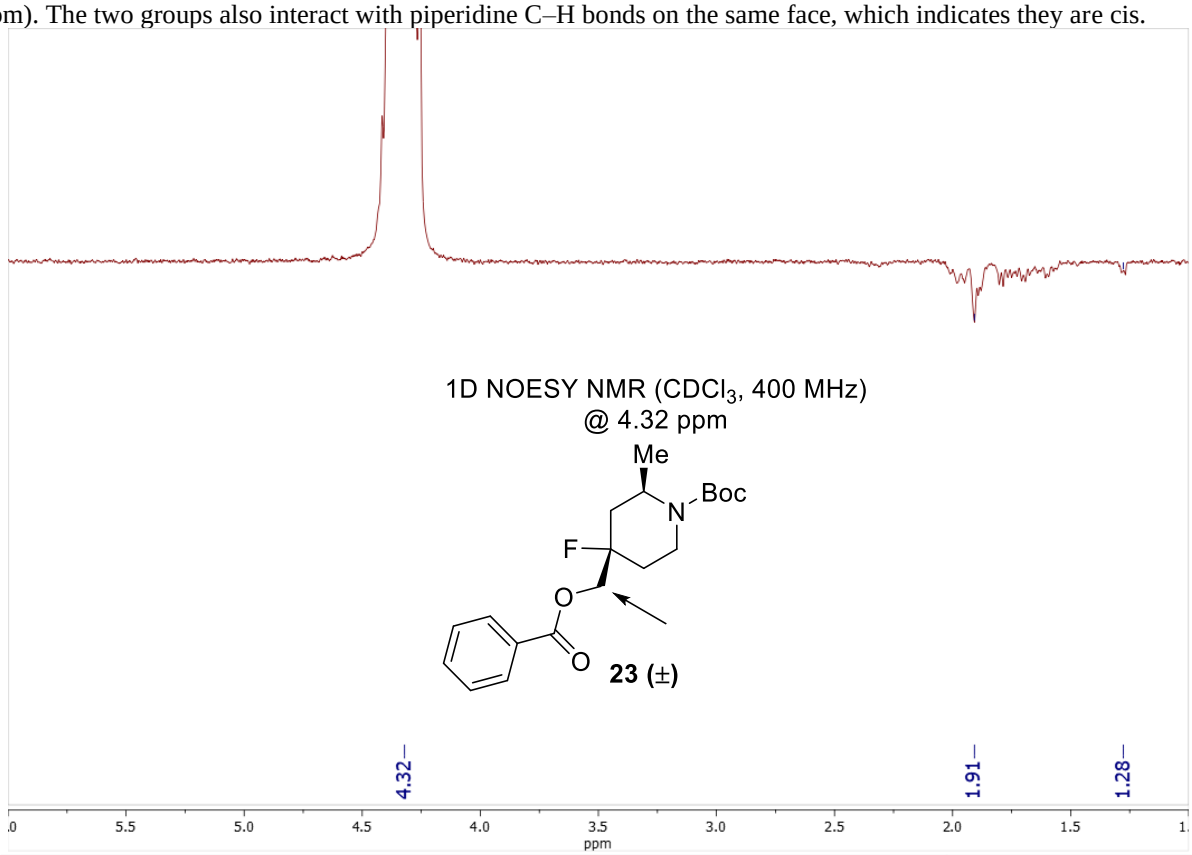

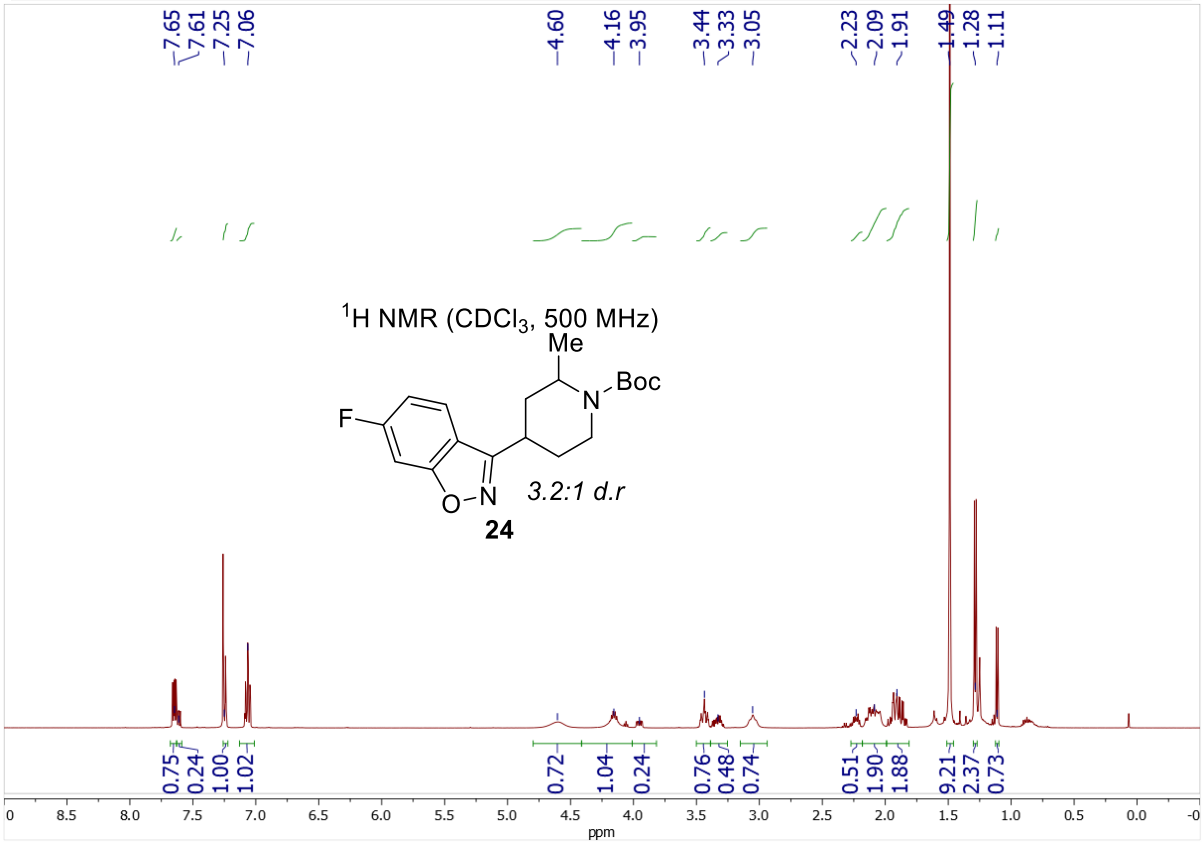

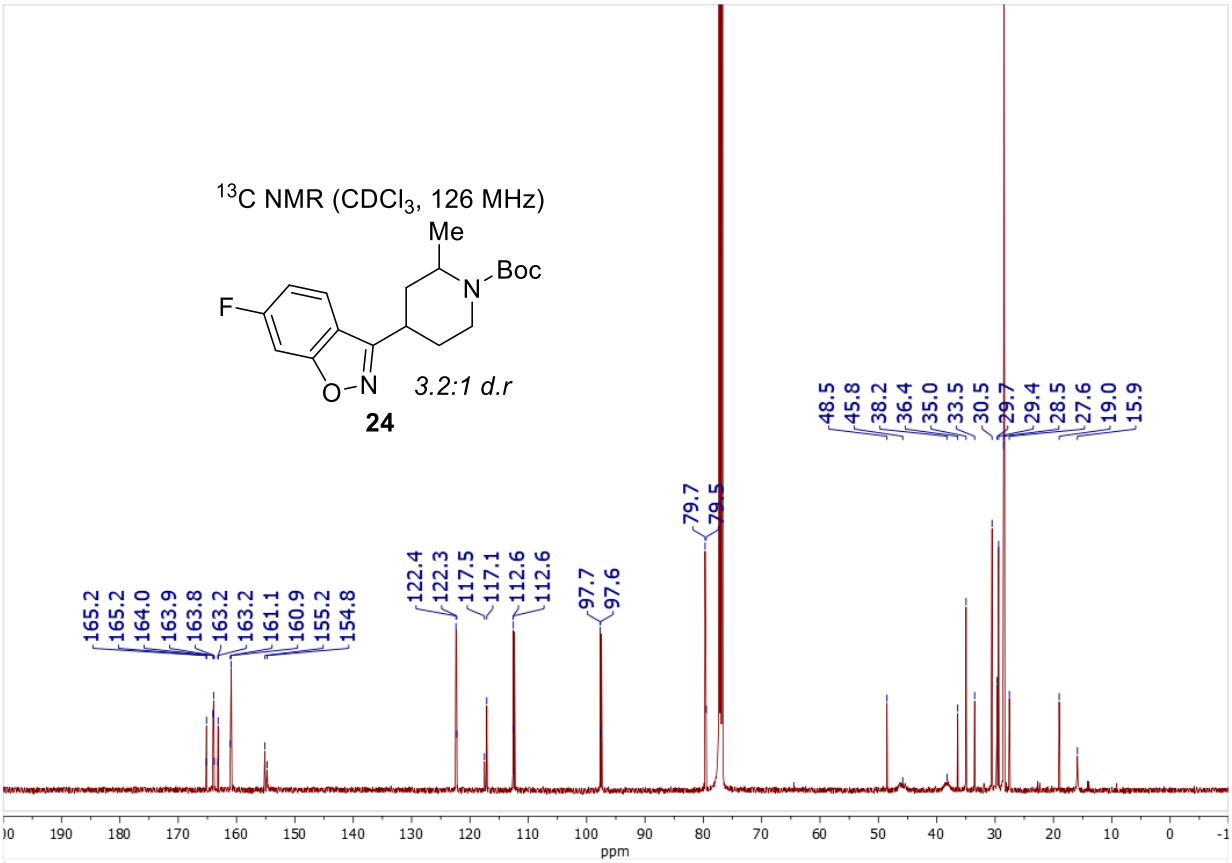
^{13}C NMR ($CDCl_3$, 126 MHz)
Me
Boc
N
F
O
N
3.2:1 d.r
24
165.2
165.2
164.0
163.9
163.8
163.2
163.2
161.1
160.9
155.2
154.8
122.4
122.3
117.5
117.1
112.6
112.6
97.7
97.6
79.7
79.5
48.5
45.8
38.2
36.4
35.0
33.5
30.5
29.7
29.4
28.5
27.6
19.0
15.9
ppm

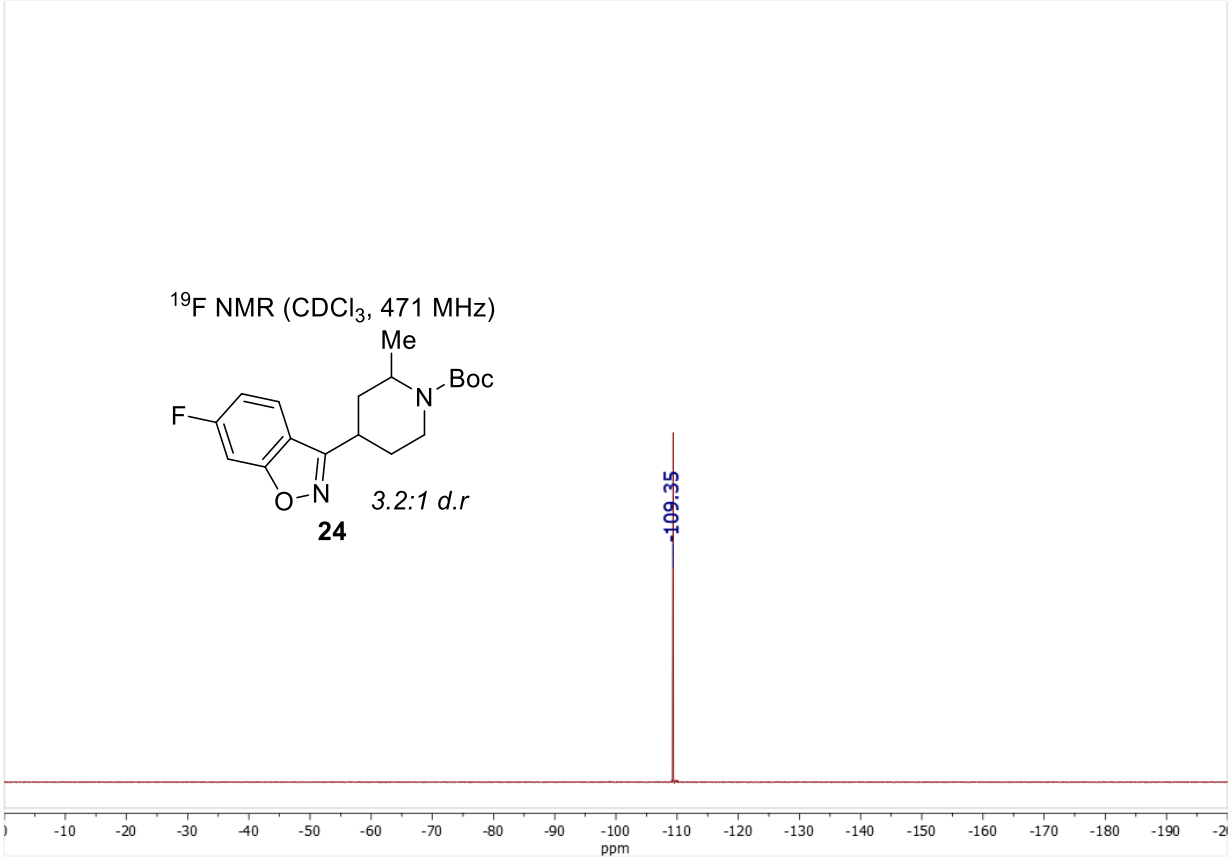
^{19}F NMR ($CDCl_3$, 471 MHz)
Me
Boc
N
F
O
N
3.2:1 d.r
24
-109.35
ppm

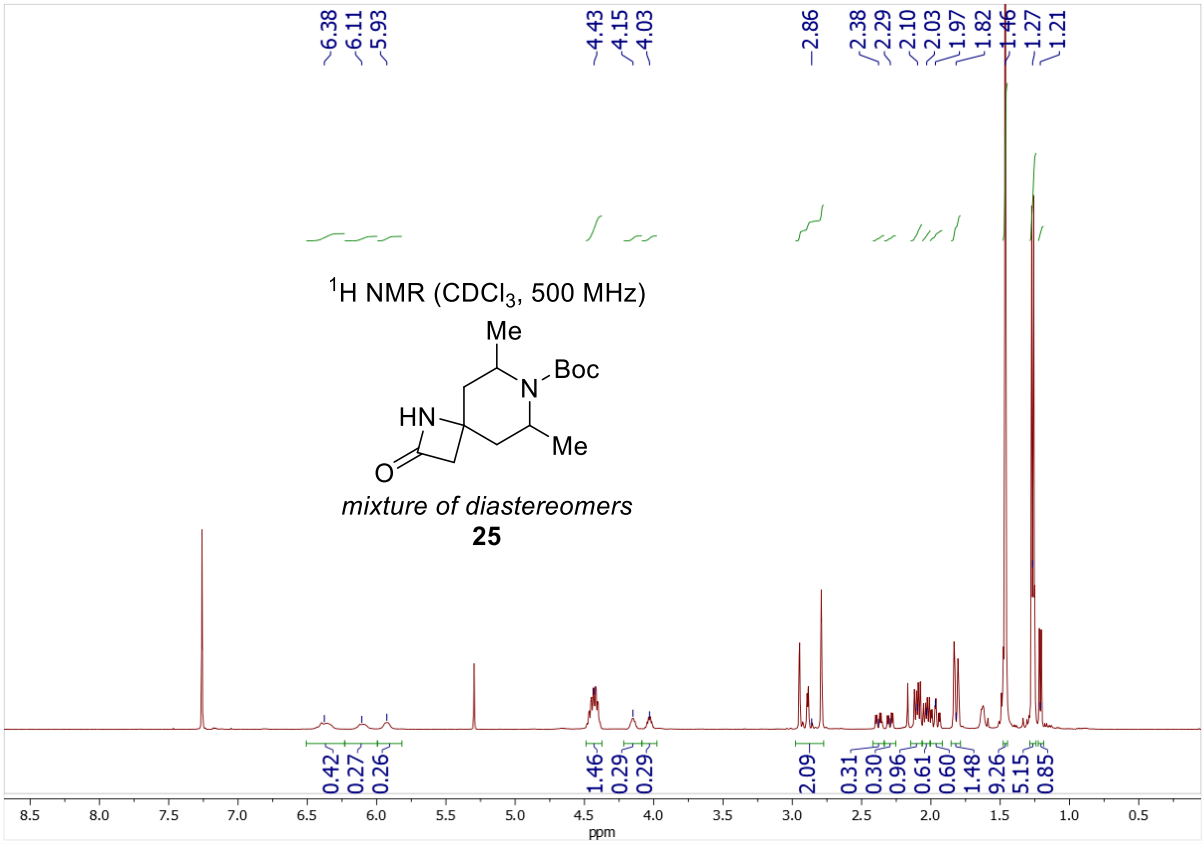
6.38
6.11
5.93
4.43
4.15
4.03
2.86
2.38
2.29
2.10
2.03
1.97
1.82
1.46
1.27
1.21
^{1}H NMR ($CDCl_3$, 500 MHz)
Me
Boc
N
HN
Me
O
mixture of diastereomers
25
0.42
0.27
0.26
1.46
0.29
0.29
2.09
0.31
0.30
0.96
0.61
0.60
1.48
9.26
5.15
0.85
8.5 8.0 7.5 7.0 6.5 6.0 5.5 5.0 4.5 4.0 3.5 3.0 2.5 2.0 1.5 1.0 0.5
ppm

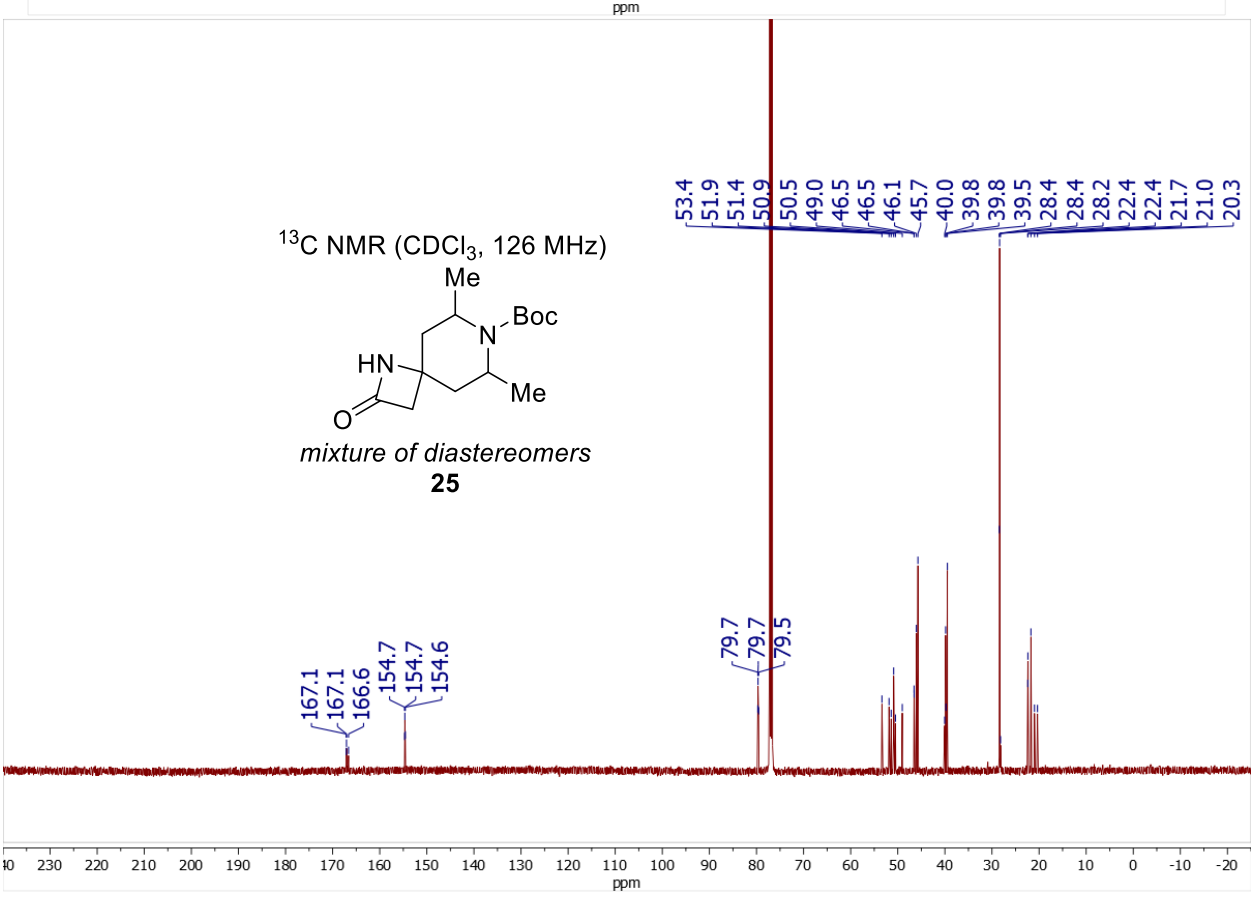
53.4
51.9
51.4
50.9
50.5
49.0
46.5
46.5
46.1
45.7
40.0
39.8
39.8
39.5
28.4
28.4
28.2
22.4
22.4
21.7
21.0
20.3
^{13}C NMR ($CDCl_3$, 126 MHz)
Me
Boc
N
HN
Me
O
mixture of diastereomers
25
79.7
79.7
79.5
167.1
167.1
166.6
154.7
154.7
154.6
240 230 220 210 200 190 180 170 160 150 140 130 120 110 100 90 80 70 60 50 40 30 20 10 0 -10 -20
ppm

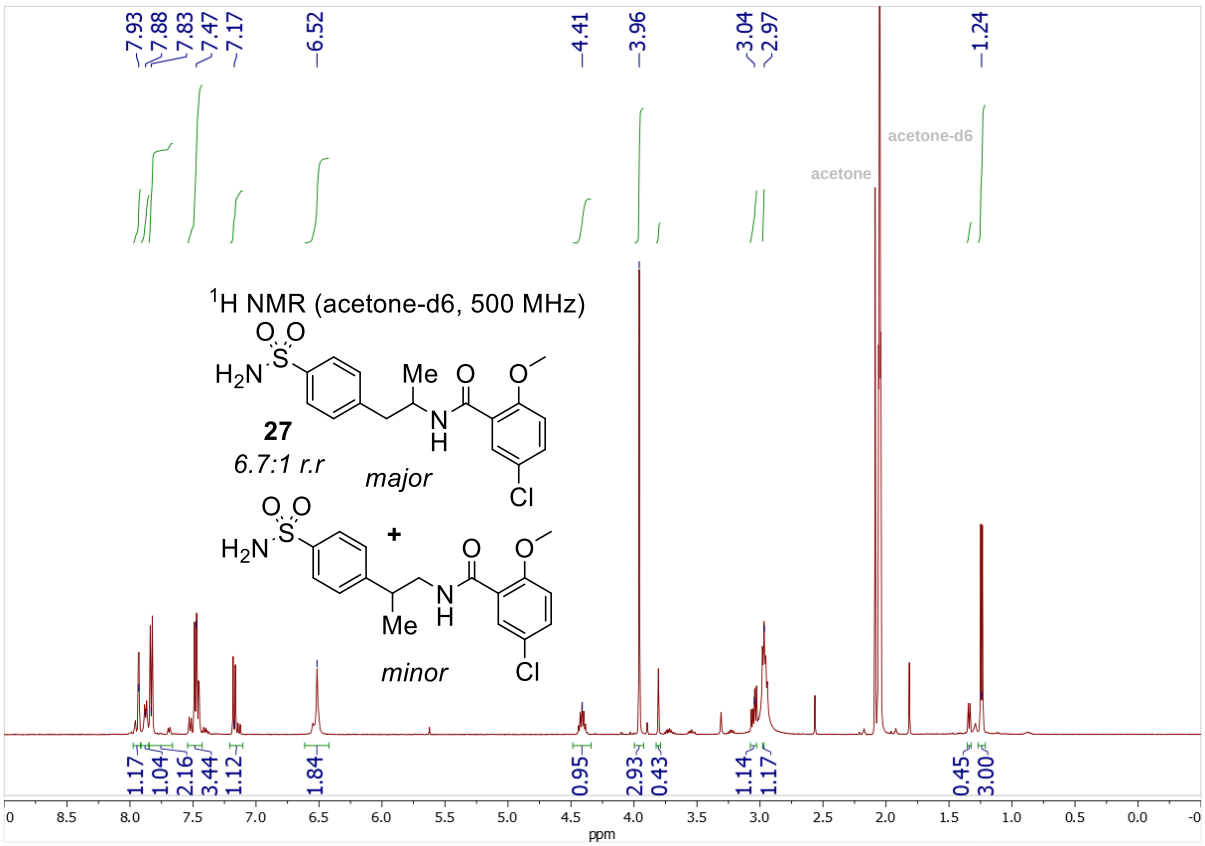
7.93
7.88
7.83
7.47
7.17
6.52
4.41
3.96
3.04
2.97
1.24
acetone-d6
acetone
1H NMR (acetone-d6, 500 MHz)
27
6.7:1 r.r
major
minor
1.17
1.04
2.16
3.44
1.12
1.84
0.95
2.93
0.43
1.14
1.17
0.45
3.00
ppm

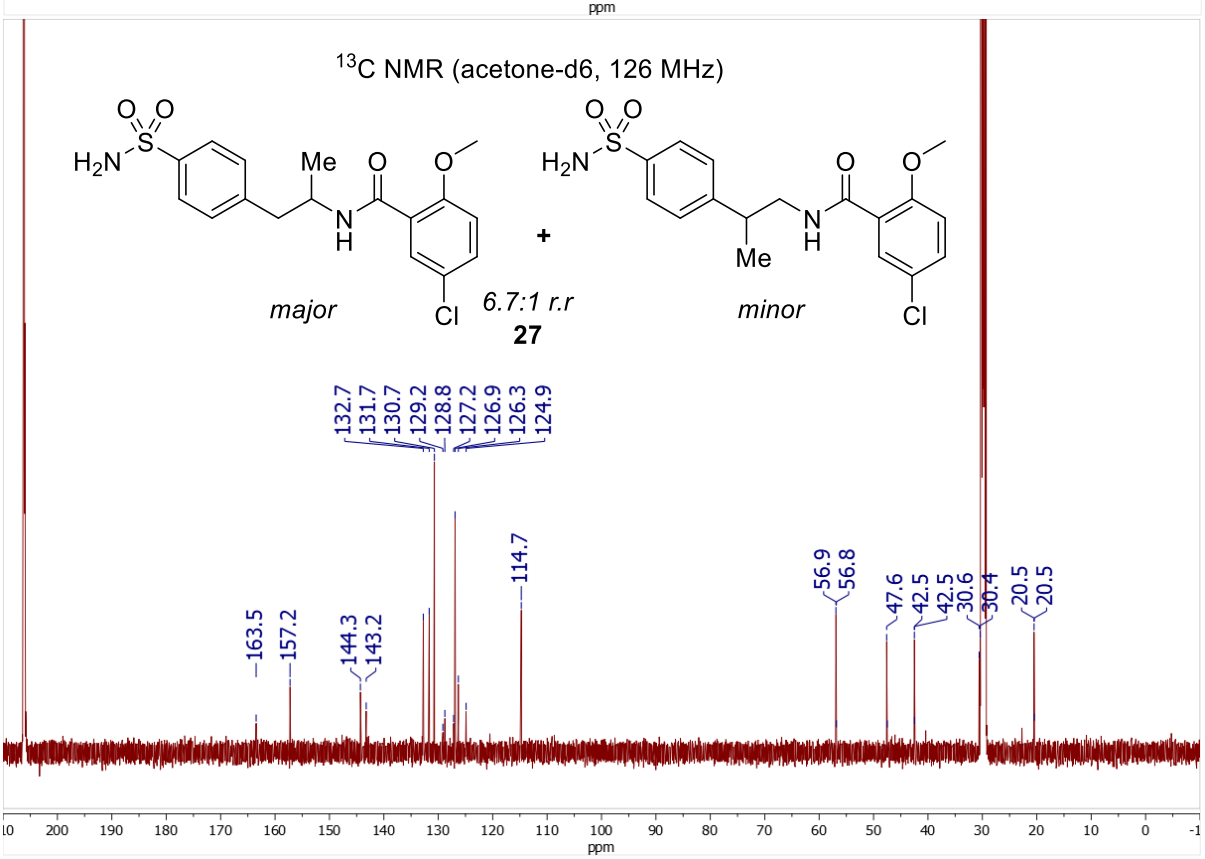
13C NMR (acetone-d6, 126 MHz)
major
6.7:1 r.r
27
minor
132.7
131.7
130.7
129.2
128.8
127.2
126.9
126.3
124.9
163.5
157.2
144.3
143.2
114.7
56.9
56.8
47.6
42.5
42.5
30.6
30.4
20.5
20.5
ppm

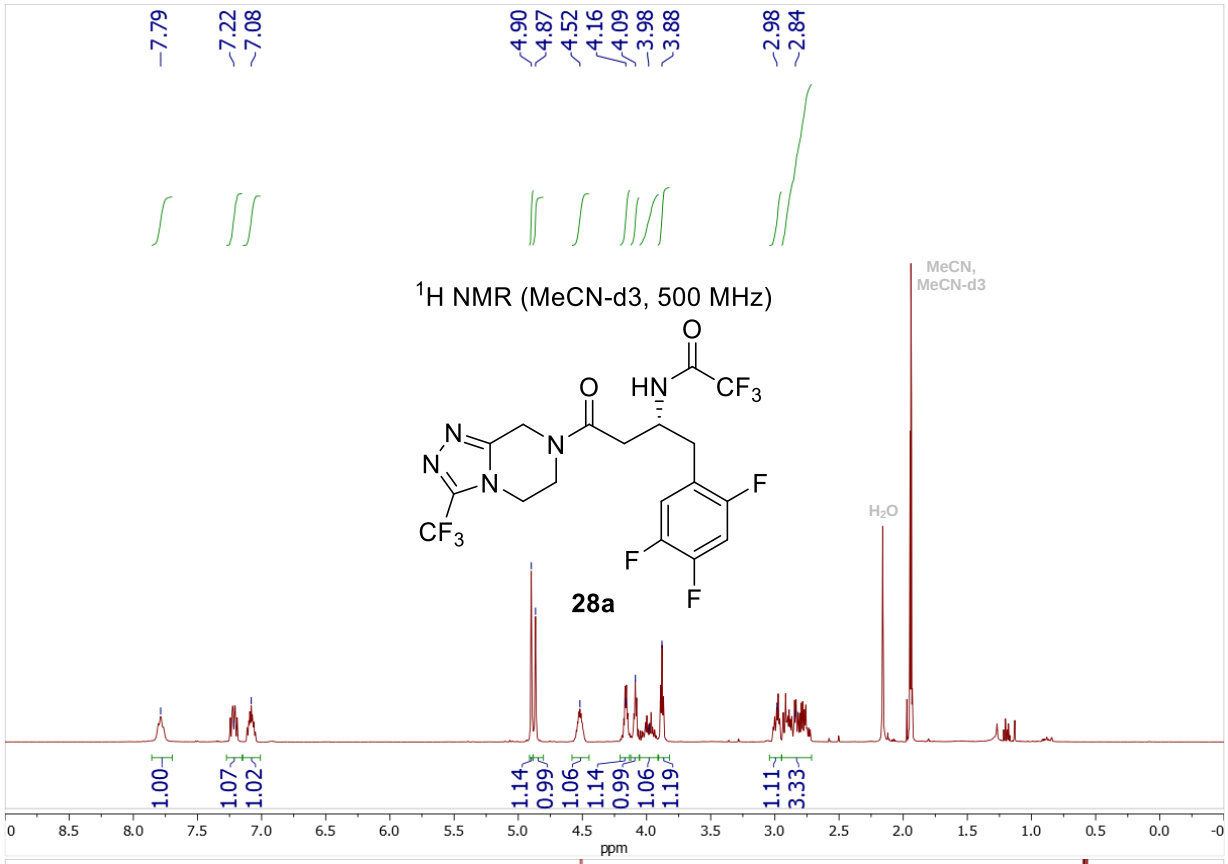
7.79
7.22
7.08
4.90
4.87
4.52
4.16
4.09
3.98
3.88
2.98
2.84
MeCN,
MeCN-d3
H2O
1H NMR (MeCN-d3, 500 MHz)
28a
1.00
1.07
1.02
1.14
0.99
1.06
1.14
0.99
1.06
1.19
1.11
3.33
ppm

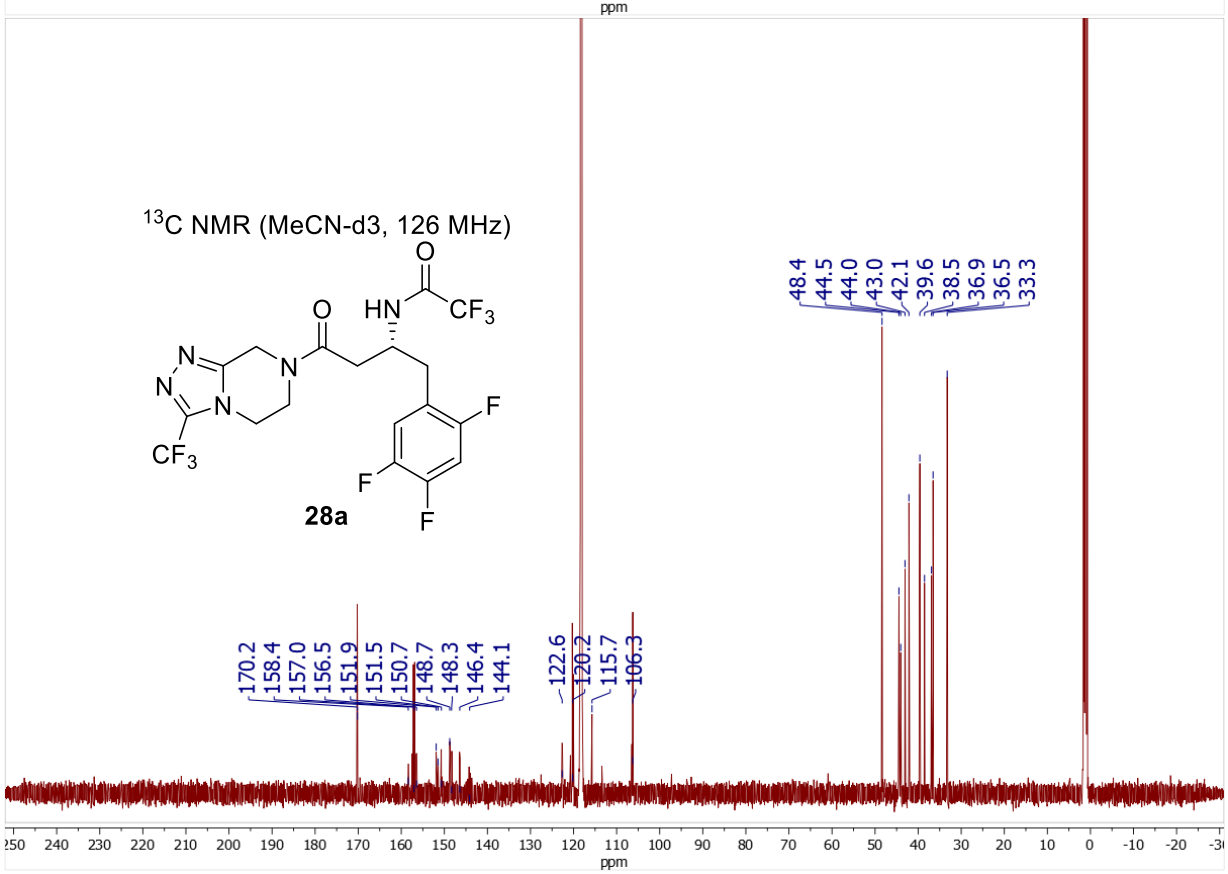
13C NMR (MeCN-d3, 126 MHz)
28a
48.4
44.5
44.0
43.0
42.1
39.6
38.5
36.9
36.5
33.3
170.2
158.4
157.0
156.5
151.9
151.5
150.7
148.7
148.3
146.4
144.1
122.6
120.2
115.7
106.3
ppm

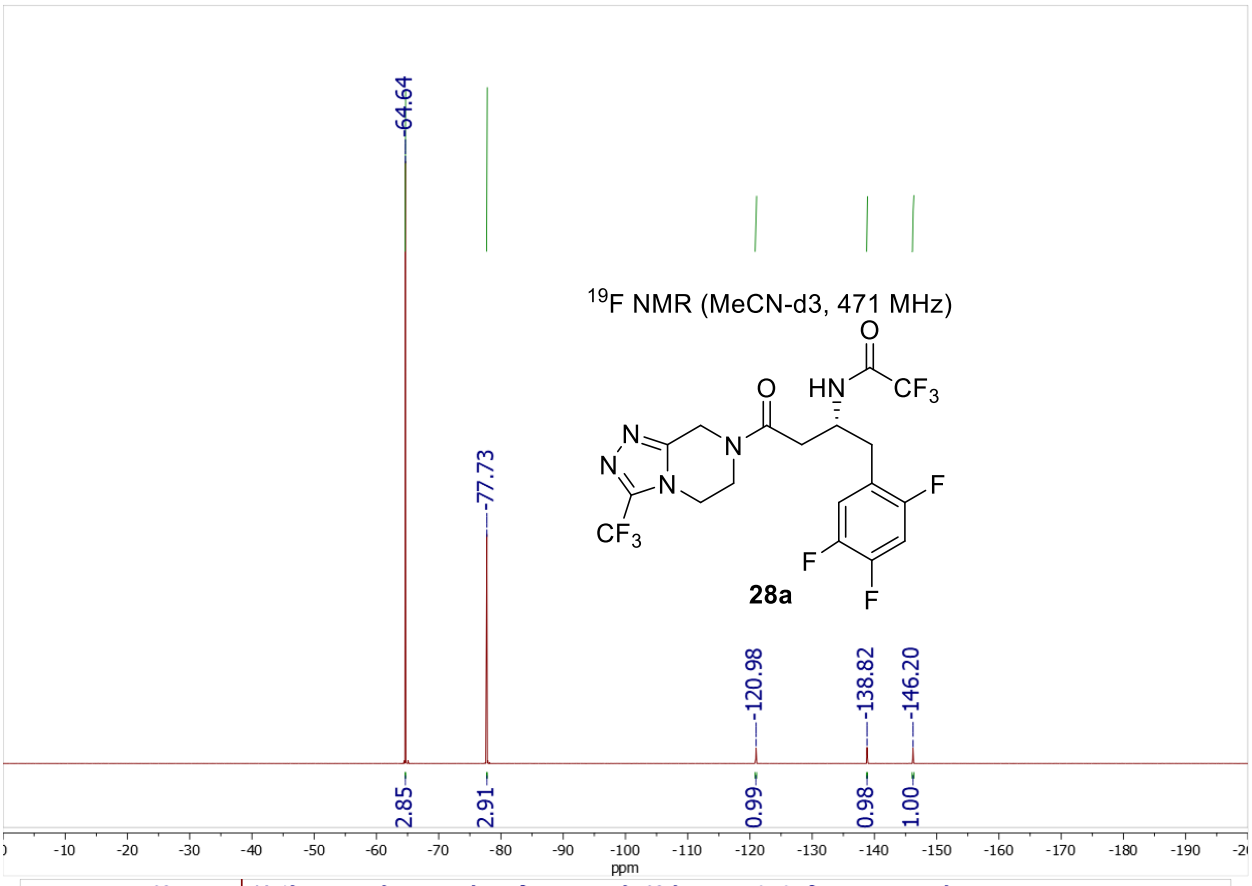
^{19}F NMR (MeCN-d3, 471 MHz)
-64.64
-77.73
-120.98
-138.82
-146.20
2.85
2.91
0.99
0.98
1.00
ppm
28a

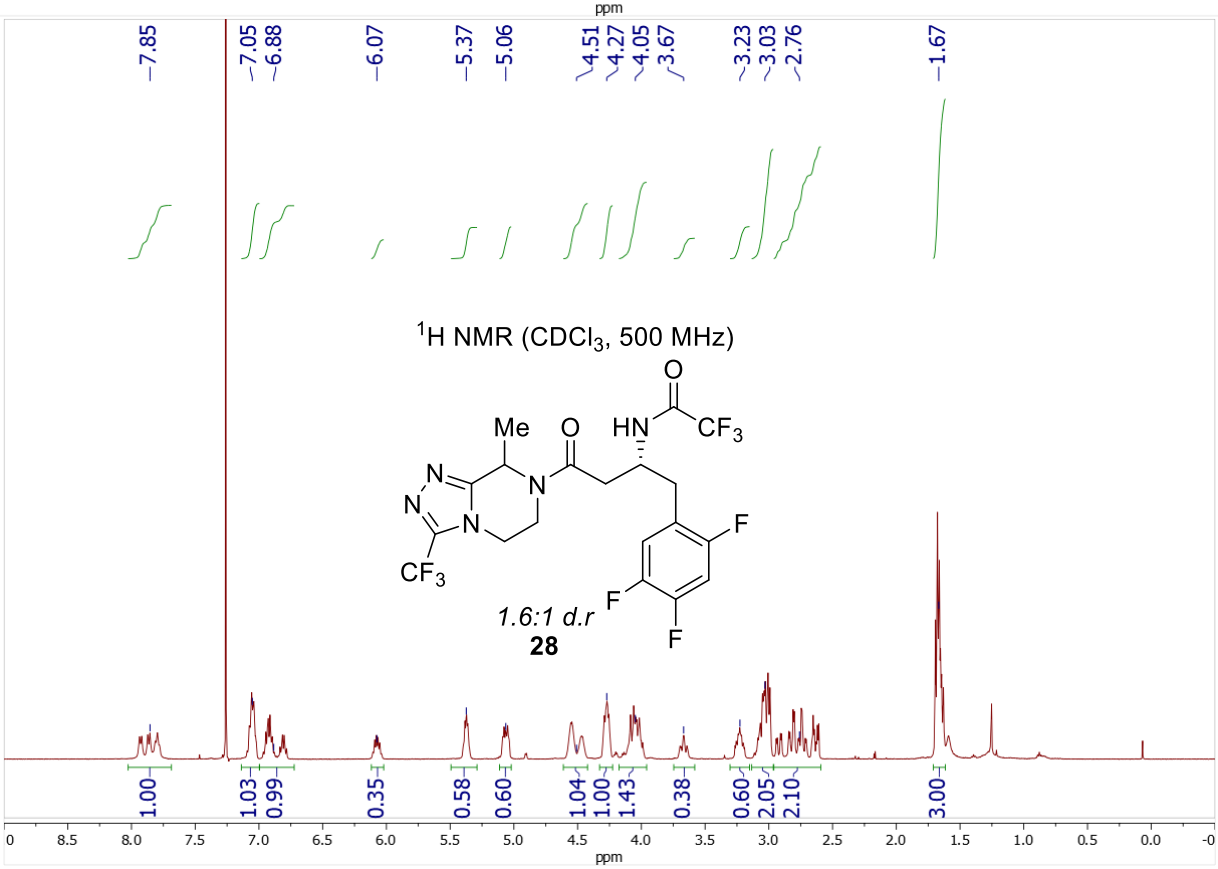
^{1}H NMR ($CDCl_3$, 500 MHz)
7.85
7.05
6.88
6.07
5.37
5.06
4.51
4.27
4.05
3.67
3.23
3.03
2.76
1.67
1.00
1.03
0.99
0.35
0.58
0.60
1.04
1.00
1.43
0.38
0.60
2.05
2.10
3.00
ppm
1.6:1 d.r
28

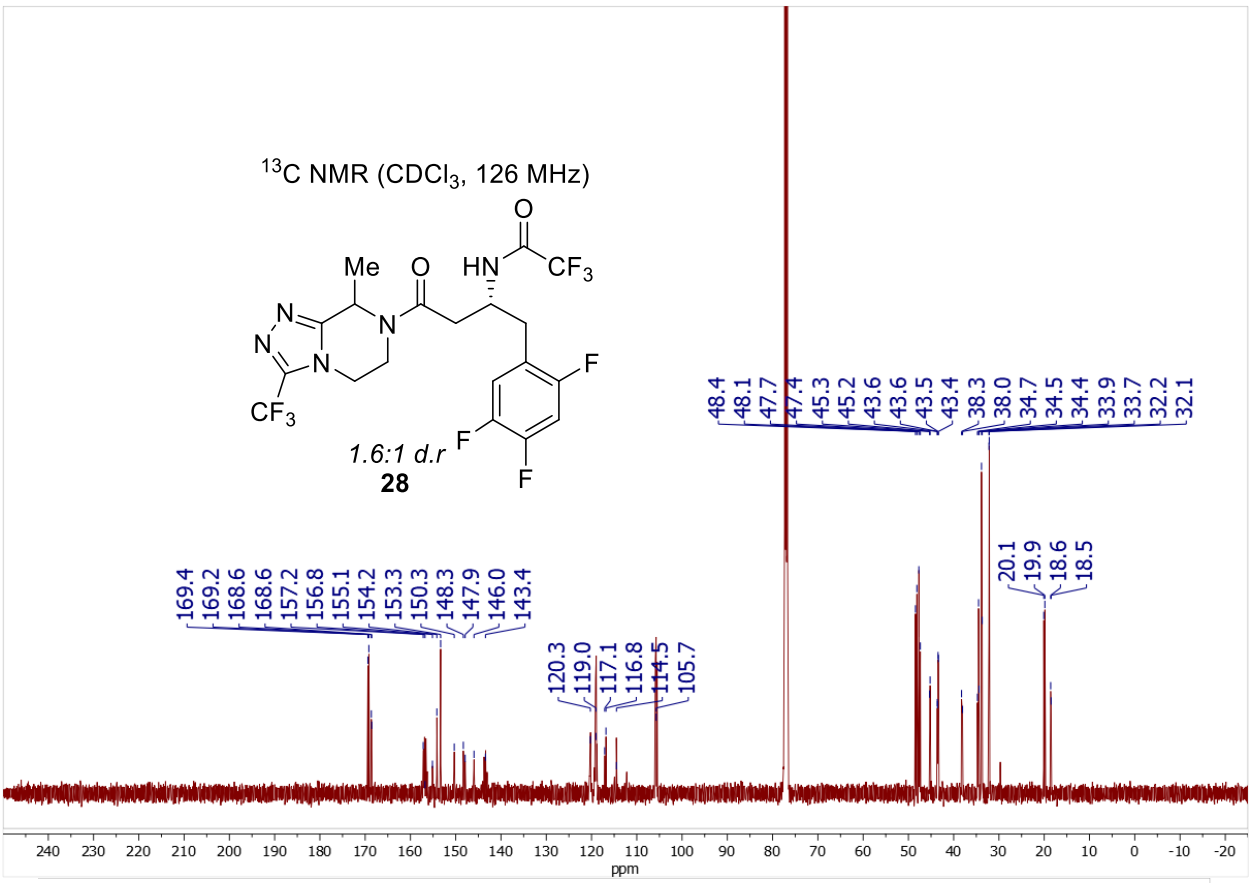
13C NMR (CDCl3, 126 MHz)
Me
O
HN
CF3
N
N
N
N
CF3
F
F
F
1.6:1 d.r
28
48.4
48.1
47.7
47.4
45.3
45.2
43.6
43.6
43.5
43.4
38.3
38.0
34.7
34.5
34.4
33.9
33.7
32.2
32.1
20.1
19.9
18.6
18.5
169.4
169.2
168.6
168.6
157.2
156.8
155.1
154.2
153.3
150.3
148.3
147.9
146.0
143.4
120.3
119.0
117.1
116.8
114.5
105.7
ppm

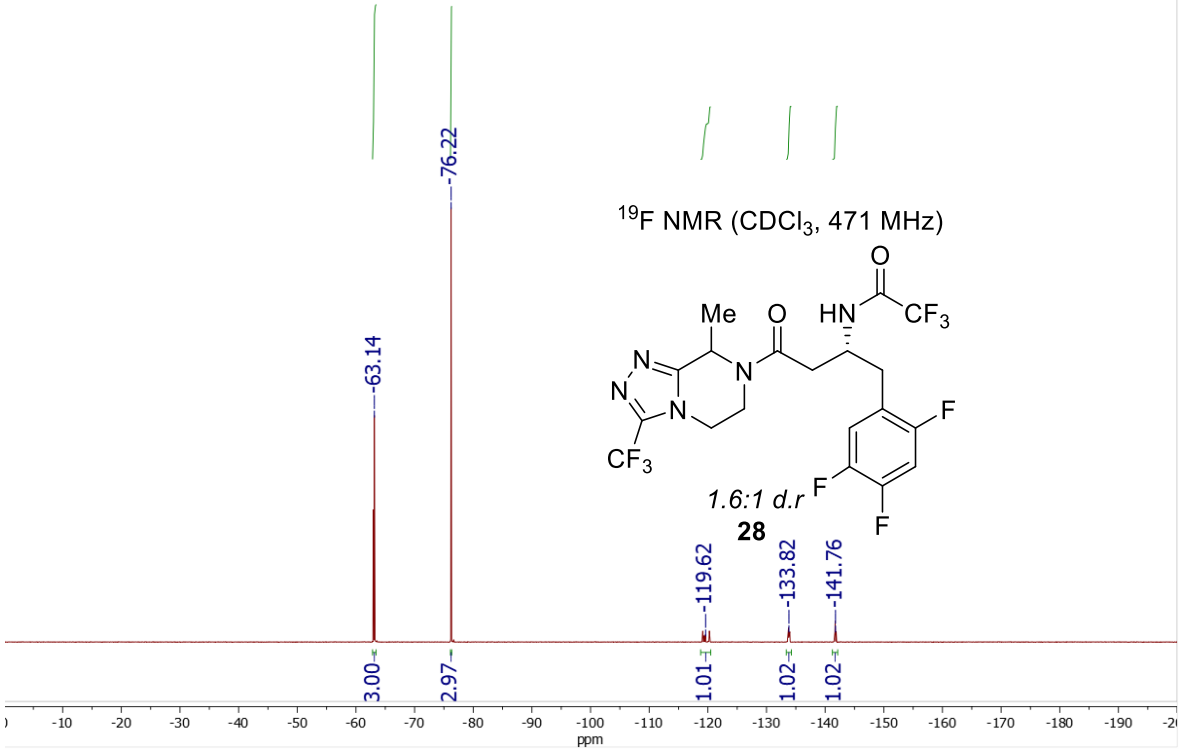
19F NMR (CDCl3, 471 MHz)
-63.14
-76.22
-119.62
-133.82
-141.76
3.00
2.97
1.01
1.02
1.02
Me
O
HN
CF3
N
N
N
N
CF3
F
F
F
1.6:1 d.r
28
ppm

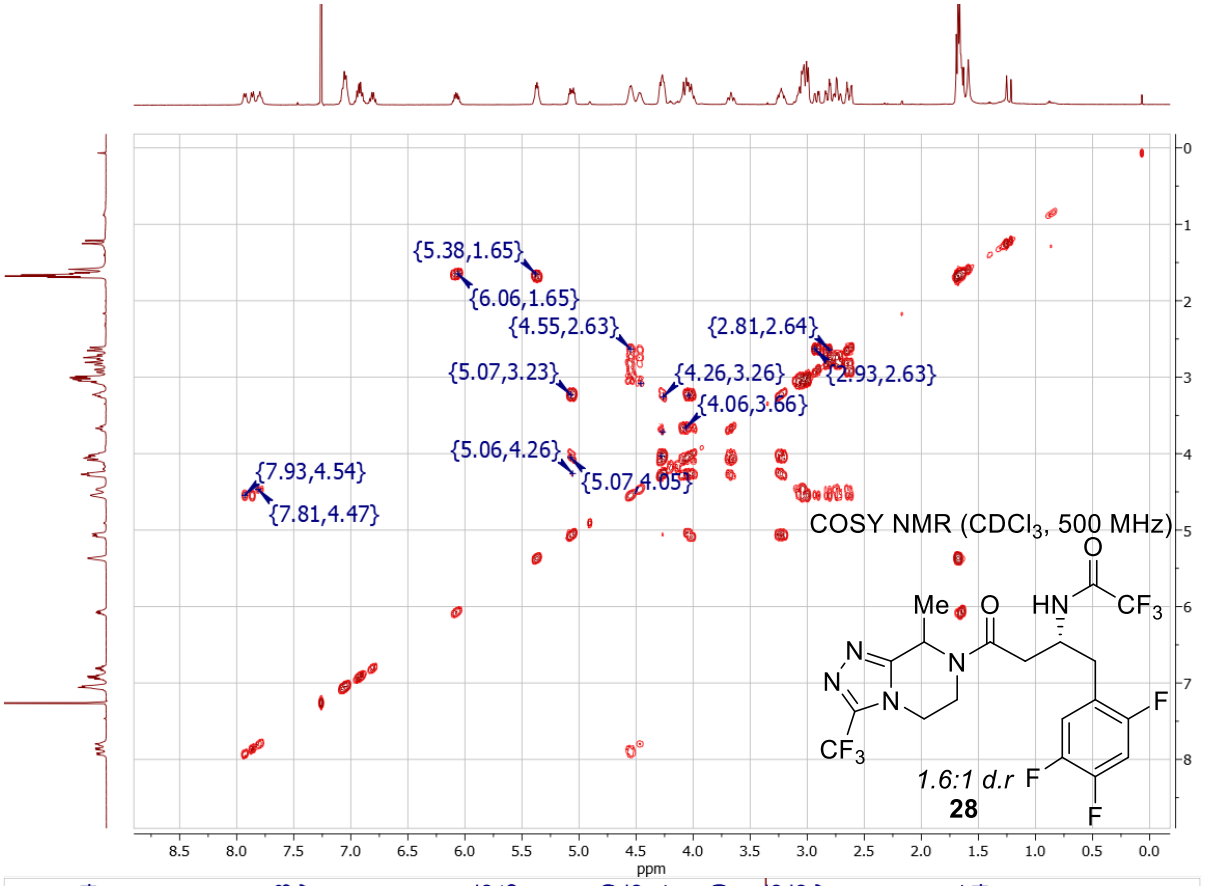
{5.38,1.65}
{6.06,1.65}
{4.55,2.63}
{2.81,2.64}
{5.07,3.23}
{4.26,3.26}
{2.93,2.63}
{4.06,3.66}
{5.06,4.26}
{7.93,4.54}
{5.07,4.05}
{7.81,4.47}
COSY NMR (CDCl3, 500 MHz)
Me
O
HN
CF3
N
N
N
CF3
F
F
F
1.6:1 d.r
28
ppm

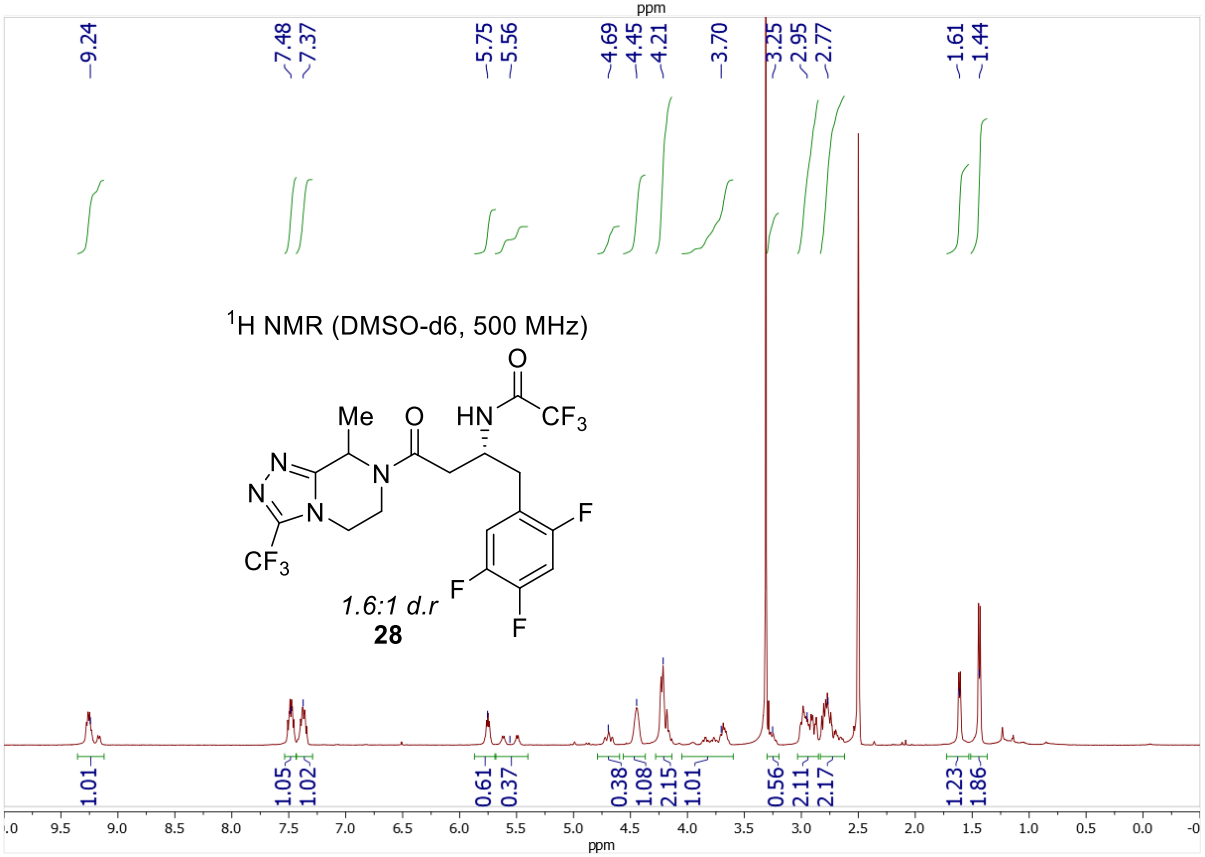
9.24
7.48
7.37
5.75
5.56
4.69
4.45
4.21
3.70
3.25
2.95
2.77
1.61
1.44
1H NMR (DMSO-d6, 500 MHz)
Me
O
HN
CF3
N
N
N
CF3
F
F
F
1.6:1 d.r
28
1.01
1.05
1.02
0.61
0.37
0.38
1.08
2.15
1.01
0.56
2.11
2.17
1.23
1.86
ppm

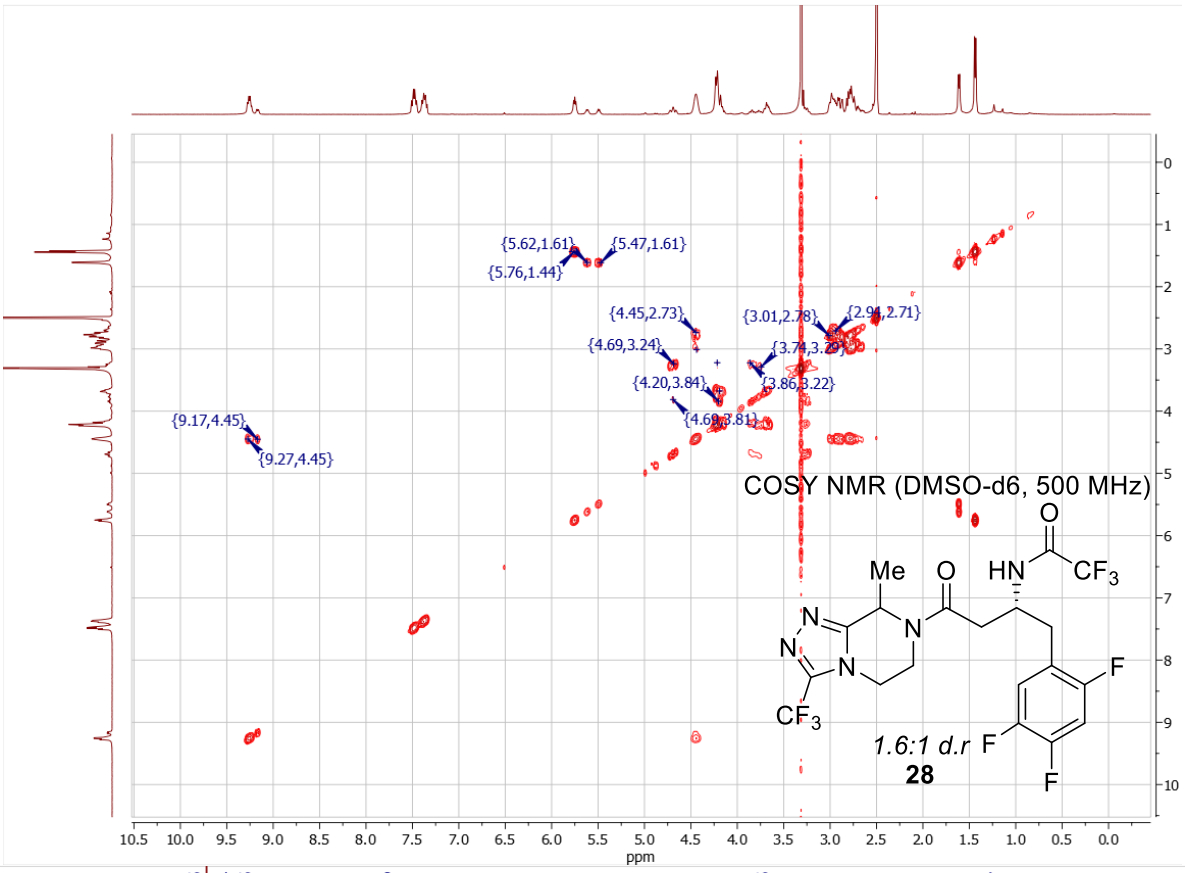
{5.62,1.61}
{5.47,1.61}
{5.76,1.44}
{4.45,2.73}
{3.01,2.78}
{2.94,2.71}
{4.69,3.24}
{3.74,3.29}
{4.20,3.84}
{3.86,3.22}
{4.69,3.81}
{9.17,4.45}
{9.27,4.45}
COSY NMR (DMSO-d6, 500 MHz)
Me
O
HN
CF3
N
N
N
N
CF3
F
F
F
1.6:1 d.r
28
ppm

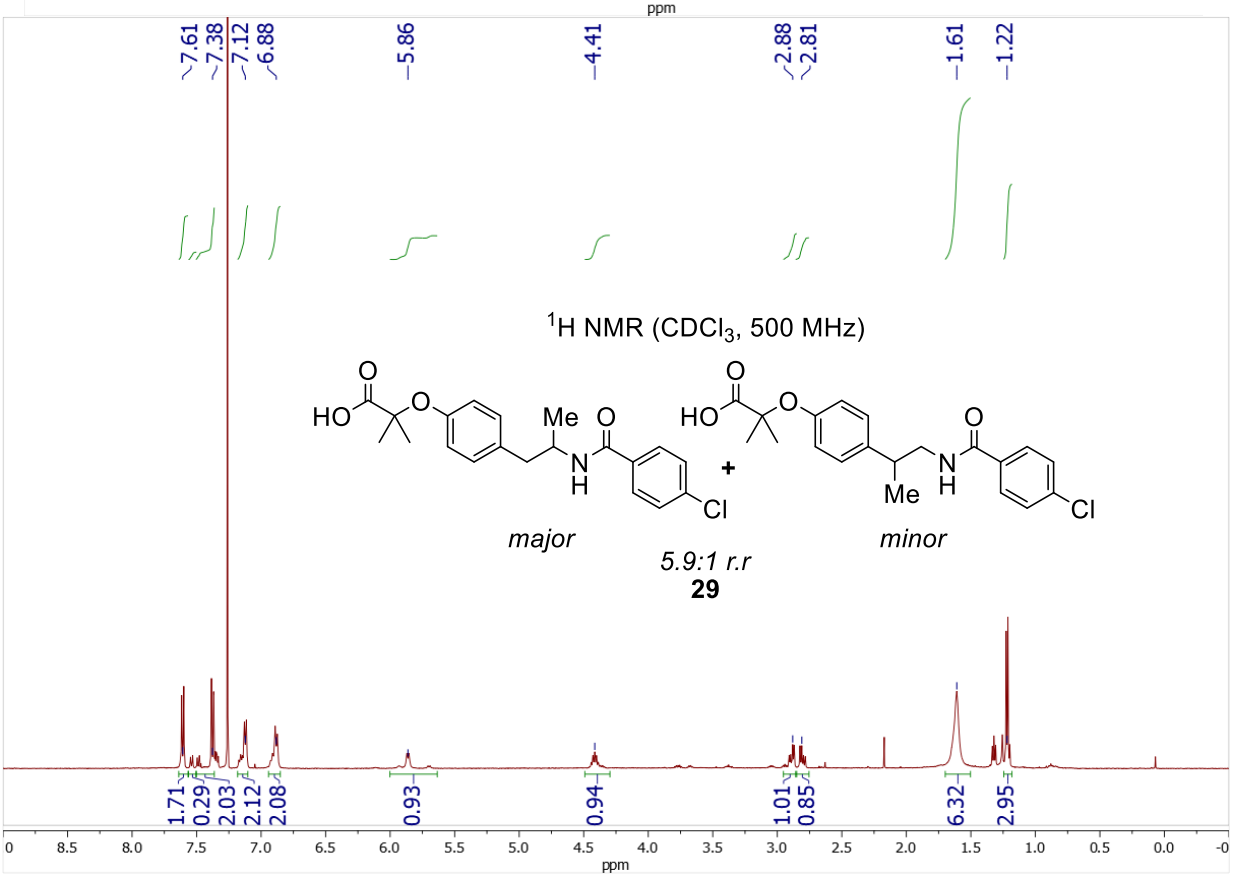
7.61
7.38
7.12
6.88
5.86
4.41
2.88
2.81
1.61
1.22
1H NMR (CDCl3, 500 MHz)
HO
O
Me
N
H
Cl
major
minor
5.9:1 r.r
29
1.71
0.29
2.03
2.12
2.08
0.93
0.94
1.01
0.85
6.32
2.95
ppm

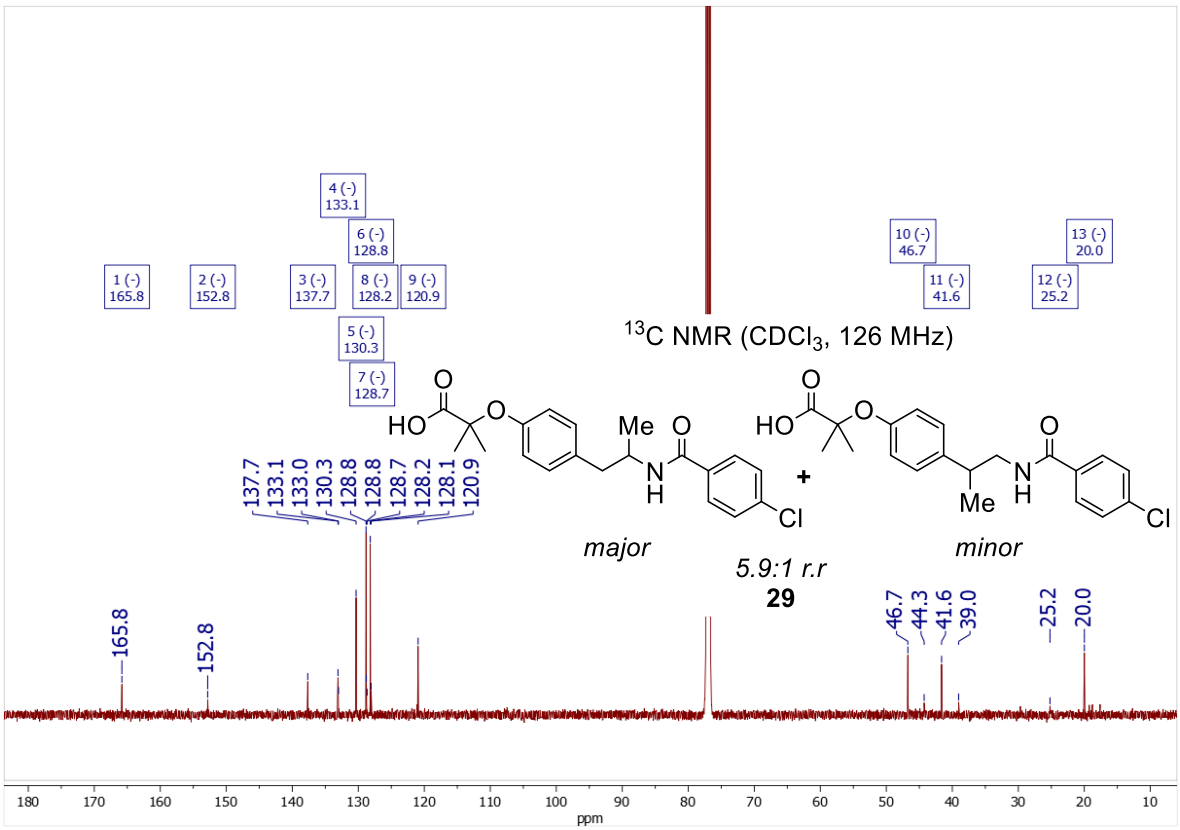

Major isomer ^{13}C peaks are shown twice (in peak picking and again in the boxes)

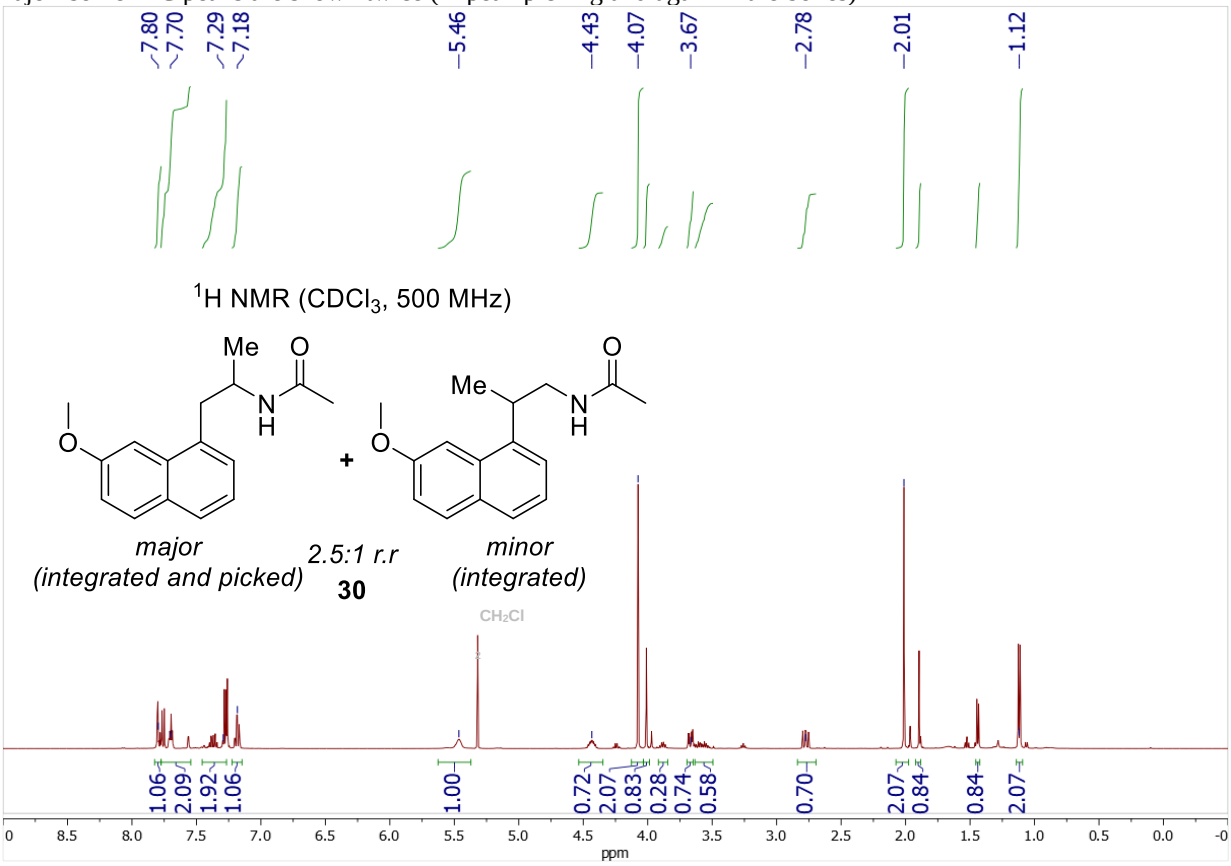

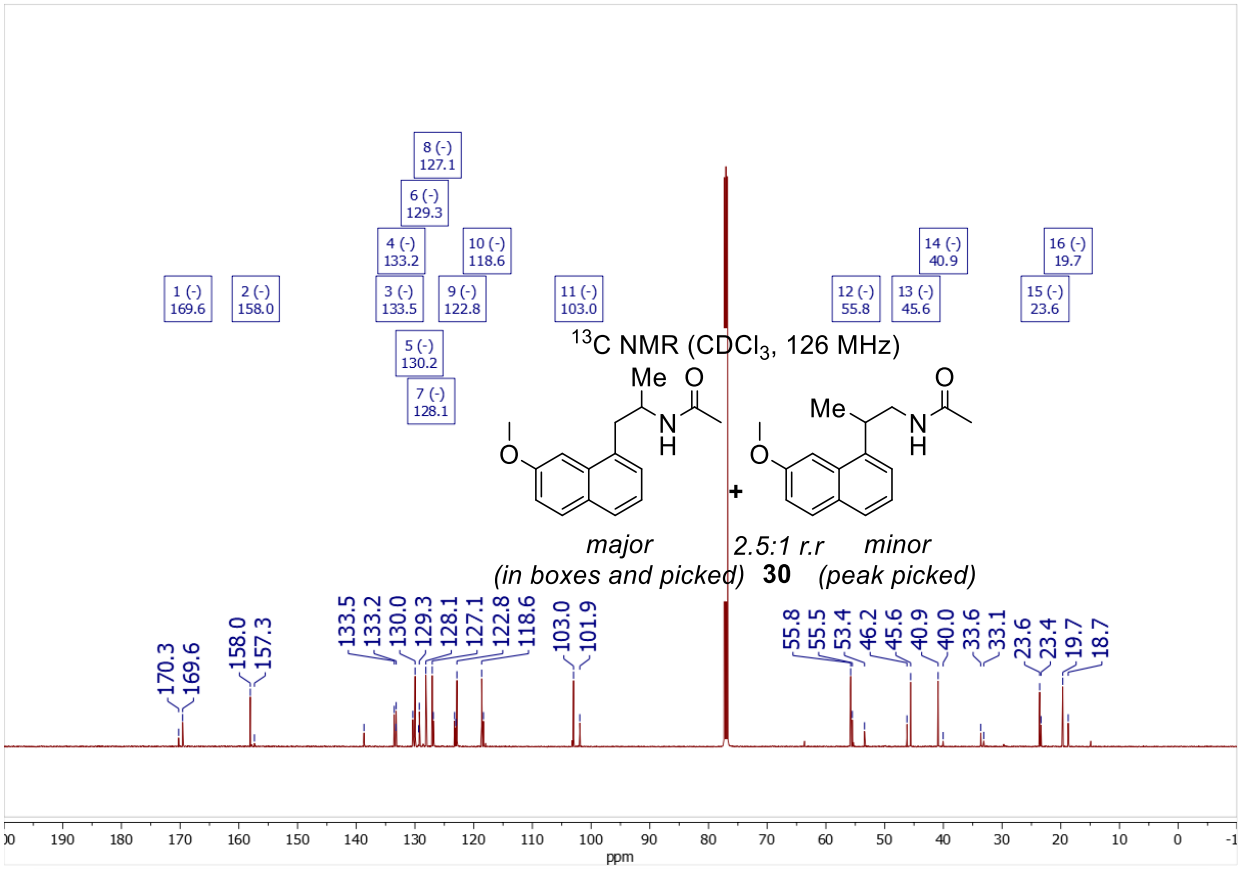
^{13}C NMR ($CDCl_3$, 126 MHz)
major
2.5:1 r.r
minor
(in boxes and picked) 30 (peak picked)
ppm

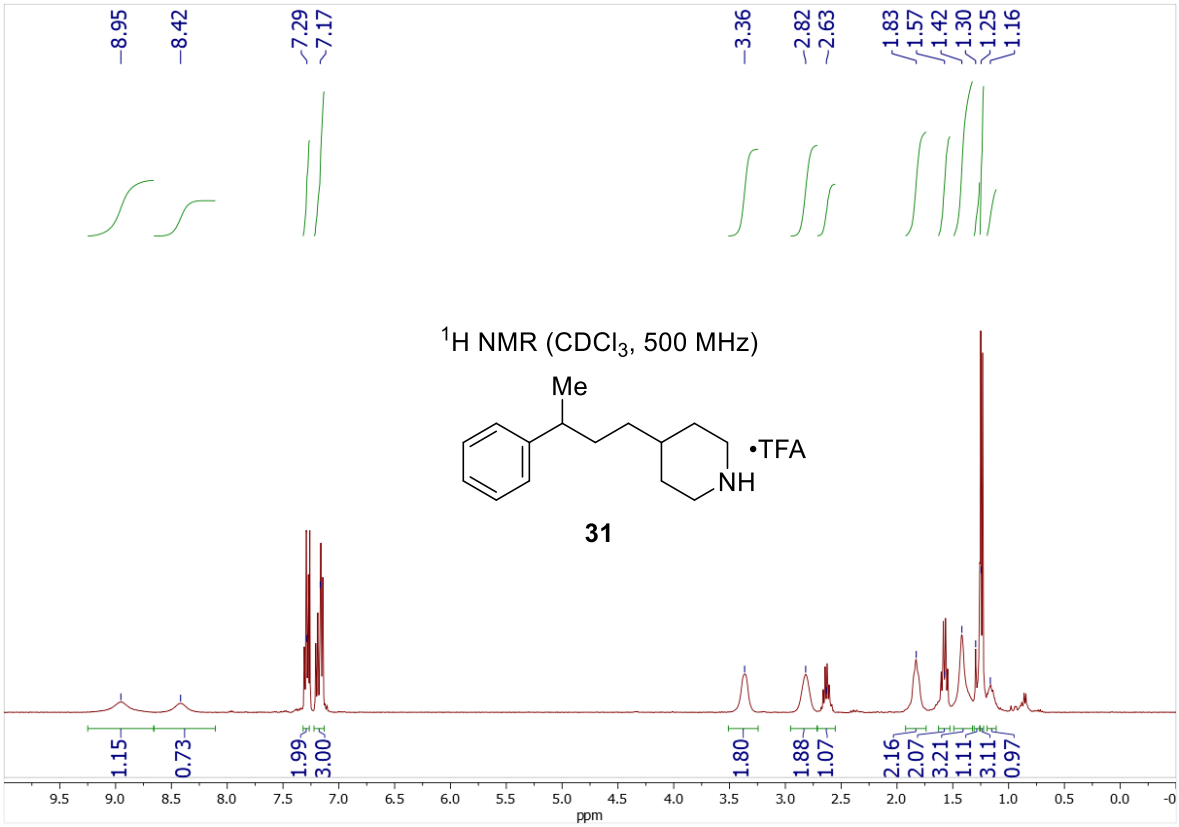
^{1}H NMR ($CDCl_3$, 500 MHz)
•TFA
31
ppm

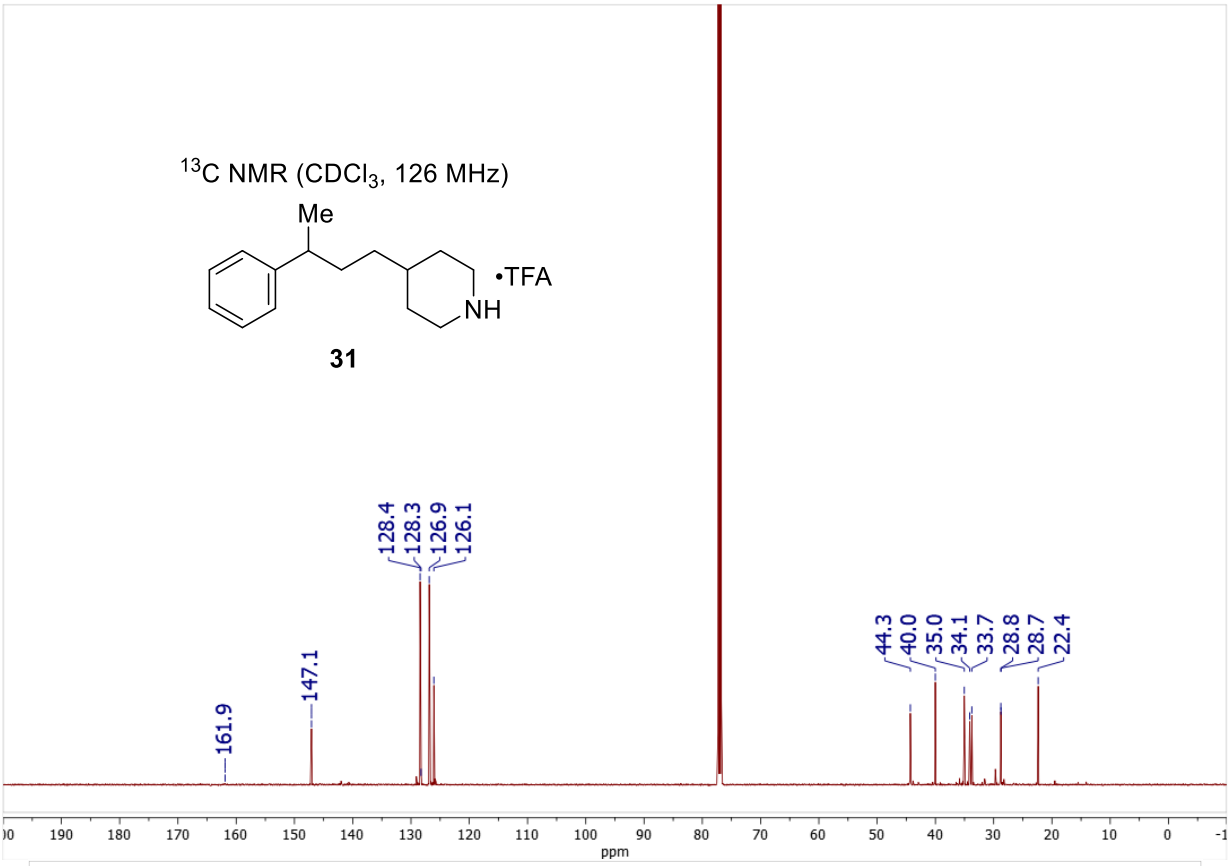
^{13}C NMR ($CDCl_3$, 126 MHz)
Me
•TFA
NH
31
161.9
147.1
128.4
128.3
126.9
126.1
44.3
40.0
35.0
34.1
33.7
28.8
28.7
22.4
ppm

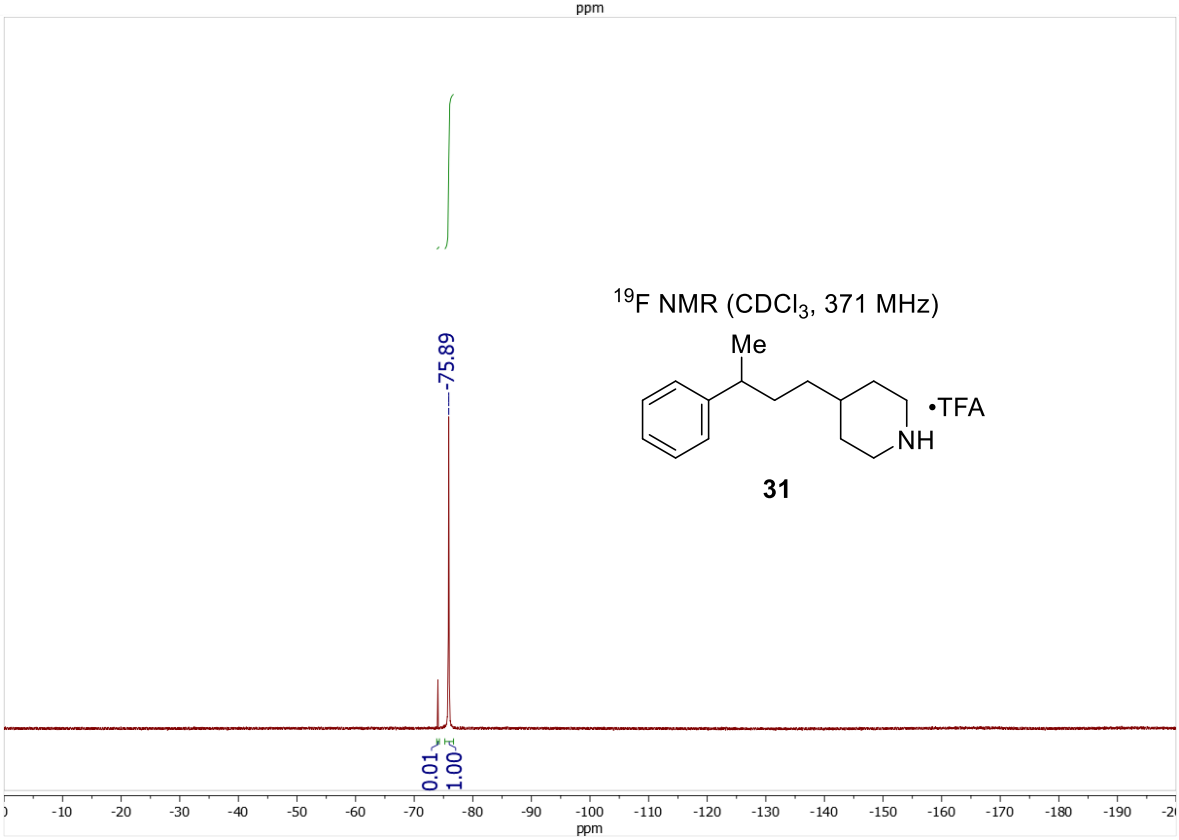
^{19}F NMR ($CDCl_3$, 371 MHz)
Me
•TFA
NH
31
-75.89
0.01
1.00
ppm

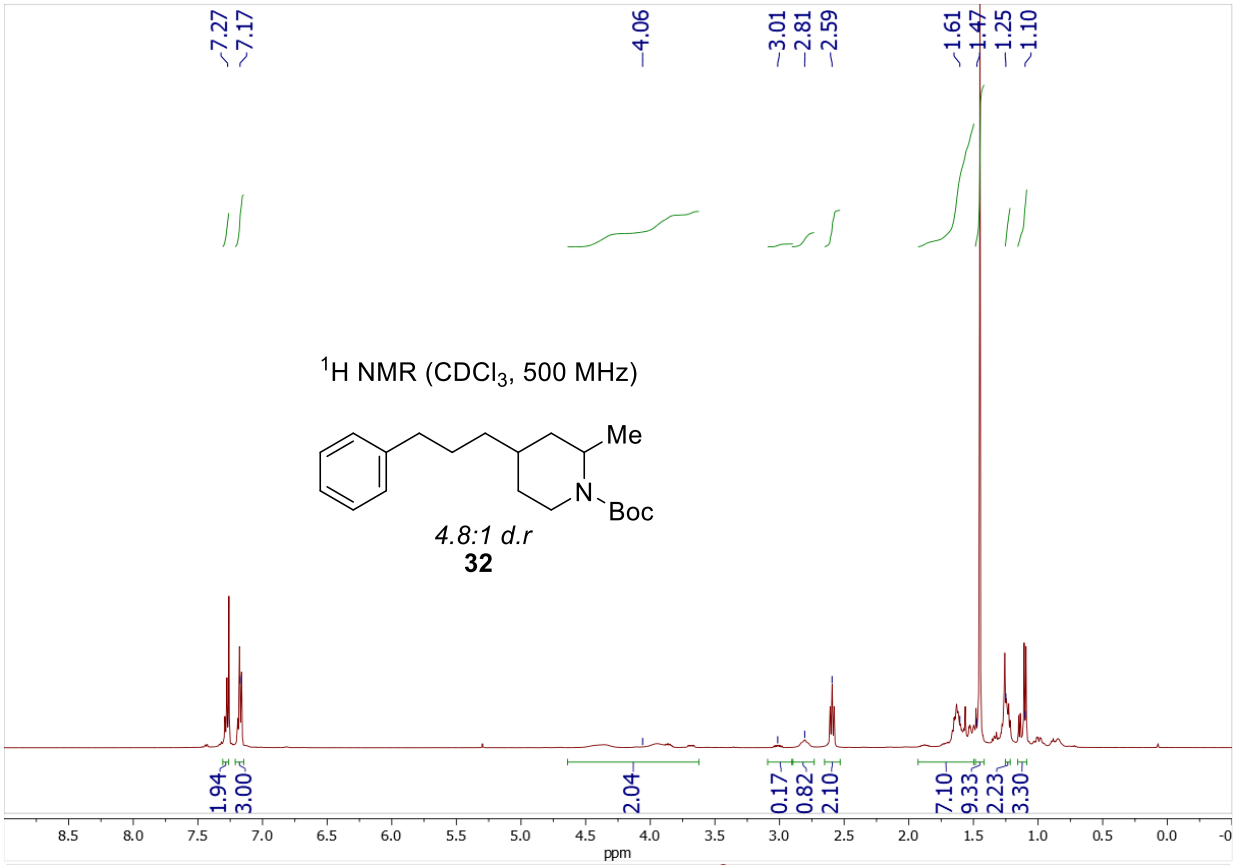
7.27
7.17
4.06
3.01
2.81
2.59
1.61
1.47
1.25
1.10
^{1}H NMR ($CDCl_3$, 500 MHz)
Me
N
Boc
4.8:1 d.r
32
1.94
3.00
2.04
0.17
0.82
2.10
7.10
9.33
2.23
3.30
ppm

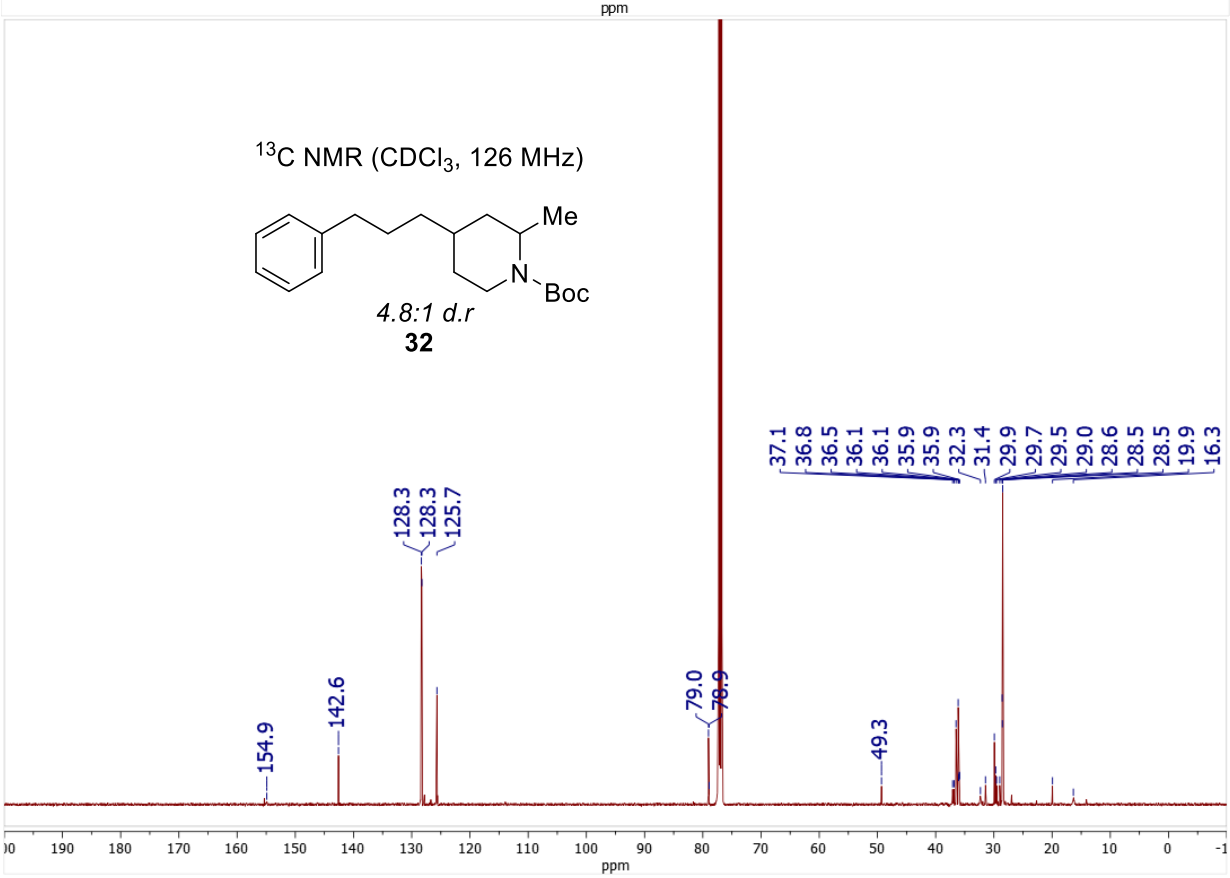
^{13}C NMR ($CDCl_3$, 126 MHz)
Me
N
Boc
4.8:1 d.r
32
37.1
36.8
36.5
36.1
36.1
35.9
35.9
32.3
31.4
29.9
29.7
29.5
29.0
28.6
28.5
28.5
19.9
16.3
128.3
128.3
125.7
154.9
142.6
79.0
78.9
49.3
ppm

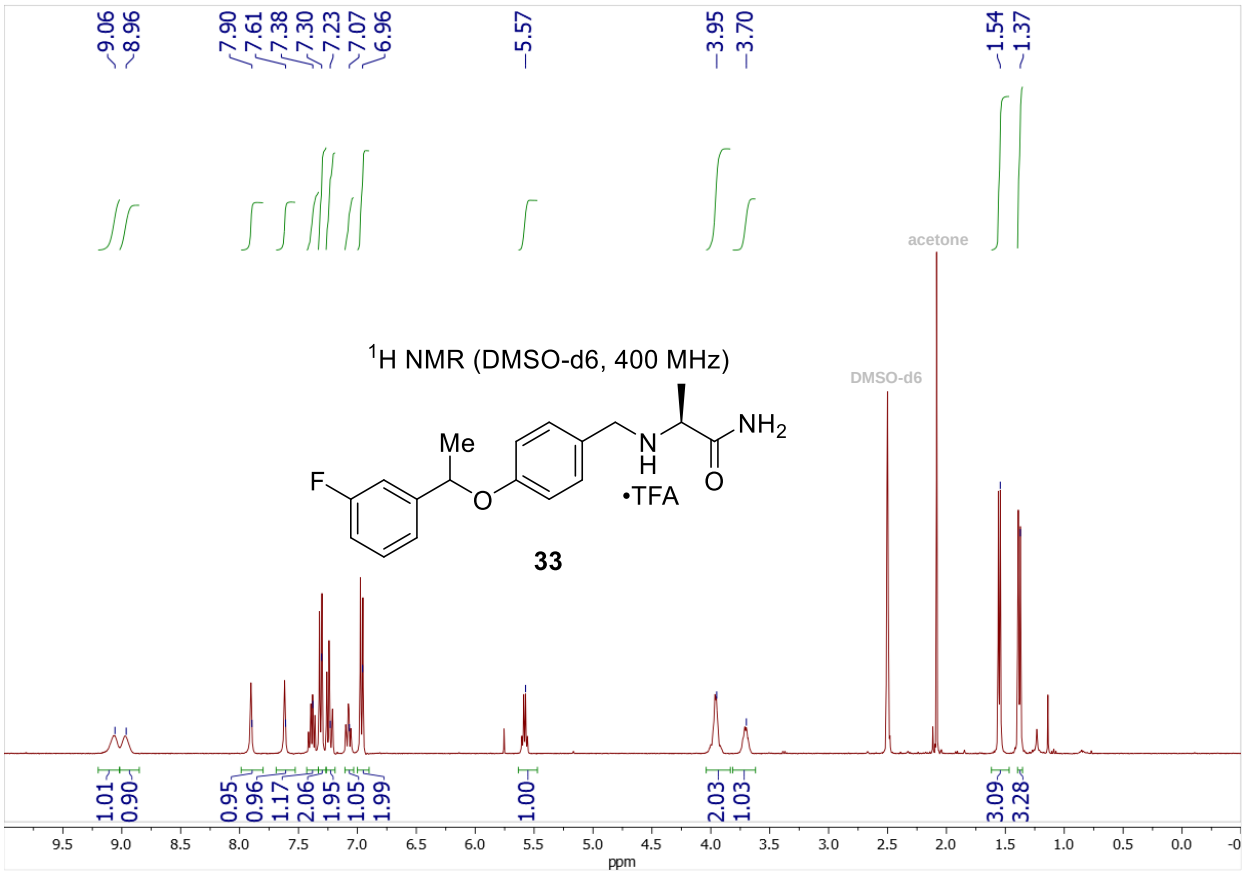

^{1}H NMR (DMSO-d6, 400 MHz)

33

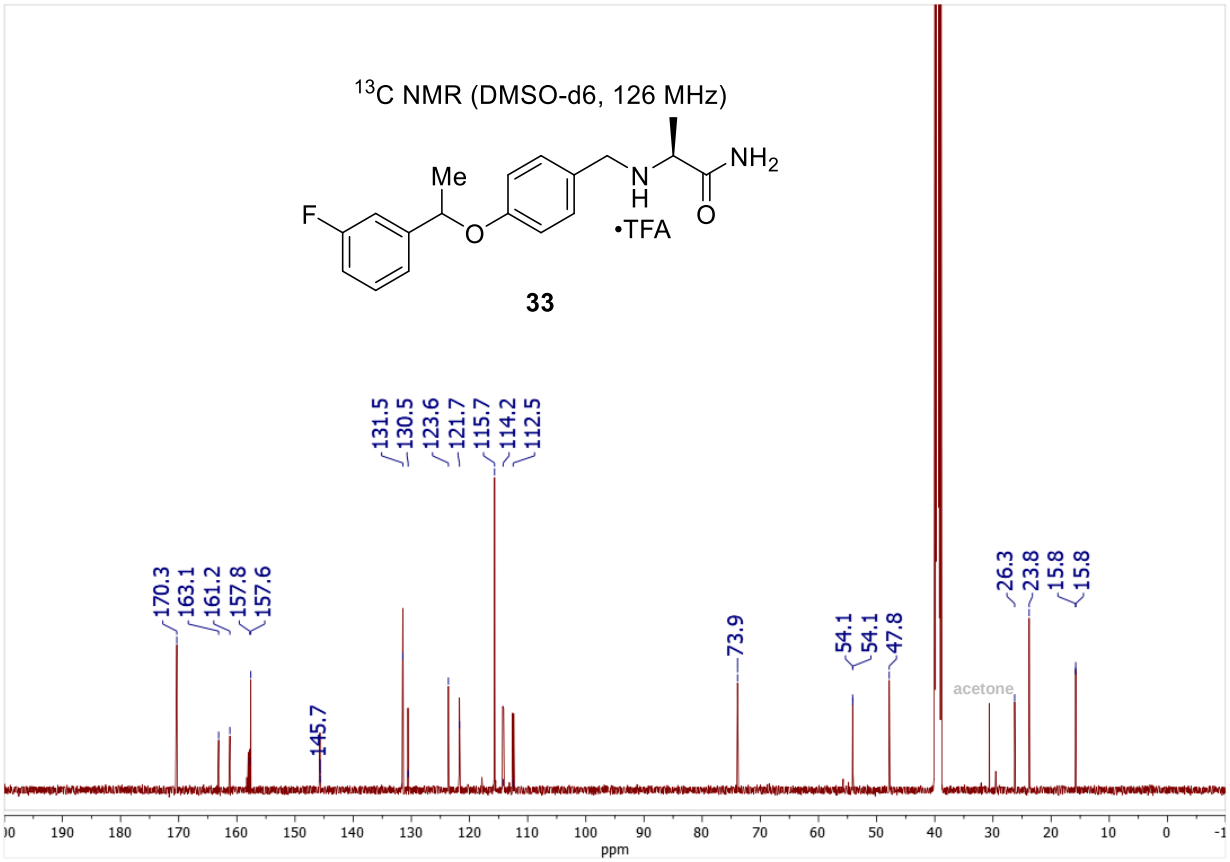

^{13}C NMR (DMSO-d6, 126 MHz)

33

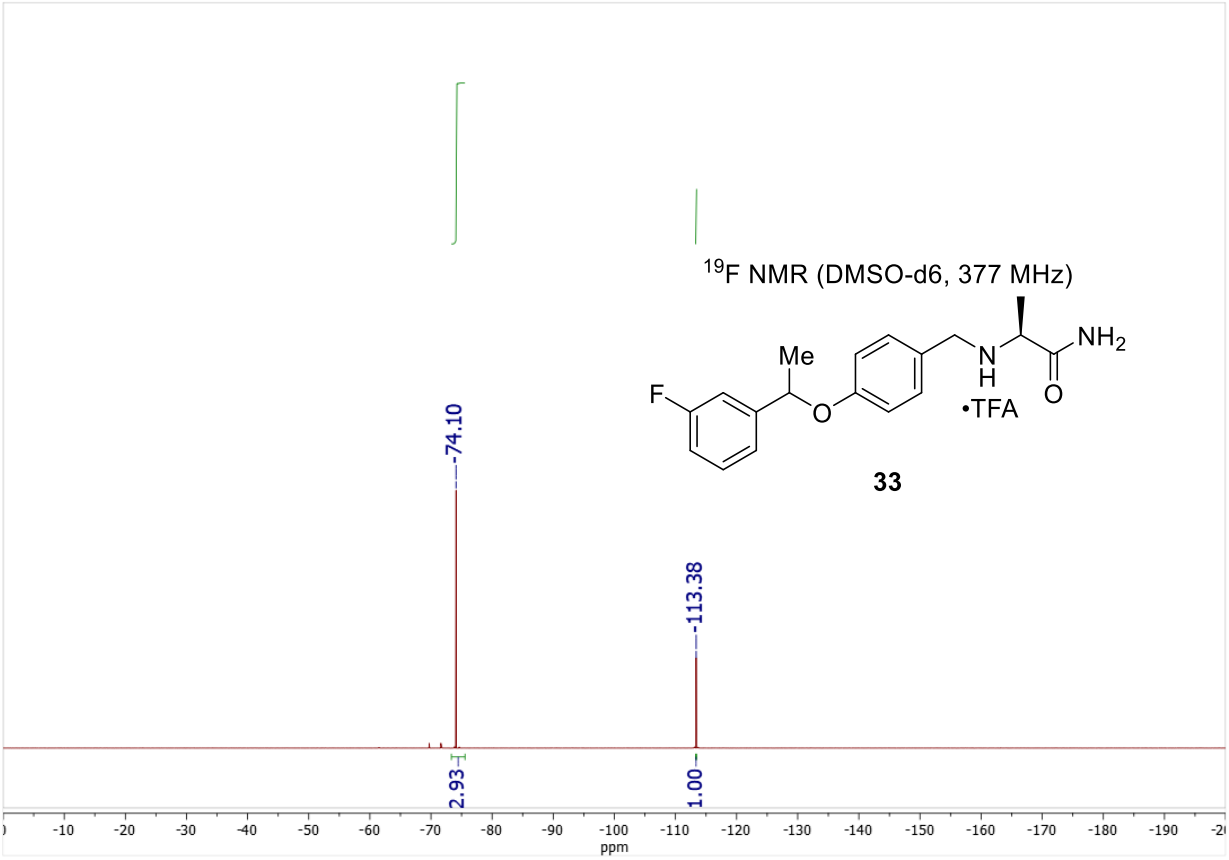
19F NMR (DMSO-d6, 377 MHz)
-74.10
-113.38
2.93
1.00
ppm
33

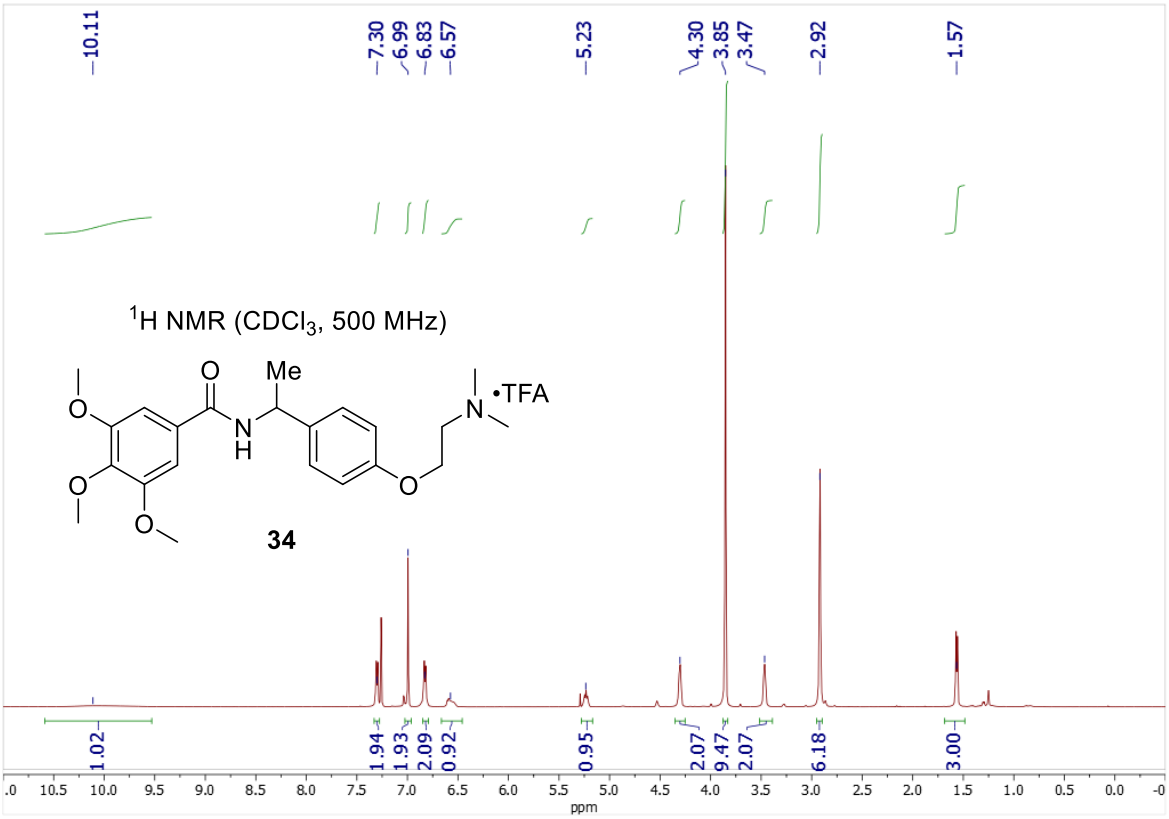
1H NMR (CDCl3, 500 MHz)
10.11
7.30
6.99
6.83
6.57
5.23
4.30
3.85
3.47
2.92
1.57
1.02
1.94
1.93
2.09
0.92
0.95
2.07
9.47
2.07
6.18
3.00
ppm
34

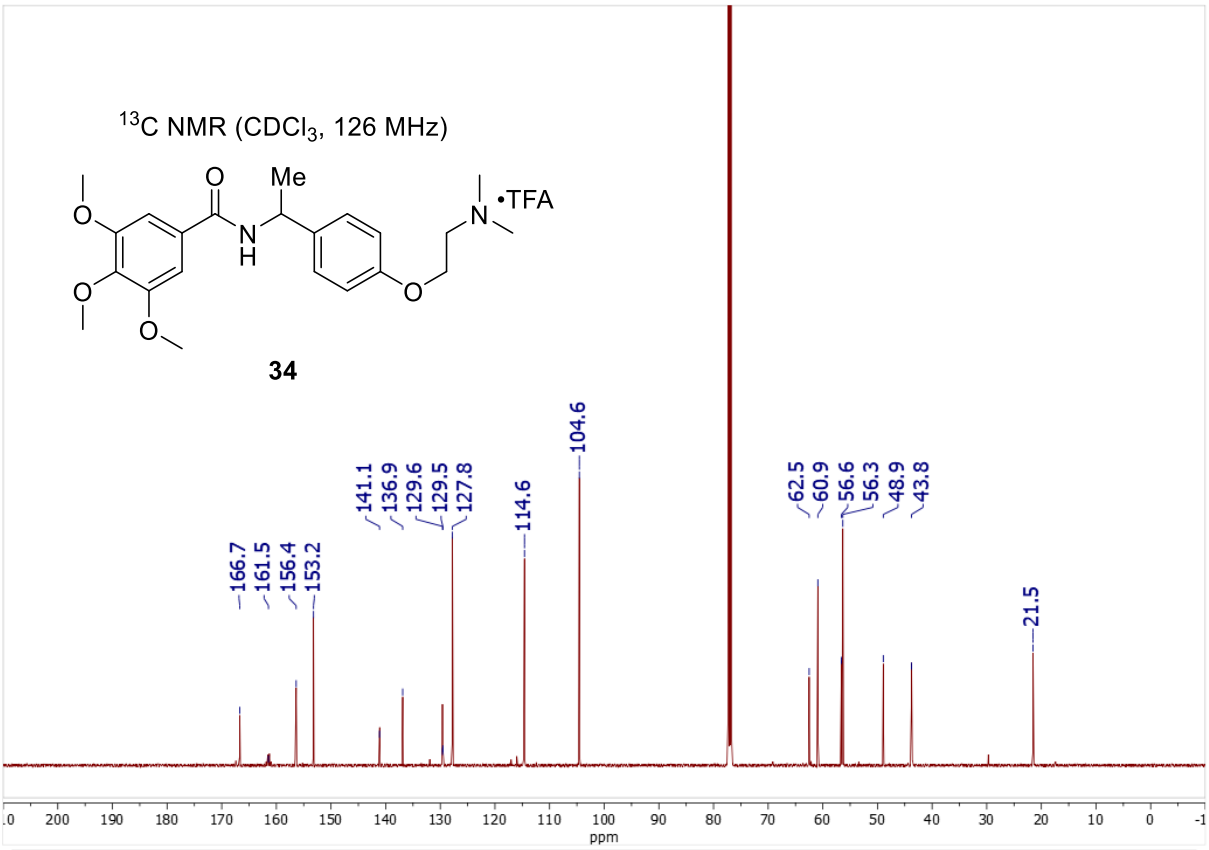
^{13}C NMR ($CDCl_3$, 126 MHz)
O
Me
O
N
H
N
•TFA
O
O
O
34
166.7
161.5
156.4
153.2
141.1
136.9
129.6
129.5
127.8
114.6
104.6
62.5
60.9
56.6
56.3
48.9
43.8
21.5
ppm

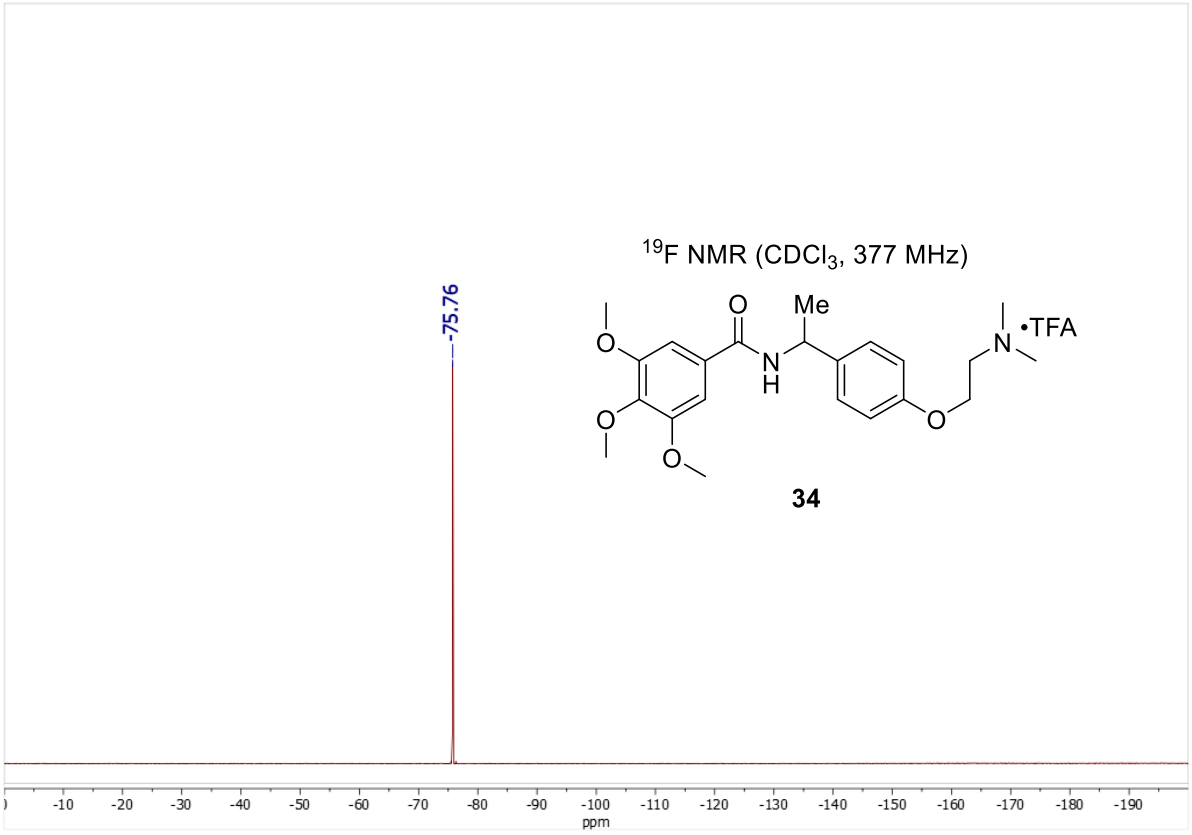
^{19}F NMR ($CDCl_3$, 377 MHz)
-75.76
O
Me
O
N
H
N
•TFA
O
O
O
34
ppm

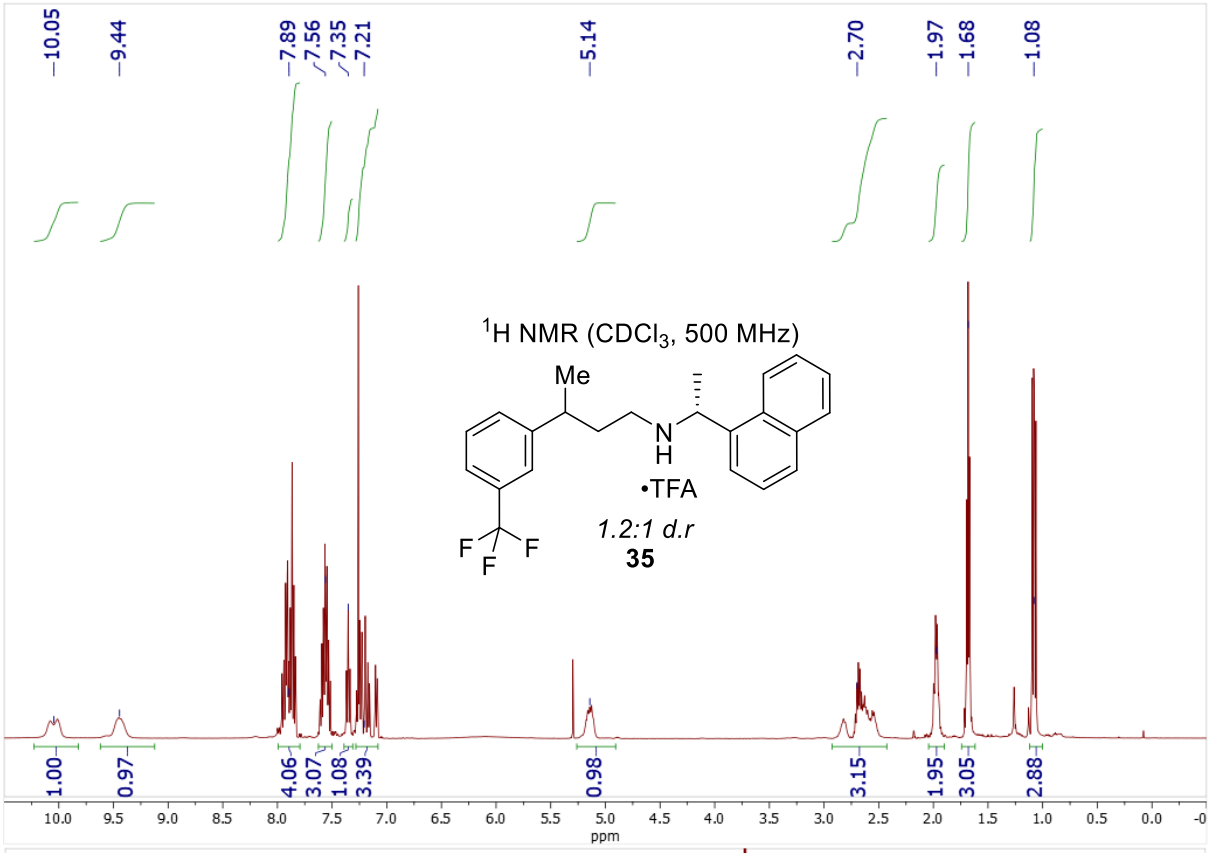
10.05
9.44
7.89
7.56
7.35
7.21
5.14
2.70
1.97
1.68
1.08
^{1}H NMR ($CDCl_3$, 500 MHz)
Me
N
H
•TFA
F
F
F
1.2:1 d.r
35
1.00
0.97
4.06
3.07
1.08
3.39
0.98
3.15
1.95
3.05
2.88
ppm

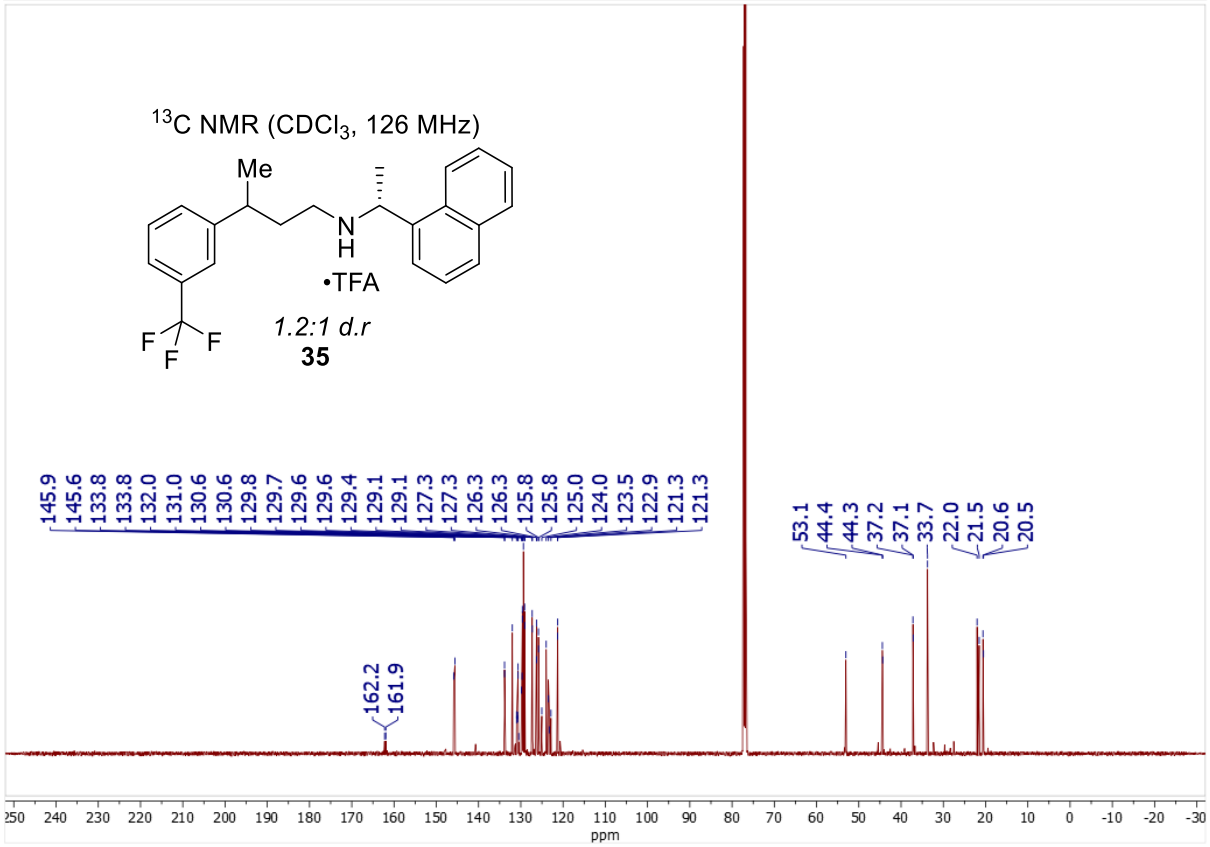
^{13}C NMR ($CDCl_3$, 126 MHz)
Me
N
H
•TFA
F
F
F
1.2:1 d.r
35
145.9
145.6
133.8
133.8
132.0
131.0
130.6
130.6
129.8
129.7
129.6
129.6
129.4
129.1
129.1
127.3
127.3
126.3
126.3
125.8
125.8
125.0
124.0
123.5
122.9
121.3
121.3
53.1
44.4
44.3
37.2
37.1
33.7
22.0
21.5
20.6
20.5
162.2
161.9
ppm

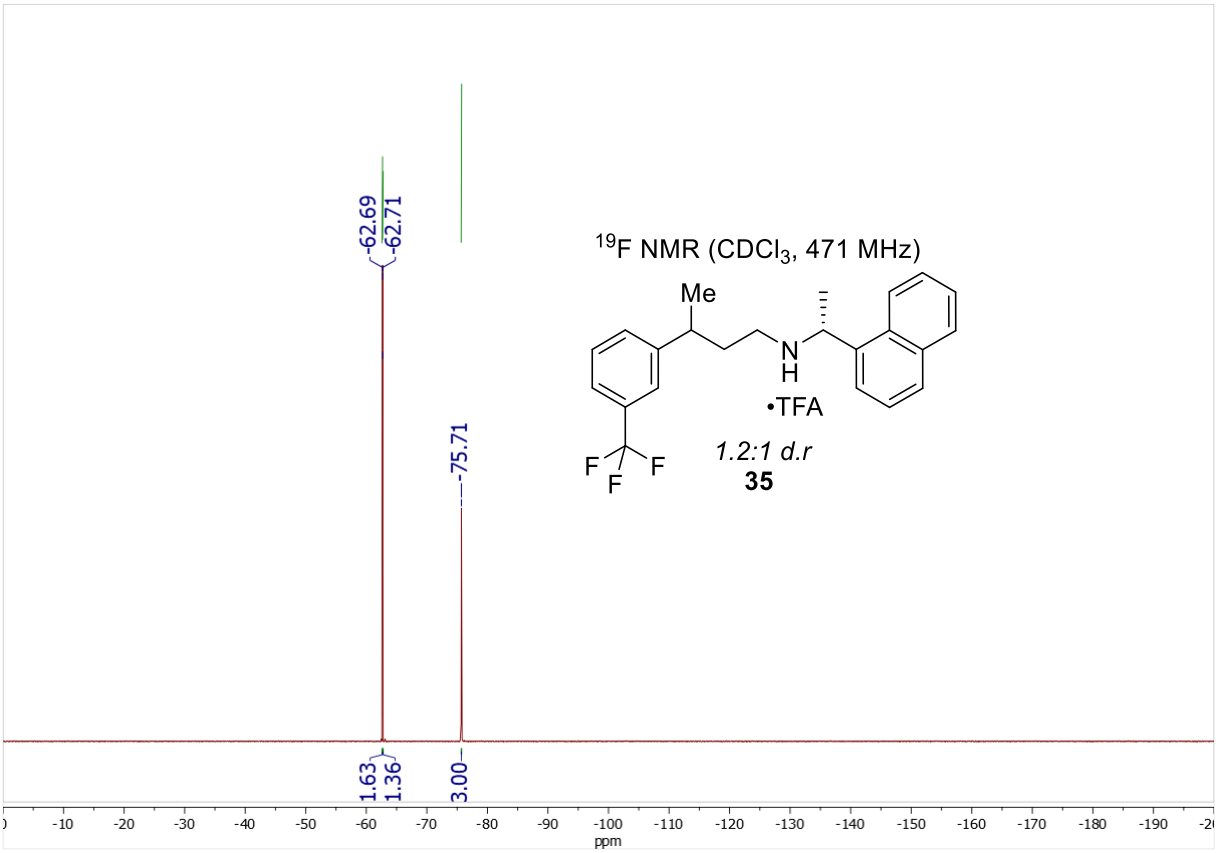
-62.69
-62.71
-75.71
1.63
1.36
3.00
ppm
19F NMR (CDCl3, 471 MHz)
Me
N
H
•TFA
F
F
F
1.2:1 d.r
35

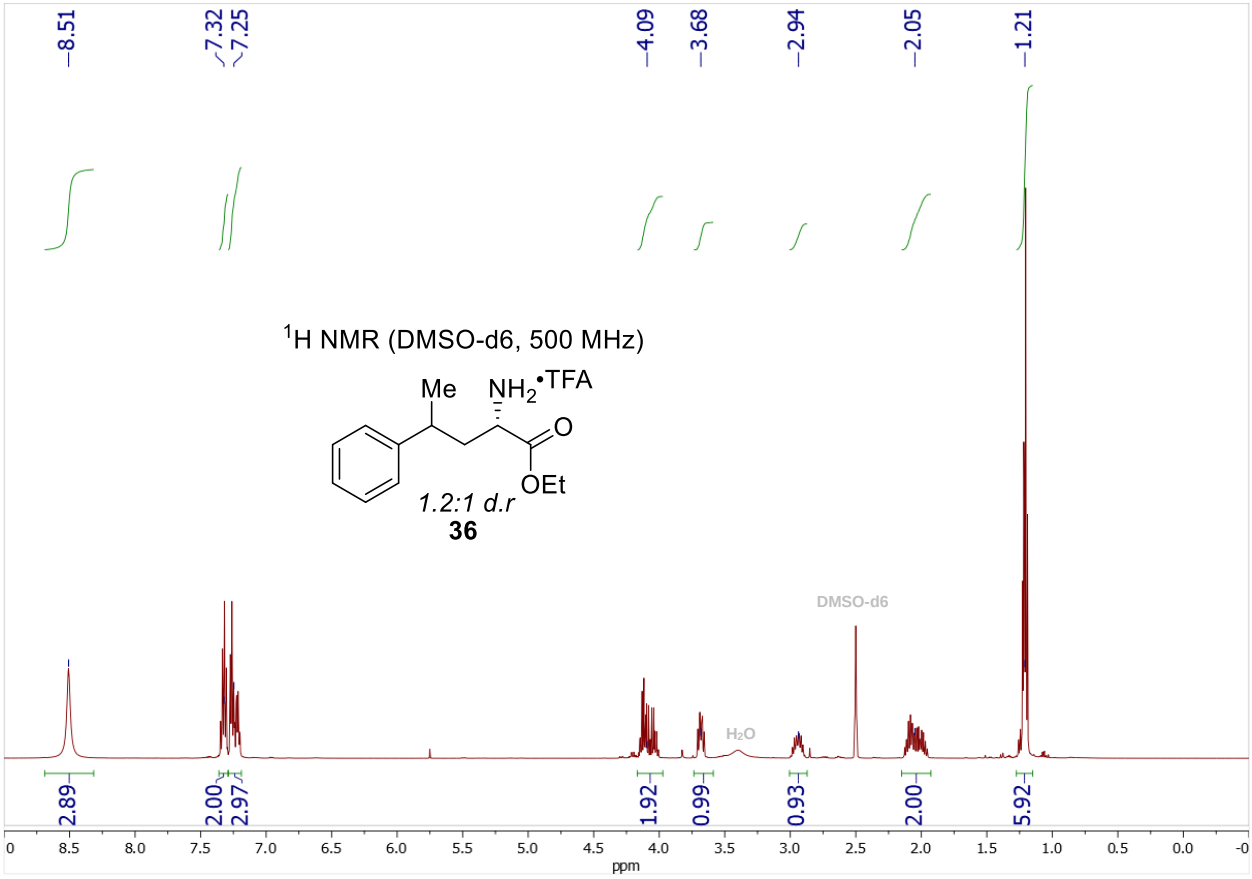
8.51
7.32
7.25
4.09
3.68
2.94
2.05
1.21
1H NMR (DMSO-d6, 500 MHz)
Me
NH2•TFA
O
OEt
1.2:1 d.r
36
DMSO-d6
H2O
2.89
2.00
2.97
1.92
0.99
0.93
2.00
5.92
ppm

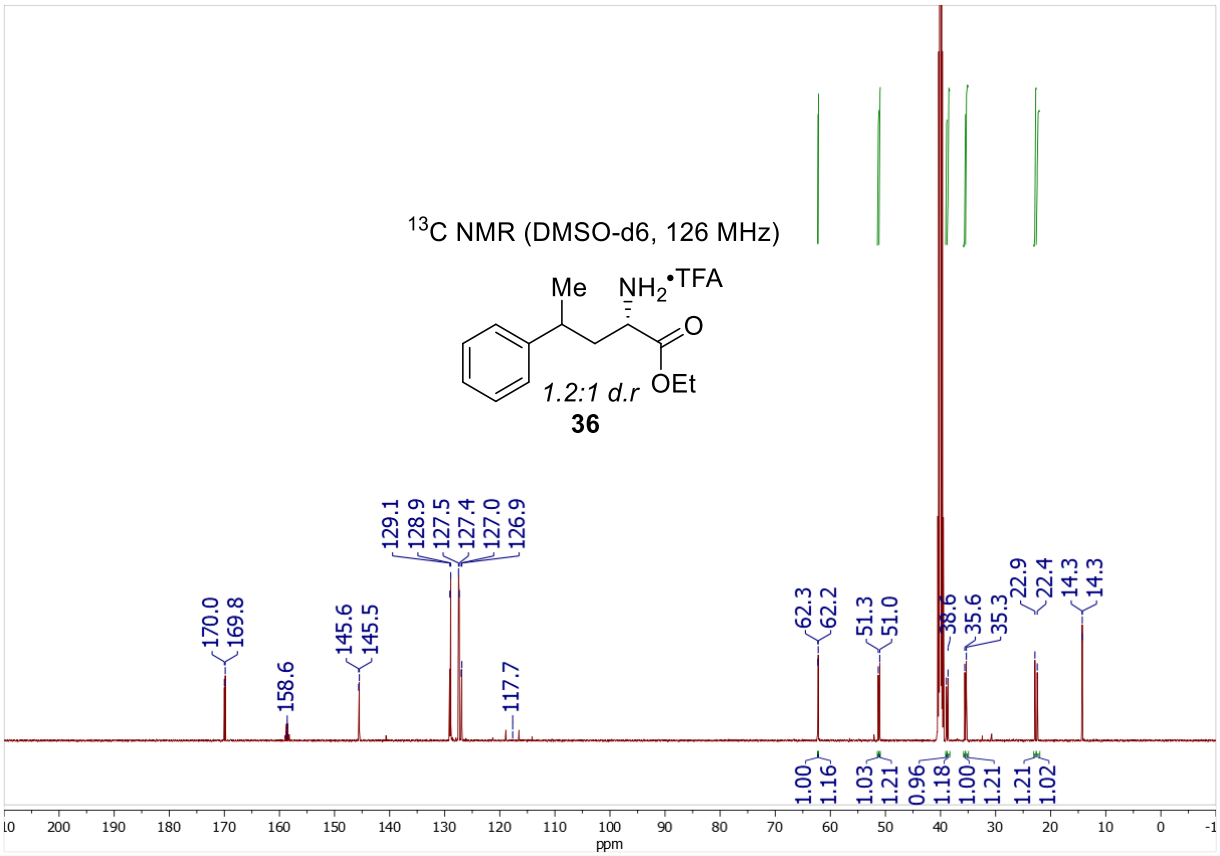
^{13}C NMR (DMSO-d6, 126 MHz)
Me
NH2•TFA
O
OEt
1.2:1 d.r
36
170.0
169.8
158.6
145.6
145.5
129.1
128.9
127.5
127.4
127.0
126.9
117.7
62.3
62.2
51.3
51.0
38.6
35.6
35.3
22.9
22.4
14.3
14.3
1.00
1.16
1.03
1.21
0.96
1.18
1.00
1.21
1.21
1.02
ppm

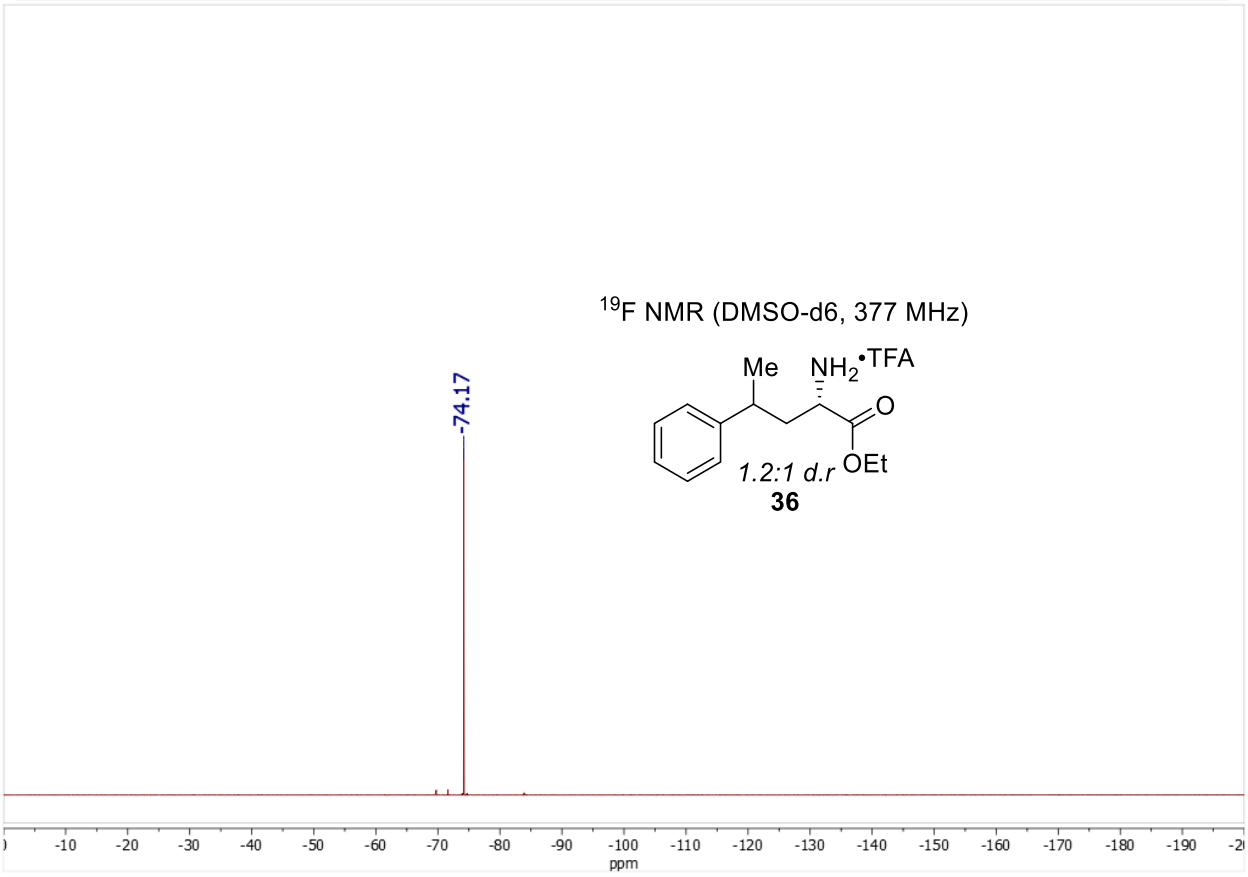
^{19}F NMR (DMSO-d6, 377 MHz)
Me
NH2•TFA
O
OEt
1.2:1 d.r
36
-74.17
ppm

5D.X. References

1. M. Xiang, Z.-K. Xin, B. Chen, C.-H. Tung, L.-Z. Wu, Exploring the reducing ability of organic dye (Acr^+-Mes) for fluorination and oxidation of benzylic C(sp^3)–H bonds under visible light irradiation. *Org. Lett.* **2017**, *19*, 3009-3012.
2. A. Varela, L. K. B. Garve, D. Leonori, V. K. Aggarwal, Stereocontrolled total synthesis of (–)-Stemaphylline, *Angew. Chem. Int. Ed.* **2017**, *56*, 2127-2131.
3. A. B. Benowitz, H. C. Eberl, C. L. Erickson-Miller, A. G. Gilmartin, E. R. Gore, M. N. Montoute, Z. Wu, A hit deconstruction approach for the discovery of fetal hemoglobin inducers, *Bioorganic Med. Chem. Lett.* **2018**, *28*, 3676-3680.
4. H. Jia, G. Dai, J. Weng, Z. Zhang, Q. Wang, F. Zhou, L. Jiao, Y. Cui, Y. Ren, S. Fan, J. Zhou, W. Qing, Y. Gu, J. Wang, Y. Sai, W. Su, Discovery of (*S*)-1-(1-(imidazo[1,2-*a*]pyridin-6-yl)ethyl)-6-(1-methyl-1*H*-pyrazol-4-yl)-1*H*-[1,2,3]triazolo[4,5-b]pyrazine (Volitinib) as a highly potent and selective mesenchymal-epithelial transition factor (c-Met) inhibitor in clinical development for treatment of cancer. *J. Med. Chem.* **2014**, *57*, 7577-7589.
5. J. Luo, J. Zhang, Donor-acceptor fluorophores for visible-light promoted organic synthesis: photoredox/Ni dual catalytic C(sp^3)–C(sp^2) cross-coupling. *ACS Catal.* **2016**, *6*, 873-877.
6. K. Hanson, L. Roskop, P. I. Djurovich, F. Zahariev, M. S. Gordon, M. E. Thompson, A paradigm for blue- or red-shifted absorption of small molecules depending on the site of π-extension. *J. Am. Chem. Soc.* **2010**, *132*, 16247-16255.
7. R. L. Donkers, F. Maran, D. D. M. Wayner, M. S. Workentin, Kinetics of the reduction of dialkyl peroxides. New insights into the dynamics of dissociative electron transfer[1]. *J. Am. Chem. Soc.* **1999**, *121*, 7239-7248.
8. C. K. Prier, D. A. Rankic, D. W. C. MacMillan, Visible light photoredox catalysis with transition metal complexes: applications in organic synthesis. *Chem. Rev.* **2013**, *113*, 5322-5363.
9. N. A. Romero, D. A. Nicewicz, Organic photoredox catalysis. *Chem. Rev.* **2016**, *116*, 10075-10166.
10. X.-Y. Cao, J.-C. Zheng, Y.-X. Li, Z.-C. Shu, X.-L. Sun, B.-Q. Wang, Y. Tang, Pyrrolidine-ureas as bifunctional organocatalysts for asymmetric Michael addition of ketone to nitroalkenes: unexpected hydrogen bonding effect. *Tetrahedron* **2010**, *66*, 9703-9707.
11. P. E. Piszel, A. Vasilopoulos, S. S. Stahl, Oxidative amide coupling from functionally diverse alcohols and amines using aerobic copper/nitroxyl catalysis. *Angew. Chem. Int. Ed.* **2019**, *58*, 12211-12215.
12. S. Wang, Q. Qian, H. Gong, Nickel-catalyzed reductive coupling of aryl halides with secondary alkyl bromides and allylic acetate. *Org. Lett.* **2012**, *14*, 3352-3355.
13. P. Beak, R. J. Trancik, D. A. Simpson, Reactions of chloroformates with silver fluoro salts. *J. Am. Chem. Soc.* **1969**, *91*, 5073-5080.
14. C. Liu, C. He, W. Shi, M. Chen, A. Lei, Ni-catalyzed mild arylations of α-halocarbonyl compounds with arylboronic acids. *Org. Lett.* **2007**, *9*, 5601-5604.
15. H. Pines, N. E. Sartoris, Base-catalyzed reactions. XXXIV.[1] The alkali metal catalyzed side-chain aralkylation of 2- and 4-alkylpyridines with styrene, α-methylstyrene, and cis- and trans-β-methylstyrene. *J. Org. Chem.* **1969**, *34*, 2113-2118.
16. Y. Wang, W. Ren, J. Li, H. Wang, Y. Shi, Facile palladium-catalyzed hydrocarboxylation of olefins without external CO gas. *Org. Lett.* **2014**, *16*, 5960-5963.

17. M. Leeman, G. Brasile, D. Gelens, T. Vries, B. Kaptein, R. Kellogg, Structural aspects of nucleation inhibitors for diastereomeric resolutions and the relationship to dutch resolution. *Angew. Chem. Int. Ed.* **2008**, *47*, 1287-1290.
18. B. Z. Costa, J. L. Galman, I. Slabu, S. P. France, A. J. Marsaioli, N. J. Turner, Synthesis of 2,5-disubstituted pyrrolidine alkaloids via a one-pot cascade using transaminase and reductive aminase bioacatalysts. *ChemCatChem* **2018**, *10*, 4733-4738.
19. F. Berthiol, H. Doucet, M. Santelli, Synthesis of β-aryl ketones by tetraphosphine/palladium catalysed Heck reactions of 2- or 3-substituted allylic alcohols with aryl bromides. *Tetrahedron* **2006**, *62*, 4372-4383.

Appendix E: Supporting Information Chapter 6

6E.I. General Considerations

All reagents were purchased from commercial sources and used as received unless otherwise noted. Cu salts were purchased from Aldrich. Alcohol and amine substrates were purchased from Oakwood, Combi-Blocks, Chem-Impex, Enamine, Ark-Pharm, AvaChem Scientific, or Aldrich. 4,4'-di-*tert*-butyl-2,2'-bipyridine ($^{t\text{Bu}}$bpy) was purchased from Aldrich and 9-azabicyclo[3.3.1]nonane *N*-oxyl (ABNO) was generously donated from Merck & Company, Inc.

All coupling reactions were set up on the benchtop. ^{1}H, ^{13}C, and ^{19}F NMR spectra were recorded on a Bruker Avance III 400 spectrometer (^{1}H 400.1 MHz, ^{13}C 100.6 MHz, ^{19}F 376.5 MHz) or a Bruker Avance III 500 spectrometer (^{1}H 500.1 MHz, ^{13}C 125.7 MHz, ^{19}F 470.6 MHz) and chemical shifts are reported in parts per million (ppm). NMR spectra were referenced to $CDCl_3$ at 7.26 ppm (^{1}H) and 77.16 ppm (^{13}C), and or d^6-DMSO at 2.50 ppm (^{1}H) and 39.52 ppm (^{13}C). All ^{19}F NMR spectra were absolutely referenced to their respective solvent peaks in the ^{1}H NMR spectrum. See the online publication for complete NMR spectra.[1] Chromatography was performed using an automated Biotage Isolera® or Teledyne Isco Combiflash Rf with reusable 25 g Redisep Rf cartridges hand packed with standard silica or Biotage® SNAP Ultra C18 60 g prepacked cartridges. High-resolution mass spectra were obtained using a Thermo Q Exactive™ Plus via (ASAP-MS) by the mass spectrometry facility at the University of Wisconsin. IR spectra were recorded on a Bruker Platinum-ATR ALPHA spectrometer. Melting points were determined using a DigiMelt MPA160 SRS melting point apparatus.

Efficient gas-liquid mixing typically improves reactivity in aerobic reactions. Employing reaction vessels with a large headspace, purging the headspace with O_2 (when necessary), and rapid stirring will improve gas-liquid mixing.

6E.II. Safety Warnings Regarding Toxicity of Fluorinated Alcohols

Fluorinated alcohols, especially 2-fluoroethanol, are highly toxic compounds that can be very harmful through inhalation or facile penetration of the skin. Fluorinated alcohols can easily undergo oxidation to the corresponding fluoroacetate compound, which can interfere with the citric acid cycle in the body resulting in cardiac arrest and/or death. Extreme caution was taken when using these compounds making sure to work in a very well-ventilated area with the proper personal protective equipment.

For more information on the toxicity of fluorinated alcohols, see Refs 2-4.

6E.III. General Procedure for Cu/ABNO-catalyzed Amide Formation

6E.III.1. Under an atmosphere of O_2

Set-up: On the benchtop, a disposable 15 mL glass vial was charged with CuI (0.025 mmol, 4.8 mg, 0.05 equiv), 4,4'-di-*tert*-butyl-2,2'-bipyridine ($^{t\text{Bu}}$bpy; 0.025 mmol, 6.7 mg, 0.05 equiv), 9-azabicyclo[3.3.1]nonane *N*-oxyl (ABNO; 0.015 mmol, 2.1 mg, 0.03 equiv), acetonitrile (2.5 mL, 0.2 M), and a Teflon stir bar. The vial was sealed by a PTFE-lined pierceable cap, placed on a stir plate, and allowed to stir for approximately 3 minutes. An O_2 balloon (1 atm) with an 18-gauge needle was used to purge the headspace of the vial with O_2 for approximately 1 minute. The vent needle was removed while the O_2 balloon was left intact, continuing to stir for an additional 2 minutes. The solution color changed from red/brown to green. The amine (0.5 mmol, 1 equiv or 0.55 mmol, 1.1 equiv) and alcohol (0.75 mmol, 1.5 equiv or 0.5 mmol, 1 equiv respectively) were injected via Hamilton syringes simultaneously through the pierceable septum, turning the solution red/brown. *Adding the reagents simultaneously is very important*. The reaction was allowed to stir at room temperature for 4 hours.

For reactions where the amine and/or alcohol coupling partners are solid: Only 1.0 mL out of 2.5 mL of acetonitrile was added to the disposable 15 mL glass vial containing CuI, $^{t\text{Bu}}$bpy, ABNO, and the Teflon stir bar. The solid coupling partner is dissolved in the remaining acetonitrile (1.5 mL) to form a 0.33 M stock solution, which is injected simultaneously with the liquid coupling partner to the stirring catalyst solution under O_2. If both coupling partners are solids, they are both dissolved in acetonitrile (0.33 M each) prior to injection.

Work-up: At the end of the reaction, the mixture turns green. The O_2 balloon was removed, the vial was removed from the stir plate, and the reaction was diluted with ethyl acetate (5.0 mL) then pushed through a plug of silica. For substrates that possessed functional groups that might prevent passage of the product through silica, a solution of 10% triethylamine in ethyl acetate was used as the eluent. Solvent was then removed in vacuo using a ThermoFisher Scientific Savant™ SPD131DDA Speedvac™ Concentrator (typical rotary evaporation is also suitable). Products insoluble in ethyl acetate and acetonitrile were immediately concentrated in vacuo at the end of the reaction. Dimethyldiphenylsilane was then added via syringe as a ^{1}H NMR external standard (0.083 mmol, 18 μL, 0.166 equiv) and the crude mixture was dissolved in *d*-chloroform. An aliquot of the mixture was taken for analysis by ^{1}H NMR spectroscopy to determine the reaction yield. After recombining the NMR sample, the reaction mixture was concentrated by rotary evaporation and purified using automated normal phase column chromatography or automated reverse phase column chromatography.

Reactions performed in DMF were set up as reported above, using DMF in place of MeCN as the solvent. These reactions are washed with a saturated aqueous solution of LiCl (3 x 3.0 mL) to remove DMF following the ethyl acetate silica plug filtration.

6E.III.2. Under air

Set-up: On the benchtop, a 25 x 150 mm test tube was charged with CuI (0.025 mmol, 4.8 mg, 0.05 equiv), 4,4'-di-*tert*-butyl-2,2'-bipyridine ($^{t\text{Bu}}$bpy; 0.025 mmol, 6.7 mg, 0.05 equiv), 9-

azabicyclo[3.3.1]nonane *N*-oxyl (ABNO; 0.015 mmol, 2.1 mg, 0.03 equiv), acetonitrile (2.5 mL, 0.2 M), and a Teflon stir bar. The test tube was placed on a stir plate in an aluminum block and allowed to stir for 10 minutes (*aids with reproducibility*). The solution changed from red/brown to green. The amine (0.5 mmol, 1 equiv or 0.55 mmol, 1.1 equiv) and alcohol (0.75 mmol, 1.5 equiv or 0.5 mmol, 1 equiv respectively) were injected via Hamilton syringes simultaneously, turning the solution red/brown. The reaction was allowed to stir at room temperature for 4 hours.

For reactions where the amine and/or alcohol coupling partners were solid, only 1.0 mL of acetonitrile was added to the 25 x 150 mm test tube containing CuI, $^{t\text{Bu}}$bpy, ABNO, and the Teflon stir bar. The test tube was placed on the stir plate and allowed to stir for 10 minutes. A 0.33 M stock solution of the solid coupling partner in acetonitrile (0.5 mmol in 1.5 mL) was prepared and injected simultaneously with the other coupling partner via Hamilton syringe. If both coupling partners are solids, they are both added in the 0.33 M stock solution. The reaction was allowed to stir at room temperature for 4 hours.

Work-up: At the end of the reaction, the mixture turns green. The test tube was removed from the stir plate, and the reaction was diluted with ethyl acetate (5.0 mL) then pushed through a plug of silica. For substrates that possessed functional groups that might prevent passage of the product through silica, a solution of 10% triethylamine in ethyl acetate was used as the eluent. Solvent was then removed in vacuo using a ThermoFisher Scientific Savant™ SPD131DDA Speedvac™ Concentrator (typical rotary evaporation is also suitable). Products insoluble in ethyl acetate and acetonitrile were immediately concentrated in vacuo at the end of the reaction. Dimethyldiphenylsilane was then added via syringe as a ^{1}H NMR external standard (0.083 mmol, 18 μL, 0.166 equiv) and the crude mixture was dissolved in *d*-chloroform. An aliquot of the mixture was taken for analysis by ^{1}H NMR to determine the reaction yield. After recombining the NMR sample, the reaction was condensed by rotary evaporation and purified using automated normal phase column chromatography or automated reverse phase column chromatography.

Reactions performed in DMF were set up as reported above, using DMF in place of MeCN as the solvent. These reactions are washed with a saturated aqueous solution of LiCl (3 x 3.0 mL) to remove DMF following the ethyl acetate silica plug filtration.

6E.IV. General Procedure for Inter- and Intramolecular Competition Experiments

6E.IV.1. Stoichiometric Trifluoroacetylation using Trifluoroacetic Anhydride (Condition A & B):

These reactions were performed by using a protocol adapted from the literature.[5]

Set-up: On the benchtop, a 6 mL vial was charged with the amine(s):
Intramolecular: 4-(aminomethyl)piperidine (0.5 mmol, 57.1 mg, 1.0 equiv)
Intermolecular: 3-phenylpropylamine (0.5 mmol, 71 μL, 1.0 equiv) and piperidine (0.5 mmol, 49 μL, 1.0 equiv)
Base (0.75 mmol, 1.5 equiv), solvent (0.83 mL, 0.6 M), and a Teflon stir bar were then added to the same vial. The vial was capped with a PTFE-lined pierceable cap and placed in an ice bath on a stir plate until cooled to 0 °C. Trifluoroacetic anhydride (TFAA; 0.5 mmol, 1 equiv) was injected via syringe under vigorous stirring, and left to react overnight.

Work-up: At the end of the reaction, a 1.0 mL solution of 0.05 M 4,4'-difluorobiphenyl in $CDCl_3$ was injected into the crude reaction mixture. A 50 μL aliquot of the reaction mixture was taken and further diluted with $CDCl_3$, then submitted for analysis by ^1H NMR and ^{19}F NMR spectroscopy to determine the reaction yield. In order to distinguish TFA byproduct salt peaks from the desired product, the NMR sample was recombined with the crude reaction mixture, and the organic phase was washed with deionized water (3 x 2.0 mL), concentrated in vacuo, and a 50 μL aliquot was taken for analysis by ^1H NMR and ^{19}F NMR spectroscopy.

Conditions A: Base = 1,8-Diazabicyclo[5.4.0]undec-7-ene (DBU; 0.75 mmol, 112.5 μL, 1.5 equiv), solvent = DCM (0.6M, 0.83 mL).

Conditions B: Base = 1,1,3,3-Tetramethylguanidine (TMG; 0.75 mmol, 94 μL, 1.5 equiv), solvent = Et_2O (0.6M, 0.83 mL).

6E.IV.2. Cu/ABNO-Catalyzed Trifluoroacetylation under air (Condition C):

Intramolecular Competition Experimental Set-Up: On the benchtop, a 25 x 150 mm test tube was charged with CuI (0.05 mmol, 9.5 mg, 0.1 equiv), 4,4'-di-*tert*-butyl-2,2'-bipyridine ($^{t\text{Bu}}$bpy; 0.05 mmol, 13.4 mg, 0.1 equiv), 9-azabicyclo[3.3.1]nonane *N*-oxyl (ABNO; 0.03 mmol, 4.2 mg, 0.06 equiv), acetonitrile (1.0 mL, 0.2 M), and a Teflon stir bar. The test tube was placed on the stir plate and allowed to stir for 10 minutes (*aids with reproducibility*). The solution changed from red/brown to brown/green. A 0.33 M stock solution of 4-(aminomethyl)piperidine (0.5 mmol, 57.1 mg, 1.0 equiv) and 2,2,2-trifluoroethanol (0.5 mmol, 37 μL, 1.0 equiv) in acetonitrile (1.5 mL) was prepared, and then injected via syringe at the 10 minute mark. The reaction was allowed to stir at room temperature for 4 hours.

Intermolecular Competition Experimental Set-Up: On the benchtop, a 25 x 150 mm test tube was charged with CuI (0.05 mmol, 9.5 mg, 0.1 equiv), 4,4'-di-*tert*-butyl-2,2'-bipyridine ($^{t\text{Bu}}$bpy; 0.05 mmol, 13.4 mg, 0.1 equiv), 9-azabicyclo[3.3.1]nonane *N*-oxyl (ABNO; 0.03 mmol, 4.2 mg, 0.06 equiv), acetonitrile (2.5 mL, 0.2 M), and a Teflon stir bar. The test tube was placed on the stir

plate and allowed to stir for 10 minutes (*aids with reproducibility*). The solution changed from red/brown to green. Then, 3-phenylpropylamine (0.5 mmol, 71 μL, 1.0 equiv), piperidine (0.5 mmol, 49 μL, 1.0 equiv), and 2,2,2-trifluoroethanol (0.5 mmol, 37 μL, 1.0 equiv) were injected via syringe simultaneously at the 10 minute mark. The reaction was allowed to stir at room temperature for 4 hours.

Work-up: At the end of the reaction, the mixture turned green. A 1.0 mL solution of 0.05 M 4,4'-difluorobiphenyl in $CDCl_3$ was injected into the crude reaction mixture. A 50 μL aliquot of the reaction mixture was taken and further diluted with $CDCl_3$, then submitted for analysis by ^1H NMR and ^{19}F NMR spectroscopy to determine the reaction yield.

6E.V. General Procedure for 15 mmol Scale Reaction Under Air

Set-up: On the benchtop, a 250 mL round bottom flask was charged with CuI (0.75 mmol, 142.8 mg, 0.05 equiv), 4,4'-di-*tert*-butyl-2,2'-bipyridine ($^{t\text{Bu}}$bpy; 0.75 mmol, 201.3 mg, 0.05 equiv), 9-azabicyclo[3.3.1]nonane *N*-oxyl (ABNO; 0.45 mmol, 63.1 mg, 0.03 equiv), acetonitrile (75.0 mL, 0.2 M), and a Teflon stir bar. This mixture was stirred for 5 minutes, and then 3-phenylpropylamine (15 mmol, 2.13 mL, 1 equiv) was added via syringe, immediately followed by trifluoroethanol (22.5 mmol, 1.64 mL, 1.5 equiv). Upon substrate addition, the reaction turned from a green to a red/brown color (Figure 6E.1). The reaction was then stirred open to air at room temperature for 4 hours.

Figure 6E.1. Reaction mixture 10 minutes after substrate addition (red/brown color).

Work-up: Over the course of the reaction, the color changes from red to green. Solvent was then removed using rotary evaporation and the remaining material was purified by column chromatography over silica using a gradient of 5%→30% EtOAc in pentane. The desired product was obtained as a white solid from the column following rotary evaporation (3.20 g, 92% yield).

6E.VI. Screening Tables

General Procedure for Optimization of Reactions from Past Conditions for Aliphatic Alcohol-1° Amine Coupling (Table 6E.1):

Set-up: On the benchtop, a disposable 15 mL glass vial (O_2 atmosphere) or 25 x 150 mm test tube (air atmosphere) was charged with Cu, ligand, ABNO, flame-dried 3Å molecular sieves (if applicable; 450 mg/mmol substrate), solvent, and a Teflon stir bar (experimental details listed in each entry of Table 6E.1). The vial was sealed by a PTFE-lined pierceable cap. The reaction vessel (vial or test tube) was placed on a stir plate and allowed to stir for approximately 3 minutes. For the reaction under an atmosphere of O_2, an O_2 balloon (1 atm) with an 18-gauge needle was used to purge the headspace of the vial with O_2 for approximately 1 minute. The vent needle was removed while the O_2 balloon was left intact, continuing to stir for an additional 2 minutes before substrate addition. For the reaction under an atmosphere of air, the reaction vessel was left stirring for a total of 10 minutes before substrate addition. Tetrahydropyran-2-methanol (0.4 mmol, 45 μL, 1 equiv) and 3-phenylpropylamine (0.44 mmol, 63 μL 1.1 equiv) were injected via Hamilton syringes simultaneously through the pierceable septum or into the open test tube, turning the solution red/brown. *Adding the reagents simultaneously is very important*. The reaction was allowed to stir at room temperature for 4 hours.

Work-up: At the end of the reaction, the O_2 balloon was removed from the vial and the reaction vessel (vial or test tube) was removed from the stir plate. The reaction was then diluted with ethyl acetate (5.0 mL) and pushed through a plug of silica. The reaction performed in DMF was washed with a saturated aqueous solution of LiCl (3 x 3.0 mL) to remove DMF following the ethyl acetate silica plug filtration. Solvent was then removed in vacuo using a ThermoFisher Scientific Savant™ SPD131DDA Speedvac™ Concentrator (typical rotary evaporation is also suitable). Dimethyldiphenylsilane was then added via syringe as a ^{1}H NMR spectroscopy external standard (0.067 mmol, 14.5 μL, 0.166 equiv) and the crude mixture was dissolved in *d*-chloroform. An aliquot of the mixture was taken for analysis by ^{1}H NMR spectroscopy to determine the reaction yield.

General Procedure for Optimization of Reactions Conducted using a Large Capacity Mixer (Tables 6E.2-4):

Set-up. Disposable culture tubes were charged with Cu source (0.01 mmol, 0.05 equiv), ligand (0.008 mmol, 0.04 equiv or 0.016 mmol, 0.08 equiv as indicated in the table), and additive (if applicable), and the reaction tubes were placed into an aluminum block mounted on a Large Capacity Mixer (Glas-Col) that enabled several reactions to be performed simultaneously under a constant pressure of (approx.) 1 atm O_2 with orbital agitation. A stock solution containing tetrahydropyran-2-methanol (1 equiv, 0.2 M), 3-phenylpropylamine (1.1 equiv, 0.22 M), and ABNO (0.03 equiv, 6 mM) in acetonitrile was prepared. To each disposable culture tube, 1 mL of the stock solution containing alcohol, amine, and ABNO was added. The headspace above the tubes was filled and purged with oxygen gas for about 2 minutes at room temperature, and then left under constant pressure of O_2 for 4 hours.

Work-up: Upon completion, the tubes were removed and diluted with ethyl acetate (2.0 mL) then pushed through a plug of silica. Solvent was then removed in vacuo using a ThermoFisher Scientific Savant™ SPD131DDA Speedvac™ Concentrator. Dimethyldiphenylsilane was then

added via syringe as a ^{1}H NMR spectroscopy external standard (0.033 mmol, 7.1 μL, 0.166 equiv) and the crude mixture was dissolved in *d*-chloroform. An aliquot of the mixture was taken for analysis by ^{1}H NMR spectroscopy to determine the reaction yield.

General Procedure for Optimization of Reactions Conducted on the Benchtop in Vials (Tables 6E.5-8):

Set-up: On the benchtop, a disposable 15 mL glass vial was charged with CuI, $^{t\text{Bu}}$bpy, ABNO, solvent, and a Teflon stir bar (experimental details depicted in tables). The vial was sealed by a PTFE-lined pierceable cap, placed on a stir plate, and allowed to stir for approximately 3 minutes. An O_2 balloon (1 atm) with an 18-gauge needle was used to purge the headspace of the vial with O_2 for approximately 1 minute. The vent needle was removed while the O_2 balloon was left intact, continuing to stir for an additional 2 minutes. The solution color changed from red/brown to green. Tetrahydropyran-2-methanol (0.4 mmol, 45 μL, 1 equiv) and 3-phenylpropylamine (0.44 mmol, 63 μL 1.1 equiv) were injected via Hamilton syringes simultaneously through the pierceable septum (except in Table 6E.8), turning the solution red/brown. *Adding the reagents simultaneously is very important (as evident in Table 6E.8).* The reaction was allowed to stir at room temperature for 4 hours.

Work-up: At the end of the reaction, the O_2 balloon was removed and the vial was removed from the stir plate. The reaction was then diluted with ethyl acetate (5.0 mL) and pushed through a plug of silica. The reaction performed in DMF was washed with a saturated aqueous solution of LiCl (3 x 3.0 mL) to remove DMF following the ethyl acetate silica plug filtration. Solvent was then removed in vacuo using a ThermoFisher Scientific Savant™ SPD131DDA Speedvac™ Concentrator (typical rotary evaporation is also suitable). Dimethyldiphenylsilane was then added via syringe as a ^{1}H NMR spectroscopy external standard (0.067 mmol, 14.5 μL, 0.166 equiv) and the crude mixture was dissolved in *d*-chloroform. An aliquot of the mixture was taken for analysis by ^{1}H NMR spectroscopy to determine the reaction yield.

Table 6E.1. Optimization of Prior Conditions for Aliphatic Alcohol-1° Amine Coupling

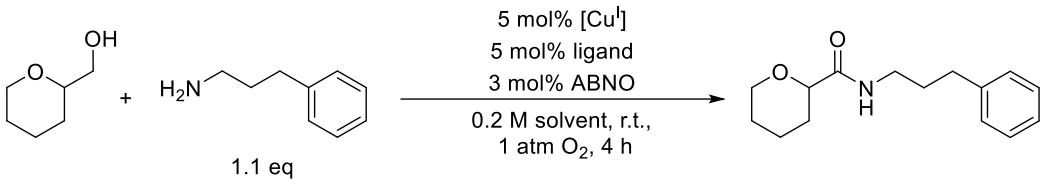

entry	Cu^{I}	ligand	solvent	additive	% yield
1	CuCl	TPA	THF	3 Å MS	35%
2	CuCl	$^{t\text{Bu}}$bpy	THF	3 Å MS	35%
3	CuI	$^{t\text{Bu}}$bpy	THF	3 Å MS	62%
4	CuI	$^{t\text{Bu}}$bpy	MeCN	3 Å MS	69%
5	CuI	$^{t\text{Bu}}$bpy	MeCN	–	77%
6	CuI	$^{t\text{Bu}}$bpy	DMF	–	71%
7[a,b]	**CuI**	**$^{t\text{Bu}}$bpy**	**MeCN**	**–**	**91%**
8[a,c]	CuI	$^{t\text{Bu}}$bpy	MeCN	–	74%

Reactions at 0.4 mmol scale. Calibrated ^{1}H NMR yields using dimethyldiphenylsilane as an internal standard. [a] 10 mol% [Cu^{I}], 10 mol% ligand, and 6 mol% ABNO. [b] When conducted at a 0.5 mmol scale, a 94% yield was obtained (cf. Scheme 2). [c] Run under air instead of O_2.

Table 6E.2. Copper Source Screening Table

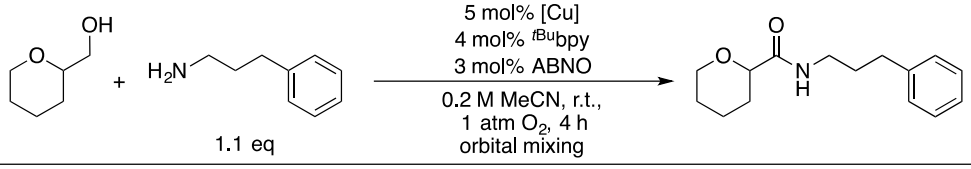

entry	Cu Source	% yield
1	CuCl	36%
2	CuBr	36%
3	CuBr•DMS	48%
4	**CuI**	**66%**
5	**$(CuI)_4 \cdot 3DMS$**	**65%**
6	$Cu(MeCN)_4PF_6$	31%
7	$Cu(MeCN)_4OTf$	34%
8	CuOAc	23%
9	Cu(2-thiophene carboxylate)	23%
10	Cu(3-methyl-salicylate)	no observable product
11	CuSPh	28%
12	CuCN	39%
13	$CuBr_2$	9%
14	$Cu(OAc)_2$•H_2O	no observable product

Reactions at 0.2 mmol scale. Calibrated ^{1}H NMR yields using dimethyldiphenylsilane as an internal standard.

CuI was chosen over $(CuI)_4$•3DMS as it was more cost effective and available from a variety of vendors.

Table 6E.3. Ligand Source Screening Table

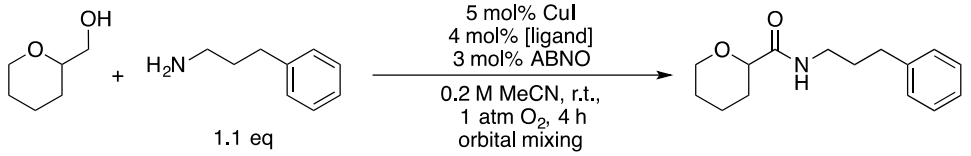

entry	Ligand	% yield	entry	Ligand	% yield
1	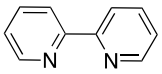	61%	9[b]	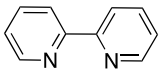 + 	67%
2	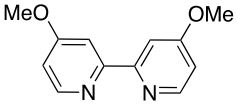	69%	10[b]	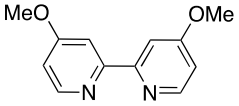 + 	67%
3	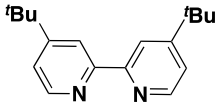	**73%**	11[b]	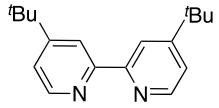 + 	71%
4	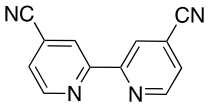	39%	12[b]	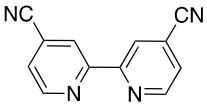 + 	40%
5	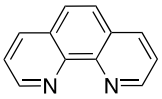	60%	13[a]	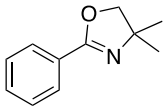	41%
6	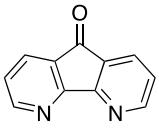	40%	14[a]		42%
7	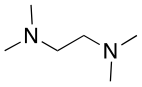	58%	15[a]	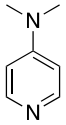	46%
8[a]		41%	16	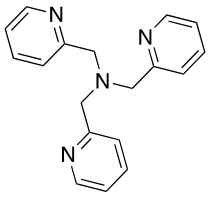	32%

Reactions at 0.2 mmol scale. Calibrated ^{1}H NMR yields using dimethyldiphenylsilane as an internal standard. [a] Ligand catalyst loading increased to 8 mol%. [b] Bipyridine derivative catalyst loading at 4 mol%, NMI catalyst loading at 8 mol%.

Table 6E.4. Additive Screening Table

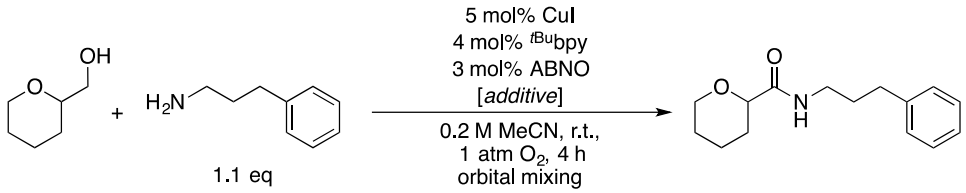

entry	Additive	% yield
0	**none**	**73%**
1	1.5 equiv. $NaHCO_3$	71%
2	1.5 equiv. Li_2CO_3	68%
3	1.5 equiv. Na_2CO_3	70%
4	1.5 equiv. K_2CO_3	67%
5	1.5 equv. Cs_2CO_3	46%
6	1.5 equiv. LiOAc	61%
7	1.5 equiv. LiF	67%
8	1.5 equiv. LiCl	17%
9	1.5 equiv. LiBr	17%
10	1.5 equiv. LiI	complex mixture
11	1.5 equiv. $LiNO_3$	40%
12	1.5 equiv. LiOTf	28%
13	1.5 equiv. LiOH	56%
14	1.5 equiv. $MgSO_4$	72%
15	powder sieves	71%
16	pellet sieves	66%
17	5 mol% hexafluoroisopropanol	51%
18	5 mol% tetrabutylammonium iodide	70%
19	1 equiv. H_2O	65%
20	2 equiv. H_2O	45%
21	3 equiv. H_2O	40%
22	no ligand	34%

Reactions at 0.2 mmol scale. Calibrated ^1H NMR yields using dimethyldiphenylsilane as an internal standard.

Table 6E.5. Solvent Screening Table

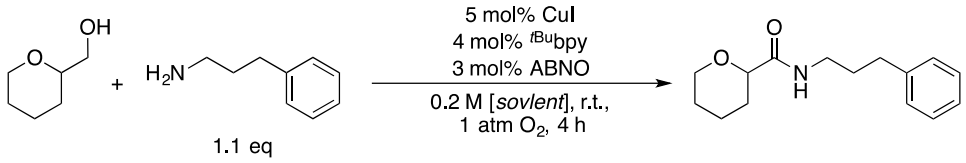

entry	Solvent	% yield
1	EtOAc	22%
2	DCE	12%
3	DMF	71%
4	Acetone	25%
5	t-amyl alcohol	12%
6	THF	32%
7	**MeCN**	**76%**
8	DCM	19%

Reactions at 0.4 mmol scale. Calibrated ^{1}H NMR yields using dimethyldiphenylsilane as an internal standard.

Table 6E.6. Catalyst Loading Screening Table

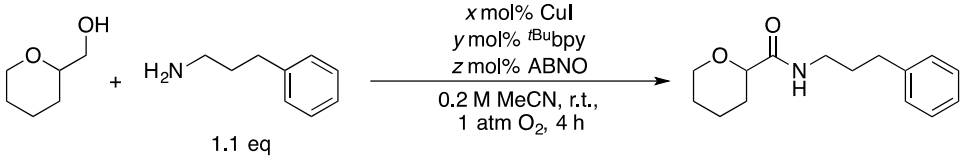

entry	*x* CuI	*y* $^{t\text{Bu}}$bpy	*z* ABNO	% yield
1	5 mol%	4 mol%	3 mol%	78%
2	5 mol%	8 mol%	3 mol%	77%
3	5 mol%	5 mol%	3 mol%	78%
4	**10 mol%**	**8 mol%**	**6 mol%**	**91%**
5	10 mol%	8 mol%	3 mol%	86%
6	**10 mol%**	**10 mol%**	**9 mol%**	**92%**
7	**10 mol%**	**10 mol%**	**6 mol%**	**89%**
8	10 mol%	10 mol%	3 mol%	81%
9	10 mol%	10 mol%	1 mol%	74%
10	10 mol%	5 mol%	3 mol%	76%
11	15 mol%	15 mol%	3 mol%	83%
12	20 mol%	20 mol%	3 mol%	80%
13	20 mol%	20 mol%	6 mol%	82%

Reactions at 0.4 mmol scale. Calibrated ^{1}H NMR yields using dimethyldiphenylsilane as an internal standard.

Table 6E.7. Concentration Screening Table

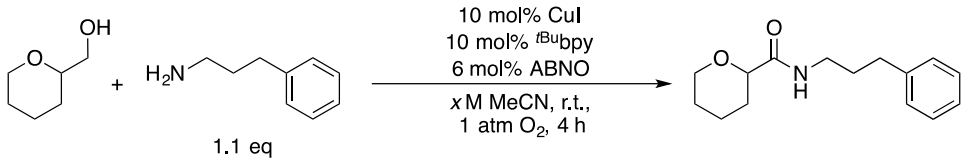

entry	Concentration (M)	% yield
1	0.1	87%
2	0.2	87%
3	0.4	76%
4	0.6	72%

Reactions at 0.4 mmol scale. Calibrated ^{1}H NMR yields using dimethyldiphenylsilane as an internal standard.

Table 6E.8. Order of Addition Screening Table

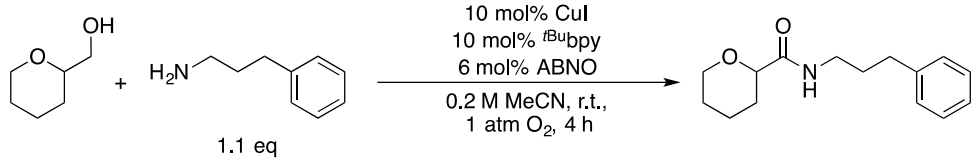

entry	Order of Addition	% yield
1	Amine, then alcohol	87%
2	Alcohol, then amine	80%
3	Simultaneous	87%

Reactions at 0.4 mmol scale. Calibrated ^{1}H NMR yields using dimethyldiphenylsilane as an internal standard. Time between addition is 4 seconds.

6E.VII. Challenging Alcohol and Amine Substrates

Not all substrates tested were effective in the reaction, and the examples of problematic alcohols and amines are summarized in Table 6E.9 and Table 6E.10. The origin of the challenges in most of these cases were not determined, but various considerations are summarized below.

Table 6E.9. Challenging Alcohol Substrates

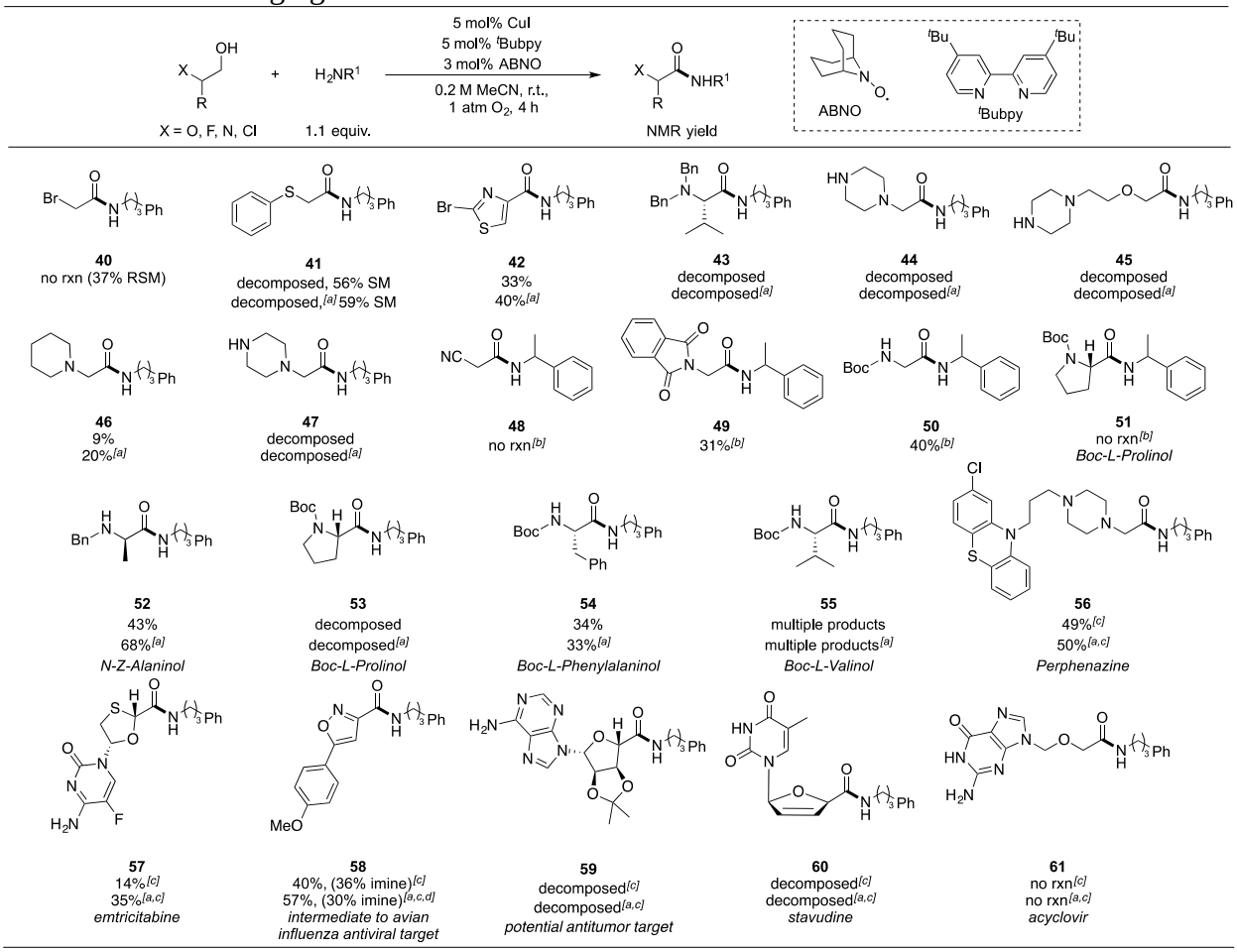

Reactions at 0.5 mmol scale. Calibrated ^{1}H NMR yields using dimethyldiphenylsilane as an internal standard. [a] Catalyst loading doubled. [b] 4 mol% ^{t}Bubpy. [c] DMF used as solvent. [d] Average of two runs.

Commentary on challenging substrates. This chemistry could not be expanded to include β-bromo alcohols (**40**) due to competing S_N2 side reactions. Chelation to copper by sulfur seems to impede successful amidation of alcohols (**41**, **56**, **57**). Alcohol substrates containing β-amino groups were also challenging, possibly due to chelation (**43**–**47**), and the β-imide alcohol (cf. **49**) proceeded in a lower yield than when 3-phenylpropylamine was used as the coupling partner (**15**, 80%), perhaps reflecting the steric sensitivity of the reaction. Boc-protected amino alcohols performed better than their benzyl-protected counterparts (at double catalyst loading, benzyl-protected Alaninol **52** proceeded in 68% yield while Boc-protected Alaninol **17** proceeded in 80% yield). Furthermore, the steric sensitivity of this reaction is apparent when comparing amino alcohol side chains with increasing steric bulk. Doubling the catalyst loading often leads to increased yields for substrates where chelation may have impeded reactivity (**12** and **17**), and thus

increased catalyst loading can be employed in certain cases to overcome limitations. Substrates containing purine and pyrimidine units (**59**–**61**) often decomposed or presented problems with solubility in MeCN and DMF.

Table 6E.10. Challenging Amine Substrates

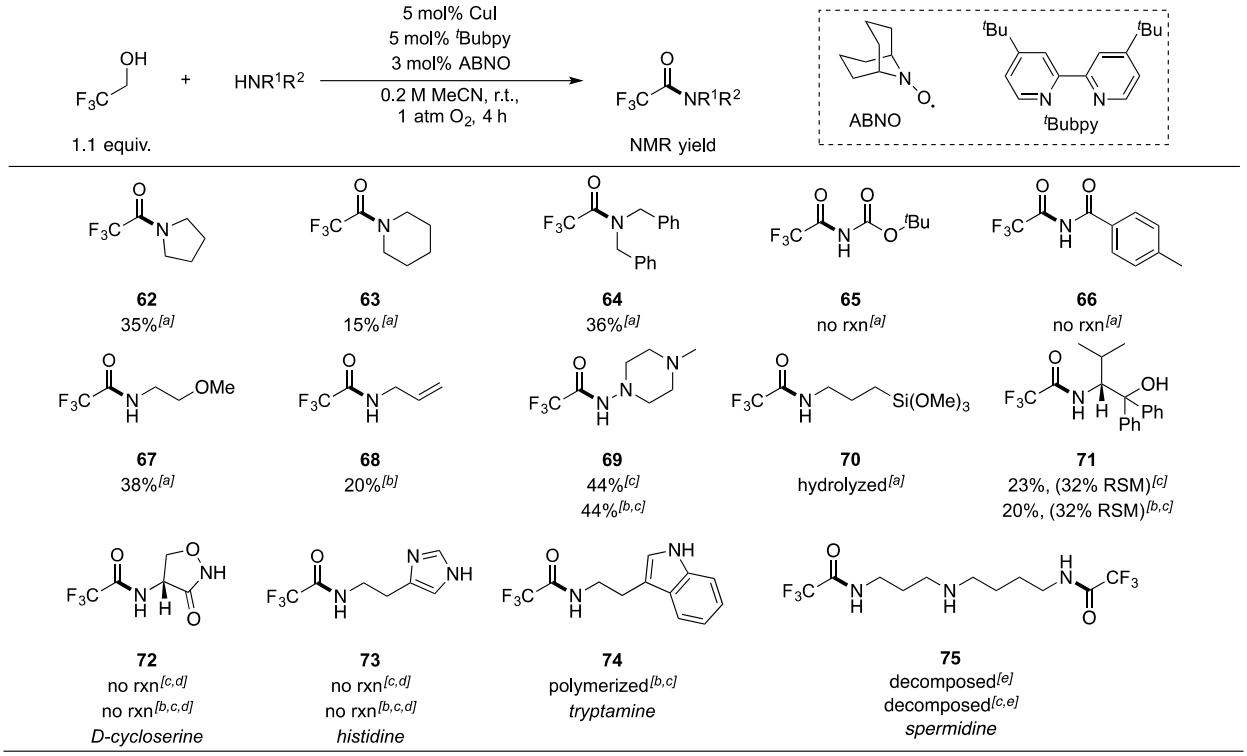

Reactions at 0.5 mmol scale. Calibrated ^{1}H NMR yields using dimethyldiphenylsilane as an internal standard. [a] 4 mol% ^{t}Bubpy. [b] Catalyst loading doubled. [c] 1.5 equiv. alcohol. [d] DMF used as solvent. [e] 2.1 equiv. of alcohol.

Due to the steric sensitivity of our catalyst system, secondary amines, both cyclic and acyclic, were poor coupling partners (**62**–**64**). This observation led us to test chemoselectivity for primary amines in the presence of secondary amines. Our catalytic system could not be applied to amide substrates for the formation of imides (**65**, **66**).[6] The electron deficient amine in **67** proceeded in moderate yield, and allylamine in **68** suffered from oxidative decomposition pathways. Our catalyst system could be applied for the formation of acyl hydrazines in moderate yield (**69**).[7-9] Siloxane derivative **70** hydrolyzed under our catalytic conditions. Either sterics or chelation to the nearby tertiary alcohol resulted in decreased yield for the formation of **71**. Limited solubility in both MeCN and DMF for bioactive molecules **72** and **73**, prevented successful amidation, while **74** and **75** suffered from alternative oxidative decomposition pathways.

6E.VIII. Experimental Data for Amide Products

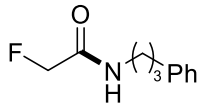

(1) 2-fluoro-*N*-(3-phenylpropyl)acetamide: Prepared according to general procedure, using alcohol (1 equiv, 0.5 mmol) and amine in excess (1.1 equiv, 0.55 mmol). The reaction was performed using 5 mol% CuI, 5 mol% $^{t\text{Bu}}$bpy, and 3 mol% ABNO.
Purification: SiO_2 plug w/ EtOAc, removed catalyst components; normal phase silica gel chromatography was used with a gradient of 20% to 40% EtOAc in pentanes.
Yield: quantitative NMR yield; 98% isolated yield, 95.7 mg of light yellow powder.
^{1}H NMR (500 MHz, $CDCl_3$) δ 7.29 (t, *J* = 7.5 Hz, 2H), 7.23 – 7.15 (m, 3H), 6.26 (s, 1H), 4.77 (d, *J* = 47.4 Hz, 2H), 3.38 (q, *J* = 6.8 Hz, 2H), 2.68 (t, *J* = 7.6 Hz, 2H), 1.90 ppm (p, *J* = 7.4 Hz, 2H).
^{13}C NMR (126 MHz, $CDCl_3$) δ 167.46, 141.04, 128.50, 128.30, 126.10, 80.27, 38.49, 33.17, 30.99 ppm.
^{19}F NMR (376 MHz, $CDCl_3$) δ -224.58 ppm.
M.P. = 47-49 °C
IR (thin film) ν_{max}/cm^{-1}: 3297, 3901, 3061, 3028, 2920, 2851, 1736, 1650, 1554, 1494, 1444, 1362, 1303, 1238, 1183, 1086, 1027, 941, 899, 768, 721, 693, 633, 601, 576, 486.
HRMS (ESI) Calculated for $C_{11}H_{15}FNO^+$ ($[M+H]^+$): 196.1132, measured: 196.1132.

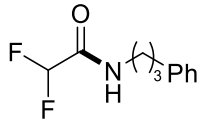

(2) 2,2-difluoro-*N*-(3-phenylpropyl)acetamide: Prepared according to general procedure, using alcohol (1 equiv, 0.5 mmol) and amine in excess (1.1 equiv, 0.55 mmol). The reaction was performed using 5 mol% CuI, 5 mol% $^{t\text{Bu}}$bpy, and 3 mol% ABNO.
Purification: SiO_2 plug w/ EtOAc, removed catalyst components; normal phase silica gel chromatography was used with an isocratic run at 25% to 50% EtOAc in pentanes.
Yield: quantitative NMR yield; 99% isolated yield, 105.4 mg of clear viscous oil.
^{1}H NMR (500 MHz, $CDCl_3$) δ 7.30 (t, *J* = 7.6 Hz, 2H), 7.23 – 7.16 (m, 3H), 6.25 (s, 1H), 5.85 (t, *J* = 54.4 Hz, 1H), 3.38 (q, *J* = 6.8 Hz, 2H), 2.68 (t, *J* = 7.6 Hz, 2H), 1.92 ppm (p, *J* = 7.3 Hz, 2H).
^{13}C NMR (126 MHz, $CDCl_3$) δ 162.52, 140.77, 128.58, 128.29, 126.23, 108.46, 38.98, 33.10, 30.60 ppm.
^{19}F NMR (377 MHz, $CDCl_3$) δ -126.27 ppm.
IR (thin film) ν_{max}/cm^{-1}: 3296, 3088, 3028, 2941, 2862, 1680, 1603, 1551, 1496, 1454, 1343, 1286, 1185, 1138, 1095, 1059, 950, 911, 855, 792, 745, 698, 573, 493.
HRMS (ESI) Calculated for $C_{11}H_{13}F_2NONa^+$ ($[M+Na]^+$): 236.0857, measured: 236.0855.

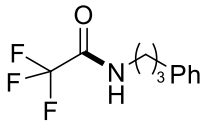

(3) 2,2,2-trifluoro-*N*-(3-phenylpropyl)acetamide: Prepared according to general procedure, using alcohol (1 equiv, 0.5 mmol) and amine in excess (1.1 equiv, 0.55 mmol). The reaction was performed using 5 mol% CuI, 5 mol% $^{t\text{Bu}}$bpy, and 3 mol% ABNO.
Purification: SiO_2 plug w/ EtOAc, removed catalyst components; normal phase silica gel chromatography was used with a gradient of 20% to 40% EtOAc in pentanes.
Yield: quantitative NMR yield; 99% isolated yield, 114.9 mg of light yellow powder.
^{1}H NMR (500 MHz, $CDCl_3$) δ 7.30 (t, *J* = 7.5 Hz, 2H), 7.24 – 7.15 (m, 3H), 6.22 (s, 1H), 3.39 (q, *J* = 6.7 Hz, 2H), 2.69 (t, *J* = 7.5 Hz, 2H), 1.94 ppm (p, *J* = 7.3 Hz, 2H).
^{13}C NMR (126 MHz, $CDCl_3$) δ 157.12, 140.53, 128.64, 128.25, 126.34, 115.85, 39.59, 33.08, 30.33 ppm.
^{19}F NMR (377 MHz, $CDCl_3$) δ -76.04 ppm.
M.P. = 41-43 °C
IR (thin film) ν_{max}/cm^{-1}: 3295, 3097, 3028, 2924, 2855, 1699, 1556, 1496, 1446, 1370, 1342, 1205, 1173, 888, 838, 741, 696, 591, 523, 488.
HRMS (ESI) Calculated for $C_{11}H_{12}F_3NONa^+$ ($[M+Na]^+$): 254.0763, measured: 254.0761.
Previously reported compound.[10]

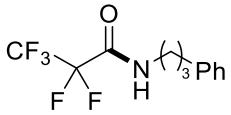

(4) 2,2,3,3,3-pentafluoro-*N*-(3-phenylpropyl)propanamide: Prepared according to the general procedure, using alcohol (1 equiv, 0.5 mmol) with the amine in excess (1.1 equiv, 0.55 mmol). The reaction was performed using 5 mol% CuI, 5 mol% $^{t\text{Bu}}$bpy, and 3 mol% ABNO.
Purification: SiO_2 plug w/ EtOAc to remove catalyst components; normal phase silica gel chromatography was used with a gradient of 15% to 40% EtOAc in pentane.
Yield: 95% NMR yield; 88% isolated yield, 123.3 mg of white powder.
Yield using 10 mol% CuI, 10 mol% $^{t\text{Bu}}$bpy, and 6 mol% ABNO: 99% NMR yield
^{1}H NMR (500 MHz, Chloroform-d) δ 7.31 (dd, J = 8.1, 6.9 Hz, 2H), 7.25 – 7.20 (m, 1H), 7.20 – 7.15 (m, 2H), 6.38 (s, 1H), 3.41 (q, J = 6.7 Hz, 2H), 2.68 (t, J = 7.5 Hz, 2H), 1.93 ppm (p, J = 7.3 Hz, 2H).
^{13}C NMR (126 MHz, Chloroform-d) δ 157.61 (t, J = 25.4 Hz), 140.53, 128.65, 128.27, 126.34, 117.79 (qt, J = 286.7, 34.7 Hz), 106.79 (tq, J = 265.8, 38.8 Hz), 39.68, 33.03, 30.40 ppm.
^{19}F NMR (377 MHz, Chloroform-d) δ -82.91, -123.19 ppm.
M.P. = 51-54 °C
IR (thin film) ν_{max}/cm^{-1}: 3286, 3087, 3028, 2925, 2855, 1697, 1553, 1497, 1448, 1366, 1334, 1209, 1155, 1074, 1043, 1016, 900, 827, 798, 731, 699, 582, 539, 486.
HRMS (ESI) Calculated for $C_{12}H_{12}F_5NONa^+$ ($[M+Na]^+$): 304.0731, measured: 304.0726.

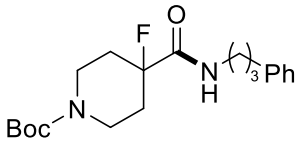

(5) *tert*-butyl 4-fluoro-4-((3-phenylpropyl)carbamoyl)piperidine-1-carboxylate: Prepared according to general procedure, using alcohol (1 equiv, 0.5 mmol) and amine in excess (1.1 equiv, 0.55 mmol). The reaction was performed using 5 mol% CuI, 5 mol% $^{t\text{Bu}}$bpy, and 3 mol% ABNO.
Purification: SiO_2 plug w/ EtOAc, removed catalyst components; normal phase silica gel chromatography was used with a gradient of 20% to 25% EtOAc in pentanes.
Yield: 92% NMR yield; 90% isolated yield, 164.4 mg of cream solid.
^{1}H NMR (500 MHz, $CDCl_3$) δ 7.29 (dd, *J* = 8.2, 6.8 Hz, 2H), 7.23 – 7.15 (m, 3H), 6.38 (q, *J* = 6.0 Hz, 1H), 4.05 (s, 2H), 3.32 (q, *J* = 6.7 Hz, 2H), 3.02 (s, 2H), 2.66 (t, *J* = 7.6 Hz, 2H), 2.14 (dddd, *J* = 39.9, 14.4, 12.7, 5.3 Hz, 2H), 1.94 – 1.81 (m, 2H), 1.73 ppm (t, *J* = 12.8 Hz, 2H), 1.46 (s, 9H).
^{13}C NMR (126 MHz, $CDCl_3$) δ 171.45, 154.49, 141.10, 128.51, 128.31, 126.09, 95.45, 79.85, 39.30, 38.77, 38.43, 33.17, 32.16, 31.99, 31.07, 28.40 ppm.
^{19}F NMR (377 MHz, $CDCl_3$) δ -167.94 ppm.
M.P. = 85-90 °C
IR (thin film) ν_{max}/cm^{-1}: 3330, 2964, 2925, 2876, 1689, 1645, 1535, 1466, 1423, 1365, 1283, 1241, 1170, 1139, 1109, 1084, 1029, 1003, 958, 931, 858, 800, 764, 740, 694, 676, 539, 494, 452.
HRMS (ESI) Calculated for $C_{20}H_{29}FN_2O_3Na^+$ ($[M+Na]^+$): 387.2054, measured: 387.2052.

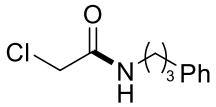

(6) 2-chloro-*N*-(3-phenylpropyl)acetamide: Prepared according to general procedure, using alcohol (1 equiv, 0.5 mmol) and amine in excess (1.1 equiv, 0.55 mmol). The reaction was performed using 5 mol% CuI, 5 mol% $^{t\text{Bu}}$bpy, and 3 mol% ABNO.
Purification: SiO_2 plug w/ EtOAc, removed catalyst components; normal phase silica gel chromatography was used with a gradient of 20% to 40% EtOAc in pentanes.
Yield: 97% NMR yield; 92% isolated yield, 97.3 mg of cream powder.
^{1}H NMR (500 MHz, $CDCl_3$) δ 7.29 (t, *J* = 7.6 Hz, 2H), 7.20 (ddd, *J* = 8.7, 7.2, 1.6 Hz, 3H), 6.54 (s, 1H), 4.02 (s, 2H), 3.35 (td, *J* = 7.2, 6.0 Hz, 2H), 2.68 (t, *J* = 7.6 Hz, 2H), 1.90 ppm (p, *J* = 7.4 Hz, 2H).
^{13}C NMR (126 MHz, $CDCl_3$) δ 165.73, 141.02, 128.52, 128.30, 126.12, 42.65, 39.45, 33.18, 30.78 ppm.
M.P. = 56-58 °C
IR (thin film) ν_{max}/cm^{-1}: 3341, 3057, 3027, 2949, 2920, 2855, 1645, 1541, 1495, 1451, 1409, 1366, 1315, 1261, 1179, 1091, 1034, 961, 925, 898, 804, 764, 732, 699, 624, 599, 571, 486, 463.
HRMS (ESI) Calculated for $C_{11}H_{15}ClNO^+$ ($[M+H]^+$): 212.0837, measured: 212.0836.
Previously reported compound.[11]

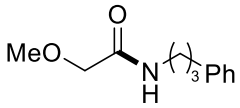

(7) 2-methoxy-*N*-(3-phenylpropyl)acetamide: Prepared according to general procedure, using alcohol (1 equiv, 0.5 mmol) and amine in excess (1.1 equiv, 0.55 mmol). The reaction was performed using 5 mol% CuI, 5 mol% $^{t\text{Bu}}$bpy, and 3 mol% ABNO.
Purification: SiO_2 plug w/ EtOAc, removed catalyst components; normal phase silica gel chromatography was used with a gradient of 20% to 40% to 100% EtOAc in pentanes.
Yield: 96% NMR yield; 92% isolated yield, 95.5 mg of light yellow powder.
^{1}H NMR (500 MHz, $CDCl_3$) δ 7.28 (dd, *J* = 8.7, 6.6 Hz, 2H), 7.21 – 7.16 (m, 3H), 6.51 (s, 1H), 3.87 (s, 2H), 3.40 (s, 3H), 3.34 (q, *J* = 6.8 Hz, 2H), 2.71 – 2.63 (m, 2H), 1.92 – 1.83 ppm (m, 2H).
^{13}C NMR (126 MHz, $CDCl_3$) δ 169.41, 141.29, 128.44, 128.32, 125.98, 72.00, 59.13, 38.38, 33.23, 31.16 ppm.
M.P. = 38-39 °C
IR (thin film) ν_{max}/cm^{-1}: 3319, 3061, 3026, 2931, 2856, 2827, 1655, 1531, 1447, 1364, 1311, 1270, 1197, 1111, 1028, 980, 800, 742, 696, 608, 583, 481.
HRMS (ESI) Calculated for $C_{12}H_{18}NO_2^+$ ($[M+H]^+$): 208.1332, measured: 208.1331.

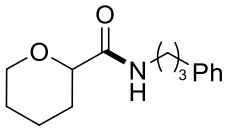

(8) *N*-(3-phenylpropyl)tetrahydro-2*H*-pyran-2-carboxamide: Prepared according to the general procedure, using alcohol (1 equiv, 0.5 mmol) with the amine in excess (1.1 equiv, 0.55 mmol). The reaction was performed using 5 mol% CuI, 5 mol% $^{t\text{Bu}}$bpy, and 3 mol% ABNO.
Purification: SiO_2 plug w/ EtOAc to remove catalyst components; normal phase silica gel chromatography was used with a gradient of 5%→30% EtOAc in pentane.
Yield: 91% NMR yield; 90% isolated yield, 110.1 mg of light yellow solid.
Yield using 10 mol% CuI, 10 mol% $^{t\text{Bu}}$bpy, and 6 mol% ABNO: 95% NMR yield
^{1}H NMR (500 MHz, Chloroform-d) δ 7.31 – 7.25 (m, 2H), 7.21 – 7.16 (m, 3H), 6.56 (s, 1H), 4.02 (ddt, J = 11.4, 3.6, 1.8 Hz, 1H), 3.75 (dd, J = 11.6, 2.5 Hz, 1H), 3.54 – 3.38 (m, 1H), 3.34 – 3.24 (m, 2H), 2.65 (t, 2H), 2.12 (ddd, J = 13.3, 4.4, 2.5 Hz, 1H), 1.93 – 1.85 (m, 1H), 1.85 (dt, J = 14.9, 7.2 Hz, 2H), 1.63 – 1.47 (m, 3H), 1.42 – 1.29 ppm (m, 1H).
^{13}C NMR (126 MHz, Chloroform-d) δ 171.94, 141.42, 128.41, 128.34, 125.92, 77.36, 68.27, 38.32, 33.22, 31.18, 29.27, 25.65, 23.20 ppm.
M.P. = 37-41 °C
IR (thin film) ν_{max}/cm^{-1}: 3318, 3026, 2932, 2852, 2331, 1650, 1532, 1443, 1368, 1291, 1263, 1204, 1176, 1089, 1045, 936, 904, 728, 696, 656, 587, 537, 483, 445.
HRMS (ESI) Calculated for $C_{15}H_{22}NO_2^+$ ($[M+H]^+$): 248.1645, measured: 248.1641.

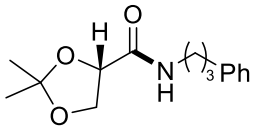

(9) (*S*)-2,2-dimethyl-*N*-(3-phenylpropyl)-1,3-dioxolane-4-carboxamide: Prepared according to general procedure, using alcohol (1 equiv, 0.5 mmol) and amine in excess (1.1 equiv, 0.55 mmol). The reaction was performed using 5 mol% CuI, 5 mol% $^{t\text{Bu}}$bpy, and 3 mol% ABNO. Purification: SiO_2 plug w/ EtOAc, removed catalyst components; normal phase silica gel chromatography was used with a gradient of 20% to 40% to 100% EtOAc in pentanes.
Yield: 92% NMR yield; 89% isolated yield, 116.9 mg of light yellow solid.
^{1}H NMR (500 MHz, $CDCl_3$) δ 7.29 (dd, *J* = 8.2, 6.9 Hz, 2H), 7.23 – 7.15 (m, 3H), 6.61 (s, 1H), 4.47 (dd, *J* = 7.6, 5.3 Hz, 1H), 4.29 (dd, *J* = 8.8, 7.6 Hz, 1H), 4.09 (dd, *J* = 8.7, 5.3 Hz, 1H), 3.38 – 3.26 (m, 2H), 2.66 (dd, *J* = 8.5, 6.9 Hz, 2H), 1.86 (p, *J* = 7.3 Hz, 2H), 1.48 ppm (s, 3H), 1.39 (s, 3H).
^{13}C NMR (126 MHz, $CDCl_3$) δ 171.09, 141.15, 128.47, 128.32, 126.05, 110.79, 75.05, 67.78, 38.47, 33.14, 31.23, 26.21, 25.01 ppm.
M.P. = 31-32 °C
IR (thin film) ν_{max}/cm^{-1}: 3419, 3348, 3061, 3026, 2987, 2932, 1662, 1604, 1528, 1451, 1375, 1254, 1214, 1151, 1063, 965, 907, 844, 793, 746, 697, 602, 571, 509.
HRMS (ESI) Calculated for $C_{15}H_{21}NO_3Na^+$ ($[M+Na]^+$): 286.1414, measured: 286.1411.
$[\alpha]_D^{25}$ (deg $cm^3g^{-1}dm^{-1}$) = -9.3 (c = 1.0 gcm^{-3}, MeOH)

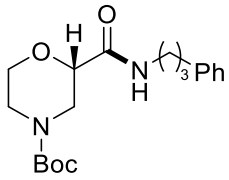

(10) *tert*-butyl (*S*)-2-((3-phenylpropyl)carbamoyl)morpholine-4-carboxylate: Prepared according to general procedure, using alcohol (1 equiv, 0.5 mmol) and amine in excess (1.1 equiv, 0.55 mmol). The reaction was performed using 10 mol% CuI, 10 mol% $^{t\text{Bu}}$bpy, and 6 mol% ABNO.

Purification: SiO_2 plug w/ EtOAc, removed catalyst components; normal phase silica gel chromatography was used with a gradient of 20% to 40% to 100% EtOAc in pentanes.

Yield: 92% NMR yield; 86% isolated yield, 149.6 mg of pale yellow oil.

Yield using 5 mol% CuI, 5 mol% $^{t\text{Bu}}$bpy, and 3 mol% ABNO: 80% NMR yield

^{1}H NMR (500 MHz, $CDCl_3$) δ 7.29 (dd, *J* = 8.6, 6.6 Hz, 2H), 7.22 – 7.16 (m, 3H), 6.54 (s, 1H), 4.34 (s, 1H), 3.93 (dd, *J* = 11.3, 3.3 Hz, 2H), 3.86 (dd, *J* = 10.9, 3.1 Hz, 1H), 3.55 (td, *J* = 11.7, 2.9 Hz, 1H), 3.31 (qd, *J* = 7.0, 3.1 Hz, 2H), 2.91 – 2.68 (m, 2H), 2.66 (t, 2H), 1.93 – 1.80 ppm (m, 2H), 1.47 (s, 9H).

^{13}C NMR (126 MHz, $CDCl_3$) δ 168.73, 154.58, 141.26, 128.46, 128.33, 126.00, 80.46, 75.09, 66.43, 46.38, 42.61, 38.44, 33.23, 31.06, 28.35 ppm.

M.P. = 64-69 °C

IR (thin film) ν_{max}/cm^{-1}: 3338, 2973, 2925, 2860, 1697, 1660, 1533, 1451, 1413, 1366, 1248, 1165, 1128, 1100, 1030, 990, 905, 880, 761, 740, 701, 652, 557, 480.

HRMS (ESI) Calculated for $C_{19}H_{29}N_2O_4^+$ ($[M+H]^+$): 349.2122, measured: 349.2118.

$[\alpha]_D^{25}$ (deg $cm^3g^{-1}dm^{-1}$) = +8.3 (c = 1.0 gcm^{-3}, MeOH)

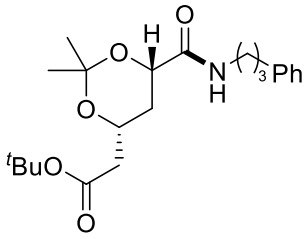

(11) *tert*-butyl 2-((4*R*,6*S*)-2,2-dimethyl-6-((3-phenylpropyl)carbamoyl)-1,3-dioxan-4-yl)acetate: Prepared according to the general procedure, using alcohol (1 equiv, 0.5 mmol) with the amine in excess (1.1 equiv, 0.55 mmol). The reaction was performed using 5 mol% CuI, 5 mol% $^{t\text{Bu}}$bpy, and 3 mol% ABNO.
Purification: SiO_2 plug w/ EtOAc to remove catalyst components; normal phase silica gel chromatography was used with a gradient of 5%→30% EtOAc in pentane.
Yield: 94% NMR yield; 91% isolated yield, 177.5 mg of light yellow oil.
^{1}H NMR (500 MHz, Chloroform-d) δ 7.28 (dd, J = 8.4, 6.8 Hz, 2H), 7.21 – 7.16 (m, 3H), 4.32 (tdd, J = 9.8, 5.8, 2.7 Hz, 2H), 3.30 (q, J = 6.8 Hz, 2H), 2.70 – 2.62 (m, 2H), 2.49 – 2.25 (m, 2H), 2.07 (dt, J = 13.0, 2.7 Hz, 1H), 1.87 (p, J = 7.4 Hz, 2H), 1.46 (s, 3H), 1.44 (s, 9H), 1.42 (s, 3H), 1.34 – 1.22 ppm (m, 1H).
^{13}C NMR (126 MHz, Chloroform-d) δ 171.05, 169.72, 141.30, 128.33, 126.00, 99.27, 80.77, 69.42, 66.31, 42.44, 38.36, 33.57, 33.19, 31.11, 29.89, 28.08, 19.60 ppm.
IR (thin film) ν_{max}/cm^{-1}: 3422, 3364, 2979, 2932, 1727, 1670, 1529, 1453, 1372, 1309, 1255, 1200, 1150, 1046, 982, 954, 926, 877, 846, 748, 699, 581, 547, 518, 454.
HRMS (ESI) Calculated for $C_{22}H_{33}NO_5Na^+$ ($[M+Na]^+$): 414.2251, measured: 414.2243.
$[\alpha]_D^{25}$ (deg $cm^3g^{-1}dm^{-1}$) = -12.9 (c = 1.0 gcm^{-3}, MeOH)

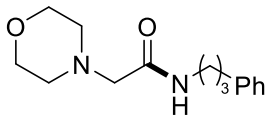

(12) 2-morpholino-*N*-(3-phenylpropyl)acetamide: Prepared according to general procedure, using alcohol (1 equiv, 0.5 mmol) and amine in excess (1.1 equiv, 0.55 mmol). The reaction was performed using 10 mol% CuI, 10 mol% $^{t\text{Bu}}$bpy, and 6 mol% ABNO.
Purification: SiO_2 plug w/ 10% NEt_3 in EtOAc, removed catalyst components; reverse phase chromatography using 100% acetonitrile followed by normal phase silica gel chromatography using a gradient of 2.5% MeOH and 2.5% NEt_3 in DCM.
Yield: 38% NMR yield; 38% isolated yield, 49.5 mg of yellow oil.
Yield using 5 mol% CuI, 5 mol% $^{t\text{Bu}}$bpy, and 3 mol% ABNO: 20% NMR yield
^{1}H NMR (500 MHz, $CDCl_3$) δ 7.29 (t, *J* = 7.5 Hz, 2H), 7.22 – 7.16 (m, 3H), 7.12 (s, 1H), 3.74 – 3.68 (m, 4H), 3.33 (q, *J* = 6.8 Hz, 2H), 2.98 (s, 2H), 2.66 (t, *J* = 7.7 Hz, 2H), 2.51 (t, *J* = 4.7 Hz, 4H), 1.86 ppm (p, *J* = 7.6 Hz, 2H).
^{13}C NMR (126 MHz, $CDCl_3$) δ 169.70, 141.32, 128.49, 128.33, 126.05, 67.00, 62.03, 53.85, 38.54, 33.34, 31.38 ppm.
IR (thin film) ν_{max}/cm^{-1}: 3326, 3026, 2927, 2856, 2819, 1659, 1522, 1449, 1372, 1330, 1293, 1146, 1114, 1073, 1013, 908, 865, 810, 745, 698, 575, 499.
HRMS (ESI) Calculated for $C_{15}H_{23}N_2O_2^+$ ($[M+H]^+$): 262.1754, measured: 262.1753.

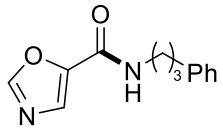

(13) *N*-(3-phenylpropyl)oxazole-5-carboxamide: Prepared according to the general procedure, using alcohol (1 equiv, 0.5 mmol) with the amine in excess (1.1 equiv, 0.55 mmol). The reaction was performed using 5 mol% CuI, 5 mol% $^{t\text{Bu}}$bpy, and 3 mol% ABNO.
Purification: SiO_2 plug w/ EtOAc to remove catalyst components; normal phase silica gel chromatography was used with a gradient of 5% to 40% EtOAc in pentane.
Yield: 84% NMR yield; 80% isolated yield, 92.1 mg of yellow-brown powder.
Yield using 10 mol% CuI, 10 mol% $^{t\text{Bu}}$bpy, and 6 mol% ABNO: 70% NMR yield
^{1}H NMR (500 MHz, Chloroform-d) δ 7.87 (s, 1H), 7.68 (s, 1H), 7.29 (dd, J = 8.1, 7.0 Hz, 2H), 7.23 – 7.17 (m, 3H), 6.19 (s, 1H), 3.48 (q, J = 6.8 Hz, 2H), 2.72 (t, J = 7.5 Hz, 2H), 1.97 ppm (p, J = 7.2 Hz, 2H).
^{13}C NMR (126 MHz, Chloroform-d) δ 156.70, 151.01, 145.53, 141.07, 130.04, 128.54, 128.32, 126.11, 38.98, 33.28, 30.99 ppm.
M.P. = 83-87 °C
IR (thin film) ν_{max}/cm^{-1}: 3352, 3268, 3108, 3064, 3028, 2923, 2854, 1643, 1601, 1522, 1476, 1444 1366, 1304, 1245, 1172, 1111, 1027, 961, 893, 862, 822, 784, 742, 695, 638, 601, 491.
HRMS (ESI) Calculated for $C_{13}H_{14}N_2O_2Na^+$ ($[M+Na]^+$): 253.0948, measured: 253.0942.

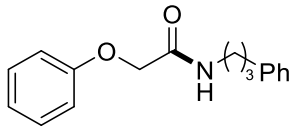

(14) 2-phenoxy-*N*-(3-phenylpropyl)acetamide: Prepared according to general procedure, using alcohol (1 equiv, 0.5 mmol) and amine in excess (1.1 equiv, 0.55 mmol). The reaction was performed using 5 mol% CuI, 5 mol% $^{t\text{Bu}}$bpy, and 3 mol% ABNO.
Purification: SiO_2 plug w/ EtOAc, removed catalyst components; normal phase silica gel chromatography was used with a gradient of 20% to 40% to 100% EtOAc in pentanes.
Yield: 93% NMR yield; 92% isolated yield, 123.5 mg of cream powder.
^{1}H NMR (500 MHz, $CDCl_3$) δ 7.36 – 7.30 (m, 2H), 7.28 (d, *J* = 7.5 Hz, 1H), 7.21 – 7.13 (m, 3H), 7.03 (t, *J* = 7.4 Hz, 1H), 6.94 – 6.89 (m, 2H), 6.56 (s, 1H), 4.48 (s, 2H), 3.45 – 3.30 (m, 2H), 2.64 (t, *J* = 7.7 Hz, 2H), 1.89 ppm (p, *J* = 7.4 Hz, 2H).
^{13}C NMR (126 MHz, $CDCl_3$) δ 168.16, 157.19, 141.19, 129.81, 128.48, 128.34, 126.06, 122.14, 114.65, 67.35, 38.62, 33.18, 31.09 ppm.
M.P. = 85-88 °C
IR (thin film) ν_{max}/cm^{-1}: 3326, 3028, 2920, 2851, 2315, 1737, 1657, 1594, 1540, 1489, 1434, 1360, 1297, 1235, 1172, 1084, 1062, 886, 833, 748, 695, 607, 583, 496, 447.
HRMS (ESI) Calculated for $C_{17}H_{20}NO_2^+$ ($[M+H]^+$): 270.1489, measured: 270.1487.

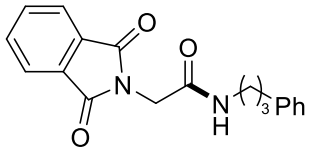

(15) 2-(1,3-dioxoisoindolin-2-yl)-*N*-(3-phenylpropyl)acetamide: Prepared according to general procedure, using alcohol (1 equiv, 0.5 mmol) and amine in excess (1.1 equiv, 0.55 mmol). The reaction was performed using 10 mol% CuI, 10 mol% $^{t\text{Bu}}$bpy, and 6 mol% ABNO.
Yield using 5 mol% CuI, 5 mol% $^{t\text{Bu}}$bpy, and 3 mol% ABNO: 54% NMR yield
Purification: Normal phase silica gel chromatography was used with a gradient of 60% to 80% EtOAc in pentanes.
Yield: 80% NMR yield; 79% isolated yield, 127.4 mg of light cream powder.
Yield using 5 mol% CuI, 5 mol% $^{t\text{Bu}}$bpy, and 3 mol% ABNO: 54% NMR yield
^{1}H NMR (500 MHz, $CDCl_3$) δ 7.88 (dd, *J* = 5.5, 3.1 Hz, 2H), 7.75 (dd, *J* = 5.4, 3.0 Hz, 2H), 7.29 – 7.27 (m, 1H), 7.26 – 7.24 (m, 1H), 7.20 – 7.13 (m, 3H), 5.68 (s, 1H), 4.28 (s, 2H), 3.32 (td, *J* = 7.1, 5.9 Hz, 2H), 2.65 (t, *J* = 7.6 Hz, 2H), 1.86 ppm (p, *J* = 7.3 Hz, 2H).
^{13}C NMR (126 MHz, $CDCl_3$) δ 167.75, 165.90, 141.22, 134.26, 131.97, 128.47, 128.35, 126.02, 123.64, 40.94, 39.49, 33.21, 30.97 ppm.
M.P. = 181-184 °C
IR (thin film) ν_{max}/cm^{-1}: 3295, 3099, 2933, 2864, 1773, 1721, 1658, 1567, 1458, 1421, 1394, 1317, 1260, 1189, 1114, 952, 850, 742, 708, 625, 563, 532, 497.
HRMS (ESI) Calculated for $C_{19}H_{19}N_2O_3^+$ ($[M+H]^+$): 323.1390, measured: 323.1385.

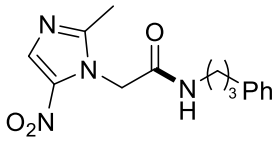

(16) 2-(2-methyl-5-nitro-1*H*-imidazol-1-yl)-*N*-(3-phenylpropyl)acetamide: Prepared according to general procedure, using alcohol (1 equiv, 0.5 mmol) and amine in excess (1.1 equiv, 0.55 mmol). The reaction was performed using 10 mol% CuI, 10 mol% $^{t\text{Bu}}$bpy, and 6 mol% ABNO in DMF.
Purification: SiO_2 plug w/ 10% NEt_3 in EtOAc, removed catalyst components; normal phase silica gel chromatography was used with a gradient of 1% to 2% to 5% MeOH in DCM.
Yield: 81% NMR yield; 81% isolated yield, 123.6 mg of beige solid.
Yield using 5 mol% CuI, 5 mol% $^{t\text{Bu}}$bpy, and 3 mol% ABNO: 67% NMR yield
^{1}H NMR (500 MHz, $CDCl_3$) δ 7.97 (s, 1H), 7.29 (t, *J* = 7.5 Hz, 2H), 7.23 – 7.13 (m, 3H), 5.79 (t, *J* = 5.5 Hz, 1H), 4.83 (s, 2H), 3.33 (q, *J* = 6.7 Hz, 2H), 2.65 (t, *J* = 7.6 Hz, 2H), 2.50 (s, 3H), 1.87 ppm (p, *J* = 7.3 Hz, 2H).
^{13}C NMR (126 MHz, $CDCl_3$) δ 164.79, 151.52, 141.02, 138.33, 133.02, 128.56, 128.33, 126.16, 48.67, 39.68, 33.19, 30.87, 14.26 ppm.
M.P. = 126-131 °C
IR (thin film) ν_{max}/cm^{-1}: 3302, 3108, 3026, 2923, 2857, 1658, 1569, 1530, 1463, 1426, 1357, 1264, 1192, 1151, 1092, 1032, 981, 933, 899, 825, 797, 745, 696, 581, 551, 519, 461.
HRMS (ESI) Calculated for $C_{15}H_{18}N_4O_3Na^+$ ($[M+Na]^+$): 325.1271, measured: 325.1270.

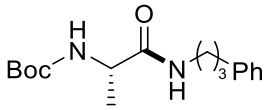

(17) *tert*-butyl (*S*)-(1-oxo-1-((3-phenylpropyl)amino)propan-2-yl)carbamate: Prepared according to general procedure, using alcohol (1 equiv, 0.5 mmol) and amine in excess (1.1 equiv, 0.55 mmol). The reaction was performed using 10 mol% CuI, 10 mol% $^{t\text{Bu}}$bpy, and 6 mol% ABNO.

Purification: SiO_2 plug w/ EtOAc, removed catalyst components; normal phase silica gel chromatography was used with an isocratic run of 2% MeOH in DCM.

Yield: 80% NMR yield; 75% isolated yield, 115.4 mg of yellow viscous oil.

Yield using 5 mol% CuI, 5 mol% $^{t\text{Bu}}$bpy, and 3 mol% ABNO: 70% NMR yield

^{1}H NMR (500 MHz, $CDCl_3$) δ 7.28 (t, *J* = 7.6 Hz, 2H), 7.22 – 7.16 (m, 3H), 6.15 (s, 1H), 4.92 (s, 1H), 4.09 (s, 1H), 3.29 (hept, *J* = 6.7 Hz, 2H), 2.65 (t, *J* = 7.6 Hz, 2H), 1.90 – 1.79 (m, 2H), 1.44 (s, 9H), 1.33 ppm (d, *J* = 9.0 Hz, 3H).

^{13}C NMR (126 MHz, $CDCl_3$) δ 172.46, 155.57, 141.38, 128.47, 128.36, 126.00, 80.16, 50.11, 39.06, 33.18, 31.07, 28.32, 18.18 ppm.

IR (thin film) ν_{max}/cm^{-1}: 3342, 3312, 3026, 2979, 2931, 2871, 1680, 1649, 1526, 1451, 1367, 1318, 1249, 1164, 1069, 1034, 940, 904, 856, 756, 693, 667, 633, 544, 465, 425.

HRMS (ESI) Calculated for $C_{17}H_{26}N_2O_3Na^+$ ($[M+Na]^+$): 329.1836, measured: 329.1835.

$[\alpha]_D^{25}$ (deg $cm^3g^{-1}dm^{-1}$) = -9.6 (c = 1.0 gcm^{-3}, MeOH)

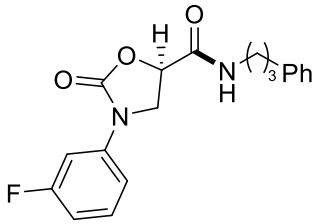

(18) (*R*)-3-(3-fluorophenyl)-2-oxo-*N*-(3-phenylpropyl)oxazolidine-5-carboxamide: Prepared according to general procedure, using alcohol (1 equiv, 0.5 mmol) and amine in excess (1.1 equiv, 0.55 mmol). The reaction was performed using 5 mol% CuI, 5 mol% $^{t\text{Bu}}$bpy, and 3 mol% ABNO.

Purification: SiO_2 plug w/ EtOAc, removed catalyst components; normal phase silica gel chromatography was used with a gradient of 30% to 50% to 100% EtOAc in pentanes.

Yield: quantitative NMR yield; 96% isolated yield, 164.4 mg of cream powder.

^{1}H NMR (500 MHz, $CDCl_3$) δ 7.45 (dt, *J* = 11.1, 2.2 Hz, 1H), 7.34 (td, *J* = 8.2, 6.5 Hz, 1H), 7.30 – 7.27 (m, 2H), 7.22 – 7.14 (m, 4H), 6.88 (td, *J* = 8.2, 2.4 Hz, 1H), 6.56 (s, 1H), 4.94 (dd, *J* = 9.8, 5.9 Hz, 1H), 4.27 (t, *J* = 9.5 Hz, 1H), 4.16 (dd, *J* = 9.3, 5.9 Hz, 1H), 3.37 (ddt, *J* = 37.7, 13.4, 6.6 Hz, 2H), 2.67 (t, *J* = 7.6 Hz, 2H), 1.91 ppm (p, *J* = 7.3 Hz, 2H).

^{13}C NMR (126 MHz, $CDCl_3$) δ 168.11, 163.04, 152.78, 140.85, 138.87, 130.42, 128.52, 128.27, 126.17, 113.33, 111.47, 105.99, 70.02, 48.11, 39.16, 33.19, 30.70 ppm.

^{19}F NMR (376 MHz, $CDCl_3$) δ -110.46 ppm.

M.P. = 144-147 °C

IR (thin film) ν_{max}/cm^{-1}: 3296, 3103, 3027, 2924, 2855, 2334, 1736, 1656, 1511, 1565, 1490, 1456, 1411, 1316, 1258, 1227, 1197, 1166, 1117, 1089, 1042, 997, 908, 865, 771, 742, 696, 670, 654, 589, 518, 456.

HRMS (ESI) Calculated for $C_{19}H_{23}FN_3O_3^+$ ($[M+NH_4]^+$): 360.1718, measured: 360.1717.

$[\alpha]_D^{25}$ (deg $cm^3g^{-1}dm^{-1}$) = -13.4 (c = 1.0 gcm^{-3}, MeOH)

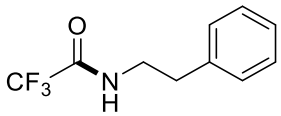

(19) 2,2,2-trifluoro-*N*-phenethylacetamide: Prepared according to general procedure, using amine (1 equiv, 0.5 mmol) and alcohol in excess (1.5 equiv, 0.75 mmol). The reaction was performed using 5 mol% CuI, 5 mol% $^{t\text{Bu}}$bpy, and 3 mol% ABNO.
Purification: SiO_2 plug w/ EtOAc, removed catalyst components; normal phase silica gel chromatography was used with a gradient of 10% to 20% EtOAc in pentanes.
Yield: 98% NMR yield; 96% isolated yield, 104.3 mg of white powder.
^{1}H NMR (500 MHz, $CDCl_3$) δ 7.34 (dd, *J* = 8.2, 6.8 Hz, 2H), 7.30 – 7.26 (m, 1H), 7.19 (dd, *J* = 7.0, 1.7 Hz, 2H), 6.25 (s, 1H), 3.63 (q, *J* = 6.7 Hz, 2H), 2.89 ppm (t, *J* = 6.9 Hz, 2H).
^{13}C NMR (126 MHz, $CDCl_3$) δ 157.12, 137.48, 128.91, 128.64, 127.02, 115.99, 40.98, 34.96 ppm.
^{19}F NMR (377 MHz, $CDCl_3$) δ -76.06 ppm.
M.P. = 56-58 °C
IR (thin film) ν_{max}/cm^{-1}: 3298, 3098, 3030, 2924, 2856, 1697, 1596, 1555, 1493, 1455, 1367, 1339, 1295, 1204, 1177, 1149, 1030, 858, 748, 694, 611, 519, 497, 435.
HRMS (ESI) Calculated for $C_{10}H_{10}F_3NONa^+$ ($[M+Na]^+$): 240.0607, measured: 240.0607.
Previously reported compound.[12]

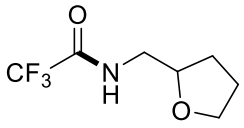

(20) 2,2,2-trifluoro-*N*-((tetrahydrofuran-2-yl)methyl)acetamide: Prepared according to general procedure, using amine (1 equiv, 0.5 mmol) and alcohol in excess (1.5 equiv, 0.75 mmol). The reaction was performed using 5 mol% CuI, 5 mol% $^{t\text{Bu}}$bpy, and 3 mol% ABNO.
Purification: SiO_2 plug w/ EtOAc, removed catalyst components; normal phase silica gel chromatography was used with a gradient of 20% to 40% EtOAc in pentanes.
Yield: 96% NMR yield; 91% isolated yield, 90.1 mg of yellow liquid.
^{1}H NMR (500 MHz, $CDCl_3$) δ 6.84 (s, 1H), 4.02 (qd, *J* = 7.3, 3.3 Hz, 1H), 3.88 (dt, *J* = 8.5, 6.7 Hz, 1H), 3.78 (dt, *J* = 8.5, 6.9 Hz, 1H), 3.65 (ddd, *J* = 13.7, 6.6, 3.2 Hz, 1H), 3.24 (ddd, *J* = 13.2, 7.6, 5.0 Hz, 1H), 2.03 (dt, *J* = 12.3, 6.8 Hz, 1H), 1.93 (p, *J* = 7.0 Hz, 2H), 1.56 ppm (dq, *J* = 12.2, 7.7 Hz, 1H).
^{13}C NMR (126 MHz, $CDCl_3$) δ 157.32, 115.87, 68.23, 43.46, 28.63, 25.76 ppm.
^{19}F NMR (377 MHz, $CDCl_3$) δ -75.92 ppm.
IR (thin film) ν_{max}/cm^{-1}: 3432, 3291, 3093, 2951, 2879, 1710, 1556, 1439, 1346, 1148, 1074, 1015, 924, 883, 809, 722, 669, 520, 479.
HRMS (ESI) Calculated for $C_7H_{10}F_3NO_2Na^+$ ($[M+Na]^+$): 220.0556, measured: 220.0554.

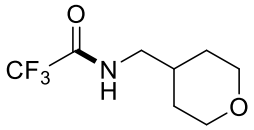

(21): 2,2,2-trifluoro-*N*-((tetrahydro-2*H*-pyran-4-yl)methyl)acetamide: Prepared according to general procedure, using amine (1 equiv, 0.5 mmol) and alcohol in excess (1.5 equiv, 0.75 mmol). The reaction was performed using 5 mol% CuI, 5 mol% $^{t\text{Bu}}$bpy, and 3 mol% ABNO.
Purification: SiO_2 plug w/ EtOAc, removed catalyst components; normal phase silica gel chromatography was used with a gradient of 20% to 40% to 100% EtOAc in pentanes.
Yield: 96% NMR yield; 94% isolated yield, 99.0 mg of cream crystals.
^{1}H NMR (500 MHz, $CDCl_3$) δ 6.39 (s, 1H), 3.99 (ddd, *J* = 11.4, 5.0, 1.8 Hz, 2H), 3.38 (td, *J* = 11.8, 2.1 Hz, 2H), 3.28 (t, *J* = 6.6 Hz, 2H), 1.84 (ttt, *J* = 11.0, 7.0, 3.8 Hz, 1H), 1.62 (ddd, *J* = 13.0, 4.1, 2.0 Hz, 2H), 1.35 ppm (dtd, *J* = 13.3, 11.8, 4.5 Hz, 2H).
^{13}C NMR (126 MHz, $CDCl_3$) δ 157.42, 115.99, 67.33, 45.41, 34.88, 30.30 ppm.
^{19}F NMR (377 MHz, $CDCl_3$) δ -75.83 ppm.
M.P. = 51-55 °C
IR (thin film) ν_{max}/cm^{-1}: 3302, 3110, 2960, 2919, 2846, 2758, 1703, 1562, 1446, 1366, 1265, 1207, 1176, 1148, 1091, 1014, 986, 961, 908, 861, 834, 799, 704, 604, 529, 446.
HRMS (ESI) Calculated for $C_8H_{13}F_3NO_2^+$ ($[M+H]^+$): 212.0893, measured: 212.0894.

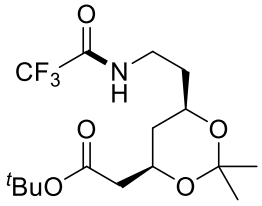

(22): *tert*-butyl 2-((4*R*,6*R*)-2,2-dimethyl-6-(2-(2,2,2-trifluoroacetamido)ethyl)-1,3-dioxan-4-yl)acetate: Prepared according to general procedure, using amine (1 equiv, 0.5 mmol) and alcohol in excess (1.5 equiv, 0.75 mmol). The reaction was performed using 5 mol% CuI, 5 mol% $^{t\text{Bu}}$bpy, and 3 mol% ABNO.
Purification: SiO_2 plug w/ EtOAc, removed catalyst components; normal phase silica gel chromatography was used with an isocratic run of 25% EtOAc in pentanes.
Yield: 94% NMR yield; 89% isolated yield, 164.9 mg of clear tacky oil.
^{1}H NMR (500 MHz, $CDCl_3$) δ 7.61 (s, 1H), 4.29 (dtd, *J* = 11.5, 6.6, 2.4 Hz, 1H), 4.11 (ddt, *J* = 11.3, 8.4, 2.7 Hz, 1H), 3.66 (dtd, *J* = 13.1, 6.3, 3.8 Hz, 1H), 3.33 (ddt, *J* = 13.4, 9.3, 3.7 Hz, 1H), 2.45 (dd, *J* = 15.3, 6.9 Hz, 1H), 2.32 (dd, *J* = 15.3, 6.2 Hz, 1H), 1.82 (ddt, *J* = 14.7, 6.5, 3.3 Hz, 1H), 1.74 – 1.63 (m, 1H), 1.57 (dt, *J* = 12.8, 2.5 Hz, 1H), 1.48 (s, 3H), 1.45 (s, 9H), 1.38 (s, 3H), 1.33 ppm (dt, *J* = 12.8, 11.6 Hz, 1H).
^{13}C NMR (126 MHz, $CDCl_3$) δ 169.99, 156.73, 116.01, 99.01, 80.81, 69.91, 66.01, 42.40, 38.13, 35.74, 33.44, 29.84, 28.08, 19.71 ppm.
^{19}F NMR (377 MHz, $CDCl_3$) δ -76.36 ppm.
IR (thin film) ν_{max}/cm^{-1}: 3327, 3098, 2985, 2939, 1171, 1551, 1456, 1373, 1316, 1258, 1149, 1046, 1004, 959, 875, 843, 764, 723, 650, 520, 464, 426.
HRMS (ESI) Calculated for $C_{16}H_{30}F_3N_2O_5^+$ ($[M+NH_4]^+$): 387.2101, measured: 387.2100.
$[\alpha]_D^{25}$ (deg $cm^3g^{-1}dm^{-1}$) = +2.1 (c = 1.0 gcm^{-3}, MeOH)

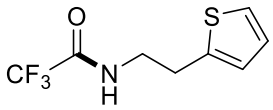

(23): 2,2,2-trifluoro-*N*-(2-(thiophen-2-yl)ethyl)acetamide: Prepared according to general procedure, using amine (1 equiv, 0.5 mmol) and alcohol in excess (1.5 equiv, 0.75 mmol). The reaction was performed using 5 mol% CuI, 5 mol% $^{t\text{Bu}}$bpy, and 3 mol% ABNO.
Purification: SiO_2 plug w/ EtOAc, removed catalyst components; normal phase silica gel chromatography was used with a gradient of 10% to 40% EtOAc in pentanes.
Yield: 98% NMR yield; 92% isolated yield, 102.9 mg of white powder.
^{1}H NMR (500 MHz, $CDCl_3$) δ 7.20 (dd, *J* = 5.2, 1.2 Hz, 1H), 6.97 (dd, *J* = 5.1, 3.5 Hz, 1H), 6.86 (dd, *J* = 3.4, 1.1 Hz, 1H), 6.39 (s, 1H), 3.64 (q, *J* = 6.4 Hz, 2H), 3.16 – 3.07 ppm (m, 2H).
^{13}C NMR (126 MHz, $CDCl_3$) δ 157.17, 139.63, 127.29, 125.82, 124.54, 115.79, 41.13, 29.16 ppm.
^{19}F NMR (377 MHz, $CDCl_3$) δ -76.04 ppm.
M.P. = 56-57 °C
IR (thin film) ν_{max}/cm^{-1}: 3301, 3101, 2920, 2852, 1698, 1556, 1445, 1346, 1309, 1247, 1148, 1011, 859, 827, 691, 519, 495, 438.
HRMS (ESI) Calculated for $C_8H_9F_3NOS$ ($[M+H]^+$): 224.0352, measured: 224.0350.

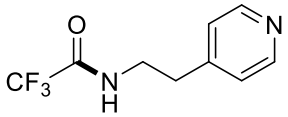

(24): 2,2,2-trifluoro-*N*-(2-(pyridin-4-yl)ethyl)acetamide: Prepared according to general procedure, using amine (1 equiv, 0.5 mmol) and alcohol in excess (1.5 equiv, 0.75 mmol). The reaction was performed using 5 mol% CuI, 5 mol% $^{t\text{Bu}}$bpy, and 3 mol% ABNO.
Purification: SiO_2 plug w/ 10% NEt_3 in EtOAc, removed catalyst components; normal phase silica gel chromatography was used with an isocratic run of 50% EtOAc in pentanes with 10% NEt_3.
Yield: 98% NMR yield; 89% isolated yield, 97.0 mg of tan powder.
^{1}H NMR (500 MHz, $CDCl_3$) δ 8.53 – 8.43 (m, 2H), 7.14 – 7.06 (m, 2H), 6.92 (s, 1H), 3.66 (q, *J* = 6.7 Hz, 2H), 2.91 ppm (t, *J* = 7.0 Hz, 2H).
^{13}C NMR (126 MHz, $CDCl_3$) δ 157.38, 150.03, 146.81, 124.02, 115.60, 40.20, 34.37 ppm.
^{19}F NMR (377 MHz, $CDCl_3$) δ -75.88 ppm.
M.P. = 105-109 °C
IR (thin film) ν_{max}/cm^{-1}: 3174, 2922, 2853, 2763, 1707, 1602, 1561, 1461, 1418, 1379, 1181, 1145, 1065, 1003, 843, 807, 745, 719, 614, 574, 521, 435.
HRMS (ESI) Calculated for $C_9H_{10}F_3N_2O$ ($[M+H]^+$): 219.0740, measured: 219.0739.
Previously reported compound.[13]

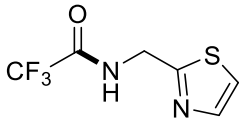

(25): 2,2,2-trifluoro-*N*-(thiazol-2-ylmethyl)acetamide: Prepared according to general procedure, using amine (1 equiv, 0.5 mmol) and alcohol in excess (1.5 equiv, 0.75 mmol). The reaction was performed using 10 mol% CuI, 10 mol% $^{t\text{Bu}}$bpy, and 6 mol% ABNO.
Purification: SiO_2 plug w/ 10% NEt_3 in EtOAc, removed catalyst components; normal phase silica gel chromatography was used with a gradient of 5%→40% EtOAc in pentane.
Yield: 78% NMR yield; 70% isolated yield, 72.8 mg of green-brown powder.
Yield using 5 mol% CuI, 5 mol% $^{t\text{Bu}}$bpy, and 3 mol% ABNO: 31% NMR yield
^{1}H NMR (500 MHz, Chloroform-d) δ 7.76 (d, J = 3.2 Hz, 1H), 7.64 – 7.50 (m, 1H), 7.37 (d, J = 3.2 Hz, 1H), 4.85 ppm (d, J = 5.4 Hz, 2H).
^{13}C NMR (126 MHz, Chloroform-d) δ 163.67, 157.12 (q, J = 37.8 Hz), 142.53, 120.35, 115.68 (q, J = 287.6 Hz), 40.83 ppm.
^{19}F NMR (377 MHz, Chloroform-d) δ -75.72 ppm.
M.P. = 89-93 °C
IR (thin film) ν_{max}/cm^{-1}: 3189, 3131, 3023, 2962, 2920, 2889, 2849, 2356, 2186, 1710, 1606, 1540, 1500, 1419, 1354, 1276, 1184, 1143, 1055, 1015, 975, 889, 829, 749, 728, 591, 521, 437.
HRMS (ESI) Calculated for $C_6H_6F_3N_2OS^+$ ($[M+H]^+$): 211.0147, measured: 211.0144.

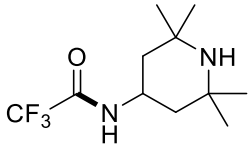

(26): 2,2,2-trifluoro-*N*-(2,2,6,6-tetramethylpiperidin-4-yl)acetamide: Prepared according to the general procedure, using the amine (1 equiv, 0.5 mmol) with the alcohol in excess (1.5 equiv, 0.75 mmol). The reaction was performed using 10 mol% CuI, 10 mol% $^{t\text{Bu}}$bpy, and 6 mol% ABNO.
Purification: 1 mL of ammonium hydroxide was used in an extraction with EtOAc to remove copper; organic phase was dried with $MgSO_4$ and concentrated then the oil was subjected to normal phase silica gel chromatography with a 30%→100% gradient of EtOAc in pentanes to remove the other catalyst components. Finally, the product was flushed off the column using 10% TEA/90% EtOAc.
Yield: 91% NMR yield, 80% isolated yield, 101 mg of white powder.
^{1}H NMR (500 MHz, Chloroform-d) δ 6.09 (s, 1H), 4.29 (tdt, J = 12.2, 7.9, 3.9 Hz, 1H), 1.93 (dd, J = 12.7, 3.8 Hz, 2H), 1.27 (s, 6H), 1.16 (s, 6H), 1.05 ppm (t, J = 12.2 Hz, 2H).
^{13}C NMR (126 MHz, Chloroform-d) δ 156.32 (q, J = 36.7 Hz), 115.77 (q, J = 288.1 Hz), 51.17, 44.34, 43.84, 34.68, 28.35 ppm.
^{19}F NMR (377 MHz, Chloroform-d) δ -76.05 ppm.
M.P. = 118-122 °C
IR (thin film) ν_{max}/cm^{-1}: 3515, 3192, 3059, 2965, 2925, 2857, 1705, 1558, 1460, 1382, 1300, 1190, 1152, 1010, 861, 812, 766, 733, 617, 573, 530, 486.
HRMS (ESI) Calculated for $C_{11}H_{20}F_3N_2O^+$ ($[M+H]^+$): 253.1522, measured: 253.1519.
Previously reported compound.[14]

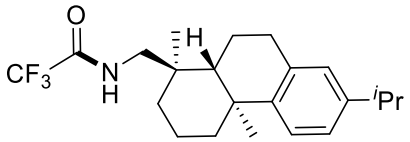

(27): 2,2,2-trifluoro-*N*-(((1*R*,4a*S*,10a*R*)-7-isopropyl-1,4a-dimethyl-1,2,3,4,4a,9,10,10a-octahydrophenanthren-1-yl)methyl)acetamide: Prepared according to general procedure, using amine (90% purity, 1 equiv, 0.5 mmol) and alcohol in excess (1.5 equiv, 0.75 mmol). The reaction was performed using 10 mol% CuI, 10 mol% $^{t\text{Bu}}$bpy, and 6 mol% ABNO.
Purification: SiO_2 plug w/ EtOAc, removed catalyst components; normal phase silica gel chromatography was used with a gradient of 0% to 10% EtOAc in pentanes.
Yield: 99% isolated yield, 170.2 mg of white powder.
Yield using 5 mol% CuI, 5 mol% $^{t\text{Bu}}$bpy, and 3 mol% ABNO: 87% NMR yield
^{1}H NMR (500 MHz, $CDCl_3$) δ 7.16 (d, *J* = 8.2 Hz, 1H), 7.00 (dd, *J* = 8.2, 2.0 Hz, 1H), 6.90 (d, *J* = 1.9 Hz, 1H), 6.21 (s, 1H), 3.35 – 3.22 (m, 2H), 2.98 – 2.89 (m, 1H), 2.87 – 2.76 (m, 2H), 2.31 (dq, *J* = 13.0, 2.8 Hz, 1H), 1.88 – 1.66 (m, 4H), 1.47 (dtd, *J* = 12.8, 3.4, 1.4 Hz, 1H), 1.39 (tq, *J* = 9.6, 5.0, 4.0 Hz, 2H), 1.29 – 1.16 (m, 10H), 0.98 ppm (s, 3H).
^{13}C NMR (126 MHz, $CDCl_3$) δ 157.43, 146.67, 145.84, 134.43, 126.95, 124.18, 124.02, 115.92, 50.40, 45.91, 38.18, 37.54, 37.48, 36.18, 33.44, 30.14, 25.33, 23.97, 23.95, 19.08, 18.46, 18.45 ppm.
^{19}F NMR (377 MHz, $CDCl_3$) δ -75.67 ppm.
M.P. = 81-85 °C
IR (thin film) ν_{max}/cm^{-1}: 3298, 2957, 2924, 2881, 1702, 1554, 1498, 1459, 1384, 1162, 955, 886, 820, 725, 633, 510, 438.
HRMS (ESI) Calculated for $C_{22}H_{34}F_3N_2O$ ($[M+NH_4]^+$): 399.2618, measured: 399.2619.
$[\alpha]_D^{25}$ (deg $cm^3g^{-1}dm^{-1}$) = +14.6 (c = 1.0 gcm^{-3}, MeOH)
Previously reported compound.[15]

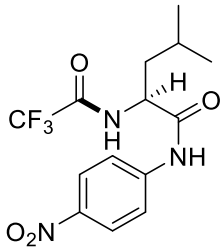

(28): (*S*)-4-methyl-*N*-(4-nitrophenyl)-2-(2,2,2-trifluoroacetamido)pentanamide: Prepared according to the general procedure, using the amine (1 equiv, 0.5 mmol) with the alcohol in excess (1.5 equiv, 0.75 mmol). The reaction was performed using 10 mol% CuI, 10 mol% $^{t\text{Bu}}$bpy, and 6 mol% ABNO.

Purification: SiO_2 plug w/ EtOAc, removed catalyst components; normal phase silica gel chromatography was used with a gradient of 5%→40% EtOAc in pentane.

Yield: 80% NMR yield; 73% isolated yield, 134.3 mg of off-white powder.

Yield using 5 mol% CuI, 5 mol% $^{t\text{Bu}}$bpy, and 3 mol% ABNO: 24% NMR yield

^{1}H NMR (500 MHz, Chloroform-d) δ 8.60 (s, 1H), 8.19 (d, J = 9.2 Hz, 2H), 7.68 (d, J = 9.1 Hz, 2H), 7.14 (d, J = 8.2 Hz, 1H), 4.78 (td, J = 8.3, 6.0 Hz, 1H), 1.87 (ddd, J = 13.7, 7.8, 6.0 Hz, 1H), 1.82 – 1.60 (m, 2H), 1.01 (d, J = 6.4 Hz, 3H), 0.99 ppm (d, J = 6.4 Hz, 3H).

^{13}C NMR (126 MHz, Chloroform-d) δ 168.96, 157.85 (q, J = 38.2 Hz), 144.06, 142.73, 125.03, 119.48, 115.57 (q, J = 287.2 Hz), 53.27, 40.99, 30.58, 24.83, 22.69, 22.15 ppm.

^{19}F NMR (377 MHz, Chloroform-d) δ -75.54 ppm.

M.P. = 146-154 °C

IR (thin film) ν_{max}/cm^{-1}: 3285, 8172, 3111, 3087, 2960, 2877, 2319, 1680, 1600, 1562, 1509, 1468, 1408, 1342, 1311, 1253, 1176, 1114, 967, 887, 856, 829, 781, 751, 727, 659, 524, 499, 460.

HRMS (ESI) Calculated for $C_{14}H_{16}F_3N_3O_4Na^+$ ($[M+Na]^+$): 370.0985, measured: 370.0978.

$[\alpha]_D^{25}$ (deg $cm^3g^{-1}dm^{-1}$) = -13.9 (c = 1.0 gcm^{-3}, MeOH)

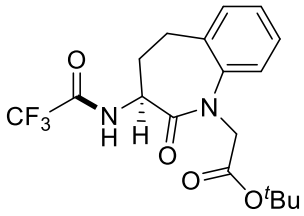

(29): *tert*-butyl (*S*)-2-(2-oxo-3-(2,2,2-trifluoroacetamido)-2,3,4,5-tetrahydro-1*H*-benzo[*b*]azepin-1-yl)acetate: Prepared according to general procedure, using amine (1 equiv, 0.5 mmol) and alcohol in excess (1.5 equiv, 0.75 mmol). The reaction was performed using 5 mol% CuI, 5 mol% $^{t\text{Bu}}$bpy, and 3 mol% ABNO.

Purification: SiO_2 plug w/ EtOAc, removed catalyst components; normal phase silica gel chromatography was used with an isocratic run of 10% EtOAc in pentanes.

Yield: quantitative NMR yield; 98% isolated yield, 189.9 mg of foamy white solid.

^{1}H NMR (500 MHz, $CDCl_3$) δ 7.48 (d, *J* = 6.3 Hz, 1H), 7.32 (td, *J* = 7.5, 2.0 Hz, 1H), 7.31 – 7.21 (m, 2H), 7.12 (dd, *J* = 7.9, 1.2 Hz, 1H), 4.62 (d, *J* = 17.0 Hz, 1H), 4.47 (dt, *J* = 11.0, 7.4 Hz, 1H), 4.30 (d, *J* = 17.0 Hz, 1H), 3.39 (td, *J* = 13.4, 8.1 Hz, 1H), 2.81 (tt, *J* = 12.9, 7.6 Hz, 1H), 2.65 (dd, *J* = 13.6, 7.1 Hz, 1H), 2.02 (dddd, *J* = 12.4, 11.1, 8.0, 1.4 Hz, 1H), 1.44 ppm (s, 9H).

^{13}C NMR (126 MHz, $CDCl_3$) δ 169.56, 167.18, 156.13, 139.98, 135.11, 129.88, 128.23, 127.64, 122.64, 115.17, 82.51, 51.31, 50.26, 35.53, 27.99, 27.76 ppm.

^{19}F NMR (377 MHz, $CDCl_3$) δ -75.93 ppm.

M.P. = 112-114 °C

IR (thin film) ν_{max}/cm^{-1}: 3356, 3003, 2974, 2938, 2365, 1732, 1666, 1596, 1550, 1491, 1460, 1420, 1403, 1353, 1223, 1162 1003, 942, 909, 847, 760, 729, 693, 614, 580, 514, 474, 426.

HRMS (ESI) Calculated for $C_{18}H_{25}F_3N_3O_4^+$ ($[M+NH_4]^+$): 404.1792, measured: 404.1792.

$[\alpha]_D^{25}$ (deg $cm^3g^{-1}dm^{-1}$) = -109.4 (c = 1.0 gcm^{-3}, MeOH)

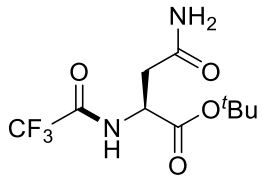

(30): *tert*-butyl (2,2,2-trifluoroacetyl)-*L*-asparaginate: Prepared according to general procedure, using amine (1 equiv, 0.5 mmol) and alcohol in excess (1.5 equiv, 0.75 mmol). The reaction was performed using 5 mol% CuI, 5 mol% $^{t\text{Bu}}$bpy, and 3 mol% ABNO.
Purification: SiO_2 plug w/ EtOAc, removed catalyst components; normal phase silica gel chromatography was used with an isocratic run of 66% EtOAc in pentanes.
Yield: 89% NMR yield; 88% isolated yield, 124.4 mg of white powder.
^{1}H NMR (500 MHz, $CDCl_3$) δ 7.76 (d, *J* = 8.1 Hz, 1H), 5.54 (d, *J* = 16.7 Hz, 2H), 4.68 (dt, *J* = 8.1, 4.1 Hz, 1H), 3.03 (dd, *J* = 16.5, 4.0 Hz, 1H), 2.77 (dd, *J* = 16.4, 4.2 Hz, 1H), 1.48 ppm (s, 9H).
^{13}C NMR (126 MHz, $CDCl_3$) δ 171.65, 168.08, 157.01, 115.68, 83.46, 49.58, 35.76, 27.76 ppm.
^{19}F NMR (377 MHz, $CDCl_3$) δ -76.10 ppm.
M.P. = 129-130 °C
IR (thin film) ν_{max}/cm^{-1}: 3447, 3358, 3333, 3191, 3043, 2988, 2938, 2892, 1735, 1709, 1675, 1611, 1565, 1459, 1407, 1375, 1339, 1270, 1191, 1155, 1049, 977, 901, 872, 839, 783, 731, 636, 555, 480, 437.
HRMS (ESI) Calculated for $C_{10}H_{15}F_3N_2O_4Na^+$ ($[M+Na]^+$): 307.0876, measured: 307.0871.
$[\alpha]_D^{25}$ (deg $cm^3g^{-1}dm^{-1}$) = -24.4 (c = 1.0 gcm^{-3}, MeOH)

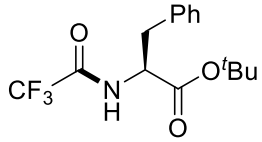

(31): *tert*-butyl (2,2,2-trifluoroacetyl)-*L*-phenylalaninate: Prepared according to general procedure, using amine (1 equiv, 0.5 mmol) and alcohol in excess (1.5 equiv, 0.75 mmol). The reaction was performed using 5 mol% CuI, 5 mol% $^{t\text{Bu}}$bpy, and 3 mol% ABNO.
Purification: SiO_2 plug w/ EtOAc, removed catalyst components; normal phase silica gel chromatography was used with an isocratic run of 5% EtOAc in pentanes.
Yield: quantitative NMR yield; 98% isolated yield, 155.7 mg of pale yellow clear crystals.
^{1}H NMR (500 MHz, $CDCl_3$) δ 7.29 (dddd, *J* = 11.5, 7.0, 4.6, 2.4 Hz, 3H), 7.18 – 7.07 (m, 2H), 6.79 (d, *J* = 7.5 Hz, 1H), 4.73 (dt, *J* = 7.5, 5.8 Hz, 1H), 3.23 – 3.13 (m, 2H), 1.44 ppm (s, 9H).
^{13}C NMR (126 MHz, $CDCl_3$) δ 168.96, 156.38, 134.88, 129.39, 128.59, 127.41, 115.48, 83.61, 53.85, 37.29, 27.90 ppm.
^{19}F NMR (377 MHz, $CDCl_3$) δ -76.05 ppm.
M.P. = 35-37 °C
IR (thin film) ν_{max}/cm^{-1}: 3354, 3086, 3029, 2980, 2932, 1703, 1548, 1496, 1454, 1367, 1285, 1244, 1167, 1021, 977, 918, 874, 841, 785, 750, 726, 697, 665, 567, 537, 482.
HRMS (ESI) Calculated for $C_{15}H_{22}F_3N_2O_3$ ($[M+NH_4]^+$): 335.1577, measured: 335.1576.
$[\alpha]_D^{25}$ (deg $cm^3g^{-1}dm^{-1}$) = -8.8 (c = 1.0 gcm^{-3}, MeOH)
Previously reported compound.[16]

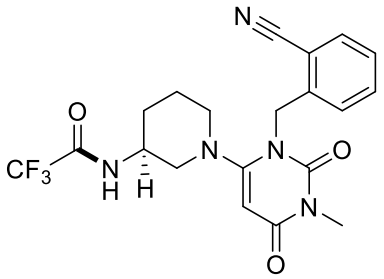

(32): (*S*)-*N*-(1-(3-(2-cyanobenzyl)-1-methyl-2,6-dioxo-1,2,3,6-tetrahydropyrimidin-4-yl)piperidin-3-yl)-2,2,2-trifluoroacetamide: Prepared according to general procedure, using amine (1 equiv, 0.5 mmol) and alcohol in excess (1.5 equiv, 0.75 mmol). The reaction was performed using 10 mol% CuI, 10 mol% $^{t\text{Bu}}$bpy, and 6 mol% ABNO.
Purification: SiO_2 plug w/ EtOAc, removed catalyst components; normal phase silica gel chromatography was used with a gradient of 50% to 70% EtOAc in pentanes.
Yield: 94% NMR yield; 94% isolated yield, 205.3 mg of cream powder.
Yield using 5 mol% CuI, 5 mol% $^{t\text{Bu}}$bpy, and 3 mol% ABNO: 85% NMR yield
^{1}H NMR (500 MHz, T = 80°C, DMSO-d_6) δ 9.09 (d, *J* = 7.4 Hz, 1H), 7.79 (dd, *J* = 7.7, 1.3 Hz, 1H), 7.64 (td, *J* = 7.7, 1.4 Hz, 1H), 7.45 (td, *J* = 7.6, 1.1 Hz, 1H), 7.25 (d, *J* = 7.9 Hz, 1H), 5.37 (s, 1H), 5.25 – 5.10 (m, 2H), 3.89 – 3.68 (m, 1H), 3.17 – 3.12 (m, 1H), 3.12 (s, 3H), 3.03 (d, *J* = 12.2 Hz, 1H), 2.66 (dt, *J* = 11.5, 9.1 Hz, 2H), 1.91 – 1.71 (m, 2H), 1.66 – 1.42 ppm (m, 2H).
^{13}C NMR (126 MHz, T = 80°C, DMSO-d_6) δ 161.99, 159.17, 155.86, 151.99, 140.94, 133.19, 132.97, 127.74, 126.94, 116.94, 114.54, 109.97, 89.94, 53.90, 51.01, 46.33, 45.91, 28.28, 27.21, 22.75 ppm.
^{19}F NMR (377 MHz, DMSO-d_6) δ -74.68 ppm.
M.P. = 204-207 °C
IR (thin film) ν_{max}/cm^{-1}: 3280, 3102, 2956, 2921, 2851, 2760, 2364, 2223, 2187, 2088, 1698, 1657, 1605, 1559, 1432, 1361, 1305, 1184, 1107, 1035, 964, 891, 865, 811, 766, 697, 602, 556, 526, 494, 457, 428.
HRMS (ESI) Calculated for $C_{20}H_{21}F_3N_5O_3^+$ ($[M+H]^+$): 436.1591, measured: 436.1589.
$[\alpha]_D^{25}$ (deg $cm^3g^{-1}dm^{-1}$) = +26.3 (c = 1.0 gcm^{-3}, MeOH)

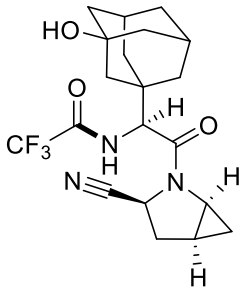

(33): *N*-((*S*)-2-((1*S*,3*S*,5*S*)-3-cyano-2-azabicyclo[3.1.0]hexan-2-yl)-1-((1*r*,3*R*,5*R*,7*S*)-3-hydroxyadamantan-1-yl)-2-oxoethyl)-2,2,2-trifluoroacetamide: Prepared according to general procedure, using amine (1 equiv, 0.5 mmol) and alcohol in excess (1.5 equiv, 0.75 mmol). The reaction was performed using 5 mol% CuI, 5 mol% $^{t\text{Bu}}$bpy, and 3 mol% ABNO.
Purification: SiO_2 plug w/ EtOAc, removed catalyst components; normal phase silica gel chromatography was used with an isocratic run of 66% EtOAc in pentanes.
Yield: 94% NMR yield; 87% isolated yield, 179.0 mg of white powder.
^{1}H NMR (500 MHz, $CDCl_3$) δ 7.11 (d, *J* = 9.5 Hz, 1H), 5.05 (dd, *J* = 10.6, 2.3 Hz, 1H), 4.83 (d, *J* = 9.4 Hz, 1H), 3.77 (td, *J* = 5.5, 5.1, 3.4 Hz, 1H), 2.60 (ddd, *J* = 13.7, 10.6, 5.7 Hz, 1H), 2.41 (dd, *J* = 13.7, 2.3 Hz, 1H), 2.29 (t, *J* = 3.4 Hz, 2H), 1.96 (dq, *J* = 8.0, 6.1 Hz, 1H), 1.76 (dd, *J* = 11.4, 2.5 Hz, 1H), 1.74 – 1.64 (m, 6H), 1.62 – 1.58 (m, 3H), 1.54 (ddd, *J* = 15.6, 10.7, 5.0 Hz, 3H), 1.19 – 1.08 ppm (m, 2H).
^{13}C NMR (126 MHz, $CDCl_3$) δ 167.59, 157.21, 118.84, 115.85, 68.39, 57.51, 46.15, 45.28, 44.16, 44.13, 41.79, 38.20, 37.57, 37.19, 34.95, 30.33, 30.05, 30.04, 17.96, 13.52 ppm.
^{19}F NMR (377 MHz, $CDCl_3$) δ -75.48 ppm.
M.P. = 163-168 °C
IR (thin film) ν_{max}/cm^{-1}: 3530, 3423, 3331, 2921, 2855, 2359, 2239, 2050, 1712, 1645, 1538 1450, 1346, 1308, 1251, 1213, 1151, 1039, 965, 916, 894, 827, 763, 721, 688, 629, 583, 522, 479.
HRMS (ESI) Calculated for $C_{20}H_{24}F_3N_3O_3Na^+$ ($[M+Na]^+$): 434.1662, measured: 434.1660.
$[\alpha]_D^{25}$ (deg $cm^3g^{-1}dm^{-1}$) = +5.3 (c = 1.0 gcm^{-3}, MeOH)

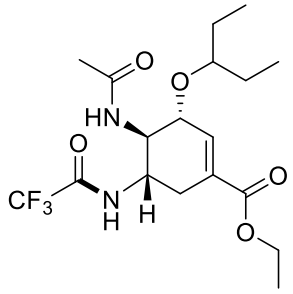

(34): ethyl (3*R*,4*R*,5*S*)-4-acetamido-3-(pentan-3-yloxy)-5-(2,2,2-trifluoroacetamido)cyclohex-1-ene-1-carboxylate: Prepared according to general procedure, using amine (1 equiv, 0.5 mmol) and alcohol in excess (1.5 equiv, 0.75 mmol). The reaction was performed using 10 mol% CuI, 10 mol% $^{t\text{Bu}}$bpy, and 6 mol% ABNO.
Purification: SiO_2 plug w/ EtOAc, removed catalyst components; normal phase silica gel chromatography was used with a gradient of 25% to 40% EtOAc in pentanes.
Yield: 90% NMR yield; 90% isolated yield, 184.3 mg of foamy white solid.
Yield using 5 mol% CuI, 5 mol% $^{t\text{Bu}}$bpy, and 3 mol% ABNO: 86% NMR yield
^{1}H NMR (500 MHz, $CDCl_3$) δ 8.25 (d, *J* = 7.7 Hz, 1H), 6.87 – 6.82 (m, 1H), 5.85 (d, *J* = 8.0 Hz, 1H), 4.27 – 4.14 (m, 4H), 4.08 – 4.02 (m, 1H), 3.40 (p, *J* = 5.7 Hz, 1H), 2.79 (ddt, *J* = 18.1, 5.0, 1.5 Hz, 1H), 2.52 (ddt, *J* = 18.0, 8.0, 2.6 Hz, 1H), 1.98 (s, 3H), 1.57 – 1.45 (m, 4H), 1.30 (t, *J* = 7.1 Hz, 3H), 0.89 ppm (td, *J* = 7.4, 2.9 Hz, 6H).
^{13}C NMR (126 MHz, $CDCl_3$) δ 171.46, 165.68, 157.59, 136.33, 129.30, 115.76, 82.34, 74.47, 61.18, 52.60, 48.94, 29.10, 26.17, 25.70, 22.98, 14.17, 9.39, 9.21 ppm.
^{19}F NMR (377 MHz, $CDCl_3$) δ -76.17 ppm.
M.P. = 168-173 °C
IR (thin film) ν_{max}/cm^{-1}: 3338, 3284, 3211, 3060, 2967, 2925, 2877, 1709, 1659, 1549, 1460, 1374, 1311, 1247, 1186, 1158, 1128, 1091, 1055, 1016, 947, 862, 803, 729, 690, 652, 603, 568, 521, 465, 436.
HRMS (ESI) Calculated for $C_{19}H_{28}F_3N_2O_5^+$ ($[M+H]^+$): 409.1945, measured: 409.1942.
$[\alpha]_D^{25}$ (deg $cm^3g^{-1}dm^{-1}$) = -50.4 (c = 1.0 gcm^{-3}, MeOH)

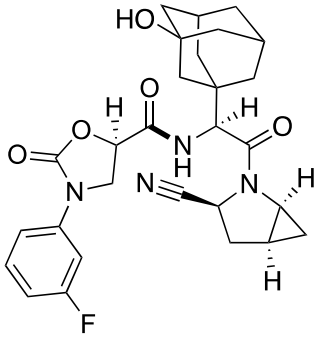

(35): (*R*)-*N*-((*S*)-2-((1*S*,3*S*,5*S*)-3-cyano-2-azabicyclo[3.1.0]hexan-2-yl)-1-((1*r*,3*R*,5*R*,7*S*)-3-hydroxyadamantan-1-yl)-2-oxoethyl)-3-(3-fluorophenyl)-2-oxooxazolidine-5-carboxamide:
Prepared according to general procedure, using amine (1 equiv, 0.5 mmol) and alcohol in excess (1.1 equiv, 0.55 mmol). The reaction was performed using 5 mol% CuI, 5 mol% $^{t\text{Bu}}$bpy, and 3 mol% ABNO.
Purification: Normal phase silica gel chromatography was used with a gradient of 1% to 6% to 10% MeOH in DCM.
Yield: 77% NMR yield; 70% isolated yield, 183.8 mg of white powder.
^{1}H NMR (500 MHz, $CDCl_3$) δ 7.42 (dt, *J* = 11.0, 2.3 Hz, 1H), 7.36 – 7.30 (m, 2H), 7.21 (dd, *J* = 8.3, 1.8 Hz, 1H), 6.87 (td, *J* = 8.2, 2.4 Hz, 1H), 5.16 – 4.98 (m, 2H), 4.87 (d, *J* = 9.4 Hz, 1H), 4.27 (t, *J* = 9.5 Hz, 1H), 4.15 (dd, *J* = 9.2, 6.6 Hz, 1H), 3.80 (dt, *J* = 6.5, 4.1 Hz, 1H), 2.56 (ddd, *J* = 13.7, 10.6, 5.7 Hz, 1H), 2.37 (dd, *J* = 13.6, 2.3 Hz, 1H), 2.29 (q, *J* = 3.2 Hz, 2H), 1.91 (p, *J* = 6.3 Hz, 1H), 1.83 – 1.49 (m, 13H), 1.14 – 1.08 ppm (m, 2H).
^{13}C NMR (126 MHz, $CDCl_3$) δ 168.15, 168.12, 163.02, 152.54, 138.93, 130.39, 119.05, 113.29, 111.37, 105.88, 69.93, 68.48, 57.14, 47.64, 46.33, 45.23, 44.33, 44.15, 41.58, 38.07, 37.70, 37.09, 35.05, 30.36, 30.16, 30.10, 17.88, 13.52 ppm.
^{19}F NMR (376 MHz, $CDCl_3$) δ -110.41 ppm.
M.P. = >260 °C
IR (thin film) ν_{max}/cm^{-1}: 3535, 3490, 3414, 3086, 2912, 2852, 2363, 1755, 1681, 1635, 1587, 1516, 1452, 1401, 1319, 1218, 1185, 1144, 1116, 1081, 1030, 949, 924, 898, 863, 829, 779, 751, 684, 658, 616, 55, 526, 511, 445.
HRMS (ESI) Calculated for $C_{28}H_{35}FN_5O_5^+$ ($[M+NH_4]^+$): 540.2617, measured: 540.2625.
$[\alpha]_D^{25}$ (deg $cm^3g^{-1}dm^{-1}$) = -11.6 (c = 1.0 gcm^{-3}, DCM)

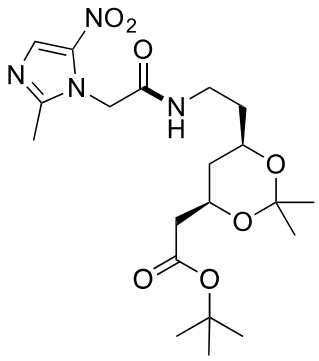

(36): *tert*-butyl 2-((4*R*,6*R*)-2,2-dimethyl-6-(2-(2-(2-methyl-5-nitro-1*H*-imidazol-1-yl)acetamido)ethyl)-1,3-dioxan-4-yl)acetate: Prepared according to general procedure, using alcohol (1 equiv, 0.5 mmol) and amine in excess (1.1 equiv, 0.55 mmol). The reaction was performed using 20 mol% CuI, 20 mol% $^{t\text{Bu}}$bpy, and 12 mol% ABNO in DMF.
Purification: Normal phase silica gel chromatography was used with an isocratic run of 4% MeOH in DCM.
Yield: 78% NMR yield; 76% isolated yield, 167.2 mg of yellow solid.
Yield using 10 mol% CuI, 10 mol% $^{t\text{Bu}}$bpy, and 6 mol% ABNO: 56% NMR yield
Yield using 15 mol% CuI, 15 mol% $^{t\text{Bu}}$bpy, and 9 mol% ABNO: 62% NMR yield
^{1}H NMR (500 MHz, $CDCl_3$) δ 7.97 (s, 1H), 6.54 (s, 1H), 4.87 (q, *J* = 15.9 Hz, 2H), 4.27 (dddd, *J* = 11.6, 9.2, 6.4, 2.4 Hz, 1H), 4.02 (ddt, *J* = 11.3, 8.5, 2.9 Hz, 1H), 3.56 (dtd, *J* = 13.3, 6.7, 4.9 Hz, 1H), 3.29 (ddt, *J* = 13.0, 8.5, 4.5 Hz, 1H), 2.52 (s, 3H), 2.46 – 2.27 (m, 2H), 1.76 (dddd, *J* = 14.7, 7.5, 4.6, 3.2 Hz, 1H), 1.62 (dtd, *J* = 13.4, 8.2, 4.7 Hz, 1H), 1.55 (dt, *J* = 12.8, 2.5 Hz, 1H), 1.47 (s, 3H), 1.45 (s, 9H), 1.37 (s, 3H), 1.27 ppm (dt, *J* = 12.7, 11.5 Hz, 1H).
^{13}C NMR (126 MHz, $CDCl_3$) δ 170.07, 164.50, 132.91, 98.89, 80.74, 69.00, 66.07, 48.75, 42.51, 37.65, 35.99, 34.66, 30.11, 28.09, 19.71, 14.27 ppm.
M.P. = 92-98 °C
IR (thin film) ν_{max}/cm^{-1}: 3299, 3116, 2982, 2939, 2872, 2364, 1721, 1663, 1563, 1531, 1468, 1429, 1368, 1327, 1267, 1192, 1147, 1036, 1008, 949, 839, 744, 679, 645, 585, 546, 464.
HRMS (ESI) Calculated for $C_{20}H_{32}N_4O_7Na^+$ ($[M+Na]^+$): 463.2163, measured: 463.2166.
$[\alpha]_D^{25}$ (deg $cm^3g^{-1}dm^{-1}$) = +5.2 (c = 1.0 gcm^{-3}, MeOH)

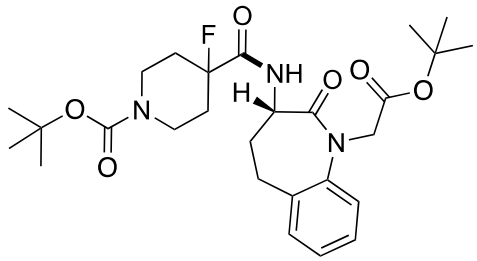

(37): *tert*-butyl (*S*)-4-((1-(2-(*tert*-butoxy)-2-oxoethyl)-2-oxo-2,3,4,5-tetrahydro-1*H*-benzo[*b*]azepin-3-yl)carbamoyl)-4-fluoropiperidine-1-carboxylate: Prepared according to general procedure, using amine (1 equiv, 0.5 mmol) and alcohol in excess (1.1 equiv, 0.55 mmol). The reaction was performed using 10 mol% CuI, 10 mol% $^{t\text{Bu}}$bpy, and 6 mol% ABNO. Purification: SiO_2 plug w/ EtOAc, removed catalyst components; normal phase silica gel chromatography was used with a gradient of 25% to 45% EtOAc in pentanes.
Yield: 88% NMR yield; 87% isolated yield, 225.2 mg of white powder.
^{1}H NMR (500 MHz, $CDCl_3$) δ 7.36 (t, *J* = 6.0 Hz, 1H), 7.29 (td, *J* = 7.6, 1.8 Hz, 1H), 7.23 (ddd, *J* = 17.3, 7.9, 2.0 Hz, 2H), 7.11 (dd, *J* = 7.9, 1.2 Hz, 1H), 4.66 (d, *J* = 17.0 Hz, 1H), 4.48 (dt, *J* = 11.1, 7.4 Hz, 1H), 4.26 (d, *J* = 17.1 Hz, 1H), 4.02 (s, 2H), 3.39 (td, *J* = 12.9, 8.0 Hz, 1H), 3.03 (s, 2H), 2.74 – 2.56 (m, 2H), 2.17 – 1.90 (m, 3H), 1.83 – 1.66 (m, 2H), 1.45 (s, 9H), 1.43 ppm (s, 9H).
^{13}C NMR (126 MHz, $CDCl_3$) δ 170.66, 170.65, 167.46, 154.53, 140.40, 135.49, 129.73, 127.98, 127.28, 122.64, 95.58, 94.09, 82.26, 79.81, 51.18, 49.39, 39.20, 38.50, 36.11, 32.08, 31.85, 28.39, 28.00 ppm.
^{19}F NMR (376 MHz, $CDCl_3$) δ -168.25 ppm.
M.P. = 66-71 °C
IR (thin film) ν_{max}/cm^{-1}: 3410, 3346, 2972, 2930, 2870, 2186, 2076, 1997, 1740, 1663, 1604, 1516, 1457, 1417, 1365, 1280, 1227, 1147, 1058, 1004, 941, 859, 761, 695, 642, 585, 546, 519, 461, 423.
HRMS (ESI) Calculated for $C_{27}H_{42}FN_4O_6$ ($[M+NH_4]^+$): 537.3083, measured: 537.3083.
$[\alpha]_D^{25}$ (deg $cm^3g^{-1}dm^{-1}$) = -72.0 (c = 1.0 gcm^{-3}, MeOH)

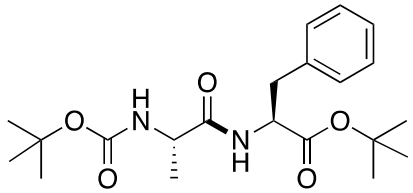

(38): *tert*-butyl (*tert*-butoxycarbonyl)-*L*-alanyl-*L*-phenylalaninate: Prepared according to general procedure, using alcohol (1 equiv, 0.5 mmol) and alcohol in amine (1.5 equiv, 0.75 mmol). The reaction was performed using 15 mol% CuI, 15 mol% $^{t\text{Bu}}$bpy, and 9 mol% ABNO. Purification: SiO_2 plug w/ EtOAc, removed catalyst components; normal phase silica gel chromatography was used with a gradient of 10% to 25% to 50% EtOAc in pentanes.
Yield: 72% NMR yield; 68% isolated yield, 134.4 mg of fluffy pale yellow solid.
Yield using 10 mol% CuI, 10 mol% $^{t\text{Bu}}$bpy, and 6 mol% ABNO: 60% NMR yield, 57% isolated yield.
^{1}H NMR (500 MHz, $CDCl_3$) δ 7.32 – 7.26 (m, 2H), 7.25 – 7.20 (m, 1H), 7.18 – 7.12 (m, 2H), 6.45 (d, *J* = 7.7 Hz, 1H), 4.93 (s, 1H), 4.71 (dt, *J* = 7.7, 6.0 Hz, 1H), 4.13 (q, *J* = 7.8 Hz, 1H), 3.17 – 3.00 (m, 2H), 1.44 (s, 9H), 1.40 (s, 9H), 1.33 ppm (d, *J* = 7.1 Hz, 3H).
^{13}C NMR (126 MHz, $CDCl_3$) δ 171.95, 170.24, 136.06, 129.54, 128.35, 126.96, 82.40, 53.55, 38.02, 28.29, 27.94, 18.47 ppm.
M.P. = 47-52 °C
IR (thin film) ν_{max}/cm^{-1}: 3343, 3295, 2974, 2931, 1732, 1691, 1651, 1522, 1450, 1389, 1363, 1325, 1248, 1156, 1072, 1040, 961, 852, 747, 696, 650, 604, 560, 493, 463.
HRMS (ESI) Calculated for $C_{21}H_{33}N_2O_5^+$ ($[M+H]^+$): 393.2384, measured: 393.2381.
$[\alpha]_D^{25}$ (deg $cm^3g^{-1}dm^{-1}$) = -11.7 (c = 1.0 gcm^{-3}, MeOH)
Previously reported compound.[17]

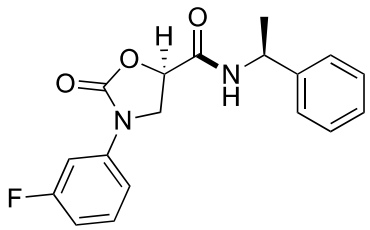

(39): (*R*)-3-(3-fluorophenyl)-2-oxo-*N*-((*S*)-1-phenylethyl)oxazolidine-5-carboxamide:
Prepared according to general procedure, using alcohol (1 equiv, 0.5 mmol) and amine in excess (1.1 equiv, 0.55 mmol). The reaction was performed using 10 mol% CuI, 10 mol% $^{t\text{Bu}}$bpy, and 6 mol% ABNO.
Purification: SiO_2 plug w/ EtOAc, removed catalyst components; normal phase silica gel chromatography was used with a gradient of 33% to 50% to 75% EtOAc in pentanes.
Yield: 90% NMR yield; 89% isolated yield, >20:1 d.r., 146.1 mg of white powder.
^{1}H NMR (500 MHz, $CDCl_3$) δ 7.42 (dt, *J* = 11.0, 2.3 Hz, 1H), 7.36 – 7.27 (m, 6H), 7.18 – 7.13 (m, 1H), 6.87 (tdd, *J* = 8.2, 2.5, 0.8 Hz, 1H), 6.82 (d, *J* = 8.1 Hz, 1H), 5.16 (p, *J* = 7.1 Hz, 1H), 5.02 (dd, *J* = 9.8, 6.3 Hz, 1H), 4.27 (t, *J* = 9.6 Hz, 1H), 4.14 (dd, *J* = 9.4, 6.3 Hz, 1H), 1.56 ppm (d, *J* = 7.0 Hz, 3H).
^{13}C NMR (126 MHz, $CDCl_3$) δ 167.18, 163.01, 152.82, 141.96, 138.81, 130.39, 128.91, 127.80, 126.01, 113.42, 111.51, 106.07, 70.13, 49.19, 48.09, 21.86 ppm.
^{19}F NMR (377 MHz, $CDCl_3$) δ -110.48 ppm.
M.P. = 214-215 °C
IR (thin film) ν_{max}/cm^{-1}: 3298, 3096, 3032, 2977, 2929, 2874, 1740, 1656, 1611, 1556, 1494, 1471, 1411, 1333, 1319, 1256, 1224, 1198, 1168, 1112, 1044, 1012, 911, 867, 803, 771, 751, 692, 543, 458.
HRMS (ESI) Calculated for $C_{18}H_{18}FN_2O_3^+$ ($[M+H]^+$): 329.1296, measured: 329.1294.
$[\alpha]_D^{25}$ (deg $cm^3g^{-1}dm^{-1}$) = -40.8 (c = 1.0 gcm^{-3}, DCM)

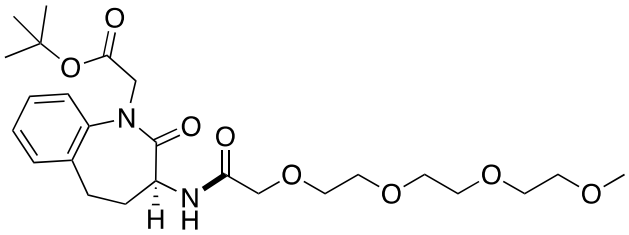

(40): *tert*-butyl (*S*)-2-(2-oxo-3-(2,5,8,11-tetraoxatridecan-13-amido)-2,3,4,5-tetrahydro-1*H*-benzo[*b*]azepin-1-yl)acetate:

Prepared according to general procedure, using alcohol (1 equiv, 0.5 mmol) and alcohol in amine (1.1 equiv, 0.55 mmol). The reaction was performed using 10 mol% CuI, 10 mol% $^{t\text{Bu}}$bpy, and 6 mol% ABNO.

Purification: SiO_2 plug w/ EtOAc, removed catalyst components; normal phase silica gel chromatography was used with a gradient of 80% to 100% EtOAc in pentanes followed by 5% MeOH in EtOAc to flush the remainder of product off the column.

Yield: quantitative NMR yield; 96% isolated yield, 236.9 mg of dark yellow oil.

^{1}H NMR (500 MHz, $CDCl_3$) δ 7.55 (d, *J* = 7.7 Hz, 1H), 7.29 (dd, *J* = 7.5, 1.8 Hz, 1H), 7.26 – 7.17 (m, 2H), 7.11 (dd, *J* = 7.9, 1.3 Hz, 1H), 4.69 (d, *J* = 17.0 Hz, 1H), 4.57 (dt, *J* = 11.1, 7.5 Hz, 1H), 4.23 (d, *J* = 17.0 Hz, 1H), 4.04 – 3.89 (m, 2H), 3.75 – 3.61 (m, 10H), 3.56 (dd, *J* = 5.7, 3.7 Hz, 2H), 3.43 – 3.33 (m, 4H), 2.63 (ddt, *J* = 18.7, 10.3, 7.2 Hz, 2H), 2.02 (td, *J* = 11.5, 8.0 Hz, 1H), 1.42 ppm (s, 9H).

^{13}C NMR (126 MHz, $CDCl_3$) δ 170.88, 168.91, 167.56, 140.51, 135.61, 129.75, 127.90, 127.14, 122.59, 82.12, 71.91, 71.03, 70.70, 70.59, 70.56, 70.52, 70.40, 59.05, 51.06, 49.03, 36.25, 28.14, 28.00 ppm.

IR (thin film) ν_{max}/cm^{-1}: 3504, 3396, 2927, 2874, 1740, 1661, 1603, 1518, 1457, 1396, 1365, 1294, 1226, 1149, 1102, 1025, 943, 846, 760, 694, 648, 561, 476.

HRMS (ESI) Calculated for $C_{25}H_{38}N_2O_8Na^+$ ($[M+Na]^+$): 517.2520, measured: 517.2519.

$[\alpha]_D^{25}$ (deg $cm^3g^{-1}dm^{-1}$) = -71.4 (c = 1.0 gcm^{-3}, MeOH)

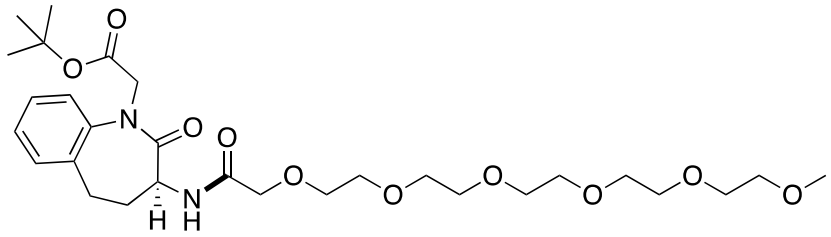

(41): *tert*-butyl (*S*)-2-(3-(2,5,8,11,14,17-hexaoxanonadecan-19-amido)-2-oxo-2,3,4,5-tetrahydro-1*H*-benzo[*b*]azepin-1-yl)acetate:

Prepared according to general procedure, using alcohol (1 equiv, 0.5 mmol) and alcohol in amine (1.1 equiv, 0.55 mmol). The reaction was performed using 10 mol% CuI, 10 mol% $^{t\text{Bu}}$bpy, and 6 mol% ABNO.

Purification: SiO_2 plug w/ EtOAc, removed catalyst components; normal phase silica gel chromatography was used with a gradient of 80% to 100% EtOAc in pentanes followed by 5% MeOH in EtOAc to flush the remainder of product off the column.

Yield: quantitative NMR yield; 99% isolated yield, 290.1 mg of orange yellow oil.

^{1}H NMR (500 MHz, $CDCl_3$) δ 7.55 (d, *J* = 7.7 Hz, 1H), 7.32 – 7.27 (m, 1H), 7.26 – 7.23 (m, 1H), 7.20 (td, *J* = 7.4, 1.2 Hz, 1H), 7.11 (dd, *J* = 7.9, 1.2 Hz, 1H), 4.69 (d, *J* = 17.0 Hz, 1H), 4.57 (dt, *J* = 11.1, 7.5 Hz, 1H), 4.23 (d, *J* = 17.0 Hz, 1H), 4.04 – 3.87 (m, 2H), 3.71 – 3.63 (m, 18H), 3.57 – 3.53 (m, 2H), 3.43 – 3.34 (m, 4H), 2.63 (ddt, *J* = 18.7, 10.3, 7.3 Hz, 2H), 2.10 – 1.97 (m, 1H), 1.42 ppm (s, 9H).

^{13}C NMR (126 MHz, $CDCl_3$) δ 170.89, 168.90, 167.57, 140.52, 135.62, 129.76, 127.91, 127.15, 122.60, 82.12, 71.93, 71.05, 70.71, 70.57, 70.55, 70.50, 70.41, 59.05, 51.07, 49.04, 36.26, 28.15, 28.01 ppm.

IR (thin film) ν_{max}/cm^{-1}: 3506, 3398, 2871, 1740, 1662, 1602, 1518, 1457, 1396, 1363, 1294, 1227, 1147, 1100, 1031, 944, 846, 761, 694, 648, 563, 477.

HRMS (ESI) Calculated for $C_{29}H_{50}N_3O_{10}^+$ ($[M+NH_4]^+$): 600.3491, measured: 600.3490.

$[\alpha]_D^{25}$ (deg $cm^3g^{-1}dm^{-1}$) = -66.1 (c = 1.0 gcm^{-3}, MeOH)

6E.IX. References

1. Piszel, P. E.; Vasilopoulos, A.; Stahl, S. S. Oxidative Amide Coupling from Functionally Diverse Alcohols and Amines using Aerobic Copper/Nitroxyl Catalysis. *Angew. Chem. Int. Ed.* **2019**, *58*, 12211-12215.
2. F. L. M. Pattison, W. C. Howell, A. J. McNamara, J. C. Schneider, J. F. Walker, *J. Org. Chem.* **1956**, *21*, 739–747.
3. B. C. Saunders, G. J. Stacey, I. G. E. Wilding, *J. Chem. Soc.* **1949**, *0*, 773–777.
4. G. W. Gribble, *J. Chem. Educ.* **1973**, *50*, 460–462.
5. A. Welle, F. Billard, J. Marchand-Brynaert, *Synth.* **2012**, *44*, 2249–2254.
6. K. Kataoka, K. Wachi, X. Jin, K. Suzuki, Y. Sasano, Y. Iwabuchi, J. Y. Hasegawa, N. Mizuno, K. Yamaguchi, *Chem. Sci.* **2018**, *9*, 4756–4768.
7. M. J. Tomaszewski, L. Boisvert, S. Jin, *Tetrahedron Lett.* **2009**, *50*, 1435–1437.
8. J. M. Li, Y. Yu, J. Weng, G. Lu, *Org. Biomol. Chem.* **2018**, *16*, 6047–6056.
9. H. M. Marsden, K. Yasufuku, J. M. Shreeve, *Inorg. Chem.* **1983**, *22*, 1202–1204.
10. H. J. Davis, G. R. Genov, R. J. Phipps, *Angew Chem. Int. Ed.* **2017**, *56*, 13351–13355; *Angew. Chem.* **2017**, *179*, 13536–13540.
11. F. Cumine, S. Zhou, T. Tuttle, J.A. Murphy, *Org. Biomol. Chem.* **2017**, *15*, 3324–3336.
12. A. R. Katritzky, B. Yang, G. Qui, Z. Zhong, *Synthesis* **1999**, 55–57.
13. I. Parikh, H. Hilpert, K. Hermann, A. S. Dreiding, *Helv. Chim. Acta* **1986**, *69*, 1588–1596.
14. T. Weinrich, E. A. Jaumann, U. Scheffer, T. F. Prisner, M. W. Göbel, *Chem. Eur. J.* **2018**, *24*, 6202–6207.
15. E. McNeill, J. Du Bois, *Chem. Sci.* **2012**, *3*, 1810–1813.
16. D. Albanese, F. Corcella, D. Landini, A. Maia, M. Penso, *J. Chem. Soc., Perkin Trans. 1* **1997**, 247–250.
17. P. Strazzolini, T. Melloni, A. G. Guimanini, *Tetrahedron* **2001**, *57*, 9033-9043.